SEISMIC PARAMETERS FOR THE CENTRAL UNITED STATES BASED ON PALEOLIQUEFACTION EVIDENCE IN THE WABASH VALLEY

by

Eric C. Pond

Dissertation submitted to the Faculty of the

Virginia Polytechnic Institute and State University

in partial fulfillment of the requirements for the degree of

DOCTOR OF PHILOSOPHY

in

Civil Engineering

APPROVED:

Prof. James R. Martin II, Chairman

Prof. J. Michael Duncan

Prof. Thomas L. Brandon

Prof. George M. Filz

Prof. M. P. Singh

June, 1996
Blacksburg, Virginia

Keywords: Earthquakes, Paleoliquefaction, Seismicity, Central United States

SEISMIC PARAMETERS FOR THE CENTRAL UNITED STATES BASED ON PALEOLIQUEFACTION EVIDENCE IN THE WABASH VALLEY

by

Eric C. Pond

Prof. James R. Martin II, Chairman

Department of Civil Engineering

(ABSTRACT)

Seismicity in the central United States has typically been defined by the New Madrid Seismic Zone. Recent discoveries of paleoliquefaction evidence outside that Zone suggest prehistoric earthquake magnitudes in the Wabash Valley far exceed historical events. This geotechnical engineering study of paleoliquefaction sites in southern Indiana and along the Wabash River in Illinois has provided an opportunity to estimate magnitudes and attenuation characteristics associated with strong prehistoric Wabash Valley earthquakes.

In-situ soil strength parameters have been measured at 22 sites over an area in the Wabash River drainage approximately 250 km N-S, and 180 km E-W. These parameters have been used in liquefaction susceptibility analyses to estimate moment magnitude (**M**) and surficial ground motion amplitudes associated with each of four separate paleo-earthquakes. In addition, site response studies based on a semi-theoretical model of

eastern North America bedrock motions have been used to compare results of the engineering study with seismological predictions of ground motions associated with large earthquakes in the region. The site response study has been used to develop an attenuation relationship for eastern North America soil sites that mirrors attenuation relationships for the western United States.

Minimum magnitude estimates are based on both distribution of paleoliquefaction evidence and on geotechnical estimates of stresses required to induce the evidence observed. A seismic energy intensity approach is then used to help improve the magnitude and surface acceleration estimates. The approach allows revised magnitude estimates by comparing peak accelerations required to induce the liquefaction effects observed to the peak surface motions predicted by the seismological model.

The results of this study suggest the Wabash Valley paleoseismic events had magnitudes of M6.9, M7.1, M7.3 and M7.8. Uncertainty exists in the analysis, but these estimates are considered reliable to within 0.25 to 0.5 magnitude unit. The geotechnical estimates of peak meizoseismal accelerations and regional attenuation characteristics were also found to be consistent with seismological predictions. The estimates of seismic parameters based on this study greatly exceed those of all historical events, suggesting the Wabash Valley seismic hazard may be underestimated by local building codes, and that seismic design requirements should be reassessed.

Acknowledgments

I would like to express my sincere appreciation for all of the assistance I received over the years that have been invested in this research. It is true that without the support of all involved it would not have been possible to complete this study. Following is a note of thanks to but a brief list of the people to whom I owe a debt of gratitude.

Many thanks to my advisor Prof. James Martin whose guidance and constant support throughout the project are greatly appreciated. Thank you for the many insights into the phenomenon of liquefaction and approaches to paleoseismic studies that proved to be invaluable in completing this research.

Thank you also to each of the members of my committee, Professors J. M. Duncan, T. L. Brandon, G. M. Filz, and M. P. Singh, whose valued suggestions and support throughout the project allowed me to make progress when the road appeared to have reached a dead end. Thank you also to all the faculty at Virginia Tech for the outstanding education offered. The background provided by the curriculum truly enhanced this project.

Thank you to Prof. G. Wayne Clough for suggesting the value of this project in the first place.

Thank you to Dr. Steve Obermeier of the U.S. Geological Survey whose initial field work lead to the discovery of the paleoliquefaction evidence, who provided supplemental outside soil profile data, and for the many hours of discussion on liquefaction that helped to improve my understanding of the phenomenon.

Thank you to Drs. Pat and Cheryl Munson of Indiana University whose field work lead to the discovery of many of the sites investigated for this study. Thank you also for the many days spent in the field pointing out identified paleoliquefaction sites possibly useful to this research project. Thank you also for the many nights' accommodations. And thank you for the many hours of discussion on local geology and site conditions

associated with the liquefaction evidence, and for the assistance with maps of site conditions and feature locations. All of this assistance truly enhaced the geotechnical research effort.

Thank you to Mr. Martin Chapman of the Virginia Tech Seismological Observatory who provided many enlightening hours of discussion on seismology and the seismic environment in the central U.S., and whose assistance in developing the synthetic ground motion records for the region proved to be a great benefit contributing to the eventual success of the project.

Many thanks to each of the property owners and farmers who were gracious enough to allow the drilling equipment access to their property, in many cases even when it required sacrifice on their part in terms of the timing of planting or harvesting.

Thank you to each of my colleagues in graduate school for the many hours of discussion and the many suggestions, both in the office and over a cold beer. Thank you especially to Messrs. Clark Morrison, Andy Rose, Alan Rauch, Kord Wissmann, Jon Porter, Jacob Esterhuizen, Carmine Polito, Vinnie Perrone, Harry Cooke, and Chris Baxter. Our discussions were truly valuable to furthering this research, and our friendship enhanced my experience in graduate school.

Thank you to the Virginia Tech support staff whose efforts kept both me and the project afloat: Judy Dumin, Clark Brown, Vickie Graham, and Judy Brown. And thank you especially to Mary Ruth McDonald, whose daily assistance and words of encouragement provided tremendous support leading to completion of this project.

And most importantly, thank you to my wife, Jami, my son, Spencer, and to each of our extended families. Without Jami's backing and support this could never have been accomplished. She has had as much to do with getting this project completed as anyone. Thank you to Spencer who provided much enthusiasm and inspiration. Thank you to each of our extended families, who provided much needed support and encouragement.

Table of Contents

List of Figures

List of Tables

1. Introduction

Until very recently, seismic hazard evaluations in the central United States have generally been associated with large historical earthquakes occurring within the New Madrid Seismic Zone (NMSZ) located in the lower Mississippi Valley. Historical earthquakes outside this zone have been infrequent and small. However, ancient liquefaction artifacts recently discovered over a widespread area of the Wabash Valley have called into question our current evaluation of the seismic hazard in this region. Of particular importance, the liquefaction findings suggest that large prehistoric earthquakes have occurred in the Wabash Valley region, far north of the New Madrid area. Evidence in the form of ancient sand boils, sand-filled dikes, and sills indicates that as many as nine moderate to large earthquakes occurred in the Wabash Valley since the late Pleistocene. These new findings are of great importance to an improved evaluation of the seismic hazard in the central U.S. region. More importantly, these findings could mean that current National Earthquake Hazard Reduction Program (NEHRP) design practices in this region are inadequate, and may contribute to a much larger seismic risk than previously recognized. The primary objective of this study therefore, is to provide a geotechnical engineering perspective on the liquefaction findings that can be used to estimate the magnitude and ground shaking levels that produced the widespread liquefaction. Importantly, this work can ultimately provide quantitative seismic parameters that can be considered in the design of constructed facilities and lifelines in the Wabash region.

Historical seismicity of the central U.S. region dates back to the end of the 17th century (Nuttli, 1979). The great New Madrid earthquakes with moment magnitudes (**M**) of approximately 8.4 in 1811-12 stand out as the largest historical seismic events in this region. As indicated in Figure 1.1, the Wabash Valley Seismic Zone (WVSZ) is located in southwest Indiana and southeast Illinois, approximately 200 km (120 mi.) northeast of the New Madrid Seismic Zone. The WVSZ runs north to south from near the confluence of the Ohio and Wabash Rivers to near Terre Haute, Indiana. In the east-west direction, the

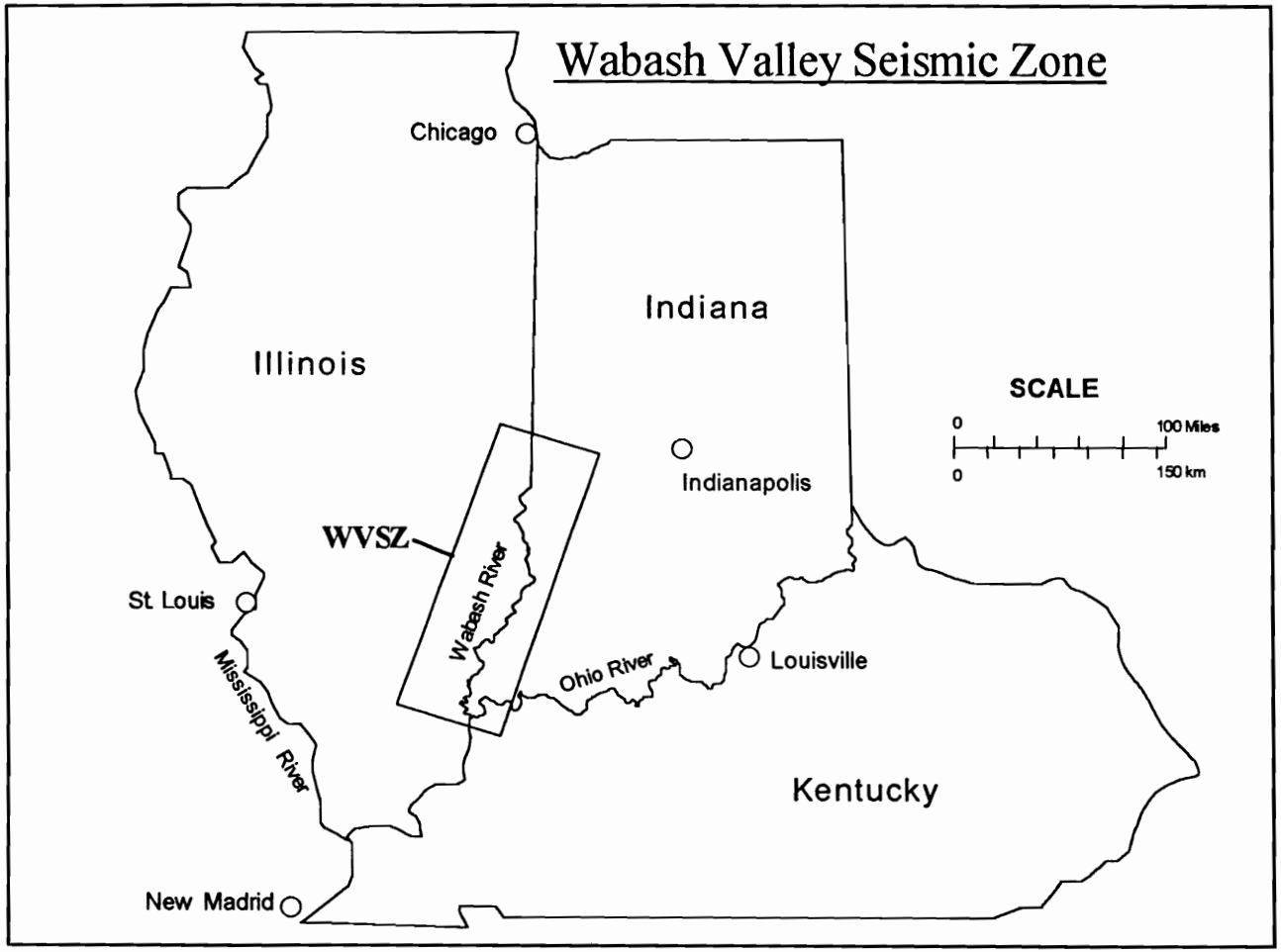

Figure 1.1. Wabash Valley Seismic Zone location map.

seismic zone is coincident with the border of Indiana and Illinois, extending approximately 50 km (30 mi.) east and west of the Wabash River.

The earliest documented earthquakes in the Wabash Valley region occurred in the early 19th century. Since that time, 15 slightly-damaging earthquakes with body wave magnitudes (m_b) in the range of $4.5 \leq m_b \leq 5.5$ have been documented in the region. Although these historical events have been small to moderate, the continuing seismic activity and the overall tectonic structure of the region suggests the capability of much larger events (Nuttli, 1979). The results of the present study strongly support this speculation.

Recent field studies of exposed soil profiles in river banks, canals, trenches, and gravel pits have revealed hundreds of prehistoric liquefaction features throughout the Wabash Valley and beyond (Obermeier, et al, 1993; Munson and Munson, 1996). Dating of the features and delineation of discreet liquefaction episodes using stratigraphic, pedological, archaeological, and geotechnical techniques, suggests that several moderate to very strong earthquakes events have occurred in the region (Munson and Munson, 1996). Although the paleoseismic liquefaction features have been associated with nine separate prehistoric events dating from approximately 20,000 BP, the majority of the liquefaction features appear to be due to a single event that occurred between approximately 6,000 and 6,200 years BP (Munson, 1994) near Vincennes, Indiana.

In making a general assessment of the ground shaking that produced the liquefaction evidence, an important consideration is that no liquefaction effects were reported due to the shaking associated with any of the historical events in the WVSZ. Thus, the presence of widespread paleoliquefaction evidence suggests that the prehistoric shaking levels exceed the largest of the historical events (**M** 5 .5). A second consideration is that many of the soils involved with the liquefaction were clean gravelly soils which generally require relatively large ground motions to liquefy and vent. A preliminary estimate of the minimum magnitude of the 6000-year old earthquake (the largest of the identified prehistoric events) has been made by Obermeier et al. (1993) based on areal

distribution and maximum epicentral distance to liquefaction evidence. Their results suggested a **M**7.5 earthquake, which far exceeds any historical event in the WVSZ. Estimates for the smaller liquefaction-producing prehistoric earthquakes suggest all these events are equal to or greater than **M**6.5 (Munson and Munson, 1996). This minimum magnitude estimate for the prehistoric liquefaction-producing events is also significnantly larger than historical seismic events within the region.

Of particular significance, the levels of prehistoric ground shaking required to produce the liquefaction artifacts were much larger than current NEHRP building design requirements for the Wabash region. It should be noted that a number of major industrial facilities and power plants, and at least one large city (population > 125,000) are located within the region. Further, soils in this region include alluvial and lacustrine deposits that may allow amplification of seismic motions. Thus, it is conceivable that significant earthquake ground motions could occur in distant populated areas such as Indianapolis, Indiana due to a large earthquake occurring within the WVSZ.

This geotechnical investigation provides information that can be used to extend the seismic record of the WVSZ into prehistoric times. The study provides seismic ground shaking parameters associated with each of four liquefaction-producing prehistoric earthquakes. This work is similar to a study of liquefaction evidence to estimate seismic shaking levels associated with the 1886 Charleston, SC (Martin and Clough, 1994). Specifically, the objectives of the current study are designed to answer the following questions:

1.) What is the extent and severity of liquefaction within the Wabash valley, and specifically, at each study site? Detailed accounts of the paleoliquefaction evidence at all identified Wabash Valley liquefaction sites are provided elsewhere (Obermeier, et al. 1993; Munson and Munson, 1996). This report focuses on using these data, in conjunction with the results of additional field reconnaissance efforts accomplished specifically for this study, to characterize the severity of liquefaction at each site.

2.) What is the liquefaction susceptibility of the gravelly Wabash soils at the study sites where these coarse-grained soils exist? Are these soils unique in terms of liquefaction susceptibility, and what liquefaction prediction method(s) are best suited to evaluating that susceptibility?

3.) What was likely the influence of local and regional geologic/geotechnical conditions upon the ground shaking patterns from past earthquakes? For instance, are the soil conditions at the studied liquefaction sites prone to strongly amplify or deamplify earthquake ground motions?

4.) Based on the answers to questions 1, 2, and 3, what magnitude, peak ground acceleration, and attenuation patterns would be consistent with the liquefaction evidence observed at each of the studied liquefaction sites?

5.) What are the primary implications of the findings from this study? What do these findings indicate with regard to seismic hazard evaluation in the central U.S., and specifically, in the Wabash Valley Region?

To answer these question, a three-year study was undertaken that involved field reconnaissance, drilling and sampling, Standard Penetration Testing (SPT), Oversize Penetration Testing (OPT), seismic wave velocity tests, in-situ density measurements, a compilation of boring logs and well drilling data, laboratory testing, dynamic site response analyses, and analytical work. The field testing and drilling program involved 22 liquefaction sites associated with 4 earthquakes, although the majority of the work was focused upon the 6000-year BP Vincennes event. The field work performed for this study extended over an area extending approximately 250 km north to south, and more than 100 km east to west. The data collected has allowed estimates of the seismic ground shaking parameters that produced the liquefaction evidence.

The remainder of this report is organized in six major sections. Chapter 2 provides background information on the regional seismicity, the geologic environment, and the mechanism of liquefaction. This section also provides background information on the

specific liquefaction evidence observed in the Wabash Valley. Chapter 3 outlines the field investigation and explains the testing procedures used. In Chapter 4, the laboratory testing procedures are described and the results discussed. The soil conditions at the study sites are presented in Chapter 5. The analysis procedures used to estimate the seismic parameters are explained in Chapter 6, and the results briefly discussed. A summary of the results and the conclusions drawn from them are presented in Chapter 7.

2. Background

2.1. Historical Seismicity

The historical record of the Wabash Valley Seismic Zone dates back to 1827 and shows only 15 moderate earthquakes ($4.5 \leq m_b \leq 5.5$, or $3.5 \leq \mathbf{M} \leq 5.5$), though many smaller events have also occurred (Nuttli, 1982; Stover and Coffman, 1993; Atkinson, 1984). Only three of the historical events have exceeded $m_b = 5.0$ (**M**4.5), but the seismic environment has long been suspected of the potential for much larger events (Nuttli, 1979). Liquefaction evidence recently identified in the Wabash River valley indicates that prehistoric seismic shaking exceeded all of the historical events, and also suggests that the Wabash Valley Seismic Zone (WVSZ) may be subject to strong shaking in the future (Obermeier, 1993).

The Wabash Valley Seismic Zone extends approximately 200 km along the lower Wabash River, a length similar to that of the New Madrid Seismic Zone. It has been suggested that the source of the seismicity in the Wabash Valley is associated with a southwest Indiana arm of the Reelfoot Rift System (Sexton et al., 1986), which is the source of the seismic activity in the New Madrid Seismic Zone (Obermeier et al., 1991). There is some controversy over this theory (Obermeier, 1993), but the presence to the Commerce Geophysical Lineament (Hildenbrand, 1996) would seem to suggest that there may be a potential for shaking of a magnitude similar to that of the 1811-1812 series of great earthquakes in the New Madrid region. There is, however, no evidence that faults in the Wabash Valley Seismic Zone are continuous over its entire length. The seismological community has suggested that an event of $m_b = 6.5$ (**M**7.5) appears to be a reasonable estimate of the region's potential (Nuttli, 1979; Atkinson, 1984).

The largest historical event to occur near the Wabash Valley was the Charleston, Missouri $m_b = 6.2$ (**M**6.8) earthquake of 1895 (Obermeier et al., 1993). The largest historical Wabash Valley Seismic Zone events had magnitudes of $m_b < 5.5$ (**M** < 5.5)

(Stover and Coffman, 1993; Nuttli, 1982; Atkinson, 1984) and produced no liquefaction effects that were reported (Obermeier et al., 1993). The Charleston, MO event produced reported liquefaction over a 16 km diameter area, and may have induced features over an area approximately 32 km in diameter (Obermeier et al., 1993).

Recently, newspaper accounts of an earthquake occurring in the New Madrid area in 1851 were discovered (Metzger, 1996). This event was reported to have produced only a single liquefaction feature (Memphis Daily Appeal, 1851). Correlations of felt area with moment magnitude of ENA events predicts that this event was a **M**5.6 earthquake (Metzger, 1995). This suggests that a lower bound on the magnitude required to induce liquefaction effects in the CUS region is approximately a **M**5.5 to **M**5.6 earthquake.

2.2. Geology

2.2.1. Tectonic Framework

The surface of the earth consists of rigid lithospheric plates into which the continental and oceanic crust is embedded. These plates are in turn floating on the hotter, lower density asthenosphere below. The lithosphere, from below the crust, and combined with the asthenosphere, forms the outermost layer of the mantle of the earth. The asthenosphere is at a range of temperatures and pressures close to the melting point and allows plastic deformations to occur. This provides a lubricating layer over which movement of the rigid lithospheric plates can occur. The asthenosphere is a likely source for upwelling magma and for isostatic adjustment through uplift and downdropping of the overriding lithospheric plates (Summerfield, 1991; Plummer and McGeary, 1993).

Plate tectonics was originally believed to be driven by convection of heat from deep within the earth toward the surface. Recent tomographic surveys of seismic wave velocities interpreted to indicate rock temperature with depth tend to discount the full-depth mantle convection theory (Dziewonski and Anderson, 1984). This research tends to support the argument that plate motion drives convection within the mantle, rather than mantle convection driving plate motion. Several theories have been proposed, but a

thorough explanation of the mechanics of tectonic motions has not been developed (Summerfield, 1991). Figure 2.1 illustrates some of the mechanisms that have been proposed. The greatest driving force in plate tectonics appears to be the sinking leading edges of subducting lithospheric plates dragging the plates down into the asthenosphere (slab-pull). The leading edge of the lithospheric plate remains much denser and cooler than the asthenosphere into which it sinks and can exert a significant pull on the remainder of the plate. This induces a spreading center where lithospheric plates are being pulled apart, allowing an upwelling of material from the asthenosphere below. This upwelling forms a ridge of new lithosphere as material from the asthenosphere reaches the surface. As this new lithosphere cools and thickens, it undergoes an isostatic adjustment to maintain equilibrium between the denser, more rigid lithosphere and the more plastic asthenosphere below. New material being added at the spreading center forces movement down the ridge formed by the upwelling (ridge-push), and the sinking due to isostatic adjustment produces an additional gravity force (sliding) driving the plate motions. It has also been theorized that a tensile stress can be induced in an overriding lithospheric plate if the plate being subducted is sinking faster than the subduction is occurring (trench suction). Tensile stress is induced as the point where the subduction is initiated, and where the subduction trench occurs, is forced further from the overriding plate.

Several theories have also been proposed as to the mechanisms driving the initial rifting of continental crust to initiate the process (Plummer and McGeary, 1993; Summerfield, 1991). Two models for rift formation are those of passive and active rifting. Passive rifting results from tensile stresses developed within the lithosphere (see Figure 2.2). Thinning of the lithosphere through stretching or faulting allows upwelling of material from the asthenosphere, which in turn produces uplifting of the lithosphere. This can then lead to formation of a ridge and a potential spreading center.

The active rifting model proposes that hot spots develop beneath the lithosphere. These hot spots then induce domal uplifts associated with isostatic adjustment of the lithosphere/asthenosphere boundary. This thins the lithosphere and induces further uplift

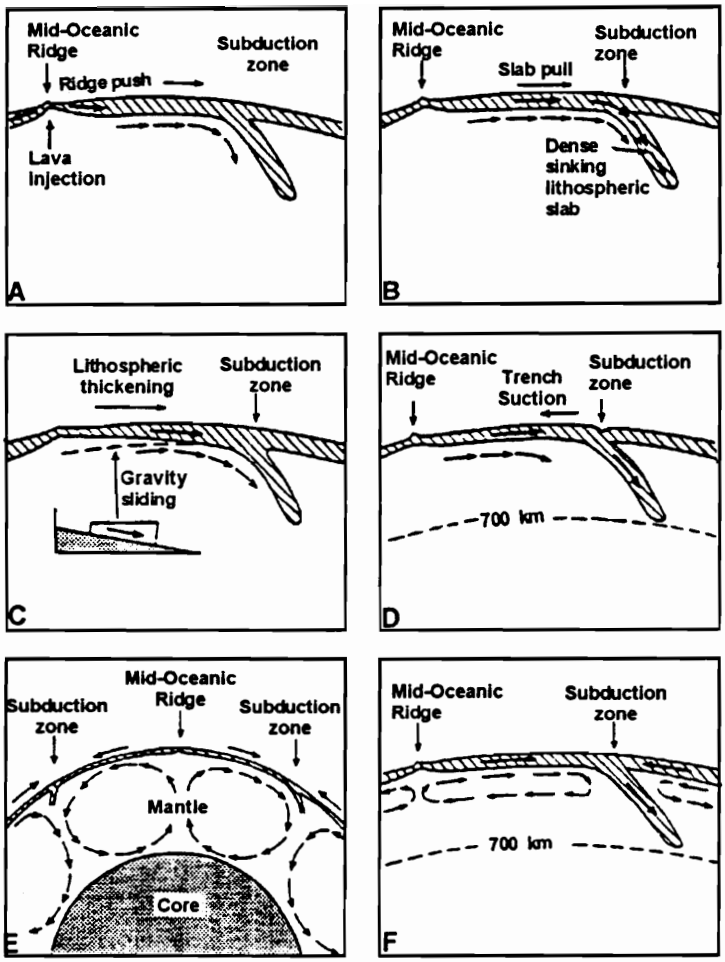

Figure 2.1. Proposed mechanisms driving tectonic plate motions: (A) ridge push; (B) slab pull; (C) gravity sliding; (D) trench suction; (E) whole mantle convection; and (F) shallow convection confined to the asthenosphere (from Summerfield, 1991; and Plummer and McGeary, 1993).

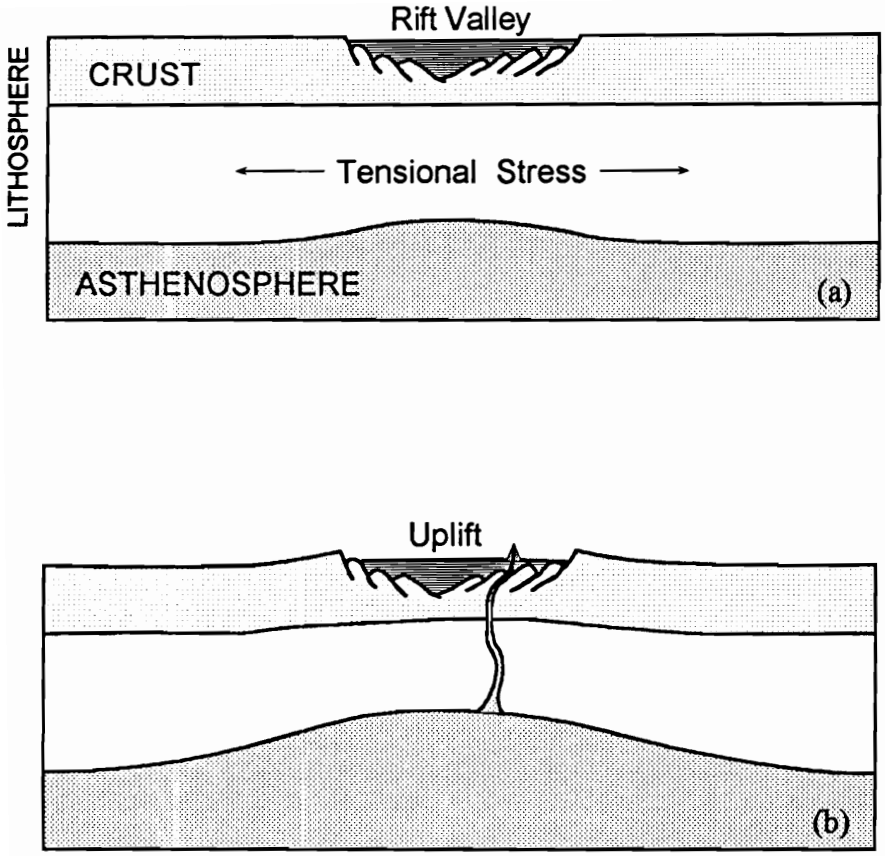

Figure 2.2. Passive rifting as a consequence of tensional stresses within the lithosphere (a). Following rifting, thinning of the lithosphere allows an upwelling of the athenosphere (b) inducing uplift and volcanic activity (from Summerfield, 1991).

of the overlying crust. As the upwelling continues, rifting will occur in a 3-armed radial pattern originating at the center of the uplift. These radial rift arms can propagate between adjacent uplifts and a series of uplifts can become joined. Where the global plate motions are suitable, a spreading center may develop along the series of uplifts. Figure 2.3 illustrates schematically how this may occur. Typically, 2 of the 3 radial rift arms will remain active as the spreading center develops. The third failed rift arm, or aulacogen, will become inactive, but remain a zone of weakness where faulting has occurred. Where these aulacogens are present they become sediment-filled valleys and strike nearly directly into the continental interior, approximately perpendicular to the new continental margin forming at the spreading center. An example of a recently-formed aulacogen is the East African Rift Valley (see Figure 2.4). This forms the inactive arm of a radial rift that has now developed into a spreading center splitting the Arabian Peninsula from the African Continent (Plummer and McGeary, 1993). If the proper stress regime develops at a later time, aulacogens may provide the mechanism for stress relief leading to earthquake motions at passive continental margins and within continental interiors.

During periods of lithospheric continental plate collisions, great mountain ranges are built up at the plate boundaries. As the continents begin to drift apart after the mountain-building episode is concluded, rifting initially occurs at several locations over a wide region. Eventually, a predominant rift zone develops and spreading ceases at the failed rifts. The stress regime within these failed rifts is then reversed from tensile to compressive, but zones of weakness remain, developed by normal faulting in the basement rock during the initial rifting process (Johnston, 1989). These areas provide a zone where stress relief is likely to occur if the direction of the major principle stress and the strike of the fault structures are appropriate (Hinze and Braile, 1988).

During periods of continental spreading, the mountain ranges formed during collisions of the lithospheric plates are eroded away and redeposition leads to sequential deposits of various sedimentary rock formations in interior continental basins and along the continental margins. These deposits tend to obscure the faulting produced in the

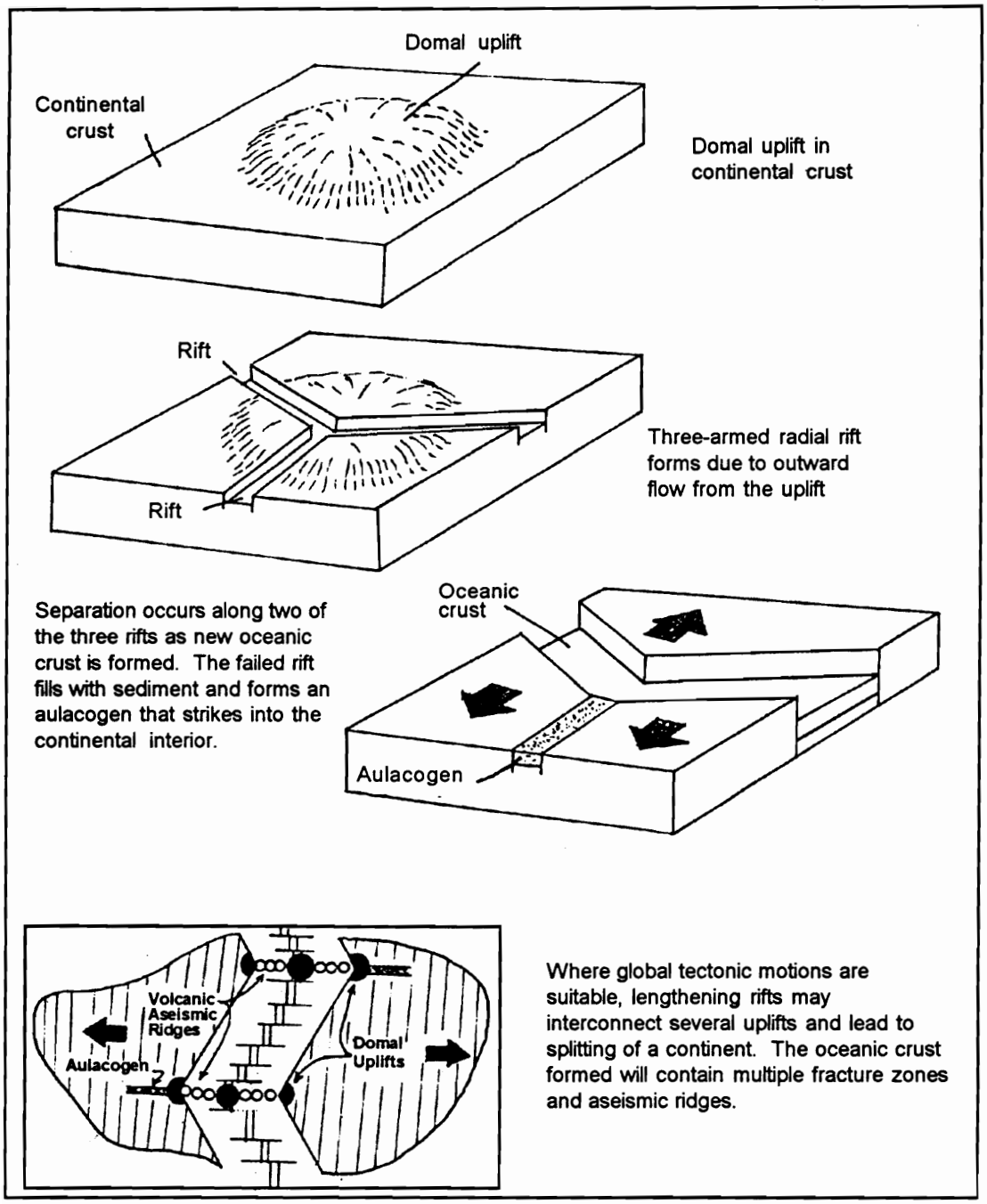

Figure 2.3. Active rifting is characterized by continental spreading preceded by uplift and volcanism. (from Summerfield, 1991; and Plummer and McGeary, 1993).

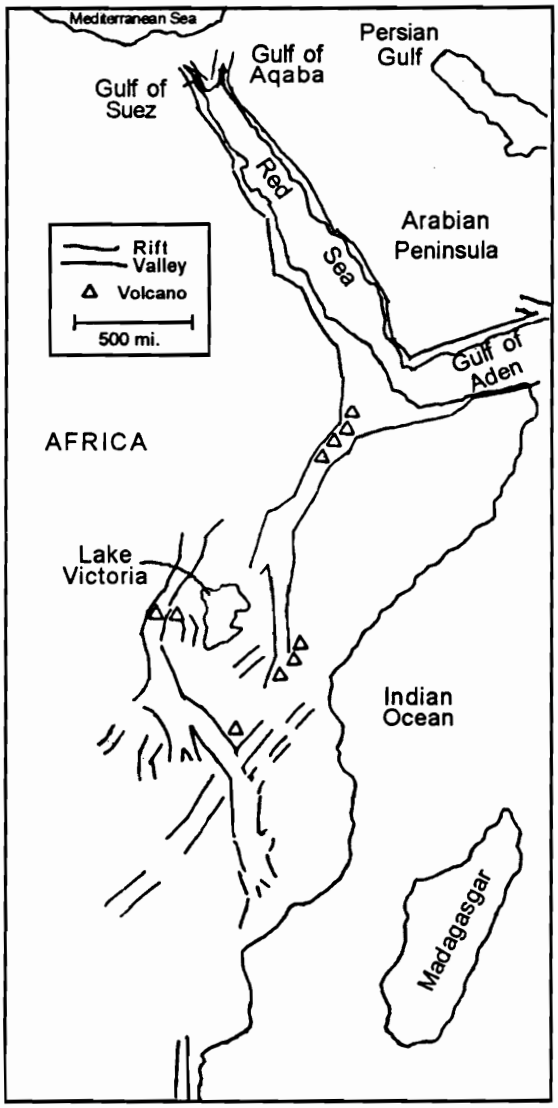

Figure 2.4. East African rift valley. Three arm rift with third failing arm extending into the continental interior (after Plummer and McGeary, 1993).

basement rock along aulacogens formed during the initial rifting process, though subsequent displacements in the basement material likely will also be represented in the overlying sedimentary deposits. This process leaves identification of the location of failed rift zones to speculation aided by near-surface faulting observed in the sedimentary rock, the presence of regional historical seismic activity, and geophysical techniques that can be used to identify tectonic structures in the basement rock (Plummer and McGeary, 1993).

2.2.2. Geophysical Environment

2.2.2.1. Basement and Sedimentary Bedrock Geology

The Central United States (CUS) bedrock geology consists of a platform area of the central North American craton. The Precambrian basement material of metamorphic and plutonic igneous rock is overlain by several kilometers of Paleozoic and later sedimentary deposits originally eroded from the Appalachian orogenic belt and Canadian shield (Plummer and McGeary, 1993).

The tectonic history of the CUS region consists of a series of continental collision and rifting episodes over the past 2.5 billion years. During the late Precambrian, rifting occurred in the region of the lower Mississippi River valley and left an aulacogen now known as the Reelfoot rift system (Braile and Hinze, 1988). Figure 2.5 shows the likely location of the coastline and aulacogens formed along the southeast North American continent during this rifting episode. The Reelfoot Rift system was reactivated during the most recent episode of continental rifting in the Mesozoic Era (Johnston, 1989) as the current Atlantic Ocean began to form. This most recent rifting episode and the continuing continental drift has led to the continental configuration we see today.

Significant intraplate seismicity typically occurs in regions where past tectonic activity has induced zones of weakness during continental rifting. Subsequent tectonism then produces reversals in the stress regime as continental drift continues (Johnston, 1989). The principle stress direction in Eastern North America (ENA) is compressive in an ENE to NE orientation and the majority of the normal faults identified in the Wabash

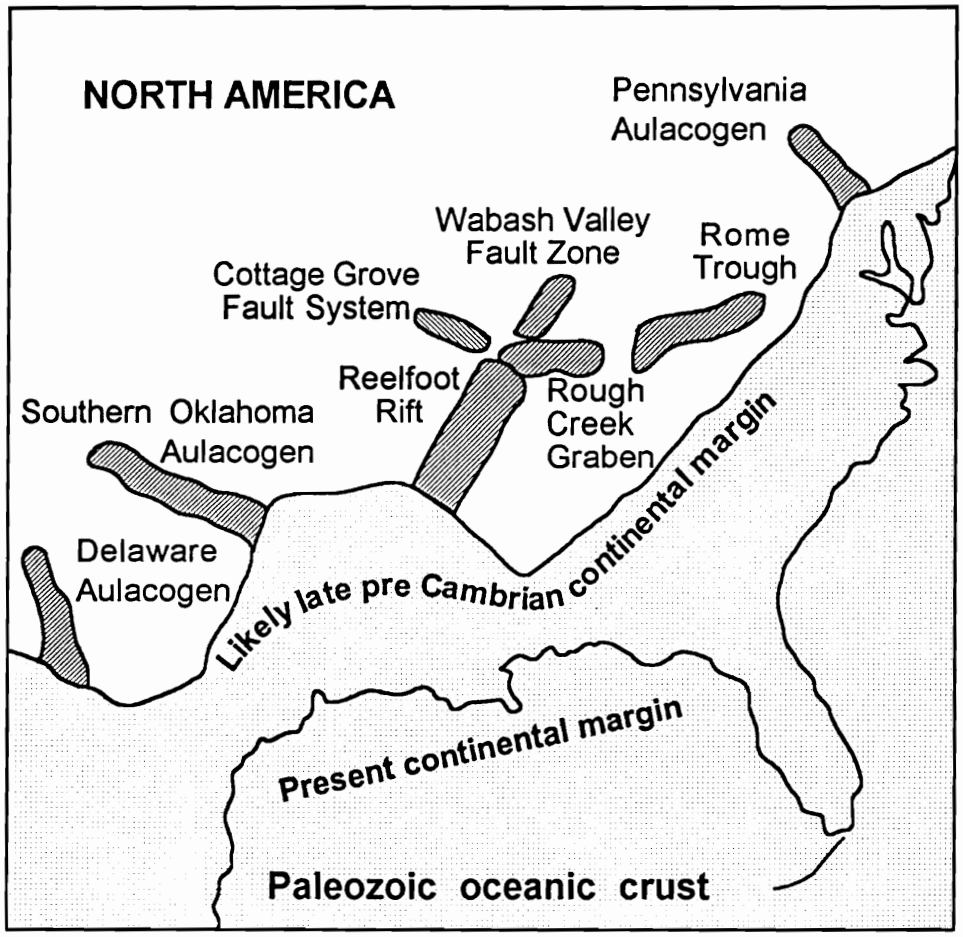

Figure 2.5. Possible southeast North American continental margin following late pre-Cambrian rifting episode (after Hinze and Braile, 1988).

Valley Seismic Zone strike NE (Collinson et al., 1988). This stress regime and fault orientation is suitable for development of strike-slip fault displacements. Earthquake motions in the region have been associated with strike-slip displacements that are then followed by aftershocks on adjacent or subsidiary faults that experience normal or reverse faulting. Talwani (1989) suggests that these aftershocks are a result of readjustments of the stress regime to make it consistent throughout the region following the strike-slip displacements.

The bedrock geology of the Wabash Valley Seismic Zone consists of several kilometers of sedimentary rock overlying the Precambrian igneous and metamorphic basement material. The sedimentary rock consists of sequences of shale, limestone, siltstone, sandstone, and coal, which dip to the southwest from the Kankakee Arch into the Illinois Basin (Gray, Ault, and Keller; 1987). These sedimentary deposits obscure the structure of the basement rock, but numerous faults have been identified in the region (Sexton et al., 1986). Figure 2.6 indicates the location of many of the known fault structures in the region. A recently-identified fault structure extends to the southwest from the vicinity of Vincennes, Indiana into northeast Arkansas (Hildenbrand and Hendricks, 1995). This is the Commerce Geophysical Lineament (Hildenbrand, 1996), and may be the source of the seismic activity that induced many of the paleoliquefaction features identified in southwest Indiana and southeast Illinois. Faults have also been identified in the central portion of Indiana that may be the source for the seismic activity inducing the liquefaction features found to the east of the Wabash Valley Seismic Zone (i.e., south of Indianapolis, and of Columbus, Indiana).

A magnetic survey map showing the location of the tectonic structure recently identified by Hildenbrand and Hendricks (1995) is shown in Figure 2.7. The feature is believed to be a strike-slip fault possibly extending continuously from the northern boundary of the New Madrid Seismic Zone to near Vincennes, Indiana. The north end of this feature coincides with the apparent epicentral region of the $M \geq 7.5$, 6,000 year BP event; apparently the largest of the prehistoric seismic events associated with the

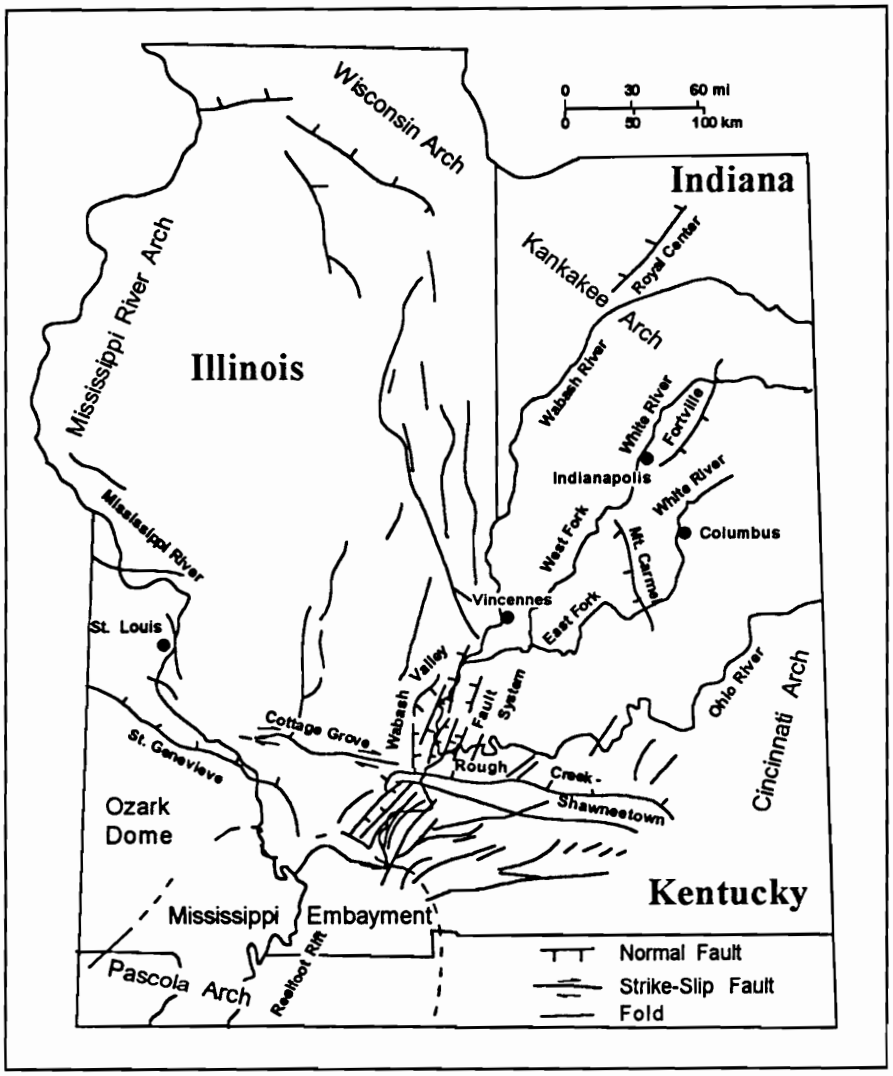

Figure 2.6. Tectonic map of the region surrounding the Wabash Valley Seismic Zone (After Collinson et al., 1988).

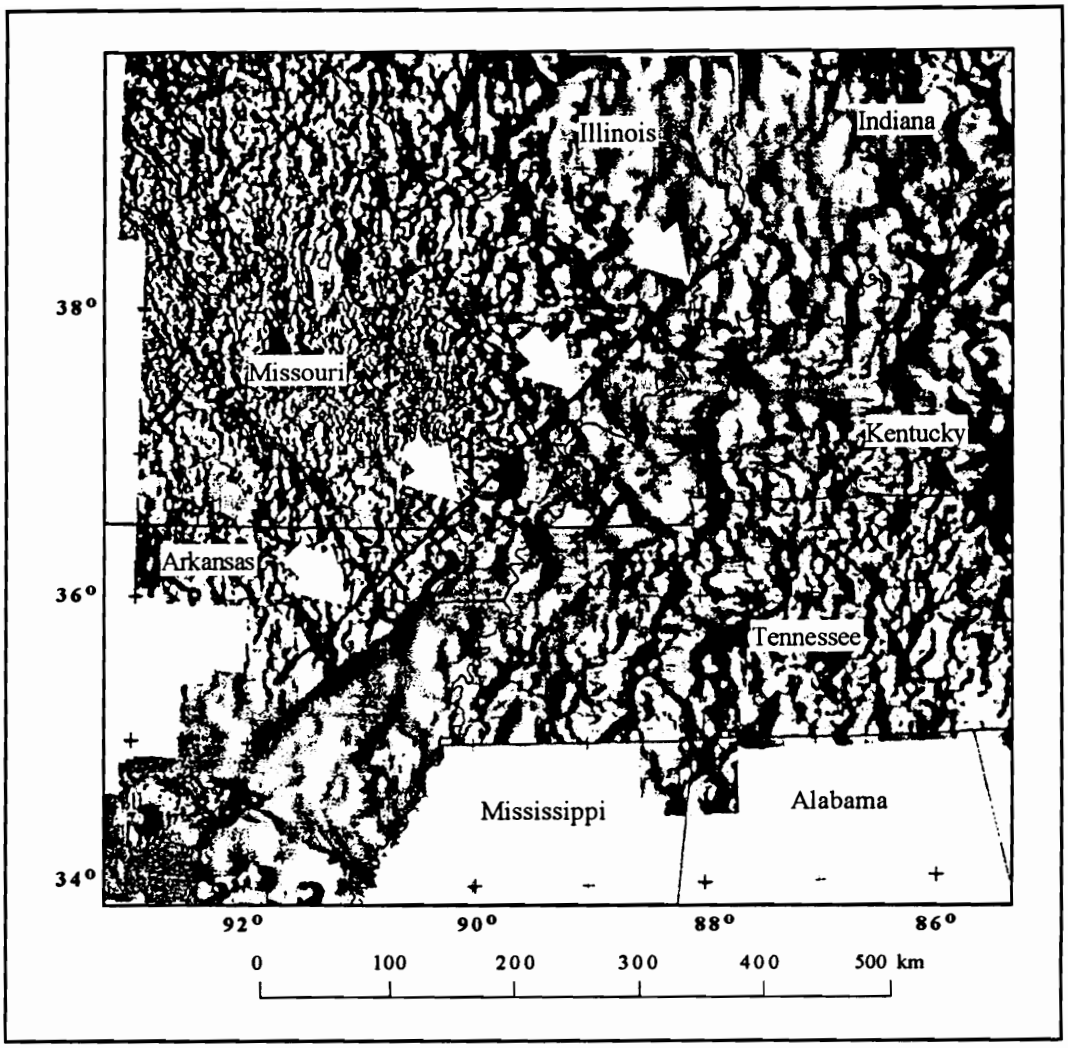

Figure 2.7. Magnetic anomaly map with approximate location of Commerce Geophysical Lineament enhanced to show relation to the Wabash Valley Seismic Zone (modified from Hildenbrand and Hendricks, 1995).

liquefaction evidence in the Wabash Valley. The feature displaces the Cottage Grove fault system in southern Illinois relative to the Rough Creek Graben in western Kentucky by approximately three miles as a strike-slip displacement (see Figure 2.6), and many instrumentally-located strike-slip earthquake epicenters are coincident with the feature.

The distribution of liquefaction features in the central and south-central portions of Indiana may be associated with the Fortville and Mt. Carmel faults, which are also indicated on Figure 2.6. The Fortville fault extends to near Indianapolis, and is nearly coincident with the center of the northern of these liquefaction feature distributions. The Mt. Carmel fault extends north from near the apparent epicenter of a seismic event that could have induced the liquefaction features centered south of Columbus, Indiana. While no conclusive evidence exists that these faults actually induced the seismic activity that produced the liquefaction evidence observed, the existence of these features adds credibility to the idea that the tectonic environment is capable of producing significant shaking in the regions where liquefaction evidence has been identified. Further, the continuing seismicity, the faulting in the region, and the recently discovered liquefaction evidence identified in the Wabash Valley collectively support the possibility of larger shaking than has been documented in the historical record.

2.2.2.2. Geomorphology of Unconsolidated Deposits

Soil deposits are present to depths of between 0 and 60 meters in the lower and middle Wabash, and the White River Valleys. Figure 2.8 shows the geology of soil deposits in the study region. In the south-central portion of Indiana, bedrock is exposed at the surface with little or no soil cover. Where surficial, unconsolidated upland soil deposits are found, they consist of pre-Wisconsinan glacial tills overlain by glacial lacustrine deposits, loess, and wind-blown sand. River valley sediments consist of diluvial glacial outwash and fluvial deposits of the Wabash River system. The majority of the outwash sediments were deposited in the late Pleistocene at the height of the Wisconsinan glaciation, and possibly with occasional small deposits of Illinoian age sediments also

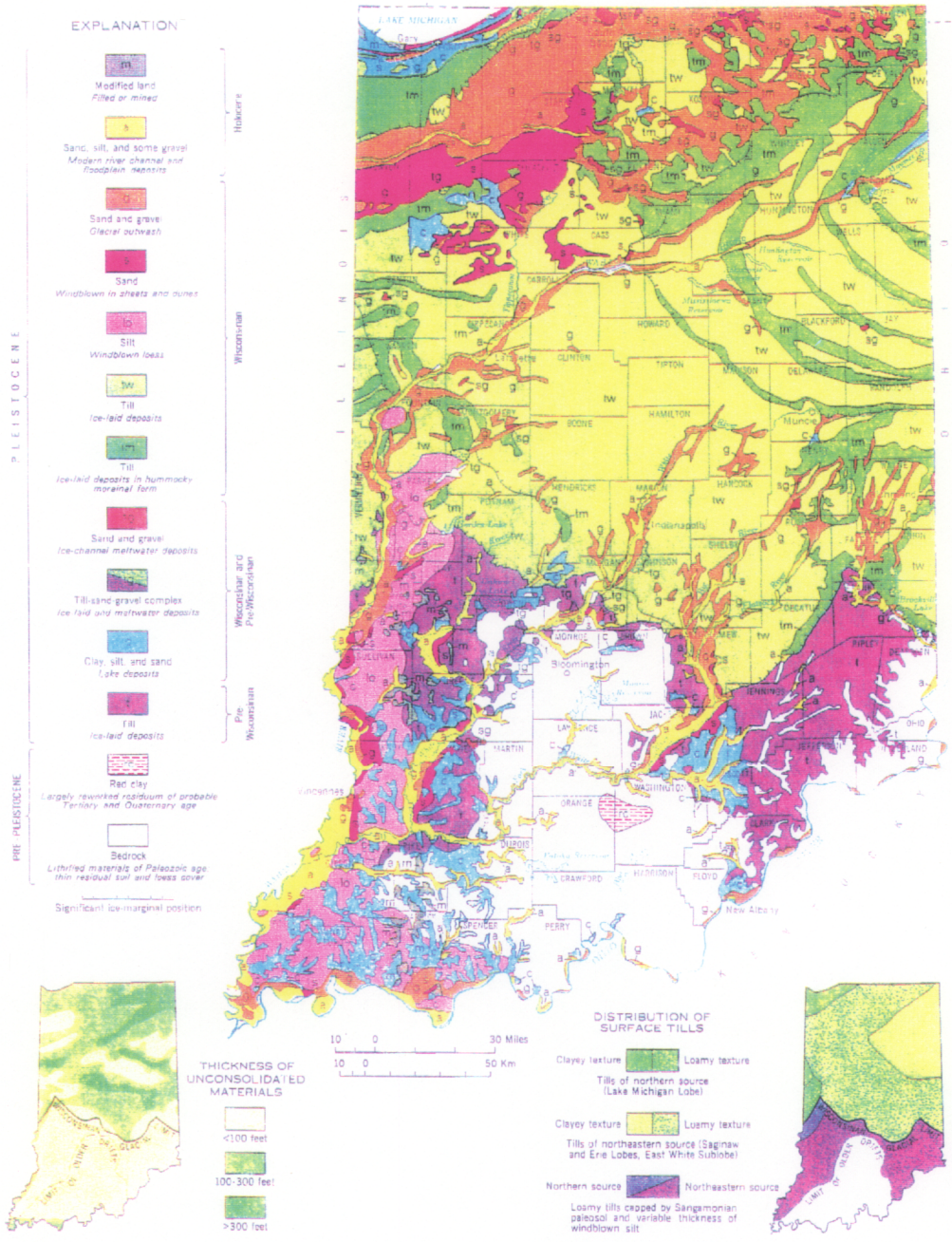

Figure 2.8. Geologic map of unconslidated deposits in Indiana.

present. The Wisconsinan-age valley-train sediments were deposited during a series of advances and retreats of the glacial ice (Frasier, 1993). Both the Illinoian and Wisconsinan glaciations produced lacustrine deposits that were laid down as a result of the advancing ice (Thornbury, 1950). The Illinoian glaciation produced ice-contact lakes, and the Wisconsinan glaciation produced both contact and non-contact lakes. Ice contact lakes were formed as the advancing lobes of ice blocked the outlet of adjacent non-glaciated valleys. Non-contact lakes were formed behind the valley-train sediments laid down in the main glacial sluiceways of the Wabash, Eel and White Rivers. The valley train sediment dammed the tributaries to those streams that did not carry melt water (Frasier and Gray, 1992).

The Wabash and White Rivers and their tributaries have subsequently reworked the outwash sediments throughout the late Pleistocene and Holocene Epochs. The rivers have become incised in the original outwash flood plain and have left the glacial sediments as terrace deposits (Thornbury, 1950). The highest terrace was deposited at the height of the Wisconsinan glaciation. A lower terrace also exists due to continued high flows while the glaciers retreated. During this time the St. Lawrence River drainage remained blocked with ice. The flow during this time carried a reduced sediment load and allowed degrading of the flood plain (Shaver, 1979). The current flood plain is made up of the fluvial deposits resulting from deposition of the reworked outwash sediments in a lower-energy environment. The coarse-grained point-bar and braid-bar sediments are overlain by low-permeability flood plain, channel fill, and backswamp deposits of silts and clays (Gray, 1989). Maximum soil depth in the river valleys is typically on the order of 15 to 45 meters (Fidlar, 1948). These sediments provide an ideal environment for the development of liquefaction due to seismic ground motions.

The soil deposits where past ground failures have been observed were typically formed as point-bar or braid-bar deposits of sand and gravel that were subsequently overlain by low-permeability floodplain deposits. The soil deposits generally consist of a suficial layer of generally massive clay and silt overlynig interbedded clay and fine sand,

which in turn overlie coarse-grained sediments. This depositional sequence is typical of meandering stream valleys. The interbedded silts and sands are natural levee sediments deposited adjacent to the river during floods. As the river continues to meander, the sediments laid down during floods become finer-grained backswamp deposits. The sand lenses observed at Wabash Valley liquefaction sites generally vary from less than one to approximately 5 to 10 cm in thickness.

Many of the Wabash Valley liquefaction sites contain soils with a significant gravel content. Particle sizes of up to 7.5 cm have been observed in the vented material. Soils of this type are have typically been believed to be difficult to liquefy and vent (Wong et al., 1975; Stokoe et al., 1988) and would require exceptionally strong shaking. This is especially true if the gravelly soil is not confined by low-permeability zones and is relatively clean (less than 5% fines). Andrus and Youd (1987) and Hardman and Youd (1987) report that the Borah Peak, Idaho (M7.3) earthquake of 1983 induced liquefaction in some of the coarsest and cleanest soils to be documented to have liquefied. Figure 2.9 compares the grain size distribution of some of the liquefied gravelly Wabash soils with the grainsize distribution of some of the coarsest of the liquefied Borah Peak, Idaho soils. Many of the Wabash soils are nearly as coarse and can be much cleaner than the liquefied gravelly Borah Peak soils. It should be also be noted the liquefaction of gravelly soils due to the largest of the Wabash events was much more widespread than that due to the Borah Peak earthquake. Other factors aside, this tends to suggest a stronger level of prehistoric seismic shaking has occurred in the Wabash Valley than that which occurred during the Borah Peak event.

2.3. Paleoseismic Investigation

Recent field searches of exposed soil profiles along river banks, canals, trenches and gravel pits by the United States Geological Survey and Indiana University personnel have revealed a total of 330 earthquake-induced liquefaction features in Indiana and along the Illinois bank of the Wabash River. These features consist of sand- or gravelly-sand-

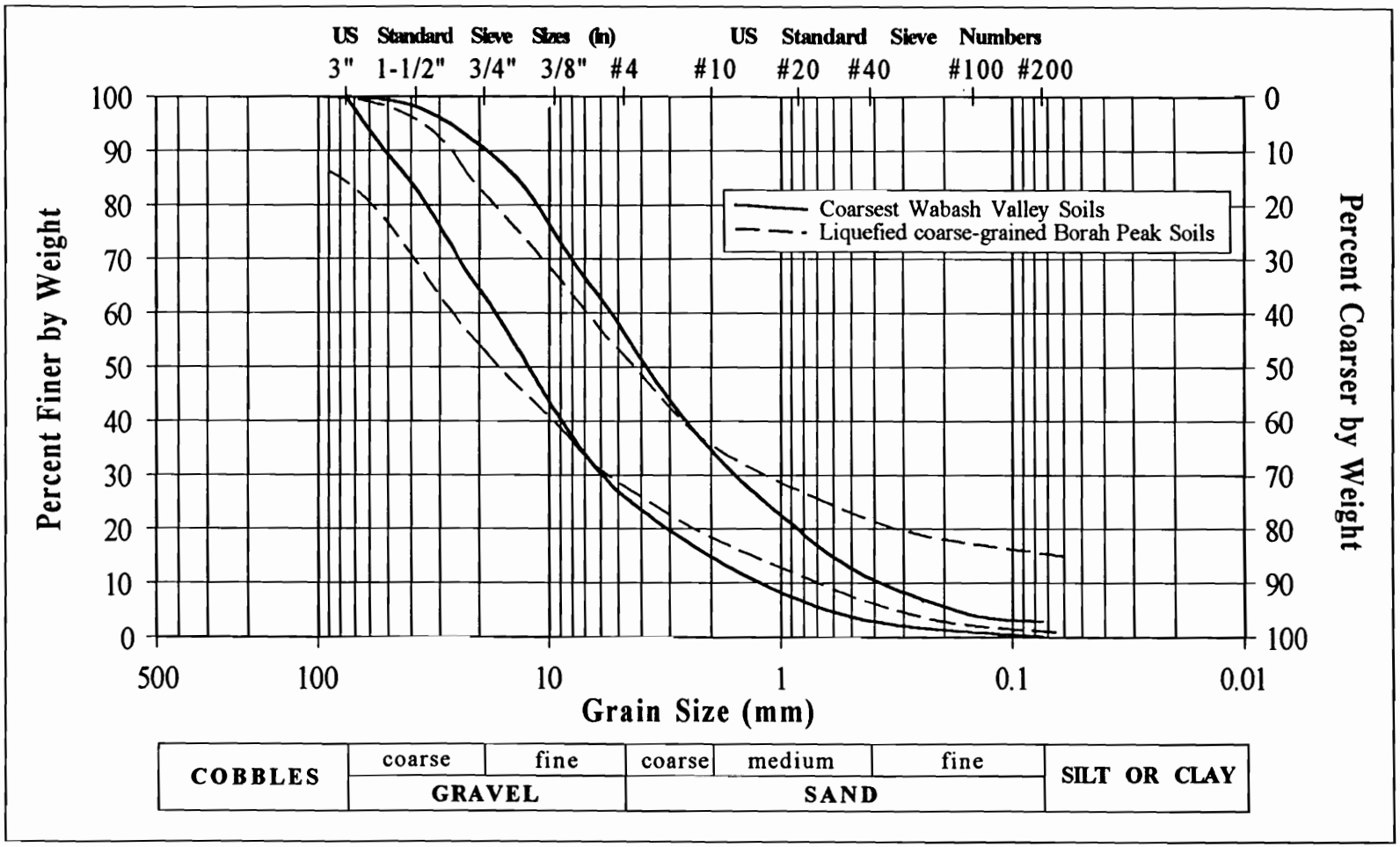

Figure 2.9. Comparison of maximum grain sizes liquefied in Wabash Valley with sediments from sites liquefied due to the 1983 M6.9 Borah Peak, Idaho earthquake.

filled dikes, sills, and/or blows of vented sands and gravels at 83 sites (Munson and Munson, 1996) throughout the Wabash and White River drainages of Indiana and Illinois. The largest dike features, up to 2.5 meters in width, occur along a 35 km stretch of the Wabash River near Vincennes, Indiana. This focal area of the largest features is the inferred epicenter of the 6,000 year BP event. The features attenuate in size and number from this apparent epicentral region, with smaller features identified over a total distance extending about 275 km from near Evansville, Indiana to north of Terre Haute, Indiana. Features have also been identified more than 100 km to the east and approximately 200 km west of the Vincennes epicentral zone (Munson et al., 1994; Obermeier, 1995).

The geotechnical setting associated with the liquefaction features generally consists of middle Holocene to late Pleistocene fluvial sediments. These soils are mainly silty-to-clean sand and gravelly sand overlain by a low-permeability surficial deposit of silt- and clay-rich flood plain soil deposits. The water table, which fluctuates with the river level, is typically within a few meters of the ground surface, usually above the top of the liquefiable sediments. The soil and water table conditions tend to be uniform among the liquefaction sites identified. At many of the sites, the ground surface that existed at the time of the earthquake has been buried by up to several meters of more recent alluvial deposits, thereby preserving the vented material as a visible bed of sand- and gravelly-sand-rich sediment. Where the source beds are exposed at liquefaction sites, it is often possible to trace nearly-vertical dikes directly from the liquefied sand stratum, through the surficial fine-grained sediments, to the vented material.

Based on the age of the features and soil strength parameters obtained at many of the liquefaction sites, it appears that four earthquakes have occurred in the Wabash Valley Seismic Zone over the past 12,000 years that were of sufficient strength to induce liquefaction evidence over significant regions (Munson, 1994). Additional recently-discovered liquefaction sites not included in this study have also been identified (Munson and Munson,1996). These additional sites have been associated with events producing less-well-defined distributions. This evidence indicates at least six liquefaction-inducing

earthquakes have occurred in the eastern portion of the Wabash Valley Seismic Zone over the past 12,000 years.

The spans of observed liquefaction effects for the prehistoric Wabash Valley events investigated for this study range from 32 km to 250 km, suggesting the largest of these events may have been similar in size to the 1886 Charleston, South Carolina **M**7.5 earthquake (Obermeier et al., 1993). Preliminary magnitude estimates for the four well-defined events, based on Liquefaction Severity Index (Youd and Perkins, 1987; Youd et al., 1989) and the data of Ambraseys (1988) modified by Obermeier et al. (1993) for the Wabash Valley, indicate magnitudes ranging from **M**6.8 to **M**7.8. Again, these events are larger than any in the historical record, and suggest the possibility of very strong shaking with epicenters throughout southwest Indiana and into southeast Illinois.

Of the other paleoseismic events inducing liquefaction in the region, only isolated sites have been associated with those earthquakes to date. Possible explanations for this may be that the earthquakes were only large enough to induce incipient liquefaction near the epicenter, or they may have been of such an age that the natural meandering of rivers in the region has erased any other liquefaction evidence that may have been produced. Also, it is possible to observe only the sediments in those areas where the soil profile is exposed in river banks and in isolated man-made excavations. Large areas of the river valley sediments and terrace deposits are not cut by the rivers and excavations, making it impractical to fully investigate the entire extent of liquefiable sediments for the presence of paleoseismic liquefaction evidence. Studies of paleoliquefaction evidence for prehistoric seismic events are limited primarily to the evidence naturally exposed.

2.4. Liquefaction Overview

In recent years there has been some inconsistency in the use of the term liquefaction. Castro (1987) has suggested that liquefaction should be defined based on the behavior of a soil mass in response to seismic loading. He suggests that the original definition was given by A. Hazen when he described "liquefied" soil behavior as the

mechanism for the 1920 Calaveras Dam failure. Since that time the term liquefaction has been used in many ways. These definitions include: 1.) Development of 100% excess pore pressure ratio (effective stress goes to zero) (Seed and Idriss, 1971), 2.) Development of a specified single amplitude cyclic strain under an applied cyclic loading (i.e., 2.5%, 5%) (Lee and Seed, 1967), 3.) The condition where externally-applied shear stresses become greater than the undrained shear resistance of the soil mass and flow deformation occurs (Castro, 1987), or 4.) The point where a granular material begins to act as a viscous liquid rather than a solid (Youd, 1984).

Each of these definitions is based on the development of excess pore pressures during undrained shear of a saturated granular soil mass leading to a reduction in the shear strength available within the soil mass. They all have their application, however, they are also limited in their applicability. In this study the term liquefaction will be used to refer to the development of excess pore pressure and the associated loss of shear strength only, with no restriction on the degree of pore pressure development required. The behavior of a soil mass due to the pore pressure development will also not be implied by use of the term. The response of the soil mass to the pore pressure development and any applied loading will be assumed to be a secondary phenomenon requiring a separate description based on the behavior mechanism associated with the response.

2.4.1. Mechanism of Liquefaction

During initial shear of granular materials, the individual particles have a tendency to rearrange themselves into a denser, or more compact, state. Where saturated conditions exist, in order for the soil particles to reach a denser state, pore fluid must be expelled from the soil mass. If flow of the pore water is impeded, high excess pore pressures will develop, transferring the vertical stresses initially supported by the soil skeleton to the pore water. The mechanism of pore pressure development is based on this tendency for contraction of the soil skeleton and the subsequent rebound as stresses are transferred to the pore water (Seed and Idriss, 1982). The amount of pore pressure

development that can be expected due to the tendency for a given amount of consolidation is conceptually illustrated in Figure 2.10. During initial cyclic loading the tendency for consolidation occurs at a constant confining stress. Since the volume must remain constant, rebound must take place, and will occur along the recompression curve. This happens by development of excess pore pressures to reduce the confining stress to the point where the void ratio can be maintained. The pore pressures developed in this way may approach the value of the initial effective confining stress, greatly reducing the frictional strength of the soil mass (Ishihara, 1985; NRC, 1985). Once the effective stress within the soil mass is reduced to near zero, the soil particles have become suspended in the pore water. As the particles begin to settle out of this suspension and the water is forced upward, the soil ends up in a denser state than the original condition (Ishihara, 1985; Castro, 1987). This process is represented schematically by the series of diagrams in Figure 2.11. Diagram (a) in the figure represents an initial loose soil condition. In (b), the soil has been "liquefied." During pore pressure dissipation the soil consolidates to a condition illustrated by diagram (c). The generation of excess pore pressures due to this suspension of soil particles under cyclic loading is dependent on the initial relative density of the soil mass and on the cyclic shear strain applied by the seismic loading (Castro and Poulos, 1977). In loose soils, excess pore pressures develop rapidly and lead to large deformations under externally applied shear stresses. Very little shear resistance exists within the liquefied soil mass. In dense soils, pore pressure development occurs much more slowly and only limited displacements occur compared to those experienced by loose soils under the same loading.

Castro and Poulos (1977) describe the two different phenomena associated with cyclic undrained loading of granular soils as "true liquefaction" and cyclic mobility. They describe the difference between these cases through the use of the state diagram for a given soil (see Figure 2.12). "True liquefaction" can occur only in those soils where the initial conditions plot to the right of the steady state line. This also requires a total applied

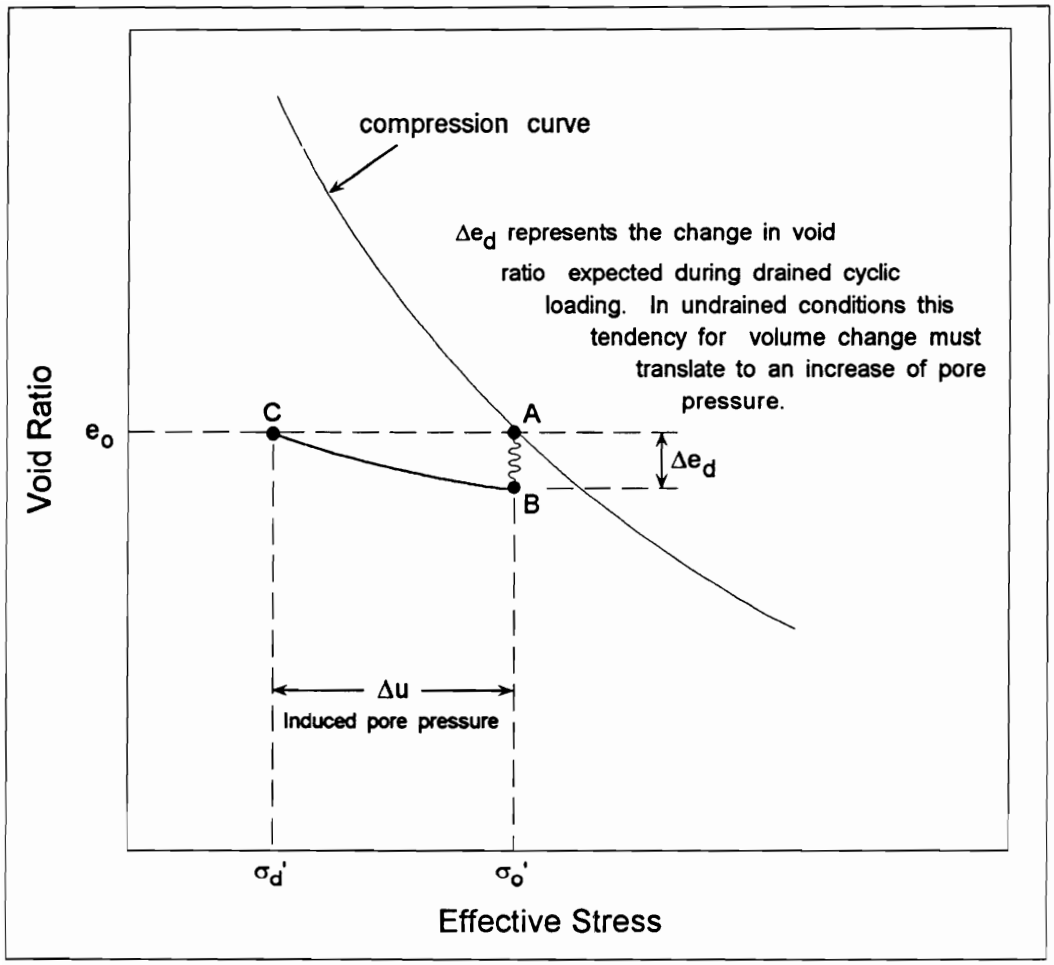

Figure 2.10. Schematic representation of excess pore pressure generation due to the tendency for volume change during cyclic loading (after Seed, 1979).

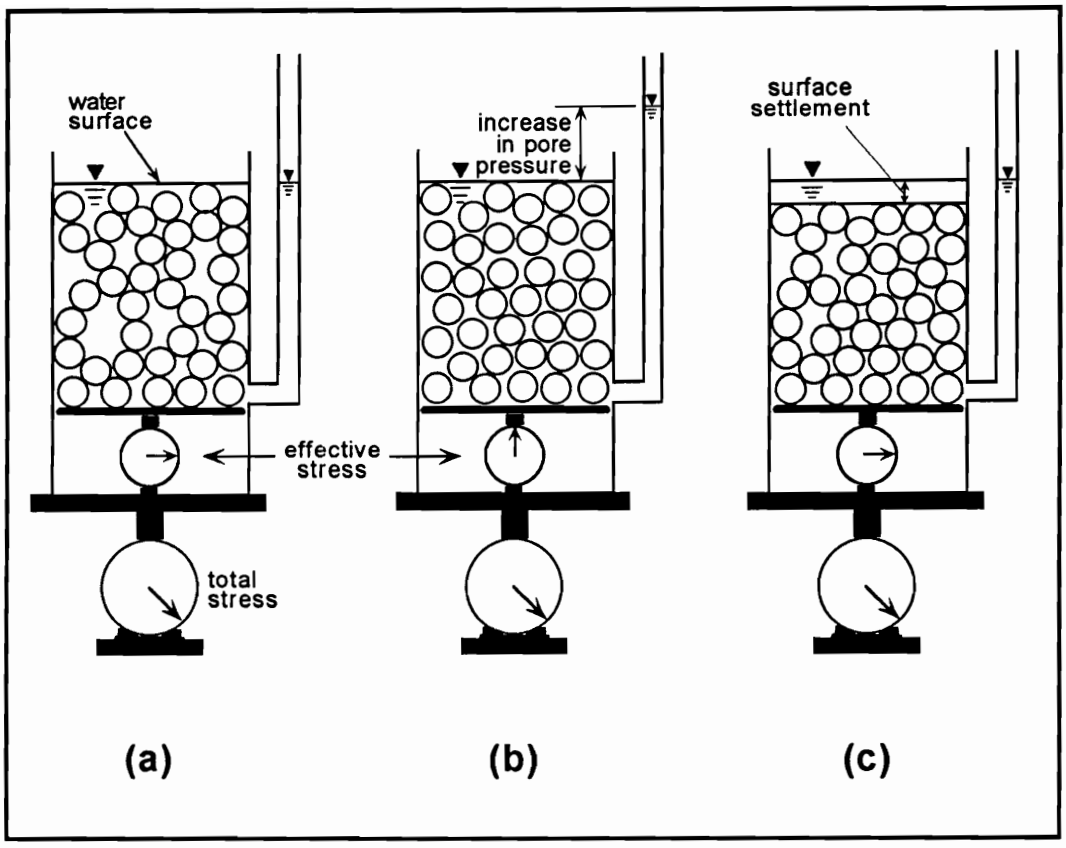

Figure 2.11. Illustration of particle suspension during liquefaction, and of surface settlement following pore pressure dissipation and reconsolidation. (after Ishihara, 1985)

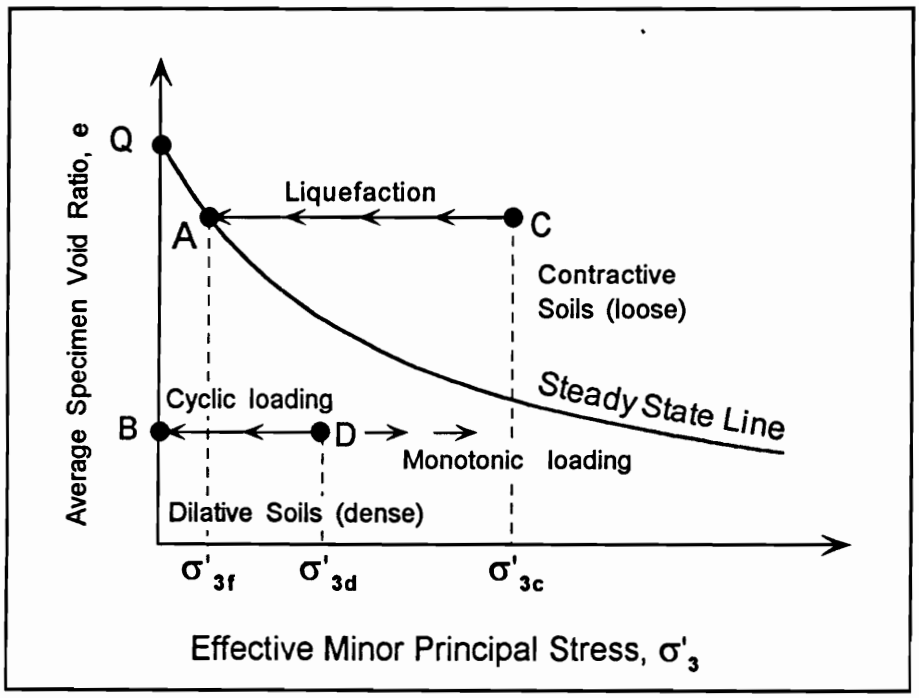

Figure 2.12. State diagram indicating undrained response to monotonic and cyclic loading (after Castro and Poulos, 1977).

cyclic stress, consisting of both the earthquake loading and the in-situ static stress, that exceeds the undrained strength of the soil.

Medium dense to dense soils initially plot near or to the left of the steady state line and tend to dilate under monotonic undrained loading after a small initial tendency for contraction. Once dilative behavior begins, pore pressures are reduced and the frictional strength available within the soil mass is increased. Pore pressure reduction continues, with the stress path following the failure envelope, until enough shear strength has been achieved to support the applied load. Figure 2.13 illustrates the behavior of saturated sand in response to monotonic simple shear loading for both drained and undrained conditions. In this diagram, the stress paths and stress-strain response for drained and undrained conditions are used to illustrate the behavioral response of loose and dense soils. Pore pressure development in undrained conditions and void ratio changes in drained conditions are also indicated.

Loose soils plot to the right of the steady state line (shown in Figure 2.12) and will undergo a tendency for contraction during both cyclic and monotonic undrained shear. Pore pressures increase in these soils until the effective stress is reduced to a steady state condition. These soils will undergo flow deformations once the peak strength has been reached. The stress path and stress-strain response for this condition is also shown in Figure 2.13. The shear stress increases to a peak strength and then decreases to the residual strength of the soil mass, where steady state deformation occurs. Poulos (1981) describes this as the state where continuous deformation occurs at constant volume, effective confining and shear stress, and constant velocity.

Alarcon-Guzman et al. (1988) have refined the state diagram described by Castro and Poulos (1977) to include both the steady state line and a critical state line. These are the F- and S-lines as shown in Figure 2.14. Alarcon-Guzman et al. attribute the difference between these lines to a structural collapse that occurs when the peak strength is reached during loading of a metastable soil structure. For a given soil, as the void ratio is

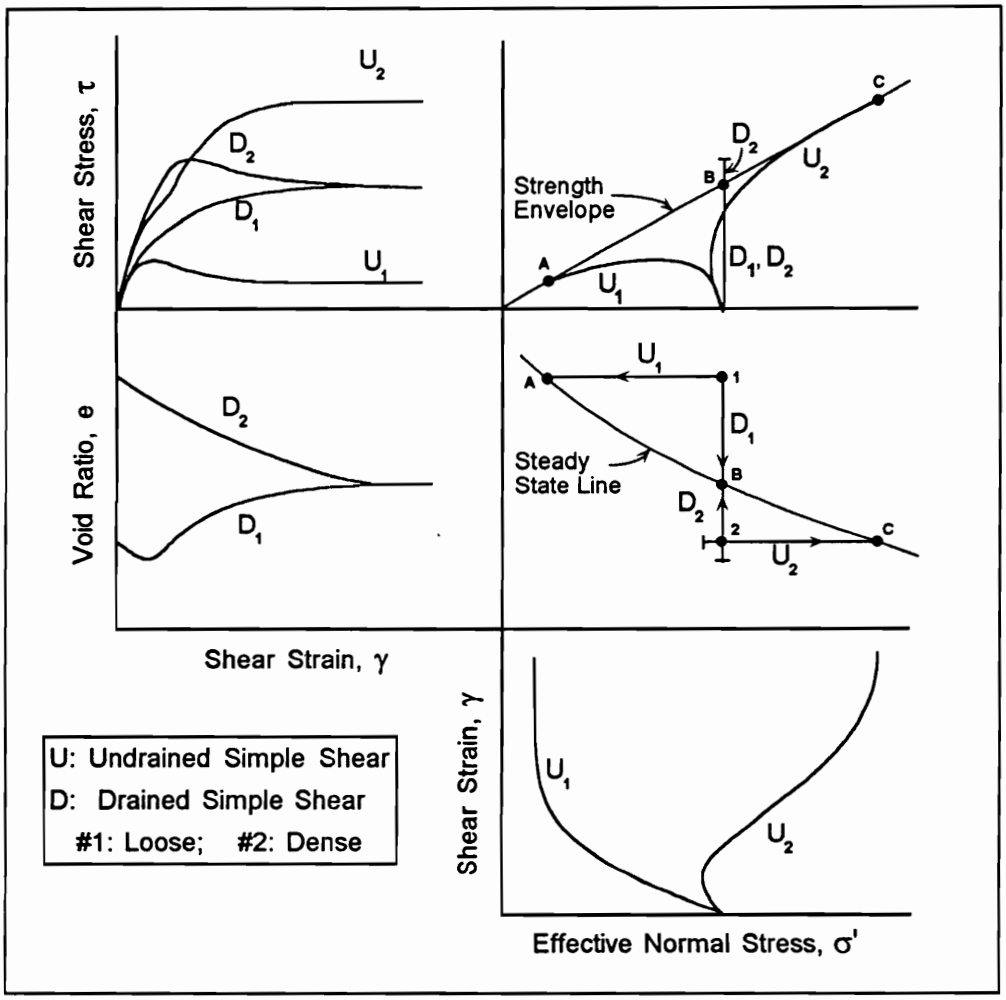

Figure 2.13. Stress-strain response of loose and dense soils to drained and undrained monotonic loading (after Castro, 1987).

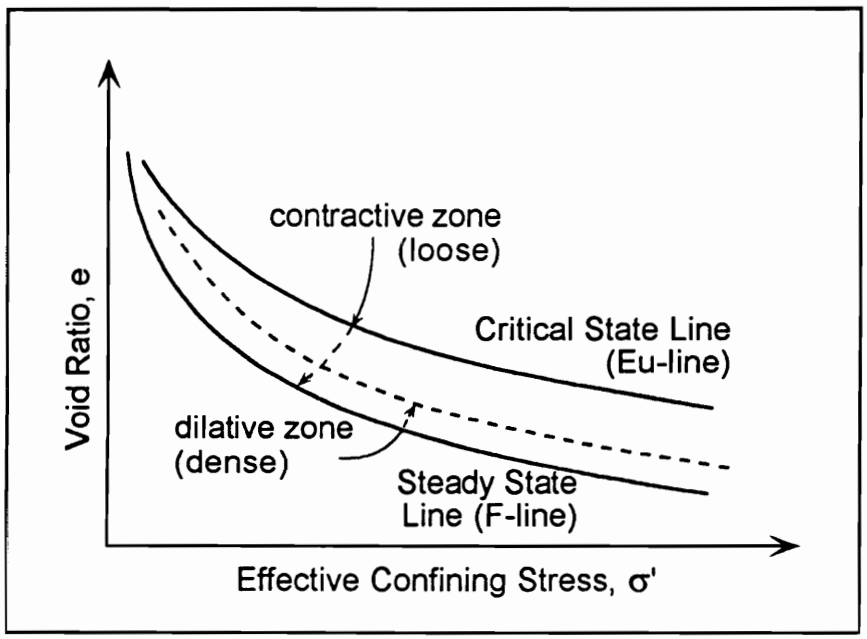

Figure 2.14. State diagram including both steady state and critical state lines (after Casagrande, 1975; Alarcon-Guzman et al., 1988).

increased the structure becomes more metastable, and the jump in pore pressure that occurs once the peak strength has been reached will also increase. This says that excess pore pressure generation is dependent on the tendency for a sudden breakdown in structure as well as on the volume change potential. If the structure is not brittle, pore pressure development will depend on volume change only, and the F- and S-lines will tend to converge.

The F-line (or steady state line) corresponds to the results of undrained load-controlled tests on loose specimens to the residual effective confining stress and shear strength for a given void ratio. The S-line (or critical state line) is determined from drained tests to the residual void ratio and shear strength for a given confining stress. The S-line is the E_u line in the state diagram as defined by Casagrande (1975). In this state diagram, dense soils plot to the left of the F-line and will not experience flow deformation during undrained loading. Loose soils plot to the right of the S-line in the state diagram and will show unlimited flow deformation under a constant applied load once the peak undrained strength has been reached. The final void ratio and effective stress relationship for the loose soils will plot on the F-line. Casagrande (1975) defines the F-line as the locus of points describing the failure conditions where a "flow structure" has developed within the soil mass.

The S-line marks the boundary between the initial conditions where unlimited flow deformation may occur under undrained loading (loose soils) and those conditions where only limited flow will occur (medium dense soils) before strain hardening returns (Alarcon-Guzman et al., 1988). Initial effective stress and void ratio conditions in medium dense soils initially plot between the F- and S-lines, with limited flow deformation occurring once the peak strength has been reached. This occurs at an effective shear stress greater than would be supported by a "loose" soil at the same void ratio. However, dilative behavior returns at some level of strain and shear strength is regained, eventually exceeding the original peak strength value. At the point where dilative behavior returns,

the stress path has reached the line of phase transformation in the stress space (Ishihara, 1985; Alarcon-Guzman et al., 1988) and turns to follow the failure envelope until the shear strength matches the applied load.

Alarcon-Guzman et al. (1988) attribute the magnitude of the difference between the state lines to the structure and "collapse potential" of the soil skeleton. A metastable soil skeleton is more likely to experience a sudden loss of structure than a soil in a more compact configuration. This tendency for sudden collapse of the entire soil structure in metastable soils will lead to a large sudden increase in pore pressures under undrained loading, and confining stresses will be rapidly transferred from the soil skeleton to the pore water. Once this has occurred, interparticle contact has been eliminated and the particles are placed in suspension (see Figure 2.11 b.). The more metastable a soil mass is, the greater the interparticle spacing within the suspension, and therefore the lower the interaction between soil particles during deformation. Under drained conditions, however, this collapse has no effect; a flow structure can not develop because volume change and particle rearrangement leads to consolidation of the soil mass during loading. As a soil structure becomes less metastable, or more compact, the tendency for a sudden collapse of the soil skeleton under undrained conditions is reduced (Alarcon-Guzman et al.). For soils that are not metastable, pore pressure increases are based on a tendency for gradual compression only, and the difference between the state lines disappears.

Loose soils subjected to cyclic loading may experience 100% excess pore pressure generation leading to soil strength reduced to a low steady state condition. This will occur in conditions where the applied peak cyclic loading exceeds the steady state undrained shear strength of the soil. This is illustrated in Figure 2.15(a). As cyclic loading continues from the initial condition (shown here for an isotropic consolidation stress condition), pore pressures gradually increase with little loss of shear resistance until the stress path reaches the monotonic stress path. At this point pore pressure generation has reduced the shear strength of the soil mass to where it is exceeded by the applied cyclic load (Alarcon-Guzman et al., 1988). Large deformations begin to occur in the stress-controlled test

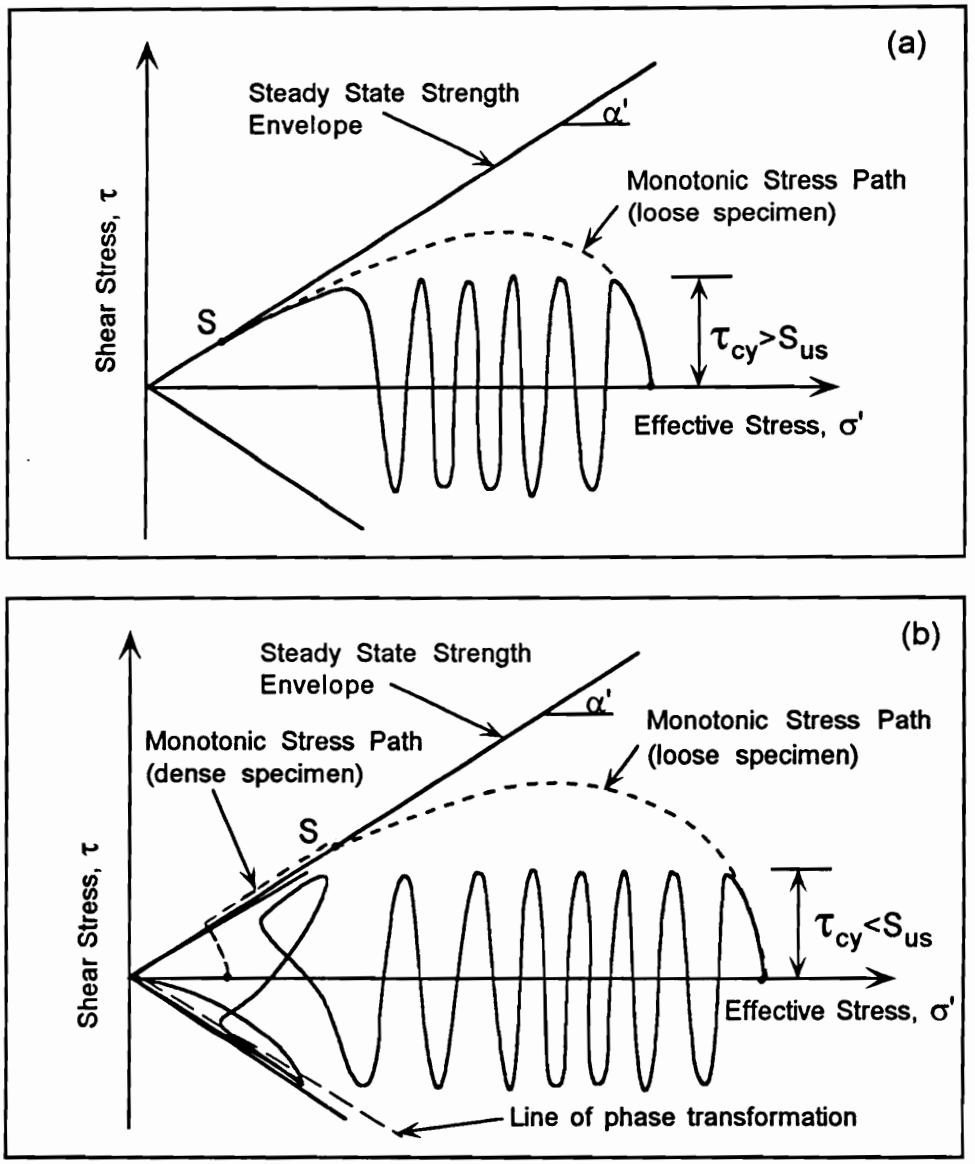

Figure 2.15. Comparison of stress paths for cyclic and monotonic undrained loading (after Alarcon-Guzman et al., 1988; and Mohamad and Dobry, 1986).

procedure and failure conditions can be said to have occurred. When in-situ soil deposits experience this type of loading, only small external loads are required to induce displacements of the soil mass (Zeghal and Elgamal, 1994). Under seismic loading of level or near-level ground conditions, lateral displacements may occur due to the minor stresses applied at the end of the loading sequence. Zeghal and Elgamal showed that the majority of lateral spreading displacements occurring at the Wildlife site due to the 1987 Superstition Hills earthquake occurred after 90% of the Arias energy intensity induced by the earthquake had passed.

Under cyclic loading of dense soils, or loose to medium dense soils where the steady state strength is greater than the applied cyclic stress, initially only contraction and an associated increase in pore pressure occurs. As the cyclic loading continues, pore pressures continue to increase and will eventually develop to the point that the stress path reaches the failure envelope and the soil skeleton will tend to dilate on each cycle of loading. Continued loading at this point induces a reduction in pore pressure and an associated increase in strength. Figure 2.15 (b) shows the stress path for this condition of loading (again shown for isotropic consolidation stress conditions). Where the applied cyclic stresses exceed the in-situ static stress on the failure plane, stress reversals will occur and excess pore pressures (u_{xs}) may develop such that the effective confining stress (σ'_o) passes through zero during each one-half cycle of loading (Mohamad and Dobry, 1986). This corresponds to an excess pore pressure ratio of 100% ($R_u = u_{xs} / \sigma'_{oi}$) and occurs at the isotropic stress condition (shear stress on the failure plane goes to zero).

Continued loading following initial development of 100% excess pore pressure in dense soil condition do not lead to large deformations because it takes only a small additional strain to mobilize dilative behavior within the soil mass. The stress path follows the failure envelope, with shear strength developing to match the applied cyclic loading due to the dilatant tendency of the soil skeleton. Once this dilative behavior begins to occur, pore pressures are reduced and soil strength increased. The cumulative effect of

the small cyclic strains producing the pore pressure reduction may lead to failure in engineered structures, but a loss of strength that could lead to the "true liquefaction" defined by Castro and Poulos (1977) has not occurred. This type of deformation within a soil mass has been defined as cyclic mobility (Casagrande, 1975; Castro and Poulos, 1977). Seed described this as a peak cyclic pore pressure ratio of 100% with limited strain potential (Seed, 1979). In this situation, the shear strength of the sand is reduced as the pore pressure increases, but then rapidly increases again once shear strains induced by the applied cyclic and static loads become large enough to reduce the excess pore pressures. Large flow slide deformations are avoided, but small cyclic displacements remain possible.

The stress-strain and pore pressure response of an in-situ loose granular soil to seismic loading is illustrated in Figure 2.16. Ground motions and pore pressure development were recorded at the Wildlife site in southern California during the 1987 Superstition Hills earthquake (Dobry et al., 1989). The response seen at this site is in good agreement with the laboratory test results seen above. Pore pressures are seen to begin to increase gradually when the threshold strain (approximately $\gamma = 0.04\%$) occurs (at time t = a of diagrams (a), (b), and (c)). Rapid pore pressure development does not begin to occur until the peak shear stress and acceleration occurs at time t = b. This is consistent with the collapse mechanism, as described by Alarcon-Guzman et al.(1988), that occurs in metastable soils when the peak strength is reached. At time t = c in the earthquake record, the majority of the shaking has ended, however, pore pressure continues to a rise rapidly. Zeghal and Elgamal (1994) report a drastic shear modulus (G) reduction, and corresponding increase in soil column period (T) at this time in the record. By time t = d in the earthquake record, the shear modulus has been reduced to a low "steady state" value, allowing the minor stresses remaining in the earthquake record to induce strains and continued increases in pore pressures. Following the conclusion of all seismic motions, the excess pore pressure remains high, and depending on drainage conditions thickness of the liquefied deposit, may remain high for quite some time. Holzer et al. (1989) report a 100% excess pore pressure ratio remained at 19 minutes after the

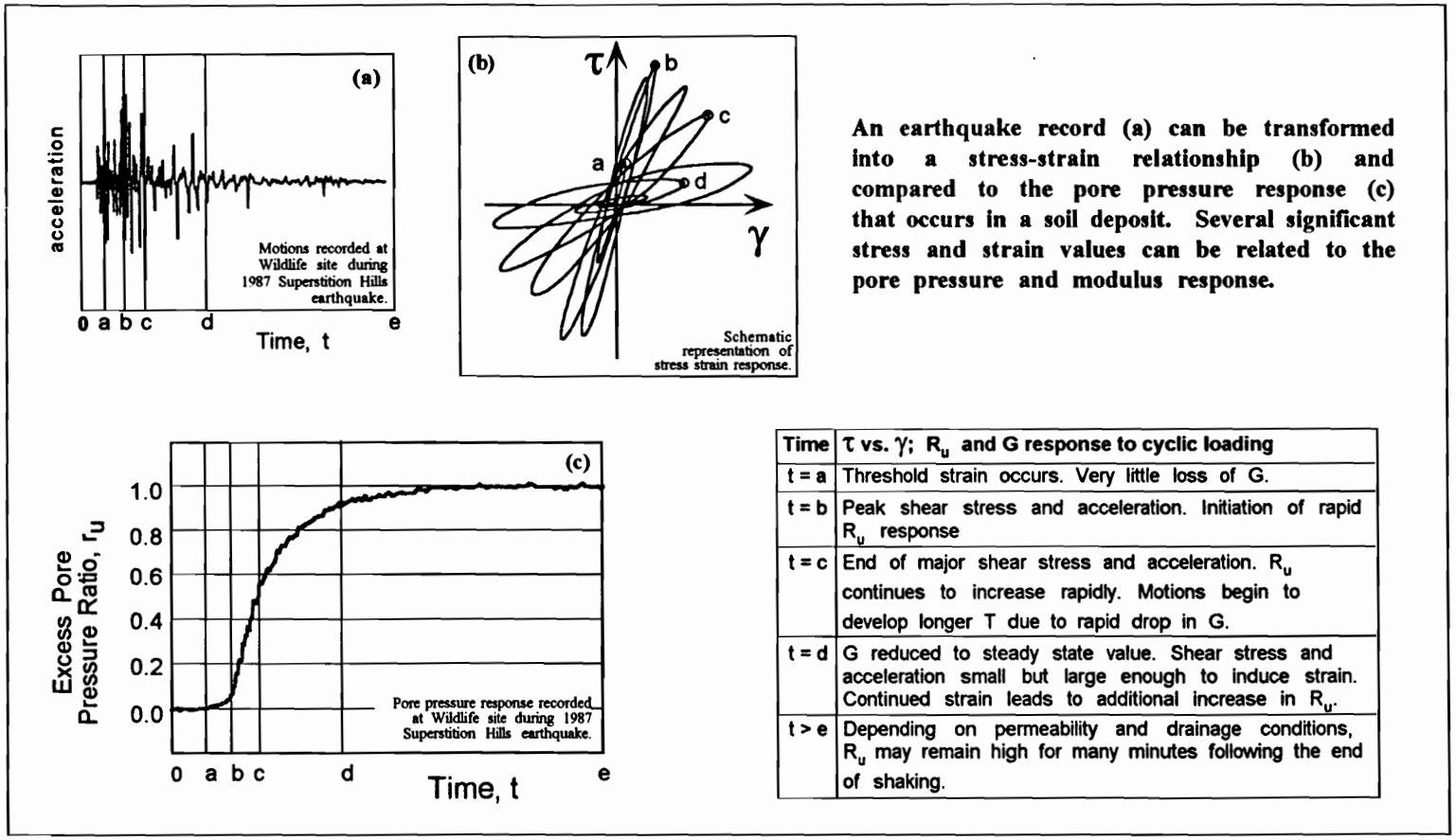

An earthquake record (a) can be transformed into a stress-strain relationship (b) and compared to the pore pressure response (c) that occurs in a soil deposit. Several significant stress and strain values can be related to the pore pressure and modulus response.

Time	τ vs. γ; R_u and G response to cyclic loading
t = a	Threshold strain occurs. Very little loss of G.
t = b	Peak shear stress and acceleration. Initiation of rapid R_u response
t = c	End of major shear stress and acceleration. R_u continues to increase rapidly. Motions begin to develop longer T due to rapid drop in G.
t = d	G reduced to steady state value. Shear stress and acceleration small but large enough to induce strain. Continued strain leads to additional increase in R_u.
t > e	Depending on permeability and drainage conditions, R_u may remain high for many minutes following the end of shaking.

Figure 2.16. Schematic representation of stress-strain and pore pressure response of a loose granular soil subjected to seismic loading. (After Holzer et al., 1989; Ishihara and Nagase, 1985; and Zeghal and Elgamal, 1994).

event began. By 29 hours after the event, a hydrostatic condition had been regained, but this shows that excess pore pressures can remain for a substantial period following the end of shaking.

2.4.2. Soil Behavior Due to Liquefaction

Castro (1987) has refined the "true liquefaction" definition described by Casagrande (1975) and Castro and Poulos (1977). This is based on the behavior of a soil and the excess pore pressure development during earthquake shaking. He suggests three types of soil behavior are possible for soils with initial stress states and densities that plot above and to the right of the steady state line. These consist of failure due to: 1.) complete loss of stability, 2.) limited shear distortions, and 3.) increased pore pressures and ground settlements.

Soils where the initial state of stress and density plots to the right of the critical void ratio (S) line are considered loose (Alarcon-Guzman et al., 1988; Casagrande, 1975). These soils tend to collapse under both monotonic and cyclic loading. In undrained conditions these soils will allow rapid development of excess pore pressures during shear. As the excess pore pressures approach the value of the initial confining stress, the soil strength may be reduced to the point that even small externally-applied loads will overcome the shear resistance available in the soil mass and allow a catastrophic failure. This can take the form of a flow slide, large settlements of buildings, or floating of buried structures. This remains what Castro (1987) describes as true liquefaction. In this case, once the failure begins to occur, displacements will continue until the external shear stresses are reduced to match the strength available within the liquefied soil mass (the steady state undrained shear strength), or the soil strength is increased through drainage to overcome the applied shear stress (Stark and Mesri, 1992). This type of failure may continue long after the seismic loading has ceased.

In cases where the undrained shear strength exceeds the value of the externally applied loads, catastrophic flow failures can not occur. However, during seismic shaking,

the earthquake-induced inertial forces combined with the external gravity loads applied to the soil mass may be sufficient to temporarily overcome the undrained strength of the soil. This type of failure can occur in any soil where the initial conditions plot above and to the right of the steady state (F) line. In this case, limited deformations of the soil mass will occur, but only when the combined inertial and gravity forces exceed the undrained strength of the soil mass for a given level of strain. Displacements due to this type of behavior result in slumping of slopes, building settlements, and lateral spreading (Castro, 1987).

The third type of failure occurs in soils loose of the steady state line during seismic loading where no externally applied loads exist. This situation exists in level ground conditions where no structures are present. Under seismic loading the soil grains become suspended in the pore water as the excess pore pressure approaches the value of the initial effective confining stress (Castro, 1987). The soil particles then begin to settle into a denser state and water is forced vertically out of the soil/water suspension. Where an overlying less-permeable soil deposit exists, large pore pressure gradients may be developed between the top of the granular deposit and the ground surface. These large gradients, combined with the seismic shaking, can lead to fracturing of, or progressive propagation of a flow path through, the overlying soil, allowing dissipation of the excess water pressures by flow to the surface. This flow can carry particles of the granular soil to the surface as well. This type of ground disruption is typically known as a sand blow or sand boil and is accompanied by settlement of the ground surface (Castro, 1987).

2.4.3. Earthquake-Induced Ground Failures In The Wabash Valley

The ground failures associated with the liquefaction that occurred in the Wabash Valley Seismic Zone most often takes the form of the dikes and blows associated with lateral spreading. Some locations also contain individual sand boils, but these are not as readily identified in the field due to the nature of their formation and the age of the earthquake events being studied. The dikes associated with lateral spreading are generally

continuous for large distances, while sand boils form in isolated locations with a single flow channel developing to the surface and allowing material to erupt from below in a manner similar to a volcano. The material ejected to the surface provides the most obvious evidence in many cases. However, subsequent deposition of floodplain deposits has obscured the vented material by a meter or more of flood plain sediments in many areas. The features are now visible only in vertical exposures of the soil profile such as river banks and excavations that extend below the paleosurface present at the time of the earthquake.

The lateral spreading features observed in the Wabash and White River Valleys developed due to displacements of the overlying low-permeability soils following excess pore pressure development during seismic shaking. The shear stresses existing at the interface of the liquefiable sand and gravel point bar deposits and overlying flood plain deposits are altered by the seismically-induced inertial stresses, and overcome the undrained strength of the soil mass in the failure zone. Lateral movement is induced in this manner and fracturing of the overlying soil occurs. The excess pore pressures developed in the liquefied soils are then dissipated by flow to the surface through the fissures. Large hydraulic gradients present at these locations then carry sand and gravel particles to the surface with the pore water. Once the earthquake shaking ceases, the undrained strength again exceeds the applied stresses and the soil mass regains a stable configuration. No further displacement will occur though excess pore pressures may remain high for a long time following the end of shaking. Flow to the surface will continue until the pore pressures are dissipated. Surface settlement will be associated with both reconsolidation of the liquefied sand stratum and loss of material by flow to the surface.

Once the excess pore pressure has been dissipated, nearly-vertical dikes filled with sand and gravel remain, cutting through the fine-grained flood plain deposits. Features of this type have been observed up to 2.5 meters in width (Obermeier et al., 1993) in the

Wabash Valley. At the surface above these features is a cap of vented material that may extend several meters or more beyond the dike through which the material was vented.

Traditional field liquefaction susceptibility analyses have been based on the Seed and Idriss (1971) simplified procedure. This type of procedure can also be used to back-calculate seismic parameters associated with prehistoric liquefaction events. The simplified procedure is described elsewhere (Seed and Idriss, 1982; Seed et al., 1983; Seed et al., 1985), and is duscussed only in Chapter 6 of this report as it relates to this study. However, a number of researchers have been working on the relationship between energy dissipation and pore pressure development during undrained cyclic loading. This type of approach to liquefaction susceptibilty provides an alternative analysis method that can be used to supplement the simplified procedure. Background for an energy approach is discussed below, with the implementation of the procedure in relation to a palwoliqn study discussed in Chapter 6.

2.4.4. Energy Approach To Liquefaction Susceptibility Analyses

Since 1979, research has been conducted assessing the relationship between accumulated energy dissipation and pore pressure development during shear of saturated cohesionless sands (Figueroa et al., 1994). An initial study established the theoretical relationship between volume change or pore pressure development and the dissipated energy per unit volume given by the area enclosed within the hysteresis loops of a stress strain diagram of cyclic shear loading (Nemat-Nasser and Shokooh, 1979). Subsequent research has been directed at identifying a direct relationship between the development of excess pore pressures and the dissipated energy per unit volume by looking at parameters that influence the relationship (Davis and Berrill, 1982; Figueroa et al., 1994), and relating the laboratory results to observed in-situ liquefaction effects to predict liquefaction development during future seismic events (Berrill and Davis, 1985; Law et al., 1990).

An energy method of assessing liquefaction potential appears to offer advantages over the Seed et al. (1983) stress method in that a measure of the total seismic energy is

used rather than an estimated peak horizontal ground surface acceleration. The frequency associated with peak ground motion amplitudes will vary depending on earthquake source characteristics and competency of the regional basement rock (Atkinson and Boore, 1995). The ground motion amplitudes will also be amplified or deamplified at different frequencies depending on site specific effects such as soil conditions and topography. The energy associated with deamplified motions at a particular frequency, however, will be balanced by amplification of the motions at other frequencies (Law et al., 1990). The total input energy applied to a soil column is unchanged by the amplification and deamplification effects. An energy approach, therefore, allows consideration of the complete spectrum of ground motions.

2.4.4.1.Laboratory Studies Of The Energy Approach

Nemat-Nasser and Shokooh (1979) developed a theoretical relationship between energy expenditure per unit volume and either volume change or excess pore pressure generation during cyclic loading. Their comparison of the theoretical predictions with published experimental data shows excellent agreement between the two. Figueroa, Saada, Liang and Dahisaria (1994) also looked at the energy approach to liquefaction potential. They performed isotropically consolidated undrained (ICU) hollow cylinder torsional simple shear tests on a poorly-graded fine sand. They varied amplitude of shear strain, relative density and confining pressure. The test results were used to establish relationships between the total energy dissipation per unit volume required for 100% excess pore pressure development and the relative density, confining pressure and shear strain amplitude. Regression analyses of the results showed the parameters of relative density and confining pressure to be statistically significant. The test results also indicate strain amplitude has no apparent effect on energy dissipation. Based on this they present the following equation to describe the energy dissipation required to produce liquefaction:

$$\mathrm{Log}(\delta W) = 2.002 + 0.00477\sigma_o' + 0.0116D_r; \quad \text{with } R^2 = 0.937.$$

In this equation, δW is the total energy dissipated per unit volume to produce liquefaction. The coefficient of determination equal to 0.937 suggests that consolidation stress and relative density adequately describe the energy dissipation required to liquefy a particular soil deposit subject to the range of conditions tested. Since their study indicates that the energy required for liquefaction is unaffected by shear strain amplitude, Figueroa, et al. (1994) conclude that the energy method can be applied to the non-uniform loading conditions that occur during seismic events. Liang et al. (1995) compare the cumulative energy per unit volume required to induce liquefaction in laboratory tests under random loading to the results reported by Figueroa et al. for sinusoidal loading tests. They conclude that there is no statistical difference at a 95% confidence level between the two loading mechanisms in the relationship between pore pressure generation and the accumulated energy per unit volume.

The conclusion that can be drawn from these studies is that an energy approach can be effectively utilized to evaluate liquefaction susceptibility of a soil deposit subjected to a seismic loading. However, a practical approach using this type of procedure will require a reliable measure of the available seismic energy that is produced by a given earthquake and affects a unit volume of a given soil deposit. In addition, a dependable method to measure the energy per unit volume required to induce liquefaction in the soil deposit is required.

2.4.4.2.Energy Approach To Field Liquefaction Susceptibility

Davis and Berrill (1982) used the relationship of Nemat-Nasser and Shokooh (1979) to predict field liquefaction probabilities based on a linear relationship between pore pressure generation and energy dissipation. Their model assumes an empirical representation of the seismic energy arriving at a site, and an empirical description of the parameters affecting liquefaction susceptibility of an in-situ soil deposit, will mirror the effects of the important parameters as measured in the laboratory tests. Their model was developed by correlating an empirical seismic energy function of magnitude and distance

with published N_1 values for sites where liquefaction did and did not occur. Berrill and Davis (1985) then revised the original model based on parametric studies of small variations in the source energy function and inclusion of material properties in the attenuation function. This work showed the Gutenberg and Richter (1956) formulation for total radiated energy provides reliable prediction of liquefaction effects, and inclusion of anelastic attenuation effects provides only small changes in model reliability.

The revised Berrill and Davis (1985) model incorporates a non-linear pore pressure vs. dissipated energy relationship based on the work of Simcock et al. (1983). From ICU cyclic triaxial tests on a poorly-graded medium sand, they found a power relationship between excess pore pressure development and dissipated energy when both are normalized by the consolidation stress. This relationship is given as:

$$\frac{\Delta u}{\sigma_o'} = \alpha \left[\frac{\Delta E}{\sigma_o'} \right]^{\beta};$$

where Δu is the excess pore pressure developed, σ_o' is the consolidation stress, ΔE is the dissipated energy, and α and β are empirical constants.

Law et al. (1990) then modified the energy model to incorporate the effects of consolidation ratio on pore pressure development. They performed isotropically and anisotropically consolidated undrained (ICU and ACU) cyclic triaxial and cyclic hollow cylinder torsional simple shear laboratory tests on a poorly-graded medium sand. They used the results to establish a new relationship between accumulated dissipated energy and excess pore pressure development. Their results are consistent with those of Berrill and Davis (1985), showing a direct relationship between excess pore pressure development and accumulated dissipated energy for constant values of minor principal consolidation stress when the effects of consolidation ratio and relative density on the energy dissipation function are also considered. Plotting the normalized test results, they found a unique relationship between the energy function and excess pore pressure development. This lead them to a dimensionless energy function normalized by these parameters to describe the

relationship between accumulated dissipated energy and excess pore pressure development. Using a log-log scale they were able to define a power relationship similar to that of Berrill and Davis (1985):

$$\frac{\Delta u}{\sigma_c'} = \alpha W_N^{\beta};$$

$$\text{for } \mathbf{W_N} = F_1(K_c) \cdot F_2(D_r) \cdot \sum \omega / \sigma_c';$$

where W_N is the normalized accumulated dissipated energy function, σ_c' is minor principal consolidation stress, K_c is the consolidation ratio relating the maximum and minimum principal consolidation stresses, D_r is the relative density of the specimen, and ω is dissipated energy per unit volume.

Use of the energy method to assess field liquefaction potential requires a comparison of the energy per unit volume expected to be applied during dynamic loading of a soil deposit with the energy per unit volume required for liquefaction of that soil deposit. Extending the findings of the laboratory studies and the model of Berrill and Davis (1985); Law et al. (1990) propose a field liquefaction susceptibility evaluation procedure based on empirical measures of both the seismic energy expected at a site during an earthquake event and the soil strength parameters related to liquefaction resistance. Using a seismic energy attenuation relationship to estimate the energy reaching each site in an existing liquefaction vs. non-liquefaction database they propose a liquefaction prediction boundary based on measured in-situ soil conditions and a seismic energy intensity function. This boundary represents the in-situ condition required to suppress liquefaction for a given seismic energy intensity. The method requires knowledge of earthquake magnitude, hypocentral site distance and near surface soil conditions, as well as an estimate of seismic energy attenuation characteristics of the region.

In order to apply their energy method to liquefaction potential in the field, Law et al. (1990) assume that the energy released at the source of an earthquake can be given by the empirical relationship proposed by Gutenberg and Richter (1956):

$$E = 10^{4.8+1.5M}$$

Berrill and Davis (1985) showed that this relationship provides good reliability in an energy model. This estimate of the energy released at the source is not related to a physical measure of ground motion parameters, but is based on empirical relationships. However, in a field liquefaction susceptibility prediction, a precise measure of energy is not needed. It is sufficient to use a relationship that results in a consistent representation of the energy arriving at any site within hypocentral distances where liquefaction effects can be expected to occur.

Law et al. (1990) assume attenuation of seismic energy will result in the energy reaching a site, E_I, being given as:

$$E_I(E,R) = \Phi E/R^B \text{ ; or } E_I(E,R) = \Phi\left[10^{(4.8+1.5M)}\right]R^{-B}.$$

where E is seismic energy in Joules, **M** is Richter or moment magnitude, R is hypocentral distance in km, Φ is assumed to be a constant, and B is an attenuation coefficient describing both geometric spreading and hysteresis damping (anelastic attenuation). Here, the attenuation function is based on the assumption that hypocentral distance is equal to the distance to the center of energy release and B=2 for geometric spreading alone. Additionally, Law et al. point out, since hypocentral distance is on the order of 10's of km and the thickness of the soil profile is generally limited to 10's of meters, the variation of the energy arriving at different depths within the soil deposit will be insignificant. Based on this, the energy available for pore pressure development can be assumed to be constant throughout the depth of the soil column. The accumulated energy loss in the soil column can then be represented by adding an energy dissipation function, λ, to the site energy function, E_I, resulting in:

$$\sum \omega = \lambda\left(\sigma_c', K_c, D_r\right) \cdot E_l(E, R).$$

Substituting this relationship into the pore pressure vs. accumulated dissipated energy per unit volume relationship developed from laboratory test results, Law et al. (1990) propose the following relationship for excess pore pressure development in the field:

$$\frac{\Delta u}{\sigma_c'} = \alpha \left[\frac{F_1(K_c) F_2(D_r) \lambda\left(\sigma_c', K_c, D_r\right) \Phi \times 10^{1.5M+4.8}}{\sigma_c' R^B} \right]^{\beta}$$

Combining the terms containing the constants, σ_c', K_c and D_r, a single function, η, can be used to represent the combined effect of these parameters. Assuming that a function of the corrected in-situ SPT blowcount value, $(N_1)_{60}$, can be used to represent these parameters, a liquefaction resistance function can then be defined as:

$$\eta\left[(N_1)_{60}\right] = \frac{\alpha^{-1/\beta} \sigma_c' \times 10^{-4.8}}{F_1(K_c) F_2(D_r) \lambda\left(\sigma_c', K_c, D_r\right) \Phi}$$

If u_{xs} is multiplied by $\eta\left[(N_1)_{60}\right]^{\beta}$ we are left with:

$$\frac{\Delta u}{\sigma_c'} = \left[\frac{10^{1.5M}}{\eta\left[(N_1)_{60}\right] R^B} \right]^{\beta}$$

Assuming the condition of liquefaction can be defined as that where the ratio of excess pore pressure to the in-situ effective confining stress becomes 1.0:

$$\frac{\Delta u}{\sigma_c'} = \left[\frac{10^{1.5M}}{\eta\left[(N_1)_{60}\right] R^B} \right]^{\beta} = \left[1.0\right]^{\beta} = 1.0;$$

the following energy equation can be written describing the threshold liquefaction condition:

$$\frac{10^{1.5M}}{\eta\left[(N_1)_{60}\right]R^B} = 1.0.$$

This allows an empirical determination of the critical value of $\eta\left[(N_1)_{60}\right]$ representing incipient liquefaction.

Law et al.(1990) define the relationship between magnitude and distance as an empirical seismic energy intensity function T(**M**,R), where:

$$T(\mathbf{M}, R) = 10^{1.5M}/R^B$$

Liquefaction is predicted to occur when the seismic energy intensity function, $T(\mathbf{M}, R)$, exceeds the liquefaction resistance function, $\eta\left[(N_1)_{60}\right]$. The condition of liquefaction can therefore be represented as:

$$\frac{T(\mathbf{M}, R)}{\eta\left[(N_1)_{60}\right]} \geq 1.0.$$

This definition of liquefaction susceptibility provides a rational method for predicting blowcounts susceptible to liquefaction occurrence based solely on magnitude and distance estimates. This procedure will be developed further in Chapter 6 based on published liquefaction catalogs. The approach will then be used to help identify the portion of the soil profile involved in producing the paleoliquefaction evidence found in the Wabash Valley.

3. Field Investigation

The field investigation performed for this study was designed to allow assessment of the seismic parameters associated with a series of ancient earthquakes inducing significant liquefaction distributions in the Wabash region. The study sites were chosen to represent a variety of epicentral distances and severity of liquefaction effects. At all sites, testing was performed adjacent to the observed liquefaction features, and where possible, at locations away from observed features. At sites showing extensive liquefaction, disturbance of the source sediments is likely to have been most severe immediately adjacent to the features. Test locations away from the features were investigated in an effort to obtain test results more representative of soil strengths present prior to the earthquake. This helps to place reasonable limits on the level of shaking that occurred at these sites. Extensive liquefaction is considered to have occurred at sites with large individual liquefaction features or many small features observed at short intervals along an exposed soil profile. Test sites with only a single moderate feature, or only a few small features, were chosen to represent the case of marginal liquefaction. The minimal amount of liquefaction evidence at these sites suggests ground motions which only marginally exceeded the threshold values required for liquefaction features to develop. The source sediments at these sites are assumed to have been less disturbed than those at the severe liquefaction sites.

Progressive densification of the sediments in the Wabash Valley Seismic Zone due to seismic events of moderate strength is assumed to be minimal due to the infrequent seismic activity in the region and observed soil density patterns. Moderate as well as severe seismic activity is infrequent. Additionally, only a narrow range of ground motions is likely to be appropriate for partial pore pressure generation that does not lead to full liquefaction and an expression of failure at the surface. Where pore pressure generation does not occur during seismic loading, there has been no tendency for differential particle motion. Therefore, no densification will have occurred. This is consistent with laboratory testing showing no change in void ratio, and field studies showing no measurable

settlement when pore pressure development does not occur (Tokimatsu and Seed, 1987). Progressive densification due to partial development of excess pore pressures is likely to be minimal in low seismicity environments. At the Wildlife site in California, 100% excess pore pressure development was measured following the 1987 M6.6 Superstition Hills earthquake, with a_p=0.21g. The previous day, however, the M6.2 Elmore Ranch event produced a_p=0.13g and no pore pressure development occurred (Zeghal and Elgamal, 1994). The response reported by Zeghal and Elgamal for the Superstition Hills event suggests that $a_p \approx 0.14$g is the threshold acceleration (Dobry et al., 1982) required to induce pore pressure development at this site due to a M6.6 event. It also appears that $a_p \approx 0.21$g is the threshold for 100% excess pore pressure generation. Progressive densification due to partial pore pressure development will therefore only occur over the range of cyclic stresses between these values. It is likely that this range of accelerations inducing partial pore pressure development is a function of grain size and other factors, but these results suggest the range of accelerations leading to only partial pore pressure development for a given magnitude event is small.

The liquefaction evidence observed in the Wabash region suggests a return period of approximately 6000 to 7000 years for events large enough to induce widespread liquefaction (M>7). Other smaller events occur more frequently, but induce liquefaction over more limited areas (Munson and Munson, 1996). Where liquefaction occurs during any of these events, the grain structure induced by progressive densification due to prior non-liquefaction events is likely destroyed. The result could be that the resistance to subsequent liquefaction is either greater or lesser than prior to the liquefaction event. This depends on the initial condition, the extent of liquefaction disturbance due to lateral spreading or venting, amount and direction of pore pressure migration, and amount of shear displacement due to the seismic loading itself. Obermeier (1995) references unpublished USGS data showing that the Superstition Hills liquefaction event did not induce an increase in penetration resistance due to the liquefaction event. The cumulative

result of these potential effects is that progressive densification is not likely to play a major role in the soil conditions measured relative to the pre-event conditions.

Changes in soil strength due to chemical alteration or aging of the soils in the Wabash region are also assumed to be negligible. The source materials involved in the liquefaction effects were initially deposited as outwash sediments from the receding Wisconsinan glaciation. This glacial episode was at its peak approximately 20,000 years ago (Plummer and McGeary, 1993). The sediments have subsequently been transported and re-deposited several times by meandering of the rivers in the region. These sediments are therefore relatively young, and insufficient time has passed to allow significant weathering. Additionally, the regional groundwater table has generally been at or above the top of the terminal Pleistocene and Holocene-age liquefiable sediments throughout the Holocene, suppressing weathering effects by limiting the available oxygen.

However, at some Holocene-age sites the river level occasionally drops below the top of the source. At most late Pleistocene-age sites the river level regularly remains a short distance below the top of the source. This has allowed direct observation of the sediments involved in the liquefaction at some sites. No significant weathering of the sediments at the Holocene sites was apparent, and only minor weathering in some of the late Pleistocene sediments was observed. The weathering is present near the top of the liquefiable deposit, and the blowcount values were also found to be the lowest at those depths. This may be due to disturbance effects that occur during liquefaction events, or strength increases associated with cementation due to weathering effects could be inconsequential. Regardless, the effect of weathering of the Wabash Valley soils can be assumed to have little or no effect on measured liquefaction resistance.

These issues and others relating to in-situ soil property measurements will be discussed in greater detail in the chapter 5, where the observed in-situ soil conditions are described.

3.1.Scope of Field Investigation

The objectives of the field work were to:

- Define the vertical and lateral extent of the soil strata where liquefaction features have been identified.
- Determine the extent of the liquefaction at each of the study sites and which sediments were involved.
- Look at the site stratigraphy as it relates to the liquefaction behavior of the soil deposit.
- Determine the in-situ soil parameters for liquefaction susceptibility analyses.
- Obtain samples of the soils where liquefaction occurred. This included both sands and gravelly soils, as well as the surficial fine-grained, low-permeability soils. Samples from below the liquefied zones were obtained to provide soil strength and deformation parameters for site response studies.
- Compare the geotechnical conditions and field behavior between sites containing sands and gravelly sands.

The majority of the field work involved obtaining Standard Penetration Test (SPT) blowcount data and penetration test data using a three-inch California-type oversize sampler (OPT). Seismic shear and surface wave velocity testing were also accomplished to provide additional input data for the site response analyses. To provide specimens for the laboratory testing program, soil samples were retained from the penetration test procedures, the in-situ density tests, and obtained as bulk samples of the exposed near-surface soils where obtainable.

3.2.Field Reconnaissance

Initial identification of potential study sites in the Wabash region was accomplished by USGS and Indiana University personnel. This involved thorough searches of exposed soil profiles in river banks, gravel pits, and other excavations throughout southwest

Indiana and portions of Illinois. During periods of low water these locations provide many excellent exposures of the near-surface sediments where liquefiable soils are present. The search and identification procedures are described by Munson and Munson (1996). Once the sites were identified, additional field reconnaissance was required to identify those sites most important to this study. This site reconnaissance looked for locations where access could be obtained for a geotechnical engineering analysis of the soils present at the site. The vast majority of identified liquefaction sites are located on private property and permission for access had to be obtained from the individual property owners. Selection of testing sites was therefore based on a variety of criteria including: 1.) the extent and severity of the liquefaction evidence present, 2.) the importance of the site to the results of the study, 3.) the ability to gain permission for access, and 4.) accessibility of the site to drilling equipment.

The initial site investigations therefore consisted of identifying the soils involved in the observed liquefaction evidence and the extent of that liquefaction. At many of the study sites (particularly near the inferred epicenter) the liquefaction evidence extended over a large lateral extent, involving all of the near-surface soils present at the site. At sites of greater epicentral distance, the liquefaction evidence may be limited to only the most susceptible soils and site conditions. An assessment of the importance of the site relative to other sites in the vicinity could then be made based on the soil types and site conditions involved in the liquefaction.

Sediments involved in the liquefaction observed in the Wabash region are of late Pleistocene to middle Holocene age. They were originally deposited as an outwash plain at the height of the Wisconsinan glaciation approximately 20,000 years BP. As the glaciers receded, outwash flows remained high, but sediment loads decreased, leading to downcutting of the rivers in the region. As outflow was reduced, rivers in the region eventually began to meander in the outwash sediments with a lower surface elevation, leaving terraces of the original braided stream outwash deposits. The rivers have reworked the outwash sediments into typical meander belt fluvial and alluvial deposits. At

some sites a sequence of the Wabash Valley fluvial sediments can be differentiated into late Pleistocene, early Holocene, or late Holocene origins based on the elevation of the interface between the coarse and fine-grained sediments. The top of the liquefiable material is at the greatest elevation in the Pleistocene deposits. In deposits of the upper Wabash and White rivers the top of the early Holocene sand and gravel deposits are at a lower elevation than those of mid to late Holocene age.

Once a site was deemed important to successful completion of the study, access concerns were addressed. Many of the sites were located in areas on the river side of flood control levies and/or in farmers' fields. These locations presented obstacles to access in terms of forested areas, presence of corn and/or soybean crops, lack of roads, inclement weather of all types, and worst of all flooding. Sites where access would be exceptionally difficult were eliminated from consideration unless no other site in the vicinity could be accessed to provide similar data.

Once the most important sites were identified, property owners were approached to obtain permission for equipment access and soil sampling. In almost all cases, this permission was granted with little hesitation. However, it generally came with the stipulation that equipment access be limited to those times when no crops were present. This was certainly generous enough on the part of the property owner, but limited the drilling and sampling work to the winter months in many cases. This lead to problems with access in terms of rain, snow and flooding. To address this issue, drilling equipment mounted on a four-wheel-drive or all-terrain vehicle was required at many sites.

3.3.Testing Program

3.3.1.Drilling and Sampling Procedure

Over the last 20 years a standard test procedure has been developed to determine in-situ blowcount values for use in liquefaction analyses. This procedure is summarized by Seed et al. (1985). The procedure includes using a 4- to 5-inch diameter rotary borehole with bentonite drilling mud for stability. Blowcounts are obtained using 2 inch OD split

spoon samplers with a constant $1^3/_8$ inch ID, and without liners. The blowcount rate should be maintained between 30 to 40 blows per minute, with the energy delivery at 60% of the theoretical maximum. The procedure utilizes a 140 lb. hammer dropped a distance of 30 inches. The energy ratio of 60% is based on minimizing the correction required for the most common hammer type (safety) and drop procedure (rope and pulley with approximately $2^1/_4$ or $2^3/_4$ wraps of the rope around the cathead) used in the United States.

The drilling and sampling procedures utilized for this study were performed in general accordance with the Seed et al. (1985) recommendations. However, there are two notable exceptions. In many of the Wabash valley soils a significant gravel content is present. An oversize penetration test (OPT) procedure was to minimize the potential effect of large particle sizes on penetration test results. It should also be noted that the blowcount rate was similar for the two tests, but that three wraps of the rope around the cathead were used for the OPT procedure, compared to the two wraps used for the SPT procedure. Also, a hollow stem auger was used to advance the borings to the sample depths of interest. The effect of these changes in the recommended sampling procedure are addressed below.

3.3.1.1.Standard and Oversize Penetration Testing

Most of the field data was obtained through use of the Standard Penetration Test procedure. In those soil deposits where gravel-sized particles are present, SPT data may be inflated with no true increase in liquefaction resistance. Tokimatsu and Yoshimi (1983) found that liquefaction could occur at higher average corrected SPT blowcount values in gravelly sands than in sands with no gravels. This was also found to be the case by Harder (1988) at the Pence Ranch site associated with the Borah Peak earthquake, though at the same site Stokoe et al. (1988) found no indication of significant change in blowcount values due to gravels. Andrus and Youd (1991) also reported no apparent influence due to larger particle sizes on SPT results.

In an attempt to avoid any potential for misrepresentation of liquefaction susceptibility associated with inflated blowcount data due to large particle sizes,

penetration testing in gravelly soils was accomplished using a three-inch California-type split spoon sampler driven with a 300-pound hammer. The sampler had an outer diameter 3-inches, and a 2-inch inside diameter. Use of this sampling procedure, however, introduced the problem of developing a method to obtain equivalent SPT data with the non-standard equipment. This was accomplished for this study by adjusting the hammer drop height. Several approaches to obtaining OPT data equivalent to SPT results were reviewed prior to initiation of the testing program. An approach suited to the Wabash valley soils was initially chosen and tests performed using both the SPT and OPT to assess the ability of the OPT procedure to produce results equivalent to the SPT procedure.

Fang (1991) presents penetration test conversion factors based on a relationship called the sampler ratio. In coarse-grained soils the following relationship is used to determine the sampler ratio, R_S:

$$R_S = \frac{\left(D_o^3 - D_i^3\right)}{144 \cdot W \cdot H};$$

where W is hammer weight in pounds, H is hammer drop height in inches, and D is sampler diameter in inches. Using this relationship, an estimate of the required drop height can be obtained in a manner similar to the energy per unit area approach above.

An approach based on the energy applied to the sampler (Karol, 1960), simply involves relating the energy applied over the cross-sectional tip area of the oversize spoon to that applied over the cross-sectional tip area of the two-inch split spoon sampler during the Standard Penetration Test. Differences in the total frictional resistance on the wall of the samplers are assumed to be negligible compared to the tip resistance, and ignored. The following relationship is used in the analysis:

$$\frac{N_{SPT} \cdot W_{SPT} \cdot H_{SPT}}{\left(D_o^2 - D_i^2\right)_{SPT}} = \frac{N_{OPT} \cdot W_{OPT} \cdot H_{OPT}}{\left(D_o^2 - D_i^2\right)_{OPT}};$$

where N is corrected blowcount, W is hammer weight or mass, H is hammer drop height, and D_o and D_i are the outer and inner sampler diameters, respectively. The subscripts SPT

and OPT refer to the standard and oversize test procedures. The required hammer drop height is found by equating the blowcounts for both test procedures and solving for H_{OPT}.

Karol (1960) proposed a conversion factor, Φ, derived based on SPT hammer weight and drop height, and sampler dimensions. Karol presents the following equation for conversion of OPT data to equivalent SPT results:

$$N_{SPT} = \frac{\Phi \cdot N_{OPT} \cdot W_{OPT} \cdot H_{OPT}}{\left(D_o^2 - D_i^2\right)_{OPT}};$$

where Φ is equal to 0.0005 in/lb.

The energy approach results in a recommended drop height of 33 inches (84 cm). The Fang (1991) conversion between SPT and OPT data results in a recommended drop height of 49 inches (125 cm). Neither of these drop heights were considered to be appropriate for this study, however. The conversion based on the Karol procedure has been shown to be conservative in a variety of soil conditions (Moore and Hempen, 1982; Martin and Fragaszy, 1994). This would lead to under-estimated in-situ blowcount values and was therefore deemed inappropriate for this study. The Fang conversion is more conservative, and was therefore also rejected.

Moore and Hempen (1982) performed SPT and OPT tests in glacially- and fluvially-derived sediments similar to the Wabash Valley soils for a foundation investigation related to the Lock and Dam No. 26 on the middle Mississippi River near St. Louis, MO. Test results from their work suggest a modification of the Karol (1960) conversion factor gives the best results for providing equivalent SPT data based on OPT procedures. They found conversion factors of between 0.0006 and 0.0008 in/lb were more appropriate based on their test results. However, incorrect OPT tip areas were used to estimate these conversion factors, (Fruel, 1991). Using the correct tip area leads to conversion coefficients of between 0.0007 and 0.001 in/lb. The smaller value was found for the upper soils in the Lock and Dam No. 26 investigation, with the larger ratio more appropriate for deeper soils.

The soils sampled during this study are in the upper portion of the soil profile, and it was therefore felt that the smaller penetration test conversion ratio would be appropriate to provide an initial hammer drop height estimate. Using the conversion factor of 0.0007 and the Karol approach leads to a drop height estimate of 24 inches (61 cm) for the OPT equipment used for this study. It was decided to initially use this 24-inch drop height and compare the test results with adjacent SPT tests to evaluate the appropriateness of this value.

At several sites the SPT and OPT procedures were performed at adjacent boring locations in both sands and gravelly sands, allowing evaluation of the difference between the N-values obtained using the two procedures. Initially, adjacent tests were performed in material with maximum particle sizes of approximately 1 inch (2.5 cm). The SPT and OPT procedures were also used at different elevations of individual boring locations when it was deemed appropriate based on the recovered soil samples. At no site was the OPT procedure use exclusively. Some natural variation is inherent in the nature of coarse-grained soil deposits, but the test results showed no apparent difference between the two sampling procedures for the range of grain sizes sampled and the blowcounts obtained. Comparison tests in materials with maximum particle sizes of up to 3 inches were eventually performed. Here again, no apparent difference in blowcount between the SPT and OPT procedures could be documented. Figure 3.1 presents the values of the penetration test blowcounts recorded at all sites where both test procedures were performed. Uncorrected blowcount values are plotted in this figure versus the depth within the liquefiable deposit at which they were recorded. The blowcount values measured in the liquefiable zone generally ranged between 5 and 30, with maximum particle sizes generally less than 5 cm. Using the 24-inch drop height, variations between the blowcount values measured with the two sampling procedures at similar elevations in adjacent borings were generally small and apparently random. In individual borings where the two test procedures were used, the trend in blowcount values was also consistent with adjacent boring locations. For the purposes of this study, therefore, blowcount values

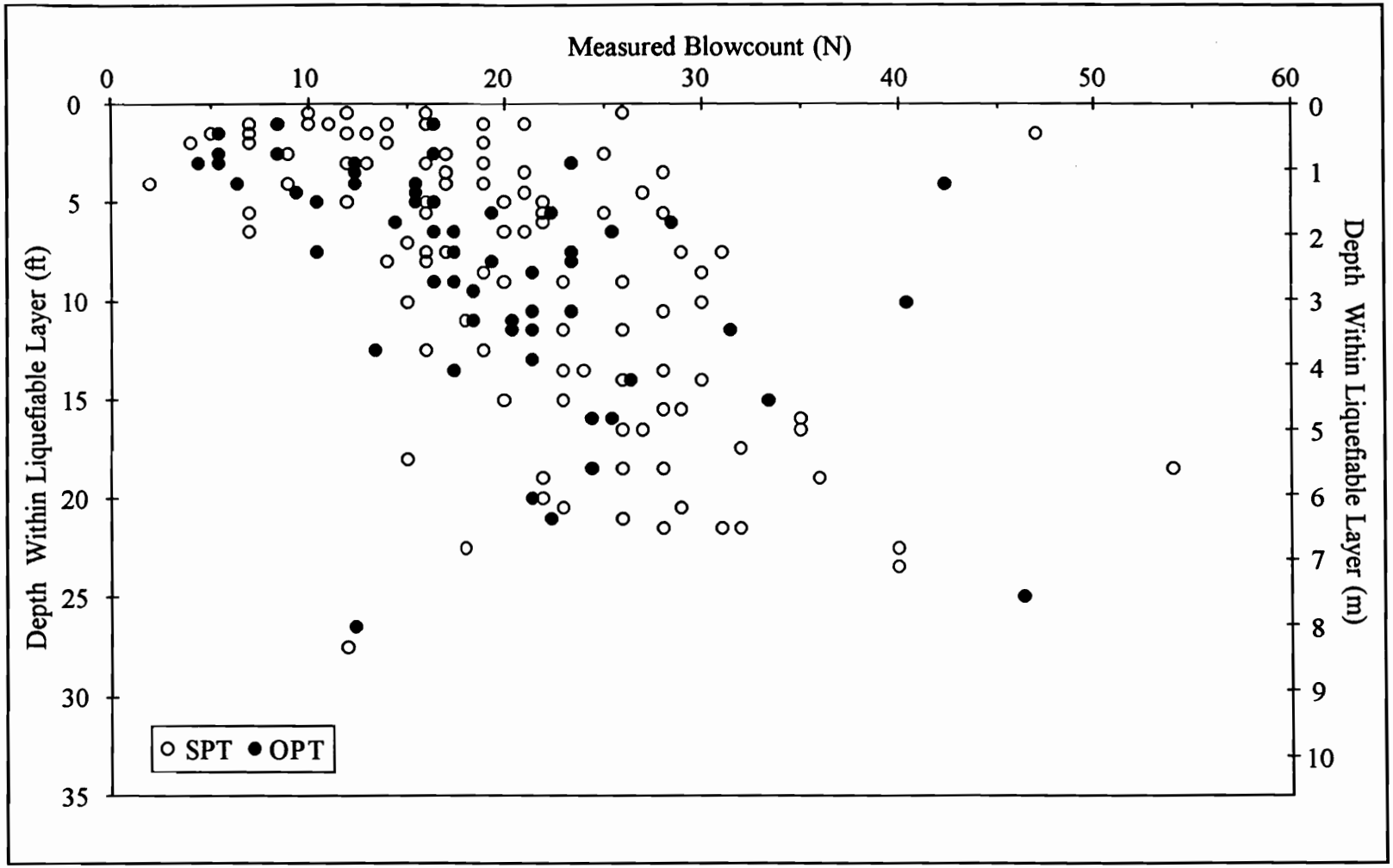

Figure 3.1. Plot of OPT and SPT results at all sites where both procedures were used.

obtained using the two methods are assumed to be equivalent and are corrected to $(N_1)_{60}$ values in the same manner.

3.3.1.2.Penetration Testing Using Hollow Stem Auger Borings

The testing program was limited by equipment readily available in the area to use of the hollow stem auger for borehole advancement. Problems associated with the use of the hollow stem auger in saturated sands can develop when steps are not taken to avoid disturbance of the cohesionless soils present at the tip of the auger prior to sampling. Hollow stem auger borings in saturated sands have the potential for producing blowcount values that are either greater or less than actual true blowcount values depending upon the drilling and sampling procedures used and any disturbance effects that might occur (Kovacs, 1994).

Hollow stem auger borings are typically advanced with a plug in the bit to prevent the cuttings from entering the auger as the bore hole is advanced. This technique is effective when the soils being sampled are above the groundwater table or are cohesive in nature. However, when cohesionless soils are encountered below the groundwater table, disturbance of the material at the tip of the auger may significantly alter the measured blowcount values. When drilling below the water table, removal of the plug prior to sampling drastically reduces the water level within the auger. When drilling in highly permeable soils, this allows groundwater to flow into the auger. When this occurs, any cohesionless soils present will also be drawn into the auger. This fills the auger with sand as well as producing disturbance of the in-situ deposit. This can lead to changes in the measured blowcount values due to two effects. The first is a reduction in blowcount due to the disturbance effect and second, any sand remaining in the inside of the auger will produce a wedging effect that increases the measured blowcounts.

For this study several techniques were used to reduce or eliminate disturbance of the cohesionless soils below the groundwater table. In all cases, once groundwater was encountered, the plug was no longer used in the center of the auger. Each study site chosen for testing was located adjacent to a river or gravel pit, and the depth of the

groundwater table could easily be determined prior to drilling based on the elevation of the water surface in the river or gravel pit adjacent to the boring location.

To keep the cuttings from entering the auger as the boring was advanced through saturated cohesionless soils, a head of water or drilling mud was maintained in the auger. The simplest method used for this was to fill the auger with water or drilling mud prior to advancement of the boring to the elevation of the next sample interval. In fine to medium sands where the depth interval to the next sample was small, this was effective in keeping all but a small amount of material from entering the auger. Where greater distances between sample intervals were used, or where the deposit contained coarser material with a high permeability, this technique would not always allow maintenance of sufficient head in the auger to exclude the cuttings. The fluid in the auger would drop to equal the head of the groundwater table quite rapidly. Once this occurred, cuttings could easily enter the auger as the boring was advanced. This was particularly true if the boring was advanced rapidly, not allowing the auger bit sufficient time to move the cuttings to the outer edge of the borehole and up the auger flights.

In those situations where sufficient head could not be maintained by filling the auger prior to advancing to the next sample interval, a more effective technique had to be utilized. The method found to be most effective at maintaining a net positive head within the auger was to maintain flow into the top of the auger as the boring was advanced. This was accomplished by installing a swivel head between the drill head and the top of the auger. The swivel head contained a quick connect fitting to allow attachment of a line from the water pump on the rig. When the water or mud level in the auger began to drop significantly during boring advancement, the pump on the rig could then be used to sustain a net positive head of drilling fluid in the auger without having to stop and pull the drill head off the top of the auger. This procedure maintained flow out of the tip of the auger and was found to be very effective at holding the cuttings out of the auger. The equipment setup for this procedure is shown in Figure 3.2. In this picture water is flowing

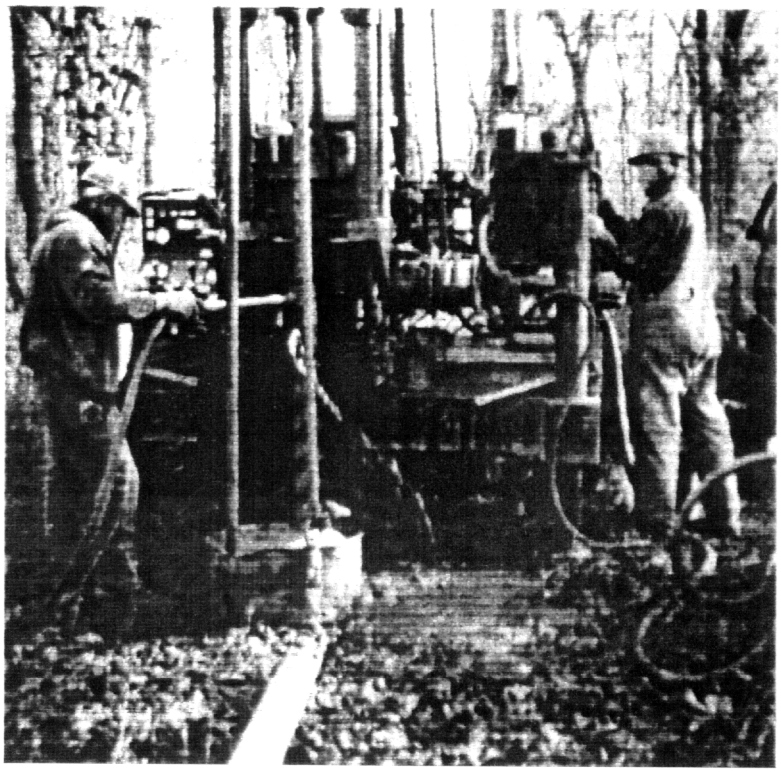

Figure 3.2. Hollow stem auger drilling in saturated cohesionless soils maintaining fluid level within the auger using a swivel head attachment.

from a screw hole in the top of the auger stem, showing that the head in the auger is being maintained at that level.

In some cases, however, it was not always possible to exclude all cuttings from entering the auger during advancement of the auger. In those cases where the measured stick-up of the drill rods indicated cuttings had entered the auger during boring advancement, they had to be removed prior to sampling. When only a few inches of material were present in the end of the auger, in many cases it was possible to drop them out of the end of the auger by lifting the auger a small distance off the bottom of the boring. This allowed the fluid in the auger to push the cuttings out of the end of the auger. They then filled the space vacated below the base of the auger. This procedure likely produces a zone of disturbed material directly below the auger bit, but it is felt that the initial 6-inch drive of the split spoon sampler extended below this zone. A comparison of blowcount values in adjacent borings and in similar materials where this technique was and was not required showed no apparent difference in the blowcount values obtained.

In some cases, the boring was advanced a significant distance without realization that a suitable head was not being maintained within the auger. In these cases it was possible for 12 inches or more of cuttings to enter the end of the auger. When this occurred, the cuttings had to be washed from the auger prior to sampling. To remove the cuttings, water was pumped through the center of the auger from the base to the surface using either a sample tube or a rotary tricone bit attached to the end of the drilling rods. The rotary bit was necessary when a large quantity or large grainsize material had entered the auger. Water was circulated through the auger until it was thoroughly cleaned, and sediment was no longer observed to be transported to the surface. Here again, some disturbance is likely to have occurred in the sediments present directly below the base of the auger, but no apparent difference in measured blowcount values could be attributed to this at adjacent boring locations where the technique was and was not required. It is therefore felt that this disturbance was limited to the upper few inches of material below the auger bit, and that the initial 6 inch drive of the sampler extended below this zone.

3.3.2.In-Situ Density Testing

In order to determine the relative density of a soil deposit, the in-situ dry density must be known. This can then be compared to minimum and maximum laboratory index densities to determine the relative density. At six sites where the liquefiable source material was exposed during periods of low water, in-situ dry densities were determined in accordance with the sand cone method of density and unit weight determination (ASTM: D 1556-90). In this procedure, a volume of in-situ soil is excavated and replaced with a sand of known density. The in-situ volume of the excavated soil is then found based on the volume of sand required to refill the excavated hole. The in-situ dry density of the native soil is found by determining the mass of the soil removed and its water content, and then dividing by the volume it occupied. Using index densities determined in the laboratory, the in-situ relative density can then be calculated. The results of the in-situ density tests showed a general trend of increasing density with depth at all sites tested.

The liquefaction susceptibility of a soil deposit can be qualitatively related to the relative density of the liquefiable soils in the deposit, however, relative density can not be directly related to liquefaction susceptibility (Seed, 1979). In general terms, however, as relative density increases, the resistance to liquefaction also increases. Sand cone density tests were performed at several sites to help estimate the in-situ void ratio of the liquefiable Wabash Valley soils and to try to correlate $(N_1)_{60}$ values with relative density. Correlations of the measured in-situ relative densities with the measured blowcount values in nearby borings were attempted. Unfortunately, the highly variable nature of the liquefiable deposit proved an insurmountable obstacle to accurate correlations of blowcount and density in the gravelly Wabash Valley soils.

3.3.3.Seismic Testing

Seismic shear-wave and surface-wave velocity tests were performed at several of the project study sites. Test procedures consisted of the cross-hole shear wave velocity tests as well as the Spectral Analysis of Surface Wave (SASW) test recently developed by Dr. Ken Stokoe of the University of Texas at Austin (Stokoe and Nazarian, 1985). The

seismic testing was performed by Dr. Glen Rix of Georgia Tech and Dr. Kevin Sutterer of the University of Kentucky. Mr. Don Eggert of the Geological Survey division of the Indiana Department of Natural Resources also provided valuable shear wave velocity data for other sites in southwest Indiana. Data obtained from these tests provided information needed to estimate the dynamic soil parameters (shear modulus, damping ratio) necessary for the one-dimensional site response (SHAKE) analyses. The seismic shear wave velocity data was also used to determine the depth of liquefiable sediments in areas where the drilling program did not extend to the full depth of the unconsolidated deposit.

3.3.3.1. SASW

Spectral Analysis of Surface Wave velocity testing was performed at four of the study sites. Three of these contain gravelly sands, with the fourth containing uniform medium sand. The advantage of SASW testing lies in that drilling is not required. Tests are performed at the surface and a vertical soil profile is obtained by analyzing data from tests where the source and receiver are placed at a range of distances. This procedure does not allow samples of the soils to be obtained, but can be an effective method to supplement penetration test data. This test procedure also has an advantage over other shear wave velocity tests in that the volume of soil sampled is much greater. This gives an average shear wave velocity that is likely to be a more representative sample of the soil column (Meier, 1993).

3.3.3.2. Cross-Hole and Down-Hole Seismic Tests

Cross hole and down hole seismic testing requires installation of cased bore holes in order to perform the tests. Each test location requires several casings to perform the cross hole test. The down hole test procedure requires only a single casing. Due to the time and expense involved in these procedures, only a single cross hole test was performed. This was performed by Dr. Kevin Sutterer of the University of Kentucky. Existing additional down hole seismic data was obtained from the Geological Survey division of the Indiana Department of Natural Resources.

3.4.Field Test Sites

Field test sites were chosen for the study of what has turned out to be four separate large prehistoric earthquakes in southern Indiana. Figure 3.3 shows the distribution of identified liquefaction sites in Indiana and Illinois. The liquefaction sites used in this study were limited to the Indiana portion of the study region. At the time of the field testing program, liquefaction sites in Illinois had not been sufficiently identified in terms of age and epicenter to allow their use in this study. Additionally, the seismic activity in southern Illinois appears to occur at a greater number of epicenters. Stratigraphic relationships leading to accurate date estimates for many of the Illinois sites are also not as prevalent. This makes it much more difficult to accurately determine the event to which each liquefaction site belongs. In addition, initial field reconnaissance to identify liquefaction sites in Illinois had not begun until well after the Indiana study was underway. Figure 3.4 provides a map of the study sites and the liquefaction distributions associated with the four events considered in this study.

3.4.1.Vincennes Event

The Vincennes event has been identified as the earthquake associated with most of the liquefaction evidence in the Wabash Valley Seismic Zone. This event occurred approximately 6000 years BP and produced liquefaction effects at sites as much as 150 km from the inferred epicenter. The epicenter has been postulated to have been located at or near Bridgeport, Illinois based on the location of the most severe liquefaction evidence, the distribution of liquefaction evidence, and historical seismicity (Munson and Munson, 1996). Bridgeport, Illinois is approximately 20 km to the west of Vincennes, Indiana.

A total of 13 sites were chosen for study of the ground motions leading to the liquefaction evidence observed for this event. These sites are located at epicentral distances of between 15 and 150 km. They are located North, South, Northeast, and East of the epicenter. No sites were available in Illinois beyond the Wabash River, and therefore no study sites extend west of the epicenter. However, the study site distribution covers approximately half of the area subjected to liquefaction effects. This is sufficient to

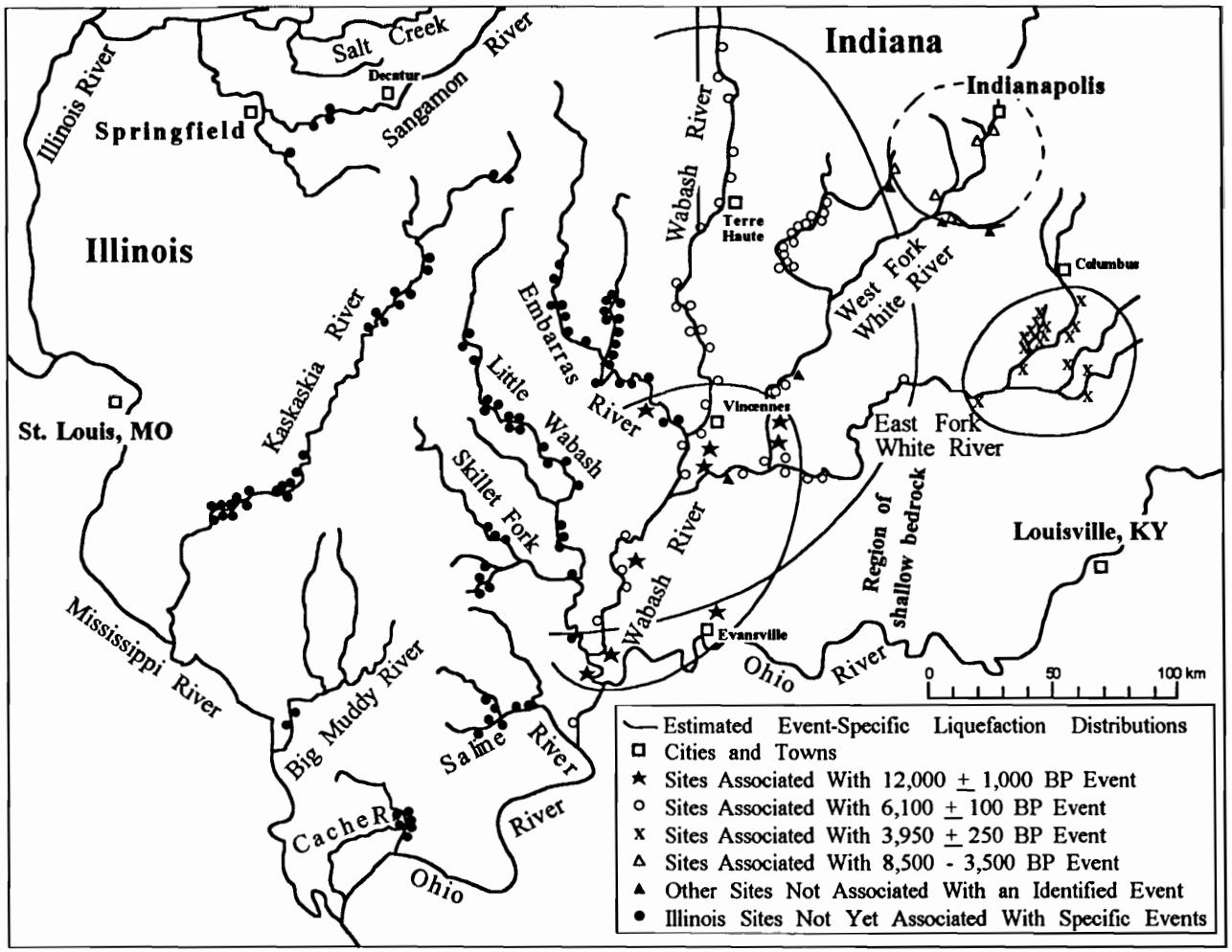

Figure 3.3. Paleoliquefaction sites and approximate event-specific distributions identified in Indiana and Illinois. (Modified from Obermeier, 1996 and Munson and Munson, 1996).

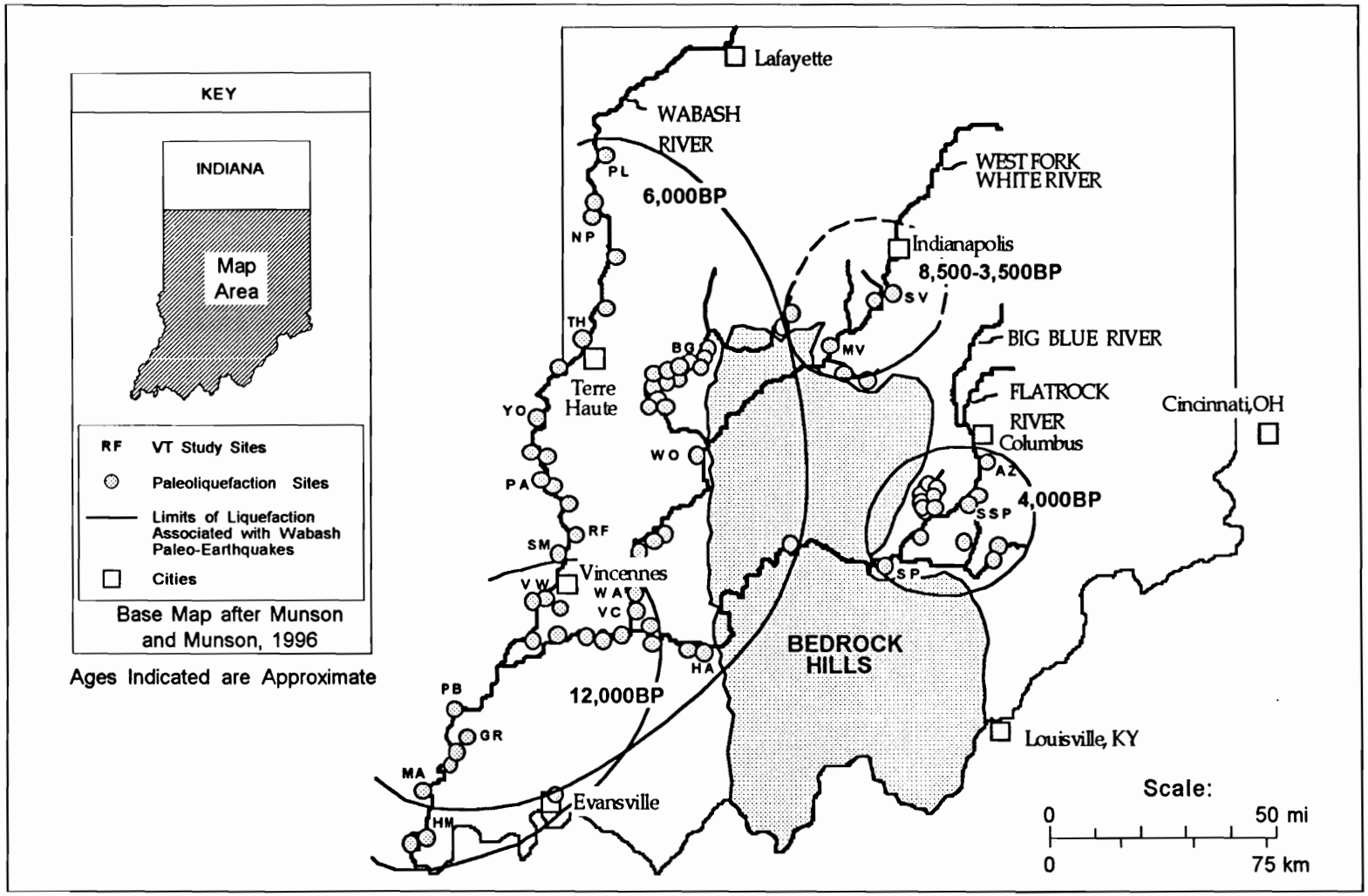

Figure 3.4. Map of Virginia Tech paleoliquefaction study sites and estimated liquefaction distributions inferred for four separate prehistoric earthquakes.

allow magnitude and surface motion estimates based on the distribution of the liquefaction effects.

3.4.2.Skelton Event

The Skelton event has been identified as a smaller and older earthquake, separate, but located near the Vincennes event. This event occurred approximately 12000 years BP and produced liquefaction effects at identified sites up to approximately 65 km from the inferred epicenter. The epicenter has been postulated to have been located at or near Mt. Carmel, Illinois based on the location of the most severe liquefaction evidence, the geotechnical investigation, the distribution of liquefaction evidence, and historical seismicity.

A total of 4 sites were chosen for study of the ground motions leading to the liquefaction evidence observed for this event. These sites are located at epicentral distances of between 28 and 63 km. They are located South and Northeast of the epicenter. Here again, no sites were available in Illinois, and therefore no study sites extend west of the epicenter. This event also occurred at such an age that the river has had ample time to eliminate much of the easily observed liquefaction evidence. Therefore, the study site distribution for this event is not as complete as for the Vincennes event. However, it provides sufficient information to allow magnitude and surface motion estimates based on the observed liquefaction effects.

3.4.3.Vallonia Event

The Vallonia event was centered in south central Indiana, nearly directly east of the Vincennes event, near the town of Columbus, Indiana. This event occurred approximately 4000 years BP and produced liquefaction effects at identified sites up to approximately 36 km from the inferred epicenter (Munson et al., 1995; Munson and Munson, 1996). The epicenter has been postulated to have been located at or near Vallonia, Indiana. This is based on the location of the most severe liquefaction evidence, the geotechnical investigation, and the distribution of liquefaction evidence.

Three sites were chosen for study of the ground motions leading to the liquefaction evidence observed for this event. These sites are located at epicentral distances of between 10.5 and 36 km. They are located Southwest and Northeast of the epicenter. The geology of the area around this event generally consists of exposed bedrock at the surface, and does not provide liquefiable sediments over most of the area that would have likely been subjected to strong shaking. However, the study sites chosen for this event provide a representative distribution of distances from the epicenter. They furnish sufficient information to allow magnitude and surface motion estimates based on the observed liquefaction effects.

3.4.4.Waverly Event

The Waverly event had an epicenter just south of Indianapolis, Indiana. This event occurred between approximately 3500 and 8500 years BP and produced surficial liquefaction effects at identified sites up to approximately 30 km from the inferred epicenter. The liquefaction in this region was initially assumed to be part of the Vincennes event at 6000 years BP. However, this area contains relatively coarse and dense sediments associated with the farthest advance of the Wisconsinan glaciation. The liquefaction susceptibility is significantly lower at most sites in this area. Thus, this has been concluded to have been a separate event with an epicenter postulated to have been located just north of Waverly, Indiana. This is based primarily on the geotechnical investigation, but also on the location of the most severe liquefaction evidence and on the distribution of liquefaction evidence.

Two study sites were chosen for an investigation that lead to the conclusion that most liquefaction in this area is not associated with the Vincennes earthquake. These sites are located at epicentral distances of approximately 3.5 and 28 km. They are located northeast and southwest of the inferred epicenter. The surficial coarse-grained sediments present over much of this region consist of end moraine or ground moraine coarse gravel and cobbles, or are glacial tills not susceptible to liquefaction. In many areas where liquefiable sediments are likely present, the rivers have been channelized or dammed,

obscuring any liquefaction evidence that may be present. This is particularly true around and to the north of Indianapolis. However, the study sites chosen for this event allow magnitude and surface motion estimates based on liquefaction effects at two significantly different epicentral distances.

3.5.Supplemental Data

In addition to the field investigations performed for this study, data on Wabash valley soil deposits were obtained from a variety of other sources. Soil boring logs were obtained from the Indiana and Illinois State Highway Departments, the Bargersville, Indiana Water Department, the United States Geological Survey, and the Indiana State Geological Survey. These data provided valuable additional information on depth to bedrock and on soil strength parameters. These drilling logs were not used directly in the liquefaction susceptibility analyses due to the fact that the boring locations relative to liquefied soil deposits is not well defined. Additionally, the soil profile at the time of the paleoevents is not as well defined as at our study sites. The supplemental data obtained was generally used to provide additional information on bedrock depths, and for comparison of blowcount values and soil profile data obtained at the study sites.

4. Laboratory Investigation

The laboratory testing program was designed to support and supplement the data obtained during the field testing program. This testing provided the data necessary for soil classification, shear strength correlations, and determination of relative densities.

4.1. Testing Program

The majority of the soil testing program was designed to provide information for classification of the soils present at the paleoliquefaction study sites. This included grain size distributions, Atterberg limits of cohesive soils, specific gravity of both fine- and coarse-grained soil solids, and angularity determinations of the coarse-grained sediments. The relative density of the in-situ granular materials has been estimated based on the results of laboratory minimum and maximum index density tests performed on the samples obtained during in-situ density determinations. The results of these tests provide the information necessary for correlation of the in-situ testing data with liquefaction susceptibility. The results of these analyses also help to confirm that traditional liquefaction susceptibility analyses can be utilized to provide reliable results at Wabash Valley paleoliquefaction sites.

4.1.1.Soil Classification

The soils present at the Wabash Valley paleoliquefaction study sites were classified in accordance with the Unified Soil Classification System. This system is described in the ASTM Standard Classification of Soils for Engineering Purposes, designation D 2487-93 (ASTM, 1994). This standard uses the results of laboratory classification test procedures to identify a soil based on its particle sizes and the plastic and liquid limits of the fine grained portion of the soil sample. These classifications can then be used with existing correlations to estimate the general engineering behavior of the soil. This classification system provides a general indication of how the soil will behave under a given loading condition based on the known response of other similar soils.

4.1.2.Grainsize Distributions

Grain size distribution analyses were performed on representative samples of the granular soil samples obtained during the field investigation. All grain size distribution analyses were performed in general accordance with ASTM standard test method designation D 422-63 (ASTM, 1994). Testing was performed on samples obtained during penetration testing and in-situ density testing, as well as on bulk samples obtained from exposed source and surficial materials. The tests were performed to allow classification of the soils present at the Wabash Valley study sites. Additionally, the distribution of particle sizes within coarse-grained soils provides an indication of the liquefaction susceptibility of the soil. The grainsize distribution can be compared to those of other soils known to have liquefied during historical seismic events. Appendix F contains plots of the grainsize distribution testing results for representative penetration test samples, as well as for the in-situ density and index density specimens.

4.1.3.Atterberg Limits of Cohesive Soils

Atterberg limits can be used to help describe the engineering properties of a cohesive soil. The two limits of greatest use to soil mechanics are the plastic and liquid limits (PL and LL). The plastic and liquid limits were determined on representative specimens of the fine-grained soils obtained during the field investigation. These Atterberg limits were determined in accordance with ASTM standard test method designation D 4318-93 (ASTM, 1994). These limits, as well as the difference between them, are used to estimate engineering properties of fine grained soils. The tests performed on the Wabash Valley flood plain sediments were performed to allow classification of those soils, as well as to provide information on the plasticity of the fines content in the granular liquefiable soil deposits. Figure 4.1 is a plasticity chart showing representative Atterberg limits test results for the Wabash soils. Appendix F contains the results for all of the test performed for this study.

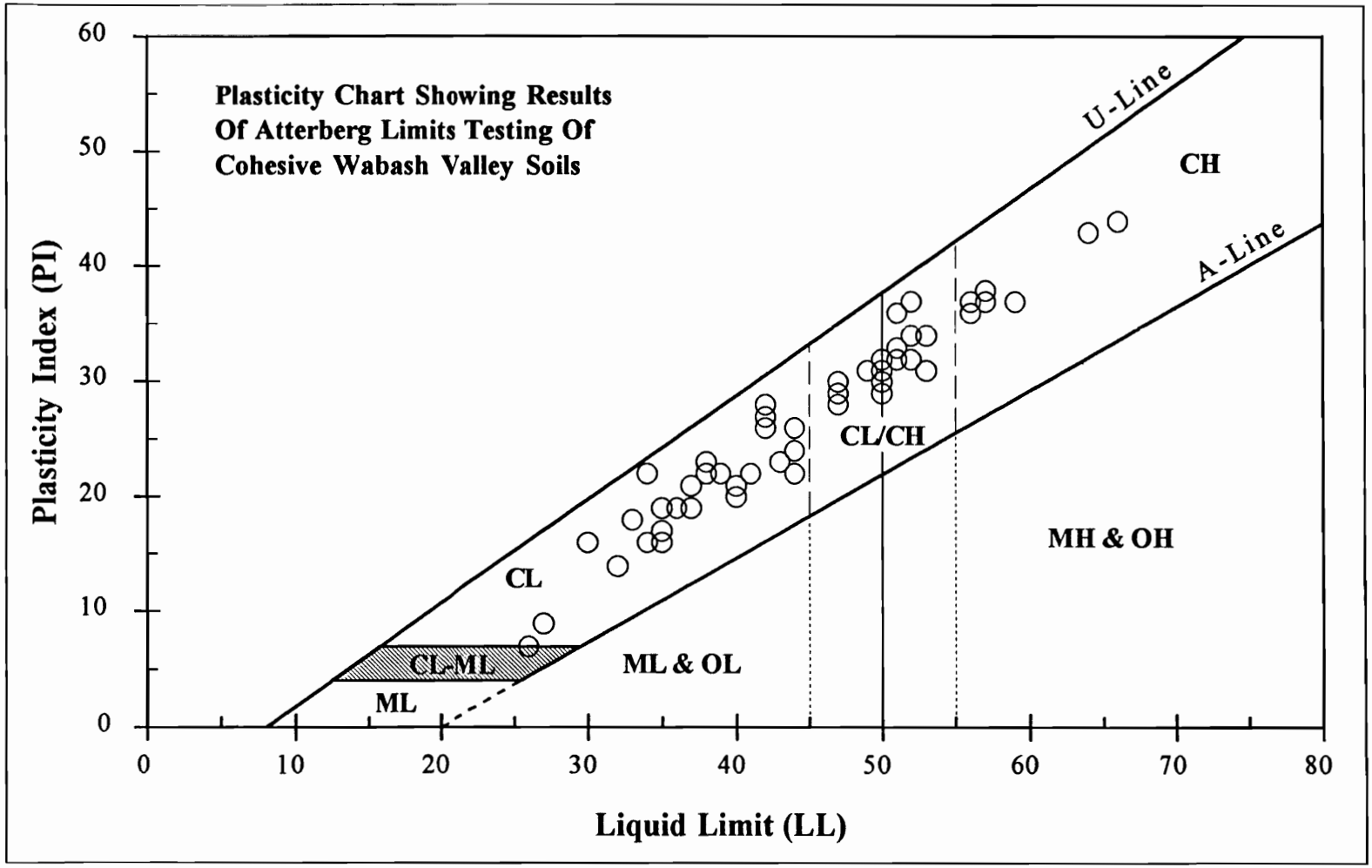

Figure 4.1. Plasticity chart showing Atterberg limits testing results for representative Wabash Valley fine-grained soils.

4.1.4.Specific Gravity of Soil Solids

Specific gravity of soil solids was determined based on the ASTM standard test method designation D 854-92 (ASTM, 1994). This test procedure provides a measure of the average density of the individual particles present in a soil deposit. The results are given as a ratio of the density of the soil particles to the density of water at a temperature of 20°C. The results of these tests were used in this study to compare the specific gravity of the Wabash soils to that of other soils where historical liquefaction has been observed. Figure 4.2 is a histogram of the results of the specific gravity tests performed on the Wabash soils from sites associated with the Vincennes 6000 year BP earthquake. Results for samples from sites associated with the other events are similar. The specific gravities range from 2.62 to 2.77 for all of the Wabash Valley alluvial soils tested. This is consistent with specific gravities of other liquefiable soils, and is the range of specific gravities expected. The majority of the Wabash Valley alluvium is made up of glacially-derived igneous and metamorphic materials transported from the Canadian Shield. Also included are particles of sedimentary materials of both indigenous and exotic origin (Fidlar, 1948). Appendix F contains a complete listing of the specific gravity test results obtained for this study.

4.1.5.Index Densities

In-situ dry densities were determined at several of the Wabash Valley study sites. Index density test results are used with the in-situ density values to estimate the relative density of a soil deposit. In order to estimate the engineering properties of a soil at its in-situ dry density it is necessary to determine maximum and minimum index densities for that soil. This allows a calculation of the relative density of the soil deposit, and provides a method, where other pertinent parameters are assumed constant, to evaluate trends in the soil strength parameters.

Liquefaction susceptibility determinations are based on correlations between in-situ measures of soil strength parameters and the cyclic loading expected to affect the soil

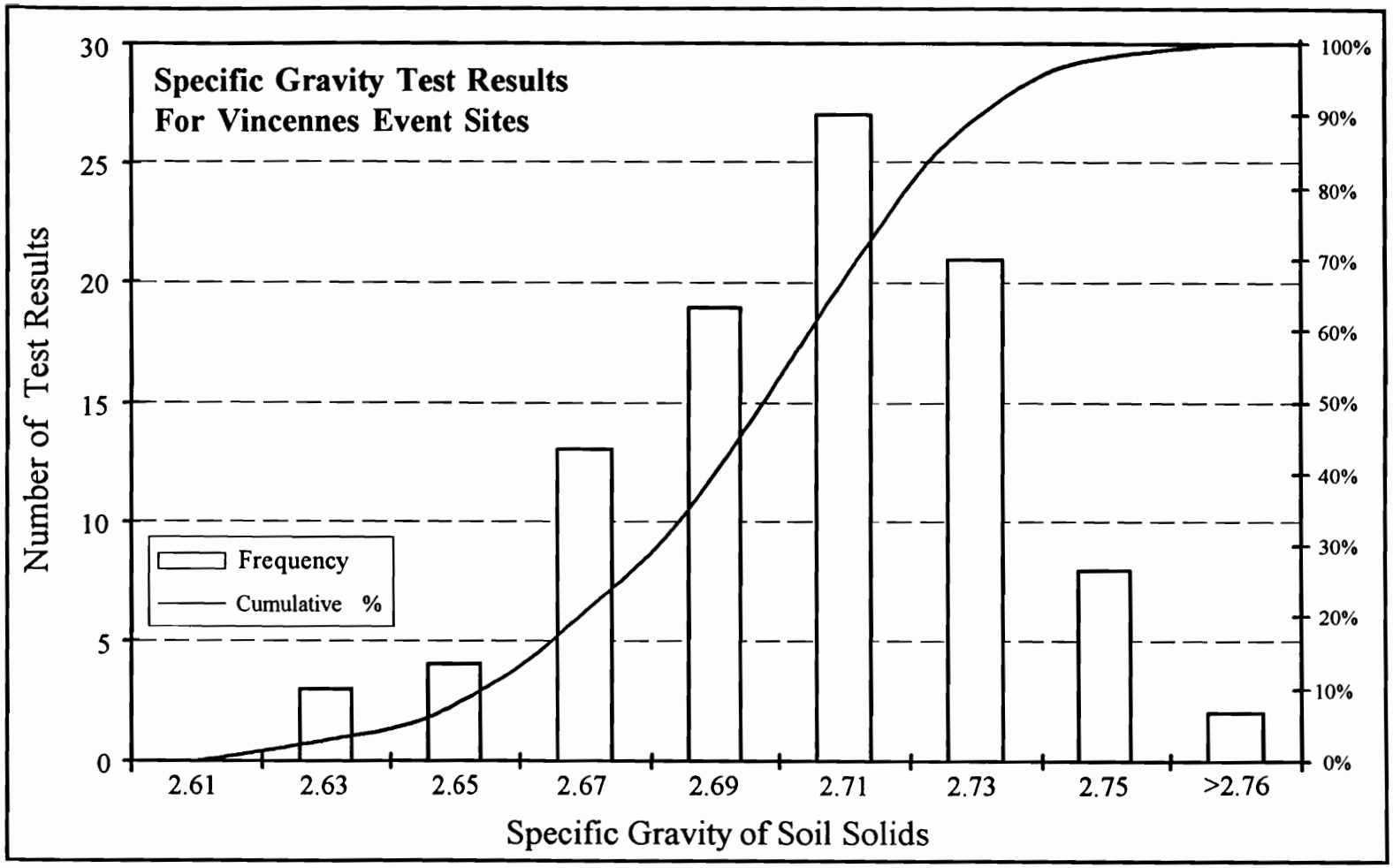

Figure 4.2. Summary of specific gravity test results for Wabash Valley soil samples for sites asociated with the Vincennes event. Results for sites associated with other events are similar.

deposit present at a particular site. To help confirm the applicability of the liquefaction susceptibility analysis procedures at Wabash Valley sites it is important to verify that the soil strength correlations are similar in Wabash Valley soils to those of the soils present at sites that make up the database used in development of the analysis procedures. The relative density can be used here to help determine if other in-situ test procedures provide results reliable in liquefaction susceptibility analyses at the Wabash sites. Published correlations of relative density values with penetration test and seismic wave velocity test results can be compared with the field data. If in-situ test results provide results similar to published correlations, the liquefaction susceptibility analyses can be assumed to be reliable.

Maximum index densities were determined in general accordance with ASTM Standard Test Method designation D 4253-93 (ASTM, 1994). This test procedure provides an upper bound on laboratory density to be used in relative density determinations. This is an index density only, and does not provide an absolute maximum value of soil density. Due to this fact, it is quite possible to attain relative density values greater than 100%. Minimum index density values were determined in general accordance with ASTM Standard Test Method designation D 4254-91 (ASTM, 1994). This test procedure provides a lower bound on laboratory density to be used in relative density determinations. Here again, this is an index density only, and does not provide an absolute minimum value of soil density. It is quite possible to obtain relative density values less than 0%. Table 4.1 summarizes the results of the index density testing.

Many of the Wabash Valley soils contain significant gravel contents. The index density test procedures call for use of a 0.5 ft^3 (0.014 m^3) mold in the test procedure, requiring a significantly larger volume of soil particles than had been obtained during the field investigation. Therefore, in performing these density determinations, a 0.1 ft^3 (0.0028 m^3) mold was used. Due to the possibility that the test results would differ from

Table 4.1. In-Situ Relative Density Test Results

Vincennes Event Sites		
In-Situ Test # (*)	D_r(%)	Depth Within Liq'd Zone (ft)
RF1	25	1.5
RF2	41	0.5
RF3	31	1.0
RF4	38	2.0
SM1	8	1.5
SM2	39	1.0
SM3	11	2.0
SM4	8	2.0
SM5	51	1.0
SM6	73	0.5
PB1	67	1.0
PB2	107	4.0
PB3	25	7.5
PB3A	19	8.0
PB4	114	1.5
PB5	60	6.5
PB6	73	6.5
PB7A	50	0.5
MA1	71	5.0
MA2	23	2.0
MA3	76	6.5
MA4	17	2.5

Skelton Event Sites		
In-Situ Test # (*)	D_r(%)	Depth Within Liq'd Zone (ft)
GR1	2	1.5
GR2	15	5.0
GR3	44	5.5
GR4	42	3.5
GR5	33	1.5
GR6	34	3.5
GR7	21	3.5
GR8	28	2.0
GR9	12	2.5
HM1	52	2.0
HM2	59	8.0
HM3	50	5.5
HM4	44	2.0
HM5	80	9.0
HM6	40	4.0
HM7	45	3.5

* First letters indicate study site. Following number and letter combination indicates specific test.

the results that would have been attained using the larger mold, a final set of index density determinations was made using a composite soil specimen made up of coarse-grained in-situ density test specimens. The index density tests were performed on this composite specimen using both the 0.1 ft^3 and 0.5 ft^3 molds. The results of these tests gave index density values within 5% of each other (see Appendix F). This suggests that for the Wabash Valley soils, the smaller mold provides reliable index density test results. Appendix F contains a listing of all index density test results including a comparison of results for the different test procedures.

4.1.6.Angularity of Granular Soils

The angularity of the coarse-grained portion of the soil deposits was determined during the testing program. The shape of the soil particles was noted during performance of the other laboratory test procedures involving the sand and gravel portions of the soil samples. Grain angularity will influence the strength of a soil sample, with an increase in strength occurring as the angularity of the particles increases. This allowed an additional check on the validity of using traditional liquefaction susceptibility analysis procedures at the Wabash Valley liquefaction sites. The liquefiable Wabash Valley soils are of fluvial origin. The coarse grained portion of the soil samples were generally subrounded to subangular, but also contained occasional angular particles. Samples obtained from sites upstream (closer to the glacial boundary) tended to have greater proportions of angular particles, but no sample was estimated to contain greater than 10% angular particles. This angularity is consistent with the angularity of other fluvial deposits where liquefaction effects have been observed in gravelly soils (Andrus et al., 1991).

4.2. Discussion of Laboratory Test Results

The laboratory test results show the Wabash Valley soils to be generally poorly graded sands and gravelly sands which are overlain by silty clays or clays. Some well graded sands and silts are also present in several locations. The coarse sediments generally have fines contents less than 10% and gravel contents in some cases range to

60%. Maximum particle sizes in the gravelly sands is generally on the order of 2-inches, with most samples containing particles no larger than 1-inch. Maximum particle sizes generally become finer downstream, but fines content of the total soil specimens was generally between 0% and 10% at all test sites. Figure 4.3 shows the range of grain size distributions measured for coarse-grained soils at the Wabash Valley study sites. Appendix F contains individual grain size curves for all samples tested. The fine grained sediments generally consist of lean and lean to fat clays with liquid limits (LL) near 50 and plasticity index (PI) values generally ranging from approximately 15 to 45. Figure 4.1 is a plot of these values for the Wabash Valley soils.

The relative density test results based on the in-situ density tests and the index densities found in the laboratory show a trend of increasing density with depth that is generally consistent with the SPT test data obtained from borings at nearby locations. A general trend of increasing relative density with blowcount, as well as the large scatter in the data, can be seen in Figure 4.4(a). This plot includes a relative density prediction based on the Gibbs and Holtz (1957) correlation, as well as two best-fit correlations from the field data. The Gibbs and Holtz prediction shown relates blowcount and relative density at overburden pressures of 1 TSF. Figure 4.4(b) shows the relationship between the measured densities and the values predicted by the Gibbs and Holtz correlation. In this case, when the prediction is compared to measured values, relative density is over-predicted for loose soils, and under-predicted in dense material. Figure 4.5 is a plot of the Gibbs and Holtz prediction (a) including a plot of the residuals (b). This shows a bias in the results when trying to relate blowcount and relative density in the liquefiable Wabash Valley soils. The fact that the residuals do not have a mean value centered at zero suggests that for these soil conditions, not all the important parameters are included. This implies that blowcount values of the Wabash soils may not be fully described based on relative density alone.

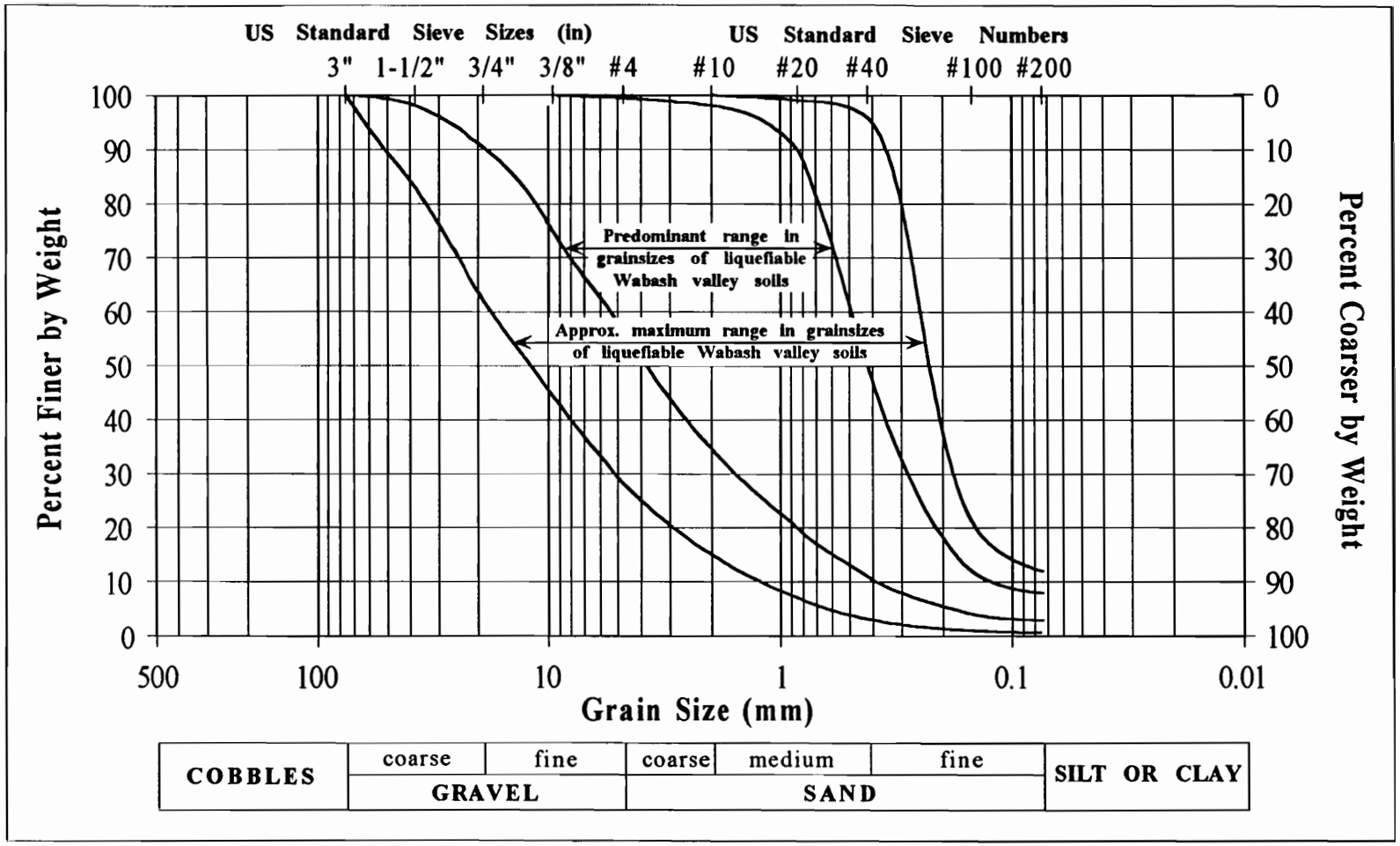

Figure 4.3. Range in grainsize distributions found for liquefiable Wabash Valley sediments.

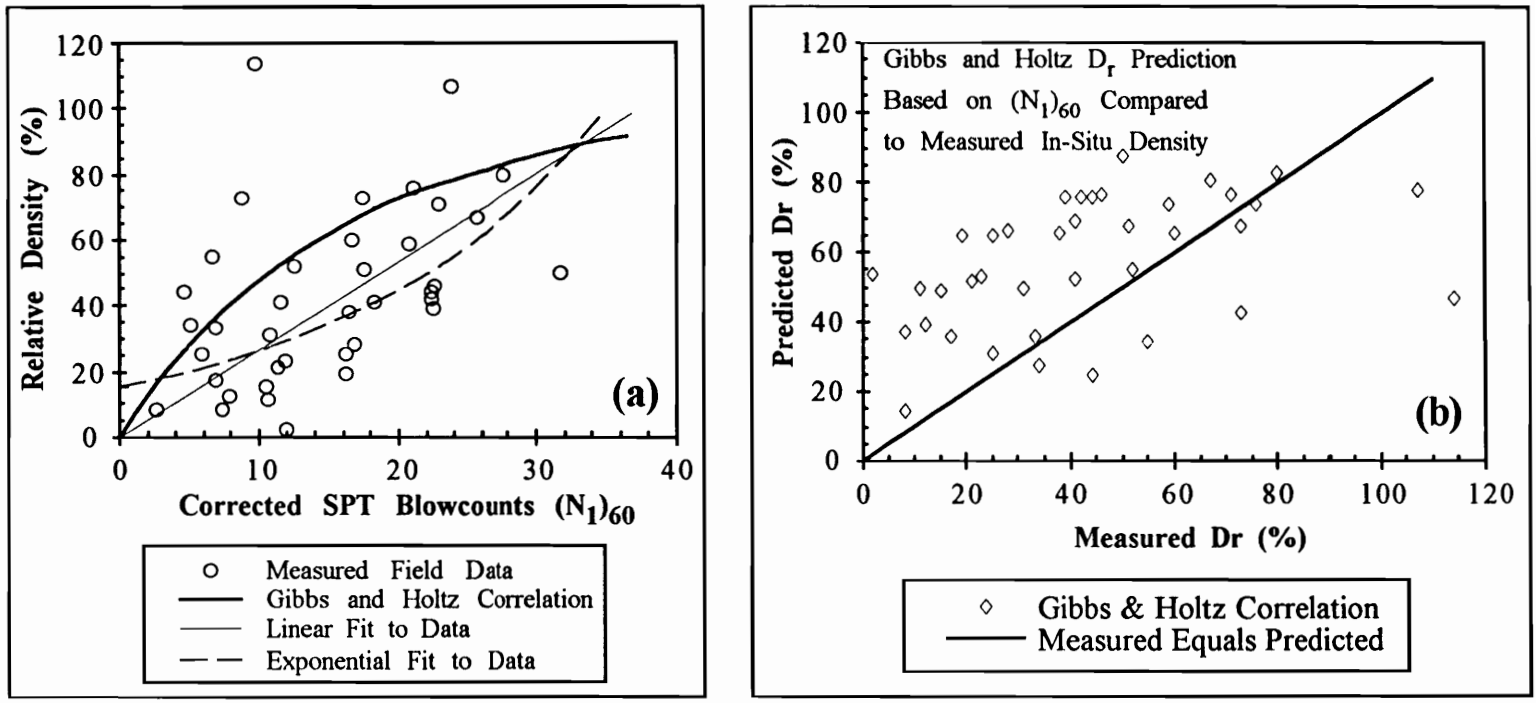

Figure 4.4. Plot of relative density vs. blowcount relationships (a) and comparison (b) of the measured Dr values to that predicted by the Gibbs and Holtz (1957) correlation. Solid line is where the predicted and measured values agree.

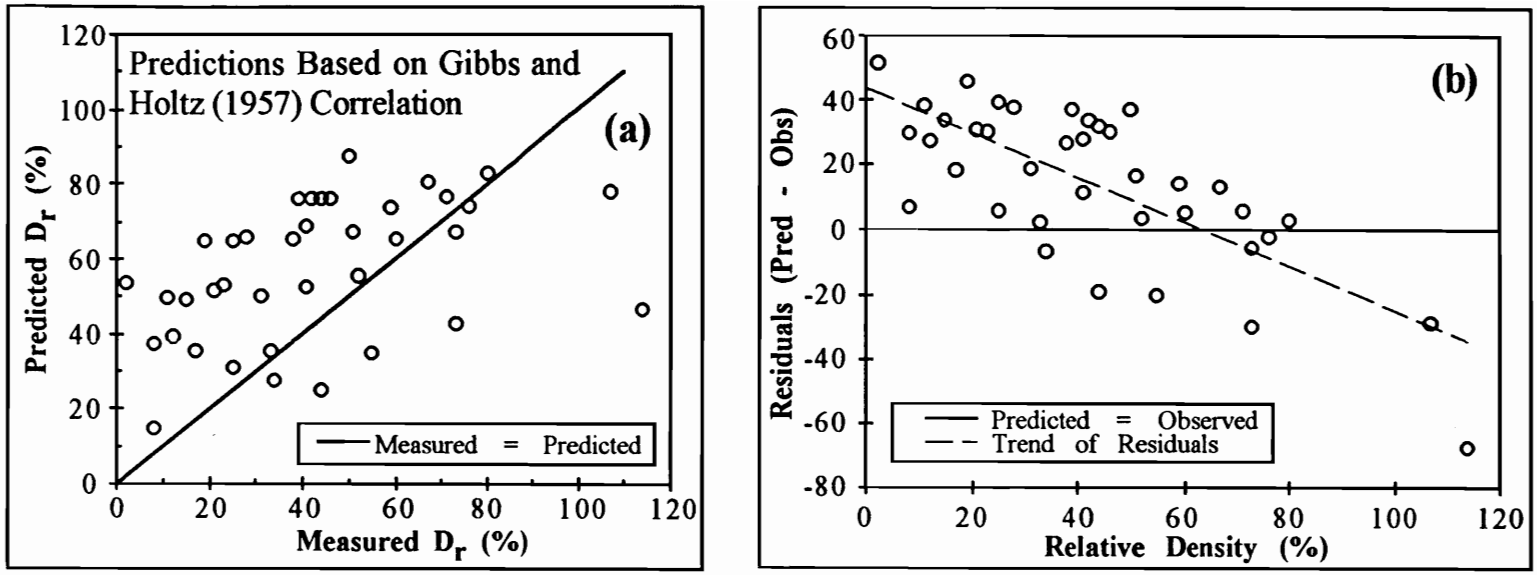

Figure 4.5. Plots comparing the Gibbs and Holtz (1957) correlation between $(N_1)_{60}$ and D_r with the field data. Predicted vs. observed values of D_r are given in (a), and residuals plotted in (b).

In an attempt to assess whether this is indicative of a difference between the Wabash soils and other liquefiable soils, similar plots were developed for exponential and linear least squares best fits to the field data. Figure 4.4(a) contains the best fit prediction curves, as well as the Gibbs and Holtz (1957) correlation. Figures 4.6 and 4.7 present assessments of the linear and exponential correlations based on the field data. These correlations show a relationship similar to the Gibbs and Holtz correlation. No reliable direct correlation between relative density and $(N_1)_{60}$ could be shown from the results of this study. Predictions of in-situ density based on blowcount data tended to over-predict density where measured relative densities were below approximately 50 percent, and to under-predict these values at greater densities. This was true for each of the correlations attempted, even when parameter transformations were used. This suggests that the relationship between relative density and blowcount in the Wabash soils is not a simple correlation. The correlation may be influenced by other parameters, even where overburden stresses are considered. This is consistent with the fact that relative density alone is not a reliable predictor of liquefaction susceptibility (Seed, 1979).

Two factors that may have influenced the density vs. blowcount correlation results were dictated by the field test conditions. First, the in-situ density testing was limited to locations where exposures of near surface liquefiable soils were accessible. The testing could therefore only be accomplished near the top of the liquefiable soil deposit. This is also the location where the liquefaction features originate, and where the greatest disturbance (due to flow associated with pore pressure dissipation) of the soil deposit has occurred. Second, blowcount data, while obtained at elevations in the soil stratum similar to the density test locations, were obtained a significant distance from the in-situ density test locations. These factors likely contributed to differences in the results of the two field test procedures that may have affected the ability to show a direct correlation between blowcount and density.

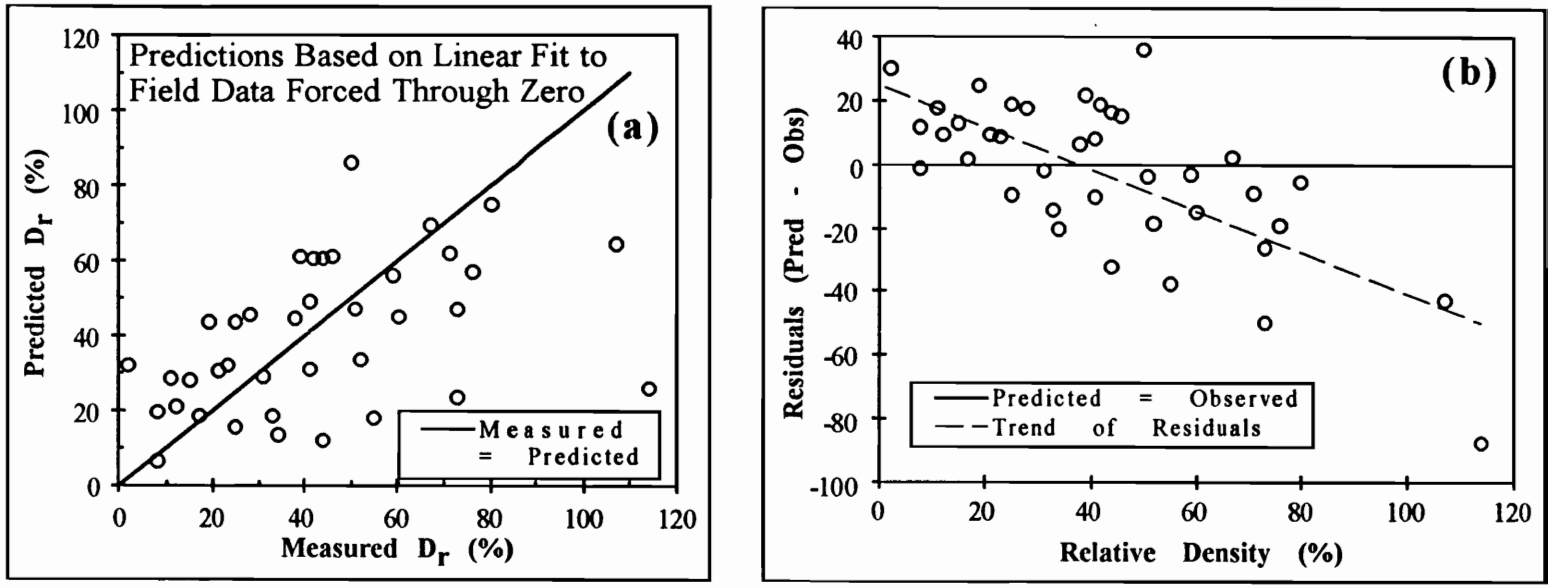

Figure 4.6. Linear least squares regression of $(N_1)_{60}$ and D_r field data (a), and the residual plot for this prediction (b).

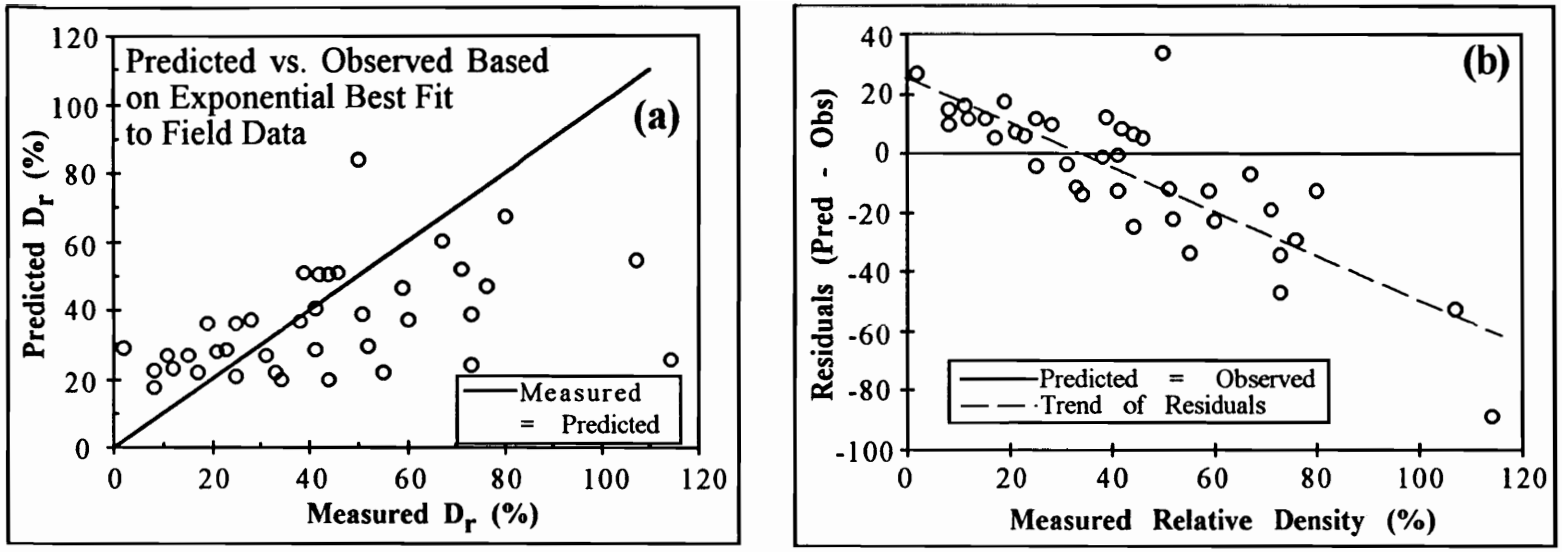

Figure 4.7. Exponential least squares regression of $(N_1)_{60}$ and D_r field data (a), and the residual plot (b) for this prediction.

The results of the density testing do, however, lend support to the use of standard liquefaction susceptibility analysis techniques for the Wabash Valley soils. The differences between predicted and measured densities were similar for correlations based on the published relationship (Gibbs and Holtz, 1957) and the correlations developed based on the field data from this study. This is seen in Figures 4.4 through 4.7. Each of the correlations show the same trend in plots of the residuals. This trend was also seen when transformed variables were used. The value of the residuals vary with the different predictions, but the tendency is consistent. In each correlation, the tendency is to over-predict density based on blowcount in loose soils, and to over-predict density in dense soils. This fact suggests that while a reliable direct relationship between blowcount and relative density could not be shown for the Wabash soils, the contribution of relative density to the measured blowcount is similar for Wabash soils and other sands. In addition, shear wave data obtained at site RF (see Fig. 3.2) are also generally consistent with the density and blowcount data. At this location, shear wave velocities at the top of the liquefiable deposit were measured at approximately 220 m/s. Average $(N_1)_{60}$ values are approximately 11, and the measured relative densities are between 25 and 40%.

The results of the laboratory and field testing program have provided the data necessary to perform liquefaction susceptibility analyses appropriate for the Wabash Valley soils. Grainsize effects on the in-situ test procedures were shown to be inconsequential using an OPT procedure. The method used in the OPT procedure has also been shown to provide equivalent SPT values. Liquefaction susceptibility analysis procedures based on the measured in-situ penetration test results will therefore be used to evaluate the liquefaction susceptibility of the Wabash Valley soils.

5. In-Situ Soil Conditions

The engineering properties of the soil deposits present in the river valleys of the Wabash River drainage have been investigated at 22 sites throughout the study region in southern Indiana and southeast Illinois. These sites have been associated with four separate paleo-earthquakes in the region based on archaeological, pedological and stratigraphic evidence, and on the results of the geotechnical investigation. The objective of this field study was to obtain the soil strength parameters necessary for performing the geotechnical analyses. There is, however, a potential for misinterpretation of the soil strength characteristics due to interbedded variations in particle size gradations or due to large particle size effects on the penetration testing procedures used to measure in-situ strengths. Also, a number of factors may contribute to changes in soil strength properties measured at the present time compared to the soil strength existing at the time of the earthquake. These issues are addressed below, followed by site-specific soil profile descriptions.

5.1. Soil Structure

Soil strength at Wabash Valley study sites is influenced by the structure of the soil deposit and is a function of both the mode of deposition and the processes that may have affected it since deposition. In the Wabash region, soil deposits involved in the paleoliquefaction evidence are products of late- and post-glacial diluvial and fluvial depositional environments. Several thousands of years may have passed between original deposition and the occurrence of the seismic events inducing the liquefaction evidence. A period of several thousand years has also elapsed between the events and the present time. The potential that these time periods may have allowed environmental effects to induce changes in the soil deposit that would cause the measured soil properties to differ from those present at the time of the liquefaction event must be considered in any paleoliquefaction study.

5.1.1.Depositional Environment

The sedimentary soil deposits present in the river valleys of the Wabash drainage consist of sands and gravels overlain by fine-grained flood plain deposits. The coarse sediments were originally laid down as braided-stream, valley-train glacial outwash deposits. The flow in this type of depositional environment typically fluctuates widely, with the fluctuations generally occurring on a seasonal and diurnal basis (Smith, 1985). This leads to a high energy deposition at times, with intervening low energy periods where flow occurs in interconnected, approximately parallel channels, and downcutting will occur. The succeeding high flow period then in many cases replaces the sediment removed during the reduced flow period. This results in broad braided plain deposits of sands and gravels with an approximately horizontal but locally irregular surface across the valley floor. At the height of the Wisconsinan glaciation, the Wabash and White River valleys were alluviated to great depths with sediments deposited in this type of high energy environment.

As the Wisconsinan glaciation began its final retreat, flow remained high but the sediment load of the glacial runoff was decreased. During this time the Wabash River served as the outlet for glacial Lake Maumee (see Figure 5.1), which served as a settling basin for sediment discharged as glacial outwash. Lacking the previous high sediment load, rivers in the glacial sluiceways began to degrade the valley-train sediments. This left the high Shelbyville terrace that remains in small areas of the upper Wabash, but is apparent in the lower Wabash due only to the presence of extensive lake plain deposits. These lake sediments were deposited in valleys impounded by the rapid alluviation of valley train sediments in the main glacial sluiceway channels (Fidlar, 1948).

The flow in the Wabash River valley remained high until the late Pleistocene due to Lake Maumee overflow. This produced a second braided stream deposit of the reworked valley train sediments below the Shelbyville terrace. This is the Maumee terrace level (Fidlar, 1948) and remains in many locations of the Wabash Valley. The difference in

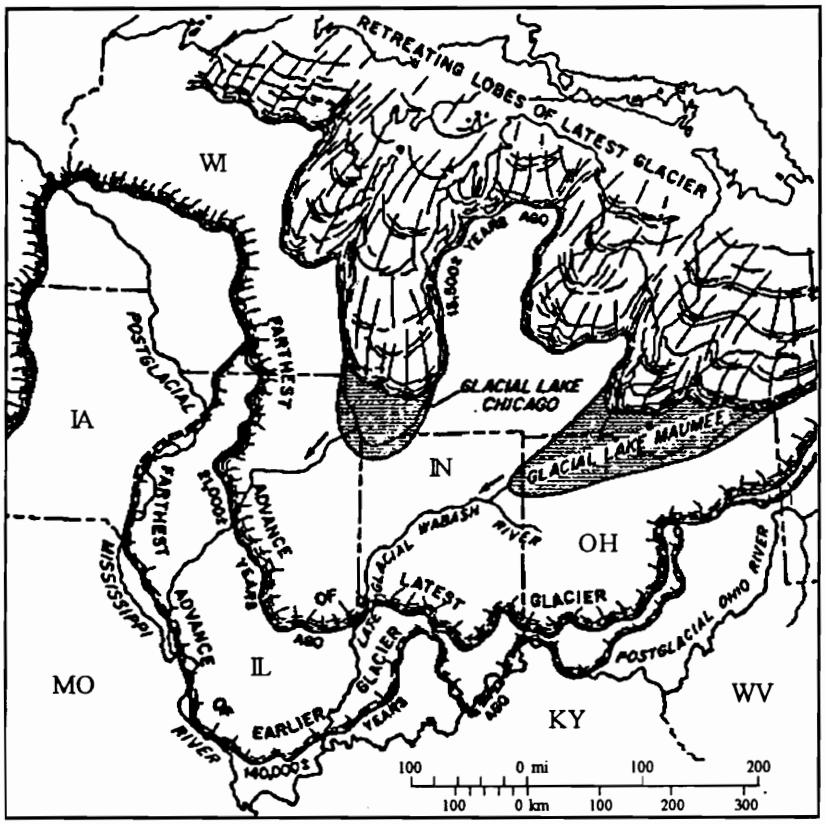

Figure 5.1. Location of late Pleistocene glacial lakes and farthest advances of two most recent glaciations (from Shaver, 1979).

elevation between the Shelbyville and Maumee terrace levels is approximately 35 feet (10.5 m) at the Shelbyville moraine (near Terre Haute, Indiana), but this decreases to approximately 20 feet (6 m) in the lower Wabash (Thornbury, 1950), near the Ohio river. While this terrace level was being formed, only the Wabash and West Fork White Rivers were carrying glacial meltwater. Flow in the other rivers and tributaries was reduced to levels induced by local precipitation only, and has remained generally consistent throughout the Holocene.

By the early Holocene, glacial meltwater was being diverted to the St. Lawrence river, and the reduced flow in all rivers of the Wabash drainage that previously carried glacial outwash were degraded below the Maumee terrace level. In the upper Wabash Valley the Maumee terrace is 4.5 to 6 m above the present floodplain, and in the lower Wabash Valley the terrace is approximately 3 to 4.5 m above the present floodplain. The lower portions of the outwash rivers had become meandering streams by this time. However, the upper portion of the Wabash and White Rivers likely remained braided streams until approximately middle Holocene time. In those locations the top of the gravel facies is at an elevation significantly below the middle to late Holocene deposits. The change in sediment level at that time likely indicates a change from braided streams to meandering river systems, with an aggradation of the sediment deposition. Since then, all of the rivers have been actively meandering, maintaining approximately constant flood plain levels (Munson and Munson, 1996).

The Holocene fluvial sediments involved in the liquefaction generally consist of point bar deposits with a relatively thin mantling of interbedded levy deposits, which are in turn overlain by generally massive deposits of silt and clay. The braided stream deposits of the Maumee terrace and of the upper river valley early Holocene deposits are similar to these soils, but generally lack the levy deposits more typical of meander belts. Each of the post-glacial depositional environments can be observed in the sediments present at the study site AZ (see Figure 5.44). A sequence of three separate depositions can be observed

in an approximately 175 meter exposure of the soil profile along the river bank at this site. the liquefaction evidence at the site originates in and cuts through sediments laid down during the early Holocene downcutting period when the river flowed as a braided stream.

5.1.2.Interbedding

The deposition associated with fluvial and diluvial environments can lead to layering within the coarse-grained soil sediments (Smith, 1985). As flow rate and volume fluctuate, the particle size and gradation of the transported sediments will vary as well. During high flow periods, the maximum particle size of the transported material will be greater than during low flow periods, and less fine-grained material will be deposited. Where deposition occurs, this leads to segregation of particle sizes into layers of relatively coarse material interbedded with sediments containing smaller maximum particle sizes and greater proportions of smaller grain sizes. This may result in a reduction of liquefaction susceptibility of the soil deposits that may not be reflected in the penetration, shear wave velocity, or in-situ density test procedures used to determine their engineering properties. It has been suggested that gravel soils are less susceptible to liquefaction than sands (NRC, 1985). However, a number of case histories have documented liquefaction in gravels (Evans et al., 1992). Wong et al. (1975) suggest that under conditions where pore pressure dissipation is impeded, generation of 100% excess pore pressure (initial liquefaction) occurs at approximately the same rate as in sands. The discussion on the liquefaction of gravels should be focused not on whether or not it will occur, but on how the damage potential associated with liquefaction of gravels differs from liquefaction of sands.

Where liquefiable sediments are visible in river banks of the Wabash drainage during periods of low water, the sediments were examined for indication of the possibility of significant effects of variation in the particle size in different layers. The soils in each of the layers generally have similar relative densities, and fines contents are less than 12%. The gradation of the samples obtained varied, but were generally consistent for all samples

obtained (see Figure 4.3). The samples obtained vary mainly in the percentage of gravel-sized particles. Siddiqi et al. (1987) found that the cyclic behavior of a gravel soil can be predicted in laboratory tests using a modeled soil gradation where oversize particles are removed. When both the model and prototype soil samples are prepared at the same relative densities, the cyclic resistance curves are identical. This suggests the interbedding of gravel contents will not significantly influence liquefaction resistances as measured by valid in-situ test procedures in the Wabash Valley soils.

The presence of gravel-sized particles may, however, influence the blowcount value obtained during penetration testing (Andrus and Youd, 1987; Stokoe et al., 1988). This may bias the liquefaction susceptibility analysis procedures toward overestimating liquefaction resistance. The results of the standard penetration test procedure may be significantly increased where large particle size material is encountered. However, Andrus and Youd, and Stokoe et al. could demonstrate no effect of gravel particles on the Standard Penetration Test (SPT) results in their studies of liquefied gravel deposits associated with the Borah Peak earthquake. Valera et al. (1994) reviewed well-documented cases of liquefaction in gravels and concluded that conventional SPT results provide reliable data for liquefaction susceptibility analyses in gravelly soils.

Not withstanding the findings above, however, in the initial stages of this study it was assumed that the presence of gravel particles could influence the SPT blowcount measurement. In order to address this issue, an oversize sampling procedure was used to minimize the potential for overestimating blowcounts due to gravels. The Oversize Penetration Test (OPT) procedure was performed in a manner designed to produce results consistent with the SPT procedure. Comparisons of the results of the SPT and OPT procedures were made for adjacent test locations in similar sand and gravelly-sand soils. These comparisons showed there is no apparent difference in the test results for any of the range of grainsizes tested.

Maximum particle sizes in any layer did not exceed that which could be effectively sampled with the OPT. This conclusion is based on the fact that no gravel particles in the samples obtained were observed to contain freshly broken facies that could be attributed to the sampling procedure. Additionally, only once did a gravel particle became lodged in the tip of the sampler during driving. Based on these observations, and the similar blowcount results obtained at adjacent test locations in sands and gravels using both the SPT and OPT test procedures, the blowcount values obtained using the OPT are assumed to be an accurate representation of equivalent SPT results. The OPT blowcount values were therefore corrected to $(N_1)_{60}$ values in the same manner as the SPT blowcount data.

The results of this study also agree with the findings of Valera et al. (1994) suggesting that SPT test results in gravelly sands can be used to provide reliable results in conventional liquefaction susceptibility analyses. The results seen in the comparison of the SPT and OPT test procedures used in this study suggest that for the grain sizes sampled the SPT procedure will provide accurate results in loose to medium dense gravelly sands. Even in the coarsest material sampled for this study (with maximum particle sizes greater than the inside diameter of the SPT split spoon sampler) the SPT and OPT results were similar. This is also consistent with the results reported by Andrus and Youd (1987) for data collected in gravelly soils that liquefied following the 1983 Borah Peak, Idaho earthquake.

5.1.3.Aging

The passage of time may contribute to a strength gain within coarse-grained soil sediments unrelated to any demonstrable recurring mechanical or other effect. This will influence the liquefaction susceptibility of a soil deposit as measured in the penetration, shear wave velocity, or in-situ density test procedures. These effects could possibly lead to an increased estimate of soil engineering properties that may not have been present at the time of the earthquake.

There is some question as to the mechanism inducing the aging effect (Mitchell, 1984; Schmertmann, 1991). However, regardless of the mechanism, this is a time dependent effect only. Other external mechanical, chemical or biological effects on soil strengths may occur as well, but constitute separate phenomena. Seed (1979) presented test results showing time-dependent increases in liquefaction resistance occurring over a period of days to years. Therefore, this is an effect that occurs in terms of engineering time as opposed to geologic time periods. Any aging effect occurring in the liquefiable soils present in the Wabash Valley would have been completed well before the occurrence of the seismic events inducing the liquefaction evidence. Following liquefaction and reconsolidation of the soil deposit, the aging effect would have again been realized prior to the testing performed for this investigation. Aging effects will therefore not have caused the soil strength parameters as measured by the in-situ test procedures to differ from what existed at the time of the earthquake inducing the liquefaction evidence.

5.1.4.Groundwater Fluctuations and Freeze/Thaw Effects

Changes in soil density may also occur due to fluctuations in water table elevation or to freeze/thaw cycles. In the Wabash region, the water table elevation may typically fluctuate seasonally over an interval of several meters. This will lead to fluctuations in stress in the deposit below. Effective stresses in the deposit will increase with a drop in the water table. This will induce consolidation of the deposit that would not occur otherwise. This is a condition that is likely to be similar over any two substantial time periods.

At the study sites, surficial deposits of silt and clay typically extend to depths of 3 to 10 feet (1 to 3 m) or more. This is generally beyond the frost depth for the region, and would typically insulate the coarse sediment from any effect of freezing and thawing on the soil density. Neither water table fluctuations nor freezing ground effects would contribute to changes in soil strength between the time of the earthquake and the field investigation that would not have been present at the time of the liquefaction events. Soil

density changes due to water table fluctuations and to freeze/thaw can therefore be assumed to be insignificant.

5.1.5.Cementation

Chemical weathering can also lead to an increase in liquefaction resistance with time (Schmertmann, 1991) and some researchers have suggested that biological processes may lead to a strength gain (Yang et al., 1992). Chemical weathering occurs due to dissolution and precipitation of carbonates in the soil particles leading to a cementation at the particle contacts. Biological processes can result in the deposition of material that leads to an increase in soil strength through adhesion between particles. These are processes that would continue with time, and could lead to an overestimation of soil strength at the time of the field investigation relative to the time of the liquefaction event.

The sediments subjected to liquefaction in the Wabash Valley were laid down during and following the most recent glacial episode. These types of sediments are not typically considered old enough to have undergone chemical weathering effects (Skinner and Porter, 1995). Chemical weathering occurs over time and requires the presence of oxygen. In the Wabash region the groundwater table is generally maintained above the top of the liquefiable sediments. This limits the potential for this type of effect to occur and there has not been enough time elapsed to allow significant weathering. Additionally, any effects that may occur in these sediments would be destroyed during any seismic event inducing liquefaction, and the process would be required to begin again.

There has not been sufficient time elapsed to allow chemical effects to contribute significantly to liquefaction resistance, although biological processes may have altered the soil characteristics and introduced a change in the soil strength. Biological processes will begin to occur in a short period of time. These effects (if any) will be realized over a time frame similar to that of engineering aging effects. Any contribution to liquefaction resistance associated with biological effects can be expected to be similar at the time of both the earthquake and the site explorations for this study.

In an effort to assess the possibility of any effect due to either chemical or biological processes, in-situ, undisturbed exposures of the liquefiable soil deposits were examined, where they were accessible, for evidence of soil characteristics that could be associated with these actions. No evidence of cementation due to either chemical or biologic effects was observed. These effects are assumed to have had no influence on changing the properties of the soil deposit between the liquefaction event and the present investigation.

5.1.6. Effect on Soil Densities by Flow During Liquefaction

Liquefaction, for the purposes of this study, can be said to have occurred in a soil deposit when excess pore pressure develops to the point that it approaches the value of the initial effective confining stress within the soil deposit and leads to some surface evidence of that pore pressure development. Lateral spreading failures are the most commonly observed liquefaction features in the Wabash valley sediments. Where a surficial low-permeability layer confines the liquefied deposit, large hydraulic gradients develop between the liquefied deposit and the ground surface. The excess pore pressures producing this hydraulic gradient are dissipated by flow to the surface through fissures or other discontinuities that develop in the surface layer. This leaves evidence at the surface in the form of sand blows, and in the soil profile as nearly vertical dikes or tubular channels through the low permeability soils. This flow to the surface occurs as water and suspended soil particles from the top of the liquefied deposit are forced from below, and intact blocks of surficial soils "sink" into the essentially viscous fluid that the soil deposit has become.

Seed (1987) suggests that a redistribution of water contents may occur within an in-situ liquefied soil deposit as is seen in liquefied laboratory samples (Castro, 1975). This occurs as a result of densification of soil at the base the deposit and a loosening of the soil at the top of the liquefied deposit. This would contribute to allowing flow to occur along the base of the capping layer toward the closest fissure or other flow path to the surface.

Obvious flow deformation disturbance of this nature was observed within the top of the liquefied deposit where liquefied sediments were exposed at the paleoliquefaction study sites. Horizontal layering was, however, maintained throughout the remainder of the observable thickness of the liquefied deposit. This type of disturbance is consistent with venting of excess pore pressures from the top of the liquefiable deposit.

As a soil deposit begins to reconsolidate following liquefaction, a consolidation front advances upward. This occurs as the soil particles fall out of the suspension induced by the liquefaction event, reconsolidating the liquefied soil deposit from the base upward. Any layering of the sediment due to the initial deposition should be maintained, since no lateral displacement occurs, and vertical mixing below the zone of venting and flow should be minimal. The horizontal layering of alluvial soil deposits will therefore be maintained, and evidence of the liquefaction will not be apparent below the depth of venting. This phenomenon was demonstrated by Liu and Qiao (1984) in shaking table tests.

The mechanism driving the flow that occurs following liquefaction is the large hydraulic gradient that develops at the top of the liquefied deposit. It is not unreasonable to assume that the density of the soil in this region is changed by the event relative to the initial state. The flows leave the deposit highly disturbed. This disturbance effect has been observed at a number of the Wabash study sites where the source materials are exposed during low water periods. The density measured in this portion of the deposit is therefore likely to be less than the pre-liquefaction density. Relative density tests performed at these locations at several of the study sites support this conclusion.

5.1.7.Stress History

Liquefaction has been shown to recur at the same site during successive large seismic events (Ambraseys and Sarma, 1969; Youd, 1984; Obermeier et al., 1993). It has long been recognized that liquefaction events will lead to settlement of a liquefied deposit (Ishihara, 1993). Martin and Clough (1990) suggest that a stress history involving recurring liquefaction events may lead to successive increases in liquefaction resistance

with each incidence of liquefaction. A progressive densification effect of this nature was documented in a liquefied soil deposit on the San Francisco waterfront based on cone penetration test results before and after the 1989 Loma Prieta earthquake (Chameau et al., 1991). Clough and Martin (1990) suggest that a top-down progression may explain the sequence of soil profile densification due to successive liquefaction events. Youd (1984) suggests density increases occur from the bottom upward and that a deposit may be either more or less susceptible to liquefaction following a liquefaction event. Koizumi (1966) reported both increased and decreased penetration resistances due to the 1968 Niigata, Japan earthquake.

It is not precisely clear how a liquefaction event affects the liquefaction resistance of a deposit relative to the contribution of aging or other progressive densification effects, or how this might be translated to other seismic events and liquefied deposits. Ambraseys and Sarma (1969) suggest that based on field evidence observed, it is not possible to densify an initially loose deposit of liquefiable soil to a dense (non-liquefiable) state through repeated liquefaction events as a progressive densification model would seem to imply. They point to the fact that liquefaction episodes have been recorded during both main and aftershocks. This could, however, be ascribed to the fact that a strength reduction occurs when the soil structure is initially disturbed (Mitchell and Solymar, 1984). Aging effects typically take place over a period of months or longer (Schmertmann, 1991), and where an aftershock liquefaction event occurs it likely happens before full strength gain due to aging can be realized. In this way, an aftershock liquefaction event may actually be induced while the soil deposit is significantly less resistant to liquefaction than was present in the original condition.

Ambraseys and Sarma (1969) also point out, however, that liquefiable soils in high seismicity regions will have been subjected to many episodes of liquefaction effects over the thousands of years since their original deposition. Youd (1984) summarizes a number of documented cases of re-liquefaction episodes for sites in California and Japan over the

past 100 years. Obermeier et al. (1990) describe paleoliquefaction evidence of this same nature in low seismicity regions of the central and eastern United States. The re-liquefaction events in each of these environments are likely to have been induced by shaking levels that would have been both larger and smaller than previous liquefaction events. The presence of deposits where many liquefaction events have taken place over hundreds to many thousands of years suggest the conclusion that coarse-grained soils cannot be densified by successive liquefaction events to a non-liquefiable condition.

Youd (1970) showed, in tests on dry sand, an equilibrium void ratio will be attained under vibrational loading, and that this is equivalent to a critical void ratio. During a seismically-induced loading of unsaturated deposits it is not certain, however, that the steady state condition would be achieved, even assuming an average value of the random loading typical of earthquakes. This suggests that successive events inducing similar loadings at a site could each induce a consolidation effect. It is conceivable that a smaller second event could also induce a densification effect. Silver and Seed (1971b) found shear strain is a more fundamental parameter than initial effective stress for describing volumetric strains that can be induced by cyclic loading of dry sands. Seed and Silver (1972) demonstrated how this idea can be used to estimate settlements due to seismic loading of natural deposits based on the shear modulus and damping degradation characteristics (Silver and Seed, 1971a) associated with the range of shear strains likely to occur.

Youd (1972) provides an example laboratory result of drained direct simple shear tests carried to 10,000 cycles. This demonstrates the change in void ratio that occurs during each cycle of loading, as well as the cumulative effect leading to a steady state condition. He also suggests an explanation of the observed behavior in terms of particle motions and the stress strain response during drained static loading. This consists of the initial strains tending to collapse any loose soil structure, and then as strain continues, deformation requires straining of progressively denser portions of the soil structure. This

leads to a consolidation followed by an expansion of the soil mass during each cycle of loading, with a finite increase in density with each cycle of loading until a maximum value is reached. This is the phenomenon that leads to progressive densification and can be extended to undrained soil conditions. Youd notes that the results obtained are also consistent with previous work showing that strain amplitudes of 0.01% or less will not induce significant volumetric strains. It has also been shown that during undrained loading at cyclic strain levels lower than this threshold value no pore pressure development is induced (Dobry et al., 1982). Significant progressive densification effects are therefore likely to occur only due to loadings sufficient to produce displacements exceeding this threshold strain level and induce pore pressure development within a soil mass.

Martin et al. (1975) have developed a closed form solution for pore pressure development during undrained cyclic loading based on the volume change that would be expected due to the same loading in a drained condition. Seed and Idriss (1982) illustrate this schematically with a diagram of void ratio vs. confining stress (see Figure 5.2). During undrained loading the tendency for volume change will transfer stresses to the pore fluid. However, the soil skeleton must maintain a constant volume and a rebound will occur. The end result of a series of these consolidation and rebound events is shown in the figure using the path from A to B to illustrate the equivalent drained consolidation, and the path from B to C the rebound that occurs. Each increment in pore pressure development will match the stress reduction required to maintain a constant void ratio within the soil skeleton during a given loading cycle.

Pore pressure development during undrained loading is induced by the tendency for particle motion, and a change in soil structure must take place to accomplish this. If the cyclic loading is removed prior to the development of full liquefaction (100% excess pore pressure generation), the changes in soil structure will primarily have been at, and adjacent to, locations within the soil mass most susceptible to disturbance. Youd (1977) describes the mechanics of this change in soil structure using a particulate model. He

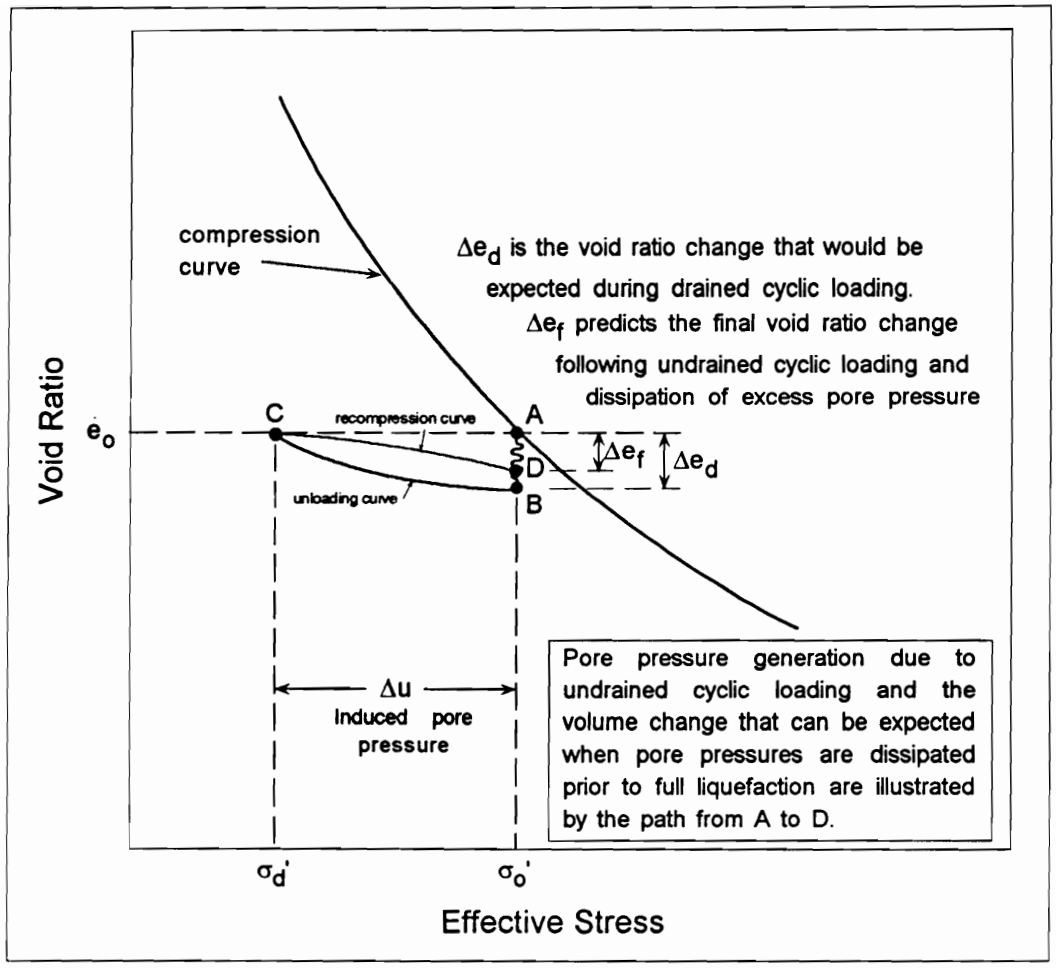

Figure 5.2. Schematic illustration of the volume change that may be expected due to partial pore pressure development during undrained cyclic loading (modified from Seed, 1979).

points out that during each successive cyclic loading event the particle motions that lead to pore pressure development will tend to collapse the most unstable contact points first. Though the overall void ratio has not been altered, a reorganization of the soil structure has occurred and subsequent dissipation of pore pressures then allows consolidation.

The increase in density produced by reconsolidation following partial excess pore pressure development is measurable, but will be small. Finn et al. (1970) measure maximum volumetric strains associated with this type of consolidation on the order of approximately one percent. Lee and Albaisa (1974) report additional test data showing similar results. These test results show that the volumetric strains following partial liquefaction are related to relative density and the excess pore pressure generated during loading. Lee and Albaisa found that this was true regardless of the means of pore pressure generation. Tokimatsu and Seed (1987) compiled field and laboratory data and also predict non-liquefaction volumetric strains will be less than one percent. This value is consistent with the model described above for pore pressure development and can be visualized as following the recompression path from C to D shown on the Seed and Idriss diagram (Figure 5.2).

Finn et al. (1970) and Lee and Albaisa (1974) also measured volumetric strains occurring following 100% excess pore pressure generation during cyclic loading. Each report a relationship between volumetric strain and maximum shear strain occurring following full liquefaction, up to a maximum volumetric strain of approximately 3%. Tokimatsu and Seed evaluated the field data on settlements associated with cyclic ground motions and found that where liquefaction occurs, maximum settlements are on the order of 10 percent. Based on a review of previous research they concluded that the major influences on volumetric strains in saturated sands will be the cyclic stress ratio, relative density and earthquake magnitude. Based on further field and laboratory data, Ishihara (1993) predicts maximum volumetric strains on the order of 4%. Hussein and Stewart (1994) show that the reconsolidation volumetric strain following liquefaction will

generally range between one and four percent for normal soil conditions. They suggest that measured field settlements beyond this upper limit have been induced by factors other than volumetric strains alone. The additional strains might be attributed to venting of subsurface material or extreme strain levels associated with liquefaction of very loose sands.

Finn et al. (1970), Lee and Albaisa (1974), and Lee and Focht (1975) all performed liquefaction resistance testing on samples that were reconsolidated following an initial pore pressure development. In samples re-tested following partial liquefaction, each of these researchers found an increased resistance to subsequent pore pressure development. The strength increase exceeded what could be expected due to the reconsolidation volumetric strain alone, and each suggest this indicates a change in soil structure occurs due to the cyclic loading. Lee and Focht found that the increase in strength occurs for each successive series of cyclic loadings following pore pressure dissipation. This result was also demonstrated by Arulanandan et al. (1983) in centrifuge model tests and is consistent with the results on dry sand reported by Youd (1972). The effect diminishes with each series of loadings and Lee and Focht conclude that a limiting value of cyclic loading resistance would eventually be attained. The test results presented by Arulanandan et al. also show that the void ratio reduction measured due to reconsolidation following cyclic loading partial liquefaction occurs only during the first loading where pore pressures are developed. Subsequent partial liquefaction cyclic loading continues to provide increased liquefaction resistance, but, based on these test results, none of this can be attributed to an increase in density. The increased liquefaction resistance must therefore be due to a change in the soil structure that allows the observed strength increase.

Excess pore pressure generation due to cyclic loading of a soil deposit may also lead to an increase in liquefaction susceptibility relative to the initial condition. The field observations and laboratory test results reviewed above suggest liquefaction resistance

will always be increased following any cyclic loading that produces excess pore pressure development. However, cyclic loading generating 100% excess pore pressure may lead to a reduction of in-situ liquefaction resistance when it is followed by additional shear strains. Finn et al. (1970) performed both cyclic triaxial and simple shear re-liquefaction tests on saturated sand specimens. While it is recognized that post-liquefaction sample disturbance and system compliance effects likely significantly influenced the results of the tests (Castro, 1975; Martin et al., 1978), the volumetric strains and general trends of the strength results are consistent with observed field behavior (Hussein and Stewart, 1994; Youd, 1977; 1984). These test results show a dramatic reduction in liquefaction resistance following full liquefaction and reconsolidation that can not be trusted in quantitative terms, but may indicate a qualitative trend that also occurs in natural deposits. Their results suggest that the magnitude of the undrained cyclic strength loss increases with the post-liquefaction maximum shear strain to a limiting shear strain value of three to four percent. This is similar to the observed value of shear strain inducing maximum volumetric strains following a liquefaction event. In this case, however, where full liquefaction occurs, liquefaction susceptibility increases with increasing volumetric strain rather than the decrease in subsequent liquefaction susceptibility seen for non-liquefied samples. Finn et al. note that this is the opposite effect of what should be expected based on the increase in density, and suggest that here too a soil structure effect influences the liquefaction resistance of a soil deposit. Castro (1975) attributes this loss in liquefaction resistance to a severe redistribution of void ratio within the lab specimen that produces a denser condition at the base and a looser condition at the top of the specimen that is inconsistent with field behavior. This is, however, qualitatively consistent with the redistribution of void ratio suggested by Seed (1987) for in-situ liquefied deposits.

The Finn et al. study suggests that the stress history of a sample can lead to negative as well as positive changes in liquefaction resistance. Cyclic liquefaction resistance losses in their strain-limited tests were obtained even though the test specimens would reconsolidate to a lower void ratio during pore pressure dissipation between tests.

They postulate that the structure of the sand is altered when the strain level exceeds a threshold value, producing a condition analogous to the flow structure suggested by Casagrande (1975). A change in soil structure of this nature may be what occurs in relatively uniform deposits of liquefied soil. As reconsolidation continues following the end of cyclic loading, the soil deposit may well be left in a looser state than the initial condition. Youd (1984) suggests this can lead to a reduced liquefaction resistance in uniform deposits where ground motions cease prior to completion of the reconsolidation process.

Finn et al. also submit that a non-uniform soil structure may result following liquefaction, and lead to a reduced soil strength. Subsequent loading then leads to non-uniform deformations and a reduced global liquefaction resistance results. Castro (1975) documented this effect in laboratory test specimens subjected to large post-liquefaction strains. Seed (1987) suggests this may occur where a confining layer induces a redistribution of water contents in the liquefied deposit. Youd (1984) documents a case where this has occurred and has likely been perpetuated through multiple events. The formation of water interlayers below an overlying low permeability soil allows formation of a loose zone at the top of the liquefiable soil layer even as the lower portion of the deposit becomes densified with successive earthquakes. This is a condition that may then persist through many liquefaction events. Using shake table tests, Liu and Qiao (1984) demonstrate that this effect can occur at multiple elevations within a stratified deposit containing impermeable layers confining the layers of liquefiable soil.

Chameau, et al. (1991) suggest stress history of an in-situ coarse-grained sediment can lead to progressive densification within that deposit as a result of ground motions. They report up to a 20% increase in penetration resistance at the Yerba Buena Cove (YBC) study site on the San Francisco waterfront based on tests performed in 1979 and 1990, before and after the 1989 Loma Prieta earthquake. They also document changes in penetration resistances at the site Telegraph Hill (TH) just to the north. An examination

of their data demonstrates densification can occur in deposits shown to have been involved in liquefaction as well as those that apparently did not liquefy. Figure 5.3 shows a portion of their data for the YBC site converted to equivalent SPT $(N_1)_{60}$ values. Figure 5.4 shows similar data for the TH site. It can be seen that a significant increase in penetration resistance was measured in the upper presumably non-liquefied portion of the soil deposit at site YBC, as well as smaller increases in penetration resistances at other elevations there and at site TH. The vertical boundary shown on the figures is the $(N_1)_{60}$ liquefaction suppression value predicted by the methodology developed for this study (see Chapter 6). Average blowcount values below this threshold indicate soils susceptible to liquefaction. This prediction also matches that of Chameau et al. using the Seed et al. (1985) simplified procedure.

The densification results reported by Chameau et al. (1991) may possibly be explained using a progressive densification model that allows a loosening effect due to a liquefaction event. In the soil deposits where full liquefaction did not occur, the ground motions experienced during the main shock of the Loma Prieta event could have induced a tendency for consolidation that allowed particle rearrangement and an improvement in liquefaction resistance. Where liquefaction occurred, the deposit would begin to reconsolidate by sedimentation of the soil particles. This produces both a consolidation front advancing from the base of the liquefied region toward the surface (Florin and Ivanov, 1961; Scott and Zuckerman, 1973; Scott, 1986) and a liquefaction front advancing from the top of the liquefied soil into the overlying non-liquefied deposit. The soil structure following liquefaction may then resemble that of a deposit recently pluviated through water, such as a hydraulic fill. Youd (1984) suggests that where this reconsolidation process continues beyond the end of shaking, a looser condition than the original state may result. Any following increases in soil strength due to stress history must therefore begin from this condition. In all cases, the post-event penetration resistances measured at the YBC and TH sites exceed the pre-event values, however, testing at the sites was conducted approximately five months following the event, and

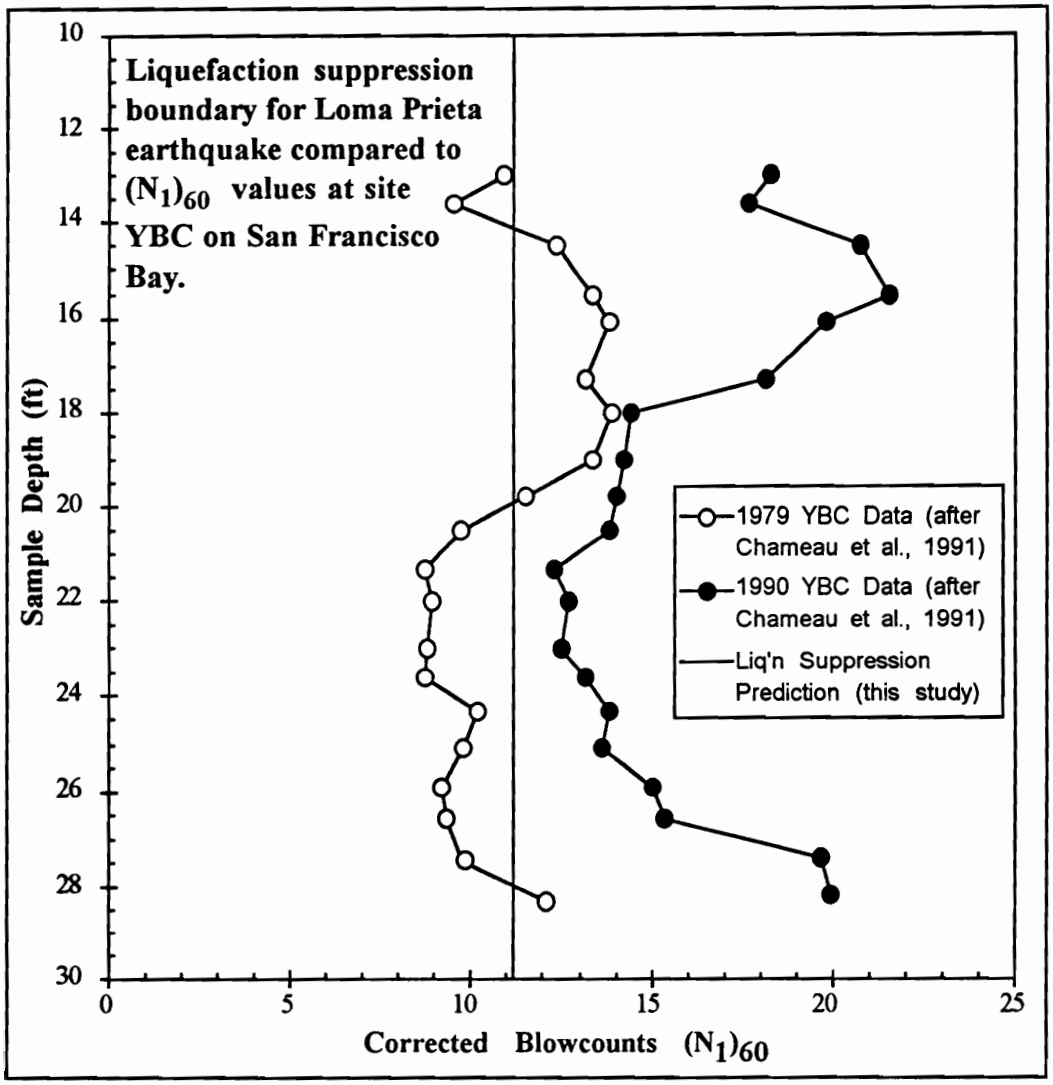

Figure 5.3. $(N_1)_{60}$ data for site YBC on the San Fransisco waterfront before and after the 1989 M7.0 Loma Prieta earthquake.

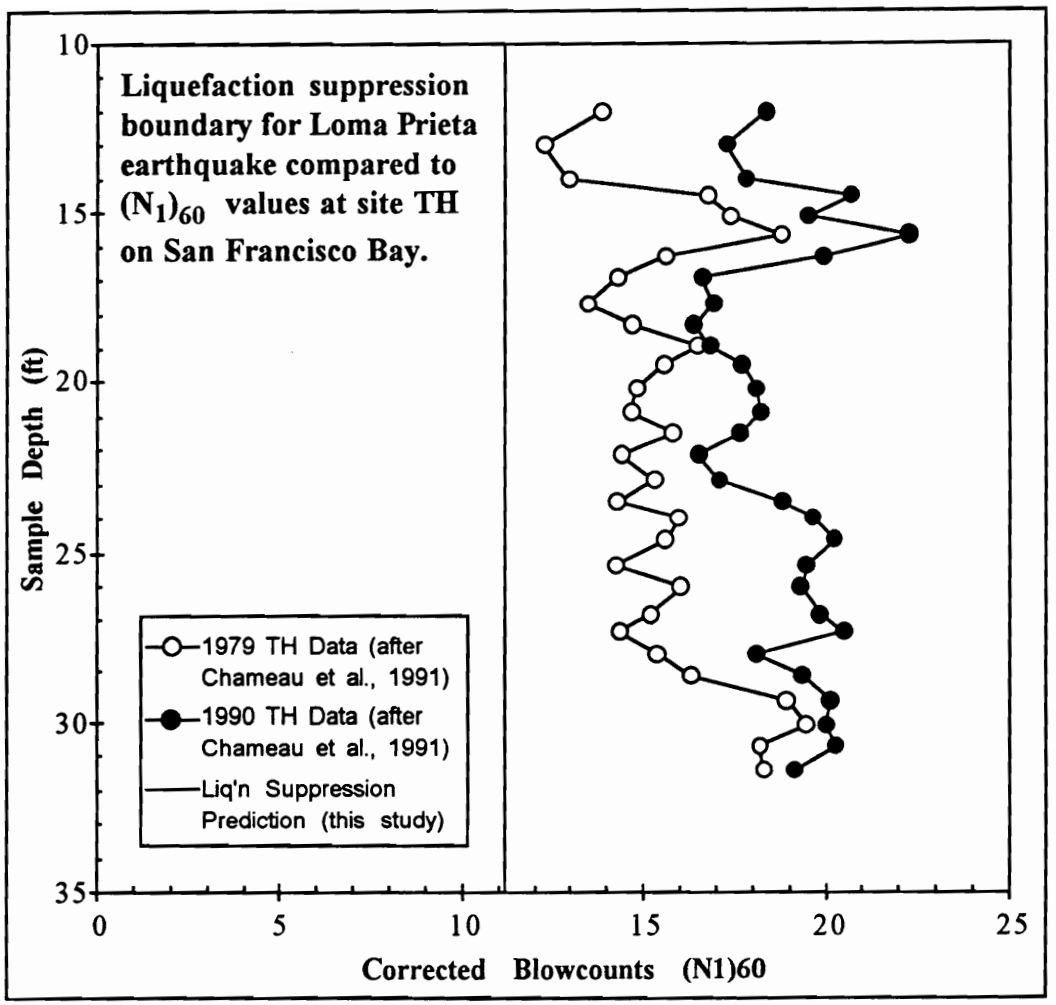

Figure 5.4. $(N_1)_{60}$ data for site TH on the San Fransisco waterfront before and after the 1989 M7.0 Loma Prieta earthquake based on CPT data from Chameau et al., 1991.

many aftershocks occurred over that time period. These events were not reported to have induced liquefaction effects but some could likely have induced stress history effects similar to the strength gain seen in repeated partial liquefaction testing. Those portions of the soil profile that did not liquefy during the main shock would have experienced a similar type of strength gain effect during that main period of shaking. The final liquefaction resistance in the non-liquefied portion of the deposit could therefore be expected to exceed that of the portion where the stress history will not have included the strengthening effect of the main shock.

There are two additional interesting effects to note associated with the penetration test results reported by Chameau et al. (1991). The first is evidence for an induced liquefaction zone at the base of the upper dense sand. In a portion of the YBC deposit predicted to not be susceptible to liquefaction, final penetration resistances are similar to the values measured in the predicted liquefied zone. This may be the result of a progressive liquefaction effect. Scott and Zuckerman (1973) demonstrate how an upper dense, coarse-grained soil can be liquefied by the presence of an underlying liquefied deposit. When a deposit liquefies, soil particles present at the base of an overlying soil layer will begin to settle into the liquefied zone. This produces an induced liquefaction front traveling toward the surface. This continues upward until the consolidation front overtakes it or the surface is reached. Scott and Zuckerman found that this can also occur in conjunction with the formation of sand blows at the surface.

The second effect of note is the similarity of the final penetration resistances measured in the apparently non-liquefied portions of the deposits. The YBC and TH sites contain similar dune sand fill sediments placed at about the same time. Both sites were reported to have experienced liquefaction effects during the 1906 San Francisco earthquake (Clough and Chameau, 1983; Chameau et al., 1991). Those portions of the deposits not subjected to liquefaction during the Loma Prieta event will likely have had similar stress histories between the 1906 event and the 1990 site investigations. The final

penetration resistances measured at the top of the YBC deposit and throughout much of the deposit at site TH (both locations where liquefaction likely did not occur) are similar. The low initial penetration resistances in the lower liquefiable portion of the YBC site may stem from the differences in severity of liquefaction effects at the two sites during the 1906 earthquake. The YBC site experienced large displacements, while only small displacements were reported for the TH site (Clough and Chameau). The disturbance of the sediments at the YBC site is likely to have been much greater, possibly producing the identified zone of greater liquefaction susceptibility. This would be consistent with the conditions detailed by Youd (1984) for a lateral spreading failure where large displacements produce a soil profile with an increased liquefaction susceptibility.

The progressive densification effect due to stress history has typically been associated with high seismicity environments (Martin and Clough, 1994), but may also occur in low seismicity regions. Any time ground motions exceed some threshold level there will be a tendency for particle rearrangement that will produce a change in the liquefaction susceptibility. This may be manifested in a soil deposit in any of the forms described above. Any ground motion exceeding the threshold strain but insufficient to produce 100% excess pore pressure generation would likely induce a strength gain effect. Ground motions producing full liquefaction of a soil deposit could lead to either an increase or decrease in liquefaction susceptibility. It is possible only to make some broad generalizations about this effect.

The liquefaction resistance of a soil deposit is also influenced by the mode of deposition. This has been clearly illustrated in laboratory test results showing the effect of sample preparation techniques on the liquefaction resistance of a specimen (Silver et al., 1976; Ishihara, 1993). These results in laboratory tests can be extrapolated to field conditions based on the fact that a natural deposit allowed to reconsolidate following liquefaction will have a different grain structure than a deposit laid down by moving water. Where ground motions cease prior to reconsolidation, the deposit can be considered

deposited by vertical sedimentation in a calm environment. A depositional environment involving moving water will produce a denser packing of the soil grains by inducing the soil grains to move into a more stable arrangement as they come to rest than would be expected in a calm environment. The energy imparted to a soil specimen as it is being deposited will in this way affect the grain arrangement within the soil matrix.

Any soil structure effects due to deposition can be considered a portion of the stress history of a soil deposit. It is apparent from laboratory test results that variations in soil structure at equal relative densities lead to significant differences in liquefaction resistance. It should also be assumed that this effect will occur in natural deposits as well. A soil deposit laid down by calm vertical sedimentation of the soil grains can be expected to allow relatively unstable inter-granular contacts to be created within the soil mass relative to what will be present following a fluvial deposition. A liquefaction event in a level ground deposit reduces the void ratio, but during liquefaction the soil particles are placed in a suspended state that continues until excess pore pressures begin to dissipate. The pore pressure dissipation occurs as the soil particles settle out of suspension, producing an upward-advancing reconsolidation front. The process produces a deposit with a lower global void ratio than the original, but this can not be directly translated into an increase in liquefaction resistance.

The energy involved in reconsolidation of a liquefied soil deposit is associated with the kinetic energy of the soil particle sedimentation. In a liquefied deposit, the soil mass reconsolidates as the particles settle out of suspension and come to rest on the particles below. The energy involved in placement of individual soil grains is related to the velocity of this settlement, and will be less than that of the same particle originally deposited by moving water. The result will be to produce less-stable inter-particle contact points at locations throughout the soil profile. In this way the global void ratio can be reduced and produce a strength reduction as well. Scott (1986) shows that as the consolidation front advances upward, the re-sedimented material below will continue to consolidate until the

effective stress is no longer increasing. This will tend to collapse the most unstable contact points, and produce a soil strength profile increasing with depth.

In a fluvial environment, the action of the water imparts a shear loading during the sedimentation process, and will have a tendency to eliminate the most unstable of the voids that could be expected in calm environments. This effect will be more pronounced as the energy of the environment increases. In a post-liquefaction depositional environment where ground motions continue during the initial stages of reconsolidation, the shear stresses may also tend to collapse the most unstable voids, resulting in a greater liquefaction resistance. However, strains will be produced even at very low shear stress levels for the level of effective confining stress induced due to initial settlement of the sand grains at the base of the liquefied zone. These strains would produce a tendency for consolidation that in turn will likely renew the full excess pore pressure ratio, maintaining the state of full liquefaction until all ground motions cease. This scenario is consistent with the pore pressure generation and liquefaction documented at the Wildlife site following the 1987 Superstition Hills earthquake (Holzer et al., 1989).

A liquefied deposit that undergoes substantial lateral spreading will experience large strains throughout the liquefied zone. As this lateral displacement occurs, there will be a tendency for dilation within the soil deposit that will tend to draw pore water from adjacent soils (Youd, 1984) outside of the shear zone. Where this redistribution of pore water occurs, the liquefied deposit will become loosened relative to its original condition and may produce a critical void ratio condition that will persist indefinitely. The large strains may also lead to a redistribution of voids within the soil mass. The result of this could be to produce a soil fabric more susceptible to liquefaction (Youd, 1977). An effect of this nature will depend on the relative permeabilities of the soil deposits and the initial condition of the deposits, as well as the seismic shaking itself.

The liquefied soil deposits identified in the Wabash Valley appear to have experienced only a single liquefaction event. Therefore, the stress history of these

deposits prior to the liquefaction event would not reflect the effect of liquefaction, and soil strength development will have been based solely on the initial deposition and subsequent stress history effects. This does, however, make the assumption that large seismic events occur only during normal or high water conditions. If a large seismic event were to occur in the Wabash Valley region during drought conditions, as was present during much of the field portion of this study, the liquefiable soils will have extended above the groundwater table at many locations, and liquefaction evidence could very likely have been suppressed.

The cumulative effect of the possibilities considered above, is that it is not precisely clear how the present condition of the Wabash soils compare with the pre-event condition. It is therefore necessary to make an educated guess as to the present soil conditions relative to the pre-liquefaction condition. In addressing this issue it is necessary to consider how the soil structure achieved during deposition compares to that attained during several thousand years of progressive densification effects. If it is assumed that the initial density based on the diluvial or fluvial deposition is greater than the density that could be induced by any potential non-liquefaction ground motion event in the region, the present condition will be looser than the pre-event condition. This is based on an assumption that liquefaction will destroy the initial fluvial deposit soil structure and substitute a vertically sedimented deposit subsequently densified by moderate seismic ground motions in the region. This could lead to an underestimation of soil strength parameters, and in turn to an underestimation of the severity of shaking required to induce liquefaction in any portion of the liquefied deposit. If this is the case, using a liquefaction susceptibility analysis to back-calculate ground motions may underestimate the actual ground motions experienced.

Where the threshold for strength increases due to stress history is exceeded by ground motions induced during moderate seismic events in the region, soil strengths will increase with time. In this case, as well that above, however, the present soil strength can differ from the pre-event condition. If seismic activity varies significantly over the

thousands of years that these deposits have been in place, it is possible that the pre- and post-event stress histories have been considerably different. If the seismic activity in the region prior to the liquefaction event includes larger events than what occurred following the liquefaction event, soil profile densities may have been greater at the time of the liquefaction event than those estimated based on the present in-situ test data. If the seismicity following the event includes greater events than prior to the event, the opposite could be true. However, if the assumption is made that seismic activity will be similar in any period of several thousand years it can also be assumed that the stress history between deposition and liquefaction will have been similar to that between liquefaction and the present. This allows the assumption that the stress history effect will lead to similar soil conditions now as were present just prior to the earthquake that induced the liquefaction.

For this study it is assumed that the threshold for stress history effects following a diluvial or fluvial deposition was exceeded by the ground motions that will have been experienced by the liquefiable deposits in the region. This is based on the fact that penetration resistances measured in the late Pleistocene and early Holocene deposits are similar. Additionally, without evidence of dissimilar seismic activity during the pre- and post-event time periods it is impossible to assess the potential difference in stress histories before and after the event. There is a possibility that aftershocks associated with the liquefaction-producing event may have been larger than any pre-liquefaction seismic event, but this is again a possibility that can not be verified or refuted based on presently-available evidence. It is reasonable to assume, however, that the stress histories will in general have been similar over time. Baring aftershocks significantly larger than other moderate (partial-liquefaction producing) events in the region, the present soil conditions are likely similar to the pre-event conditions.

In order to reliably assess the liquefaction resistance of a soil deposit it would be necessary to account for the changes in soil density that occur due to liquefaction. However, the database used to develop the liquefaction susceptibility design curves is

based on historical pre- and post-earthquake data (Seed and Idriss, 1971). This database therefore includes the effect of density changes due to liquefaction of the deposit. Based on this fact and the conclusions derived above, it is assumed that the in-situ blowcounts measured provide a representative description of the soil conditions present at the time of the earthquake.

In the analyses performed for this study it is assumed that the in-situ conditions at the paleoliquefaction study sites are generally not significantly different now than was present at the time of the liquefaction event. However, one important exception to this is the region within the soil deposit at the base of the dikes. Where the liquefiable soil is exposed during low water, obvious flow deformations were observed in these areas. The assumption made here is that the extreme disturbance in these locations will have significantly altered the original soil structure. The in-situ relative density testing performed for this study supports this conclusion. In order to address this issue, an effort was made to ensure blowcount data was obtained at locations outside of these zones.

As will be seen in the analysis section of this report, however, the assumption of similar pre- and post-liquefaction susceptibilities as measured by penetration testing is inconsequential in the back calculation procedure used to estimate surface motions. As Ambraseys (1988) points out, changes in blowcount due to liquefaction should have only a minor effect on the cyclic stress ratio estimate. This is particularly true for low blowcount material where the slope of the liquefaction prediction boundary is less than for denser soils. Additionally, the surface motion estimate is based on a threshold blowcount rather than a minimum value or finite thickness of liquefied layer. An estimate of earthquake magnitude is made and then used to predict a maximum value of corrected standard penetration resistance that would be involved in the liquefaction at a given site. This blowcount value is used to predict a liquefied layer thickness, which then allows back-calculation of surface motions at a specific site. This estimate can then be compared to ground motion predictions made by the seismological community. Small variations in the

true thickness of the liquefied deposit will not significantly affect the prediction of surface motion. The effect on surface motion predictions will be due to a small variation in the stress estimates in the liquefied zone. These potential variations from actual ground motions will not significantly alter the results. There have been no recorded strong ground motions in the region, and many assumptions must be made regarding the application of liquefaction susceptibility analysis techniques derived from plate margin data. Errors introduced here can therefore be assumed to be relatively minor in relation to the uncertainties in other portions of the analysis.

5.2.Soil Conditions at Paleoliquefaction Study Sites

5.2.1.Vincennes Event

The soil conditions were investigated at thirteen paleoliquefaction sites in order to estimate ground motions associated with this event. The liquefaction evidence at each of the study sites associated with the Vincennes event originates in the fluvial deposits laid down during the early Holocene epoch. These liquefiable sediments were laid down during the time period just following the end of the Wisconsinan glaciation, while the rivers were downcutting into the present terrace sediments. The dikes and sand blows left following the liquefaction event typically originate at or near the crests of the point-bar sediments left by the meandering of the rivers. The features are generally linear with a strike following the crests of the point-bar sediments.

5.2.1.1.Site VW

Site Vincennes West is located along the Indiana bank of the Wabash River approximately 7.5 km southwest of the town of Vincennes, Indiana. The site extends approximately 365 m northeast to southwest and contains dikes ranging in width from a few cm to 0.75 m. Figure 5.5 shows a site plan for the study site, and includes a site vicinity map.

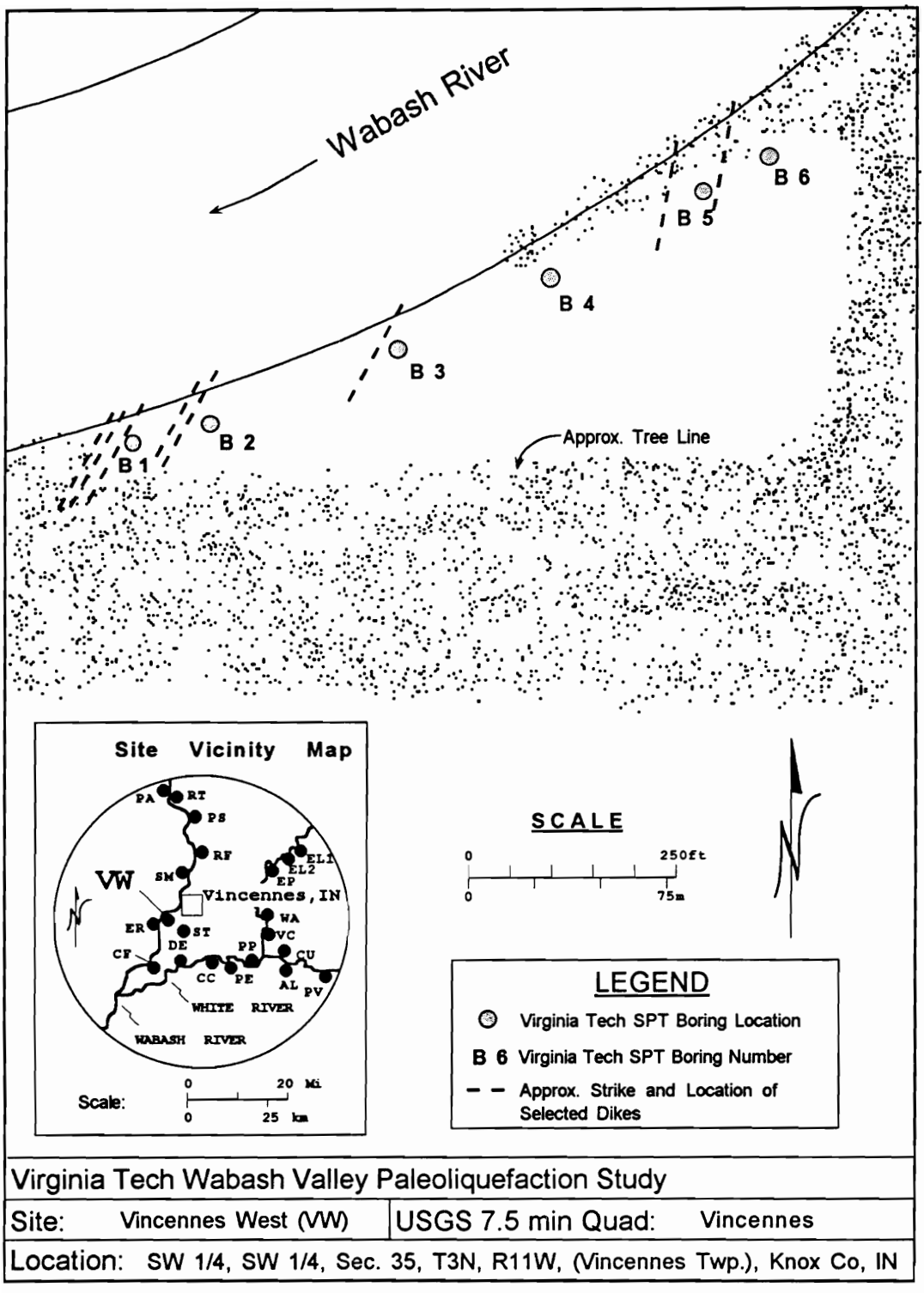

Figure 5.5. Site plan for site Vincennes West (VW)

The soil conditions present at the site consist of from 3.5 to 5 m of lean to fat clays overlying medium dense to dense gravelly sand with silt. The original ground surface at the time of the earthquake is now buried by between 2 and 4.6 m of more recent sediments. A 1 to 3 m zone of natural levee deposits containing interbedded clay and sand is present between the fine sediments and the coarse material. The liquefiable soils range from predominantly fine to medium sands at the southwest end of the site, to gravelly sands at the northeast end. The largest dike features are associated with the fine to medium sands, and the smallest with the gravelly sediments. A generalized soil profile of the site is given in Figure 5.6 The soil conditions between boring locations were interpreted based on exposed soil in the river bank and on data provided by Professor Munson (1994) of Indiana University.

5.2.1.2.Site SM

Site Seven Mile Island is located along the Illinois bank of the Wabash River approximately 7.5 km north of the town of Vincennes, Indiana. Figure 5.7 shows a site plan for the study site, and includes a site vicinity map. The site extends approximately 230 m northwest to southeast and contains several dikes up to approximately 0.3 m wide in the central portion of the site.

The surficial soil present at the site consists of from 2.5 to 3.6 m of lean to fat clays overlying a natural levee deposit, which in turn overlies loose to medium dense liquefiable sediments. Where they are present, the levee deposits of interbedded clay and sand extend to between 0.75 and 1.2 m in thickness, however, this deposit is absent in the vicinity of the observed dikes. The liquefiable soils consist of a loose fine to medium sand layer overlying a medium dense sand with some gravel. Like the levee deposit, the loose sand layer is missing in the center most portion of the site. These layers appear to have been ejected by flow to the surface during the liquefaction event. Six in-situ density tests were performed at this site. The tests performed in the vicinity of the greatest disturbance show relative densities of 8% to 39% in the upper 0.6m of the liquefiable deposit. Two

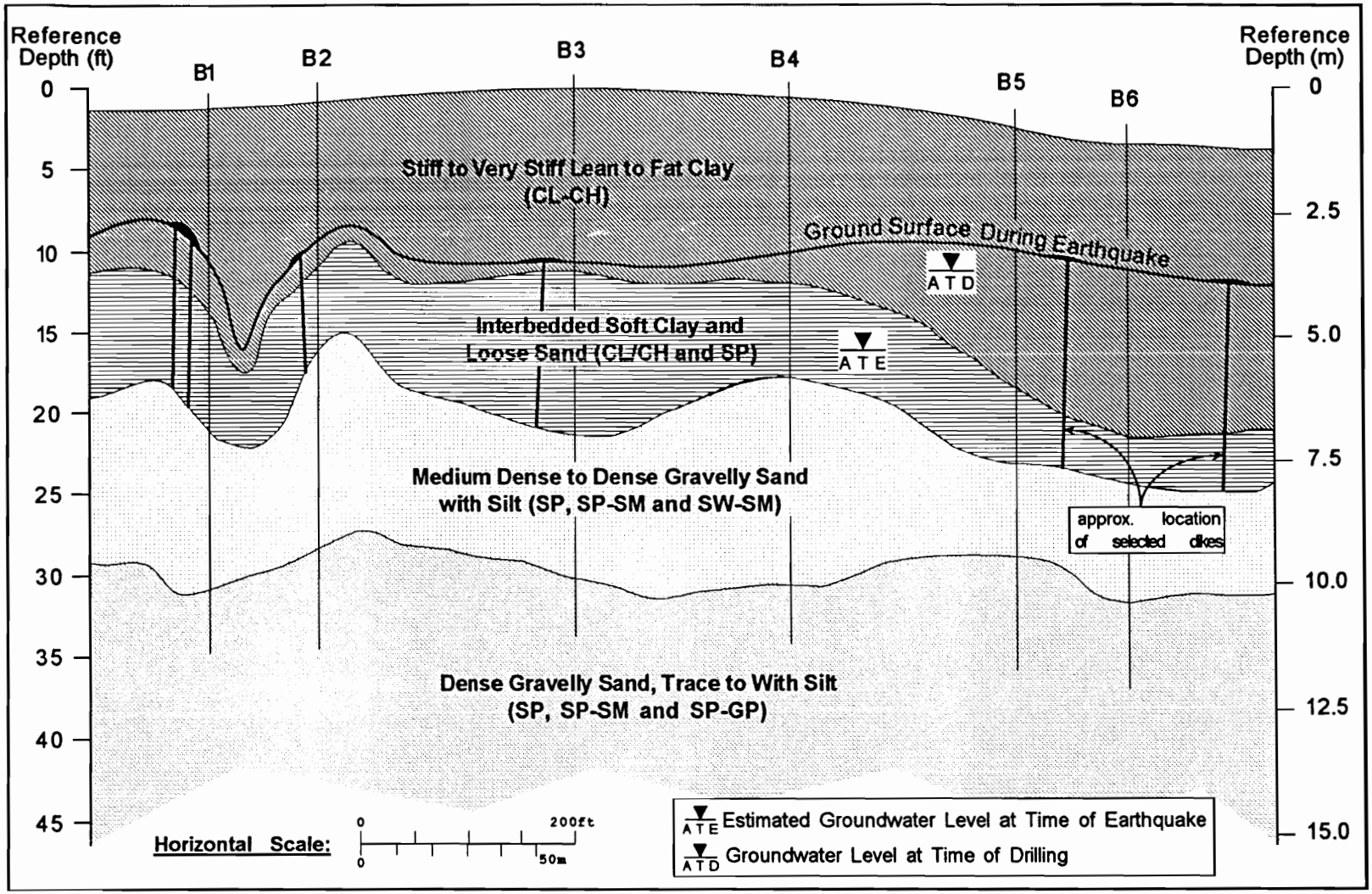

Figure 5.6. Near surface soil profile for site Vincennes West (VW)

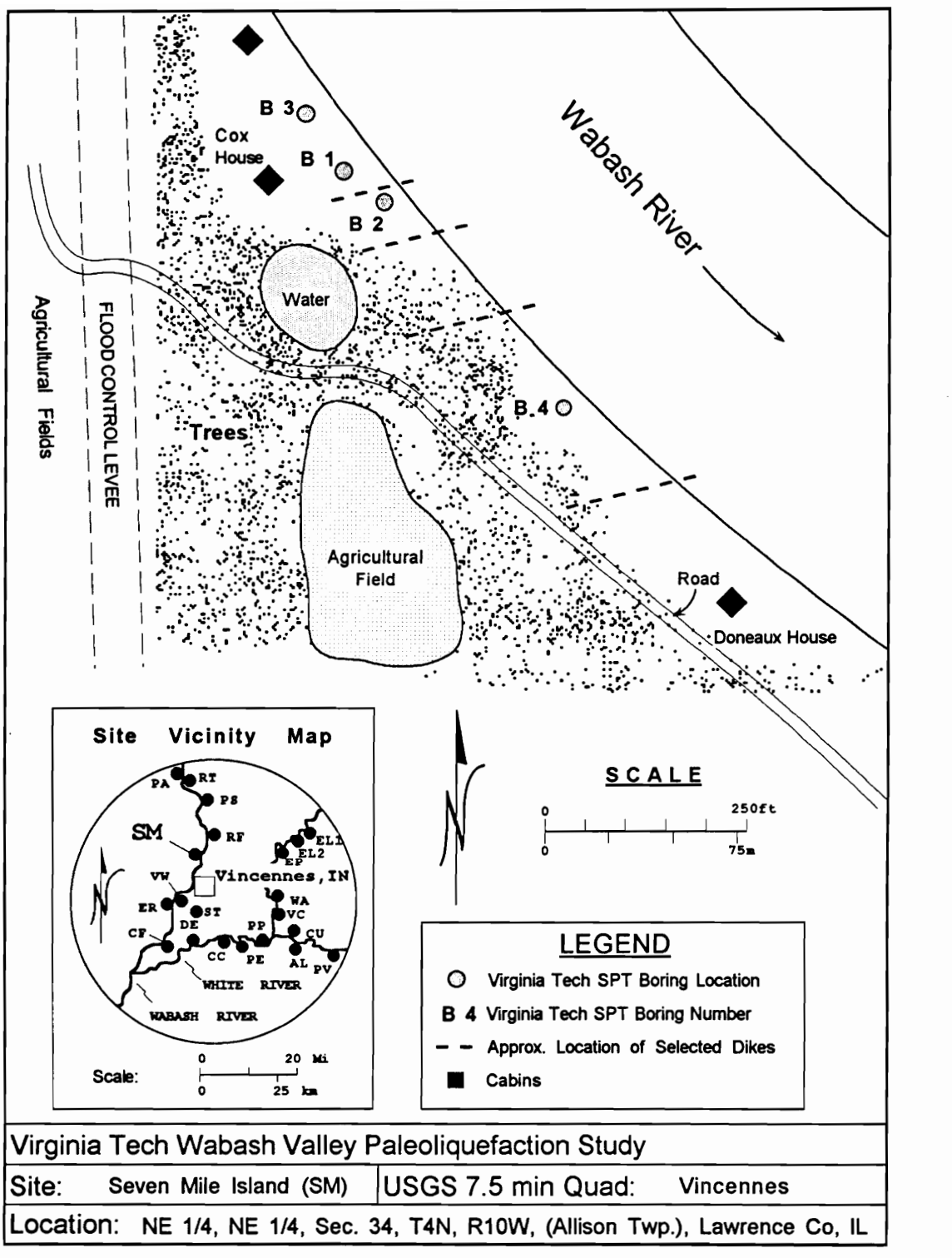

Figure 5.7. Site plan for site Seven Mile Island (SM)

tests in soil showing less evidence of disturbance revealed relative densities of 51% and 73%. These results are consistent with the penetration test data obtained in this vicinity. A generalized soil profile of the site is given in Figure 5.8. The soil conditions between boring locations were interpreted based on soil conditions exposed in the river bank and interpolation between borings.

5.2.1.3.Site RF

The Russellville Ferry site is located along the Indiana bank of the Wabash River approximately 10 km north of Vincennes, Indiana. Figure 5.9 provides a site plan for the study site, and includes a site vicinity map. The site extends approximately 300 m northeast to southwest and contains dikes ranging in width from a few centimeters to 1.5m.

The surficial soil present at the site consists of from 3.5 to 5 m of silt and lean to fat clays overlying a natural levee deposit, which then in turn overlies medium dense liquefiable sediments. The ground surface at the time of the earthquake is buried by 1.5 to 2.5 m of post earthquake flood plain deposits. The levee deposits of interbedded clay and sand extend to between 0.5 and 2.5 m below the surficial silts and clays. The liquefiable soil below generally consists of a medium dense gravelly sand. The largest dike features are typically associated with the finest site sediments, and the smallest with coarser soils. Four in-situ density tests were performed in the vicinity of the northern dikes at this site. The tests show relative densities of 25% to 41% in the upper 0.6m of the liquefiable deposit. These results are consistent with the penetration test data obtained in this vicinity. A generalized soil profile of the site is given in Figure 5.10. The soil conditions between boring locations were interpreted based on exposed soil in the river bank and on data provided by Professor Munson (1994) of Indiana University.

5.2.1.4.Site PA

The Palestine site is located along the Illinois bank of the Wabash River approximately 35 km north of Vincennes, Indiana. Figure 5.11 provides a site plan for

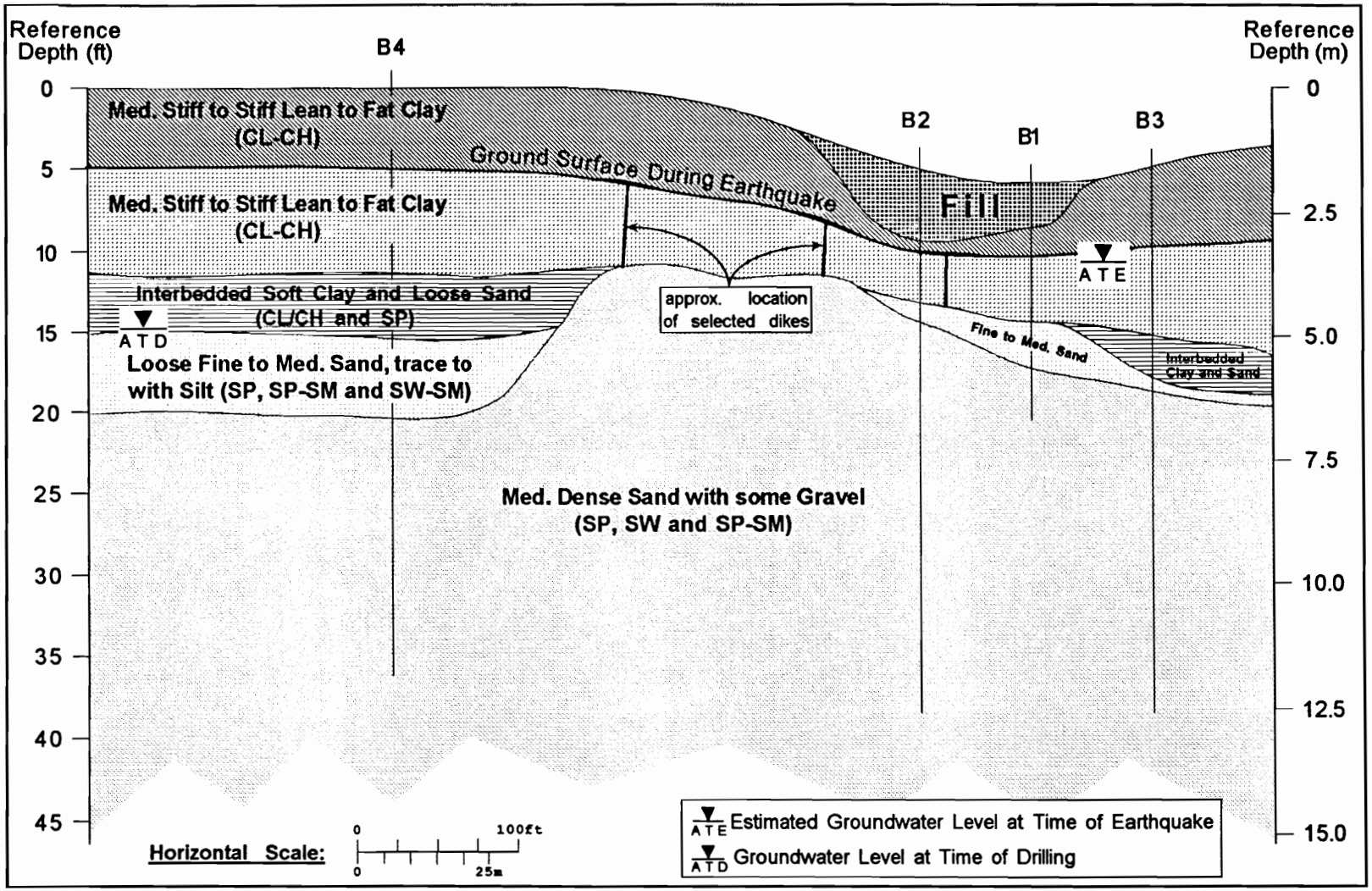

Figure 5.8. Near surface soil profile for site Seven Mile Island (SM)

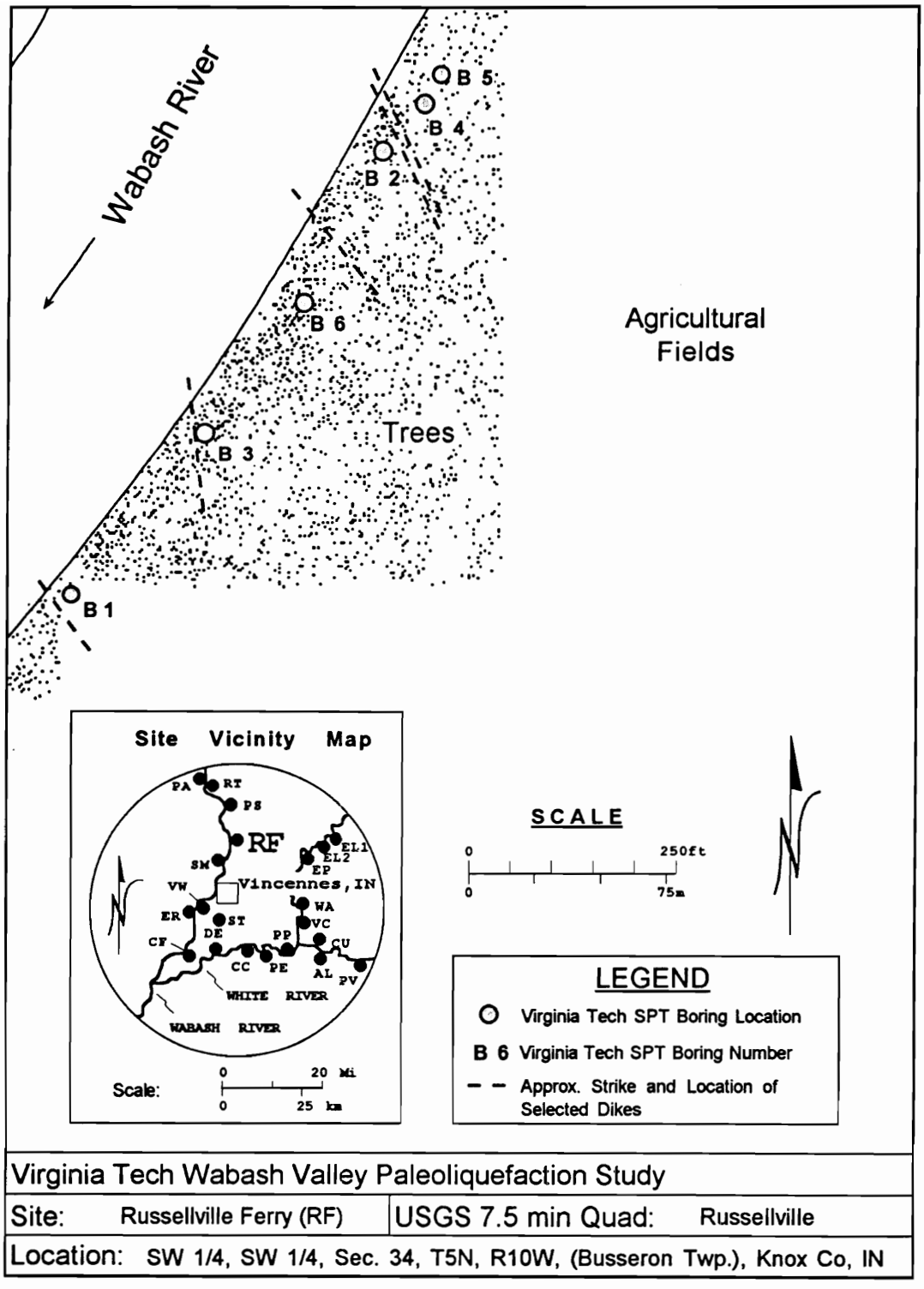

Figure 5.9. Site plan for site Russellville Ferry (RF)

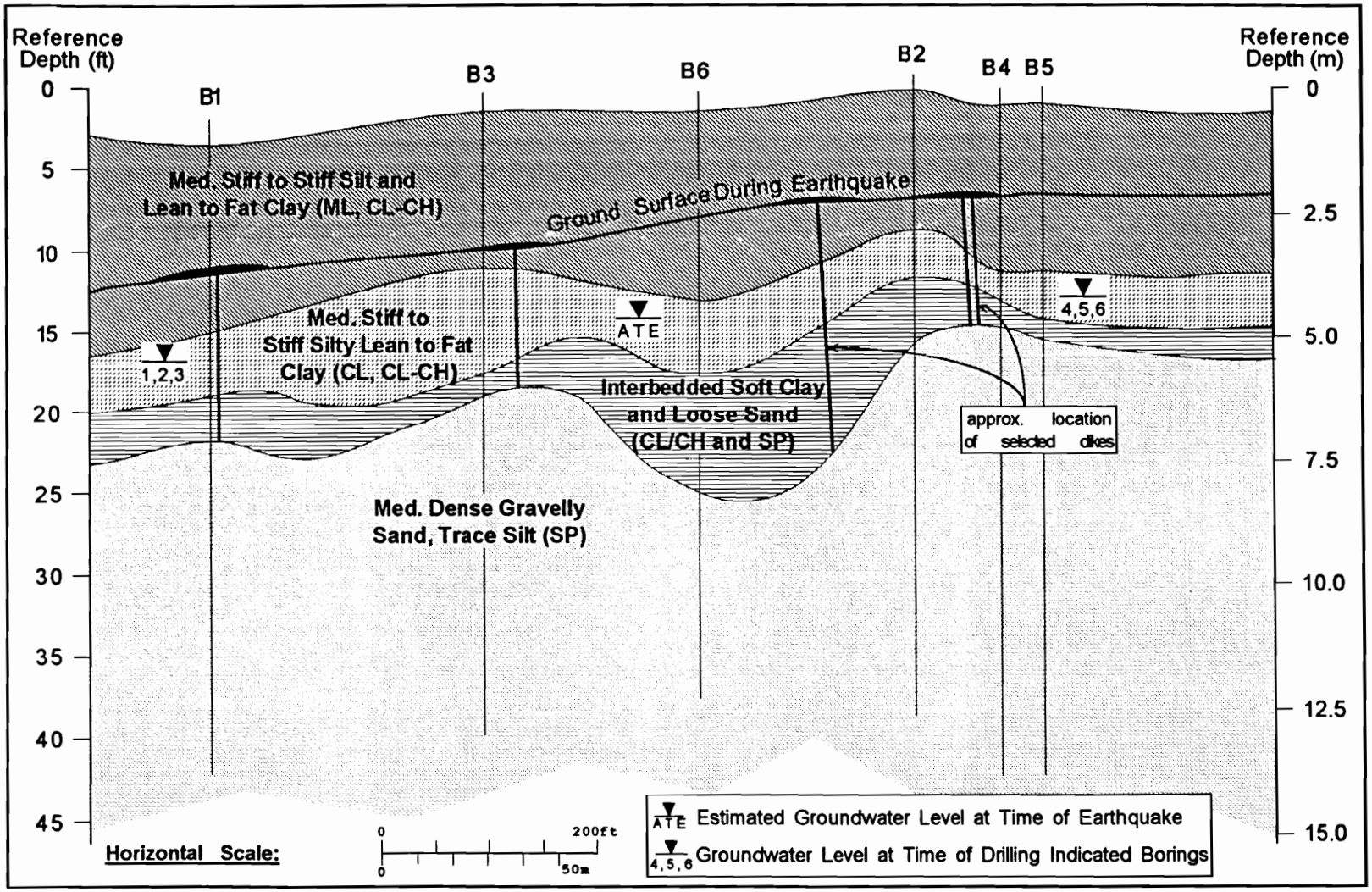

Figure 5.10. Near surface soil profile for site Russellville Ferry (RF)

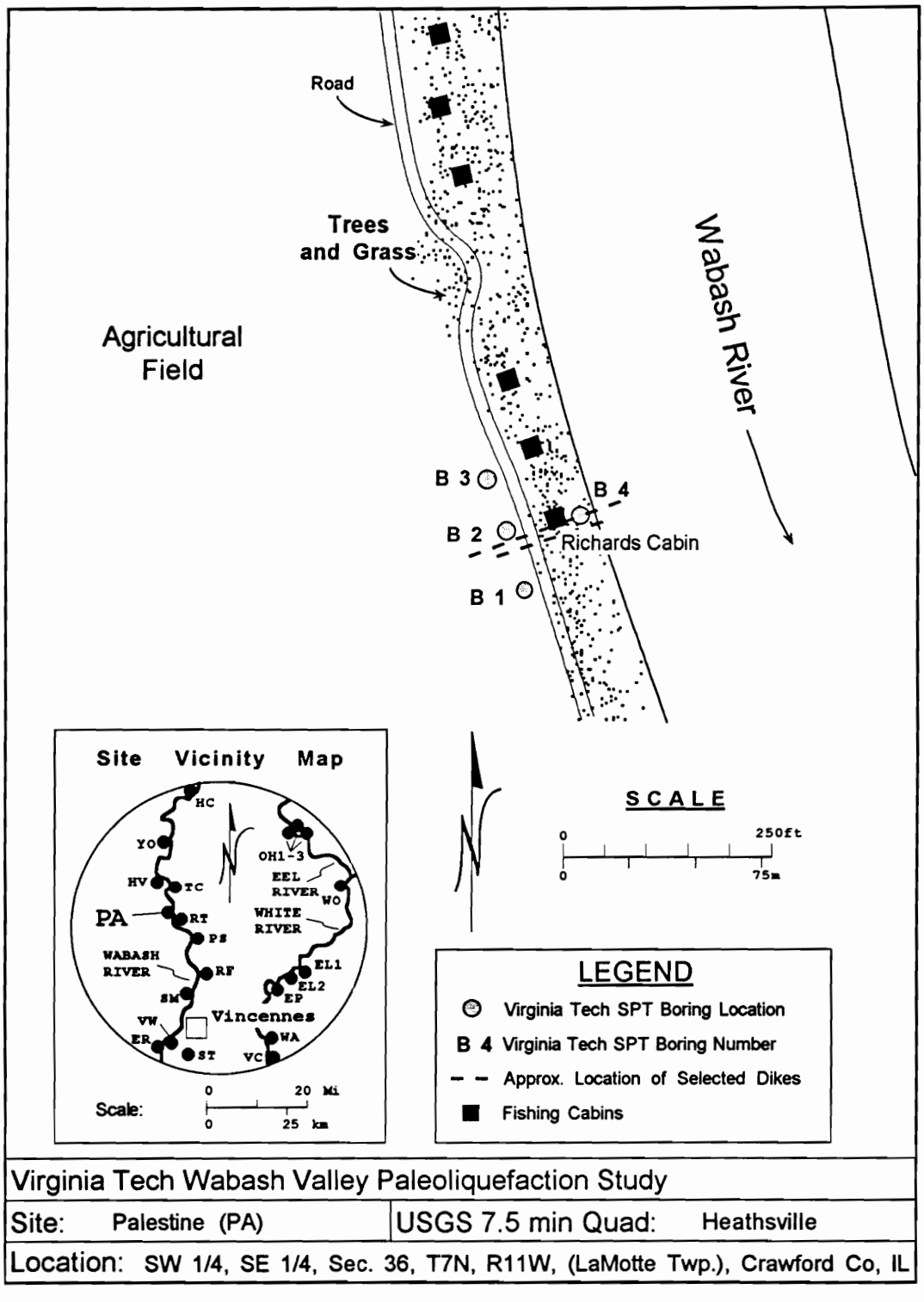

Figure 5.11. Site plan for site Palestine (PA)

the study site, and includes a site vicinity map. The site extends approximately 100 m north to south and contains two dikes approximately 0.02 and 0.15 m wide. The exposure of the sediments at this site also continues over a total length of approximately 750 m with no other observed liquefaction evidence.

The surficial soils present at the site consist of from 1.5 to 2.7 m of loose silty sand and sandy silt over 0.6 to 2 m of fat clay. These soils extend to the surface present at the time of the earthquake (approximately 3.4 to 3.8 m in depth). Beneath the paleo-surface is a 1.2 to 1.6 m thickness of lean to fat clay overlying a natural levee deposit, which in turn overlies the liquefiable sediments. The levee deposits of interbedded sand and silt are approximately 0.8 to 1.4 m in thickness. The liquefiable soil consists of a 0.5 m layer of loose to medium dense gravelly sand overlying medium dense sandy gravel and gravelly sand. A generalized soil profile of the site is given in Figure 5.12. The soil conditions between boring locations were interpreted based on exposed soil in the river bank.

5.2.1.5.Site PB

The Peankishaw Bend site is located along the Illinois bank of the Wabash River approximately 56 km southwest of Vincennes, Indiana and 46 km northwest of Evansville, Indiana. Figure 5.13 provides a site plan for the study site, and includes a site vicinity map. The site extends approximately 150 m northwest to southeast and contains 2 dikes with widths of approximately 0.02 and 0.5 m.

The surficial soil present at the site consists of from 2.4 to 4.4 m of silt and lean clay overlying a natural levee deposit, which in turn overlies medium dense liquefiable sediments. The ground surface at the time of the earthquake is buried by 1.5 to 1.8 m of post-event sediments. The levee deposits of interbedded clay and sand extend to between 1.2 and 2.6 m below the surficial silts and clay. The liquefiable soil generally consists of a medium dense sand with gravel. Silt content of the liquefiable sediments ranges up to approximately 10%. At the northern end of the site, the base of the boring extended into an interbedded silt and clay layer overlying a fine sand with interbedded, laminated silt.

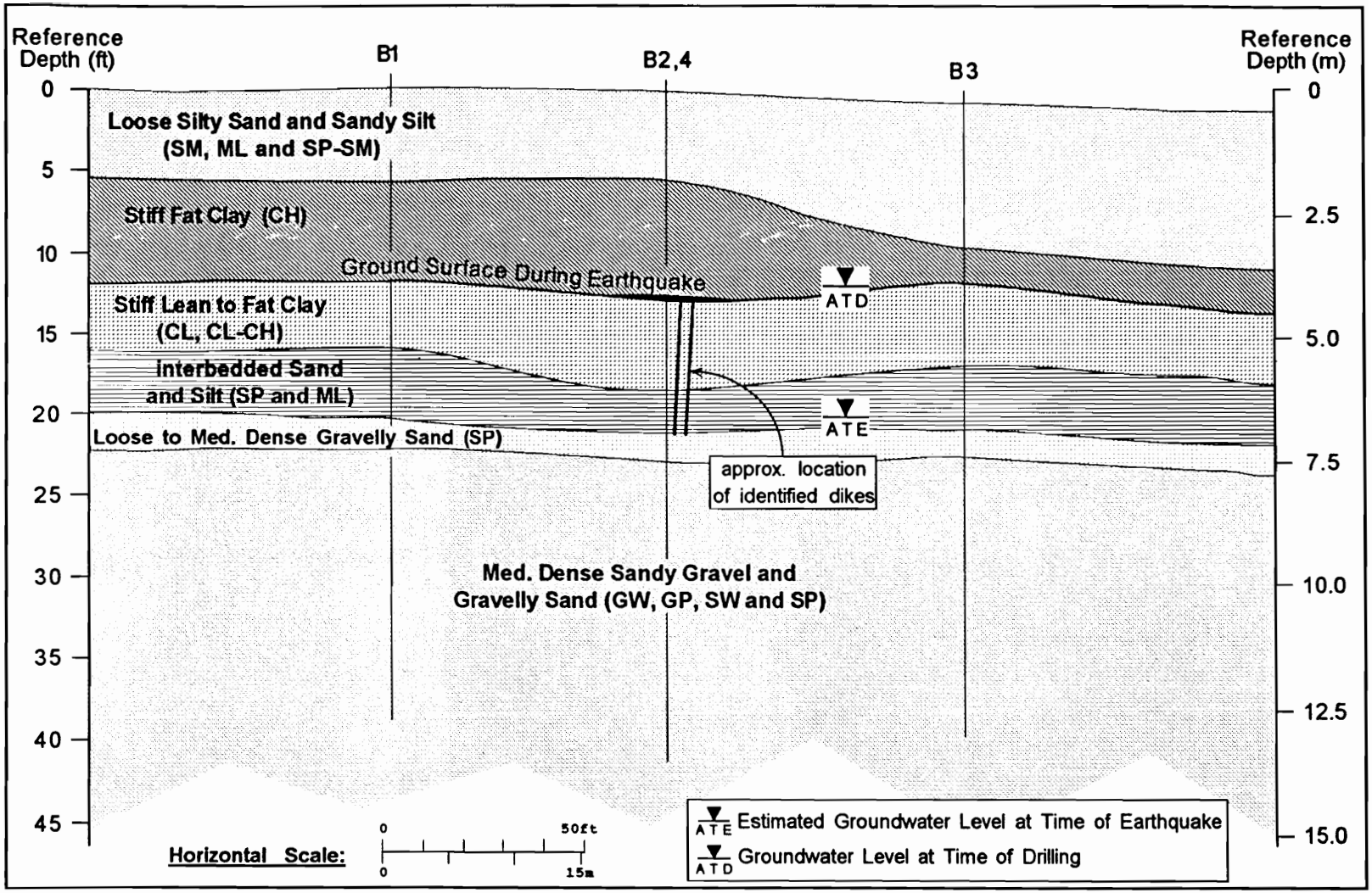

Figure 5.12. Near surface soil profile for site Palestine (PA)

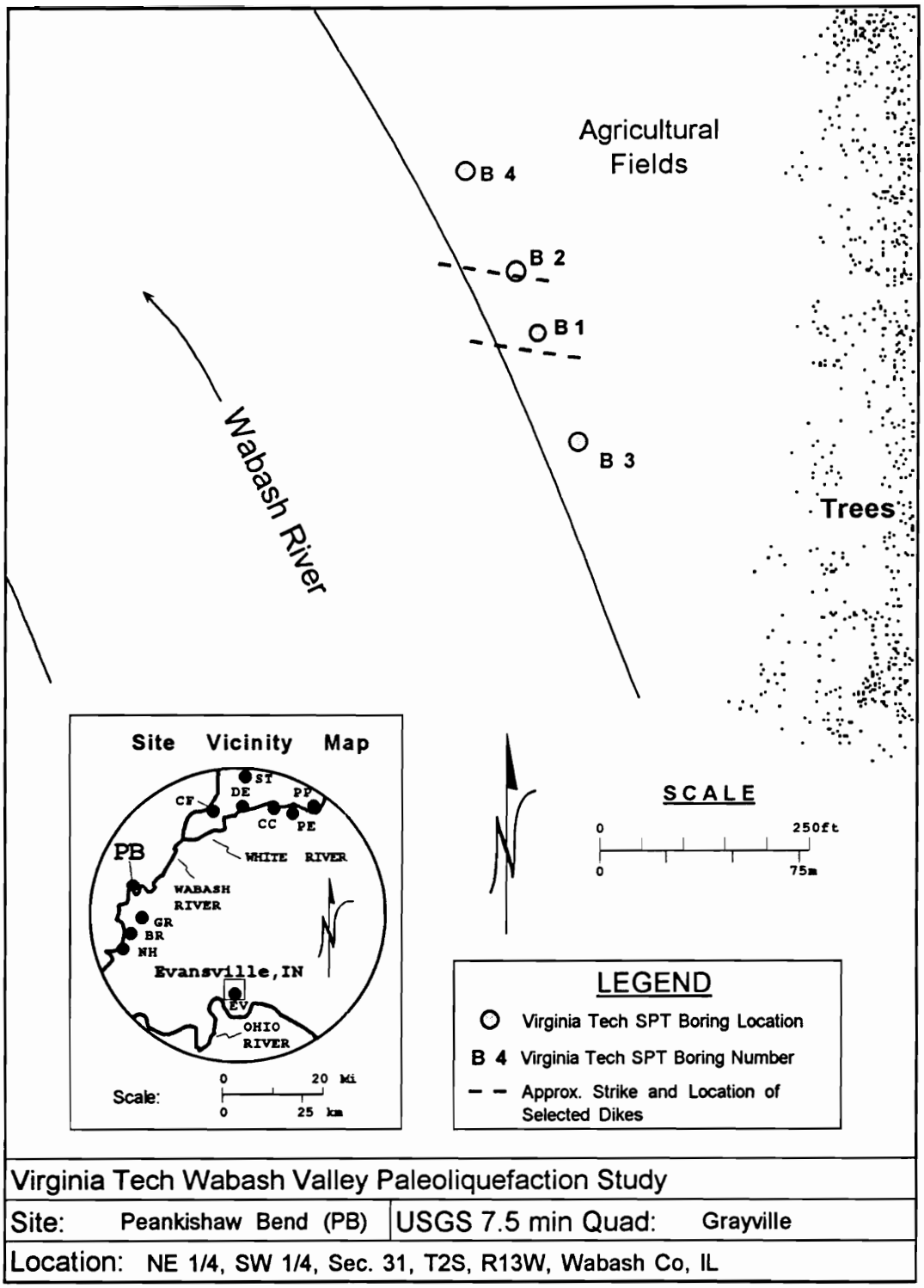

Figure 5.13. Site plan for site Peankishaw Bend (PB)

Eight in-situ density tests were performed in the vicinity of the dikes at this site. The tests show relative densities of 55% to 114% in the upper 2 m of the liquefiable deposit. The two deepest in-situ tests performed were approximately 2.5 m below the cap and appear to reveal a loose zone with relative density test results of 19% and 25% that was missed by the penetration testing. The remaining values are consistent with the penetration test data obtained, however. A generalized soil profile of the site is given in Figure 5.14. The soil conditions between boring locations were interpreted based on exposed soil in the river bank and on hand probe data provided by Professor Munson (1994) of Indiana University. The lateral and lower bounds indicated for the soils encountered at the base of exploration B4 are very rough estimates only.

5.2.1.6.Site YO

The York site is located along the Illinois bank of the Wabash River approximately 59 km north of Vincennes, Indiana and 31 km southwest of Terre Haute, Indiana. Figure 5.15 provides a site plan for the study site, and includes a site vicinity map. The site extends approximately 300 m north to south and contains dikes of approximately 0.02 to 0.10 m in width.

The surficial soils present at the site consist of from 2.4 to 3.8 m of lean to fat clay overlying 2 to 2.6 m of fat clay, which in turn overlies 0.8 to 1.5 m of another lean to fat clay. The surface present at the time of the earthquake is approximately 2.9 to 4 m below the modern surface. Levee deposits of clay and sand with a thickness of approximately 1.2 to 2.1 m are present below the surficial clay soils. The liquefiable soils consists of 2 m of loose to medium dense sand overlying medium dense gravelly sand. Silt contents of the gravelly soil range to approximately 10%. A generalized soil profile of the site is given in Figure 5.16. The soil conditions between boring locations were interpreted based on exposed soil in the river bank and on hand probe data provided by Professor Munson (1994) of Indiana University.

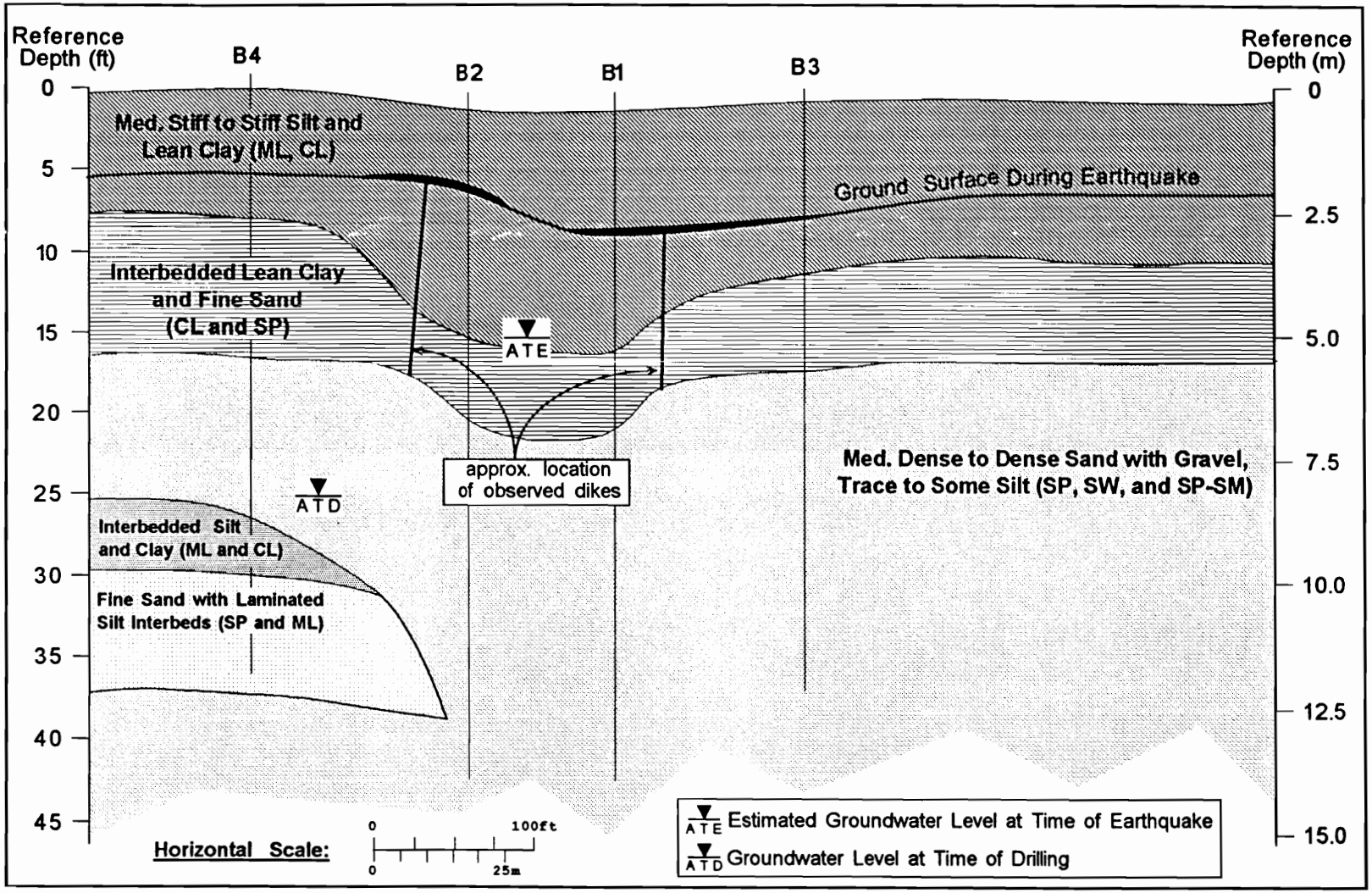

Figure 5.14. Near surface soil profile for site Peankishaw Bend (PB)

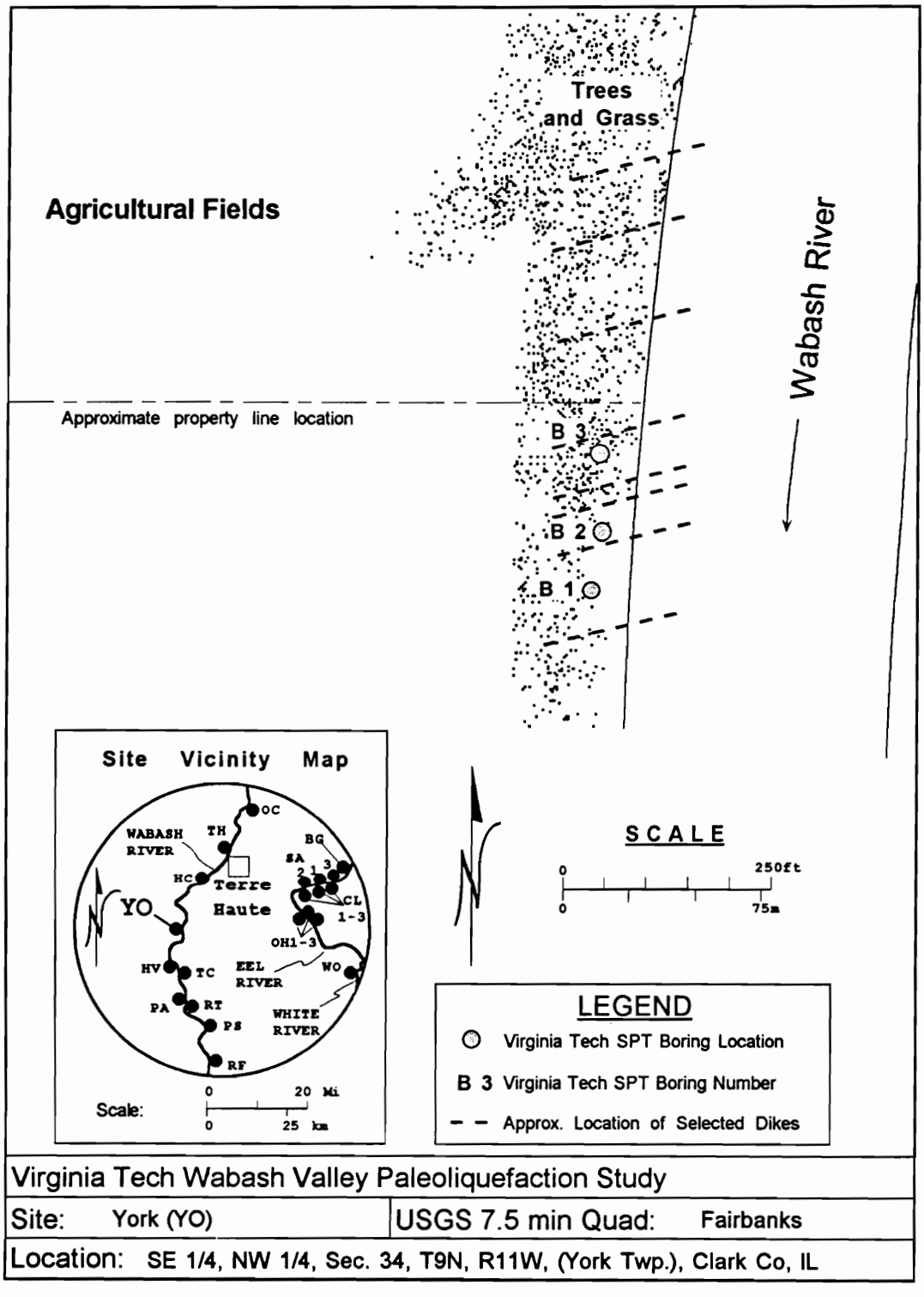

Figure 5.15. Site plan for site York (YO)

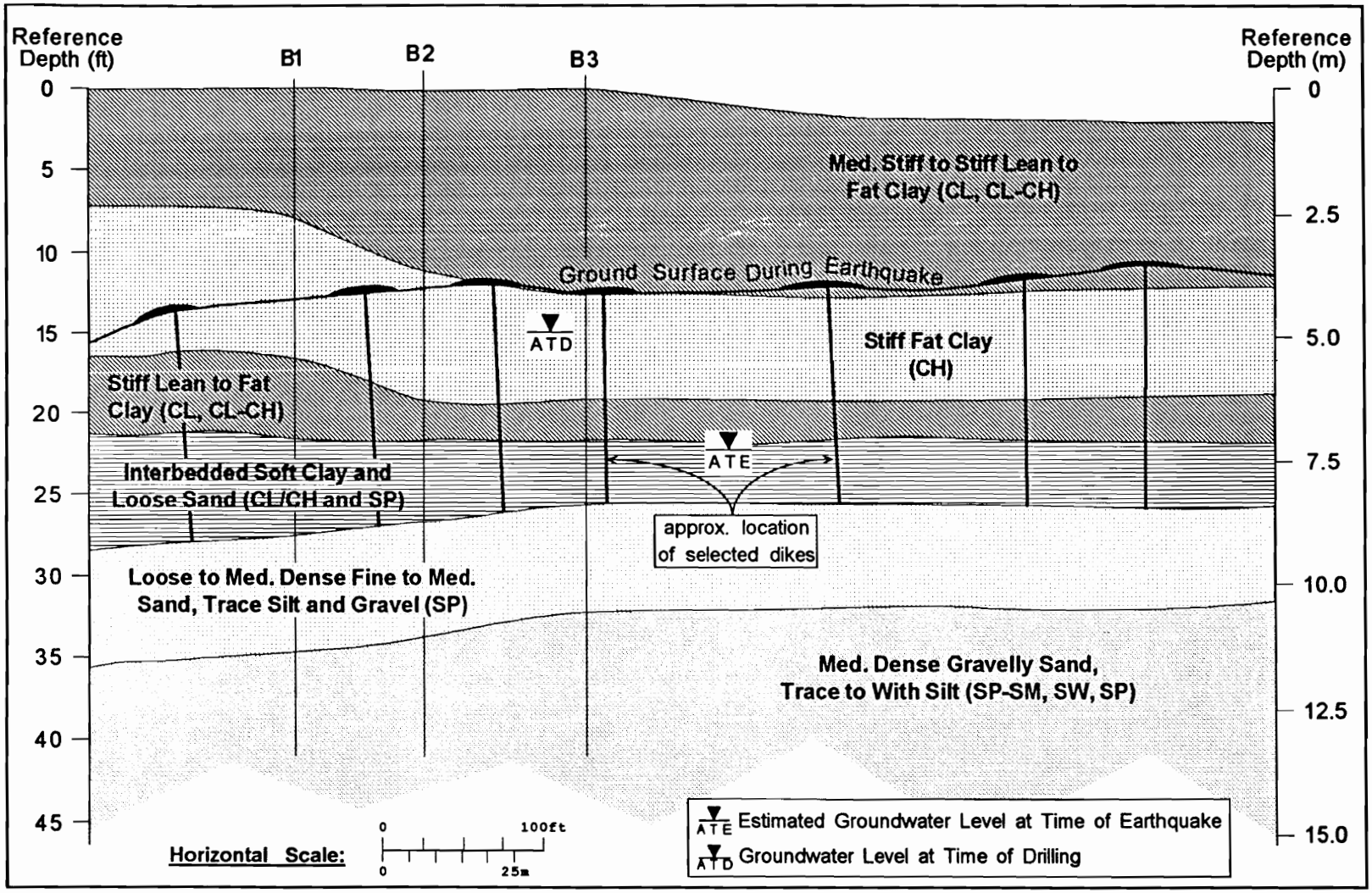

Figure 5.16. Near surface soil profile for site York (YO)

5.2.1.7.Site HA

The Haysville site is located along the southern bank of the East Fork of the White River approximately 56 km southeast of Vincennes, Indiana. Figure 5.17 provides a site plan for the study site, and includes a site vicinity map. The site extends approximately 230 m west to east. Two dikes have been identified at this site, but many more are likely to exist. The sediments extending beyond the observed dikes are contemporary with those at the dikes. Slumping of the surficial soils along the river bank has obscured the sediments containing the observed dikes along most of the exposure. The subsurface exploration at this site was limited to the vicinity of the dikes identified in the exposed soil profile in the river bank.

The surficial soil present at the site consists of approximately 5.6 m of lean clay with silt and trace to some fine sand. The surface present at the time of the earthquake is approximately 2.9 m below the modern surface. A natural levee deposit of clay and sand approximately 0.4 m thick is present below the surficial clay soil. The liquefiable soil consists of medium dense to dense predominantly fine to medium sand, with silt and a trace of gravel. A generalized soil profile of the site is given in Figure 5.18. The soil conditions beyond the boring locations were interpreted based on exposed soil in the river bank and on information provided by Professor Munson (1994) of Indiana University. Beyond the exploration locations the soil profile can be considered approximate only.

5.2.1.8.Site MA

The Maunie site is located along the Illinois bank of the Wabash River approximately 86 km southwest of Vincennes, Indiana and approximately 42 km west of Evansville, Indiana. Figure 5.19 provides a site plan for the study site, and includes a site vicinity map. The site extends approximately 610 m northwest to southeast and contains dikes ranging to approximately 0.3 m in width.

The surficial soil present at the site consists of approximately 2 to 3.5 m of fat clay with silt overlain at the eastern end of the site by up to approximately 1 m of lean clay.

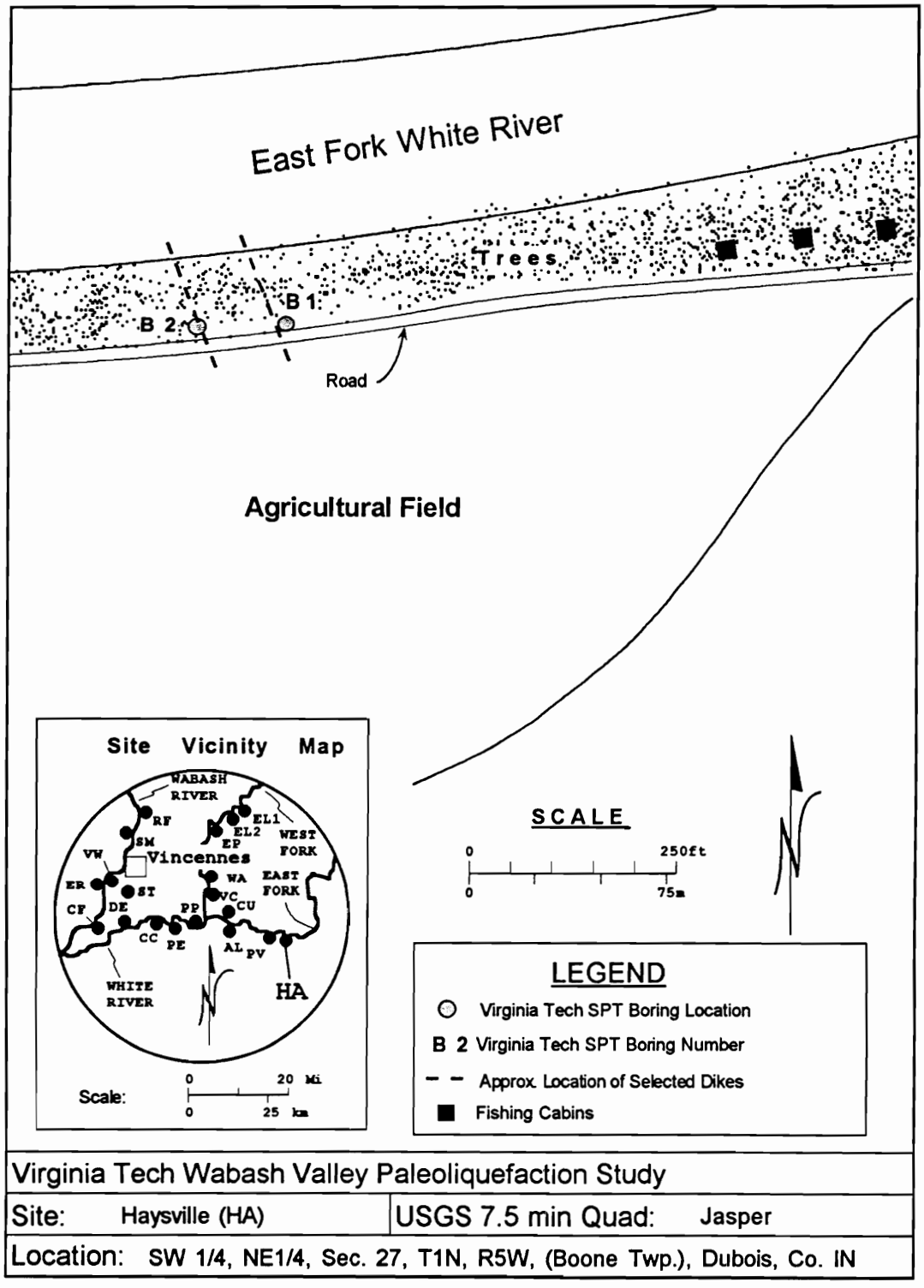

Figure 5.17. Site plan for site Haysville (HA)

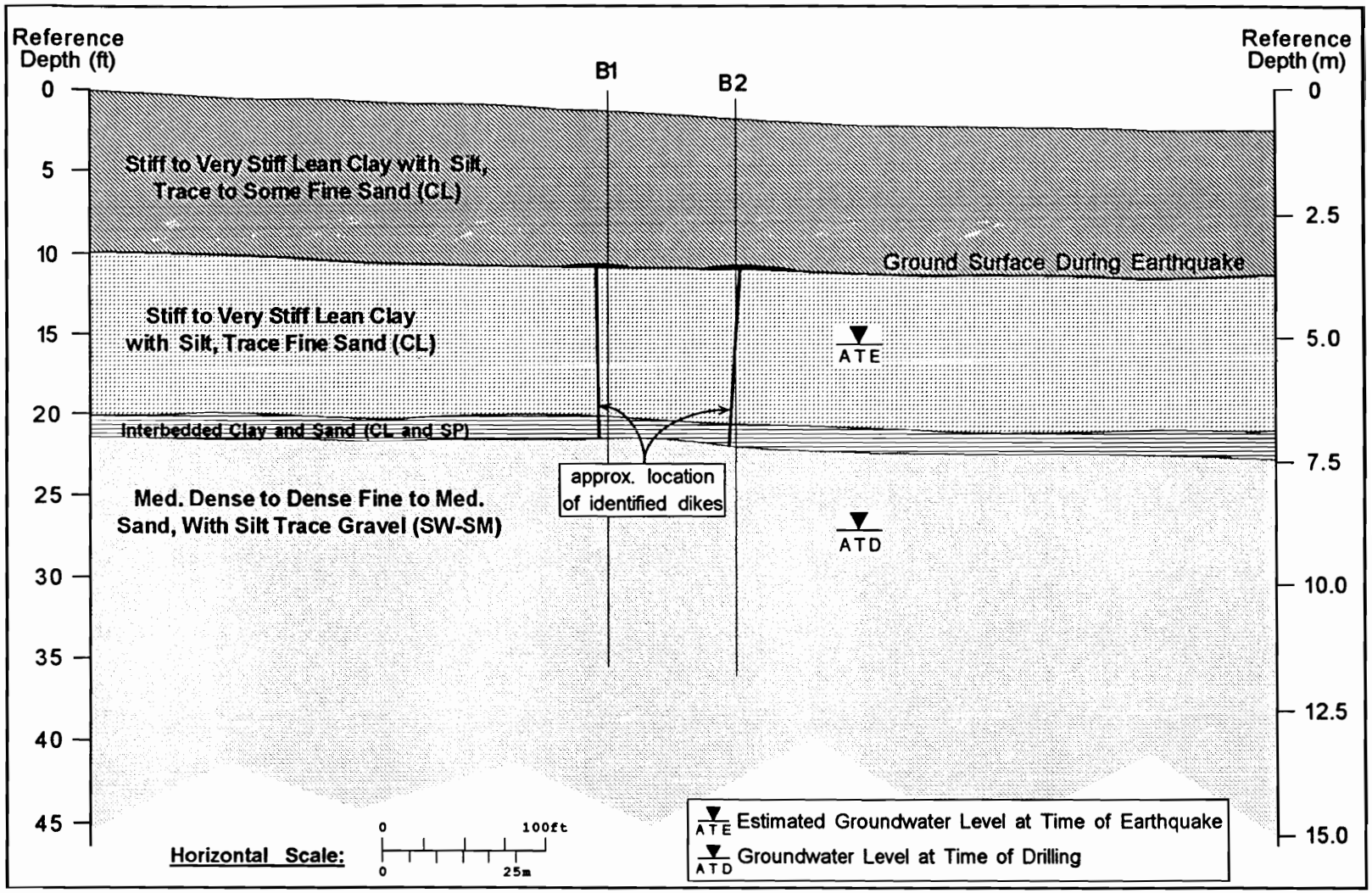

Figure 5.18. Near surface soil profile for site Haysville (HA)

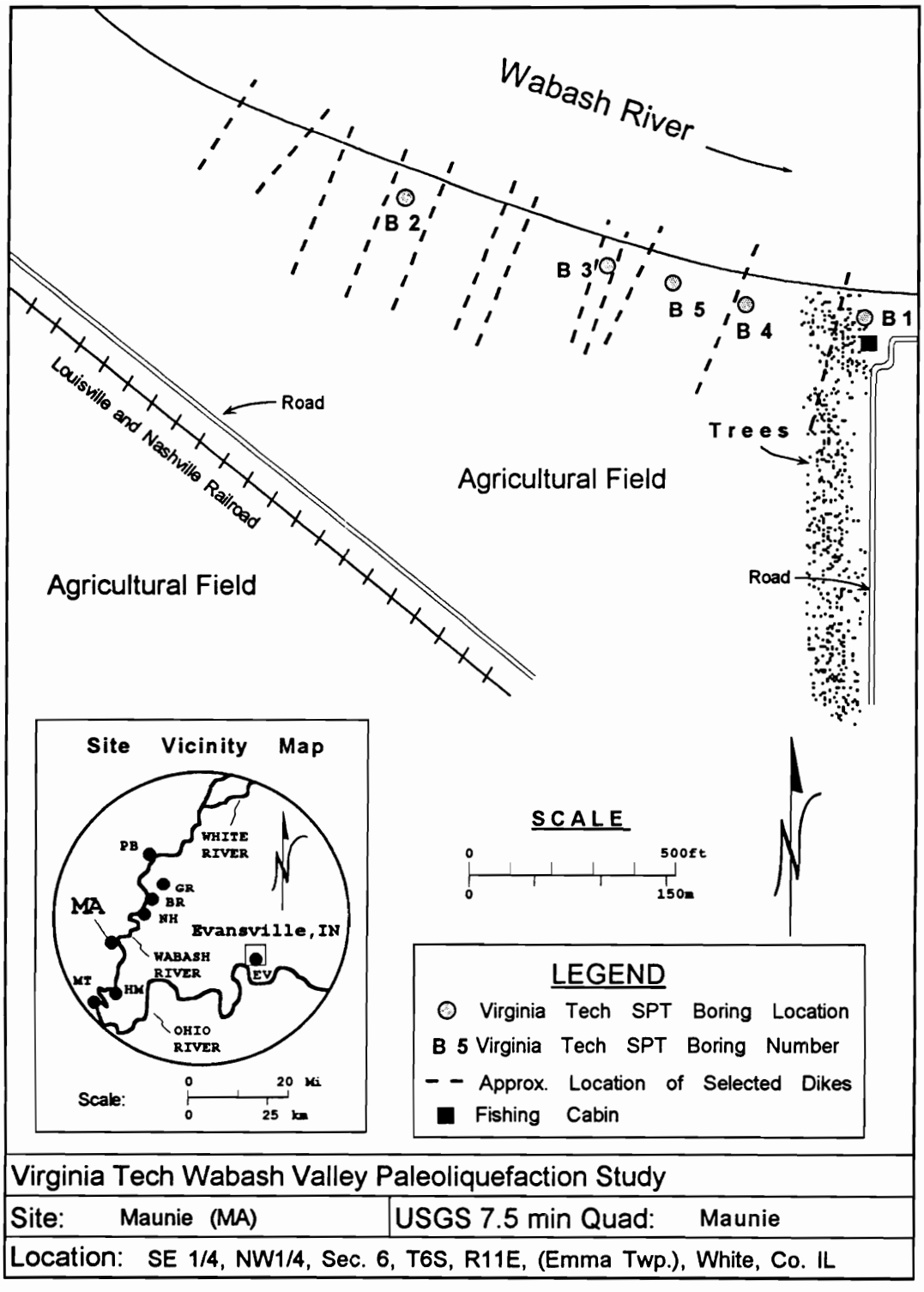

Virginia Tech Wabash Valley Paleoliquefaction Study	
Site: Maunie (MA)	USGS 7.5 min Quad: Maunie
Location: SE 1/4, NW1/4, Sec. 6, T6S, R11E, (Emma Twp.), White, Co. IL	

Figure 5.19. Site plan for site Maunie (MA)

The surface present at the time of the earthquake is between approximately 0.5 and 1.5 m below the modern surface. A levee deposit of interbedded clay and sand approximately 0.7 to 2.1 m thick is present below the surficial clay soils. The liquefaction dikes originate in the sands present within the levee deposits at this site. The soil present below the levee deposit consists of medium dense to dense predominantly fine to medium sand with trace silt, and trace to with gravel. Four in-situ density tests were performed at this site. Two just below the cap, in the sand present in the interbedded zone, and two in the medium dense to dense soils below. These tests show relative densities of 17% and 23% in the upper disturbed portion of the deposit. Two in-situ tests performed in the lower dense material gave relative density results of 71% and 76%. These values are consistent with the penetration test data obtained. A generalized soil profile of the site is given in Figure 5.20. The soil conditions between and beyond the boring locations were interpreted based on exposed soil in the river bank and on hand probe data provided by Professor Munson (1994) of Indiana University.

5.2.1.9.Site WO

The Worthington site is located along the northwest bank of a recently cut off meander of the West Fork of the White River approximately 65 km northeast of Vincennes, Indiana and 56 km southeast of Terre Haute, Indiana. Figure 5.21 provides a site plan for the study site, and includes a site vicinity map. The site extends approximately 200 m northeast to southwest and contains four dikes ranging to approximately 0.15 m in width. Only one of the dikes extends to the surface present at the time of the earthquake. To the southwest of the identified dikes the soils present at the time of the earthquake are truncated by a filled post-earthquake meander channel. The evidence of liquefaction may have been more extensive at this site than is indicated by the observed dikes.

The surficial soil present in the vicinity of the observed dikes at this site consists of approximately 2.5 m of lean clay with fine sand. The surface present at the time of the

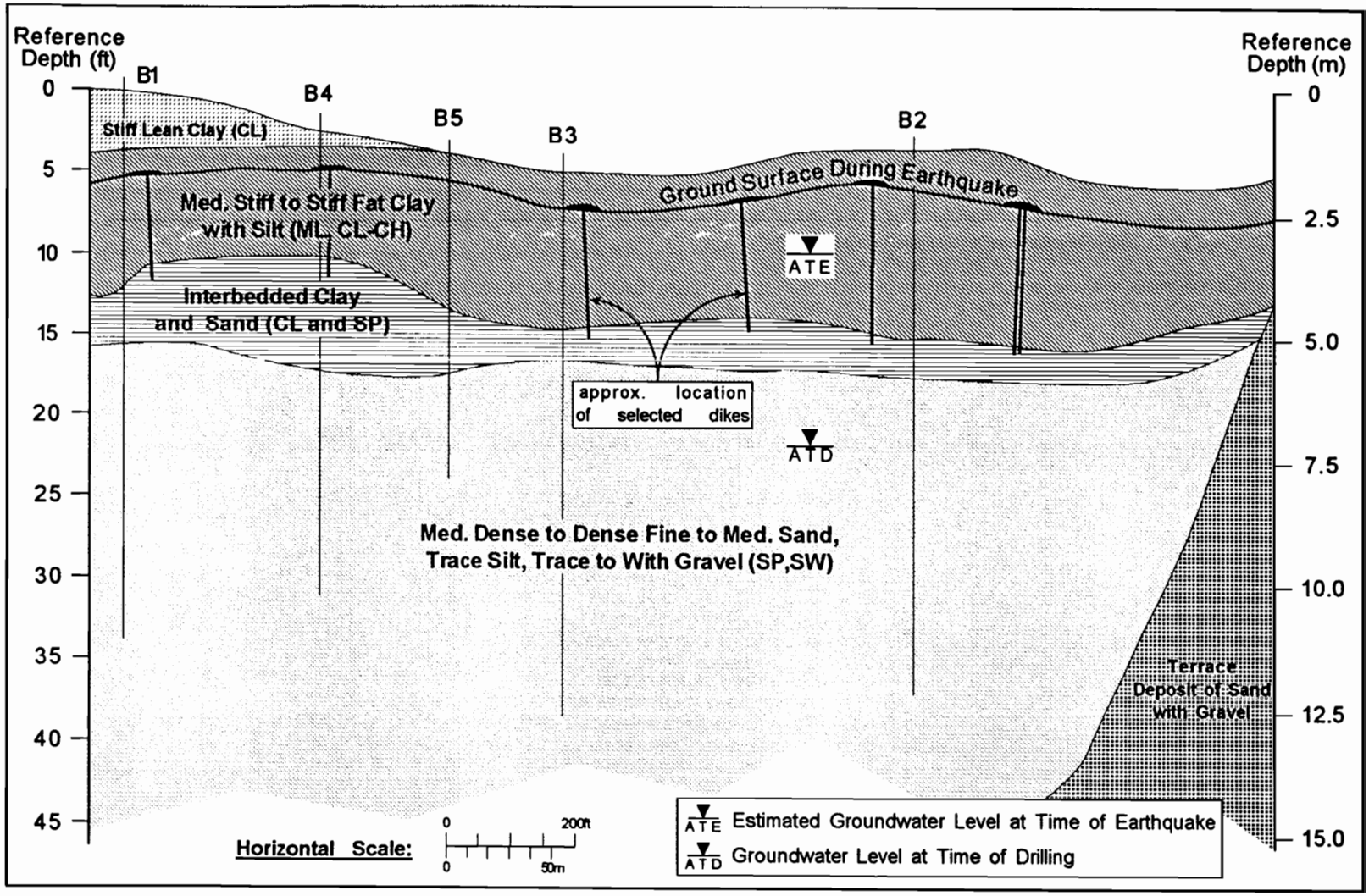

Figure 5.20. Near surface soil profile for site Maunie (MA)

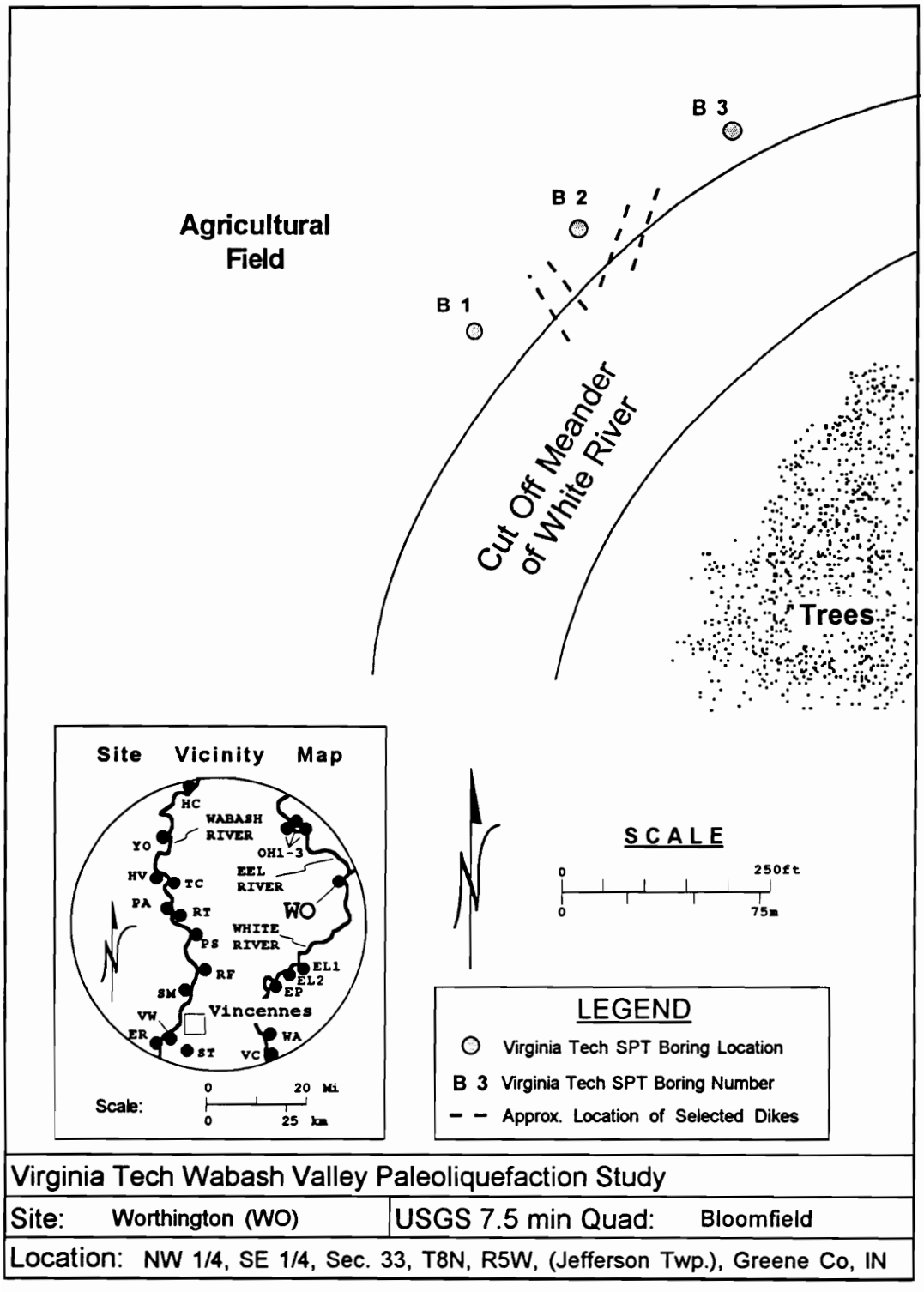

Figure 5.21. Site plan for site Worthington (WO)

earthquake is between approximately 1.6 and 1.9 m below the modern surface. A levee deposit of interbedded silty clay and silty sand with gravel approximately 1.4 to 1.6 m thick is present below the surficial clay soils. The soils present below the levee deposit consist of medium dense sand with silt and gravel overlying medium dense sand with gravel. Boring locations B1 and B2 encountered sandstone bedrock at depths of 10.8 and 12.4 m. A generalized soil profile of the site is given in Figure 5.22. The soil conditions between and beyond the boring locations were interpreted based on exposed soil in the river bank and on hand probe data provided by Professor Munson (1994) of Indiana University.

5.2.1.10.Site TH

The Terre Haute site is located in Indiana along the western bank of the Wabash River approximately 90 km north of Vincennes, Indiana and across the river from Terre Haute, Indiana. Figure 5.23 provides a site plan for the study site, and includes a site vicinity map. The site extends approximately 180 m northeast to southwest and contains four liquefaction feature with dikes ranging to approximately 0.12 m in width.

The surficial soils consist of approximately 2.3 m of lean clay with silt and trace fine sand overlying approximately 6.5 to 7.3 m of lean to fat clay with silt and trace fine sand. The surface present at the time of the earthquake is between approximately 5 and 5.4 m below the modern surface. No levee deposit was observed to be present at this site. The liquefiable soils present consist of medium dense to dense sand with gravel and silt, clayey gravel and sandy gravel with silt. A generalized soil profile of the site is given in Figure 5.24. The soil conditions between and beyond the boring locations were interpreted based on a limited exposure of soil in the river bank and should be considered approximate only.

5.2.1.11.Site BG

The Bowling Green site is located along the west bank of the Eel River approximately 90 km northeast of Vincennes, Indiana and 34 km east of Terre Haute,

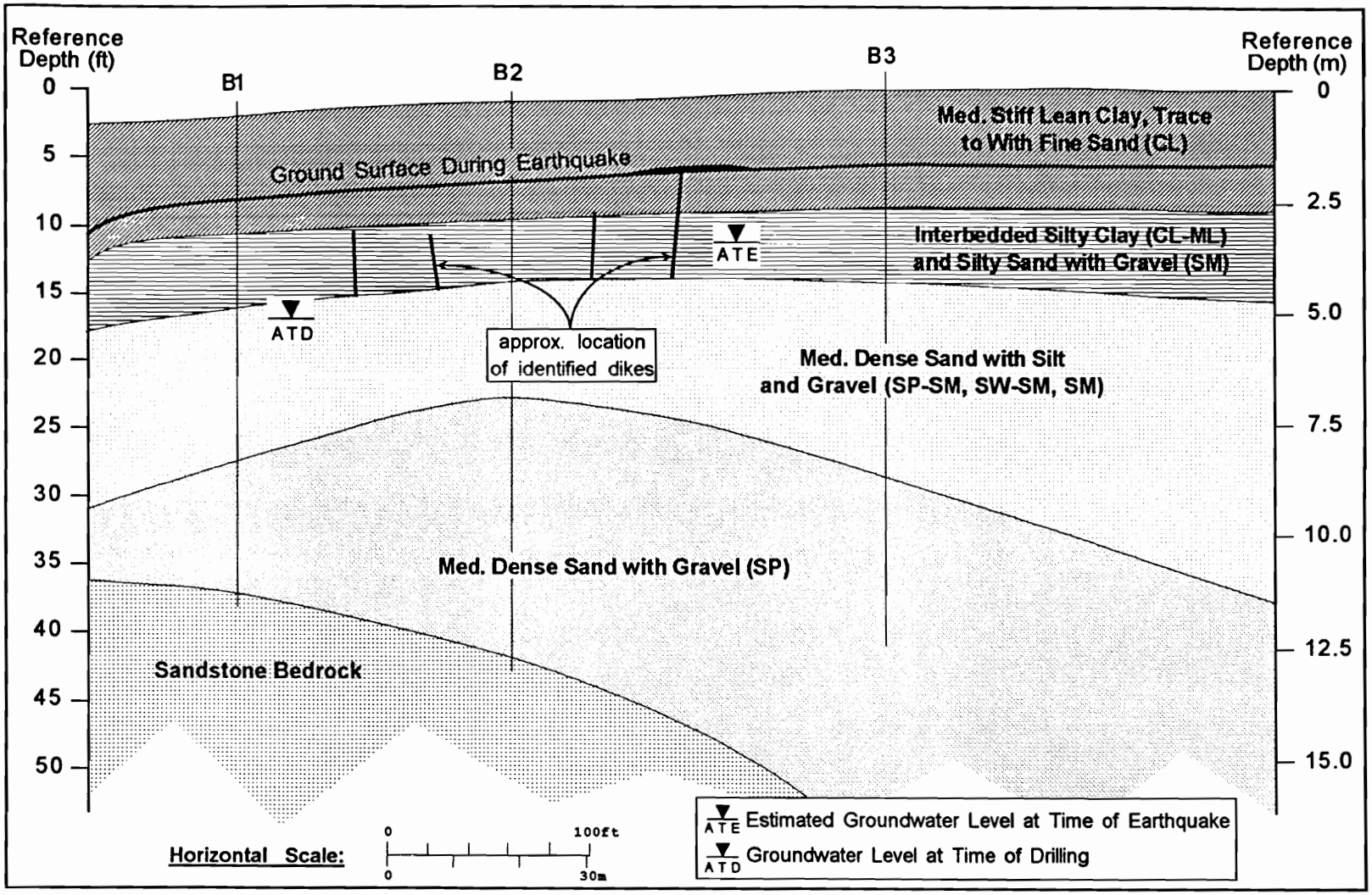

Figure 5.22. Near surface soil profile for site Worthington (WO)

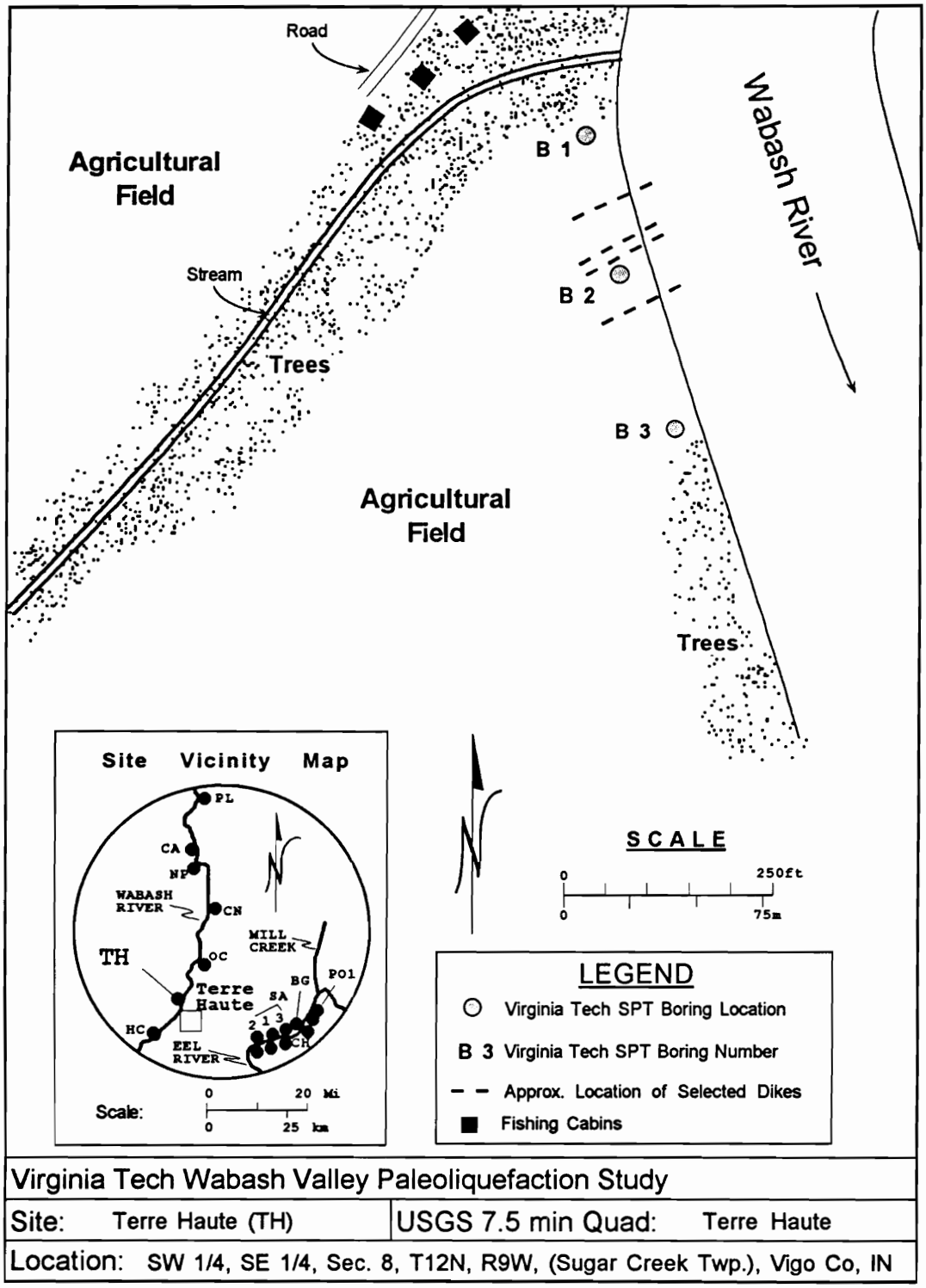

Figure 5.23. Site plan for site Terre Haute (TH)

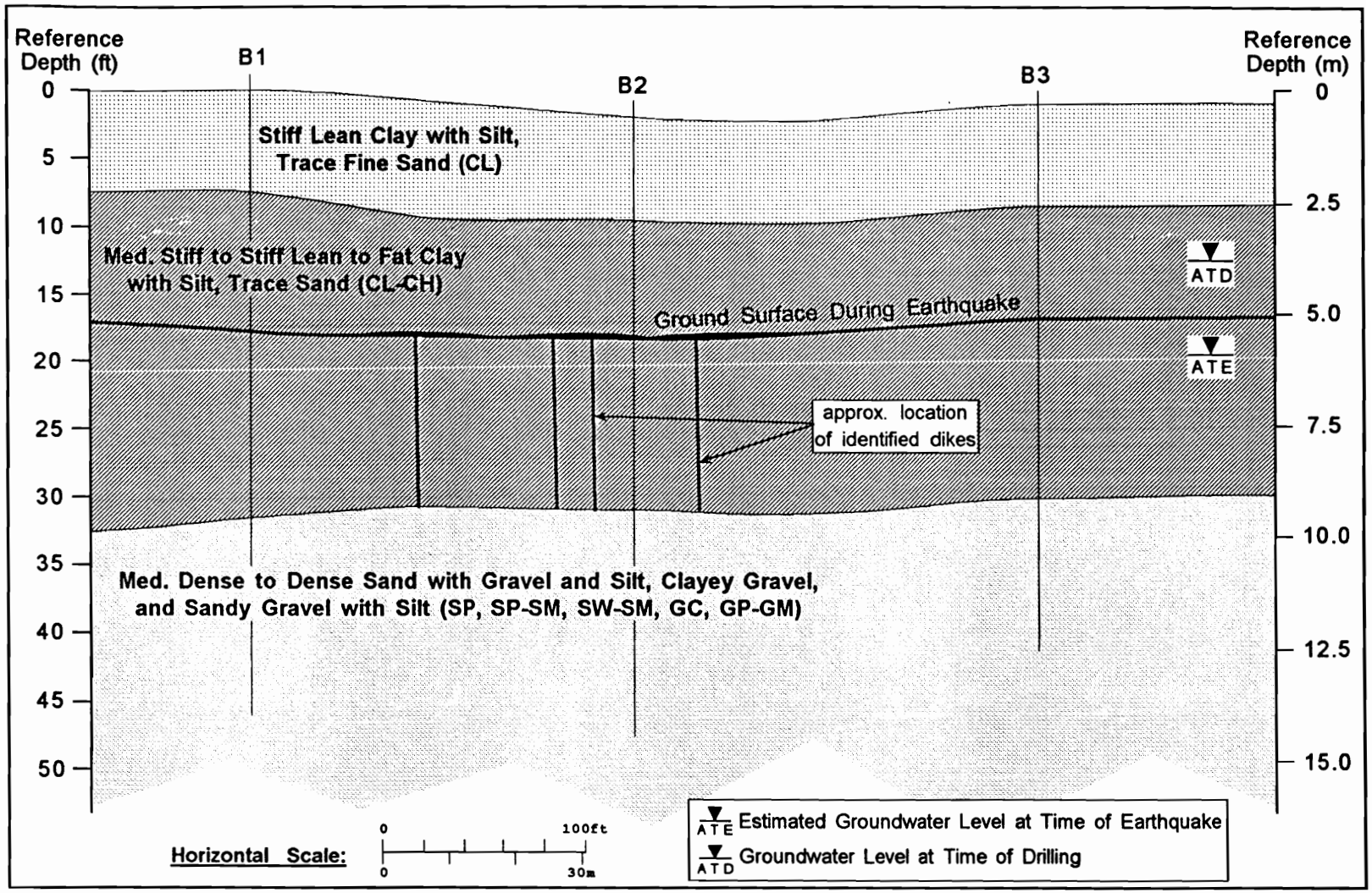

Figure 5.24. Near surface soil profile for site Terre Haute (TH)

Indiana. Figure 5.25 provides a site plan for the study site, and includes a site vicinity map. The site extends approximately 60 m north to south and contains two small dikes. The top of the dikes are truncated by a filled post-earthquake meander channel that advanced from the north and was cut off before erasing the remaining liquefaction evidence The remaining portions of the dikes point to a blow surface present just above and to the south of their location. The evidence of liquefaction may have been more extensive at this site than is indicated by the observed dikes.

The surficial soil at this site in the vicinity of the observed dikes consists of approximately 1.8 m of lean clay with fine to medium sand and silt, and extends to the surface present at the time of the earthquake. Beneath the blow surface, the dikes cut through approximately 3.5 m of lean clay with silt, trace fine sand. A levee deposit of interbedded clay and fine sand approximately 1.2 m thick is present below the clay soils. The liquefiable soil deposits consist of approximately 0.7 m of loose fine to medium sand with silt overlying medium dense to dense predominantly fine to medium sand with silt and gravel. A generalized soil profile of the site is given in Figure 5.26. The soil conditions between and beyond the boring locations were interpreted based on exposed soil in the river bank and on information provided by Professor Munson (1994) of Indiana University.

5.2.1.12.Site NP

The Newport site is located in Indiana along the western bank of the Wabash River approximately 133 km north of Vincennes, Indiana and 45 km north of Terre Haute, Indiana. Figure 5.27 provides a site plan for the study site, and includes a site vicinity map. The site extends approximately 150 m northwest to southeast and contains two liquefaction features observable in the river bank approximately 0.12 and 0.24 m in width. At this site the meander of the river nearly parallels the strike of the dikes. Only features that are being actively eroded from the river bank are exposed to view. The liquefaction evidence at this site may be now or may have been much more extensive than is apparent

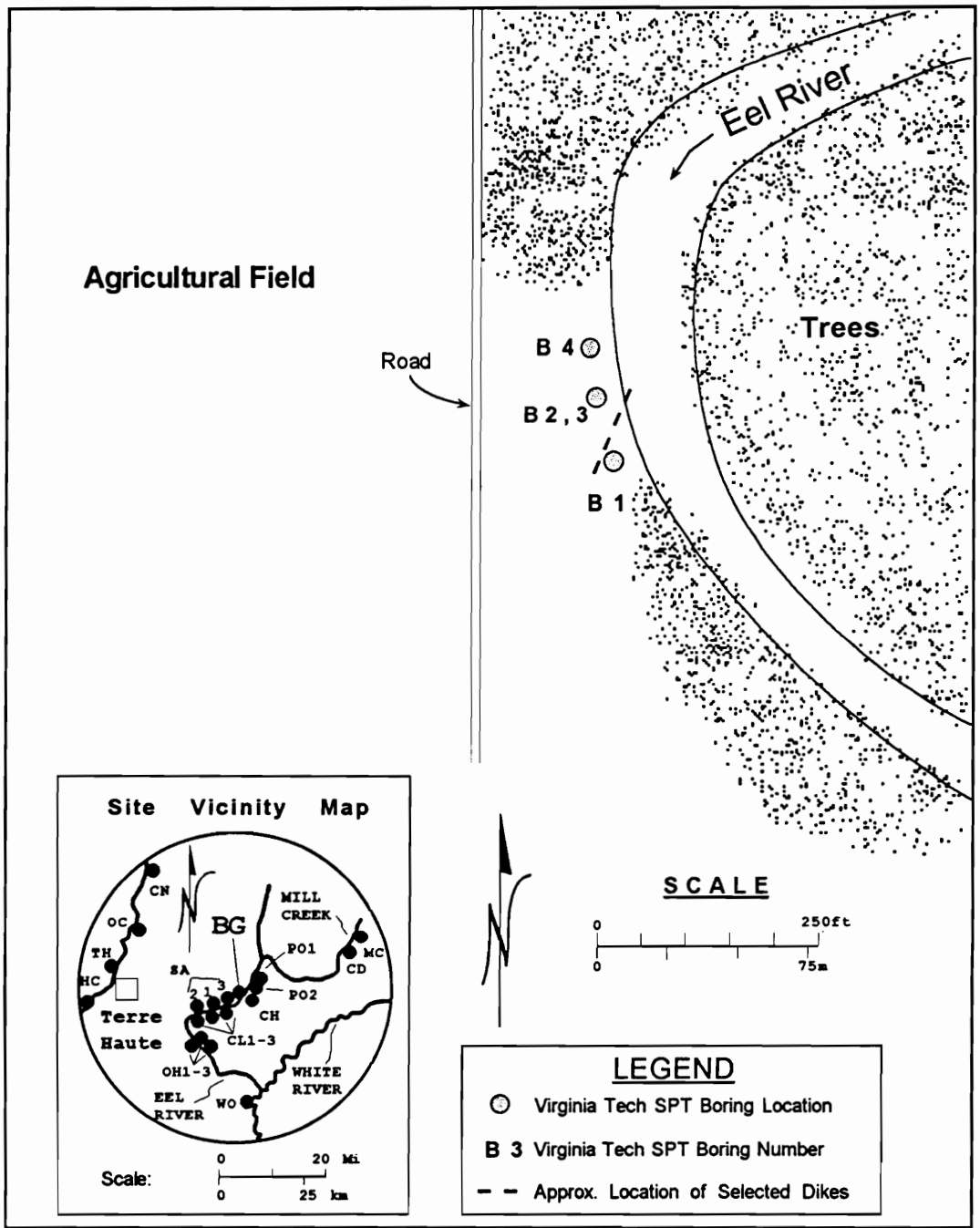

Figure 5.25. Site plan for site Bowling Green (BG)

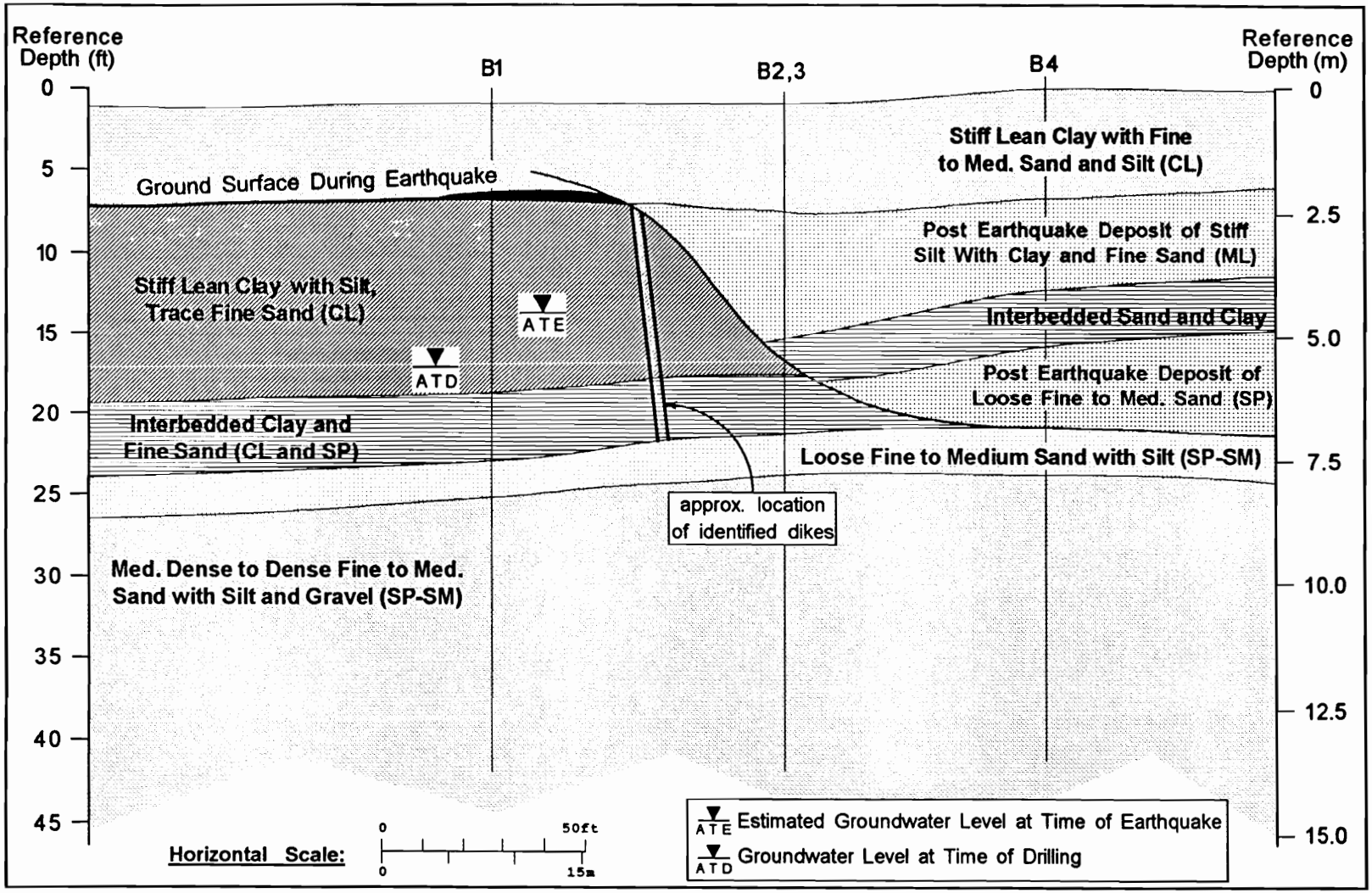

Figure 5.26. Near surface soil profile for site Bowling Green (BG)

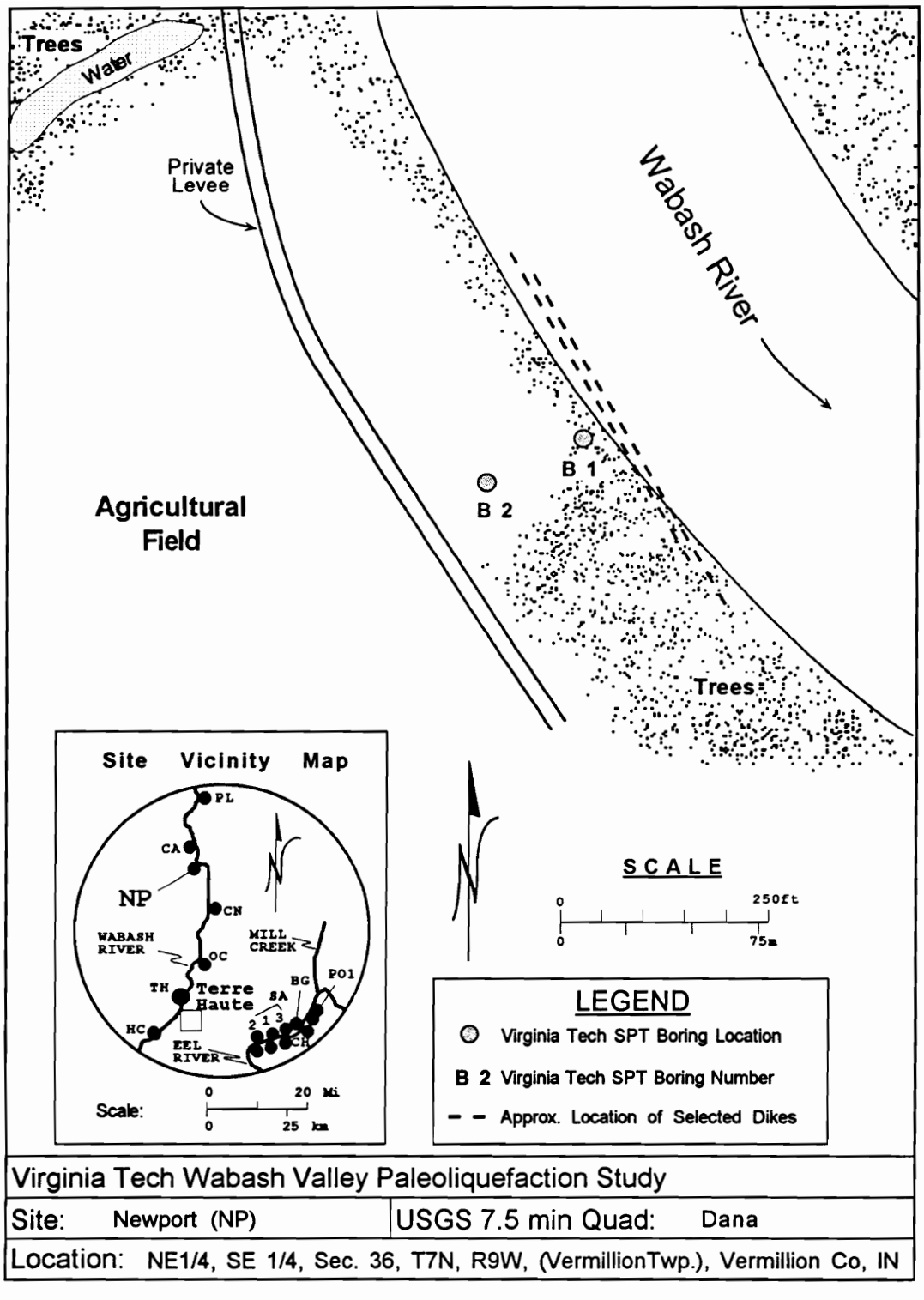

Figure 5.27. Site plan for site Newport (NP)

from the observable features. During drilling an additional feature was discovered approximately 45 from the edge of the river. Other dikes may also be present at this site, and others are likely to have been erased by the river prior to this study.

The surficial soils consist of approximately 6.5 m of fat clay with silt and trace fine sand. The surface present at the time of the earthquake is approximately 3.8 m below the modern surface. A loose silty gravelly sand layer approximately 0.3 m thick exists at a depth of 4.7 to 5.3 m. One of the dikes observed in the river bank extends to this layer only. No levee deposit was observed to be present at this site. The liquefiable soils present consist of a loose sandy gravel with trace silt 0.6 to 0.8 m thick overlying medium dense to dense gravelly sand with silt, and gravel with sand. A generalized soil profile of the site is given in Figure 5.28. The soil conditions between and beyond the boring locations were interpreted based on a limited exposure of soil in the river bank and should be considered approximate only.

5.2.1.13.Site PL

The Perrysville site is located in Indiana along the eastern bank of the Wabash River approximately 152 km north of Vincennes, Indiana and 64 km north of Terre Haute, Indiana. Figure 5.29 shows a site plan for the study site, and includes a site vicinity map. The site extends approximately 250 m northeast to southwest and contains liquefaction features observable in the river bank at each end of the site. Two levees once used for a now-abandoned canal are present at the southern end of the site. A post-event filled channel deposit is present in the central portion of the site.

The surficial soils in the vicinity of the dikes consist of approximately 2.1 to 2.7 m of clayey silt. This deposit contains an approximately 0.2 m thick loose silty gravel layer at a depth of 1.8 m at the northern end of the site. Below the surficial silt lies a layered sandy silt, and silty sand with gravel deposit approximately 2.2 m thick. The surface present at the time of the earthquake is within this layer, approximately 3.4 m below the modern surface. The dike at the southern end of the site extends to a blow surface at this

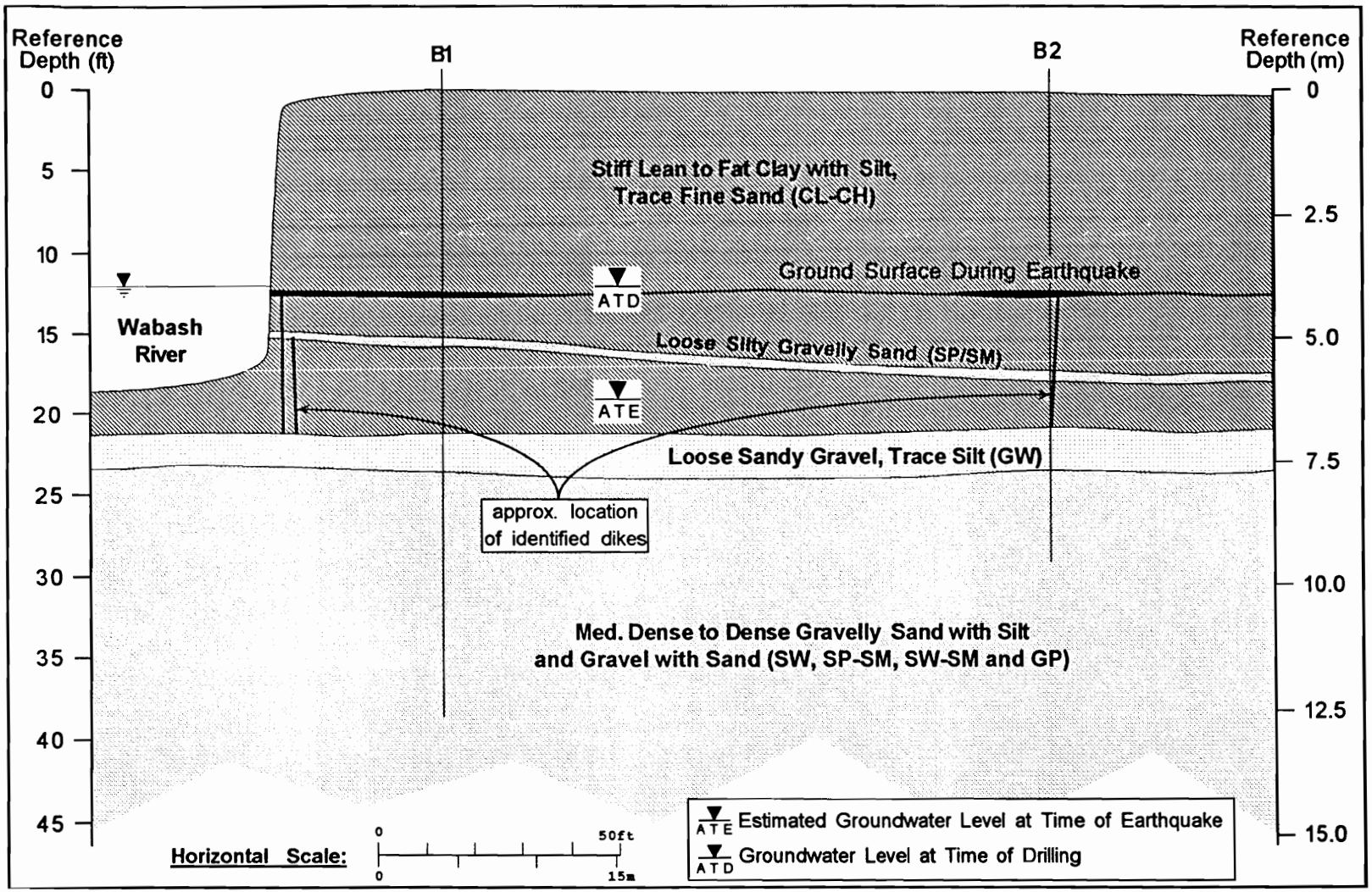

Figure 5.28. Near surface soil profile for site Newport (NP)

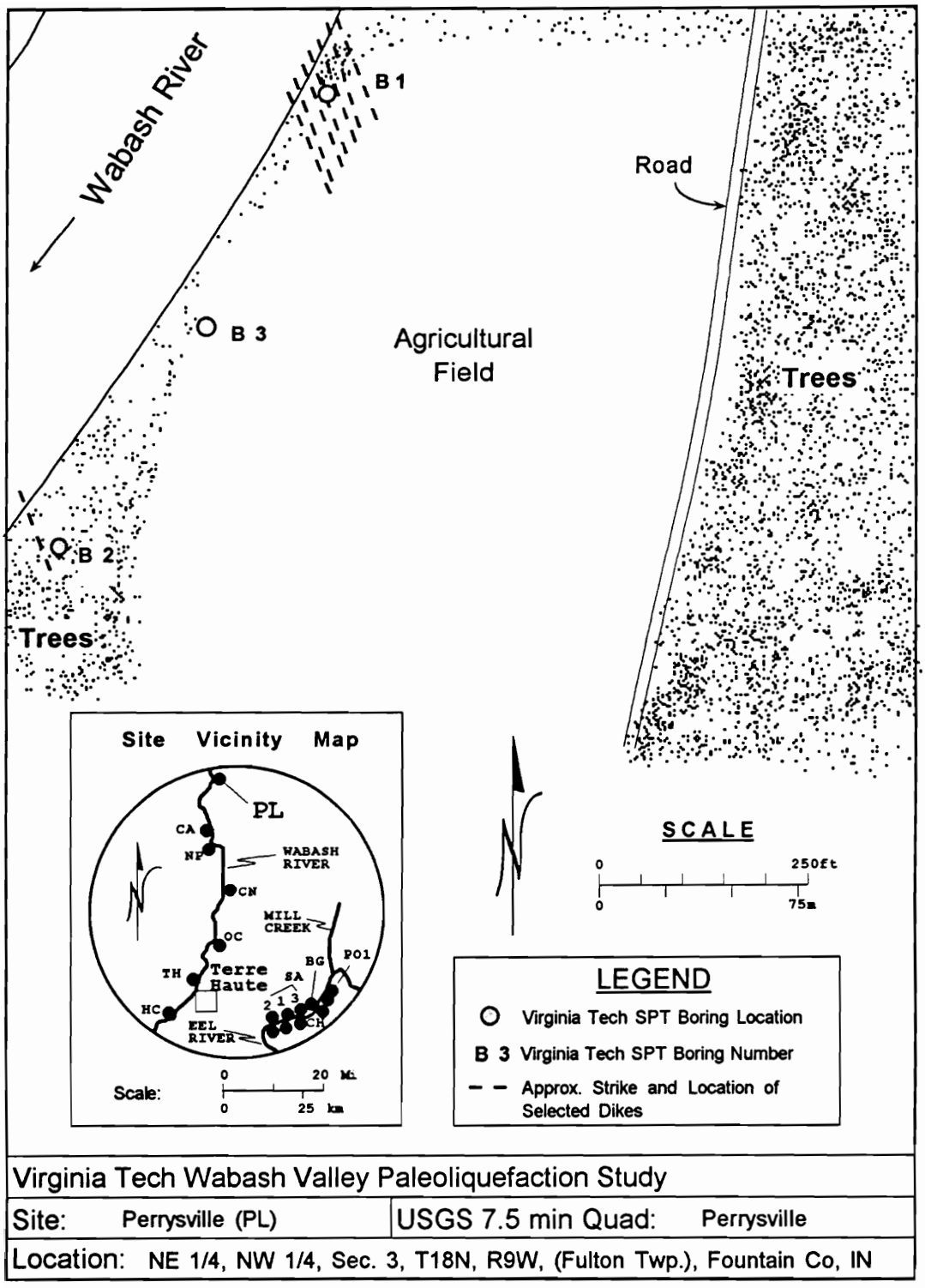

Figure 5.29. Site plan for site Perrysville (PL)

level. The dikes present at the northern end of the site terminate in a gravel lens at a depth of approximately 4.1 m. Below the layered silt and sand is an interbedded clay and sand layer between 0.4 and 0.9 m thick, overlying a lean clay layer between 1.1 and 1.3 m in thickness. This in turn overlies an interbedded sand and lean clay layer approximately 2.5 m in thickness. A fine to medium sand layer is present within this portion of the deposit at the northern end of the site. Below this layered sand and clay is a loose to medium dense fine sand layer between 1 and 2 m thick. The base of all borings encountered a sandstone bedrock.

The boring at the center of the site encountered the post-event channel fill deposit. This contained lean clay with silt and trace fine to medium sand to a depth of 3 m. Below this was a fine to medium sand with interbedded silty sand and sandy silt extending to a depth of 7.2 m. At this point the boring encountered pre-event sediments of interbedded sand and clay. This portion of the soil profile extended to a depth of 9.6 m, where sandstone bedrock was encountered. A generalized soil profile of the site is given in Figure 5.30. The soil conditions between and beyond the boring locations were interpreted based on a limited exposure depth of soil in the river bank and should be considered approximate only.

5.2.2.Skelton Event

The soil conditions were investigated at four sites in order to estimate ground motions associated with this event. The liquefaction evidence at each of the study sites associated with the Skelton event originates in the glacio-fluvial braid-bar deposits laid down during the late Pleistocene epoch. These liquefiable glacial outwash sediments were deposited during the Wisconsinan glaciation, and make up the present terrace deposit throughout the Wabash Valley. The dikes and sand blows left following the liquefaction event typically originate at or near the crests of the braid-bar sediments left by the outwash flow. The features are generally linear and have a strike following the crests of the braid-bar sediments.

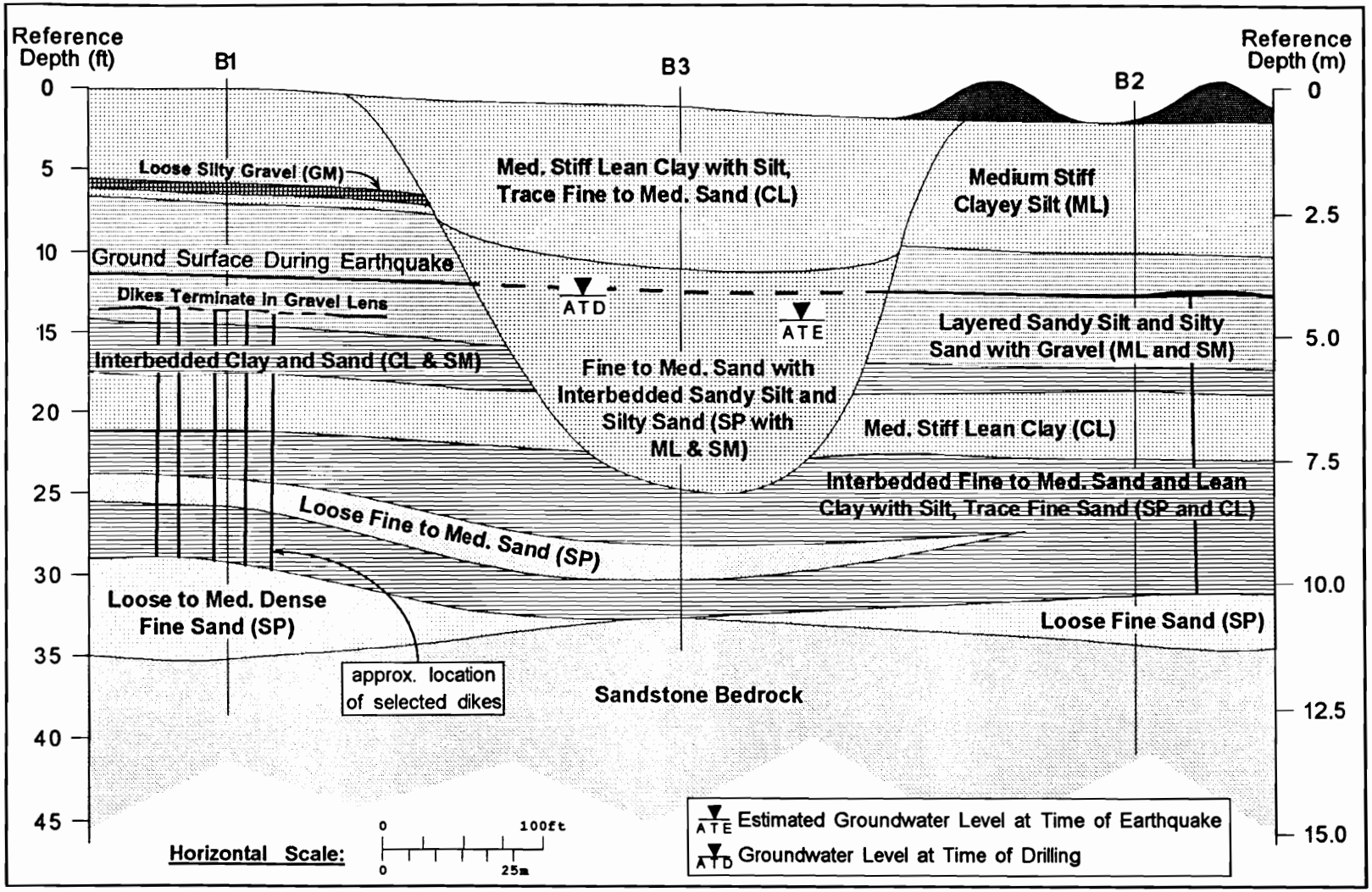

Figure 5.30. Near surface soil profile for site Perrysville (PL)

5.2.2.1.Site GR

The Griffin Gravel Pit site is located in Indiana nearly 3 km northeast of the Wabash River. This study site is approximately 66 km southwest of Vincennes, Indiana and approximately 38 km northwest of Evansville, Indiana. Figure 5.31 provides a site plan for the study site, and includes a site vicinity map. The site extends around the western end of an active gravel pit, covering an area approximately 185 m square and contains numerous dikes ranging to approximately 0.3 m in width. It is likely some of the features were originally continuous across the gravel pit between the north and west or south faces of the pit. In-situ density testing performed at this site reveals relative densities in the range of 2% to 44%. The lowest of these values were generally closest to the disturbance associated with flow toward the dikes. Away from the areas of greatest disturbance these values are consistent with the penetration test data obtained.

The surficial soil present on the north side of the gravel pit consists of approximately 2.3 m of sandy clay with silt. On the west side of the pit, this soil is approximately 1.7 m thick, and is overlain up to approximately 1.7 m of lean clay. The surface present at the time of the earthquake is coincident with the modern surface at boring locations B1 to B3. At boring locations B4 and B5 the modern surface extends approximately 0.7 and 1.1 m, respectively, above the surface at the time of the earthquake. This is likely the result of recent filling associated with the gravel pit operation and the access road for the oil well. The liquefiable sediments present beneath the clay cap consist of medium dense sand with some gravel overlying medium dense to dense sand, trace to with gravel. The upper liquefiable sediments have a thickness of between 0.8 and 2.4 m, and the medium dense to dense sand extends to the base of the explorations. A generalized soil profile of the site is given in Figure 5.32. The soil conditions between and beyond the boring locations were interpreted based on exposed soil in the pit walls.

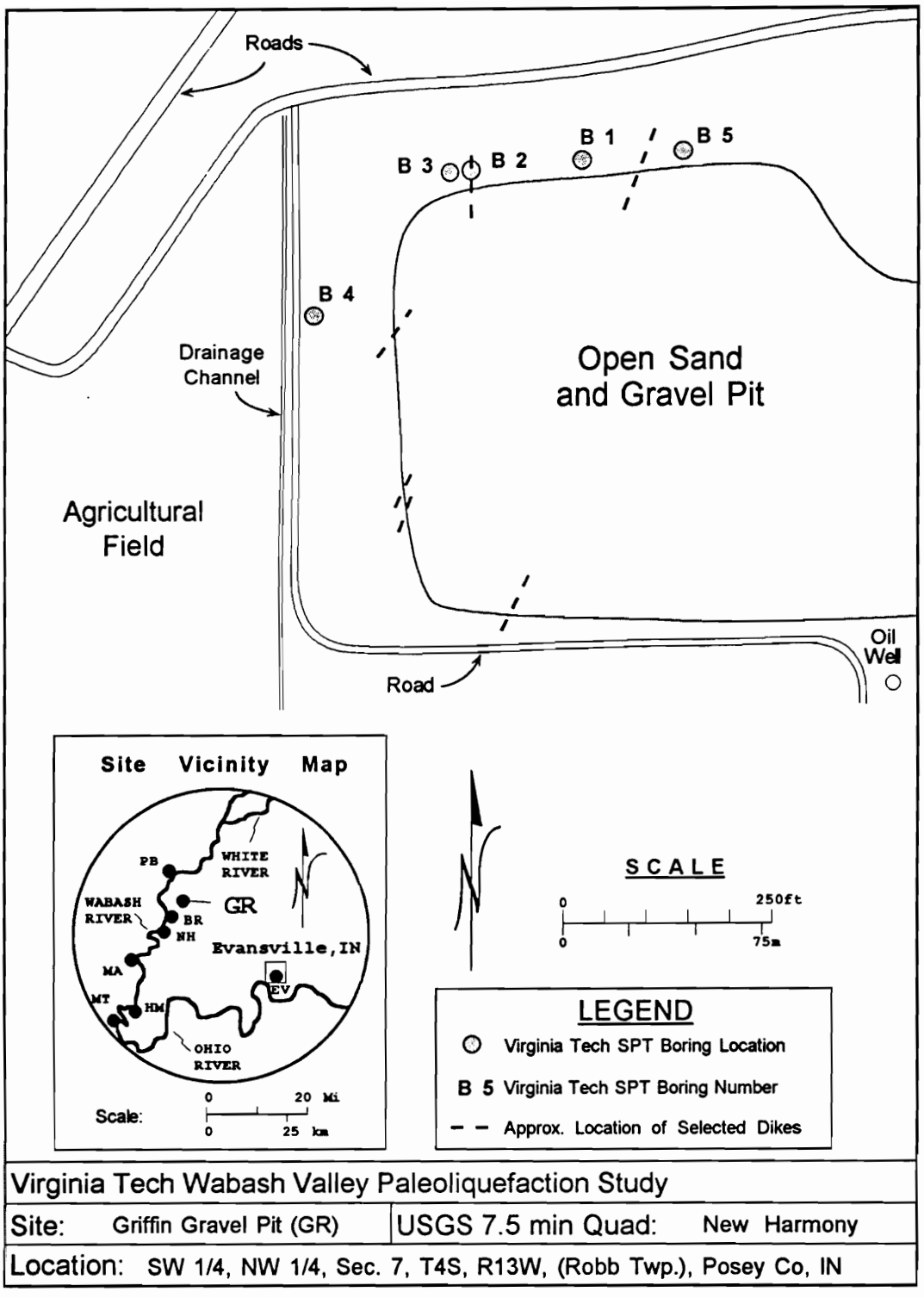

Figure 5.31. Site plan for site Griffin Gravel Pit (GR)

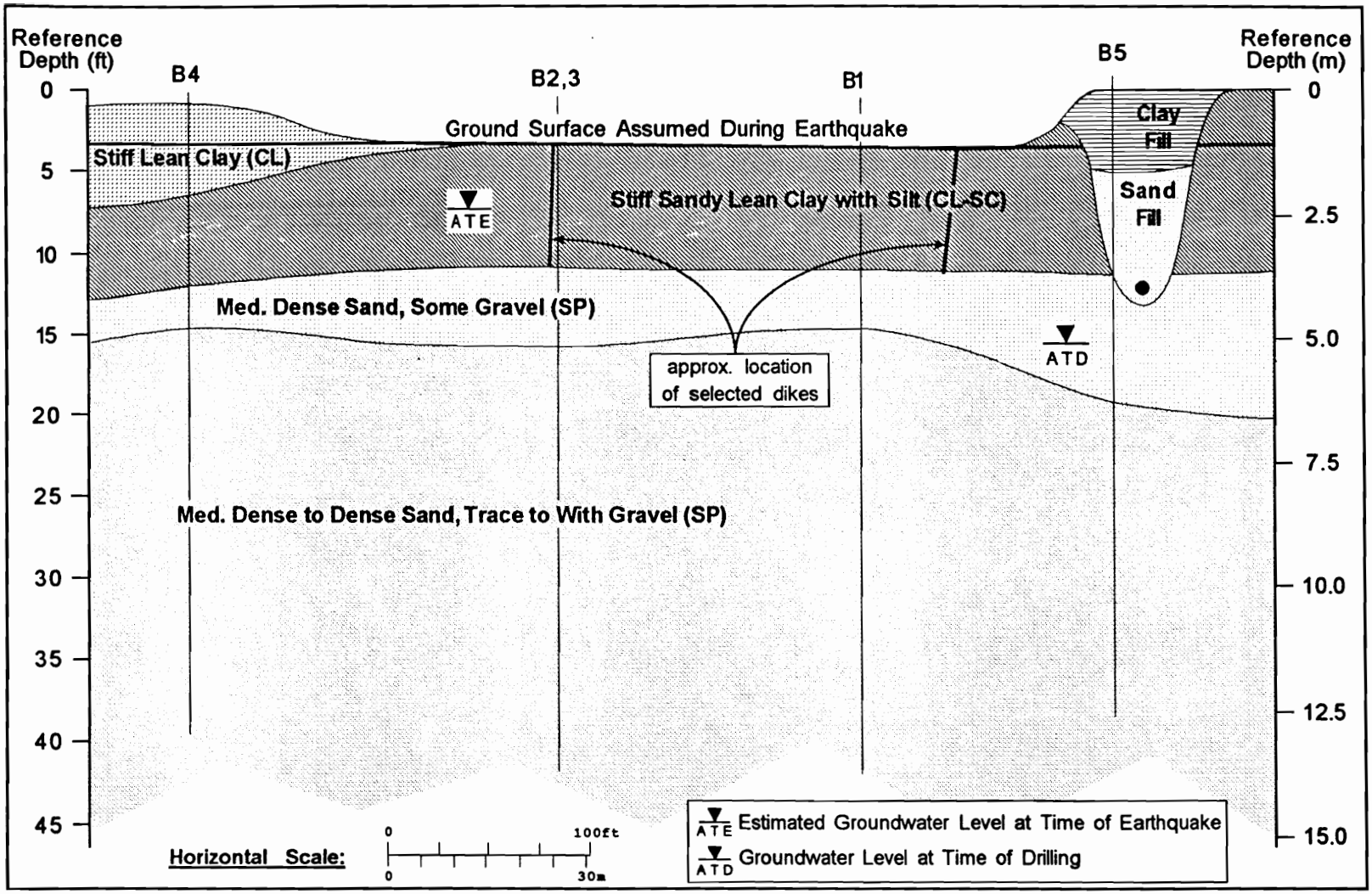

Figure 5.32. Near surface soil profile for site Griffin Gravel Pit (GR)

5.2.2.2.Site VC

The Veale Creek site is located along the eastern bank of the West Fork of the White River. This study site is approximately 26 km east of Vincennes, Indiana. Figure 5.33 provides a site plan for the study site, and includes a site vicinity map. The length of the exposure investigated for this study extends approximately 90 m northwest to southeast. The site contains at least three dikes ranging to approximately 0.6 m in width.

The surficial soil present at the site consists of approximately 1.8 to 2.4 m of lean to fat clay with silt and trace fine sand. This soil layer extends to the surface present at the time of the earthquake. Below the vent surface is a 1.2 to 1.5 m thickness of lean clay with silt and fine sand. The liquefiable sediments present beneath the clay deposits consist of a loose to medium dense predominantly medium sand with silt and trace gravel overlying a dense deposit of the same soil. The loose to medium dense potion of the deposit ranges from 1.5 to 1.8 m in thickness. The dense sand then extends to the base of the explorations. A generalized soil profile of the site is given in Figure 5.34. The soil conditions between and beyond the boring locations were interpreted based on only a limited exposure of the top of the soil profile in the river bank.

5.2.2.3.Site WA

The Washington site is also located along the eastern bank of the West Fork of the White River. This study site is approximately 24 km east of Vincennes, Indiana and is just north of site VC. Figure 5.35 provides a site plan for the study site, and includes a site vicinity map. The length of the exposure investigated for this study extends approximately 90 m north to south. The site contains two small dikes that did not reach the surface at the time of the earthquake. We are able to identify the liquefaction features due only to the presence of the exposed soil profile in the river bank. The analysis procedure used to estimate motions presumes surface evidence of liquefaction has been produced. The development of small dikes that do not penetrate to the surface would be interpreted as a negative liquefaction case. The ground surface motions estimated based

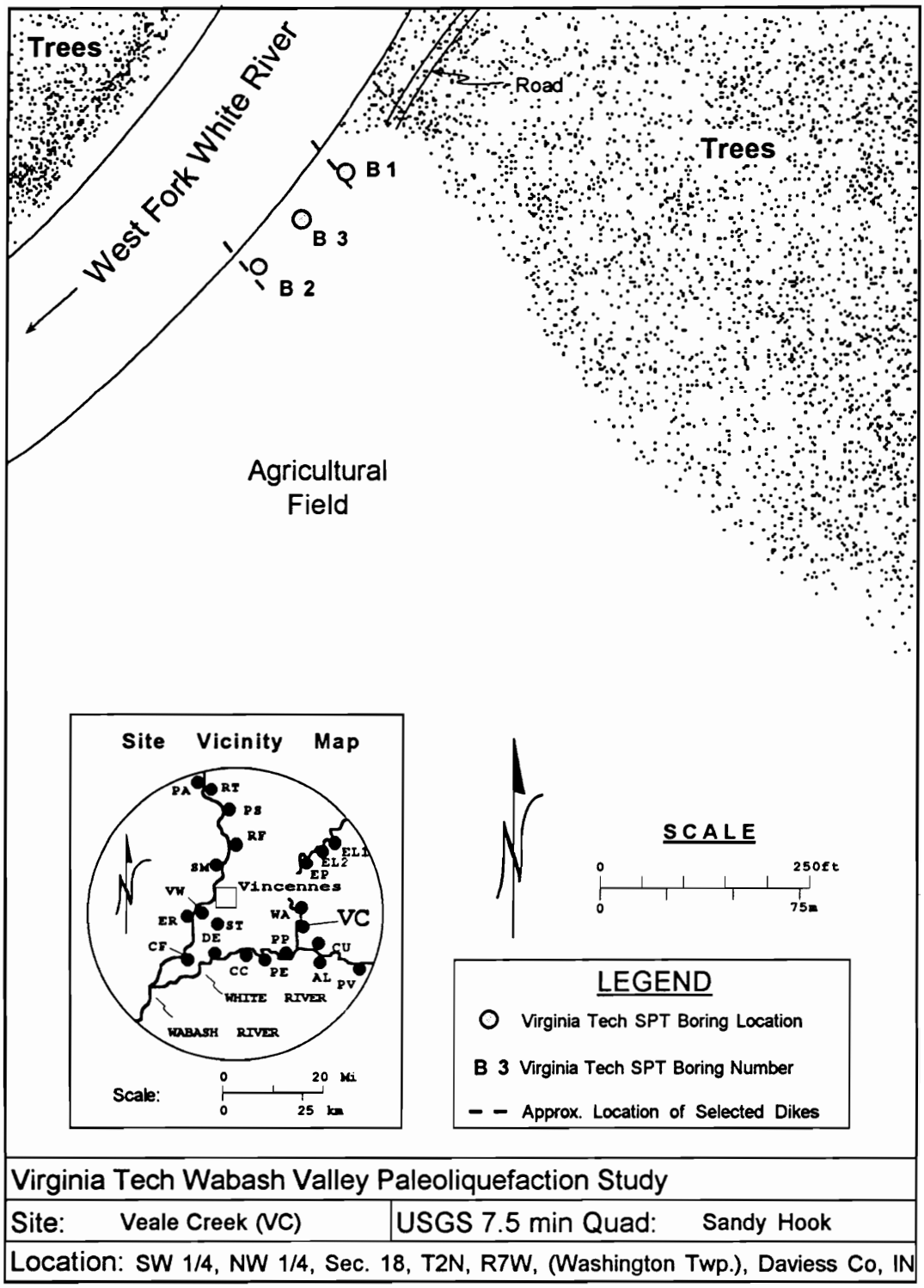

Virginia Tech Wabash Valley Paleoliquefaction Study	
Site: Veale Creek (VC)	USGS 7.5 min Quad: Sandy Hook
Location: SW 1/4, NW 1/4, Sec. 18, T2N, R7W, (Washington Twp.), Daviess Co, IN	

Figure 5.33. Site plan for site Veale Creek (VC)

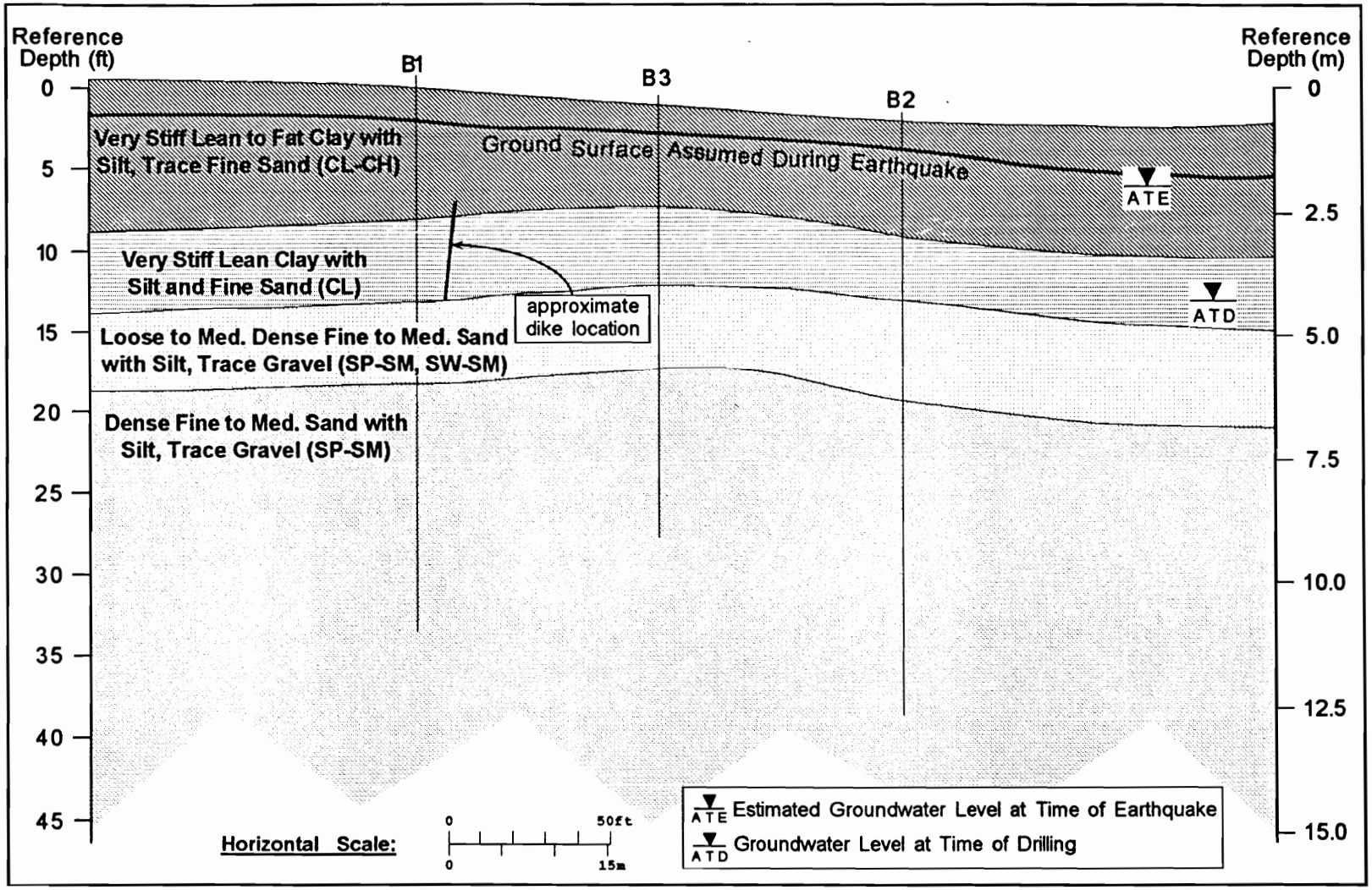

Figure 5.34. Near surface soil profile for site Veale Creek (VC)

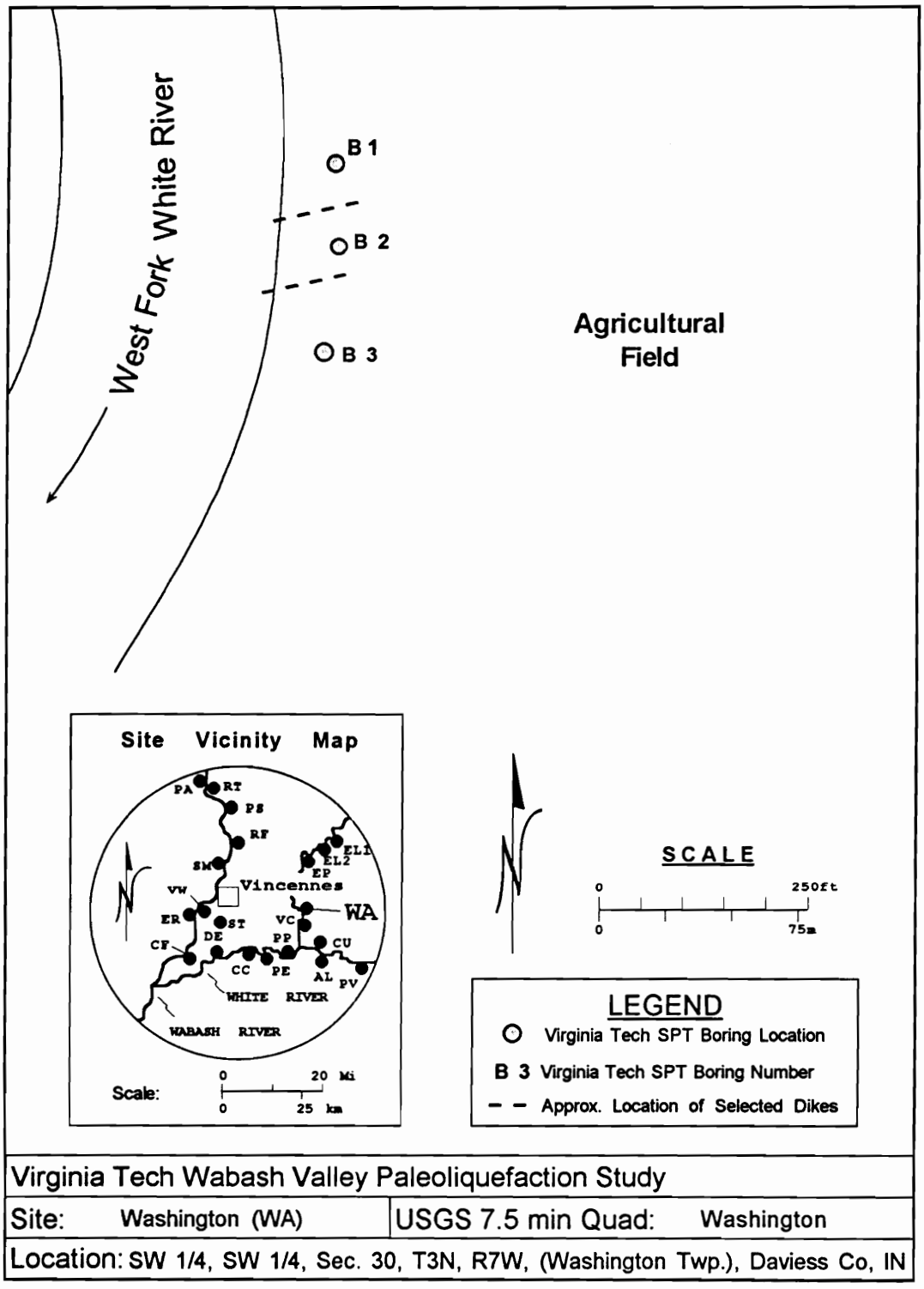

Figure 5.35. Site plan for site Washington (WA)

on the conditions at this site will therefore yield an upper bound value. It is reasonable to assume, however, that surface evidence was imminent, and that the estimated motions will not greatly exaggerate the actual motions that occurred.

The surficial soil present at the site consists of approximately 2 to 2.4 m of lean to fat clay with silt. The estimated depth to the ground surface present at the time of the earthquake is approximately 0.6 to 1 m. The liquefiable sediments present beneath the clay deposit consist of a loose grading to medium dense predominantly fine to medium sand with silt, trace gravel, overlying a dense fine sand with silt. The loose soil is 1.3 to 1.7 m thick overlying 1.2 to 2 m of the medium dense soil. The dense sand ranged from 0.2 to 1.7 m in thickness. The explorations encountered a very hard clay glacial till at the base. A generalized soil profile of the site is given in Figure 5.36. The soil conditions between and beyond the boring locations were interpreted based on the exposed soil profile in the river bank and on information provided by Professor Munson (1994) of Indiana University.

5.2.2.4.Site HM

The Half Moon Bend site is located along the Indiana bank of the Wabash River. This study site is approximately 99 km southwest of Vincennes, Indiana and 41 km west of Evansville, Indiana. Figure 5.37 provides a site plan for the study site, and includes a site vicinity map. The length of the exposure investigated for this study extends approximately 90 m east to west. The site contains three dikes on the order of 0.1 m in width. In-situ density testing performed at this site reveals relative densities of 41 to 52% in the upper loose to medium dense portion of the liquefiable soil. Two in situ tests performed in the lower dense material gave relative density results of 59 an 80%. These values are consistent with the penetration test data obtained.

The surficial soil present at the site consists of approximately 2.4 to 2.9 m of lean to fat clay with silt and fine sand. The ground surface present at the time of the earthquake is now buried by this soil deposit. Below the blow surface is approximately

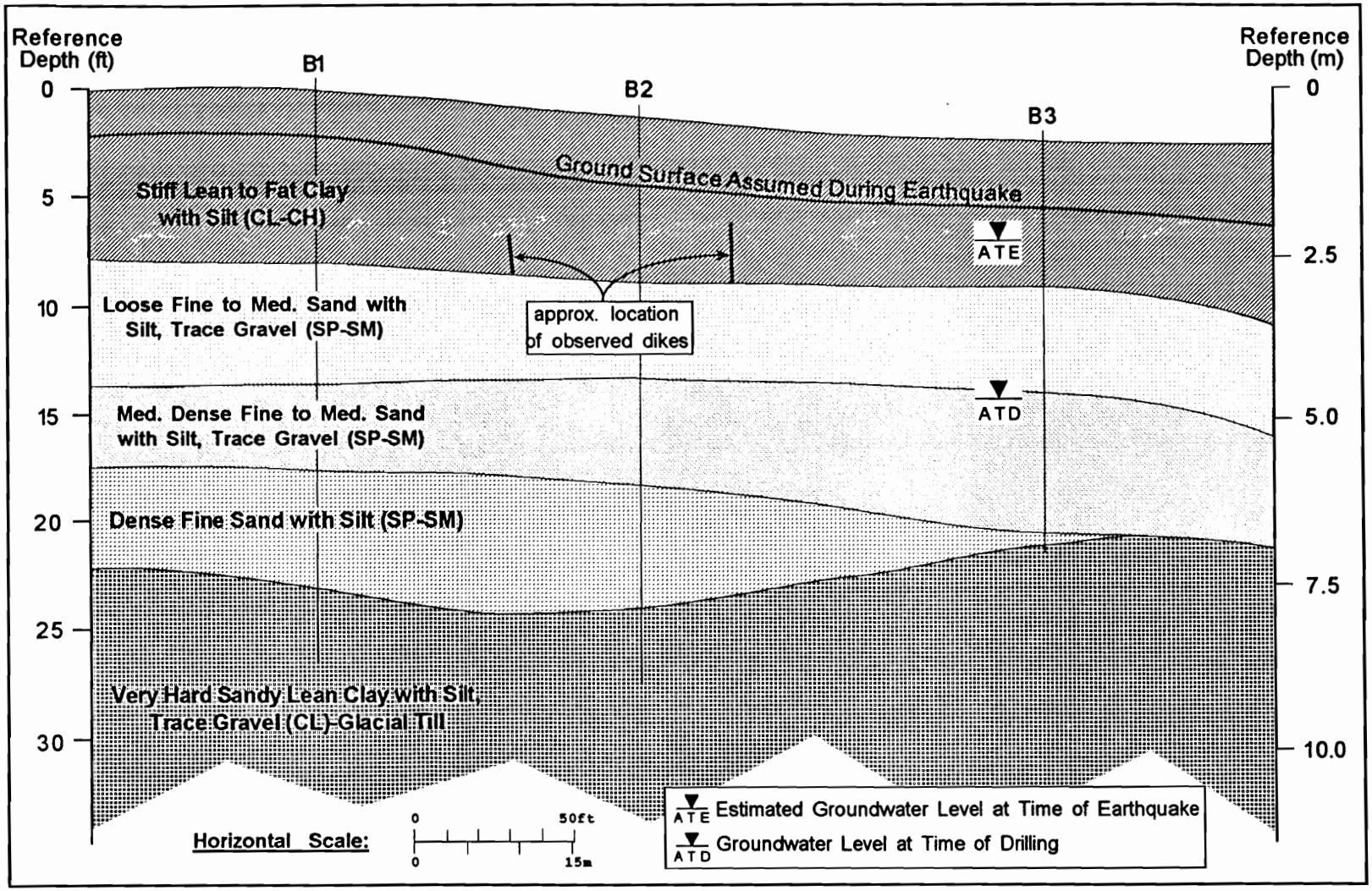

Figure 5.36. Near surface soil profile for site Washington (WA)

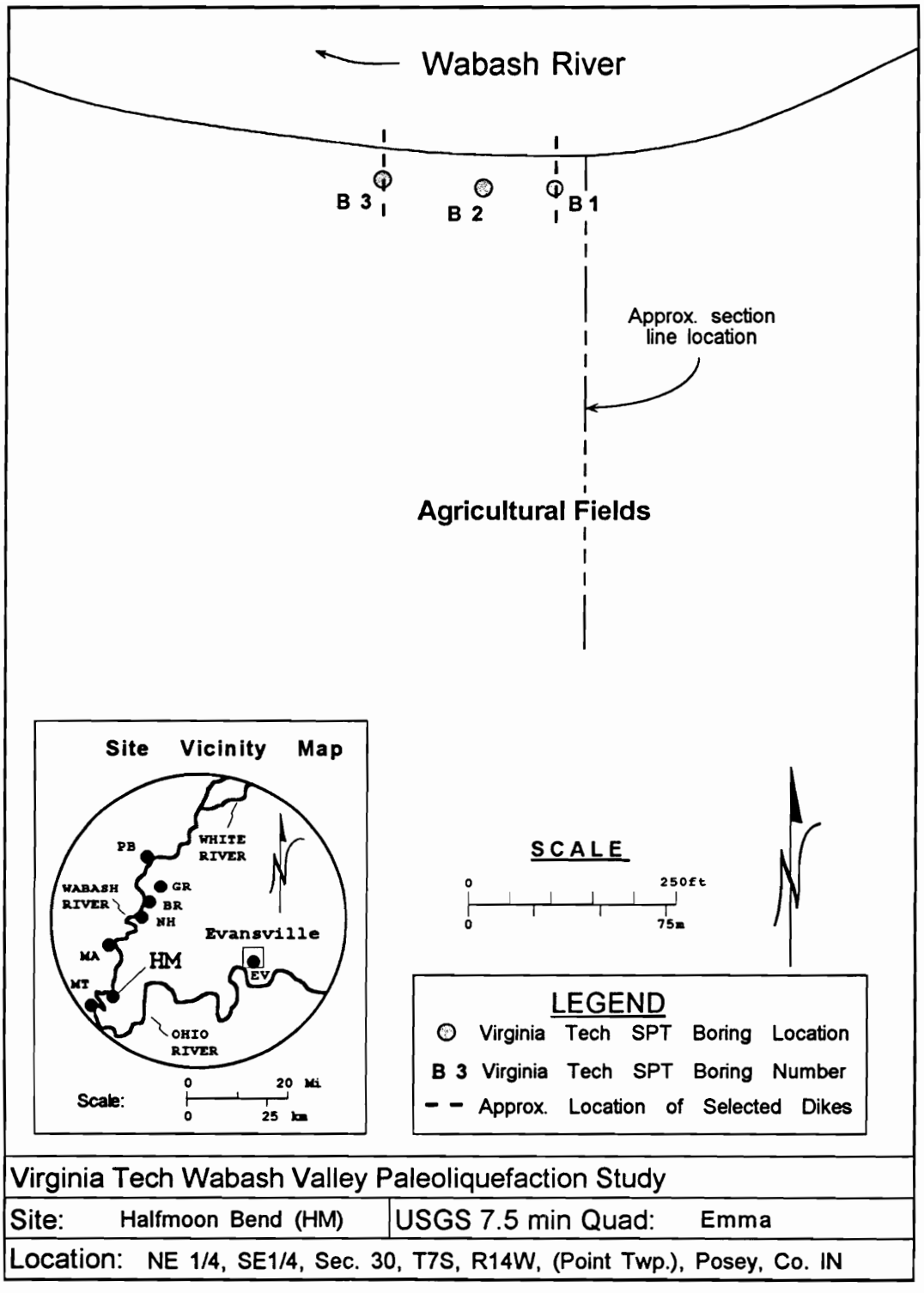

Figure 5.37. Site plan for site Halfmoon Pond (HM)

0.9 to 1.2 m of interbedded sand and clay. The liquefiable sediments consist of a loose to medium dense predominantly fine to medium sand, with trace silt and gravel overlying a medium dense sand with gravel. The loose soil is 1.3 to 1.7 m thick and the medium dense soil extends to the base of the explorations. A generalized soil profile of the site is given in Figure 5.38. The soil conditions between and beyond the boring locations were interpreted based on the exposed soil profile in the river bank and on information provided by Professor Munson (1994) of Indiana University.

5.2.3. Vallonia Event

The liquefaction evidence at each of the study sites associated with the Vallonia event is within fluvial deposits laid down during the early Holocene epoch. The soil conditions were investigated at three sites in order to estimate ground motions associated with this event. These liquefiable sediments were laid down during the time period just following the end of the Wisconsinan glaciation, while the rivers were downcutting into the present terrace sediments. The liquefaction features identified are generally linear in plan view, with a strike following the orientation of the fluvial source sediments.

The groundwater elevation at the time of the earthquake is estimated to have been at an elevation similar to that encountered at the time of the exploration program. This is based on the presence of a narrow band of oxidation near the top of the Pleistocene braid-bar deposit at site AZ, and on the top of the liquefied deposit at site SP. The oxidation in the deposit at site AZ indicates the range over which the regional groundwater table normally fluctuates. At site SP, the flow path where excess pore pressures carried liquefied soil to the surface passes through other liquefiable sands in the vicinity of the dike.

5.2.3.1. Site SP

The Sparksville site is located along the southern bank of the East Fork of the White River approximately 114 km east of Vincennes, Indiana and 54 km southwest of Columbus, Indiana. Figure 5.39 provides a site plan for the study site, and includes a site

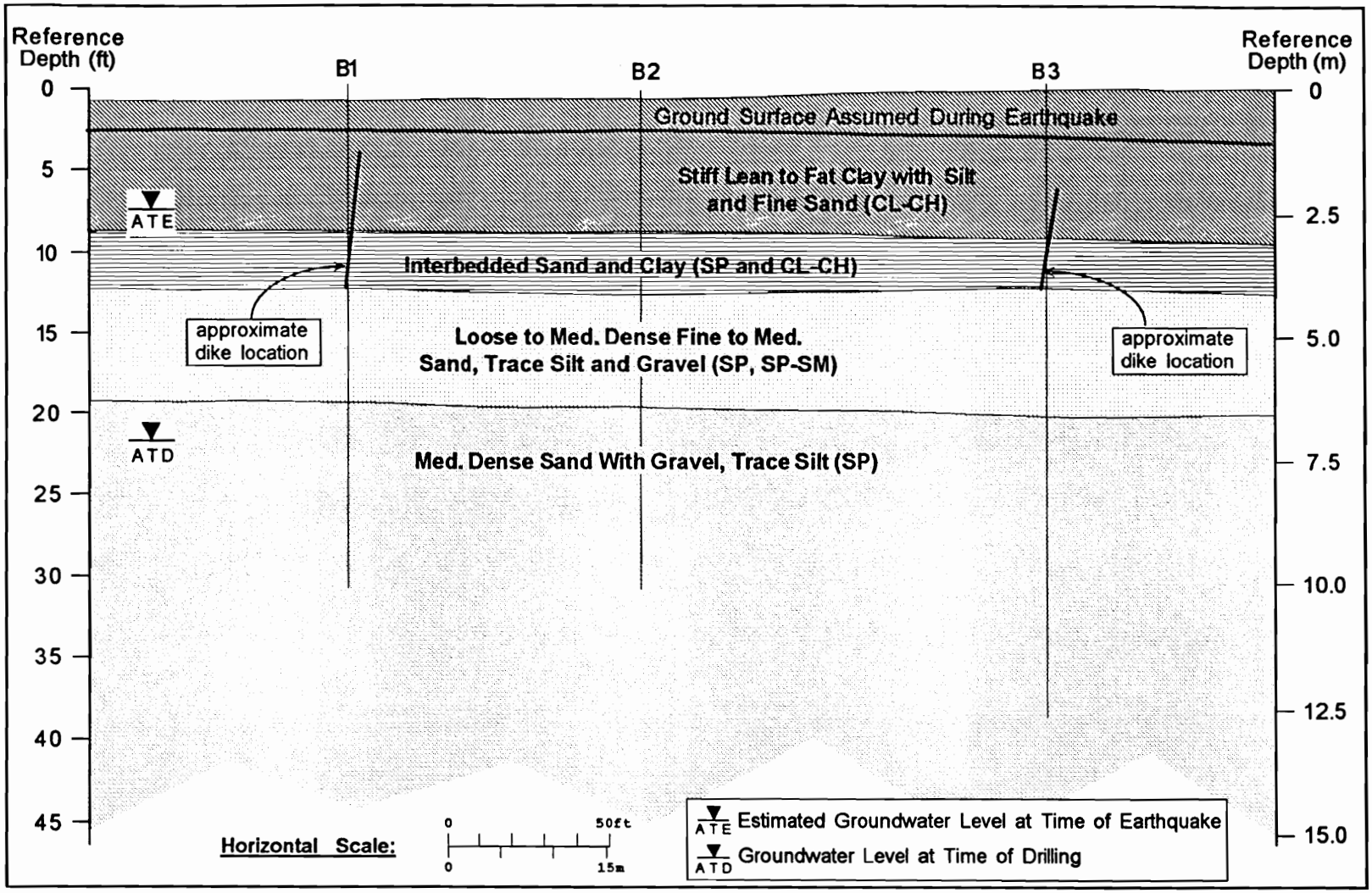

Figure 5.38. Near surface soil profile for site Halfmoon Pond (HM)

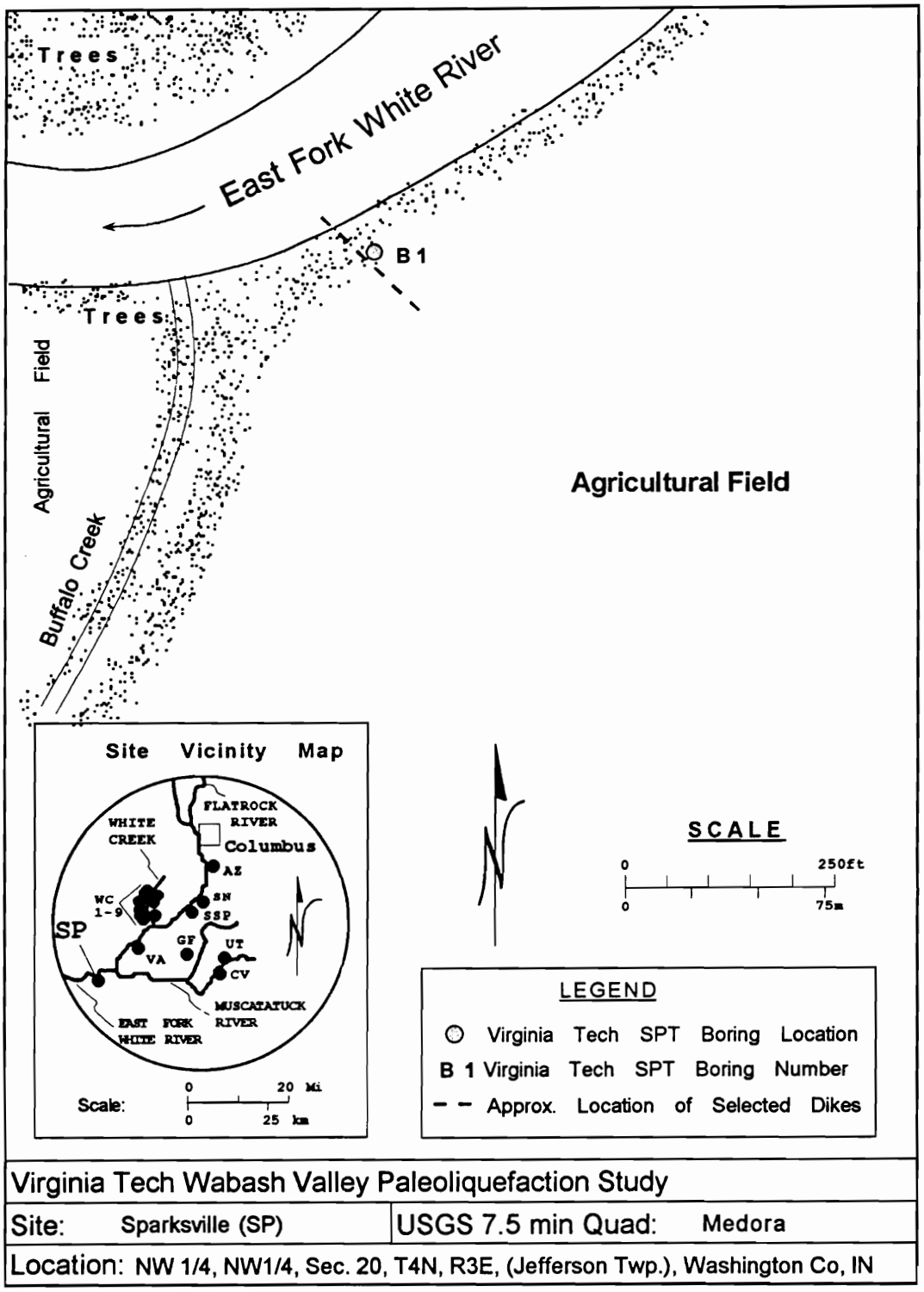

Figure 5.39. Site plan for site Sparksville (SP)

vicinity map. The site extends approximately 60 m north to south and contains a single dike approximately 0.2 m in width. The site exposure is limited in length due to the presence of an existing channel of Buffalo Creek to the west, and a post earthquake deposit to the east that has replaced the sediments present there at the time of the liquefaction event. The evidence of liquefaction may therefore have been more extensive at this site than is indicated by the observed dike.

The surficial soil at this site in the vicinity of the boring location consists of approximately 3.4 m of lean clay with silt and sand overlying a 1 m thick natural levee deposit of interbedded clay and sand. In the vicinity of the dike feature, the levee deposit is underlain by a deposit of sand with interbedded clay lenses and clasts. Liquefied sediment from below this zone was observed in the river bank to have cut through this portion of the deposit as pore pressures were vented to the surface. Additionally, flow toward the dike feature appears to have forced sand and gravel into this region beneath the levee deposit, displacing the entire deposit upward near the dike as flow toward the surface occurred.

The ground surface at the time of the earthquake is present at a depth of approximately 1.8 m within the modern soil profile. Below the levee sediments is a deposit of medium dense fine to medium sand with silt and trace gravel overlying a medium dense fine sand. The upper sand is approximately 1.5 m thick, and the lower fine sand extends approximately another 2.3 m. Below these soils, a medium dense fine to medium sand with silt and some gravel extended to the base of the exploration. A generalized soil profile of the site is given in Figure 5.40. The soil conditions away from the boring location were interpreted based on exposed soil in the river bank and on information provided by Professor Munson (1994) of Indiana University.

5.2.3.2. Site SSP

The site Seymour Sand Pit is located in Indiana approximately 0.7 km east of the East Fork of the White River. This study site is approximately 142 km east of Vincennes,

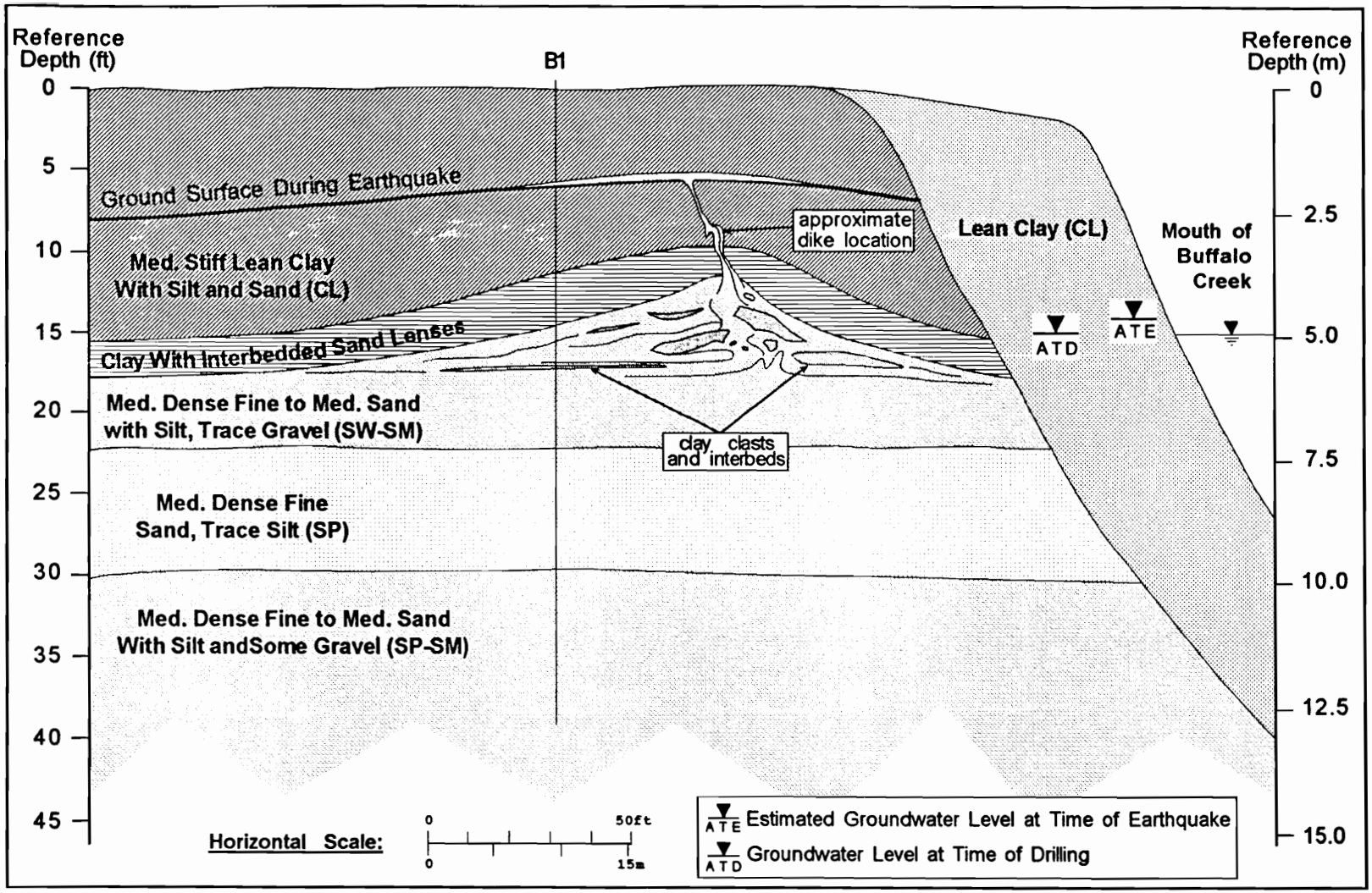

Figure 5.40. Near surface soil profile for site Sparksville (SP)

Indiana and approximately 26 km south of Columbus, Indiana. Figure 5.41 provides a site plan for the study site, and includes a site vicinity map. The site exists at the southern end of an active gravel pit. Two liquefaction features approximately 0.04 m in width are approximately 40 m apart in the south wall of the pit. The eastern dike extends approximately 1.8 m above the source material and pinches out. The western feature extends approximately 2.1 m above the source to a paleosol assumed to have been the surface at the time of the earthquake. No vented material is apparent on this paleosol, however, and the potential exists that the pit operation has reworked the surface.

The surficial soil present at this site consists of approximately 2.4 to 2.6 m of lean clay with silt and some fine sand. The surface present at the time of the earthquake is assumed to be at a depth of approximately 0.5 to 0.6 m. No levee deposits were observed at this site. The liquefiable sediments present beneath the clay cap consist of loose to medium dense gravelly sand with silt, overlying medium dense sand and medium dense to dense sand with silt and some gravel. At the base of all boring locations dense sand with a trace of silt and gravel was encountered. The upper gravelly sand layer is between 2.7 and 3 m thick. The sand layer below that extends another 2.1 to 3.2 m in depth. The medium dense to dense sand is between 0.6 and 2.3 m in thickness and the dense sand extends beyond the base of the explorations. A generalized soil profile of the site is given in Figure 5.42. The soil conditions between and beyond the boring locations were interpreted based on exposed soil in the pit walls and on interpolation between boring locations.

5.2.3.3.Site AZ

The Azalia site is located along the eastern bank of the East Fork of the White River approximately 151 km east of Vincennes, Indiana and 13 km south of Columbus, Indiana. Figure 5.43 provides a site plan for the study site, and includes a site vicinity map. The site extends approximately 100 m northwest to southeast and exhibits soils deposited during three different time periods. The northernmost deposit is a late

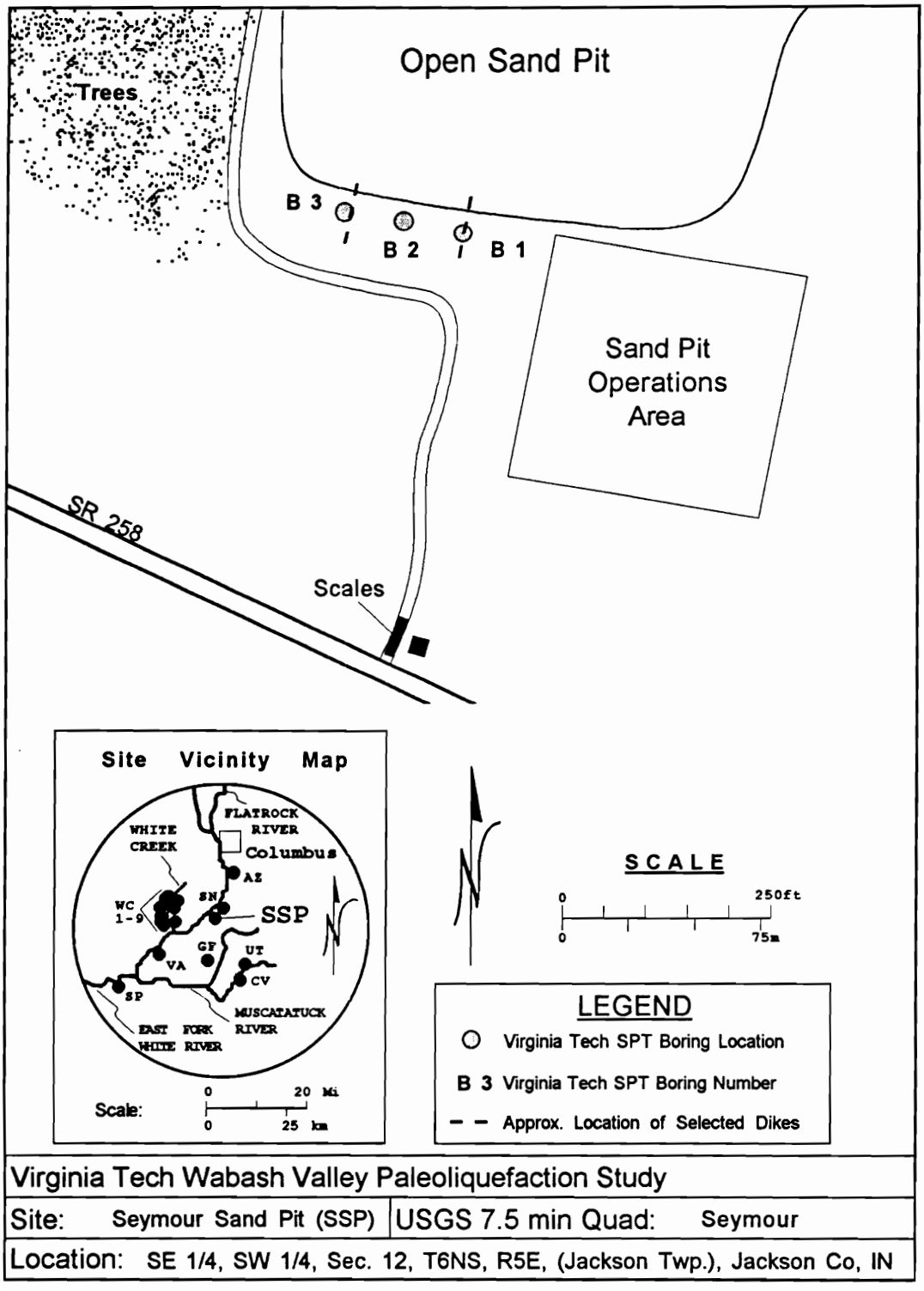

Figure 5.41. Site plan for site Seymour Sand Pit (SSP)

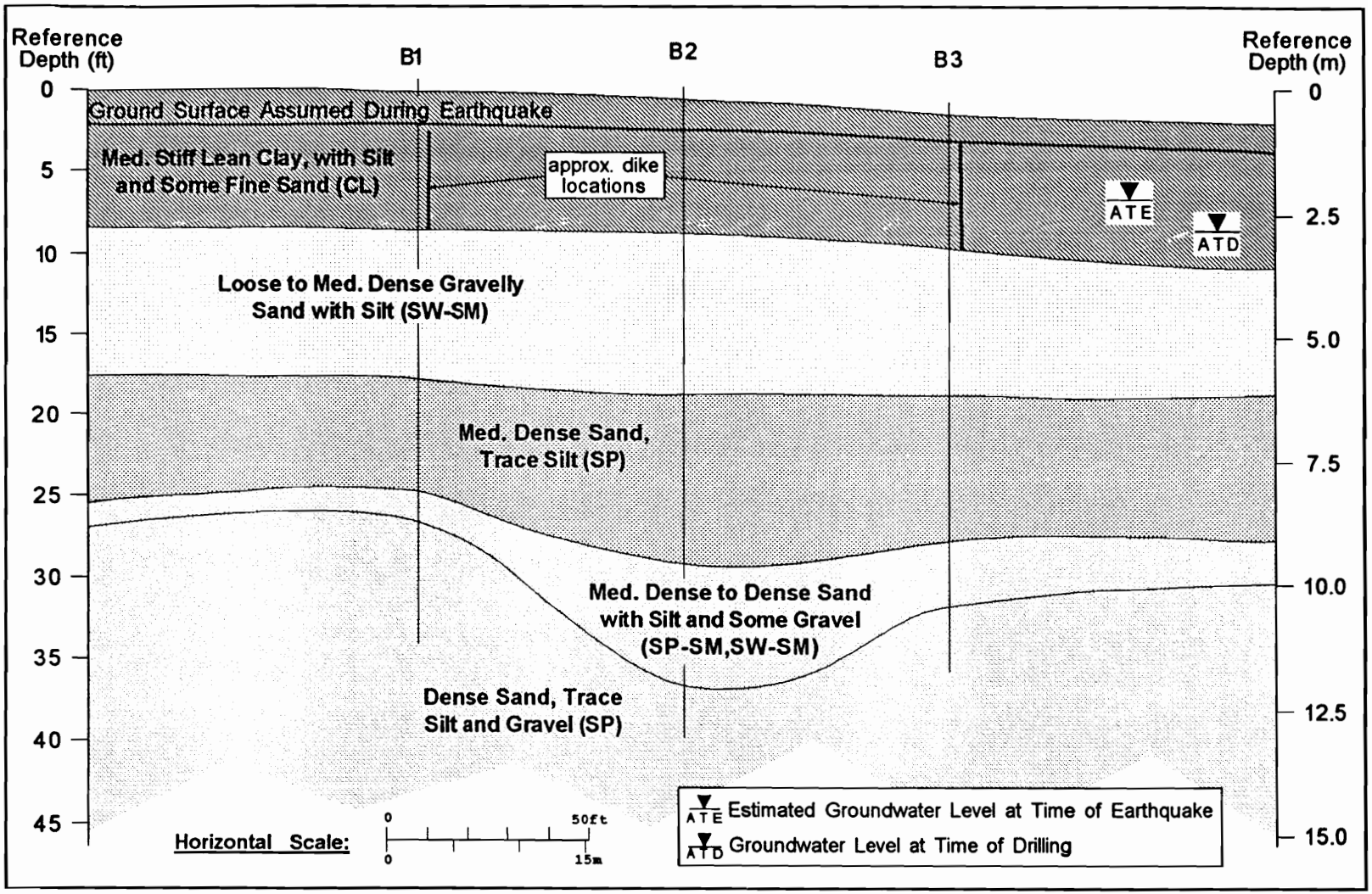

Figure 5.42. Near surface soil profile for site Seymour Sand Pit (SSP)

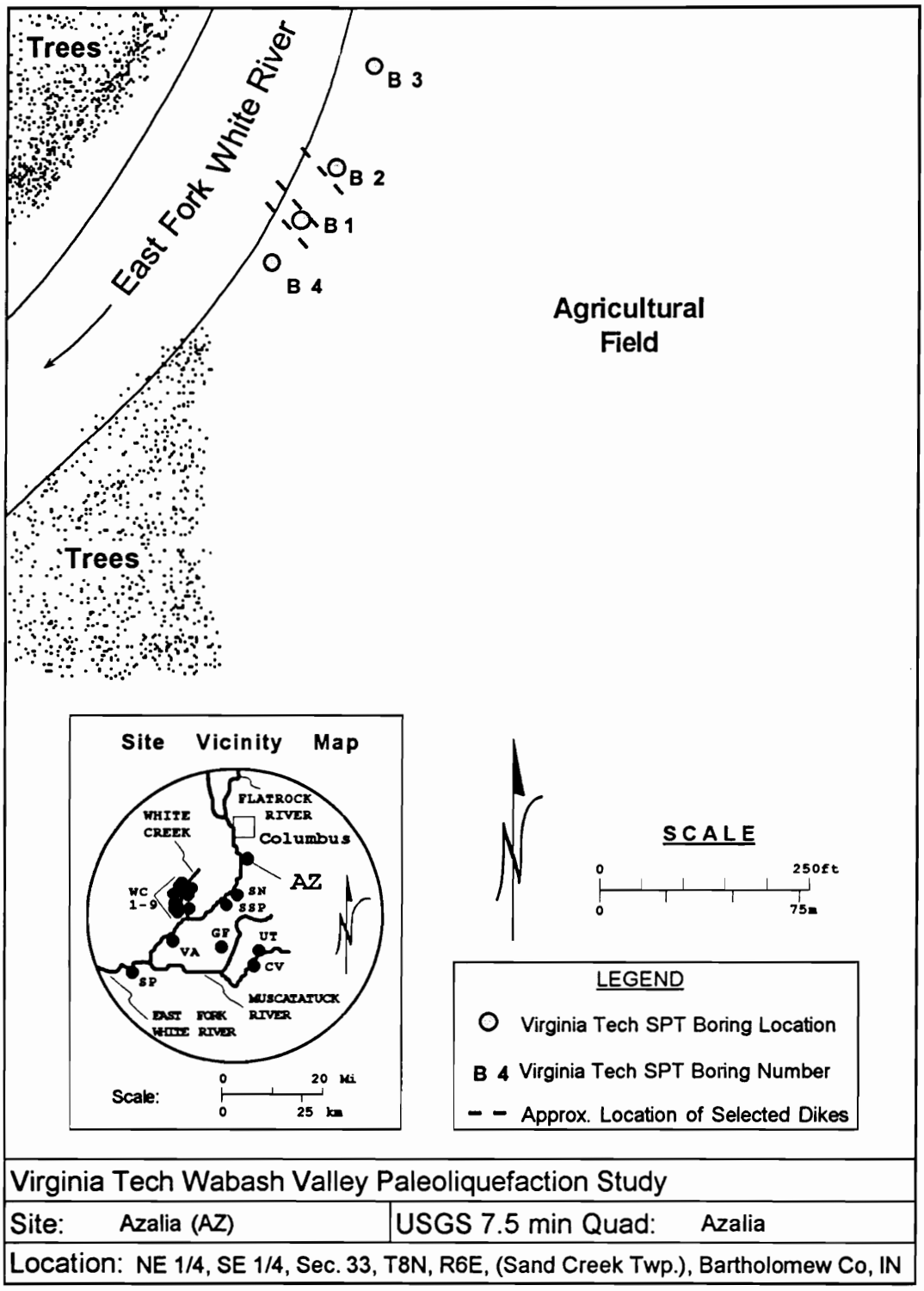

Figure 5.43. Site plan for site Azalia (AZ)

Pleistocene braid-bar terrace deposit. South of this is an early Holocene fluvial deposit laid down by the White River. The southernmost deposit is a result of a late Holocene meander of the river.

Three small dikes ranging to approximately 0.03 m in width are present in the early Holocene deposit. This deposit is in a cut-off meander belt that had been filled with sediment prior to the earthquake. A small, filled, creek channel is also present in the upper portion of this deposit. The dikes extend from the source to a deposit of sand in the base of this filled channel. The material present in this deposit matches the source material and was likely injected by the liquefaction event. The sand present here extends upward to the north and south of the dikes. To the south, the late Holocene channel fill truncates the deposit. To the north, the swale extends to what is assumed to have been the surface at the time of the earthquake. There is no evidence of vented material at this elevation, but the paleo-surface assumption is based on weathering and depositional patterns within the surficial soil deposits across the width of the entire site.

The surficial soil present in the vicinity of the observed dikes consists of a sequence of approximately 3.5 to 3.7 m of lean to fat clay with silt and fine sand overlying layers of lean clay and lean to fat clay with shells. The injected sand deposit is present within these deposits. These soils overlie a thin interbedded layer of sand and clay. This in turn overlies medium dense sands with silt to total depths of 7 to 8.2 m. The base of these explorations encountered medium dense sand with varying silt and gravel contents. The assumed surface present at the time of the earthquake is approximately 1.6 m below the modern surface. A boring advanced within the Pleistocene deposit encountered 1.7 m of lean to fat clay with silt and sand overlying the coarse-grained sediments. The coarse material consists of 0.5 m of loose clayey fine sand overlying 2.7 m of medium dense silty sand with some gravel, which in turn overlies 2.9 m of medium dense sand with gravel, trace silt. At the base of the exploration was the medium dense fine to medium sand with silt, trace to some gravel encountered at the base of borings B1 and B2. Boring B4 was

advanced through the late Holocene fluvial deposit. At this location is 2.8 m of the surficial lean to fat clay overlying post-event deposits of sand with silt and gravel, and gravelly sand. At a depth of 5.5 m this exploration encountered soils present at the time of the liquefaction event. These consist of a medium dense sand with gravel, trace silt extending 1.7 m, overlying the medium dense fine to medium sand with silt, trace to some gravel encountered at the base of each of the other boring locations. A generalized soil profile of the site is provided in Figure 5.44. The soil conditions between and beyond the boring locations were interpreted based on exposed soil in the river bank and on information provided by Professor Munson (1994) of Indiana University.

5.2.4.Waverly Event

The soil conditions were investigated at two sites associated with this event. These sites were originally assumed to be associated with the Vincennes event. The geotechnical analyses performed based on the site studies indicate that the ground motions required to induce liquefaction at these sites could only have originated with a source much closer than the Vincennes epicentral location. Based on the soil strength parameters obtained and the analyses performed for this study, the epicentral location for this event is assumed to be approximately 3.5 km north of Waverly, Indiana, at the confluence of Goose Creek and the West Fork of the White River.

The liquefaction evidence at the study sites associated with the Waverly event is within fluvial deposits laid down during the early Holocene epoch. The liquefiable sediments were deposited during the time period following the end of the Wisconsinan glaciation, while the rivers were downcutting into the present terrace sediments. The liquefaction features identified are generally linear in plan view, with a strike following the orientation of the fluvial source sediments.

The groundwater elevation at the time of the earthquake is estimated to have been at an elevation similar to that encountered at the time of the exploration program. This is based on the oxidation pattern in the surficial clay soil at the site MV, and on the elevation

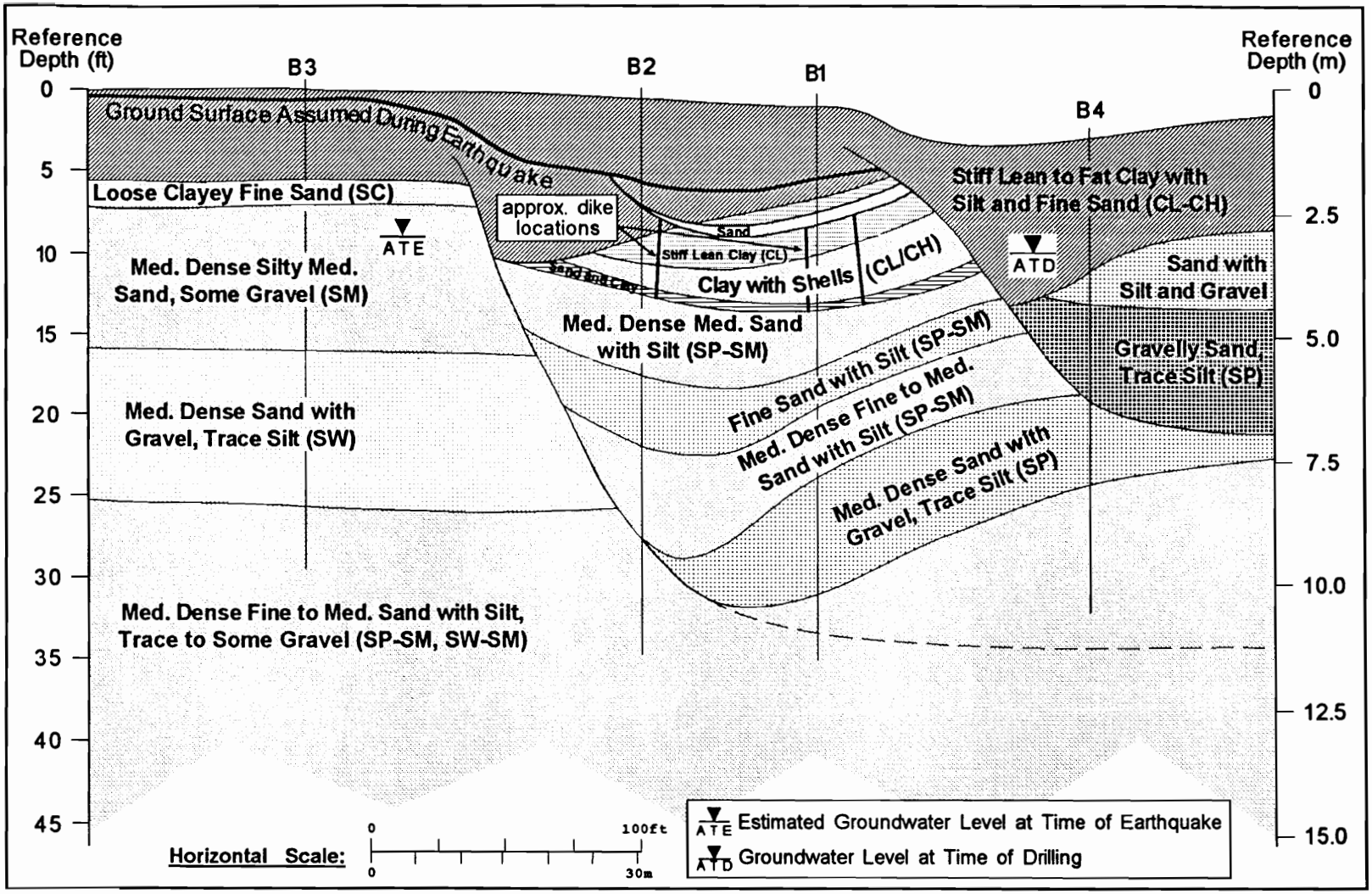

Figure 5.44. Near surface soil profile for site Azalia (AZ)

of the top of the liquefied deposit at site SV. The oxidation in the deposit at site MV indicates the range over which the regional groundwater table normally fluctuates. At site SV, the top of the liquefied deposit is stratigraphically similar in elevation to the top of the oxidized zone at site MV. This suggests the groundwater table was near the top of the oxidation zone at site MV at the time of the earthquake.

5.2.4.1.Site SV

The Smith Valley site is located along the eastern bank of the West Fork of the White River approximately 18 km southwest of downtown Indianapolis, Indiana and approximately 151 km northeast of Vincennes, Indiana. Figure 5.45 provides a site plan for the study site, and includes a site vicinity map. The site extends approximately 70 m north to south. Two dikes have been identified at this site, but more may exist. The sediments extending south of the observed dikes are obscured by rip-rap protection placed along the river bank at this location. In fact, between the time that the site was first identified and the time the geotechnical investigation was performed, the southern of the dikes identified had been obscured by this activity. The subsurface exploration at this site was limited to the vicinity of the dikes identified in the exposed soil profile in the river bank.

The surficial soil present at the site consists of approximately 2.1 to 2.4 m of lean to fat clay with silt and some fine sand. The surface present at the time of the earthquake is assumed to have been approximately 1 m below the modern surface. There is no vented material visible at this site, however, the ground surface assumption is based on the presence of a paleosol with a stratigraphic relationship to a paleosol present just beneath the vent surface identified at site MV. A natural levee deposit of interbedded sand and clay approximately 0.5 m thick is present below the surficial clay soil. The liquefiable soils consist of medium dense to dense gravelly sand with silt, or sand with silt and gravel. At boring location B1, a layer of medium dense fine to medium sand with only a trace of sand was encountered between the depths of 4 and 5 m. A generalized soil profile of the site is

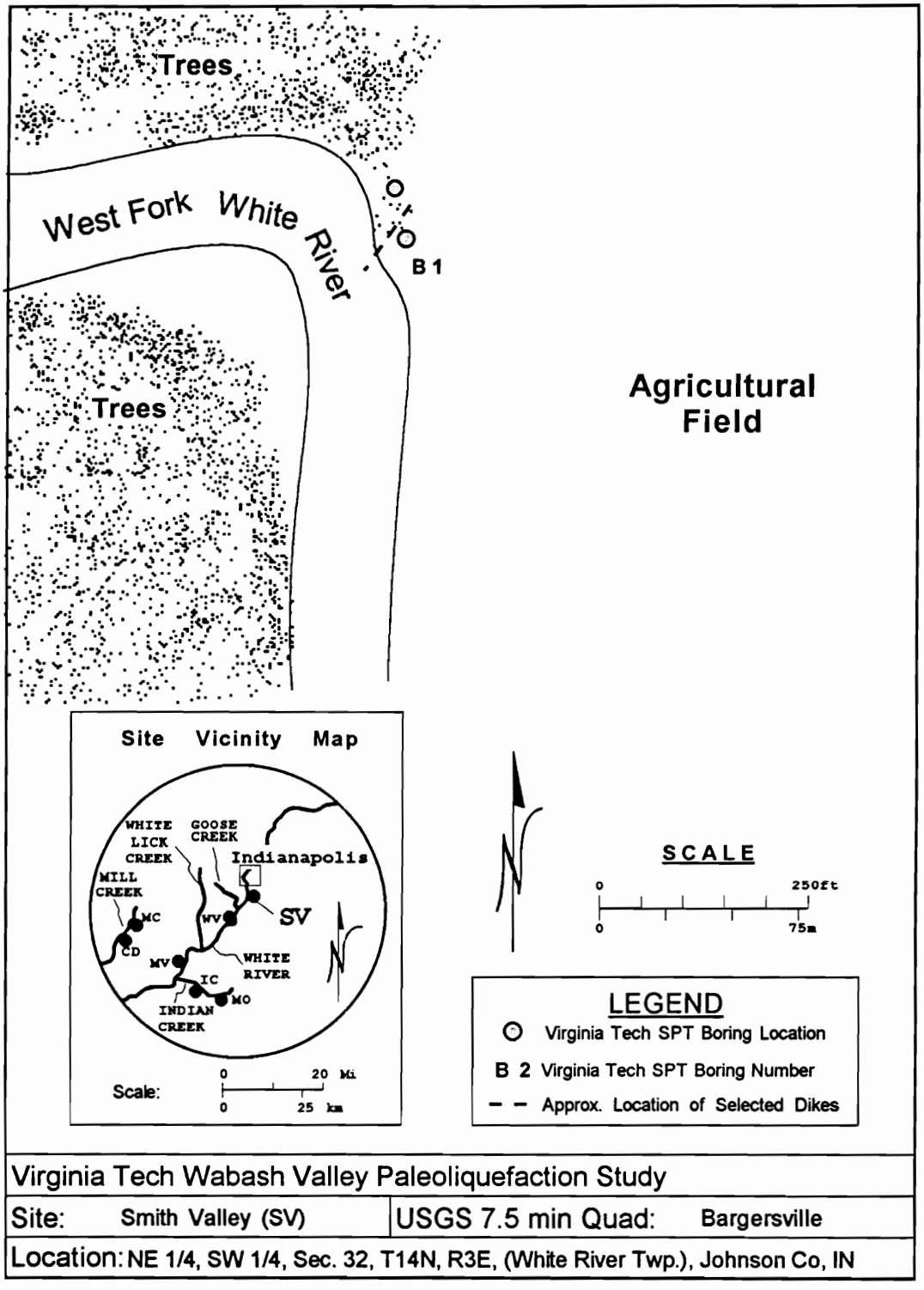

Figure 5.45. Site plan for site Smith Valley (SV)

given in Figure 5.46. The soil conditions beyond the boring locations were interpreted based on exposed soil in the river bank and on information provided by Professor Munson (1994) of Indiana University. The soil conditions between and beyond the boring locations were interpreted based on exposed soil in the river bank, and on information provided by Professor Munson (1994) of Indiana University, and on water well boring logs provided by the Bargersville Water Company. This estimate of the soil profile away from the boring locations should be considered approximate only.

5.2.4.2.Site MV

The Martinsville site is located along the western bank of the West Fork of the White River approximately 48 km southwest of downtown Indianapolis, Indiana and approximately 122 km northeast of Vincennes, Indiana. Figure 5.47 provides a site plan for the study site, and includes a site vicinity map. The site extends approximately 70 m north to south. Two dikes have been identified at this site with widths of 0.11 and 0.27 m. It is possible that other dikes exist to the north of the identified dikes The sediments extending north of the observed dikes are obscured by rip-rap protection placed along the river bank. The subsurface exploration at this site was limited to the vicinity of the dikes identified in the exposed soil profile in the river bank.

The surficial soil present at the site consists of approximately 3.2 to 3.7 m of lean clay with silt and trace fine sand. The surface present at the time of the earthquake is approximately 1.1 to 1.4 m below the modern surface. A natural levee deposit of interbedded silt and fine sand varying between approximately 0.9 and 2.1 m in thickness is present below the surficial clay soil. The liquefiable soils consist of a 1.5 to 2.5 m thick layer of medium dense sand with silt and gravel overlying medium dense gravelly sand with trace silt extending to the base of the explorations. A generalized soil profile of the site is given in Figure 5.48. The soil conditions between and beyond the boring locations were interpreted based on exposed soil in the river bank and on information provided by Professor Munson (1994) of Indiana University.

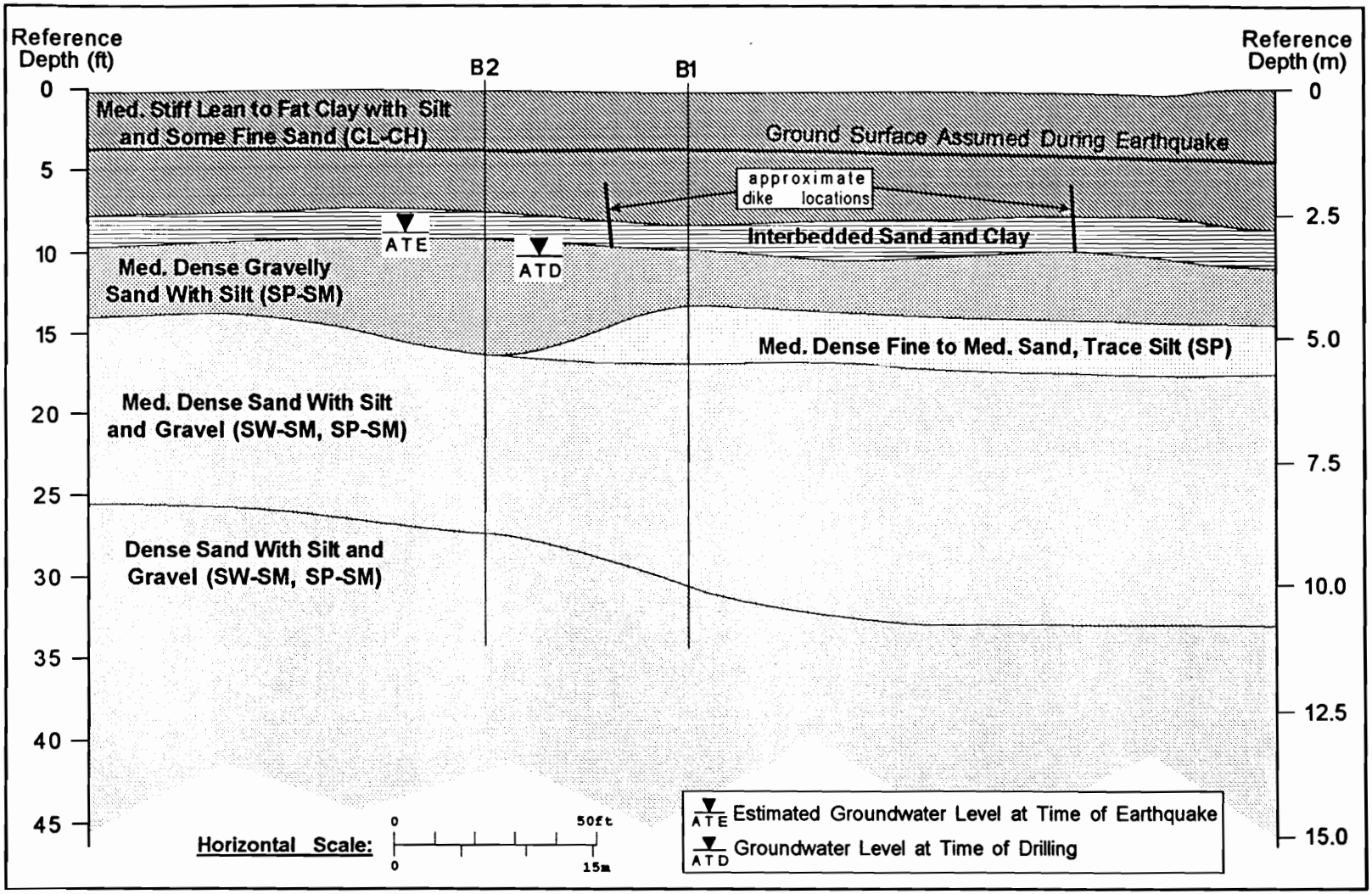

Figure 5.46. Near surface soil profile for site Smith Valley (SV)

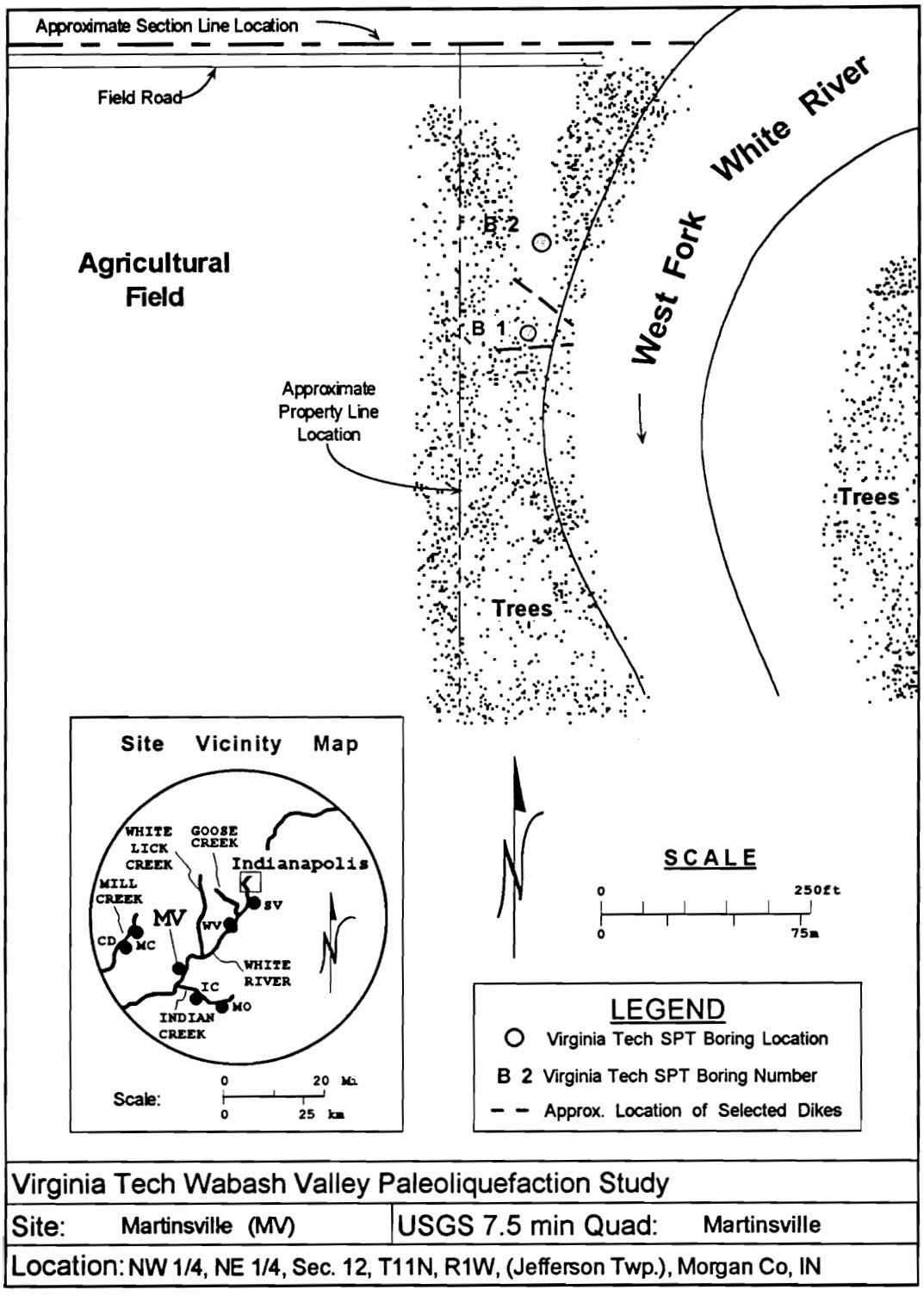

Figure 5.47. Site plan for site Martinsville (MV)

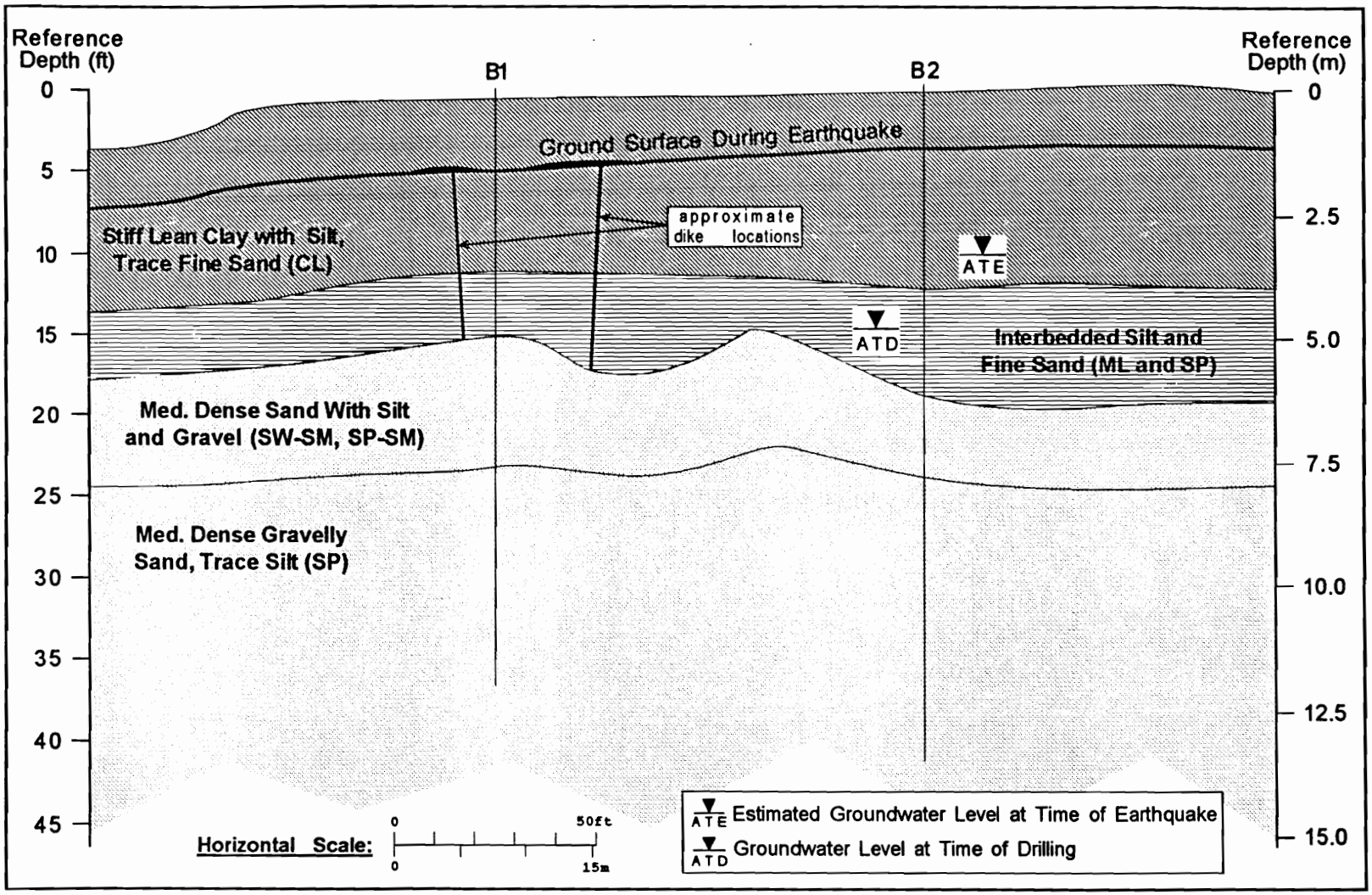

Figure 5.48. Near surface soil profile for site Martinsville (MV)

5.3.Discussion of In-Situ Soil Conditions

The in-situ testing portion of this study was performed to obtain the data necessary for estimating the surface motions that would have induced the liquefaction evidence observed. The results of these test procedures are influenced by the soil structure effects resulting from the conditions that have existed at the study sites prior to and since the liquefaction event. Changes in soil structure due to the liquefaction event itself are also a concern in any liquefaction susceptibility analysis. In an effort to asses the potential for variation in the penetration test data obtained today compared to what would have been present at the time of the earthquake, it was necessary to consider those issues that may lead to changes in the soil properties related to liquefaction susceptibility. Based on the factors involved in liquefaction, it is not possible to make a definitive conclusion as to how the soil deposit may have been altered due to the liquefaction event. From a consideration of the factors involved, and without definitive evidence otherwise, it is reasonable to assume that the penetration resistances measured at the present time are representative of the condition present at the time of the liquefaction event. Regardless of the true condition of the soil deposits prior to the liquefaction event, these issues were shown not to have a significant effect on the outcome of the results of the analysis procedure that is used for this analysis.

The soil conditions present at the Wabash Valley study sites generally show similar liquefaction susceptibilities. The evidence of liquefaction at these sites is typically manifested as a lateral spreading failure. The depositional environment is similar across the region, and the soil deposits involved with each of the liquefaction events were laid down at about the same geologic time. The oldest of the soil deposits involved in the liquefaction study consists of late Pleistocene diluvial sediments. The more recent earthquakes produced liquefaction evidence in early Holocene fluvial deposits. Soil conditions at the study sites generally consist of 2 to 3m of fine grained flood plain sediments overlying a thin (less than 1m) layer of interbedded clay and sand laid down as

levy deposits. The liquefiable soils below this vary from fine sands and silty sands to gravelly sands and sandy gravels extending to bedrock depths generally on the order of 30 to 45m, though occasional sites contain lesser soil depths.

This environment is highly susceptible to liquefaction due to strong seismic shaking, and contains many sites of liquefaction evidence. The numerous liquefaction sites present are evidence that strong seismic events have occurred at several times in the area over the past approximately 14,000 years. These sites provide an excellent opportunity to estimate the level of strong prehistoric seismic activity in the region.

6. Data Analyses

The data obtained during the field and laboratory portions of this study provide the parameters necessary for the liquefaction susceptibility analyses used to back-calculate an estimate of the ground motions that lead to the liquefaction evidence observed. A preliminary link between individual study sites and a specific earthquake event was made based on the date of occurrence of the liquefaction evidence (Munson and Munson, 1996). A reliable susceptibility analysis procedure requires a distribution of study sites that will provide ground motion estimates at reasonable epicentral distance intervals and directions. Estimates of regional attenuation characteristics consistent with the data must therefore be based on study sites located such that ground motion estimates can be made over the entire range of epicentral distances experiencing liquefaction effects. Estimates of the earthquake magnitude and associated ground surface acceleration suitable to produce the liquefaction evidence seen at each individual site must be evaluated in relation to all other sites associated with a specific event to ensure consistent results are obtained. It is also necessary to compare the estimated site-specific motions with estimates of regional ground motion attenuation characteristics. Once an attenuation relationship has been estimated based on consistent results at each of the study sites, the attenuation relationship should be compared to other proposed attenuation relationships for the region.

A previous paleoseismic study of liquefaction evidence has been successfully used to estimate combinations of earthquake magnitude and amplitude of peak surface accelerations consistent with the liquefaction evidence reported for the 1886 Charleston, South Carolina earthquake (Martin and Clough, 1994). At the time of that event, earthquakes, and the effects of the ground motions associated with them, were recorded based on intensity of the effects (Algermissen, 1983). At the time of the event, the population was well established and the distribution of ground disruptions and other effects was well documented. Using a geotechnical paleoliquefaction study allowed

estimates to be made of the magnitude, peak acceleration, and ground motion attenuation characteristics associated with the event that could not be provided elsewhere.

The Charleston study region was in the flat, low-lying coastal plain of South Carolina. This is a region with little relief and the soil deposits are generally continuous over extensive distances. The liquefaction evidence generally occurred as sand blows in soils on the lee side of Pleistocene beach ridge deposits. The study was therefore completed in an area where level ground conditions controlled the liquefaction failures and lead to the formation of individual sand blows (Martin and Clough, 1990). The liquefaction conditions present there allowed the use of traditional liquefaction analysis procedures to back-calculate the ground motion estimates. Seed's simplified procedure (Seed et al., 1983) was used to estimate whether liquefaction was possible, and the liquefied thickness was estimated based on Ishihara's (1985) relationship between thickness of liquefied deposit and the cap thickness required to suppress the formation of surface evidence of the liquefaction.

The liquefaction evidence associated with the Wabash Valley earthquakes consists of lateral spreading failures. Seed's simplified procedure (Seed and Idriss, 1971; Seed et al., 1985) has been shown to provide reliable liquefaction prediction results for this type of failure condition in silty sand (Tuttle et al., 1990) and in sediments similar to those found in the Wabash Valley (Andrus and Youd, 1987; Stokoe et al., 1988). This approach will be used here to estimate the peak surface acceleration required to produce the onset of liquefaction evidence. The Ishihara (1985) approach to liquefaction suppression prediction based on cap thickness is unreliable for lateral spreading liquefaction failures, however (Youd and Garris, 1995). The present study, therefore, requires an alternative to the Ishihara approach to estimate thickness of the liquefied deposit.

Energy intensity, or source characteristic, models for liquefaction prediction have been shown to provide results with reliability similar to that of the Seed et al. (1985) approach (Liao et al., 1988). A source characteristic model uses a function of magnitude

and distance alone to estimate the energy release associated with a seismic event and predict the occurrence of liquefaction evidence. A model of this type can be used to predict the blowcounts susceptible to liquefaction and can provide an estimate of the liquefied soil layer thickness for the Wabash Valley liquefaction sites. Once the liquefied thickness of the soil deposit has been estimated, a variation on the Seed et al. approach can be used to estimate the peak surface motion required to induce liquefaction through that thickness of the soil profile. The surface motions estimated in this way can then be compared to existing attenuation relationships proposed for the region.

6.1.Existing Ground Motion Attenuation Relationships

It has long been recognized that attenuation characteristics are different between the western and eastern portions of North America (Nuttli, 1973). It has therefore not been possible to directly translate western attenuation relationships to eastern and central portions of the continent. The fact that the study region is in a stable continental region with no recorded strong ground motions due to large earthquakes presents some difficulty in that a direct comparison of estimated attenuation characteristics and actual motions can not be made. The instrumentally-recorded seismic record for the region consists predominantly of small events. Current estimates of attenuation characteristics have been based on these events supplemented with data from a few moderate events.

6.1.1. Seismological Predictions of Ground Motions

The seismic ground motion data available for the central United States prior to 1975 is based solely on Modified Mercalli intensity (Herrmann and Nuttli, 1981). Since that time instrumentally-recorded motions have been added to the seismic record, but the low rate of significant seismic activity in the region makes this a slow process. Due to the limited amount of recorded data, early attenuation relationships proposed have been based on several approaches designed to work with the limited data set. The first approach has been to use intensity attenuation relationships and then estimate site motions based on relationships between site intensity and other ground motion parameters (McGuire, 1984).

This is useful, but contains a large degree of uncertainty due to the nature of intensity data. A second approach assumes source characteristics are similar between plate-boundary and mid-plate regions, and that only the anelastic attenuation characteristics vary. This approach is presented by Campbell (1981), but provides only near-source motion estimates. Herrmann and Nuttli (1981) use a semi-theoretical approach to extend the limited amount of recorded data beyond the magnitude range it contains. An attenuation relationship is developed based on the magnitude of recorded data and extended to other magnitudes based on theoretical relationships. Most recently a theoretical model has been developed to predict attenuation relationships for Eastern North America seismic motions (Boore and Atkinson, 1987). This model is fit to Eastern North America based on the empirical database available and improves with each new earthquake.

6.1.1.1. Bedrock Motions

The majority of the recent work of the seismological community on estimating attenuation characteristics in Eastern North America has been focused on bedrock motions (Atkinson, 1984; Atkinson and Boore, 1990; Boore and Joyner, 1991;). Ground motion attenuation estimates have been developed based on the stochastic model of source characteristics presented by Hanks and McGuire (1981) and have been calibrated for Eastern North America based on the existing seismogram database. The empirical data currently available is primarily for rock sites and is limited to events in the magnitude range of **M**3.5 to **M**6.8. As recorded data continues to be collected, the attenuation relationships are able to be improved, however. Atkinson and Boore (1995) have incorporated the results of several empirical studies of over 1500 seismograms to update the (Boore and Atkinson) 1987 model This is the most current model for ground motions in the region, but remains focused on bedrock motions. They suggest that for typical deep soil sites (> 60m) of Eastern North America, motions may be amplified by a factor of approximately two.

6.1.1.2. Soil Site Ground Surface Motions

Very few attenuation relationships exist for soil site motions in Eastern North America. Little attention has been focused on central United States soil site attenuation other than in the region of the New Madrid Seismic Zone of the lower Mississippi River valley. Campbell (1981), however, proposed a relationship for attenuation based on worldwide near-source ground motion data. This relationship represents the mean horizontal component of acceleration and applies to both rock and soil sites, excluding only extremely soft or shallow soil conditions. Campbell suggests the relationship be restricted to areas within 50 km of the epicenter due to differences in anelastic attenuation, however. Two additional attenuation relationships have been proposed specifically for soil sites in the central United States. Each of these are designed to predict motions at sites located in the Mississippi embayment region located over the Reelfoot Rift of the New Madrid Seismic Zone (see Figure 2.6). The first is the semi-theoretical relationship proposed by Herrmann and Nuttli (1984). The second is based on the Boore and Atkinson (1987) model of bedrock motions, but modified for sites with soil conditions consistent with the Mississippi embayment (Boore and Joyner, 1991). Figure 6.1 is a comparison of these attenuation relationships for a magnitude **M**7.0 earthquake. In the figure, the Campbell relationship has been increased by 13% as suggested by Joyner and Boore (1981) to predict the random component of the peak acceleration.

It is felt, however, that these relationships are inappropriate for use with soil sites in the Wabash Valley region. Soil conditions in the Wabash area typically consist of fluvial deposits of sand and gravel with depths generally in the range of 15m to 45m. This is consistent with the conditions required for the Campbell (1981) model, but covers only the near-source epicentral distances. Maximum epicentral distances of interest in this study are on the order of 150 km. The Boore and Joyner (1991) and Herrmann and Nuttli (1984) models are designed for much different soil conditions than exist in the Wabash

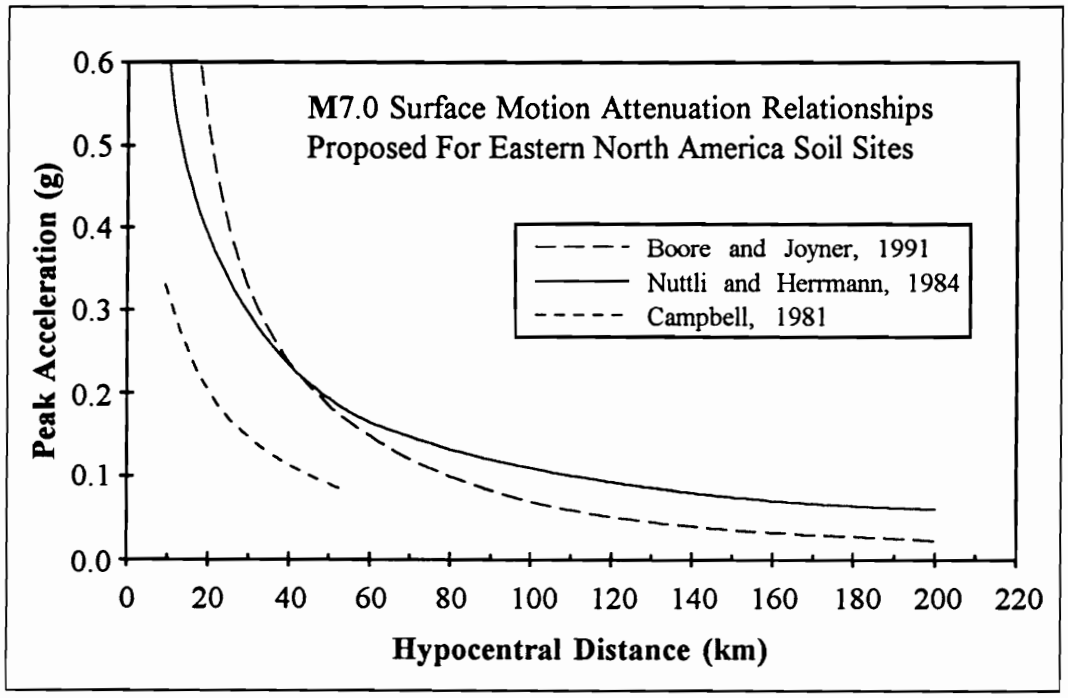

Figure 6.1. Attenuation relationships proposed for soil sites in the central United States.

Valley, and should therefore be expected to predict much different surface motions than would be consistent with soil sites in the Wabash Valley Seismic Zone.

6.2.Attenuation of Liquefaction Effects

6.2.1. Liquefaction Severity

Liquefaction effects are being used in this study to serve as evidence of large prehistoric seismically-induced ground motions. It is therefore necessary to relate the severity of ground motions to the occurrence of this type of ground disruption effect. Two recent studies have been directed toward estimating earthquake characteristics based on the attenuation of liquefaction-induced ground failures (Youd and Perkins, 1987; Youd et al., 1989). This approach suggests an attenuation relationship based on the severity of liquefaction effects as measured by the total amount of lateral spreading displacement experienced at sites with different epicentral distances. The liquefaction severity is a measure of the maximum lateral displacement that can be expected to occur at a given epicentral distance (Youd and Perkins, 1987). The Youd and Perkins study is focused on the Western United States and the Youd et al. study examines the limited data set available for Eastern North America.

Using lateral spreading displacements to estimate earthquake characteristics is an approach similar to using intensity distribution relationships to estimate magnitude and surface accelerations. The liquefaction severity approach is less subjective and is restricted to specific environments, but contains a large degree of uncertainty when trying to back-calculate seismic parameters, especially for prehistoric events. In paleoliquefaction studies, the liquefaction evidence is limited to the sites that present themselves. It would be quite fortuitous if these sites contained the maximum displacements experienced by any site at similar epicentral distances, but is highly unlikely. Paleoliquefaction studies suffer the same conditions experienced by any other paleological study in that the largest, oldest, farthest or most significant piece of evidence found can

not be used to place absolute limits on the findings. It is only the largest, oldest, farthest or most significant piece of evidence that is known to exist.

When displacement is measured as the sum of the dike widths at paleoliquefaction sites, the actual lateral displacement experienced will also be underestimated. Following a liquefaction event, and the dissipation of excess pore pressure, lateral spreading dikes will have a tendency to close up. At many Wabash Valley paleoliquefaction sites the maximum particle sizes in the blows exceed the width of the feeder dikes supplying material to the blow. In some cases where flow mainly carried water and possibly some fine sand to the surface, the dikes may have closed completely. At some locations dikes can be traced vertically to where they appear to pinch out or are lost in desiccation cracks in the cohesive soils. It is not always true, but where these conditions exist it appears that in some cases the dikes originally extended to the surface (Munson, 1994). Subsequent pedogenesis has subsequently obscured the top of the dike in these situations.

Additionally, time has allowed the meandering rivers in the region to erase portions of the evidence at some sites. The rivers in the Wabash Valley have been actively meandering for the thousands of years since the paleoliquefaction events, reworking the sediments present in the active meander belt. As the age of the event increases, the amount of remaining sediment available to be searched for liquefaction evidence is reduced. The remaining older sediments tend to be at the very edge of the meander belt and are only occasionally currently intersected by the present river channel. This greatly reduces the number of exposures available to be searched for evidence.

The cumulative effect of the factors associated with measurable lateral spreading displacements in the Wabash Valley is that maximum liquefaction severity will be underestimated when based on measured dike widths. It is also likely that the maximum distance to surface evidence of liquefaction effects may be underestimated when based on paleoliquefaction evidence. The confidence that can be placed in seismic parameters based on prehistoric liquefaction evidence will be increased as the number and distribution of

liquefaction sites is increased, however, it is unlikely that the evidence will include all representative values of liquefaction severity. Seismic parameters based on paleoliquefaction severity relationships must therefore be considered lower bound values.

6.2.2.Paleoliquefaction Attenuation in the Wabash Valley

The Wabash Valley region is located in the central United States, a stable interior region of the continental plate. This area experiences few large earthquakes, and the liquefaction severity index relationship proposed for this region (Youd et al., 1989) is based on three events, two of which are the pre-instrumental Charleston, SC and New Madrid events. The third is the Saguenay, Quebec earthquake, which had a focal depth much greater than is considered typical of Eastern North America events (Atkinson and Boore, 1995). This limited data set suggests a large degree of uncertainty in the relationship for Eastern North America. However, it should be expected that the general trend seen in attenuation of severity of liquefaction effects elsewhere will be apparent in the data associated with the attenuation of paleoliquefaction effects associated with large seismic events in the Wabash Valley.

Figure 6.2 is a plot of the total dike widths measured at sites associated with the Vincennes 6000 year BP event. It can clearly be seen that there is a consistent trend of decreasing lateral displacement with distance from the epicenter. For other events this trend is also present, but is not as clear due to the reduced number of data points available (see Munson and Munson, 1996 for a detailed presentation of this data). Maximum liquefaction severity index values for three Wabash events are shown in Figure 6.3 compared to the data presented by Youd et al. (1989) for the three large historical Eastern North America events listed above. A linear regression of the data of Youd et al. is also shown on the plot for comparison purposes. This should be used for comparisons only, but can provide a preliminary estimate of the approximate range of magnitudes involved in producing the liquefaction evidence in the Wabash Valley.

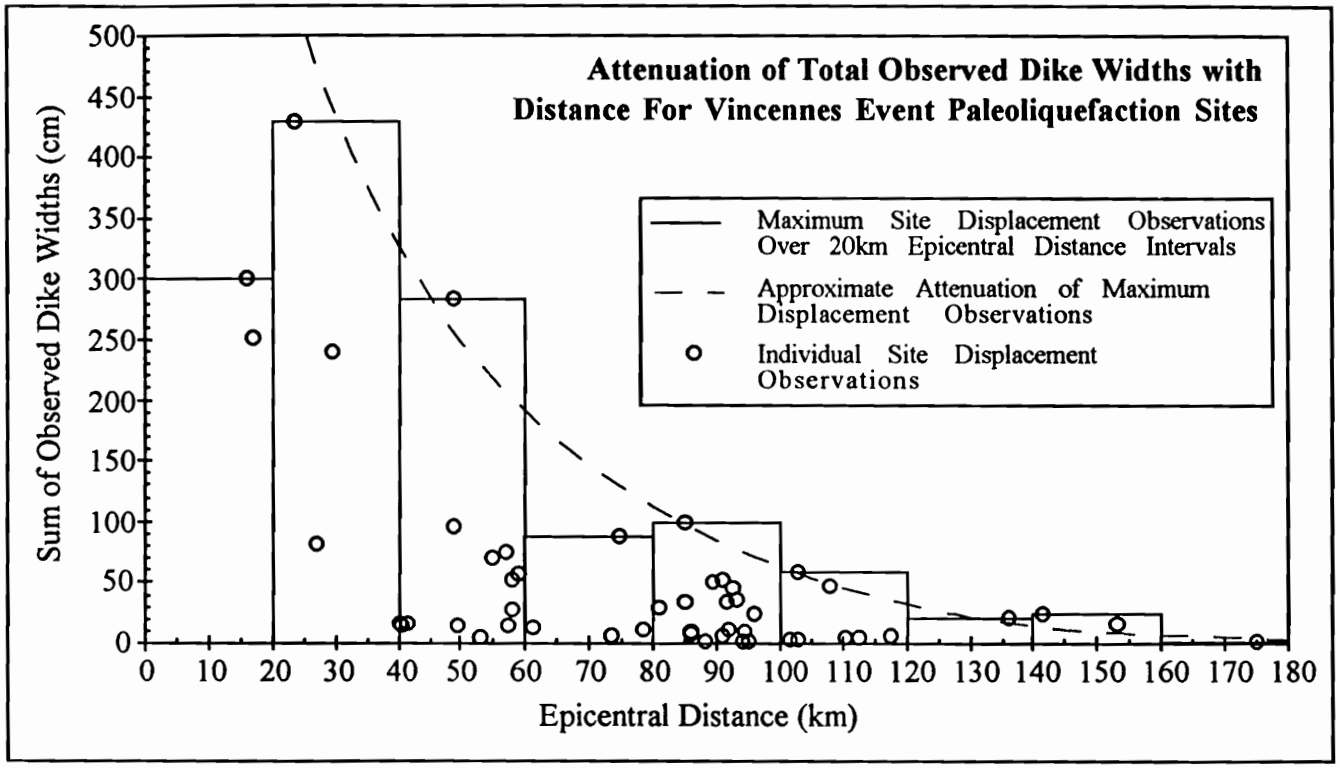

Figure 6.2. Attenuation of the total observed dike widths for sites associated with the Vincennes 6000 year BP event.

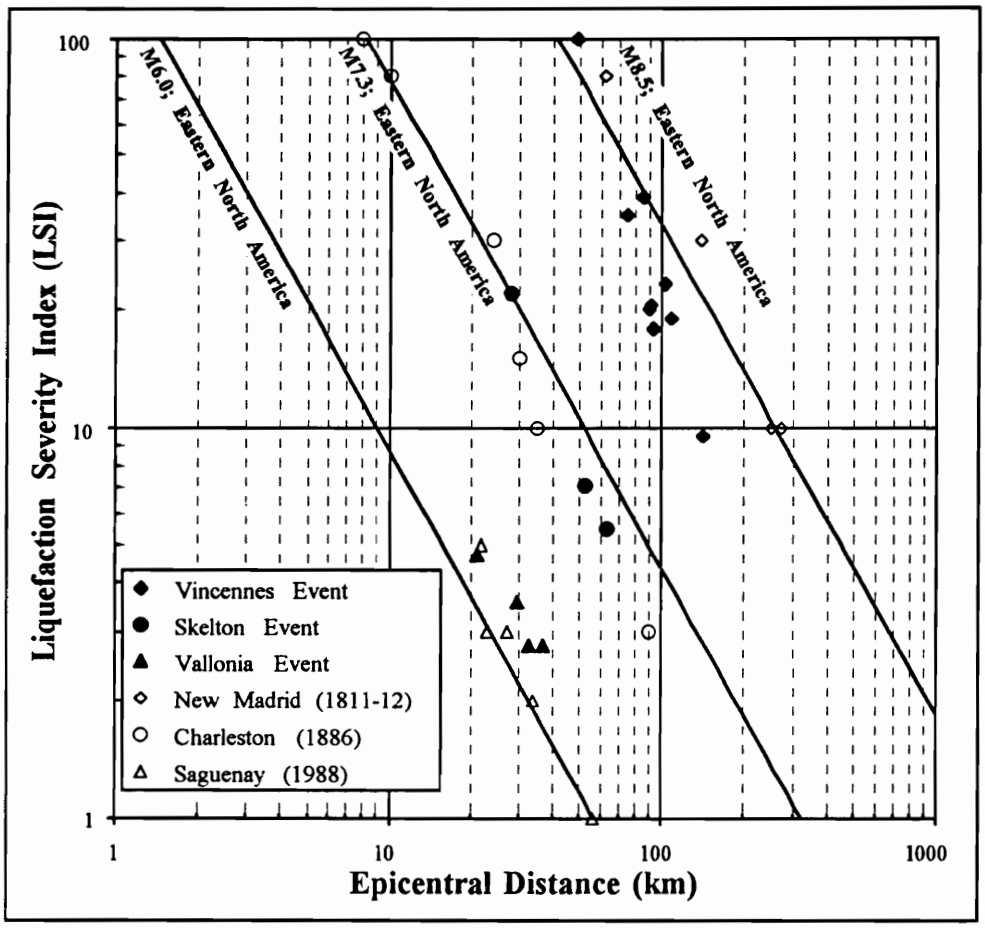

Figure 6.3. Liquefaction Severity Index for eastern North America events. (after Youd et al., 1989). This should be used for generalizations only.

The data for the Wabash Valley earthquakes shown in Figure 6.3 suggest magnitudes in the range of M6.0 to M8.5 produced the liquefaction evidence observed. The linearly-scaled relationship showing attenuation of total dike width vs. distance in Figure 6.2 is consistent with what would be expected for liquefaction sites associated with a single event. The data shown in Figure 6.3 show a similar relationship for the maximum displacement values for each of three events. The liquefaction severity index data shown suggest that the Skelton (12,000 year BP) event was similar in size to the 1886 Charleston, SC earthquake (M7.3). The data for the Vallonia event (4000 years BP) suggest that event was somewhat larger than the 1988 M6.0 Saguenay, Quebec earthquake. The data for the Vincennes earthquake show that event was likely smaller than the 1811-12 New Madrid events (M8.5). These magnitude estimates are based on a very small data set mainly from earthquakes not instrumentally recorded, and should be viewed as very approximate only.

6.3.Magnitude Estimates Based on Maximum Distance to Liquefaction Effects

Two recent studies are among those which have examined the maximum distance to surface evidence of liquefaction effects based on earthquake magnitude (Ambraseys, 1988; Obermeier et al., 1993). Ambraseys compiled data on liquefaction effects for worldwide events and found a well-defined upper bound on the maximum distance to where liquefaction effects could be anticipated for shallow-focus events. This is shown as the dark solid line in Figure 6.4. This approach has subsequently been modified to conditions specific to the Wabash Valley and other similar central United States environments by Obermeier et al. They examined data for earthquakes in the central United States and proposed an upper bound for Wabash Valley events. This is shown as the triangular region in Figure 6.4. This boundary is a suggested upper bound on liquefaction effects for events with magnitudes in the range of M6.8 to M8.3.

For this study, two additional points have been added to the range of upper bounds on distance to liquefaction effects proposed by Obermeier et al. (1993). These are also

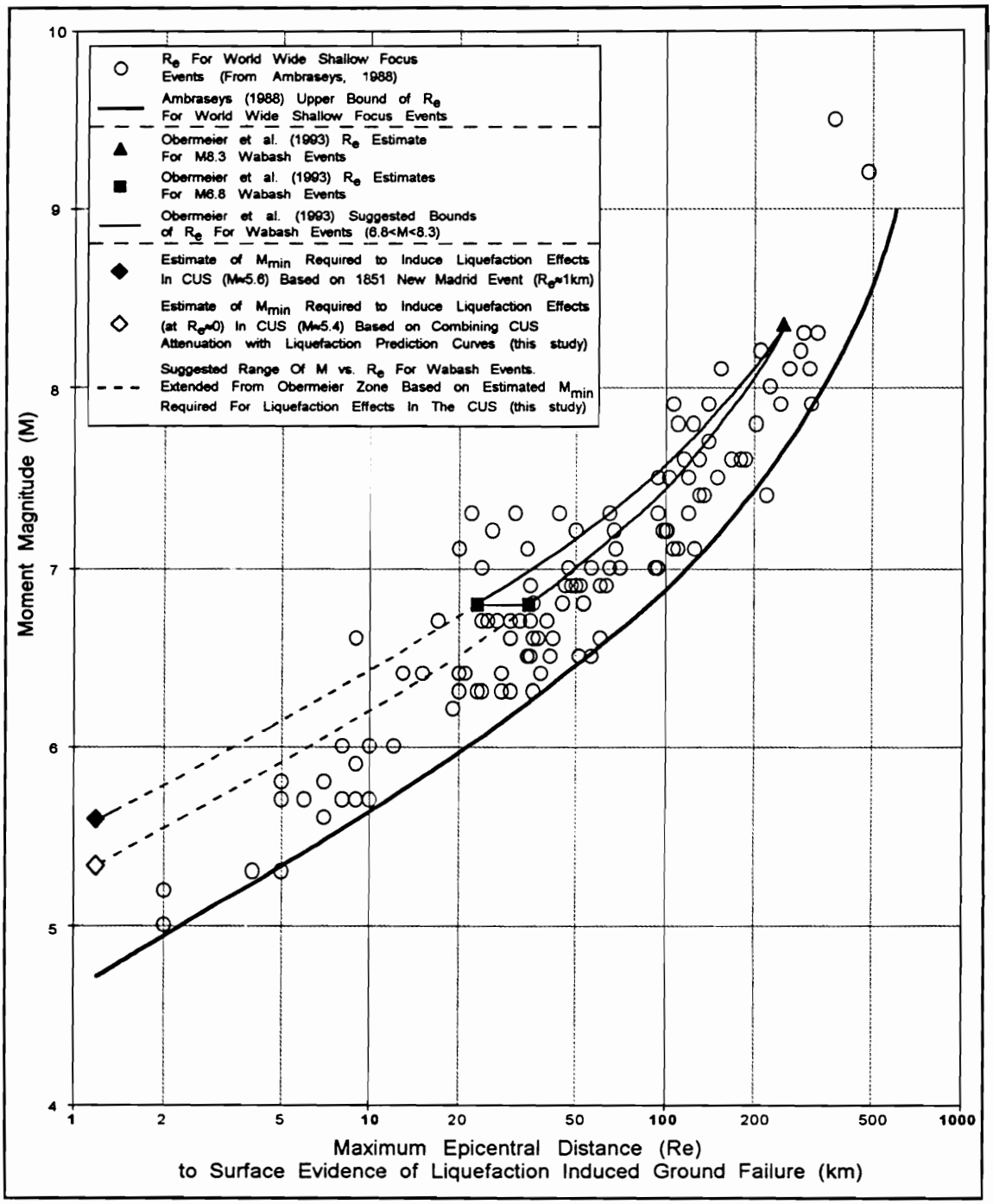

Figure 6.4. Upper bound of distance to surface evidence of liquefaction effects based on Magnitude (modified from Ambraseys, 1988; and Obermeier et al., 1993).

shown on Figure 6.4. The first is based on an earthquake in the New Madrid region in 1851 that apparently induced only a single (reported) liquefaction feature (Metzger 1995, 1996). The event magnitude is estimated to have been **M**5.6. This is assumed to be approximately the threshold for production of liquefaction effects in the central United States and is shown on the figure as a filled diamond. A second threshold estimate is based on the results of this study, which will be seen later to suggest a minimum magnitude for liquefaction effects of **M**5.4. This point is included in Figure 6.4 as an open diamond. The bounds suggested by Obermeier et al. have been extended to these points and it can be seen in Figure 6.5 that this provides a continuous extension of the original boundary that parallels the original curve suggested by Ambraseys (1988). At the present time no data exists to confirm the location of this boundary between **M**5.5 and **M**6.8, but this proposed boundary region is in good agreement with the Obermeier et al. results, and the fact that it approximately parallels the shape of the Ambraseys curve lends support to the location of the boundary curve in this region.

By adopting an average value of the shaded region shown in figure 6.5, a boundary can be drawn predicting the maximum expected extent of liquefaction effects for central United States earthquakes. This is shown in Figure 6.6. From this prediction boundary it is also possible to estimate the magnitude of prehistoric seismic events inducing liquefaction in the central United States. Use of this technique requires a reasonable knowledge of the distribution of liquefaction effects that are associated with a specific event. Liquefaction sites must be confidently associated with specific events and a site at or near the greatest epicentral distance to surface evidence of liquefaction effects is necessary to provide a reasonable estimate of prehistoric earthquake magnitudes.

Using the prediction boundary based on maximum distance to liquefaction effects, magnitude estimates can be made for the four earthquakes investigated for this study. A maximum epicentral distance to liquefaction effects for the Vincennes (6000 BP) event is approximately 141 km. This leads to a magnitude estimate of **M**7.8. Maximum epicentral

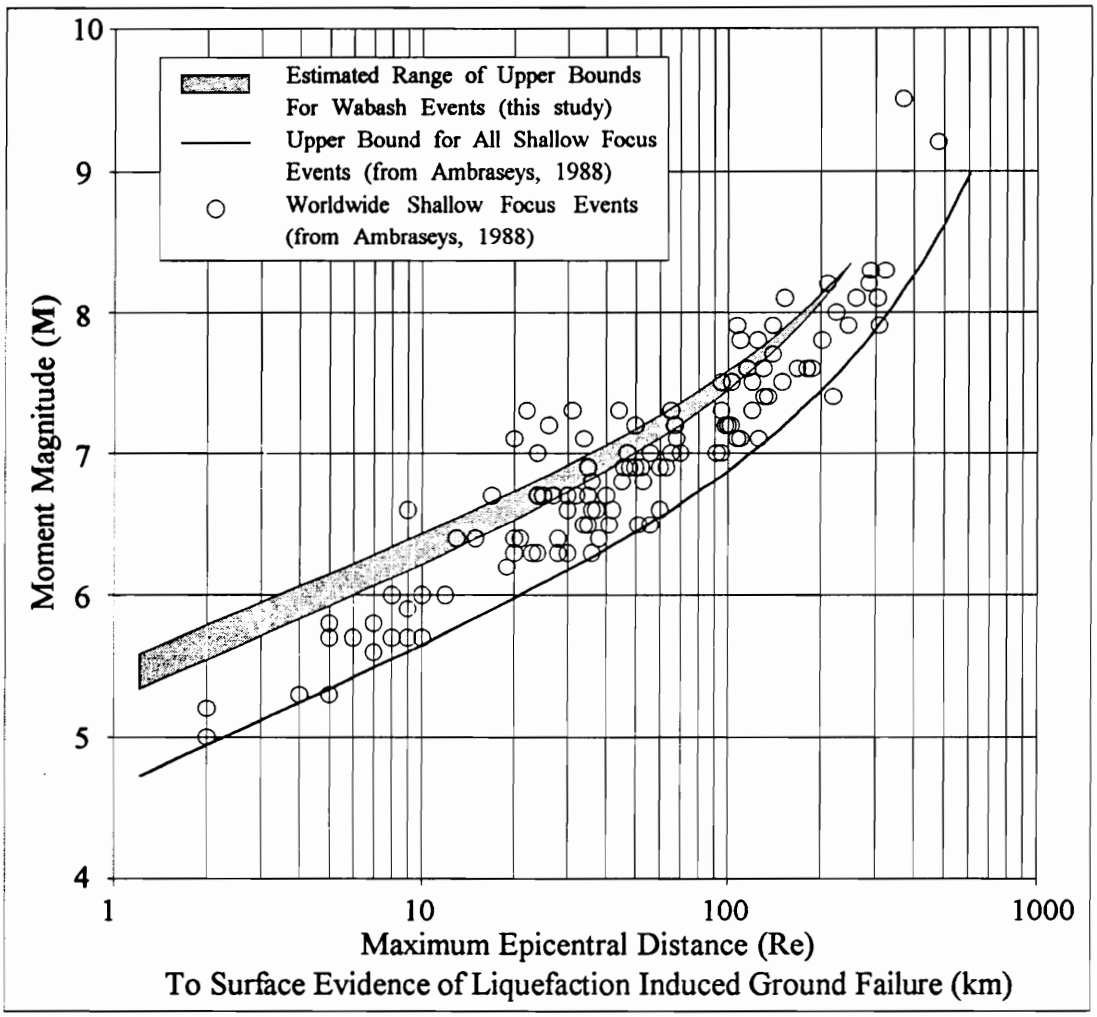

Figure 6.5. Range of upper bounds on maximum distance to liuefaction effects recommended for the central United States.

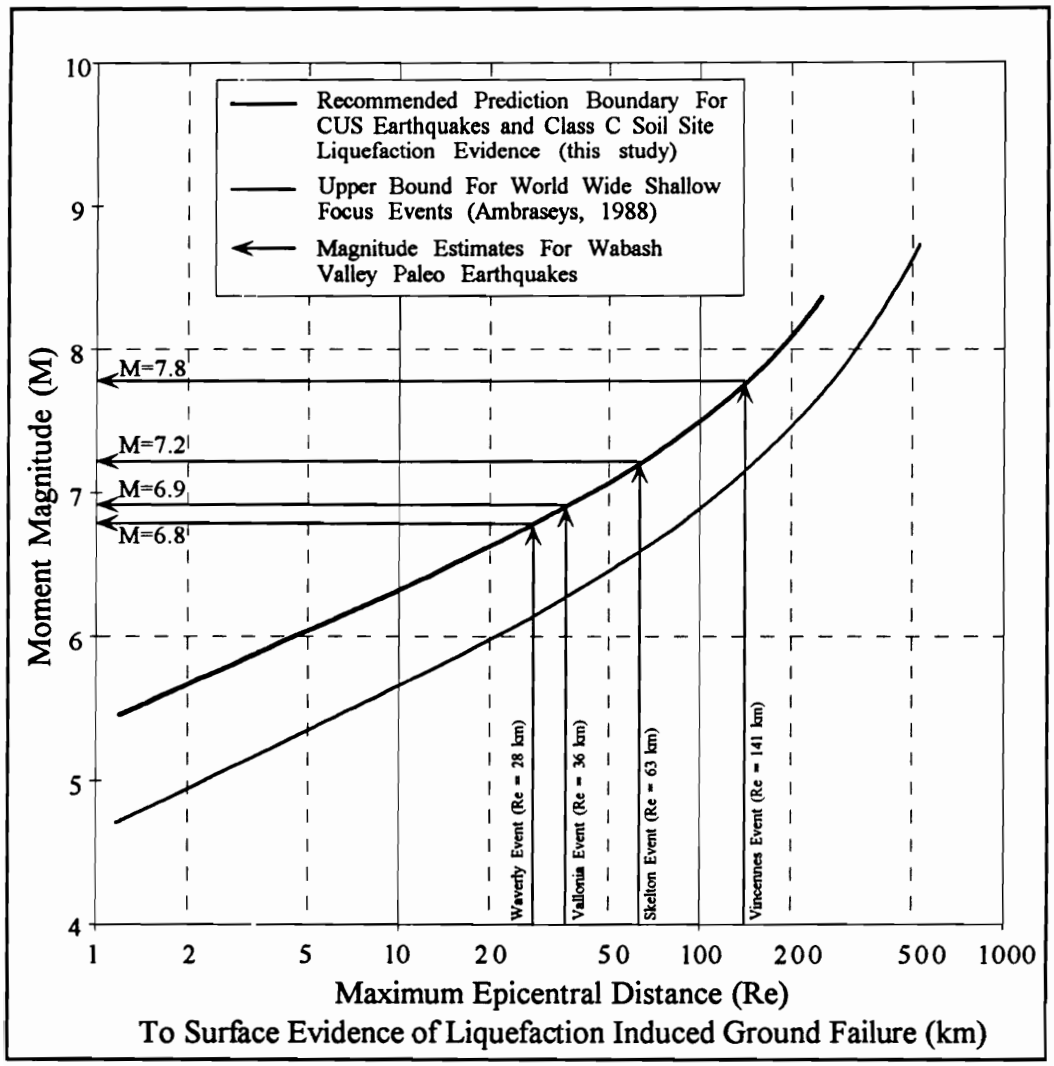

Figure 6.6. Recommended boundary for estimating magnitude of prehistoric central United States earthquakes based on liquefaction evidence.

distances to liquefaction effects for the Skelton (12,000 BP), Vallonia (4000 BP) and Waverly (8500-3500 BP) events are: 63 km, 36 km, and 28 km, respectively. These maximum distance values lead to magnitude estimates of **M**7.2, **M**6.9, and **M**6.8. The magnitude estimates obtained here are consistent with the range of magnitudes suggested previously by the Liquefaction Severity Index relationship. These magnitude estimates will be used later as preliminary estimates in site-specific liquefaction susceptibility analyses.

6.4.In-Situ Liquefaction Susceptibility Analyses of Granular Soils

In-situ liquefaction susceptibility analyses are typically based on variations of the simplified procedure first proposed by Seed and Idriss (1971). This procedure was developed and has found widespread acceptance for two main reasons. First, initial attempts to determine field liquefaction susceptibility based on laboratory tests were found to be unreliable because undisturbed samples of granular soils are, for all practical purposes, impossible to obtain. The cyclic resistance of a given soil has also been found to be highly dependent on stress history (Finn et al., 1970). Sampling procedures remove the stress history effect and drastically alter the cyclic resistance of a sample as measured by the laboratory tests. However, in-situ penetration test procedures have been shown to reliably predict the occurrence of liquefaction (Seed, 1979). Factors that affect the liquefaction susceptibility of sands, such as aging, stress history, and relative density, also affect penetration resistance in a similar manner. Secondly, the SPT has been widely used for foundation investigations for many years and can be performed relatively inexpensively. The SPT has therefore been the primary basis for in-situ liquefaction susceptibility analyses due to the large database of documented field liquefaction cases where penetration test data was available. More recently, use of the CPT and other methods such as SASW and oversize penetration tests have been gaining wider acceptance as well (Andrus and Youd, 1987).

6.4.1.Liquefaction Prediction In Level Ground Conditions

Liquefaction within a saturated granular soil due to seismic loading is induced by the upward propagation of shear waves through the soil deposit (Seed and Idriss, 1982). The mechanism by which pore pressure generation occurs due to this loading was discussed in Chapter 2. The occurrence of liquefaction evidence in the field can be related to the peak horizontal acceleration at the surface based on an initial assumption of rigid body deformation of a soil column. Seed and Idriss review development of their well-known equation relating cyclic stress ratio to the peak surface acceleration:

$$\frac{\tau_{avg}}{\sigma'_o} = 0.65 \cdot \frac{a_{max}}{g} \cdot \frac{\sigma_o}{\sigma'_o} \cdot r_d ;$$

where τ_{avg} is the average of a random loading stress equivalent to a uniform shear stress, a_{max} is the peak surface acceleration that will induce that stress level, g is acceleration due to gravity, σ_o and σ'_o are the total and effective stresses at the depth of interest, r_d is a stress reduction factor accounting for the fact that soil does not behave as truly a rigid body, and τ_{avg}/σ'_o is the cyclic stress ratio (Seed and Idriss, 1982).

Field liquefaction susceptibility analyses using the cyclic stress ratio are based on the past occurrence of liquefaction effects. Where surface motions due to seismic loading, the occurrence or non-occurrence of liquefaction, and the in-situ penetration resistances are known, values of the cyclic stress ratio can be plotted against the blowcount value. By noting the occurrence or non-occurrence of liquefaction, a boundary line can then be drawn to separate conditions allowing liquefaction from those where liquefaction is unlikely. Since this procedure was first developed, the database of liquefaction occurrence and non-occurrence has been improved with each large earthquake. Additionally, steps have been taken to standardize the penetration test procedures (Seed et al., 1985; Seed and DeAlba, 1986).

Recently, several researchers have proposed alternative liquefaction prediction boundaries based on cyclic stress ratio. The Seed et al. (1985) boundary curve is drawn

by hand using engineering judgment to provide a conservative boundary encompassing most cases of liquefaction occurrence. This curve therefore has no direct mathematical representation. In an effort to obtain a suitable mathematical representation of this curve, three other liquefaction prediction boundaries were considered as possible alternatives to provide an estimate of the Seed et al. prediction boundary. These are shown in Figure 6.7. It can be seen in this diagram that each of the prediction boundaries for M7.5 events are similar to the original Seed et al. boundary. The Liao et al. (1988) and Loertscher and Youd (1994) curves are based on a logistic regression analysis of their respective liquefaction databases. The Ambraseys (1988) curve was developed by evaluating the liquefaction database in a manner similar to that used by Seed et al., but over several 0.5 magnitude unit ranges in an effort to incorporate field evidence of magnitude effects.

None of the alternative predictive methods here are either a perfect representation of the Seed curve or a clearly superior alternative. The Ambraseys, and Loertscher and Youd curves incorporate magnitude in the predictive equation. Both the Liao et al. and Ambraseys models include the effect of fines content. The Liao et al. and Loertscher and Youd boundaries predict a cyclic stress ratio greater than zero required to induce liquefaction at minimum blowcount values. In addition, the Liao et al. and Loertscher and Youd curves provide a means to estimate probability associated with a specific boundary curve. The Liao et al. curve shown in Figure 6.7 is for p=0.18 and the Loertscher and Youd curve corresponds to p=0.32. The fact that Loertscher and Youd did not assess the effect of fines content on the results of their evaluation (Loertscher, 1994), however, suggests their probability estimate may be unreliable. The effect of including all fines contents in the regression analysis may have shifted the prediction curves to the left. This would be manifested in an overprediction of the probability of liquefaction for clean sands and an underprediction of liquefaction probability for silty soils. The uncertainty associated with the effect of fines content shown by Liao et al. (1988) suggests that the magnitude of this effect can not be clearly determined. In fact, if the p=0.18 prediction boundary of Liao et al is plotted based on the relationship for silty soils, is can be seen that

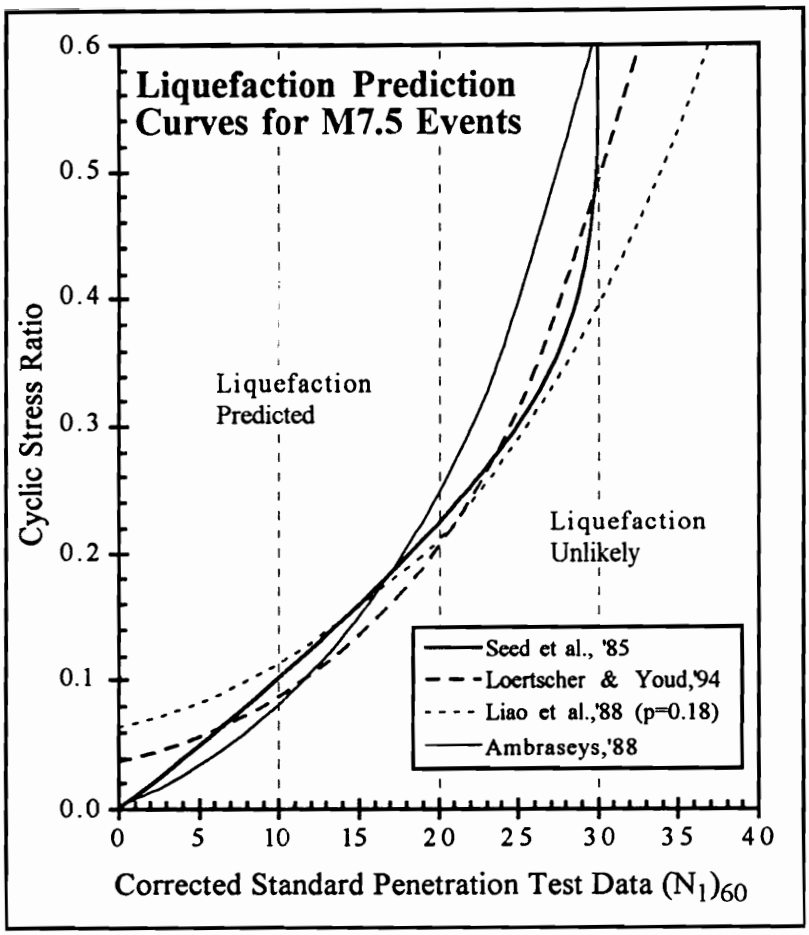

Figure 6.7. Alternative liquefaction prediction curves for M7.5 events compared to the Seed et al. (1985) liquefaction boundary.

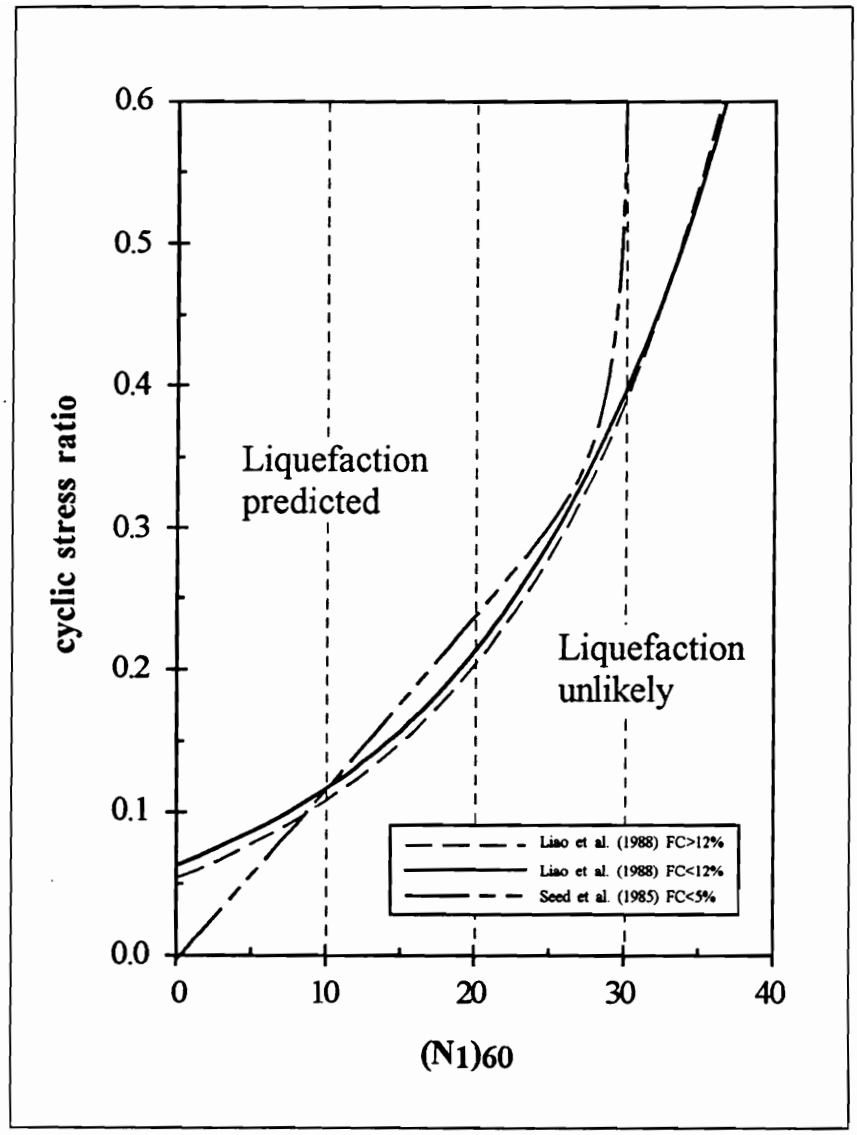

Figure 6.8. Liao et al. (1988) liquefaction prediction boundaries based on p=0.18, for both silty and clean sands compared to Seed et al. 1985 clean sand curve.

there is little or no difference between the predicted liquefaction susceptibilities (Figure 6.8). Ambraseys (1988) considered the effect of fines content and found the "clean" sand prediction boundary shown in Figure 6.7 applies for fines contents of 0% to 10%. Liao et al. also found no statistically significant difference in liquefaction susceptibility among soils with less than 12% fines at a probability of liquefaction occurrence level of p=0.50. They also note that this is a convenient demarcation for the effect of fines content because it corresponds to the separation point in the Unified Soil Classification System between silty sand (SM) and sand with silt (SP-SM or SW-SM).

The Loertscher and Youd (1994) prediction equation was originally derived as a means to evaluate the magnitude scaling factors based on laboratory test results and proposed by Seed and Idriss (1982). The Loertscher and Youd results suggest that at low magnitudes the Seed et al. prediction boundary is highly conservative. The Loertscher and Youd curves for low magnitude events suggest cyclic stress ratios much larger than those of Seed and Idriss. As noted above, it is not clear whether this is an effect of the inclusion of fines in the regression analysis or is a true representation of the cyclic stress ratio required to induce liquefaction for these smaller magnitude events. In an effort to assess how this might affect the results of this study, the Loertscher and Youd curves for the magnitude range of interest were compared to the Seed et al. curves. This is shown in Figure 6.9. The three comparisons shown are for magnitudes of M7.0, M7.5 and M8.0. These magnitude values were chosen based on the range of preliminary magnitude estimates predicted by the maximum distance to liquefaction effects approach above. It can be seen that there is very little difference between the two predictions for this range of magnitudes. Based on this, it can be assumed that the Loertscher and Youd curves will provide reliable results for the magnitude range of interest in this study.

6.4.2.Probability of Liquefaction

The Liao et al. (1988) liquefaction prediction boundary at approximately p=0.18 provides the closest match between their approach and the Seed et al. curve at magnitude

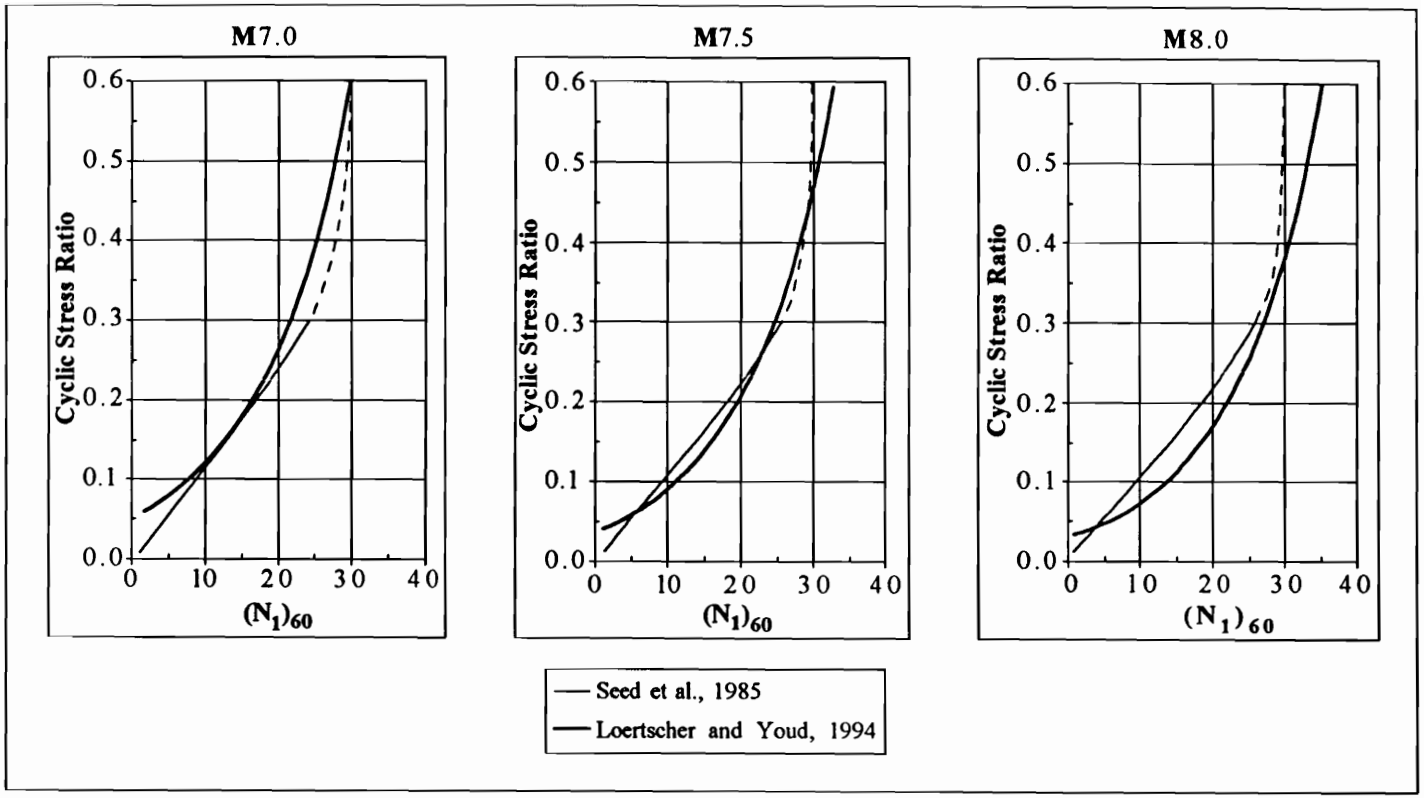

Figure 6.9. Comparison of Loertscher and Youd (1994) Liquefaction prediction boundary with Seed et al. (1985) boundary for the approximate range of magnitudes (M7 to M8) involved in the liquefaction evidence seen in the Wabash valley.

M7.5. The Loertscher and Youd prediction boundary more nearly parallels the Seed et al. (1985) boundary given their probability estimate of p=0.32. The probability associated with this prediction may not be reliable, however, due to the effect of fines content. It is therefore felt that the Liao et al. curve provides a better estimate of the probability for surface manifestation of liquefaction over all site conditions where the cyclic stress ratio and blowcount relationship falls on the Seed et al. boundary. The Loertscher and Youd boundary that most closely matches the Seed et al. curve at M7.5 may also represent a probability of liquefaction similar to p=0.18. The curves shown for the p=0.18 boundaries given by Liao et al. (1988) for silty and clean sands shown in Figure 6.8, however, suggest this may not be the case. The true probability associated with the prediction boundary is likely between these two estimates. It should be noted however, that this probability estimate applies for all cases of liquefaction failure modes. An investigation focused on a single type of failure mode will have a different level of probability associated with the occurrence of liquefaction.

As noted previously, the occurrence of lateral spreading failures will occur more readily than other types of liquefaction-induced failures. Youd and Garris (1995) examined the applicability of Ishihara's (1985) empirical relationship between the depth of a surficial non-liquefiable layer and the thickness of liquefied sediments required to produce surficial evidence of liquefaction. Their study shows lateral spreading and ground oscillation liquefaction failures occur at liquefied layer thicknesses lower than predicted by the Ishihara curves. This says that lateral spreading and ground oscillation failures will occur at cyclic stress ratios less than will be required for failures typical of the conditions examined by Ishihara (sand boils in level ground). This conclusion is based on the fact that, for all else equal, lesser liquefied layer thicknesses will require greater cyclic stress ratios to induce ground failure (Youd and Perkins, 1987). When layer thickness is held constant, the Youd and Garris findings show that lateral spreading is a failure mode with a greater likelihood of occurrence than that for level ground conditions susceptible to sand boils and settlement only. Thus, it can be concluded that at sites subject to lateral

spreading or ground oscillation failures, greater soil strengths are required to resist liquefaction effects. Conversely, for a given soil condition, sites subject to either lateral spreading or ground oscillation failures will experience those liquefaction-induced failures at lower cyclic stress ratios than similar blowcount material subject to level-ground failure conditions.

The difference in susceptibility to liquefaction effects at lateral spreading and sand boil sites has also been observed in the central United States. Outside the meizoseismal zone associated with the 1811-1812 New Madrid earthquakes, liquefaction failures are generally confined to lateral spreading and ground oscillation displacements (Obermeier, 1995), while within the meizoseismal zone liquefaction-induced surface disruptions are observed for all modes of failure. For sites in the central United States, this agrees with the findings of Youd and Garris (1995) based on predominantly plate margin events. Sites subject to sand boil development alone can resist liquefaction effects at lower soil strengths than required at sites subject to lateral spreading or ground oscillation failures. From this it can be concluded that liquefaction failures due to lateral spreading and ground oscillations will represent points in the liquefaction database that on average plot nearer to the prediction boundary than the average for all liquefied sites. This fact also increases the probability associated with the liquefaction prediction boundary for liquefaction-induced failures at sites controlled by these conditions. The p=0.18 probability of occurrence suggested based on Liao et al. (1988) will therefore likely underestimate the true probability of liquefaction associated with lateral spreading failures.

For lateral-spreading failures at sites where a free face controls the displacement, liquefaction resistance will also require greater soil strengths than for sites subject to ground oscillation failures alone. At the margins of liquefaction effects observed in the New Madrid region, the mode of failure is generally limited to lateral spreading alone. Additionally, as the distance from a free face increases, the severity of the liquefaction-induced displacement is reduced (Obermeier, 1995). The observations made in the New

Madrid region are also supported by a parametric study using the lateral spreading displacement prediction model of Bartlett and Youd (1995). If it is assumed that ground oscillation failures are represented by the Bartlett and Youd prediction of ground slope-controlled displacements, and that free-face displacements adjacent to a channel are representative of traditional lateral spreading failures, a comparison can be made of the loading conditions leading to displacements in each of these site conditions.

The results of this parametric study show that displacements adjacent to a free face (lateral spreading) are predicted to exceed those governed by ground slope (ground oscillation) for any combination of parameters consistent with the wide alluvial valleys in the Wabash and New Madrid regions. The ground conditions considered here are for slopes of less than 6%, consistent with the type of failure mode observed in the Wabash region and as recommended by Bartlett and Youd (1992) for the near-level ground conditions represented by their model. At the outer limits of predicted liquefaction effects, ground-slope controlled displacements decrease to zero before those of a free-face controlled displacement. This suggests that the lateral spreading failure condition will represent points in the liquefaction database that can be expected to fall at or very near the liquefaction prediction boundary. The probability of liquefaction associated with this type of site condition will be much higher than the approximately 20% probability estimate shown by the Liao et al. (1988) curve for all failure conditions. For sites most susceptible to liquefaction and lateral spreading failure, the prediction boundary can be considered a "best" estimate of the actual cyclic stress ratio that will induce liquefaction.

6.4.3.Back Calculation of Surface Motions

Based on the findings above, the Loertscher and Youd (1994) prediction equation was chosen to represent the Seed et al. (1985) curve for the liquefaction susceptibility evaluations of this study. The Liao et al. and Ambraseys boundaries do not match the curve of Seed et al. as well as the Loertscher and Youd curve. However, it is assumed, as suggested by both of these researchers, that for fines contents less than 10% to 12%, the

liquefiable Wabash soils could be considered clean sands. All except a few rare samples of the liquefiable Wabash soils fall below this range of fines contents.

Loertscher and Youd (1994) propose the following equation for cyclic stress ratio as a function of moment magnitude and $(N_1)_{60}$:

$$\frac{\tau_{avg}}{\sigma_o'} = e^{\left(-7.400 + 30.826/M + 0.0851(N_1)_{60}\right)};$$

Using this liquefaction prediction boundary, the threshold cyclic stress ratio required to allow liquefaction effects at the Wabash Valley paleoliquefaction study sites can be estimated for the in-situ $(N_1)_{60}$ values measured throughout the thickness of the soil deposit predicted to liquefy. Here again, it is assumed that lateral spreading due to liquefaction will provide points in the liquefaction database occurring at or near the threshold boundary, though some variation above and below the predicted threshold is likely. The deviation from the threshold prediction boundary will affect the results to some extent, but the error introduced here should be within the margin of error based on assumptions necessary in other parts of the analysis.

For each of the threshold cyclic stress ratios estimated above, a corresponding "best" estimate of peak ground surface acceleration can be back-calculated using the Seed and Idriss (1982) equation for cyclic stress ratio experienced in the field. Solving for the peak ground surface acceleration, the Seed and Idriss equation can be rewritten as:

$$\frac{a_{max}}{g} = \frac{\tau_{avg}/\sigma_o'}{0.65(\sigma_o/\sigma_o')r_d}.$$

Performing this evaluation for sites at various epicentral distances, an approximate attenuation relationship can be developed based on estimates of the minimum peak surface acceleration required to induce the liquefaction seen at each site. The peak acceleration is found at each sample interval throughout a soil profile based on the cyclic stress ratio determined from the Loertscher and Youd (1994) liquefaction prediction equation. The

in-situ stress parameters can be easily determined based on the soil profile data, and magnitude is based on the initial estimate found from the maximum distance to liquefaction effects.

The minimum value of a_{max} found at a boring location can be assumed to represent the minimum surface motion required to produce the liquefaction effects observed at that location. Alternatively, some engineering judgment can be applied to estimate a greater liquefied layer thickness based on the in-situ conditions. Neither of these are particularly satisfying alternatives, however. Using the absolute minimum value of surface acceleration leads to a low and flat attenuation relationship due to the fact that liquefaction susceptibility of the loosest soil is fairly high, and site conditions are relatively constant within the study region. All of the sites associated with specific events are of similar depositional origin and age. A few locations near the epicentral region may contain soils with higher blowcount values throughout the upper liquefied soil profile, but these conditions are the exception rather than the rule. Using engineering judgment to assess a likely liquefied thickness will provide an estimate of surface motion presumably greater than the minimum value, but is a subjective process that may introduce a bias in the results not representative of actual field experience.

An additional problem that needs to be addressed here is the reliance of the analysis on the initial assumption of magnitude proposed by the maximum distance to liquefaction effects prediction of Figure 6.6. An alternative method to estimate magnitude should be found that can confirm or refute the estimates based on this approach. This issue will be addressed below, and a method to estimate the liquefied thickness of the soil deposit will then be proposed.

6.5.Semi-Theoretical Wabash Valley Attenuation Relationship

As was noted previously there is not a reliable attenuation relationship available for Wabash Valley soil site conditions. Most attention has been directed toward the soil conditions associated with sites in the New Madrid Seismic Zone. This is the location of

the Mississippi embayment, and contains sediments much different from the Wabash region. There are also no historical strong motion records on which to build an empirical soil site attenuation relationship. At the present time reliable Wabash Valley (and Eastern North America in general) ground motion attenuation predictions are limited to rock sites. The best of these is the Atkinson and Boore (1995) update of the Boore and Atkinson (1987) model. The new version of the model has been modified based on recent empirical studies and is shown to be consistent with events of **M**5.8 and **M**6.8.

In order to develop an attenuation relationship appropriate to Wabash Valley soil sites it was necessary to use the Atkinson and Boore (1995) model to produce time series earthquake records for a range of magnitudes and hypocentral distances and propagate those motions to the ground surface through the soils present in the Wabash Valley. The time series motions required for this study have been synthesized by Mr. Martin Chapman of the Virginia Polytechnic Institute and State University Seismological Observatory based on the stochastic modeling procedure outlined by Boore (1983), and using the input parameters suggested by Atkinson and Boore (1995). A total of 13 records were produced. These time series earthquake records are for a **M**6.75 event at epicentral distances of 0, 15 and 30 km; a **M**7.0 event at epicentral distances of 3, 30, 45, and 60 km; and for a **M**7.25 event at epicentral distances of 15, 40, 60, 80, 100, and 140 km. Each of the records produced are given in Appendix G. These records were propagated to the ground surface using the computer program SHAKE (Schnabel et al., 1972). A linear regression of the results of the SHAKE analyses was then performed to determine an appropriate semi-theoretical seismological attenuation relationship for Wabash Valley soil site earthquake motions. This analysis is outlined below.

6.5.1.SHAKE Analyses

The program SHAKE performs a one-dimensional analysis of the propagation of vertically-traveling shear waves through a soil column from an elastic base. The analysis assumes a horizontally-layered system of homogeneous, visco-elastic layers of infinite

lateral extent. Each of the layers within the system are assumed to be defined by the shear modulus, critical damping ratio, density and vertical thickness. The program uses an iterative procedure to compute strain-compatible shear modulus (G) and critical damping values (D) based on the average effective strain level for each layer at each time step. Yegian et al. (1994) have shown that for sediment-filled valleys similar to those found in the Wabash Valley Seismic Zone this technique gives reliable predictions of ground surface motions propagated through the soil deposit from input seismic base motions.

Input data required by the program are the time series of the object motions; the soil profile data, including: layer type and thickness, an initial estimate of the strain-compatible shear modulus and damping ratio, unit weight of the soil layer, the value of K_{2max} for sands (Seed et al., 1986) or G_{max} for clays, and the relative dynamic modulus and damping ratio properties for each soil type (Vucetic and Dobry, 1991). The conditions present at site RF were chosen to represent an average soil profile for Wabash sites. This is the site where the greatest variety of in-situ test results was obtained.

Site RF is also located near Vincennes, Indiana, at approximately the center of the study region in the north-south direction (see Figure 3.4). The liquefiable soil conditions at this site range from gravelly sand to sand (see Figure 5.10 and grainsize distributions in Appendix F), with bedrock at a depth estimated to be approximately 150 feet (45m). The input properties used were determined based on the soil samples obtained; the penetration test data; and the cross-hole, down-hole, and SASW seismic wave velocity test results. This site is considered representative of an average site condition for the study region. The results of the near-surface testing performed at other study sites were found to be similar to the results found at site RF.

The depth to bedrock does vary, however, from approximately 15m to 45m across the study region. To assess the effect of soil depth, five different depths were analyzed for each of the synthetic motions. It was found that for each soil depth between 50 and 250 feet (15 to 75m) the results were relatively constant (generally within ±10%). Since soil

depths vary across the region, an average value of the predicted peak ground surface accelerations found for the five soil profile depths was chosen to represent the surface motion for each of the magnitude and distance combinations evaluated.

6.5.1.1.SHAKE results

The soil profile was found to generally deamplify the input motions by a factor of between 1 and 3, depending on epicentral distance. This is due to the fact that the peak bedrock motion is associated with the high frequency portion of the input motion spectrum. These peak high frequency motions tend to be attenuated out of the record with distance from the epicenter as well as being efficiently filtered out in the soil column. At the greatest source to site distances studied, some slight amplification of the peak motion was seen. At these large distances, the amplitude of the higher frequency strong motions has been reduced due to the filtering effect of the bedrock. The strongest motions at these distances are associated with frequencies closer to the natural period of the soil column.

Seismic motions in Eastern North America tend to contain a much higher frequency content than their Western United States counterparts (Atkinson and Boore, 1995). Eastern North America earthquakes contain an upper corner frequency of approximately 50 Hz compared to less than 20 Hz for Western United States events. Including the entire spectrum of frequencies in the time series records produced a numerical instability in the program SHAKE that required the input motions to be filtered to a maximum frequency of 25 Hz for the smaller events and distances, and to 12.5 Hz for the largest events and distances. For the cases where the program was stable at a maximum input frequency of 25 Hz, the maximum difference in the predicted peak surface acceleration for the two filtered input records is less than 10%. For most cases, however, the predicted peak surface motions showed no difference at all. This is due to the fact that the soil column effectively attenuates nearly all the motions associated with frequencies greater than approximately 10Hz. A comparison of the Fourier spectra of the bedrock and surface

motions for f_{max} = 12.5 Hz and 25 Hz at M7.0, R = 30 km and a soil depth of 100 ft. is included in Appendix G. This response is representative of the difference in the response seen for all of the cases where the program was stable for f_{max} equal both 12.5 and 25 Hz.

6.5.2.Wabash Region Soil Site Attenuation Relationship

The results of the SHAKE analyses were used in a multiple linear regression analysis to develop an attenuation relationship that could be used to supplement the liquefaction susceptibility analysis. The variables included in the regression were based on equations of the form given by Boore and Joyner (1991) and Atkinson and Boore (1995). Each of those studies express the log transform of surface acceleration as a function of the log transform of hypocentral distance, and as a linear function of magnitude, distance, and other higher order magnitude terms as:

$$Log(\mathrm{PGA}) = a + b \cdot (\mathrm{M} - 6) - c \cdot (\mathrm{M} - 6)^2 - d \cdot (\mathrm{M} - 6)^3 - e \cdot Log(R) - f \cdot (R);$$

where PGA is peak surface acceleration in units of gravity, **M** is moment magnitude, ***R*** is hypocentral distance in km, and ***a*** through ***f*** are regression coefficients.

The regression analysis of the SHAKE results showed the coefficients on the higher order magnitude terms and the linear distance term were not statistically different from zero at a 99% confidence level. This differs from the finding of Boore and Joyner (1991) for Eastern North America deep soil sites, but is consistent with the peak acceleration attenuation relationship proposed by Boore, et al. (1993) for Western United States class C soil sites (180 m/s $\leq V_s \leq$ 360 m/s in the upper 30m). Additionally, no improvement was seen in the coefficient of determination (r^2) by including these variables in the regression, and the F-statistic was reduced for models including these terms. The results of the regression analysis therefore leads to the following recommended relationship expressing Wabash Valley class C soil site attenuation:

$$Log(\mathrm{PGA}) = -1.129 + 0.216 \cdot (\mathrm{M}) - 0.7205 \cdot Log(R);$$

This equation results in a coefficient of determination, $r^2 = 0.97$, and an F-statistic of 174. Hypocentral distance is used for this relationship rather than epicentral distance because it provides a better fit to the data in the near field. All focal depths are assumed to be 10 km based on the average focal depth suggested by Boore and Atkinson (1987).

The regression equation prediction of attenuation and the original data found from the SHAKE analysis are shown in Figure 6.10. The curves shown in the figure are for ground motion attenuations associated with earthquake magnitudes of **M**6.75, **M**7.0, and **M**7.25, corresponding to the magnitudes used to develop the surface motion relationship. There is very good agreement between the individual surface motion estimates and the linear regression predictions of those points.

Figure 6.11 is a comparison of the attenuation relationship at magnitude **M**7.0 developed for this study and the three attenuation relationships shown in Figure 6.1. It can be seen that there is good agreement between the Wabash Valley attenuation relationship and those for the New Madrid region (Nuttli and Herrmann, 1984; Boore and Joyner, 1991) at hypocentral distances beyond approximately 80 km. In the near field, however, the Wabash Valley relationship predicts a substantially lower peak surface acceleration than either of the New Madrid relationships. The Boore and Joyner model is for stiff soil sites which will transmit a greater portion of the high frequency motion to the surface. This results in higher peak surface accelerations, but also at a higher frequency than for that produced at the Wabash Valley soil sites. The Campbell (1981) worldwide near-field relationship predicts motions lower than the Wabash relationship developed here.

Figure 6.12 presents the attenuation relationship developed here for Wabash Valley soil sites in comparison to the Boore, Joyner, and Fumal (1993) relationship for Western United States soil site attenuations of peak surface acceleration. It can be seen that the difference in attenuation predictions between eastern and western regions of North America is negligible. This is consistent with the assumptions in the Campbell (1981)

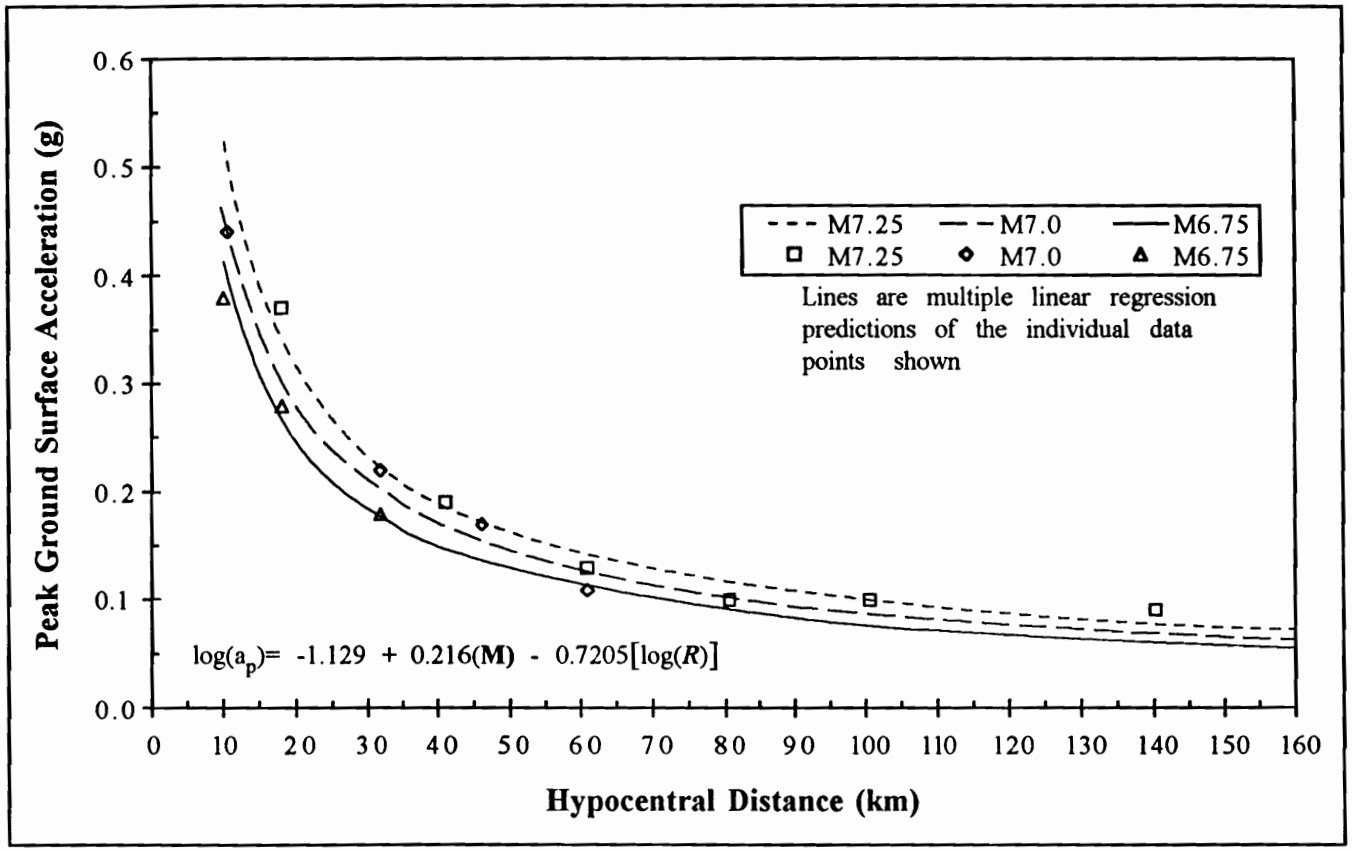

Figure 6.10. Proposed surface motion attenuation relationship for Wabash Valley Seismic Zone soil site conditions.

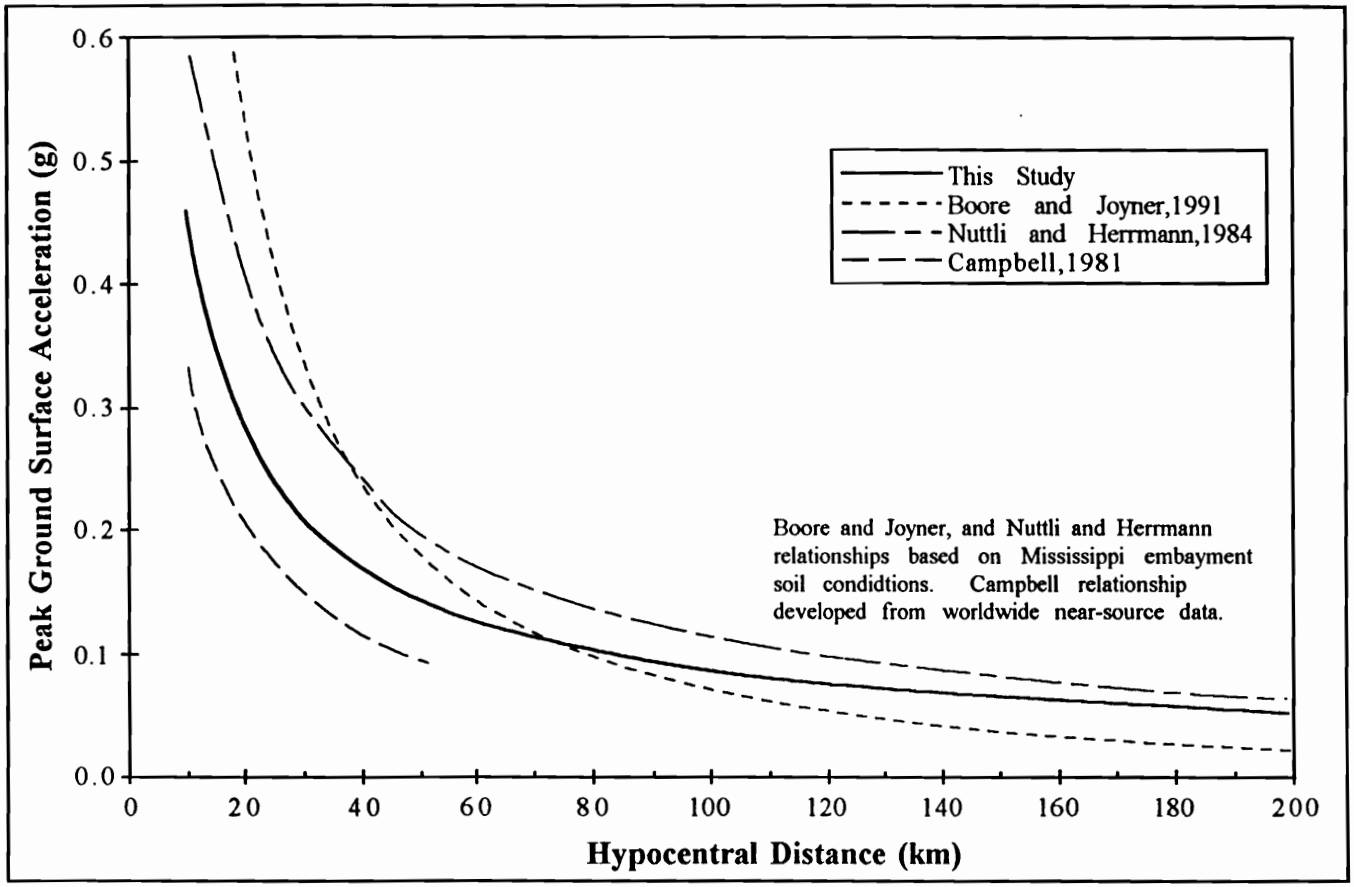

Figure 6.11. M7.0 Surface motion attenuation relationships proposed for central United States soil sites.

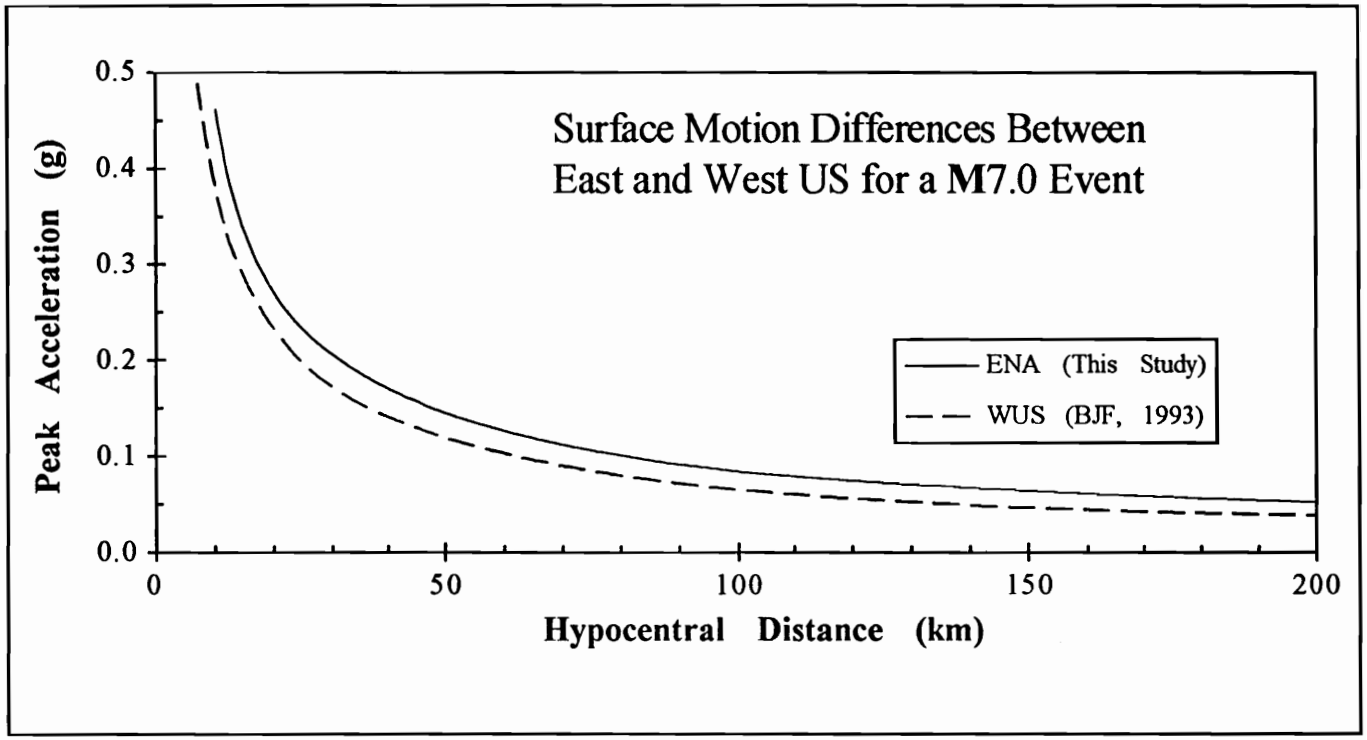

Figure 6.12. Comparison of class C soil site attenuation relationships for a M7.0 earthquake in both Eastern and Western U.S. regions. Western U.S. attenuation relationship from Boore, Joyner and Fumal (1993).

approach to attenuation prediction. Source characteristics can be assumed to be similar between plate margin and interior events, with differences only manifested in the anelastic attenuation component. The prediction of motions shown here also indicates that anelastic attenuation differences are insignificant in the distance ranges considered. Within epicentral distances subject to the occurrence of liquefaction effects, plate margin and mid-continent class C soil site peak ground motions will not be significantly different.

6.6.Seismological Magnitude Estimates

6.6.1.CUS Attenuation Linked With Liquefaction Prediction

The Wabash Valley attenuation relationship developed above based on a seismological prediction of seismic motions can be used to provide a second estimate of the magnitude required to induce the liquefaction evidence observed in the Wabash Valley. By incorporating the Seed et al. (1985) approach to liquefaction prediction based on cyclic stress ratio and in-situ blowcount with the Wabash Valley attenuation relationship, it is possible to develop an equation for magnitude based solely on blowcount and distance. This will provide a simple method to estimate magnitude based on the in-situ conditions at each of the study sites. This equation is derived below and used to estimate magnitudes for the four earthquakes investigated for this study.

6.6.1.1.Magnitude Based on Hypocentral Distance and Liquefaction Susceptibility

The Loertscher and Youd (1994) liquefaction prediction equation for cyclic stress ratio is given as:

$$Ln(CSR) = -7.4 + \frac{30.826}{M} + 0.0851 \cdot (N_1)_{60};$$

but can be written as:

$$Log(CSR) = -3.214 + \frac{13.388}{M} + 0.037 \cdot (N_1)_{60}.$$

where ***CSR*** is the cyclic stress ratio as defined by Seed and Idriss (1971), **M** is moment magnitude, and $(N_1)_{60}$ is the corrected in-situ standard penetration test blowcount.

The cyclic stress ratio equation:

$$\frac{\tau_{avg}}{\sigma_o'} = 0.65 \cdot \frac{a_{max}}{g} \cdot \frac{\sigma_o}{\sigma_o'} \cdot r_d$$

can be substituted into the Loertsher and Youd relationship, resulting in:

$$Log\left(0.65 \cdot \frac{a_{max}}{g} \cdot \frac{\sigma_o}{\sigma_o'} \cdot r_d\right) = -3.214 + \frac{13.388}{M} + 0.037 \cdot (N_1)_{60}.$$

and solving for $Log(a_{max})$ the result is:

$$Log(a_{max}) = \left(-3.214 + \frac{13.388}{M} + 0.037 \cdot (N_1)_{60}\right) - Log\left(0.65 \cdot \frac{\sigma_o}{\sigma_o'} \cdot r_d\right).$$

For the site conditions observed at the Wabash Valley study sites, the quantity: $\left(0.65 \cdot {}^{\sigma_o}/_{\sigma_o'} \cdot r_d\right)$, typically ranges between 0.95 and 1.05. This value can therefore be assumed to equal 1.0 for most cases and will drop out of the equation. By equating this relationship and the Wabash Valley attenuation prediction, the following equation is obtained:

$$\left(-3.214 + \frac{13.388}{M} + 0.037 \cdot (N_1)_{60}\right) = \left(-1.129 + 0.216 \cdot M - 0.7205 \cdot \left[Log(R)\right]\right).$$

This then results in a quadratic equation in **M**:

$$M^2 + \left(-0.1713 \cdot (N_1)_{60} + 9.653 - 3.336 \cdot \left[Log(R)\right]\right) \cdot M - 61.98 = 0;$$

that can easily be solved for **M** in terms of $(N_1)_{60}$ and R by use of the familiar quadratic formula. With an equation for **M** in terms of R and $(N_1)_{60}$ it is possible to plot contours of

magnitude required to induce liquefaction evidence at sites with known soil properties and epicentral distances.

By comparing the minimum value of $(N_1)_{60}$, measured at each boring location where liquefaction evidence has been observed, with the contours of minimum magnitude required to induce liquefaction, it is possible to estimate a minimum magnitude required to induce the liquefaction evidence at all sites associated with a specific prehistoric event. This analysis has been performed for each of the liquefaction distributions associated with the four earthquakes investigated for this study. At each site, several borings were completed during the field portion of this study. It is assumed here that the liquefaction evidence produced at each of the boring locations was governed by the blowcount values measured at that location. This assumes that each boring location can be considered to be independent, which is not strictly true. However, this assumption is reasonable based on the distance between most boring locations, and the fact that this assumption will remove some of the subjectivity inherent in other methods of choosing appropriate site specific soil parameters (Liao et al., 1988). The boring location at each site with the largest minimum blowcount value is therefore chosen to represent that site in this analysis. The assumption leading to the selection of the boring with the largest minimum blowcount is that the minimum magnitude affecting a site will have been that required to produce the liquefaction evidence seen at each boring location at a given site.

Figures 6.13 through 6.16 show the results of this analysis for the Vincennes, Skelton, Vallonia, and Waverly events. A single data point is shown for each site. This value is the minimum corrected blowcount from the boring location with the greatest value of minimum blowcount. The individual site predictions are shown compared to the contours of magnitude required for liquefaction. The dashed lines are magnitude contours that correspond to the minimum magnitude that will lead to liquefaction at all of the sites associated with a specific event. It can be seen from these figures that the predictions of minimum magnitude required to induce liquefaction at all of the sites associated with each

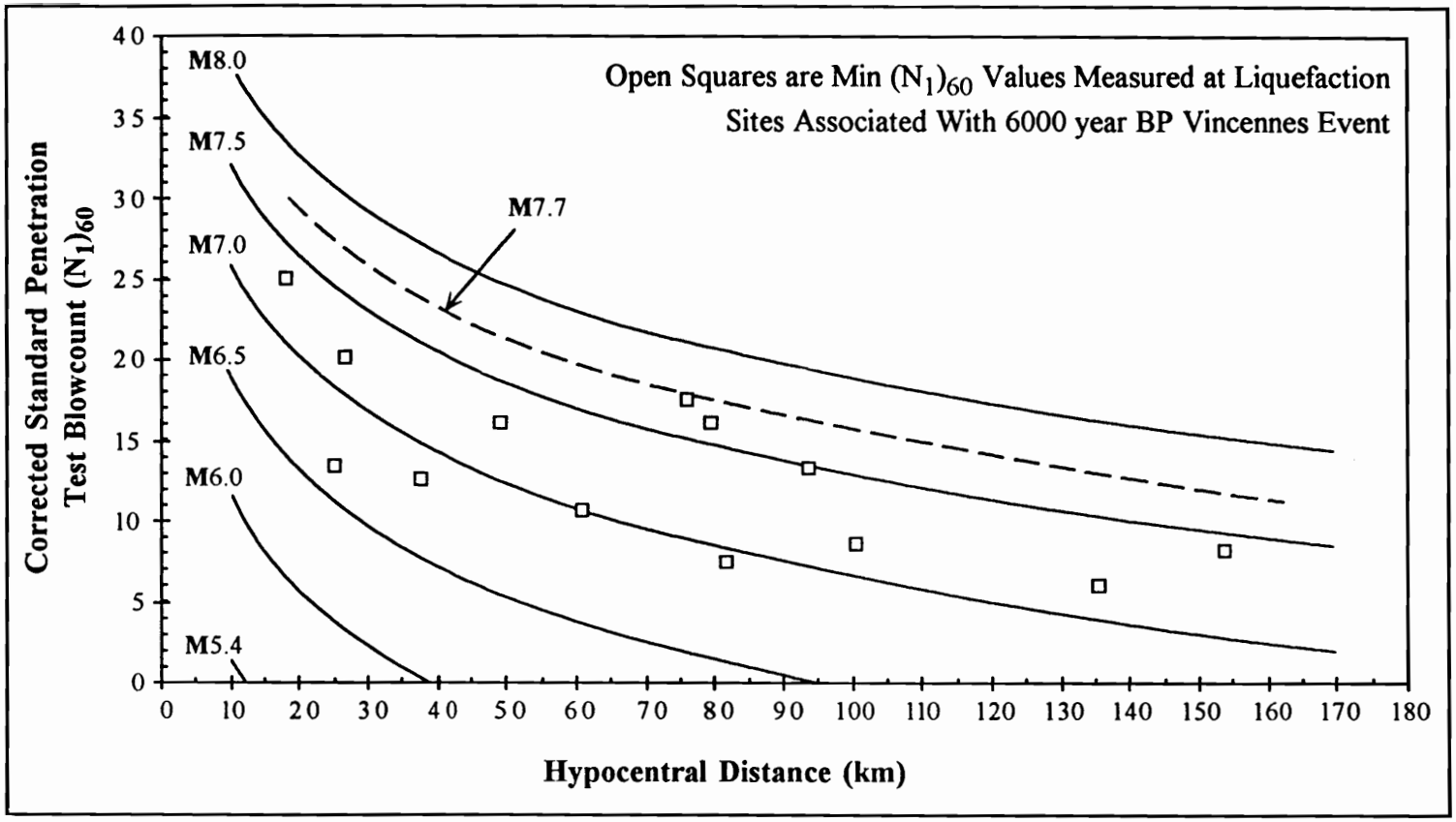

Figure 6.13. Minimum blowcount involved in liquefaction evidence at Vincennes event sites compared to the contours of minimum magnitude required to induce liquefaction. Predicted M7.7 earthquake required to liquefy all sites associated with this event.

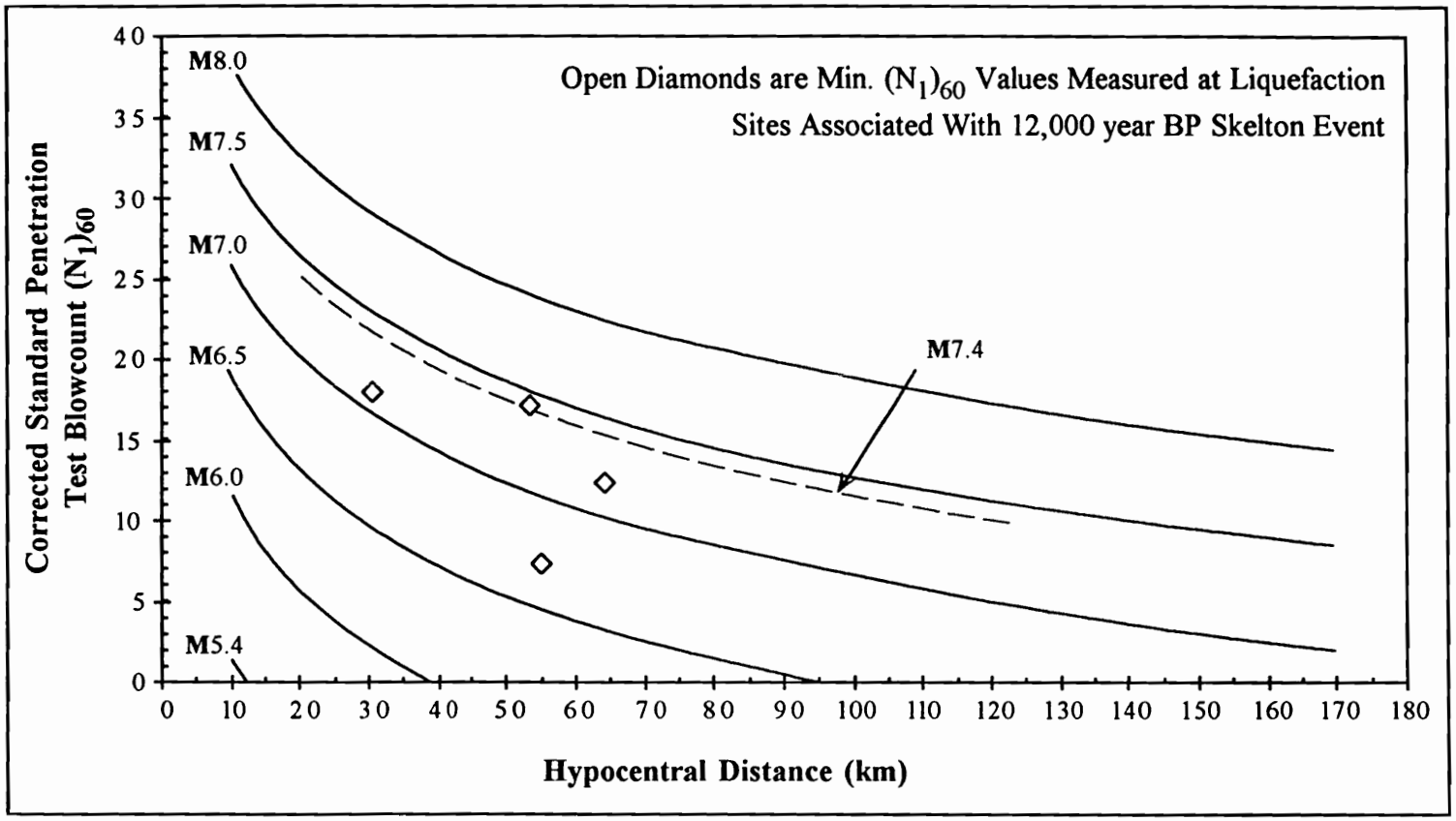

Figure 6.14. Minimum blowcount involved in liquefaction evidence at Skelton event sites compared to the contours of minimum magnitude required to induce liquefaction. Predicted M7.4 earthquake required to liquefy all sites associated with this event.

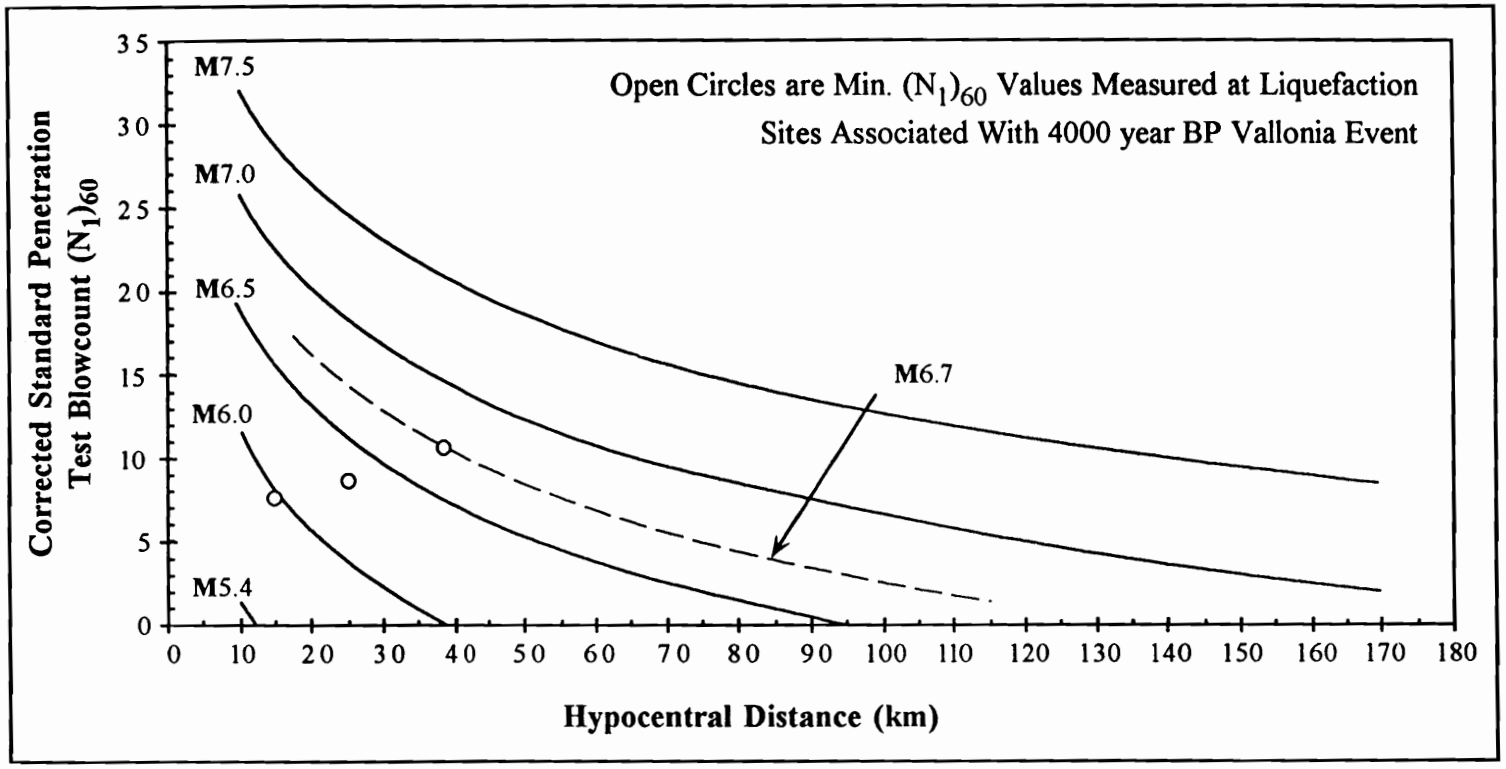

Figure 6.15. Minimum blowcount involved in liquefaction evidence at Vallonia event sites compared to the contours of minimum magnitude required to induce liquefaction. Predicted M6.7 earthquake required to liquefy all sites associated with this event.

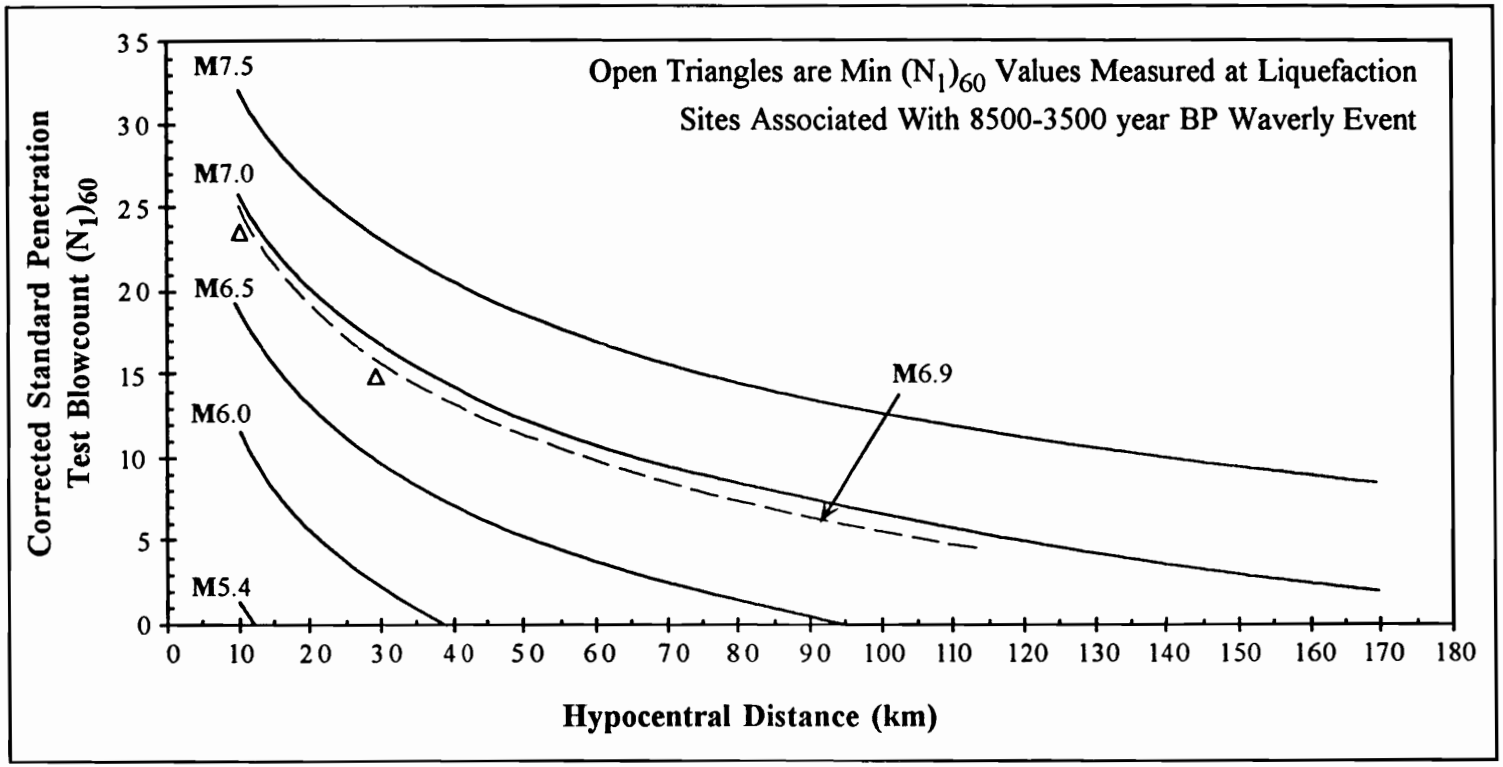

Figure 6.16. Minimum blowcount involved in liquefaction evidence sat Waverly event sites compared to the contours of minimum magnitude required to induce liquefaction. Predicted M6.9 earthquake required to liquefy all sites associated with this event.

of the four prehistoric Wabash Valley earthquakes are: **M**7.7, **M**7.4, **M**6.7, and **M**6.9, respectively. These predicted values are in very good agreement with the magnitude predictions based on the maximum distance to liquefaction effects approach above.

An additional result of this approach to magnitude estimates can also be seen based on the contours themselves. It would be useful to have an estimate of the absolute minimum magnitude that may reasonably be expected to produce liquefaction effects in the Wabash Valley. First, assume a site in a liquefiable environment with very loose soil conditions also exists at the epicentral location of a Wabash Valley earthquake. The contours of magnitude shown in Figures 6.13 through 6.16 suggest a minimum magnitude required to induce liquefaction at this site will be approximately **M**5.4. This is the minimum magnitude value used in Figure 6.4 to extend the upper bound of liquefaction effects proposed by Obermeier et al. (1993). It can be seen that this value provides a smooth extension of their boundary, which parallels the original curve proposed by Ambraseys (1988) for all worldwide shallow focus events. This consistency between the two approaches to a minimum magnitude estimate required to induce liquefaction effects lends additional support to use of this approach to estimate the minimum magnitude associated with the prehistoric Wabash events.

6.7.Empirical Energy Intensity Approach to Estimating Seismic Parameters

The two approaches above to estimating magnitude of prehistoric Wabash Valley earthquakes are in very good agreement. However, it would be desirable to have an alternative approach to estimating magnitude that will also allow an estimate of an attenuation relationship representative of soil site surface motions in the region. This can be done using the in-situ soil conditions and the Seed and Idriss (1971) approach to liquefaction susceptibility if a reliable estimate of the liquefied layer thickness can be made.

At each of the liquefaction sites identified in the Wabash Valley, a reasonable estimate of epicentral distance can be made based on the liquefaction distributions. As seen above, a magnitude estimate can be based on this distribution as well. Therefore, if a

relationship based on magnitude and distance alone can be developed to predict the maximum blowcount reasonably expected to be susceptible to liquefaction, an estimate of liquefied layer thickness can be made. This type of relationship can be developed based on an empirical energy intensity approach similar to that of Berrill and Davis (1985) and Law et al. (1990). The development of this approach is shown below, and is used to compare site specific acceleration estimates with the surface motion predictions based on the Wabash Valley attenuation relationship proposed above.

6.7.1.Development of Seismic Energy Intensity Approach

As was shown in Chapter 2, Law et al. (1990) derive the following equation describing the threshold liquefaction condition:

$$\frac{10^{1.5M}}{\eta\left[(N_1)_{60}\right]R^B} = 1.0.$$

This allows an empirical determination of the critical value of $\eta[(N_1)_{60}]$ representing incipient liquefaction. To do this, Law et al.(1990) define a seismic energy intensity function T(M,R) as:

$$T(M,R) = 10^{1.5M}/R^B$$

Liquefaction is predicted to occur when the seismic energy intensity function, T(M, R), exceeds the liquefaction resistance function, $\eta[(N_1)_{60}]$. The condition of liquefaction can therefore be represented as:

$$\frac{T(M,R)}{\eta\left[(N_1)_{60}\right]} \geq 1.0.$$

Law et al. (1990) used two existing liquefaction databases of liquefaction vs. non-liquefaction occurrence to estimate the liquefaction resistance function representing a liquefaction prediction boundary. The Seed et al. (1975) catalog containing liquefaction

data for 11 significant plate-margin earthquakes affecting 38 sites was used to initially determine the liquefaction resistance function. A second liquefaction catalog of data for two Chinese earthquakes was used to compare the reliability of the energy intensity method with that of the Seed et al. (1983, 1985) stress method. In both analyses, all standard penetration test data were corrected to $(N_1)_{60}$ values (Seed et al., 1985). Law et al. report an improvement in liquefaction and non-liquefaction prediction reliability using the energy intensity method over that of the stress method. They also suggest the method is easier to use based on the fact that it does not require an estimate of peak ground surface acceleration. The improvement noted in the reliability of the energy intensity approach may very well be due to the fact that acceleration is not required in the analysis. Most of the peak surface accelerations reported in any liquefaction database are estimates only. The actual values may vary from these reported estimates. A liquefaction susceptibility analysis procedure that eliminates this source of uncertainty should be expected to provide more reliable results.

Law et al. (1990) calculate values of the seismic energy intensity function at each site based on an attenuation exponent of B = 4.3. This is based on estimated attenuation relationships for seismic motions in western North America given by Hasegawa et al. (1981). Hasegawa et al. base this value on an assumption that energy attenuation is proportional to attenuation of Modified Mercalli Intensity (MMI) with distance. By redrawing published intensity distribution contours to enclose equivalent concentric circular areas they plot a log-linear relationship between hypocentral distance and intensity. Using data for six western and six eastern Canadian earthquakes they estimate attenuation exponents, B, for western and Eastern North America. Large errors are inherent, however, in using MMI to estimate attenuation characteristics of any seismic parameter. This approach likely provides estimates of attenuation coefficients with very large uncertainties.

Based on the parametric studies of Berrill and Davis (1985) showing only a small sensitivity in model response to anelastic attenuation, it may be a more reliable approach to assume anelastic effects on attenuation of energy will be insignificant to model results. This, however, requires the assumption that the geometric spreading component comprises the majority of the attenuation effects within the hypocentral distances where liquefaction damage will occur.

Hanks and Johnston (1992) suggest that for both Western United States and Eastern North America events, anelastic contributions to attenuation are insignificant compared to the geometric spreading effects out to hypocentral distances of 100 to 150 km. Bollinger et al. (1993) also agree that at least to distances of 100 km, attenuation is dominated by the geometric spreading component. The lack of a significant difference in the attenuation relationships shown in Figure 6.12 also supports this conclusion. Within distances of approximately 200 km, the surface motion predictions for Eastern North America and Western United States earthquakes are nearly identical. For comparable source characteristic events, the similar near-source attenuation relationships suggest that while Western United States and Eastern North America earthquakes may produce much different total felt areas (Algermissen, 1983), they will tend to experience similar areas subject to severe damage effects. Differences in anelastic attenuation between plate margin and mid-plate regions will not significantly influence the ground motions until beyond a distance where the peak motions have been attenuated to an amplitude that will not induce significant damage effects. Based on the findings above, the contribution of anelastic effects can be ignored in an energy intensity approach to liquefaction susceptibility prediction. This fact allows the use of existing databases cataloging liquefaction occurrence vs. non-occurrence in plate margin environments to be used to develop an empirical energy intensity approach to liquefaction prediction that can be applied in any tectonic region of the world.

For attenuation due to geometric spreading alone, the attenuation exponent, B, will have a value of 2 (Berrill and Davis, 1985), and the seismic energy intensity function suggested by Law et al. (1990) becomes:

$$T(M, R) = 10^{1.5M}/R^2.$$

This function can be used to determine a liquefaction prediction boundary based on existing liquefaction catalogs that will apply to all tectonic environments. This function is similar to the model proposed by Berrill and Davis, but ignores the in-situ stress term. Liao et al. (1988) performed logistic regression analyses of the Liao and Whitman (1986) liquefaction database of 278 cases of liquefaction and non-liquefaction effects for both the magnitude normalized cyclic stress ratio model (Seed et al., 1983) and the source characteristic (energy intensity) model (Berrill and Davis, 1985). They found that both models fit the data well, showing that both models provide reliable results for liquefaction susceptibility analyses. The model used here includes the stress term in the liquefaction resistance function rather than the energy intensity function as in the Berrill and Davis model. Law et al. (1990) found their model provided more reliable results than the stress-based approach when the effective stress term was included in this way.

The seismic energy intensity function given above can be evaluated for each site in a liquefaction database. By noting the occurrence or non-occurrence of liquefaction and plotting the results against a representative blowcount value for each site, a boundary can be identified separating the region where a high liquefaction potential exists from that where liquefaction is unlikely. This line represents the liquefaction resistance function $\eta[(N_1)_{60}]$ and can be used to predict the average in-situ blowcount required to suppress liquefaction in future seismic events. This results in a liquefaction prediction boundary similar to that of Seed et al. (1985), but is based on source characteristics rather than stresses experienced at the site.

It is important here to consider the definition of representative blowcount and effect the definition will have on the prediction boundary to be developed. As pointed out by

Liao and Whitman (1986), the use of a boring location as a single data point eliminates most of the correlation between data points that is inherent in using individual SPT values. It also removes the subjectivity inherent in trying to determine an average representative site value as the relevant liquefaction parameter. Using each boring location as a liquefaction data point still retains some subjectivity in deciding the representative blowcount value for that location, however. In order to address this issue, the minimum blowcount value was chosen as representative by Liao and Whitman. This approach is also used in this study to remove any subjectivity. This approach has the additional advantage of being consistent with the idea of a critical depth of liquefaction (Liao and Whitman, 1986; Seed and Idriss, 1971).

The Liao and Whitman (1986) catalog of liquefaction data is used here to develop a liquefaction prediction boundary that can be used to estimate thickness of liquefied layer. In any liquefaction catalog, the parameters documented are likely to contain significant errors. Magnitude estimates are one source of error. In this study it is assumed that the magnitudes reported by Liao and Whitman are reasonable approximations of the moment magnitude (**M**). The different magnitude relationships are not actually exactly equal, but provide a reasonable estimate of moment magnitude (Wakamatsu, 1992). Over the range where other magnitude scales are reported, they are typically similar to the moment magnitude scale and the error introduced by assuming this approximation will be within the range of the error in the original estimate. For cases where focal depth is not reported, it is assumed to be 10 km. The influence of this assumption is negligible. Where fines content is not reported it is assumed to be less than 12%. The remaining parameters are used as reported in the catalog. Only those data points containing less than 12% fines are used to find the prediction boundary. The resulting database contains 78 cases of non-liquefaction and 41 cases of liquefaction.

The data excerpted from the Liao and Whitman catalog have been used to calculate the seismic energy intensity function (T) and these values are plotted in Figure 6.17

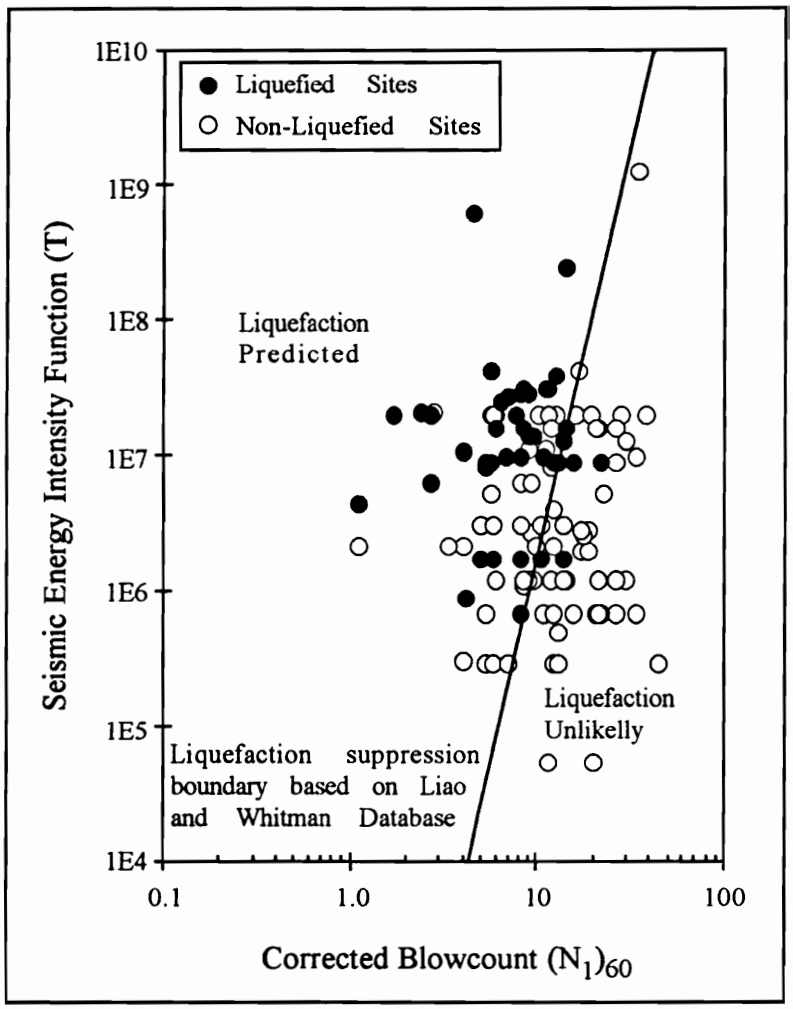

Figure 6.17. Liquefaction suppression boundary found for the Liao and Whitman (1986) database.

against their respective blowcounts. A liquefaction suppression boundary has been drawn as a predicted upper bound on liquefaction susceptibility. The equation of this line predicts, based on the seismic energy intensity value, the minimum in-situ blowcount required at a given boring location to suppress liquefaction.

To assess the validity of this curve for other liquefaction data, it is necessary to plot the seismic energy intensity function for another database and investigate the prediction reliability for that data set. The boundary found in Figure 6.17 should be able to predict liquefaction and non-liquefaction effects with reasonable accuracy for the original Law data set as well. Figure 6.18 presents the results for this data set. The Law et al. data is not strictly an independent catalog of liquefaction occurrence. Most of the earthquakes used in that data set are contained in the Liao and Whitman catalog, but a portion of the data in each catalog differs from the other. Where the same data points appear to have been used, the parameters associated with liquefaction vary somewhat between the two data sets. Therefore a comparison of the prediction boundary with the second data set will provide both an indication of the effect on the model associated with variations in parameter definition and an indication of the validity of the boundary for other data points. It can be seen in Figure 6.18 that the liquefaction suppression boundary provides good results for the Law et al. data set.

The plots of seismic energy intensity in Figures 6.17 and 6.18 show there is a transition zone between areas of liquefaction and non-liquefaction effects rather than an abrupt boundary. In this region, sites with similar seismic energy intensity vs. blowcount values may or may not exhibit liquefaction effects. The boundary line shown on the figures is drawn to provide an upper bound estimate of blowcount values required for liquefaction suppression. It can be seen in Figure 6.15 that three liquefaction sites are miss-classified as non-liquefaction conditions, and in Figure 6.16 one liquefied site falls in the area where liquefaction suppression is predicted. The type of ground disruption, local variability of in-situ deposits, topography, and effects of other regional and local site conditions not

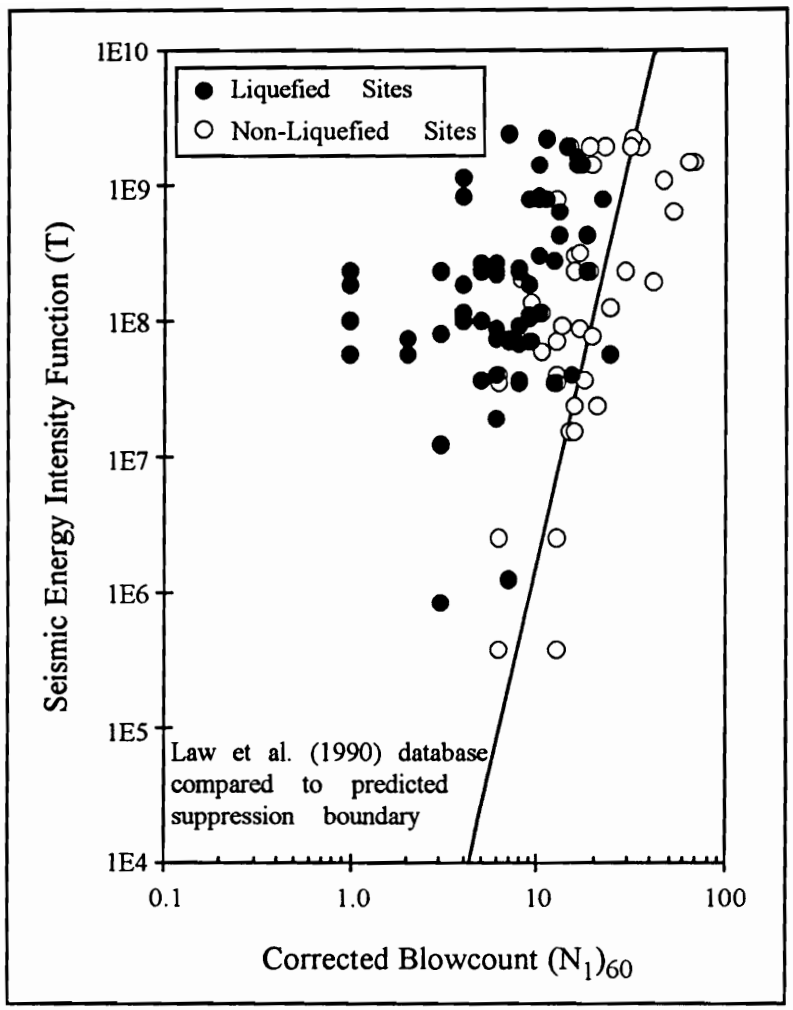

Figure 6.18. Law et al. (1990) database compared to the liquefaction suppression boundary found from the Liao and Whitman (1986) catalog.

measured by the Standard Penetration Test prevent achieving a precise upper bound. The boundary shown does, however, provide a reasonable "best" estimate of soil strength required to suppress liquefaction for all sites subjected to a given seismic energy as estimated by the seismic energy intensity function. A boundary may also be drawn, indicating a minimum blowcount value where the least susceptible sites will not experience liquefaction failure. It is necessary, therefore, to select the bound of the transition zone that will provide suppression $(N_1)_{60}$ estimates representative of the conditions in the Wabash region, and that will lead to "best" estimates of the blowcount involved in liquefaction.

The identified paleoliquefaction evidence in the Wabash Valley consists of lateral spreading failures. As noted previously, these deformations will occur at a stress, or energy, levels lower than is required for development of other types of surface effects due to liquefaction. The liquefaction database is made up of data from sites experiencing all types of liquefaction-induced ground disruption (Seed, 1979). The lateral spreading test sites utilized for this study will, therefore, plot at or near the liquefaction suppression boundary shown. This suggests use of the upper bound of the transition zone for estimation of the blowcount value required to suppress liquefaction at the Wabash Valley liquefaction sites.

The liquefaction resistance function found based on the Liao and Whitman (1986) data can be defined as:

$$\eta\left[(N_1)_{60}\right] = 1.445 \cdot (N_1)_{60}^{6.06}.$$

Where the seismic energy intensity function, T, exceeds this liquefaction resistance function, liquefaction susceptibility is predicted. Therefore, the blowcount value at the liquefaction suppression boundary can be described mathematically as:

$$(N_1)_{60} = \left[\frac{10^{1.5-M} / R^2}{1.445} \right]^{0.165}$$

This equation predicts the average in-situ $(N_1)_{60}$ value that will be involved in liquefaction for a given magnitude event influencing a site at a known hypocentral distance. However, in using this equation to predict the possible occurrence of liquefaction for design purposes, the blowcount value obtained from this equation can be viewed as the minimum value that must be achieved throughout that portion of the soil column that may be susceptible to liquefaction. The fact that the suppression boundary was developed based on the use of a database with minimum blowcount value as the representative soil parameter allows this approach to be used to predict a minimum liquefaction suppression blowcount value rather than an average for some subjective finite thickness of the deposit.

This predictive approach can be considered to apply to the upper 15 m of the soil column, which is the depth range of the data used to develop the relationship. It should be remembered that the assumption here is a site subject to lateral spreading failure. At sites subject to ground oscillation or level ground failures, this approach may be conservative, but predicts a blowcount value that will allow liquefaction suppression at all sites with a given hypocentral distance. A greater degree of uncertainty is introduced if other site conditions are considered. The current liquefaction database does not allow reliable assessment of the increased liquefaction resistance associated with failure modes other than lateral spreading. The Seed et al. (1985) prediction boundary provides a similar conservatism for sites other than lateral spreading conditions, but is based on cyclic stress ratio rather than energy intensity. The advantage of the energy intensity approach over the stress-based approach is that prior knowledge of the peak surface acceleration is not required.

An assumption in using this predictive approach is that the earthquake has "normal" source characteristics. If anomalous ground motions are produced, the response may differ from the prediction. This, however, is a problem that will also affect a stress-based approach to liquefaction prediction. Attenuation relationships used to predict surface accelerations are based on average empirical evidence. Where an earthquake produces motions that differ from the assumed motions, the predicted site response will vary as well. The effect of changes in the ground motion characteristics will produce similar results in the two approaches to liquefaction susceptibility analyses. Therefore, based on the results of the Liao et al. (1988) statistical study of the two approaches, it can be assumed that the energy intensity approach will have a reliability similar to the stress-based approach to liquefaction susceptibility.

6.7.2.Application of the Energy Intensity Approach to Paleoliquefaction

The blowcount prediction boundary defined by the seismic energy intensity function can be used in a paleoliquefaction study to improve back-calculated estimates of the seismic parameters associated with prehistoric events. By using this technique, a prediction can be made of the thickness of the layer involved in the liquefaction evidence within a soil deposit. The estimate of liquefied soil layer thickness is found for paleoliquefaction studies based on the predicted minimum blowcount value required to suppress liquefaction evidence. Where a reasonable distribution of lateral spreading liquefaction effects has been identified, this procedure will then provide "best" estimates of the seismic parameters associated with a seismic event. In a region where the liquefaction effects are limited to level ground failures (sand boils) alone, the results of the procedure are not as clearly defined. This will then result in a lower bound value, but will remain an improvement on the minimum blowcount approach.

With an initial assumption of magnitude based on the maximum distance to liquefaction effects and/or on the minimum blowcount and magnitude contours required to induce liquefaction approach above, it is possible to estimate seismic energy intensities for

each of the sites associated with a specific event. It is assumed here that the available evidence provides an estimate of the distribution of liquefaction effects that is reasonably representative of the event. This is necessary to provide a reliable initial estimate of the epicentral location. In some cases the liquefaction distribution will not be well defined due to a scarcity of liquefiable soil deposits in a region, to erosional removal of a significant portion of the evidence by meandering rivers; to a lack of available exposures in soil deposits of the proper age; or to man-made structures, such as dams and rip-rap placed on river banks, that obscure the soil profile. These types of concerns are most critical for smaller events that produce liquefaction effects over a lesser area to begin with. Each liquefaction site erased or obscured from one of these distributions represents a lost portion of the total evidence significantly larger than would be true for distributions associated with a much greater event.

When a substantial portion of the evidence for a moderate event is eliminated, it may become practically impossible to fully describe the distribution of liquefaction effects associated with the event. This is the case for the prehistoric Waverly event (near Indianapolis) investigated in this study. It can be seen from the estimated liquefaction distribution shown in Figures 3.3 and 3.4 that there is a lack of available paleoliquefaction sites in the northern portion of the distribution inferred for this event. In this area the soils are not highly susceptible to liquefaction, and in developed areas liquefiable soils have been obscured due to dams and rip-rap at many locations.

In cases where only a few paleoliquefaction sites have been identified it remains possible, however, to use an iterative procedure with the limited available evidence to provide a reasonable estimate of the epicenter. Several trial epicentral locations are assumed based on the evidence available, on knowledge of the local geologic structure, and the local historical seismicity. Evaluation of the predicted surface motions for a variety of magnitude values at each of the epicentral locations may then lead to a refined estimate of the epicentral location.

6.7.2.1.Estimating Thickness of Liquefied Layer

In order to use the energy intensity approach to predict the thickness of the portion of the soil deposit involved in liquefaction it is necessary to understand what the liquefaction suppression blowcount value represents in this analysis. When the procedure is used to predict non-liquefaction in a soil deposit during a future event it is required that the blowcount at every location within the soil deposit exceed the suppression boundary. However, this can not be directly reversed when trying to estimate the liquefied thickness of a soil deposit involved in a prior liquefaction event. Liao and Whitman (1986) used the lowest blowcount value from an individual boring location as the soil strength parameter associated with that location. In order to remain consistent with the assumptions made in compiling the Liao and Whitman liquefaction catalog, the predicted liquefaction suppression blowcount (N_ℓ) must be taken as an average of the blowcounts measured through the liquefied thickness of the soil deposit. Considering the liquefaction suppression value to be an absolute upper bound will underestimate the liquefied layer thickness except for the case where blowcount is constant through the liquefied thickness.

Figure 6.19 illustrates the rational behind using the predicted N_ℓ value to represent an average of blowcount values in the liquefied layer. Suppose three sites experiencing lateral spread liquefaction failures are located at similar hypocentral distances. The soil profiles for hypothetical sites A, B, and C are shown as diagrams (a), (b), and (c) in Figure 6.19. For the purposes of this illustration, the shape of the blowcount distributions are shown to be similar, but this is not necessary. The soil strength profiles differ only in that the minimum value increases from site A to site C. The liquefied thickness of the soil deposit will be greatest for site A and least for site C. (The severity of the lateral spreading displacement will also be greatest at site A and least at site C, but this does not affect the illustration). The liquefied thickness of the soil profile, as well as the minimum, maximum and average blowcount values involved in the liquefaction are indicated for each site.

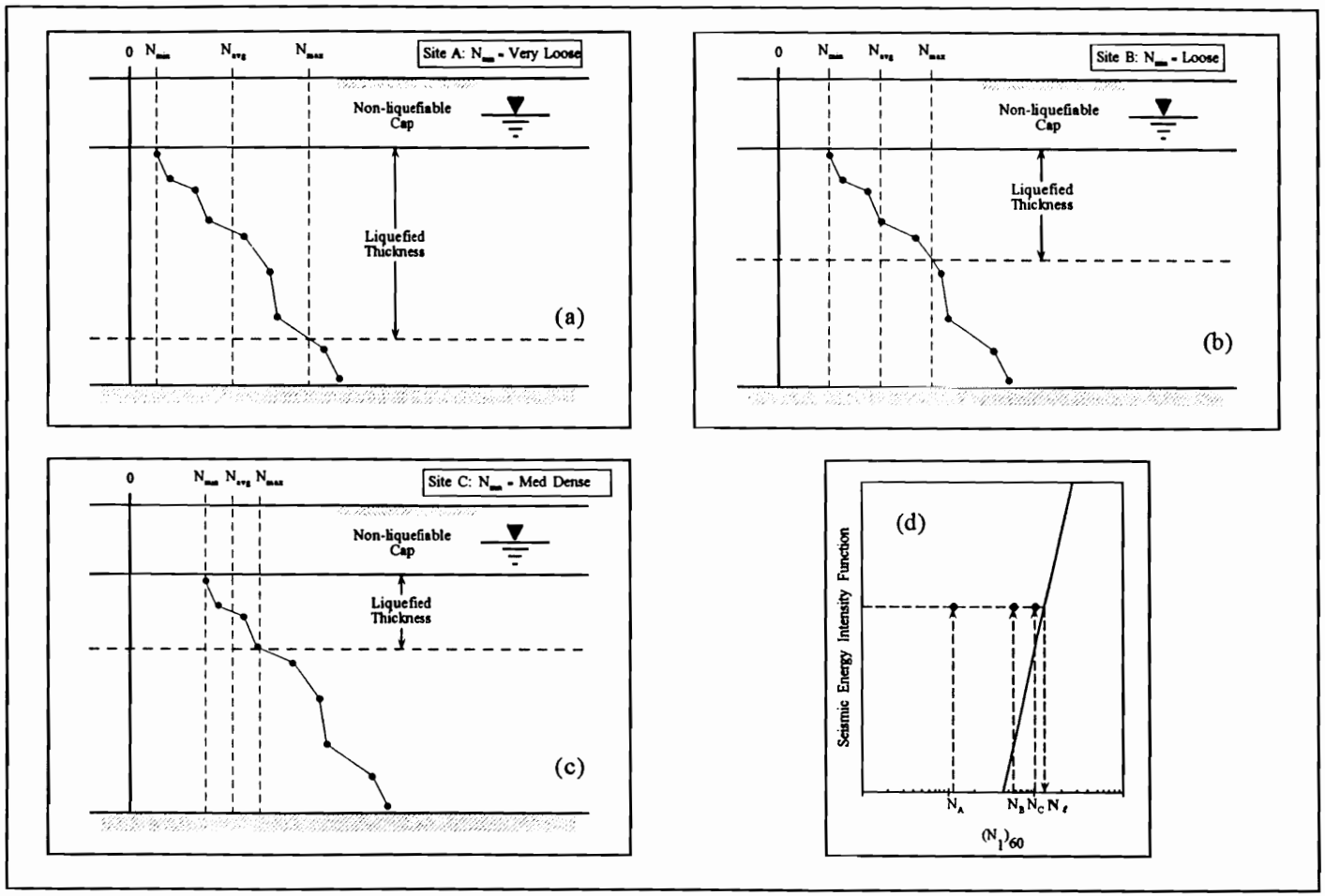

Figure 6.19. $N_\ell = N_{avg}$ predicts the liquefied layer thickness at paleoliquefaction sites when the energy intensity boundary is based on an N_{min} liquefaction catalog.

If the seismic energy intensity function affecting these sites is plotted against minimum blowcount values, the results will be as shown in diagram (d). In each of the soil profiles, N_ℓ equals N_{avg} and N_A, N_B, and N_C are the minimum blowcount values at each site. As N_{min} increases from site A to site C, the liquefied layer thickness decreases, and N_{min} approaches the average blowcount value involved in the liquefaction event. The data points in the liquefaction prediction diagram (d) can be seen to approach the liquefaction suppression boundary at the same time. Once the minimum blowcount value exceeds N_ℓ, the soil profile is no longer predicted to be susceptible to liquefaction.

This type of relationship can also be shown if the predicted N_ℓ suppression blowcount is assumed to represent the maximum value involved in liquefaction. However, if N_ℓ is assumed to equal the maximum blowcount in the liquefied layer, the progressive liquefaction phenomenon is ignored. In reality, the occurrence of liquefaction at one location will tend to increase the liquefaction potential at adjacent locations. This can be visualized conceptually as a pore pressure migration effect. Liquefaction of a contractive soil can allow migration of pore water to an adjacent, dilative soil. This then will tend to induce a loosening effect in the adjacent soil. The result of this is that the soil densities have a tendency to be altered toward an average blowcount where $N_{avg} = N_\ell$. The pore pressure migration tendency can also lead to increased pore pressures in an adjacent less-contractive soil, increasing the liquefaction tendency there. Also, as the minimum in-situ blowcount approaches the predicted suppression blowcount, it should be expected that in order for surface effects of liquefaction to be observed, the progressive liquefaction effect must occur to provide a thickness of liquefied deposit sufficient to produce observable deformations. The results presented by Holzer et al. (1989) for liquefaction at the Wildlife site due to the Superstition Hills earthquake also support this. Liquefaction susceptibility there is predicted for only the upper and lower portions of the soil deposit based on a

stress-based liquefaction analysis. During the liquefaction event, however, 100% excess pore pressure was generated throughout the entire thickness of the liquefiable soil layer.

By using the Liao and Whitman (1986) catalog in developing the liquefaction suppression boundary, subjectivity is removed from the analysis. Other catalogs contain blowcount data based on a critical value assumed to represent an average for the liquefied layer thickness. A liquefaction suppression boundary based on this type of data will predict the average blowcount value that is likely to be involved in a future liquefaction event. However, it is impossible to predict from this the minimum value that would be required to resist a future liquefaction event. Therefore, an energy intensity design procedure based on this type of liquefaction catalog would be conservative. It remains necessary that all blowcount values be improved to exceed the predicted suppression value.

In a paleoliquefaction study based on a database containing subjective estimates of blowcount values, the suppression boundary must be taken as the upper bound blowcount. However, it is not clearly apparent how the results will be affected by this subjectivity. In cases where assumptions made in selecting the database values match the conditions that occur at the paleoliquefaction sites this will provide a reasonable prediction of the past surface motions. However, where the conditions vary between the paleoliquefaction site and the database site assumptions, the predicted motions may differ substantially from the actual motions experienced. Using the minimum blowcount provided in the Liao and Whitman database removes this source of subjective uncertainty.

6.7.2.2.Estimating Peak Surface Motions Based On The Liquefied Layer Thickness

The minimum in-situ blowcount value predicted by the energy intensity approach to be required for liquefaction suppression can be used to estimate the maximum thickness of liquefied layer at lateral spreading paleoliquefaction sites. This is done by comparing the N_ℓ value required for liquefaction suppression with the $(N_1)_{60}$ blowcount values measured

throughout the soil profile at each boring location. As outlined above, this thickness is then estimated as that where the average in-situ $(N_1)_{60}$ is less than or equal to the average blowcount required to suppress liquefaction (N_ℓ). This prediction of the liquefied layer thickness can then be used to back-calculate the peak ground surface acceleration amplitude experienced at the site. The in-situ blowcount value at each sample interval is used to predict the cyclic stress ratio required for liquefaction at that elevation based on the Loertscher and Youd (1994) liquefaction prediction boundary. The Seed and Idriss (1971) equation for the cyclic stress ratio associated with a given peak acceleration is then used to back-calculate the peak surface acceleration associated with the cyclic stress ratio required to induce liquefaction at that location.

The stress-based liquefaction prediction boundary used in this back-calculation procedure represents the threshold cyclic stress ratio required to allow liquefaction effects. Here again, the nature of the type of ground failure suggests the prediction boundary will provide a "best" estimate of the ground motions experienced. Lateral spreading failures will occur at stress ratios lower than those necessary for other types of liquefaction failures and will provide points in the liquefaction database occurring at or near the threshold boundary. Any deviation from the threshold prediction boundary will affect the results to some extent, but the difference in the predicted surface acceleration will be small. Errors introduced here can be expected to be within the range of uncertainties based on assumptions necessary in other parts of the analysis

The estimated peak surface acceleration at paleoliquefaction sites is estimated based on the predicted average $(N_1)_{60}$ value required to suppress liquefaction evidence. It is possible to identify a predicted thickness of liquefied layer by first examining the soil profile data. The liquefied thickness is taken as that where the average of the corrected SPT blowcount values is less than or equal to the predicted liquefaction suppression blowcount value. The threshold cyclic stress ratio predicted for liquefaction at each of the sample intervals is then used to back-calculate the peak surface accelerations required to

liquefy the soil profile at the locations of the individual blowcount values within the estimated liquefied layer thickness. The actual peak surface acceleration experienced at the site is then estimated to be the average of the values required to induce liquefaction at each of the sample locations within the predicted liquefied layer thickness. An example of this analysis for the Wabash study site HA, a site associated with the Vincennes event, is included in Appendix A.

6.7.2.3.Model Verification Based on Recent Documented Liquefaction Occurrences

In order to asses the validity of the procedure presented here for prediction of liquefied layer thickness and peak surface accelerations, the approach was applied to several recent cases of lateral spreading liquefaction. Cases of both liquefaction and non-liquefaction occurrence were investigated in this phase of the project to assess the possibility of a bias in the procedure toward over-predicting one case or the other. All of the cases investigated were for sites in the Western United States, but as pointed out above, differences in attenuation will have no significant impact on the results for hypocentral distances within the span of liquefaction effects. In all of the cases investigated, the model accurately predicts the occurrence or non-occurrence of the liquefaction effects. Only a single site investigated for this portion of the study is included in the original Liao and Whitman (1986) database used to develop the procedure. This, therefore, provides independent verification of the model.

A total of eleven cases of liquefaction or non-liquefaction were investigated for model verification. Four earthquakes affecting the Wildlife site of southern California were investigated (the 1979 Imperial Valley, 1981 Westmorland, 1987 Elmore Ranch, and 1987 Superstition Hills earthquakes). Two of these induced liquefaction at the site and two did not. Four sites affected by the 1989 Loma Prieta earthquake were investigated where three cases of liquefaction and two cases of non-liquefaction were reported. Two cases of liquefaction due to the 1989 Borah Peak earthquake were also analyzed. The use

of the energy intensity approach prediction boundary developed above accurately predicts the seven cases of liquefaction at six sites affected by five earthquakes. Also, the procedure accurately predicts the non-occurrence of liquefaction at four sites due to three earthquakes.

In each of the cases studied here, a prediction of liquefaction or non-liquefaction was made. Where liquefaction was predicted, the peak surface acceleration estimate required to induce the liquefaction was also estimated and compared to the accelerations reported in the literature for the study sites. Where liquefaction did not occur, the peak surface acceleration required to induce liquefaction at the minimum blowcount within the soil deposit was estimated. The results were then compared to the field conditions reported for the case studies. In all cases, the energy intensity model accurately predicts the occurrence or non-occurrence of liquefaction effects. Where liquefaction is predicted (and reported), the energy intensity approach to estimated peak surface acceleration is found to be in very good agreement with the values reported in the literature. Table 6.1 summarizes the results of this analysis.

In Table 6.1, hypocentral distance (R) is given in km and N_ℓ is the liquefaction suppression blowcount. The energy intensity approach estimated average value of blowcount throughout the liquefied thickness (or the minimum suppression blowcount for a non-liquefied deposit) is given as N_{avg}. If liquefaction occurred (Liq'n ?: Y or N) at the site, the energy intensity approach prediction of surface acceleration is given under "NRG." If liquefaction did not occur, the minimum acceleration estimated to be required to induce liquefaction is reported. The Boore et al. (1993) Western United States class C soil site ($180m/s < V_s < 360m/s$ in the upper 30m) attenuation relationship prediction of surface motion (B,J,F) and the estimated surface acceleration reported in the references cited (Rept'd) are also listed for comparison. Information on motions at the Wildlife site due to the Imperial Valley and Westmorland events was also obtained from Dobry et al. (1992). Two items are worth noting regarding the analysis procedure in relation to the

Table 6.1. Results of Energy Intensity Approach For Recent Western United States Liquefaction Case Histories

EQ	Site	R (km)	N_ℓ	N_{avg}	liq'n (?)	a_p (g's) NRG	B,J,F	Rept'd	Reference
LP	YBC	98	11.2	11.1	Y	0.13	0.07	0.175	Chameau et al. (1991)
	TH	98	11.2	15.2	N	0.19	0.07	0.175	Chameau et al. (1991)
	MF1	26.9	17.1	14.9	Y	0.26	0.22	0.39	Holzer et al. (1994)
	MF2	26.9	17.1	22.4	N	0.41	0.22	0.39	Holzer et al. (1994)
	FF	26.9	17.1	17.0	Y	0.32	0.22	0.39	Holzer et al. (1994)
BP	WS	10.4	26.2	20.9	Y	0.41	0.63	0.50	Andrus and Youd (1989)
	PR	14.5	23.6	18.3	Y	0.33	0.33	0.28	Stokoe et al. (1988); Andrus et al. (1991)
IV	W	54.7	10.2	11.6	N	0.21	0.08	0.15	Holzer et al. (1989)
WM	W	11.5	12.1	11.9	Y	0.33	0.20	0.22	Holzer et al. (1989)
ER	W	24.5	9.4	11.0	N	0.33	0.11	0.13	Dobry et al. (1992)
SH	W	31.1	12.3	12.7	Y	0.21	0.12	0.21	Dobry et al. (1992)

Notes and Definitions:

Earthquakes		Sites	
LP	1989 Loma Prieta (M7.0)	W	Wildlife Site
BP	1983 Borah Peak (M6.9)	MF1	Miller Farm (young flood plain)
IV	1979 Imperial Valley (M6.5)	MF2	Miller Farm (old flood plain)
WM	1981 Westmorland (M5.9)	FF	Farris Farm
ER	1987 Elmore Ranch (M5.9)	YBC	Yerba Buena Cove
SM	1987 Superstition Hills (M6.5)	TH	Telegraph Hill
B,J,F:	Boore, Joyner and Fumal (1993)	PR	Pence Ranch
NRG:	a_p based on energy approach	WS	Whiskey Springs

case studies presented in this table: the effect of fines content, and the choice of the Loertscher and Youd (1994) liquefaction prediction boundary to predict cyclic stress ratio in the analysis.

6.7.2.3.1.Effect of Fines Content

Many of the site conditions reported for the case studies examined here contain significant fines contents. The energy intensity approach developed here to estimate liquefied layer thickness is based on the assumption that fines content is less than 12%. In order to estimate the liquefaction occurrence in soil conditions with greater than 12% fines the measured in-situ blowcount values are corrected to equivalent clean sand blowcounts. This can be accomplished using the following relationship for blowcount:

$$\left[(N_1)_{60}\right]_{cs} = \left[(N_1)_{60}\right]_{ss} + 5$$

where the subscript 'cs' refers to the equivalent clean sand blowcount and the subscript 'ss' refers to the in-situ silty sand blowcount corrected for energy ratio and confiningstress (O'Rourke et al., 1991; Ishihara, 1993). This approach assumes a bilinear relationship desribes the effect of fines content on liquefaction susceptibility and is consistent with the Liao et al. (1988) findings. Ishihara (1993) plotted a smooth curve through three points estimated from the data presented by Seed and DeAlba (1986). In Figure 6.20 this relationship is compared to the bilinear form used here. It can be seen that the difference between the two is small, and particularly for fines contents greater than 12%. The assumption was made previously, based on the Liao et al. study, that there is no real difference in liquefaction susceptibility based on penetration test data for fines contents less than 12%.

The bilinear form used here to provide equivalent clean sand blowcount values for silty soils is consistent with the Liao et al. (1988) results suggesting the 12% fines content value as the separation between clean and silty soils for liquefaction susceptibility analyses. The results of the analysis using this correction technique, where appropriate, for the case

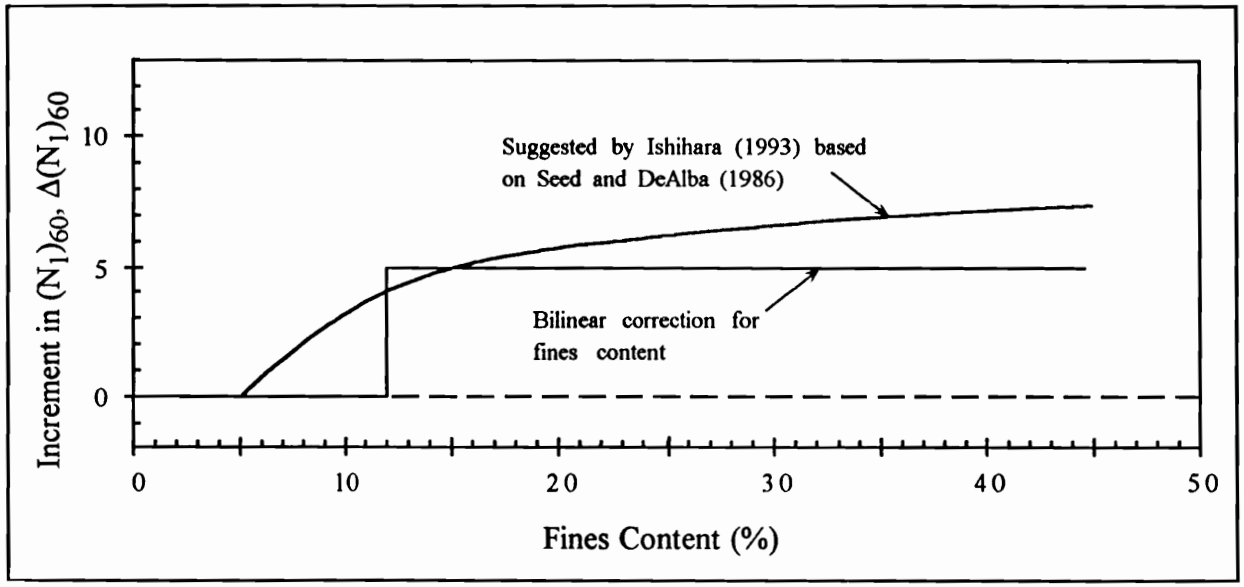

Figure 6.20. Blowcount corrections proposed to provide equivalent clean sand blowount values for a liquefaction susceptibility analysis of silty soils.

studies considered here were found to be in very good agreement with the in-situ liquefaction effects reported. Using this bilinear conversion relationship therefore provides a convenient method for extending the use of the energy intensity approach to silty soils from the model originally developed for clean sands alone.

6.7.2.3.2.Liquefaction Prediction Boundary

At the Wildlife site, the U. S. Geological Survey liquefaction array was installed in 1982 (Holzer et al., 1989a). Ground motions and pore pressure generation for both the 1987 **M**5.9 Elmore Ranch and **M**6.5 Superstition Hills events were instrumentally recorded. The Superstition Hills event produced a peak surface acceleration of 0.21g and liquefaction effects were observed through the full depth of the soil deposit. The Boore et al. (1993) attenuation relationship under-predicts the acceleration value to be a_p=0.12g. Based on the energy intensity approach estimate of liquefied soil thickness, liquefaction is predicted and the surface acceleration estimate of a_p=0.21g equals the recorded value. The peak acceleration recorded at the surface is suggested by Holzer et al. (1989) to be the peak acceleration that would have been experienced at the site even without the liquefaction event. Based on the results reported by Zeghal and Elgamal (1994), the a_p=0.21g value appears to be the threshold for generation of 100% excess pore pressure due to a **M**6.5 event at this site. Pore pressure generation prior to the peak acceleration loading was small. At the point this load occurred, excess pore pressure development increased dramatically. This is the pore pressure response shown in Figure 2.16, and occurs at time t=b in the diagrams shown in that figure. This response is also consistent with the Alarcon-Guzman et al. (1988) suggestion that breakdown of a metastable soil structure when the peak strength is exceeded leads to an increase in pore pressure development.

The results of the energy intensity approach for the 1979 **M**6.5 Imperial Valley earthquake at the Wildlife site also suggests this threshold value. Liquefaction was not reported due to the Imperial Valley event, but is shown here to require a peak surface

acceleration of a_p=0.21g to induce liquefaction at the minimum in-situ blowcount value. The fact that a threshold exists for large excess pore pressure development with generation of surficial liquefaction evidence also supports the use of a Seed et al. (1985) type of liquefaction prediction boundary as a "best" estimate of the surface motions at lateral spreading paleoliquefaction sites. At the Wildlife site no significant pore pressure generation occurred until this threshold acceleration was reached during the Superstition Hills event, and was not subsequently exceeded. During the Imperial Valley event, Dobry et al. (1992) present data suggesting a peak acceleration of 0.15g at the site. No liquefaction evidence was reported based on that event. For lateral spreading sites this suggests that once the threshold liquefaction prediction value is reached, there will be significant surface effects, but that prior to reaching this value there will be little or no pore pressure development or surface effects.

The motions associated with the **M**5.9 Elmore Ranch earthquake were also recorded at the Wildlife site. No measurable pore pressure development occurred due to this event, and peak surface motions were recorded at a_p=0.13g. The energy intensity approach suggests peak surface motions of approximately a_p=0.30g would be required to induce liquefaction effects due to this event. This event is in the magnitude range, however, where the Loertscher and Youd (1994) liquefaction prediction boundary significantly exceeds that of Seed et al. (1985). Predicting the peak surface acceleration required to induce liquefaction based on the Seed et al. boundary leads to an estimate of a_p=0.16g. This exceeds the measured acceleration as well as the predicted Boore et al. estimate, and is therefore also consistent with the field results. It is possible that the surface acceleration required to induce liquefaction is overestimated by the Loertscher and Youd prediction. It should be noted, however, that if this is the case, the ability to use the energy intensity approach outlined above to predict the occurrence or non-occurrence of liquefaction will not be affected. The only effect will be on the predicted surface accelerations for low-magnitude (**M** $\leq$ 6) events.

The 1981 M5.9 Westmorland earthquake also affected the Wildlife site. This occurred closer than the Elmore Ranch event and did induce liquefaction effects, although ground motion recordings are not available at the site for this earthquake. The energy intensity approach suggests a peak surface motion of 0.33g was associated with this liquefaction event based on using the Loertscher and Youd boundary. Predicting peak surface acceleration based on the Seed et al. (1985) boundary leads to an a_p=0.18g estimate. The Boore et al. (1993) estimate and the estimate based on Dobry et al. (1992) are 0.20g and 0.22g respectively. These agree very well with the energy intensity approach using the Seed et al. liquefaction boundary for prediction of peak acceleration. However, if the Boore et al. attenuation relationship under-predicts the surface motion due to this event by an amount similar to what was seen for the Superstition Hills event, the acceleration estimate would need to be increased to a_p=0.35g. This value is consistent with the energy intensity prediction using the Loertscher and Youd boundary. Case study data for sites associated with the Loma Prieta event also suggests the Boore et al. (1993) prediction underestimates the surface motions for that event. If the increased acceleration value is a valid assumption, this supports the validity of the Loertscher and Youd liquefaction prediction boundary for low magnitude events.

Evidence contrary to suggesting an increase in the Boore et al. acceleration prediction does, however, exist in the fact that the recorded and predicted acceleration values for the Elmore Ranch event agree very well. This event had a magnitude similar to the Westmorland event (M5.9). Further research is therefore required to fine the most appropriate stress-based liquefaction prediction boundary for low magnitude events. The data presented here does, however, suggest the Loertscher and Youd liquefaction prediction boundary is reliable for events of M≥6.5. The energy intensity approach, in conjunction with the Loertscher and Youd (1994) liquefaction prediction boundary, will therefore be used to estimate the magnitude and attenuation characteristics of the Wabash Valley paleo earthquakes.

6.7.3.Compare Site Specific Peak Acceleration Estimates With Wabash Attenuation Relationship

Performing this evaluation for all sites associated with a specific event, an attenuation relationship can be developed based on the peak ground surface acceleration estimates at each site. The predicted surface motion attenuation can then be compared to the seismologically-based attenuation relationship developed previously. Predicted surface motions are back-calculated over a range of magnitudes for each event. This allows a refined estimate of magnitude to be made. A "best" estimate of magnitude is taken as that where the seismological attenuation relationship most closely agrees with the energy intensity approach at all sites associated with a given event.

The two approaches used here to estimate surface motions are both based on magnitude and distance. The energy intensity approach, however, also incorporates local site conditions and a liquefaction susceptibility relationship to provide a ground surface acceleration estimate. Where the magnitude associated with a specific event affecting sites at a given distance is underestimated, the peak surface acceleration predicted by the energy intensity approach will exceed the seismological attenuation prediction. As the magnitude value is increased to improve the estimate, the a_p predictions will tend to converge. If magnitude is overestimated, the energy intensity prediction will again exceed the seismological attenuation prediction. This is illustrated in Figure 6.21.

Where magnitude is underestimated, the energy intensity prediction of surface acceleration exceeds the attenuation prediction due to the fact that larger accelerations are required to liquefy a given soil deposit subjected to a shorter duration event. When magnitude is overestimated, the average blowcount predicted to be involved in the liquefaction event will be overestimated as well. As blowcount increases, the cyclic stress ratio predicted to be required to induce liquefaction increases at an increasing rate. This leads to a greater increase in acceleration estimates based on the energy intensity approach than the increase in predicted surface acceleration based on the attenuation relationship.

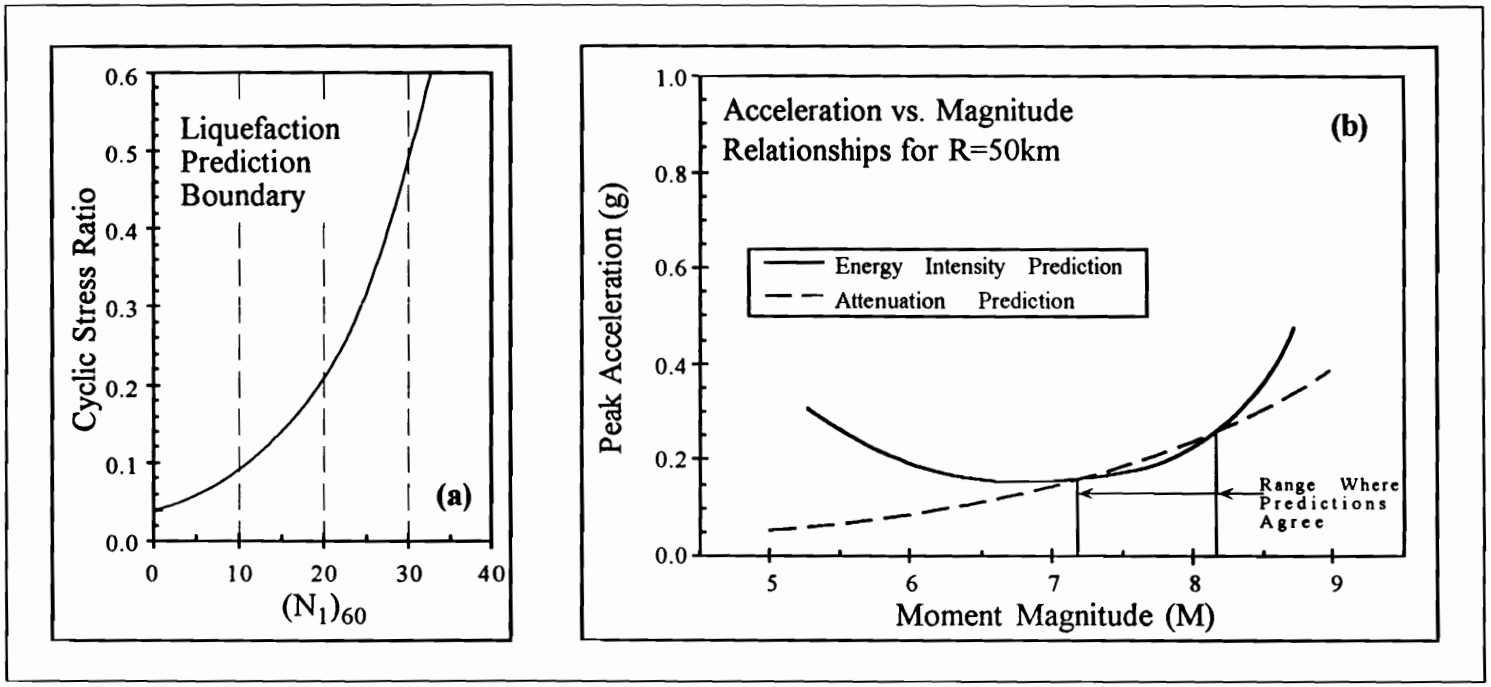

Figure 6.21. Convergence of energy intensity and attenuation predictions where magnitude estimates agree.

At low magnitudes, the slope of the energy intensity acceleration prediction curve is governed by the duration effect associated with magnitude. This is because the slope of the liquefaction prediction boundary is relatively flat for low blowcount values (see Figure 6.21a). As the magnitude estimate increases, the average blowcount predicted to be involved in liquefaction increases as well. The cyclic stress ratio begins to increase rapidly with blowcount and soon overwhelms the reduction in required cyclic stress ratio based on increased duration (Figure 6.21b).

The relationship between the two prediction methods that allows a best estimate of magnitude is based on the fact that the two predictions converge over a given magnitude range. This is also illustrated in Figure 6.21b. In this figure, the acceleration values predicted to occur at sites with hypocentral distances of 50 km are illustrated. The dashed line shows the peak surface acceleration values predicted by the Wabash Valley soil site attenuation relationship for magnitudes of M5.0 to M9.0. The solid line shows the predicted acceleration amplitudes based on the energy intensity approach. The energy intensity line drawn here for R=50 km is based on the assumption that:

$$\left(0.65 \cdot r_d \cdot \sigma_o / \sigma'_o\right) = 1.0;$$

which is an average condition. As in-situ stresses vary from this condition, the position of the energy intensity curve will vary as well, but the procedure remains valid. The two prediction approaches will agree over a range of magnitudes that can be expected to induce liquefaction at a given site.

At small hypocentral distances, the range over which the two predictions agree can be quite large. Liquefaction effects can be expected at near-source sites due to a much greater range of magnitudes. Near the outer limits of liquefaction effects, the two predictions will agree for only a small magnitude range, will eventually become tangent to one other, and at hypocentral distances beyond the limits of liquefaction effects, should not intersect at all. It is seen in Figure 6.19 that the minimum magnitude where the two predictions agree is approximately M7.2. This is also consistent with the magnitude that

is predicted based on a maximum distance to liquefaction effects of 50 km in the Wabash Valley (see Figure 6.6). At epicentral distances of 50 km or more, liquefaction effects are therefore not predicted to occur for events smaller than **M**7.1 to **M**7.2.

Four prehistoric seismic events in the Wabash Valley produced liquefaction effects that have been identified over significant regions. The approach outlined here has been used to refine the minimum magnitude estimates made previously for these events. The results of the analysis are summarized below for each of the events. An example of the analysis procedure is presented in detail for the study site Haysville (HA) in Appendix A.

6.7.3.1. Vincennes Event Results

The Vincennes earthquake (referred to as Vincennes-Bridgeport in Munson and Munson, 1996) occurred approximately 6000 years BP. Liquefaction evidence was produced over an area extending to epicentral distances of 170 km or more (see Figure 3.4). The epicenter for this event is assumed to be located at Bridgeport, IL, as suggested by Munson and Munson. The maximum distance from this location to surface evidence of liquefaction associated with the event is approximately 141 km. A total of thirteen sites associated with this event were chosen for the geotechnical study.

The present soil profile at these sites differs from that present during the earthquake. The surface at the time of the earthquake is now buried by a meter or more of post-event sediment. The surface at the time of the earthquake is therefore based on the presence of buried sand blows exposed in the banks of the river. The water table elevation is another issue that is of concern to liquefaction susceptibility. During the time period when the earthquake occurred, the regional water table was quite low (Munson and Munson, 1996). It is assumed that the water table was above the top of the source material, at the stratigraphically highest sites, but by only a very small margin. This is based on the fact that at many sites layers of clean sand in the natural levy deposits are present that show no indication of liquefaction. It is assumed that if these deposits had been involved in the liquefaction, where they are visible during low water levels there would have been some

indication of flow toward the dikes that cut across them. The evidence presented by some of these layers is that they actually tended to absorb excess pore pressures form the underlying liquefied soil layers. Stratigraphic relationships between sites are also used to limit the possible range of water table elevations based on an assumption of regionally consistent water table elevations. The elevation of the water table and its effect on the results of this study is discussed further in the context of the example calculation presented in Appendix A for study site HA. Site plans and soil profiles for the sites associated with this event are presented in Figures 5.3 through 5.30.

An initial estimate of magnitude for this event was taken as that suggested by the maximum distance to liquefaction effects approach. Using an initial magnitude estimate of **M**7.8 based on the maximum distance to liquefaction effects, liquefied layer thicknesses were estimated for each of the sites. From these layer thicknesses, the surface accelerations were then back-calculated using the Seed and Idriss (1971) stress-based approach with the Loertscher and Youd (1994) prediction of cyclic stress ratio. The results of these calculations were then compared to surface motion predictions based on the attenuation relationship developed for the Wabash Valley. The results of this evaluation for each of the sites are shown in Figure 6.22. Also included in Figure 6.22 are comparison results for initial magnitude estimates of **M**7.5 and **M**8.0. It can be seen that the M7.8 estimate provides the best match between the energy intensity approach and the attenuation prediction of surface motions.

Several of the surface acceleration estimates are shown in the figures as lower bound estimates. These acceleration estimates are lower bound values for one of two reasons. The most common reason is that the average blowcount value predicted to be involved in the liquefaction event exceeds the average corrected blowcount value measured through the depth of the soil profile sampled at these sites. The second reason for a lower bound estimate is that the liquefied layer thickness prediction is not foolproof. Blowcount profiles do not always follow the smooth increase with depth as indicated in Figure 6.19.

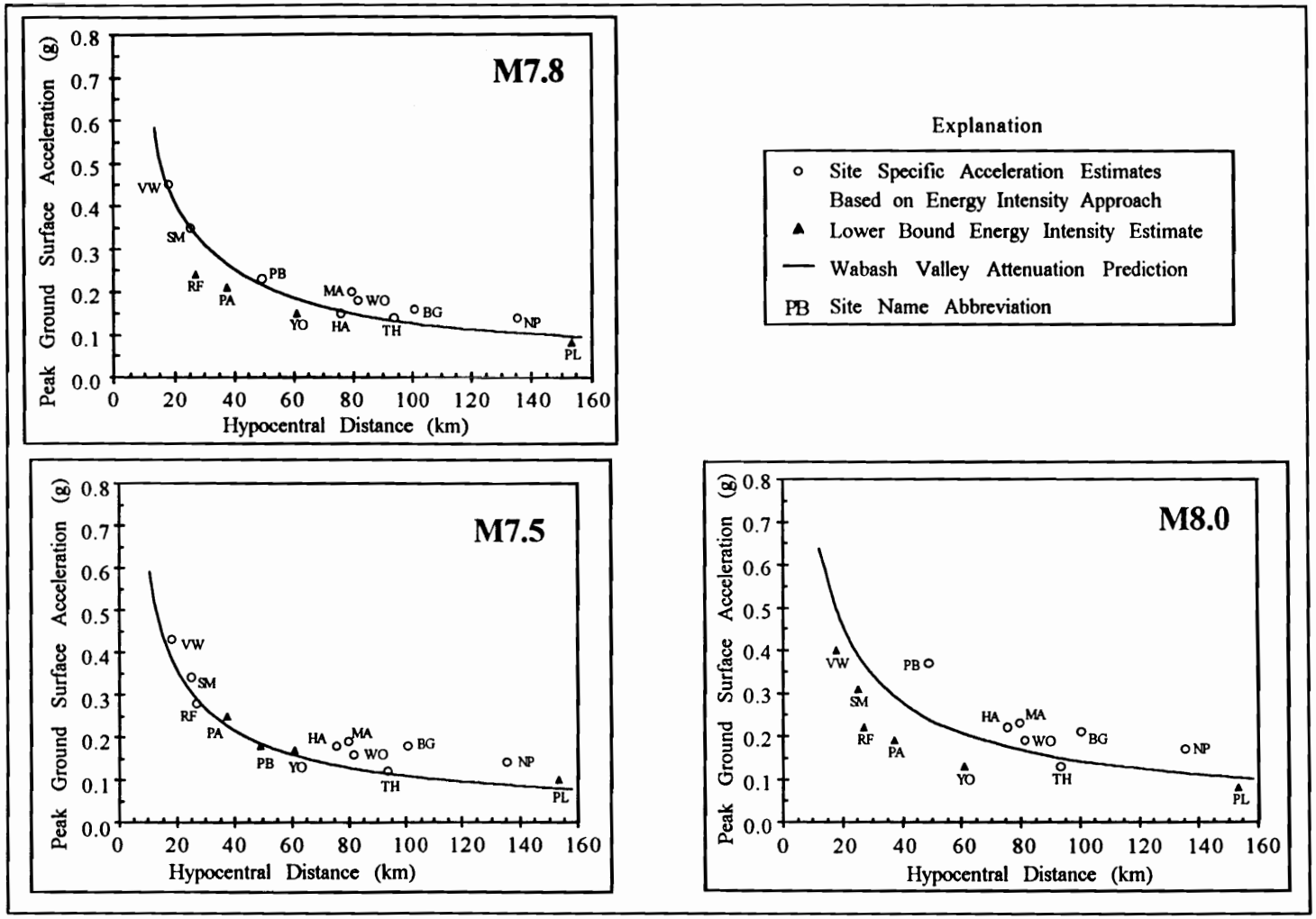

Figure 6.22. Peak surface acceleration predictions for Vincennes event based on energy intensity and attenuation convergence.

At most locations this will be true, but several of the study sites investigated for this study showed a large increase in measured blowcount at some depth within the soil profile. At these sites it is unreasonable to include the large blowcount material in the liquefied layer thickness. Including these high blowcounts in the average liquefied thickness leads to an excessively high estimate of peak surface motion. The slope of the liquefaction prediction boundary continues to increase with increasing blowcount, and these blowcounts contribute unreasonably to the surface acceleration estimates. Some engineering judgment is therefore required to estimate when this type of condition is encountered. In these cases, only the lower blowcount values are included in the surface motion estimate, and the average blowcount there may be less than the value predicted to allow liquefaction occurrence.

The results shown in Figure 6.22 clearly point to a magnitude M7.8 estimate as most appropriate for this event. Peak surface acceleration at the epicenter of this event is estimated to have been on the order of 0.68g based on the attenuation relationship developed for Wabash Valley events. The surface motion estimates reported here will be associated with frequencies generally in the range of one to three Hz. This is in the frequency range of most concern to engineered structures, and shows that soil sites in the region may suffer serious deleterious effects if an event of this magnitude occurs in the future.

6.7.3.2.Skelton Event Results

The Skelton earthquake (referred to as Skelton-Mt. Carmel in Munson and Munson, 1996) occurred approximately 12,000 years BP. It should be noted that the estimated epicentral location based on this analysis is slightly different than that suggested by Munson and Munson. They estimate an epicenter to be near Mt. Carmel, IL based on the distribution of maximum dike width. However, in order to avoid the likely possibility that the event would be associated with the Mt. Carmel fault if given that name, they chose the Hamlet of Skelton, IN as a namesake. They found that their dike width vs. distance data

fit this epicentral location well and measured their epicentral distances based on this location. They were unable to locate any sites within the immediate epicentral region, however, leaving a 45 km span between the liquefaction sites north and south of the epicenter.

The results of the analyses performed for this study suggest an epicenter located at the confluence of the Wabash and White Rivers is more consistent with the geotechnical data collected than is a Skelton, IN epicenter. The results of the analysis presented here are therefore based on epicentral distances measured from that location and differ slightly from those reported by Munson and Munson. This difference is small, but varies between 2 and 6.5 km. Based on the epicentral location assumed here, liquefaction evidence was produced over an area extending to epicentral distances of 68.5 km or more. The maximum distance to surface evidence of liquefaction associated with this event is approximately 63 km. Four of the identified liquefaction sites associated with this event were chosen for the geotechnical study.

The soil profile at sites associated with the Skelton event does not differ substantially from that present the time of the earthquake. Shortly after this event rivers began downcutting, and produced the present Maumee terrace level. These are the sediments that contain the liquefaction evidence for this event, and are well above the present flood plain level. The water table elevation during the time period when the earthquake occurred was quite high (Munson and Munson, 1996). It is assumed that the water table was at approximately the midpoint of the surficial fine-grained material. This is based on the stratigraphic relationship between sites and the relatively narrow constraints placed on the water table elevation based on the conditions at sites VC and WA. Site plans and soil profiles for the sites associated with this event are presented in Figures 5.31 through 5.38.

An initial estimate of magnitude for this event was taken as that suggested by the maximum distance to liquefaction effects. Using a preliminary M7.2 magnitude estimate, the analysis proceeds as for the Vincennes event. Liquefied layer thicknesses were

estimated for each site and a surface acceleration estimated. The results of these calculations are compared to surface motion predictions based on the Wabash Valley attenuation relationship in Figure 6.23. Comparison results for initial magnitude estimates of **M**7.3 and **M**7.4 are also presented in the figure. It can be seen that a **M**7.3 estimate provides the best match between the energy intensity approach and the attenuation prediction of surface motions. This should not be taken to imply that the magnitude estimate is accurate to within 0.1 magnitude unit. This is a numerical convergence procedure, and the results suggest only that a magnitude estimate of **M**7.3 provides a better fit to the data than either a **M**7.2 or **M**7.4 magnitude estimate.

In this case, the surface acceleration estimates at site WA are indicated as an upper bound estimate of surface motion. This is based on the fact that the liquefaction evidence identified at this site may not have been apparent at the surface. The prediction boundary used to estimate surface accelerations is based on empirical surface evidence of liquefaction occurrence. In cases where the dikes observed can not be shown to have reached the ground surface, the site would be classified as a non-liquefaction case. It should be expected, however, that the predicted motion will not significantly exceed the value that actually occurred. Surface evidence at this site was likely imminent. Based on this, the results shown in Figure 6.23 clearly point to a magnitude **M**7.3 estimate as most appropriate based on the field data for this event. Peak epicentral ground surface accelerations for this event are estimated to have been approximately 0.53g.

6.7.3.3. Vallonia Event Results

The Vallonia earthquake occurred approximately 4000 years BP. Liquefaction evidence was produced over an area extending to epicentral distances of approximately 36 km. The epicenter for the event is assumed to have been located at Vallonia, IN, as suggested by Munson and Munson. The maximum distance from this location to surface evidence of liquefaction associated with the event is approximately 36 km. Three sites associated with this event were chosen for the geotechnical study.

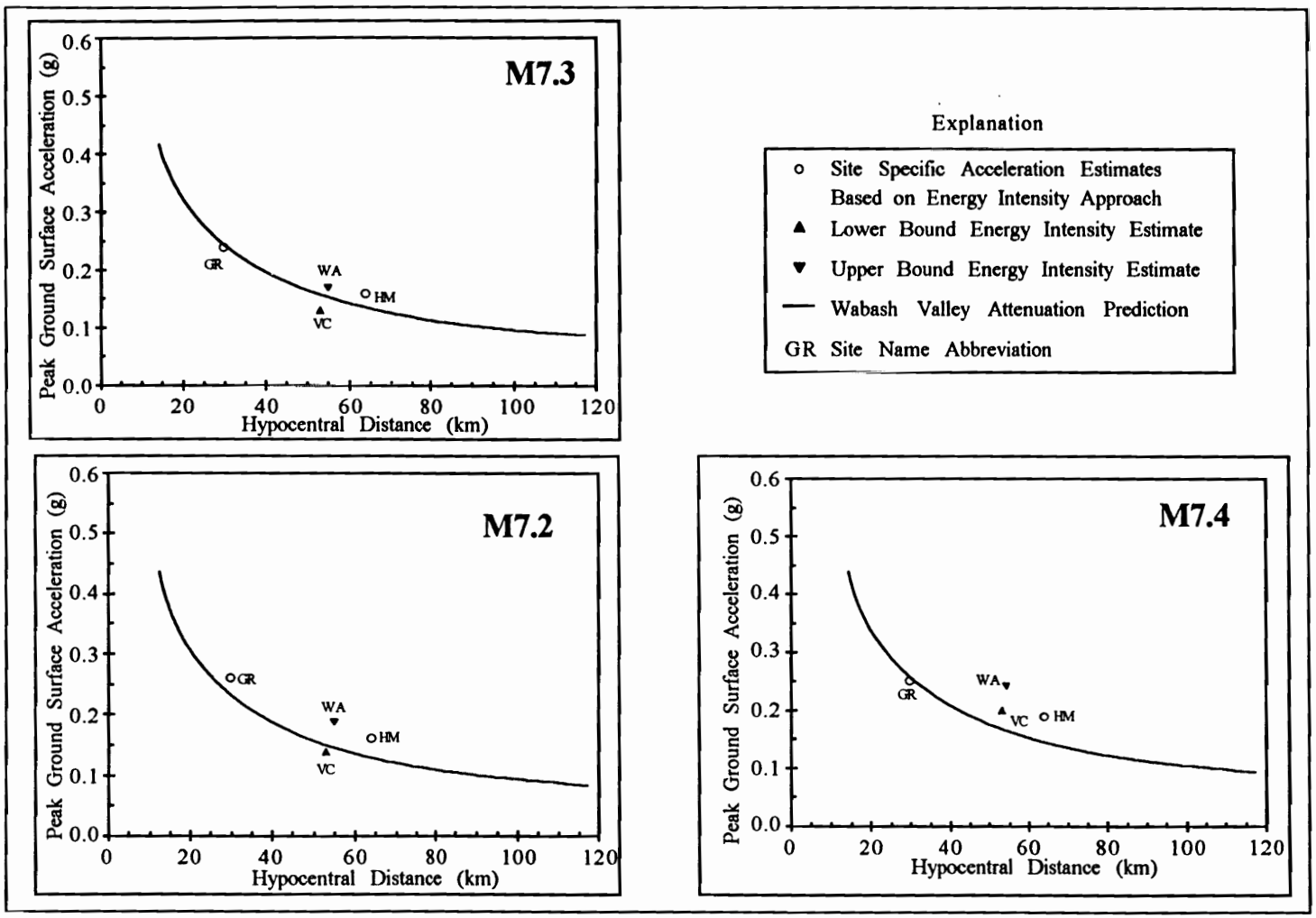

Figure 6.23. Peak surface acceleration predictions for Skelton event based on energy intensity and attenuation prediction convergence.

Here again, it was necessary to make some assumptions regarding the surface at the time of the earthquake. At site AZ there has been some post-event erosion in the vicinity of the liquefaction evidence that has obscured some of the near-surface details. At site SSP there has likely been some reworking of the surface that has obscured the top of the liquefaction dikes due to the gravel pit operations. At site SP the blow surface is inferred based on samples from the boring location only. This detail was obscured by vegetation in the river bank. The water table elevation is estimated for these sites based on the presence of weathering at the site AZ that is indicative of a long term fluctuation of the water table over a relatively narrow range just above the top of the source material. Site plans and soil profiles for the sites associated with this event are presented in Figures 5.39 through 5.44.

An initial estimate of magnitude for this event was taken as the M6.9 value suggested by the maximum distance to liquefaction effects. Using this magnitude estimate, the analysis again proceeds as for the Vincennes event. Liquefied layer thicknesses were estimated for each site and surface acceleration estimated. The results of these calculations are compared to surface motion predictions based on the Wabash Valley attenuation relationship in Figure 6.24. The results of the analysis for this event lead to an increased magnitude estimate as was seen for the Skelton event. When the magnitude estimate was increased to M7.1 a better fit was found between the two approaches to estimating surface motions. It was not until the magnitude estimate was increased to M7.2 that the two approaches began to diverge again. Comparison results for the three magnitude estimates are presented in the figure. It can be seen that the M7.1 estimate provides the best match between the energy intensity approach and the attenuation prediction of surface motions. The peak epicentral surface acceleration estimated for this event is approximately 0.48g, only slightly lower than that estimated for the Skelton event.

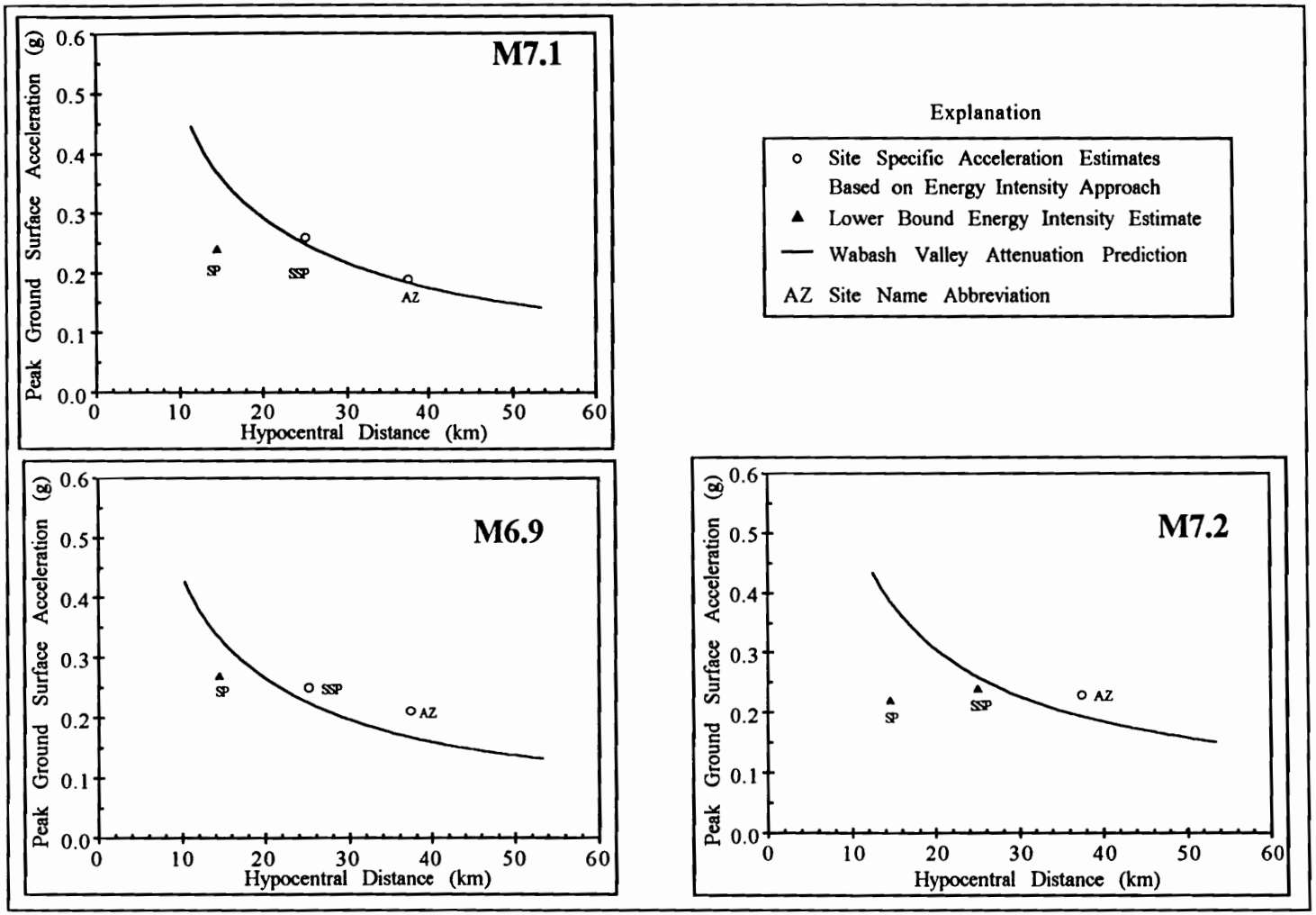

Figure 6.24. Peak surface acceleration predictions for Vallonia event based on energy intensity and attenuation predictions.

6.7.3.4.Waverly Event Results

The Waverly earthquake (referred to as Martinsville-Waverly in Munson and Munson, 1996) occurred some time between 8500 and 3500 years BP. The estimated epicentral location for this event is at the mouth of Goose creek, where it enters the White River. This is based predominantly on the geotechnical analysis. The liquefaction severity distribution associated with this event does not clearly point to an epicentral location. Additionally, the age of these sites is not well defined. For these reasons, the liquefaction seen in this area was originally assumed to be associated with the Vincennes event, which occurred at 6000 BP.

The liquefaction susceptibility of the soils in this region is much lower than for other areas of the Wabash and White River valleys. The area is located at approximately the southern terminus of the Wisconsinan glaciation, and while the grainsize distribution of the soils sampled here do not differ substantially from the distributions at other study sites, the measured blowcounts are greater. The sites are located too far from the Vincennes epicenter to have allowed liquefaction to have been induced by that event. Minimum surface motions required to induce liquefaction based on a M7.8 Vincennes event greatly exceed that which could reasonably be expected for such great epicentral distances. Neither could any anomalous soil or topographic conditions be identified that would lead to unusual amplification effects that might allow the large accelerations required.

Several epicentral location estimates were therefore postulated within this region, and surface acceleration predictions made. The epicentral location that leads to the best fit between the energy intensity approach and the attenuation prediction is Goose creek. The analysis results presented here are therefore based on epicentral distances measured from that location Based on this epicentral location, approximately 3.5 km southwest of site SV, liquefaction evidence was produced over an area extending to epicentral distances of approximately 33 km. The maximum distance to surface evidence of liquefaction

associated with this event is 28 km. Two study sites were chosen in this region for geotechnical evaluation.

The soil profile at the two sites associated with the Waverly event are quite different, with the profile less well defined at site SV. Post-event deposition is assumed to have been similar at each of these sites, however, and the surface estimate at site SV is based on this. Since only two study sites are associated with this event, the water table elevation is less well constrained than for the other events, but can still be estimated to have been in only a relatively narrow range based on the relationship between these sites. Site plans and soil profiles for the sites are presented in Figures 5.45 through 5.48.

An initial estimate of magnitude for this event was taken as that suggested by the maximum distance to liquefaction effects. Using the magnitude **M**6.8 estimate found from the prediction curve developed for the central United States, the analysis again proceeds as for the other events. Liquefied layer thicknesses were estimated for each site and surface acceleration estimated. The results of these calculations are compared to surface motion predictions based on the Wabash Valley attenuation relationship in Figure 6.25. The results for this event were similar to that found for the Vallonia event in that when the magnitude estimate was increased, a slightly better fit was found between the two approaches to surface motion estimates. Comparison results for three magnitude estimates are presented in Figure 6.25 for this event. It can be seen that the difference on the predictions over the magnitude range **M**6.8 to **M**7.1 does not vary substantially, but that a **M**6.9 estimate provides the best match between the energy intensity approach and the attenuation prediction of surface motions. The peak surface acceleration experienced at the epicentral location for this event is estimated to have been 0.44g.

6.8.Discussion

Minimum magnitude estimates of **M**6.8, **M**6.9, **M**7.2 and **M**7.8 are found for four Wabash Valley earthquakes when based on the maximum distance to observed liquefaction effects. Geotechnical estimates of the minimum magnitudes required to

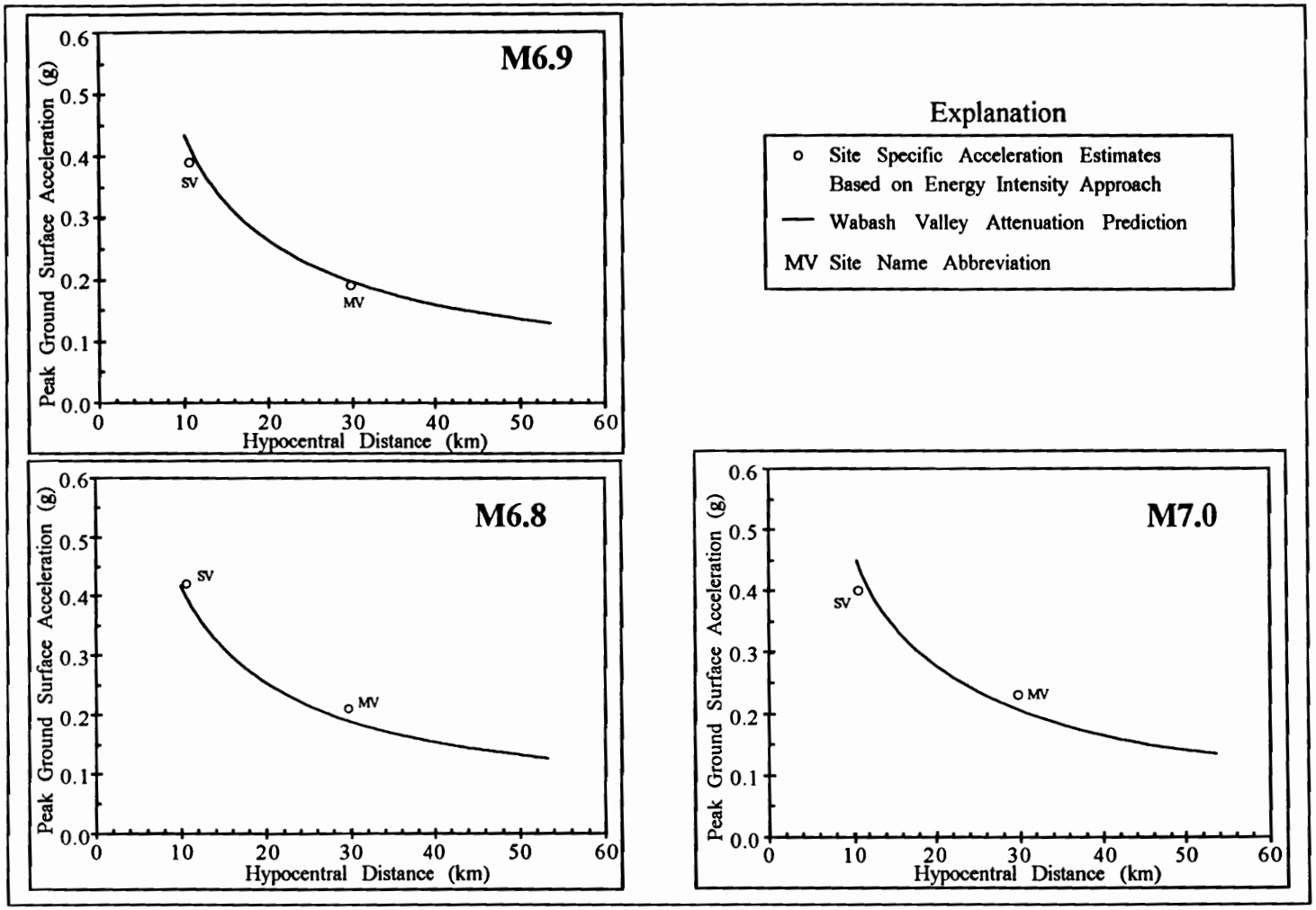

Figure 6.25. Peak surface acceleration predictions for Waverly event based on energy intensity and attenuation convergence.

induce the liquefaction evidence have also been made using the magnitude contours developed by incorporating an estimated Wabash Valley attenuation relationship in a liquefaction susceptibility analysis procedure. This suggests minimum magnitude estimates of **M**6.9, **M**6.7, **M**7.4 and **M**7.7 for the four earthquakes. In order to refine these minimum magnitude estimates, an energy intensity approach to liquefaction susceptibility analysis was developed to predict a best estimate of the peak accelerations required to induce the liquefaction effects observed at each of the study sites. The value found using this approach was then compared to the peak surface motions predicted by the attenuation relationship based on these magnitude estimates. These two approaches most closely agree for magnitude estimates of **M**6.9 for the Waverly event, **M**7.1 for the Vallonia event, **M**7.3 for the Skelton event, and **M**7.8 for the Vincennes event. The effect of variations in the water table are not shown on these figures to provide a clearer presentation of the convergence effect that occurs when the prediction methods agree. It must be understood that this involves some uncertainty, however. Based on a liberal estimate of the likely variation in the water table elevation, the predicted peak acceleration values will vary by approximately 0.02g. This translates into an uncertainty in the magnitude estimate of approximately ±0.25 moment magnitude units for the M7.8 estimate. It should be noted here as well, however, that not only do the peak acceleration estimates derived from the energy intensity approach tend toward the attenuation prediction, there also tends to be less scatter among the site specific estimates. This lends additional support to the magnitude estimate based on that where the two approaches most closely agree.

The magnitude estimates based on paleoliquefaction evidence greatly exceed the magnitude of recorded historical events. It should be pointed out, however, that these magnitude estimates are consistent with the maximum event (approximately **M**7.5) suggested for this region by the seismological community (Nuttli, 1979). The results

shown here suggest the seismic hazard assumed in the Wabash region based on historical seismicity may be significantly underestimated.

7. Summary and Conclusions

Paleoliquefaction evidence has traditionally been used to supplement other evidence of past seismic activity in high seismicity regions. The evidence has typically been used as an indication of recurrence rates in those regions. The use of the information was usually limited to areas of known surface expressions of fault displacements and/or recorded evidence of seismic events. This type of evidence has, however, been gaining acceptance in recent years as an indication of large prehistoric seismic events where no surface fault displacement expression of that seismic activity has been identified. Use of liquefaction evidence has also been extended beyond a simple estimate of recurrence rates to estimating earthquake magnitude and amplitude of ground motions. A recent study in Charleston, South Carolina (Martin and Clough, 1994) has shown that liquefaction evidence can be successfully used to estimate magnitude and ground motion parameters associated with earthquakes in low-seismicity regions.

The Wabash valley of the central United States is a region that has long been suspected of containing the potential for large earthquakes (Nuttli, 1979). However, no historical event has produced strong shaking in the region. More importantly, no historical event has been reported to have induced liquefaction effects. Additionally, no surface expression of displacements associated with geologically-recent earthquakes has been identified. This limits investigations of seismic activity in the region to use of paleoliquefaction evidence with no other evidence for strong ground motions. Recent field surveys throughout the region of southern Indiana and Illinois have identified widespread liquefaction effects that have been linked to prehistoric seismic events (Figure 3.3). This evidence suggests that the region is susceptible to seismic activity greater than that which is present in the historical record.

This study was undertaken in an effort to better describe the seismic potential associated with the tectonic environment in the Wabash Valley Seismic Zone. As the field portion of the study was begun, identification of the liquefaction effects present in the

region was also in the preliminary stages. Estimates at that time of the extent of the region that would eventually be identified as containing liquefaction evidence was grossly underestimated by all involved. As the field investigations continued, the region of liquefaction effects also continued to expand. The area of liquefaction effects shown in Figure 3.3 appears to be the limit of liquefaction effects at this time, but field searches for further evidence continue. Relatively early in this study, however, the extent of liquefaction effects in Indiana was beginning to become well defined. Field work in Illinois did not begin in earnest until much of the field work for this study had been completed. For this reason, the analysis of the available data has been focused on the Indiana portion of the study region.

Assuming a point-source event and regionally homogeneous bedrock conditions, the production of liquefaction effects can be assumed to be a reasonably symmetrical result of seismic activity. These assumptions are adopted by the seismological community when modeling ground motions due to large seismic events and have been found to provide reliable estimates of regional bedrock motions. These assumptions also allow geotechnical estimates of the seismic parameters associated with the events based on only half of a liquefaction distribution. Liquefaction distributions associated with the four events investigated for this study contain at least half of the distributions identified for those events. This fact has allowed the analysis techniques used in this study to provide reasonable estimates of seismic parameters associated with prehistoric Wabash Valley events.

This study has used field and laboratory test results to provide input parameters necessary for a liquefaction-susceptibility analysis procedure that has lead to estimates of magnitude, peak acceleration, and attenuation characteristics for four large prehistoric earthquakes occurring in the Wabash Valley Seismic Zone. Geotechnical parameters were obtained at 22 sites throughout the study region. The primary field test procedure was the Standard Penetration Test (SPT), but was supplemented in gravelly soils by the Oversize

Penetration Test (OPT). In addition, seismic shear wave velocity tests and in-situ density tests were performed at several of the study sites.

The field portion of the study was accomplished over a period of three years, expanding as necessary as the region of identified liquefaction effects was enlarged. Field test locations were chosen in an attempt to represent the greatest distribution of epicentral distances possible, and at intervals that would allow reasonable estimates of attenuation characteristics to be made. A total of 76 penetration test borings were performed at the 22 sites. In-situ density testing were performed at six study sites for a total of 38 tests. Seismic shear wave velocity testing was completed at four sites. This was based on the SASW procedure, with a cross-hole shear wave velocity test performed at one site for comparison with the SASW data. Laboratory testing performed for this study was directed toward classification of the soil samples obtained. These tests included grainsize analyses, Atterberg limits, specific gravity, angularity, and index density determinations.

This study has focused on the paleoliquefaction evidence associated with four prehistoric earthquakes in the Wabash Valley. These are the 6,000 year BP Vincennes; 12,000 year BP Skelton; 4,000 year BP Vallonia; and 8,500-3,500 year BP Waverly events. The inferred epicenters for the two largest of these Wabash Valley earthquakes are near Vincennes, Indiana. This location agrees with the location of instrumentally recorded modern seismicity and the greatest intensity for the M5.0 southeastern Illinois earthquakes of 1987 (Reagor and Brewer, 1987). A magnetic anomaly survey in the region has also revealed evidence of a structure that appears to be a large tectonic feature. Thus, three independent assessments suggest a seismic source in this region (Hildenbrand, 1996). This combined evidence suggests the potential for strong shaking that greatly exceeds that in the historical record.

Measured in-situ soil strength parameters were used in this study to estimate seismic parameters associated with four large prehistoric earthquakes in the Wabash Valley. In addition to these findings, completion of this study has lead to results of

general interest to the geotechnical and seismological communities. The findings related to seismic parameters associated with large Wabash Valley earthquakes are provided below, followed by the primary conclusions regarding the results of this research.

1.) The primary objective of this research was to estimate seismic parameters associated with four prehistoric earthquakes that induced paleoliquefaction evidence in the Wabash Valley.

- The four events investigated were the Vincennes (6,000 years BP), Skelton (12,000 years BP), Vallonia (4,000 years BP), and Waverly (8,500-3,500 years BP) events.
- Based on maximum distances to observed liquefaction effects of 141km, 63km, 36km, and 28km, minimum magnitude estimates are:

  M7.8, **M**7.2, **M**6.9, and **M**6.8, respectively.

- Based on the minimum soil strength parameters measured at sites associated with these events, the minimum magnitudes required to induce the observed liquefaction evidence are:

  M7.7, **M**7.4, **M**6.7, and **M**6.9, respectively.

2.) "Best" estimates of seismic parameters associated with these earthquakes are based on using an energy intensity approach to provide a rational approach to estimating liquefied layer thickness.

- The Seed and Idriss (1982) simplified procedure is then incorporated with the energy intensity approach to back-calculate surface motion estimates. A best estimate of seismic parameters can be taken as that where the geotechnical surface motion prediction most closely agrees with a seismological prediction of attenuation appropriate to the site conditions.

- The Vincennes event is estimated to have been an approximately **M**7.8 event. Peak surface accelerations in the epicentral region are estimated to have been greater than 0.6g. This attenuates rapidly with distance, and at a 30 km hypocentral distance is reduced to approximately 0.3g. At 150 km the surface acceleration is reduced to approximately 0.1g. This attenuation relationship is shown in Figure 6.22.

- The Skelton event is estimated to have been an approximately **M**7.3 event. Peak surface accelerations in the epicentral region are estimated to have been nearly 0.5g. The motions associated with this event will have been reduced to approximately 0.25g at a 30 km hypocentral distance. At 100 km the surface acceleration is reduced to approximately 0.13g. This attenuation relationship is shown in Figure 6.23.

- The Vallonia event is estimated to have been an approximately M7.1 event. Peak surface accelerations in the epicentral region for this event are also estimated to have been nearly 0.5g. At 50 km, the surface acceleration is attenuated to approximately 0.15g. This attenuation relationship is shown in Figure 6.24.

- The Waverly event is less well defined than the others, but is estimated to have been an approximately M6.9 event. Peak surface accelerations in the epicentral region are estimated to have been nearly 0.45g. At 50 km the surface acceleration is reduced to approximately 0.14g. This attenuation relationship is shown in Figure 6.25.

3.) The error in the magnitude predictions is estimated to be on the order of 0.25 to 0.5 magnitude units.

- These estimates are based on a semi-theoretical seismological approach combined with an approach based on liquefaction effects associated with

historical earthquakes. The errors in the magnitude estimates may be similar to the error present in magnitude estimates for historical earthquakes where magnitude is based on damage effects or felt area, however, the agreement between the geotechnical and seismological approaches suggests the uncertainty is reduced from that present in felt area vs. magnitude estimates.

- It is unlikely that the accuracy of the evaluation procedure used here could approach that achieved using worldwide measured seismic data. However, three different approaches to estimating magnitude were used here and each has lead to magnitude estimates for the individual events that fall within a very narrow range.

4.) Attenuation of eastern North America class C soil site peak surface acceleration can be described by the following relationship:

$$Log(a_p) = -1.129 + 0.216 \cdot (M) - 0.7205 \cdot Log(R);$$

where a_p is peak surface acceleration in units of gravity, M is moment magnitude and R is hypocentral distance in km. This relationship is recommended for $6.0 < M < 8.0$ events at distances of 10 km $< R <$ 200km. These ranges are an extrapolation of the relationship beyond the original data set, however, the prediction has been found to be consistent with the attenuation suggested by the Wabash Valley liquefaction evidence.

- This attenuation relationship was developed based on the Boore et al. (1993) definition of Class C soil site conditions (180 m/s $< V_s <$ 360 m/s) and for soil depths of 15 to 75 m (50 to 250 ft.).
- The attenuation relationship is similar to the Boore et al. relationship for the western United States class C soil sites (Figure 6.12). This supports the assumption of similar source characteristics and near-source attenuation characteristics for eastern and western United States soil sites.

5.) Soil conditions significantly influence site response relative to the bedrock motions associated with eastern North America earthquakes.

- The increased high frequency content of mid-continent seismic motions are greatly influenced by the filtering effect of both the regional bedrock characteristics and site specific soil conditions.
- A site response study using the computer program SHAKE suggests a maximum deamplification of peak acceleration of approximately three for the soil conditions investigated. This deamplification decreases with distance from the source, and a slight amplification is predicted at the maximum distances investigated.
- The deamplification effect is due to the fact that peak bedrock motions are associated with the high frequency portion of the earthquake record. Peak soil site accelerations are associated with much lower frequencies. The high frequency motions are attenuated with distance, and the period associated with the peak bedrock motions tends to approach that of the soil column.

6.) Liquefaction susceptibility of the Wabash Valley alluvial deposits are generally high to moderate.

- Soil conditions associated with the liquefaction evidence observed consist of medium dense sands and gravelly sands deposited in a diluvial or fluvial environment. Gravel contents generally decrease with distance downstream, but also show significant variation at individual sites.
- Liquefied gravelly soils in the Wabash Valley are similar to soils that liquefied during the Borah Peak Idaho earthquake of 1983, but maximum particle sizes tend to be slightly smaller.

7.) The SPT procedure provides reliable blowcount values for liquefaction susceptibility analyses in soil deposits with maximum grain sizes of up to 7.5 cm and blowcounts of $5 \leq (N_1)_{60} \leq 25$.

- The gravelly soil conditions present at many of the study sites dictated use of an oversize penetration testing procedure to assess the potential impact of large particle sizes on the results of the SPT procedure. Inflated blowcount values could overestimate liquefaction resistance and therefore lead to overly large estimates of the minimum magnitude required for liquefaction.

- A penetration test conversion factor based on applied energy was used to determine a penetration test procedure that would provide equivalent SPT data using OPT equipment. An energy conversion approach (Karol, 1960) was used to accomplish this. The following equation was found to provide reliable results for the Wabash soils:

$$N_{SPT} = \frac{\Phi \cdot N_{OPT} \cdot W_{OPT} \cdot H_{OPT}}{\left(D_o^2 - D_i^2\right)_{OPT}};$$

where $\Phi = 0.0007$ in/lb, N is measured in-situ blowcount, W is hammer weight in pounds, H is drop height in inches, and D is sampler diameter in inches with the subscripts 'o' and 'i' referring to outside and inside diameters.

- Figure 3.1 presents the results of comparison test results of the SPT and OPT procedures. When the OPT procedure was adjusted to give $N_{SPT}=N_{OPT}$ based on the relationship above, no apparent difference was observed between the measured SPT and OPT blowcounts.

- These results support the Andrus and Youd (1986) conclusion that SPT data in gravelly soils provides reliable liquefaction susceptibility data. This is also consistent with the results reported by Liao et al. (1988) showing no statistical difference in liquefaction resistance due to the presence of gravels.

8.) The findings of this study have implications for understanding of the seismic environment in the Wabash Valley

- The Wabash Valley Seismic Zone is shown to have produced significant seismically-induced ground motions not represented in the historical record. This suggests the seismic hazard in the region may be underestimated and should be reassessed.
- The use of paleoliquefaction evidence to estimate seismic parameters has helped to improve understanding of the overall seismic environment in the central United States and the seismic risk associated with the region. This can suggest to seismologists the scale of tectonic deformation rates and other evidence to search for in the region. In this way additional corroborative evidence may be discovered that could also indicate the region has been subject to significant deformations.

9.) The findings of this study do suggest a seismic potential consistent with that indicated by three other independent sets of evidence.

- Location of the inferred epicenters associated with the largest prehistoric events (near Vincennes, Indiana) coincide with the location of instrumentally recorded modern seismicity
- The inferred Vincennes epicenter is also coincident with the region of greatest intensity for the most recent felt earthquake (1987, M5.0 Southeastern Illinois event).
- Also, a deep magnetic survey suggests a large tectonic feature in the vicinity of these epicenters that may be capable of producing very large ground motions..

References

Alarcon-Guzman, A., Leonards, G. A. and Chameau, J. L. (1988) "Undrained Monotonic And Cyclic Strength Of Sand," JGENDZ, ASCE, 114(10), 1089-1109.

Algermissen, S. T. (1983) "An Introduction To The Seismicity Of The United States," EERI monograph, 147 p.

Ambraseys, N. N. (1988) "Engineering Seismology: Earthquake Engineering And Structural Dynamics," J. Int'l. Assoc. Earthquake Engrg., 17(1), pp. 1-105.

Ambraseys, N. N. and Sarma, S. (1969) "Liquefaction Of Soils Induced By Earthquakes," BSSA, 59(2), 651-664.

Andrus, R. D. and Youd, T. L. (1987) "Subsurface Investigation Of A Liquefaction-Induced Lateral Spread, Thousand Springs Valley, Idaho," U.S. Army Corps of Engrs. WES, Misc. Paper GL-87-8, 106 pp.

Andrus, R. D., Stokoe, D. H., and Roesset, J. M. (1991) "Liquefaction Of Gravelly Soil At Pence Ranch During The 1983 Borah Peak, Idaho Earthquake," Proc. Soil Dynamics and Earthquake Engineering, '91, pp. 251-262.

Arulanandan, K., Anandarajah, A. and Abghari, A. (1983) "Centrifugal Modeling Of Soil Liquefaction Susceptibility," JGENDZ, ASCE, 109(3), 281-300.

ASTM (1994) Annual Book of ASTM Standards, Section 4, Construction, Vol. 04.08, Soil and Rock (I): D 420-4914.

Atkinson, G. M. (1984) "Attenuation Of Strong Ground Motion In Canada From A Random Vibrations Approach," BSSA, 74(6), 2629-2653.

Atkinson, G. M. and Boore, D. M. (1995) "Ground-Motion Relations For Eastern North America," BSSA, 85 (1), 17-30.

Baladi, G., Bellotti, R., Ghionna, V., Jamiolkowski, M. and Pasqualine, E. (1985) "Penetration Resistance And Liquefaction Resistance Of Sands," Proc. 11th Int'l Conf. on Soil Mechs. and Foundation Engrg., Vol. 4, 1891-1896.

Bartlett, S. F. and Youd, T. L. (1995) "Empirical Analysis Of Horizontal Ground Displacement Generated By Liquefaction-Induced Lateral Spread," NCEER 92-0021, Buffalo, NY.

Bartlett, S. F. and Youd, T. L. (1995) "Empirical Prediction Of Liquefaction-Induced Lateral Spread," ASCE, JGENDZ, 121(4), 316-329.

Berrill, J. B. and Davis, R. O. (1985) "Energy Dissipation And Seismic Liquefaction Of Sands: Revised Model," JSSMFE, Soils and Foundations, 25(2), 106-118.

Bollinger, G. A., Chapman, M. C., and Sibol, M. S. (1993) "A Comparison Of Earthquake Damage Areas As A Function Of Magnitude Across The United States," BSSA, 83(4), 1064-1080.

Boore, D. M. (1983) "Stochastic Simulation Of High Frequency Ground Motions Based On Seismological Models Of The Radiated Spectra," BSSA, 73, 1865-1894.

Boore, D. M. and Atkinson, G. M. (1987) "Stochastic Prediction Of Ground Motion And Spectral Response Parameters At Hard Rock Sites In Eastern North America," BSSA, 77(2), 440-467.

Boore, D. M. and Atkinson, G. M. (1992) "Source Spectra For The 1988 Saguenay, Quebec Earthquakes," BSSA, 82(2), 683-719.

Boore, D. M. and Joyner, W. B. (1991) "Estimation Of Ground Motion At Deep Soil Sites In Eastern North America," BSSA, 81(6), 2167-2185.

Boore, D. M., Joyner, W. B. and Fumal, T. E. (1993) "Estimation Of Response Spectra And Peak Accelerations From Western North American Earthquakes: An Interim Report," U.S. Geological Survey, Open-File Report 93-509, 72 pp.

Braile, L. W., Hinze, W. J., Keller, G. R. and Lidiak, E. G. (1982) "The Northeastern Extension Of The New Madrid Seismic Zone," in Investigations of the New Madrid, Missouri Earthquake Region, U.S. Geological Survey Prof. Paper 1236-L, 175-184.

Braile, L. W., Hinze, W. J., Sexton, J. L., Keller, J. R. and Lidiak, E. G. (1984) "Tectonic Development Of The New Madrid Seismic Zone," US Geological Survey Open File Report 84-770, pp. 204-233.

Casagrande, A. (1975) "Liquefaction And Deformation Of Sands - A Critical Review," Fifth Pan American Conf. on Soil Mechs. and Foundation Engrg., Vol. V, 80-133.

Castro, G. (1975) "Liquefaction And Cyclic Mobility Of Saturated Sands," JGENDZ, ASCE, 101(GT6), 551-569.

Castro, G. (1987) "On The Behavior Of Soils During Earthquakes - Liquefaction," in: Developments in Geotechnical Engineering, Vol. 42, Soil Dynamics and Liquefaction, A. S. Cakmak (ed.), 169-204.

Chameau, J. L., Clough, G. W., Reyna, F. and Frost, J. D. (1991) "Liquefaction Response Of San Fransisco Bayshore Fills," BSSA, 81(5), 1998-2018.

Clough, G. W. and Chameau, J. L. (1983) " Seismic Response Of San Fransisco Waterfront Fills," ASCE, JGENDZ, 109(4), 491-506.

Clough, G. W. and Martin, J. R., II (1990) "Geotechnical Setting For Liquefaction Events In The Charleston, South Carolina Vicinity," H. Bolton Seed Memorial Symposium Proceedings, J. Michael Duncan (ed.), Vol. 2, 313-334.

Coulter, H. W. and Migliaccio, R. R. (1966) "Effects Of The Earthquake Of March 27, 1964 At Valdez, Alaska," U.S. Geological Survey Prof. Paper 542-C, 36 pp..

Davis R. O. and Berrill, J. B. (1982) "Energy Dissipation And Seismic Liquefaction In Sands," Earthquake Engineering and Structural Dynamics, Vol. 10, 59-68.

DeAlba, P., Seed, H. B. and Chan, C. K. (1976) "Sand Liquefaction In Large-Scale Simple Shear Tests," JGENDZ, ASCE, 109(GT9), 909-927.

Dobry, R., Baziar, M. H., O'Rourke, T. D., Roth, B. L. and Youd, T. L. (1992) "Liquefaction And Ground Failure In The Imperial Valley, Southern California 1979, 1981 And 1987 Earthquakes," in: Case Studies of Liquefaction and Lifeline Performance During Past Earthquakes, NCEER-92-0002, State Univ. of NY, Buffalo, NY, Vol. 2, No. 4, 85 pp.

Dobry, R., Elgamal, A.-W. and Baziar, M. (1989) "Pore Pressure And Acceleration Response Of Wildlife Site During The 1987 Earthquake," in O'Rourke, T. D. and Hamada, M., eds., Proceedings from the Second U.S.-Japan Workshop on Liquefaction, Large Ground Deformation, and Their Effects on Lifelines: State University of New York at Buffalo, Technical Report NCEER-89-0032, p. 145-160.

Dobry, R., Stokoe, K. H., Yokel, F. Y., Chung, R. M. and Powell, O. (1982) "Predictions Of Pore Water Pressure Buildup And Liquefaction Of Sands During Earthquakes By The Cyclic Strain Methods," National Bureau of Standards, Building Science Series, No. 138.

Douglas, B. J., Olsen, R. S. and Martin, G. R. (1981) "Evaluation Of The Cone Penetrometer Test For SPT-Liquefaction Assessment," Insitu Testing To Evaluate Liquefaction Susceptibility, Report. 81-544, ASCE Nat'l. Conf., St. Louis, Missouri.

Duncan, J. M., Horz, R. C., and Yang, T. L. (1989) "Shear Strength Correlations For Geotechnical Engineering," Virginia Tech Dept. of Civil Engineering, Geotechnical Engineering, 100 p.

Evans, M. D., Seed, H. B. and Seed, R. B. (1992) " Membrane Compliance And Liquefaction Of Sluiced Gravel Specimens," JGENDZ, ASCE, 118(6), 856-872.

Fang, H. (1991) "Foundation Engineering Handbook," 2nd Ed., Nostrand-Reinhold, New York, NY, pp. 38-39.

Fidlar, M. M. (1948) Physiography of The Lower Wabash Valley," Indiana Geological Survey, Bulletin No. 2, 112 p.

Figueroa, J. L., Saada, A. S., Liang, L. and Dahisaria, N. M. (1994) "Evaluation Of Soil Liquefaction By Energy Principles," ASCE, J. Getoech. Engrg., 120(9), 1554-1569.

Finn, W. D. L. (1979) "Critical Review Of Dynamic Effective Stress Analysis," Proc. 2nd U.S. National Conf. on Earthquake Engrg., 853-867.

Finn, W. D. L., Bransby, P. L. and Pickering, D. J. (1970) "Effect Of Strain History On The Liquefaction Behavior Of Sand," JSMFD, ASCE, 96(SM6), 1917-1934.

Florin, V. A. and Ivanov, P. L. (1961) "Liquefaction Of Saturated Sandy Soils," Proc. Fifth Int'l. Conf. on Soil Mechanics and Foundation Engrg., Vol. 1, 107-111.

Fragaszy, R. J., Su, J., Siddiqi, F. H. and Ho, C. L. (1992) "Modeling Strength Of Sandy Gravel," JGENDZ, ASCE, 118(6), 920-935.

Frasier, G. S. (1993) "Sedimentology And History Of Late Wisconsin Alluviation Of The Wabash Valley," Indiana Geological Survey, Special Report No. 56, 18 p.

Frasier, G. S. and Gray, H. H. (1992) "Quaternary Evolution Of The Prairie Creek Lake Basin, Davies County, Indiana," Indiana Geol. Survey, Special Report No. 53, 20 p.

Fruel, G. (1991) Written personal communication to Prof. J. R. Martin of Va. Tech., Shannon and Wilson, Inc., St. Louis, MO.

Gibbs, H. J. and Holtz, W. G. (1957) "Research On Determining The Density of Sands By Spoon Penetration Testing," Proc. Fourth Int'l Conf. on Soil Mechanics and Foundation Engineering, London,

Gray, H. H. (1989) "Quaternary Geologic Map Of Indiana," Indiana Geological Survey, Misc. Map 49.

Gray, H. H. (1987) "Bedrock Geologic Map Of Indiana," Indiana Geological Survey, Misc. Map 48.

Gutenberg, B. and Richter, C. Figure. (1956) "Magnitude And Energy Of Earthquakes," Annali de Geofisica, Vol. 9, 1-15.

Hanks, T. C. and Johnston, A. C. (1992) "Common Features Of The Excitation And Propagation Of Strong Ground Motion For North American Earthquakes," BSSA, 82(1), 1-23.

Hardman, S. L. and Youd, T. L. (1987) "State-Of-The-Art For Assessing Earthquake Hazards In The United States; Report 22: Mapping The Extent And Thickness Of Liquefiable Soil Layers At Engineering Sites," U.S. Army Corps of Engrs. WES, Misc. Paper S-73-1, 161 pp.

Hasegawa, H. S., Basham, P. W. and Berry, M. J. (1981) "Attenuation Relations For Strong Seismic Ground Motion In Canada," BSSA, 71(6), 1943-1962.

Heidari, M. and James, R. G. (1982) "Centrifuge Modeling Of Earthquake-Induced Liquefaction In A Column Of Sand," Proc. of the Conf. on Soil Dynamics and Earthquake Engrg., Vol. 1, 271-281.

Herrmann, R. B. and Nuttli, O. (1981) "Scaling and attenuation relations for strong motion in eastern North America," Proc. Eighth World Conf. on Earthquake Engineering, Vol. 2, 99. 305-309.

Hildenbrand, T. G. (1996) "Structural Setting Of The Wabash Valley Fault System Based On Magnetic-Anomaly Data," Seismological Research Letters, 67(2), p. 40.

Hildenbrand, T. G. and Hendricks, J. D. (1995) "Geophysical Setting Of The Reelfoot Rift And Relations Between Rift Structures And The New Madrid Seismic Zone," in Investigations of the New Madrid Seismic Zone, K. M. Shedlock and A. C. Johnston eds., U.S. Geological Survey Prof. Paper 1538-E, 30 p.

Holzer, T. L., Bennett, M. J., and Youd, T. L. (1989a) "Lateral Spreading Field Experiments By The U.S. Geological Survey," in O'Rourke, T. D. and Hamada, M., eds., Proceedings from the Second U.S.-Japan Workshop on Liquefaction, Large Ground Deformation, and Their Effects on Lifelines: State University of New York at Buffalo, Technical Report NCEER-89-0032, p. 82-101.

Holzer, T. L., Tinsley, J. C., III, Bennett, M. J., and Mueller, C. S.. (1994) "Observed And Predicted Ground Deformation-Miller Farm Lateral Spread, Watsonville, California," in: Proc., 5th U.S.-Japan Workshop on Earthquake Resistant Design of Lifeline Facilities and Countermeasures Against Soil Liquefaction, (O'Rourke, T. D. and Hamada, M., eds.), State University of New York at Buffalo, NCEER-94-0026, 82-101.

Holzer, T. L., Youd, T. L. and Hanks, T. C. (1989) "Dynamics Of Liquefaction During The 1987 Superstition Hills, California, Earthquake," Science, Apr. 7, Vol. 244, 56-59.

Hussein, A. K. and Stewart, H. E. (1994) " Postliquefaction Deformation Of Cohesionless Soil," in: Proc. From The Fifth US-Japan Workshop On Earthquake Resistant Design Of Lifeline Facilities And Countermeasures Against Soil Liquefaction, O'Rourke and Hamada (eds.), NCEER-94-0026, 199-215.

Ishihara, K. (1980) "Present State And Problems Of Aseismic Design And Dynamic Investigation And Testing For Soils," Geology and Investigation, No. 2.

Ishihara, K. (1985) "Stability Of Natural Deposits During Earthquakes," 11th Int'l. Conf. on Soil Mechanics and Foundation Engineering, Vol. 1, pp. 321-376.

Ishihara, K. (1993) "Liquefaction And Flow Failure During Earthquakes," Rankine Lecture, Geotechnique, 43(3), 351-415.

Joyner, W. B. and Boore, D. M. (1981) "Peak Horizontal Acceleration And Velocity From Strong-Motion Records Including Records From The 1979 Imperial Valley, California, Earthquake," BSSA, 71(6), 2011-2038.

Karol, R. H. (1960) "Soils And Soils Engineering," Prentice Hall, Englewood Cliffs, NJ, pp. 22-23.

Keefer, D. K., Wilson, R. C., Harp, E. L. and Lips, E. W. (1985) "The Borah Peak Earthquake Of October 28, 1983 - Landslides," Earthquake Spectra, 2(1), 91-125.

Koizumi, Y. (1966) "Changes In Density Of Sand Subsoil Caused By Niigata Earthquake," Soils and Foundations, JSSMFE, 6(2), 38-44.

Kovacs, W. D. (1994) "Effects Of SPT Equipment And Procedures On The Design Of Shallow Foundations On Sand," in: Vertical and Horizontal Deformations of Foundations and Embankments, (A.T. Yeung and G.Y. Felio, eds.), GT Special Publication No. 40, ASCE, Vol. 1, 121-131.

Kovacs, W. D., Yokel, F. D., Salomone, L. A. and Holtz, R. D. (1984) "Liquefaction Potential And The International SPT," Proc. 8th World Conf. on Earthquake Engrg., Vol. III, 263-268.

Ladd, R. S. (1974) "Specimen Preparation And Liquefaction Of Sands," JGENDZ, ASCE, 100(GT10), 1180-1184.

Law, K. T., Cao, Y. L. and He, G. N. (1990) "An Energy Approach For Assessing Seismic Liquefaction Potential," Can. Geotech. J., 27(3), 320-329.

Lee, K. L. and Albaisa, A. (1974) "Earthquake Induced Settlements In Saturated Sands," JGENDZ, ASCE, 100(GT4), 387-406.

Lee, K. L. and Focht, J. A., Jr. (1975) "Liquefaction Potential At Ekofisk Tank In North Sea," JGENDZ, ASCE, 101(GT1), 1-18.

Lee, K. L. and Seed, H. B.. (1967) "Cyclic Stress Conditions Causing Liquefaction Of Sand," JSMFD, ASCE, 92(SM6), 47-70.

Liang, L., Figueroa, J. L. and Saada, A. S. (1995) "Liquefaction Under Random Loading: Unit Energy Approach," ASCE, J. Geotech. Engrg., 121(11), 776-781.

Liao, S. S. C., Veneziano, D. and Whitman, R. V. (1988) "regression models for evaluating liquefaction probability," ASCE, J. Geotech. Engrg., 114(4), 389-411.

Liao, S. S. C. and Whitman, R. V. (1986) "A Catalog Of Liquefaction And Non-Liquefaction Occurrences During Earthquakes," Research report excerpted from Ph.D. thesis by S. S. C. Liao titled "statistical modeling of earthquake-induced liquefaction," Dept. of Civil Engineering, MIT, Cambridge, MA, 117 pp.

Liu, H. and Qiao, T. (1984) "Liquefaction Potential Of Saturated Sand Deposits Underlying Foundation Of Structure," Proc. Eighth World Conf. on Earthquake Engineering, EERI, Vol. III, 199-206.

Loertscher, T. W. (1994) "Magnitude Scaling Factors For Analysis Of Liquefaction Hazard," Dissertation Presented to the Department of Civil Engineering, Brigham Young University, In Partial Fulfillment of the Requirements for the Degree of Doctor of Philosophy, 136 p.

Loertscher, T. W. and Youd, T. L. (1994) "Magnitude Scaling Factors For Analysis Of Liquefaction," in: Proc. From The Fifth US-Japan Workshop On Earthquake Resistant

Design Of Lifeline Facilities And Countermeasures Against Soil Liquefaction, O'Rourke and Hamada (eds.), NCEER-94-0026, 703-715.

Marcuson, W. R. and Bieganousky, W. A. (1977) "SPT And Relative Density In Coarse Sands," JGENDZ, ASCE, 103(GT11), 1295-1309.

Martin, G. R., Finn, W. D. L. and Seed, H. B. (1975) "Fundamentals Of Liquefaction Under Cyclic Loading," JGENDZ, ASCE, 101(5), 423-438.

Martin, G. R., Finn, W. D. L. and Seed, H. B. (1978) "Effects Of System Compliance On Liquefaction Tests," JGENDZ, ASCE, 101(5), 423-438.

Martin, J. R, and Clough, G. W. (1990) "Implications From A Geotechnical Investigation Of Liquefaction Phenomena Associated With Seismic Events In The Charleston, SC Area," U.S. Geological Survey, Reston, VA.

Martin, J. R. and Clough, G. W. (1994) "Seismic Parameters From Liquefaction Evidence," JGENDZ, ASCE, 120(8), 1345-1361.

Martin, J. R. and Fragaszy, R. J. (1994) "Soil Failure/Liquefaction Susceptibility Analysis For North Anna Power Station (NAPS) -- Seismic Margin Assessment," Report submitted to Virginia Power Company, Glen Allen, Virginia.

McGuire, R. K. (1984) "Ground Motion Estimation In Regions With Few Data," EERI, Eighth World Conf. on Earthquake Engineering, Vol. II, 327-334.

Meier, L. S. (1993) "The Susceptibility Of A Gravelly Soil Site To Liquefaction," Report Submitted to Virginia Polytechnic Institute and State University, in partial fulfillment of the Master of Science in Civil Engineering Degree, 74 p.

Metzger, A. G., (1995) Personal communication

Metzger, A. G., (1996) "'New' Historical Earthquakes In The New Madrid Seismic Zone," (abstract) Seism. Soc. Am, Seism. Res. Letters, 67(2), p. 47.

Mitchell, J. K. and Solymar, Z. V. (1984) "Time Dependent Strength Gain In Freshly Deposited Or Densified Sand," JGENDZ, ASCE, 110(11), 1559-1576.

Moore, B. H., and Hempen, G. L. (1982) "Exploration Innovations At Locks And Dam No. 26," U.S. Army Corps of Engineers, St. Louis, MO District, 18 p.

Munson, P. J. (1994) personal communication.

Munson, P. J. and Munson, C. A. (1996) "Paleoliquefaction Evidence For Recurrent Strong Earthquakes Since 20,000 Years BP In The Wabash Valley Area Of Indiana," Dept. of Anthropology, Indiana University, Bloomington, IN, 137 pp.

Munson, P. J., Munson, C. A. and Pond, E. C. (1995) "Paleoliquefaction Evidence For Strong Earthquake Shaking in South-Central Indiana," Geology, 23(4), 325-328.

Nemat-Nasser, S. and Shokooh, A. (1979) "A Unified Approach To Densification And Liquefaction Of Cohesionless Sand In Cyclic Shearing," Can. Geotech. J., Vol. 16, 659-678.

NRC (National Research Council), (1985) "Liquefaction Of Soils During Earthquakes," Nat'l Academy of Sciences, Committee on Earthquake Engrg., Report No. CETS-EE-001, 240 pp.

Nuttli, O. W. (1973) "Seismic Wave Attenuation And Magnitude Relations For Eastern North America," Am. Geophys. Union, J. Geophys. Res., 78(5), 876-885.

Nuttli, O. W. (1979) "Seismicity Of The Central United States," in: Reviews in Engineering Geology, Vol. IV, Geol. Soc. Am., 67-93.

Nuttli, O. W. (1982) "Damaging Earthquakes Of The Central Mississippi Valley," in Investigations of the New Madrid, Missouri Earthquake Region, U.S. Geological Survey Prof. Paper 1236-B, pp. 15-20.

Nuttli, O. W. and Herrmann, R. B. (1984) "Ground Motion Of Mississippi Valley Earthquakes," J. of Tech. Topics, ASCE, 110(1), 54-69.

Obermeier, S. F. (1993) "Paleoliquefaction Features As Indicators Of Potential Earthquake Activity In The Southeastern And Central United States," National Research Council, Transportation Research Record 1411, 42-52.

Obermeier, S. F. (1995) "Using Liquefaction-Induced Features For Paleoseismic Analysis," U.S. Geological Survey Open-File Report 94-663A,

Obermeier, S. F. (1996) Written personal communication.

Obermeier, S. F., Bleuer, N. R., Munson, P. J., Munson, C. A., Martin, S. M., McWilliams, K. M., Tabaozynski, D. A., Rubin, M. and Eggert, D. L. (1991) "Prehistoric Liquefaction Features Indicate Strong Shaking In The Lower Wabash Valley," Science, 251, 1061-1063.

Obermeier, S. F., Jacobson, R. B., Smoot, J. P., Weems, R. E., Gohn, G. S., Monroe, J. E. and Powars, D. S. (1990) "Earthquake-Induced Liquefaction Features In The Coastal Setting Of South Carolina And In The Fluvial Setting Of The New Madrid Seismic Zone," U.S. Geological Survey Prof. Paper 1504, 44 pp.

Obermeier, S. F., Martin, J. R., Frankel, A. D., Youd, T. L., Munson, P. J., Munson, C. A., and Pond, E. C. (1993). "Liquefaction Evidence For One Or More Strong Holocene Earthquakes In The Wabash Valley Of Southern Indiana And Illinois, With A Preliminary Estimate Of Magnitude," U.S. Geological Survey Prof. Paper 1536, 27 pp.

O'Rourke, T. D., Gowdy, T. E., Stewart, H. E. and Pease, J. W. (1991) "Lifeline Performance And Ground Deformation In The Marina During 1989 Loma Prieta Earthquake," in: Proc., 3rd US-Japan Workshop on Earthquake Resistant Design of

Lifeline Facilities and Countermeasures For Soil Liquefaction, (O'Rourke and Hamada, eds.), NCEER-91-0001, 129-146.

Park, T. K. and Silver, M. L. (1975) "Dynamic Triaxial And Simple Shear Behavior Of Sands," JGENDZ, ASCE, 101(GT6), 513-530.

Peck, R. B. (1979) "Liquefaction Potential: Science vs. Practice," JGENDZ, ASCE, 105(GT3), 393-398.

Peck, R. B., Hanson, W. E., and Thornburn, T. H. (1974) "Foundation Engineering," John Wiley and Sons, publ., New York, NY, 514 p.

Plummer, C. C. and McGeary, D. (1993) "Physical Geology," (6th ed.), Dubuque, IA, Wm. C. Brown Communications, Inc.

Poulos, S. J., Castro, G. and France, J. W. (1985) "Liquefaction Evaluation Procedure," JGENDZ, ASCE, 111(GT6), 393-398.

Reagor, G. and Brewer, L. R. (1987) "Preliminary Isoseismal Map And Intensity Distribution For The Southeastern Illinois Earthquake Of June 10, 1987," U.S. Geological Survey Open-File Report 87-578, 3 pp.

Robertson, P. K. and Campanella, R. G. (1985) "Liquefaction Potential Of Sands Using The CPT," JGENDZ, ASCE, 111(GT3), 384-403.

Robertson, P. K., Campanella, R. G. and Wightman, A. (1983) "SPT-CPT Correlations," JGENDZ, ASCE, 109(GT11), 1449-1459.

Schmertmann, J. H. (1991) "The Mechanical Aging Of Soils," JGENDZ, ASCE, 117(9), 1288-1330.

Schnabel, P. B., Lysmer, J. and Seed, H. B. (1972) "SHAKE, A Computer Program For Earthquake Response Analysis of Horizontally Layered Sites," EERC Report 72-12, Univ. of Calif., Berkeley.

Scott R. F. and Zuckerman, K. A. (1973) "Sandblows And Liquefaction," in: The Great Alaskan Earthquake Of 1964, Committee on the Alaskan Earthquake, National Research Council, Vol. 6, 179-189.

Scott, R. F. (1986) "Solidification And Consolidation Of A Liquefied Sand Column," Soils and Foundations, 26(4), 23-31.

Seed, H. B. (1979) "Soil Liquefaction And Cyclic Mobility Evaluation For Level Ground During Earthquakes," JGENDZ, ASCE, 105(GT2), 201-255.

Seed, H. B. (1987) "Design Problems In Soil Liquefaction," JGENDZ, ASCE, 113(8), 827-845.

Seed, H. B. and De Alba, P. (1986) "Use Of SPT And CPT Tests For Evaluating The Liquefaction Resistance Of Sands," Proc. In-Situ '86, (Clemence, S. P., ed.), ASCE, Geot. Spec. Publ. No. 6, Use of In-Situ Tests in Geotechnical Engineering, 281-302.

Seed, H. B. and Idriss, I. M. (1967) "Analysis Of Soil Liquefaction: Niigata Earthquake," JSMFD, ASCE, 93(SM3), 83-108.

Seed, H. B. and Idriss, I. M. (1971) "Simplified Procedure For Evaluating Soil Liquefaction Potential," JSMFD, ASCE, 79(SM9), 1249-1273.

Seed, H. B. and Idriss, I. M. (1982) "Ground Motions And Soil Liquefaction During Earthquakes," EERI Monograph, 134 pp.

Seed, H. B. and Lee, K. L. (1966) "Liquefaction Of Saturated Sands During Cyclic Loading," JSMFD, ASCE, 92(SM6), 105-136.

Seed, H. B. and Silver, M. L. (1972) "Settlement Of Dry Sands During Earthquakes," JSMFD, ASCE, 98(SM4), 381-397.

Seed, H. B. and Wilson, S. D. (1967) "The Turnagain Heights Landslide, Anchorage, Alaska," JSMFD, ASCE, 93(SM4), 325-353.

Seed, H. B., Idriss, I. M. and Arango, I. (1983) "Evaluation Of Liquefaction Potential Using Field Performance Data," JGENDZ, ASCE, 109(3), 458-482.

Seed, H. B., Tokimatsu, K., Harder, L. F., and Chung, R. M. (1985) "Influence Of SPT Procedures In Soil Liquefaction Resistance Evaluations," JGENDZ, ASCE, 111(12), 1425-1445.

Seed, H. B., Wong, R. T., Idriss, I. M. and Tokimatsu, K. (1986) "Moduli And Damping Factors For Dynamic Analyses Of Cohesionless Soils," JGENDZ, ASCE, 112(11), 1016-1032.

Sexton, J. L., Braile, L. W., Hinze, W. J., and Campbell, M. J. (1986) "Seismic Reflection Profiling Studies Of A Buried Precambrian Rift Beneath The Wabash Valley Fault Zone," Geophysics, 51(3), 640-660.

Shaver, R. H. (1979) "Geologic Story Of The Lower Wabash Valley With Emphasis On The New Harmony Area," Indiana Geological Survey, Occasional Paper No. 27, 14 p.

Siddiqi, F. H., Seed, R. B., Chan, K. C., Seed, H. B. and Pyke, R. M.. (1987) "Strength Evaluation Of Coarse-Grained Soils," UCB/EERC-87/22, Berkeley, CA, 53 pp.

Silver, M. L. and Seed, H. B. (1971a) " Deformation Characteristics Of Sands Under Cyclic Loading," JSMFD, 97(SM8), 1081-1098.

Silver, M. L. and Seed, H. B. (1971b) " Volume Changes In Sands During Cyclic Loading," JSMFD, 97(SM9), 1171-1182.

Silver, M. L., Chan, C. K., Ladd, R. S., Lee, K. L., Tiedemann, D. A., Townsend, F. C., Valera, J. E. and Wilson, J. H. (1976) "Cyclic Triaxial Strength Of Standard Test Sand," JGENDZ, ASCE, 103(GT6), 517-533.

Simcock, K. J., Davis, R. O., Berrill, J. B. and Mullenger, G. (1983) "Cyclic Triaxial Tests With Continuous Measurement Of Dissipated Energy," ASTM, Geotech. Test. J., 6(1), 35-39.

Skinner, B. J. and Porter, S. C. (1995) "The Dynamic Earth-An Introduction To Physical Geology," (3rd ed.) New York, NY, John Wiley and Sons, Inc.

Smith, N. D. (1985) "Proglacial Fluvial Environment," in: Glacial Sedimentary Environments (Ashley, Shaw, and Smith, eds.), SEPM Short Course No. 16, 85-134.

Somerville, P. G., McLaren, J. P., Saikai, C. K., and Helmberger, D. V. (1990) "The 25 November 1988 Saguenay, Quebec Earthquake: Source Parameters And The Attenuation Of Strong Ground Motions," BSSA, 80(5), 1118-1143.

Stokoe, K. H. and Nazarian, S. (1985) "Use Of Raleigh Waves In Liquefaction Studies," in Measurement and Use of Shear Wave Velocity for Evaluating Dynamic Soil Properties, R. D. Woods, ed., ASCE, pp. 1-17.

Stokoe, K. H., II, Andrus, R. D., Rix, G. J., Sanchez-Salinero, I., Sheu, J.-C. and Mok, Y.-J. (1988) "Field Investigation of gravelly soils which did and did not liquefy during the 1983 Borah Peak, Idaho, Earthquake," Geotechnical Engineering Report GR87-1, Geotechnical Engineering Center, Univ. of Texas at Austin, 206 pp.

Stokoe, K. H., Roesset, P.M., Bierschwale, J. G. and Aouad, M. (1988) "Liquefaction Potential Of Sands From Shear Wave Velocity," Proc. 9th World Conf. on Earthquake Engineering, Vol. III, 213-218.

Stokoe, K. H., Rix, G. J., Sanchez-Salinero, I., Andrus, R. D., Mok, Y. (1988) "Liquefaction Of Gravelly Soils During The 1983 Borah Peak, Idaho Earthquake," Proc. of the Ninth World Conf. on Earthquake Engrg., Vol. III, 183-189.

Stover, C. W. and Coffman, J. L. (1993) "Seismicity Of The United States, 1568-1989 (Revised)," U.S. Geological Survey Prof. Paper 1527, 418 pp.

Thornbury, W. D. (1950) "Glacial Sluiceways And Lacustrine Plains Of Southern Indiana," Indiana Geological Survey, Bulletin No. 4, 21p.

Tokimatsu, K. and Seed, H. B. (1987) "Evaluation Of Settlements In Sand Due To Earthquake Shaking," JGENDZ, ASCE, 113(8), 861-878.

Tokimatsu, K. and Yoshimi, Y. (1983) "Empirical Correlation Of Soil Liquefaction Based On SPT N-Value And Fines Content," Soils and Foundations, 23(4), 56-74.

Tuttle, M., Law, K. T., Seeber, L. and Jacob, K. (1990) "Liquefaction and Ground Failure Induced By The 1988 Saguenay, Quebec, Earthquake," Can. Geotech. J., 27(5), 580-589.

Valera, J. E., Traubenik, M., Egan, J. A. and Daneshiro, M. (1994) "A Practical Perspective On Liquefaction Of Gravels," in: Ground Failures Under Seismic

Conditions, S. Prakash and P. Dakoulas (eds.), Geotechnical Special Technical Publication No. 44, ASCE, 241-257.

Vucetic, M. and Dobry, R. (1991) "Effect Of Soil Placticity On Cyclic Response," ASCE, J. Geotech. Engrg., 117(1), 89-107.

Wakamatsu, K. (1992) "Liquefaction History, 416-1991, In Japan," in: Proc. 4th Japan-US Workshop on Earthquake Resist. Design of Lifeline Facilities and Countermeasures for Soil Liquefaction," NCEER-92-0019, Vol. 1, 97-114.

Whitman, R. V. and Lambe, P. C. (1986) " Effect Of Boundary Conditions Upon Centrifuge Experiments Using Ground Motion Simulation," Geotech. Testing J., ASTM, 9(2), p. 61.

Wong, R. T., Seed, H. B. and Chan, C. K. (1975) "Cyclic Loading Liquefaction Of Gravelly Soils," JGENDZ, ASCE, 101(GT6), 571-583.

Yegian, M. K., Ghagraman, V. G., and Gazetas, G. (1994) "Seismological, Soil And Valley Effects In Kirovakan, 1988 Armenia Earthquake," JGENDZ, ASCE, 120(2), 349-365.

Youd, T. L. (1970) "Densification And Shear Of Sand During Vibration," ASCE, JSMFD, 96(SM3), 863-880.

Youd, T. L. (1977) "Packing Changes and Liquefaction Susceptibility," ASCE, JGENDZ, 103(GT8), 918-922.

Youd, T. L. (1984) "Recurrence Of Liquefaction At The Same Site," Proc. Eighth World Conference on Earthquake Engineering, EERI, Vol. III, 231-238.

Youd, T. L. and Garris, C. T. (1995) "Liquefaction-Induced Ground Surface Disruption," J. Geotech. Engrg., ASCE, 121(11), 805-809.

Youd, T. L. and Holzer, T. L.. (1994) "Piezometer Performance At Wildlife Liquefaction Site, California," J. Geotech. Engrg., ASCE, 120(6), 975-995.

Youd, T. L. and Perkins, D. M. (1987) "Mapping Of Liquefaction Severity Index," J. Geotech. Engrg., ASCE, 113(11), 1374-1392.

Youd, T. L., Harp, E. L., Keefer, D. K. and Wilson, R. C. (1985) "The Borah Peak, Idaho Earthquake Of October 28,1983 - Liquefaction," Earthquake Spectra, 2(1), 71-89.

Youd, T. L., Perkins, D. M., and Turner, W. G. (1989) " Liquefaction Severity Index For The Eastern United States," in O'Rourke, T. D. and Hamada, M., eds., Proceedings from the Second U.S.-Japan Workshop on Liquefaction, Large Ground Deformation, and Their Effects on Lifelines: State University of New York at Buffalo, Technical Report NCEER-89-0032, p. 438-452.

Zeghal, M. and Elgamal, A.-W. (1994) Analysis Of Site Liquefaction Using Earthquake Records," ASCE, JGENDZ, 120(6), 996-1017.

Appendix A:

Example of Empirical Energy Intensity Approach to Estimating Surface Motions based on Paleoliquefaction Evidence

The primary technique used for liquefaction susceptibility analyses today is based on the observed field performance of liquefaction sites and is an outgrowth of the Seed and Idriss simplified procedure (1971). The procedure has been revised to provide a degree of standardization that allows the analysis to be applied over a wide range of conditions and has gained widespread acceptance for both its ease of application and the relatively inexpensive procedure utilized to obtain the necessary field data. The application of the analysis technique is outlined and explained by Seed and Idriss (1982), Seed et al. (1985) and Seed and DeAlba (1986).

This stress-based approach to liquefaction analysis provides an effective method for estimating the susceptibility of a soil deposit to liquefaction failure where the peak surface acceleration expected at a site is known or can be reasonably estimated. It is therefore possible to use this technique to determine susceptibility of a site to liquefaction-induced failures during future seismic events using surface motion estimates based on a knowledge of the tectonic environment and an appropriate attenuation relationship. In paleoliquefaction studies, however, it is the observed evidence of a prior liquefaction event that drives the desire to estimate surface motions, rather than the anticipation of a future liquefaction event. In these cases very little is known other than the soil strength parameters and an estimate of the distribution of liquefaction effects. The desired end result of this type of analysis is an estimate of the actual motions experienced rather than a conservative minimum value that would have been required to induce the liquefaction evidence seen.

The Seed and Idriss (1982) simplified approach to liquefaction susceptibility provides the threshold value of liquefaction susceptibility. This threshold boundary was designed to provide assurance that liquefaction would not likely occur during a future seismic event. Using this approach in a paleoliquefaction study predicts the minimum cyclic stress ratio required to induce liquefaction for a given blowcount. Where liquefaction evidence has been observed, this allows an approximate minimum estimate of

the surface motions to be made. Without more information, however, surface motion estimates can be based only on the minimum blowcount in the soil profile, and therefore provides only an absolute minimum estimate of the ground motions that would have been experienced at a site. It is desirable, therefore, to be able to estimate the liquefied thickness of the soil profile using an alternative procedure that will in turn allow an improved estimate of the peak surface motions. The seismic energy intensity approach outlined here allows this type of analysis.

The computational procedure outlined here provides a method for finding a "best" estimate of the peak ground surface acceleration associated with paleoliquefaction evidence at sites experiencing lateral spreading failure. The analysis presented is provided as an example of the technique based on the energy intensity approach outlined in Chapter 6. This example provided here will be applied to a single study site, which when combined with results from a representative number of sites for a given earthquake, can be used to refine the magnitude estimate associated with a paleo-earthquake, and to estimate ground motion attenuation characteristics for the region in which it occurred. In Chapter 6 this technique was used with the Wabash Valley paleoliquefaction evidence as the basis to verify and refine magnitude estimates determined based on both the maximum extent of liquefaction evidence, and the minimum magnitude required to induce liquefaction at all sites associated with a specific event.

The application of the technique in a paleoliquefaction study involves eight basic steps. These are: 1.) Determine a preliminary magnitude estimate based on associated evidence such as maximum distance to liquefaction effects. Alternatively, an educated guess may be appropriate, but will likely require a greater number of trial calculations in order to refine the magnitude estimate. 2.) At each sample interval in the soil profile determine the threshold cyclic stress ratio required to produce liquefaction evidence based on the preliminary magnitude estimate. This value is determined based on a stress-based approach to threshold liquefaction prediction. 3.) Back-calculate individual peak ground

surface acceleration estimates associated with the cyclic stress ratio found for each of the sample locations. This calculation is performed using the relationship presented by Seed and Idriss (1971) which relates cyclic stress ratio to peak surface acceleration. 4.) For each individual paleoliquefaction site, estimate the average blowcount value involved in the liquefaction event using the seismic energy intensity function and the liquefaction suppression boundary. 5.) Find the thickness of the liquefied soil profile as that where the average corrected blowcount value is equal to the liquefaction suppression blowcount (N_c) predicted by the energy intensity function. 6.) The peak acceleration representative of a specific boring location is the average of the values required to induce liquefaction at each of the individual sample intervals making up the predicted liquefied layer thickness. 7.) The peak acceleration representative of a specific site can be taken as the value from the boring location where the average blowcount most closely matches, but does not exceed, the average blowcount value predicted to be involved in the liquefaction evidence. 8.) The magnitude estimate is then refined and the analysis performed for the new magnitude. This procedure is repeated until the magnitude estimate is shown to provide peak acceleration estimates for all study sites that most nearly match the accelerations for those sites predicted by local attenuation relationships.

Steps 1 through 3 of this procedure are straight forward and have been thoroughly reviewed previously. They will be only briefly mentioned here. The portions of this computation that differ from traditional liquefaction susceptibility analyses are contained in steps 4 through 8. These steps will be illustrated using an example site associated with the 6000 year BP Vincennes earthquake. The soil profile used for this example is that found at site HA. The site location is indicated on Figure 3.4 and a site plan with a site vicinity map is given in Figure 5.17. The modern soil profile at the site is shown in Figure 5.18. The boring logs for the site are included in Appendix B, with the logs for each of the sites associated with the Vincennes event. The logs are arranged alphabetically by site name and chronologically by boring number.

The energy intensity approach presented here is analogous to the Seed et al. stress-based approach except that the ground motion parameter used to identify liquefaction susceptibility is related to the earthquake itself rather than to the site-specific surface motions that are produced. A seismic energy intensity function is used to predict the in-situ corrected SPT blowcount value required to suppress the occurrence of liquefaction at a given site distance experiencing a specified magnitude event. This approach can be applied to future liquefaction susceptibility in exactly the same manner as using the cyclic stress ratio with the Seed et al. liquefaction prediction boundary. The boundary here, however, predicts blowcount based solely on magnitude and distance. This prediction boundary is shown in Figure A.1. Due to the nature of the seismic energy intensity function, the suppression boundary is plotted on a log-log scale, rather than the linear scale used for the stress-based approach. This boundary is based on recorded occurrences and non-occurrences of liquefaction evidence. The location was determined in a manner similar to the procedure used to locate the Seed et al. prediction boundary.

The seismic energy intensity function, T, is defined as:

$$\mathbf{T} = 10^{1.5\mathbf{M}}/\mathbf{R}^2 ;$$

where M is moment magnitude and R is hypocentral distance in km. This value of T is then used with the liquefaction suppression boundary shown in figure A.1 to estimate the average value of the in-situ blowcount that will have been involved in a paleoliquefaction event. The boundary curve shown can be represented mathematically to predict N_ℓ as:

$$\left[(N_1)_{60}\right]_\ell = \left[\frac{T}{1.445}\right]^{0.165}$$

By evaluating this function for a given site distance and magnitude, it is possible to predict the average value of blowcount involved in producing the liquefaction evidence observed at paleoliquefaction sites. The reason this represents an average blowcount value rather than an upper bound is reviewed in chapter 6.

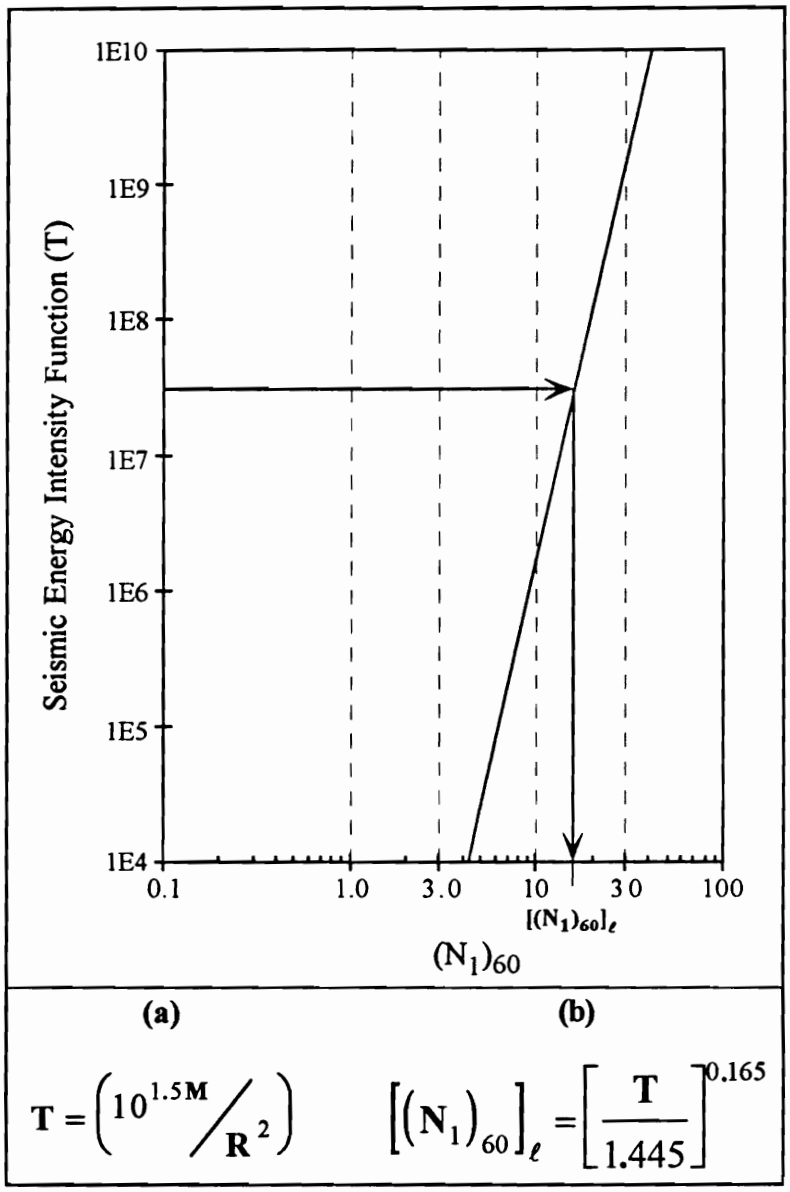

Figure A.1. Prediction of blowcount required to suppress liquefaction at site HA (R=75km) when subjected to a M7.5 earthquake. (a) is used to determine energy intensity and (b) predicts a liquefaction suppression blowcount.

In order to use this procedure to estimate a liquefaction suppression blowcount value, it is required that a preliminary estimate of magnitude be made. This can be based on a relationship such as that of Ambraseys (1988), as shown in Figure 6.6. Alternatively, the magnitude contours of Figures 6.13 through 6.16 can be used to estimate a minimum magnitude based on the minimum blowcount values from all sites associated with a given event. These contours can be used for the Class C soil site conditions (180m/s < V_s < 360 m/s in the upper 30 m) as defined by Boore et al. (1993). The Class C soil site condition is typical of sites subject to lateral spreading (see Youd and Perkins, 1987). These magnitude contours apply to any tectonic environment within the epicentral distance range subject to liquefaction effects. Within this distance range the attenuation characteristics are similar in all environments for the given soil site condition assumption (see Figure 6.12). The preliminary magnitude estimate made here then provides a starting point for the remainder of the analysis. The example of the remainder of the procedure is presented below for Wabash Valley site HA.

The soil profile estimated to have been present at site HA at the time of the earthquake is shown in Figure A.2. The corrected blowcount values, $(N_1)_{60}$, are indicated on the figure for the depth range sampled within the liquefiable soil deposit at this site. These blowcount values have been corrected from the measured blowcounts based on the modern soil profile and water table elevation. An initial magnitude estimate of M7.8 has been made for this event based on the maximum epicentral distance to surface evidence of liquefaction effects (see Figure 6.6). A summary of the results of the calculations performed for this analysis are presented in Table A.1 and are described below.

Based on the preliminary magnitude estimate, peak surface acceleration values are estimated at each sample interval within the liquefiable deposit. Cyclic stress ratios are first determined based on the in-situ blowcount value at each sample interval. These values are calculated based on the Loertscher and Youd (1994) representation of the Seed

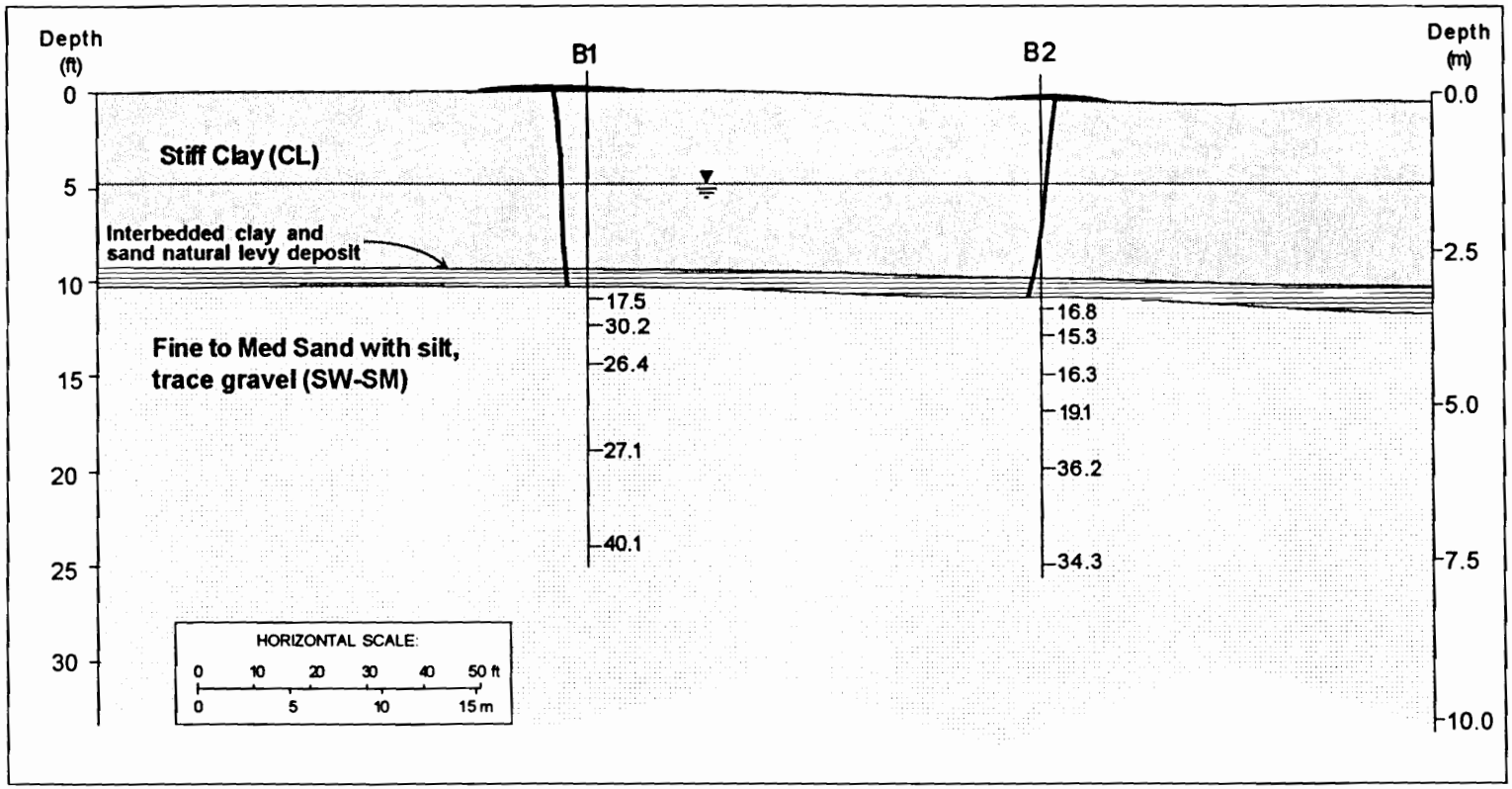

Figure A.2. Soil profile for site HA at time of earthquake. See Figure 5.18. for modern profile. Blowcounts indicated are $(N_1)_{60}$ values.

Table A.1. Liquefied thickness calculation for site HA experiencing a M7.8 Vincennes event

Site: **HA**

M = 7.8

$(N_1)_{60}$ < 19.2

Boring #	Cap (ft)	Best Est. Water Table Depth in ft. (range)		
1	10.5	4.75	0.25	10.5
2	11	4.5	0	10.25

Boring #: 1

layer thickness	Depth Below Cap	Total Depth	$(N_1)_{60}$	a (best)	a (min)	a (max)
1.25	0.5	11	**17.5**	**0.15**	0.11	0.22
3.00	2.0	12.5	30.2	0.44	0.33	0.60
6.25	4.0	14.5	26.4	0.31	0.24	0.40
11.00	8.5	19	27.1	0.31	0.26	0.39
6.75	13.5	24	40.1	0.94	0.80	1.12
1.3	<--liquefied	N_{avg}-->	**17.50**	**0.15**	0.11	0.22

Boring #: 2

layer thickness	Depth Below Cap	Total Depth	$(N_1)_{60}$	a (best)	a (min)	a (max)
1.25	0.5	11.5	**16.8**	**0.14**	0.10	0.20
1.75	2.0	13	**15.3**	**0.12**	0.09	0.16
2.00	4.0	15	**16.3**	**0.13**	0.10	0.17
2.50	6.0	17	**19.1**	**0.16**	0.13	0.20
4.00	9.0	20	36.2	0.67	0.56	0.83
5.00	14.0	25	34.3	0.56	0.48	0.67
7.5	<--liquefied	N_{avg}-->	**16.88**	**0.14**	0.10	0.18

et al. (1985) liquefaction prediction boundary. The form of their equation for cyclic stress ratio used here is:

$$\mathbf{CSR} = exp^{\left[-7.4 + 30.826/\mathbf{M} + 0.0851(\mathbf{N}_1)_{60}\right]}.$$

The value of cyclic stress ratio found from this prediction is then used with the Seed and Idriss (1982) relationship between cyclic stress ratio and peak surface acceleration to back-calculate the threshold acceleration required to induce liquefaction at each sample interval through the soil profile. This relationship, rearranged to estimate peak acceleration, is:

$$\frac{\mathbf{a_p}}{\mathbf{g}} = \frac{\mathbf{CSR} \cdot \sigma'_o}{0.65 \cdot \mathbf{r_d} \cdot \sigma_o}.$$

where $\mathbf{r_d}$ is the stress reduction factor to account for the fact that the soil column does not act as a truly rigid column, σ_o and σ'_o are the total and effective stress conditions at the sample depth, $\mathbf{a_p}$ is peak surface acceleration, and **g** is acceleration due to gravity.

As a means to illustrate the effect of possible variations in the water table elevation at the time of the earthquake, the minimum and maximum values of peak acceleration have also been included here. This maximum range is based on the possibility of the water table elevation varying between the ground surface and the top of the liquefiable soil. This is considered the maximum possible range for two reasons. First, the water table must have been below the ground surface at the time of the event or the vented sand observed at the blow surface would have tended to have been carried away or dispersed by the flood waters. Second, the water table also must have been above the top of the source soils or liquefaction evidence would have been suppressed by the presence of the unsaturated material at the top of the deposit.

It can be seen that the peak acceleration estimate shown in Table A.1 will vary by approximately ± 0.05g for the maximum range of water table conditions at this site. This

site contains one of the greatest cap thicknesses, however, and by relating this site to other sites in the region, the actual uncertainty in the water table elevation becomes much smaller. The techniques used to estimate refined limits on the potential water table elevation were introduced in Chapter 6 and are reviewed further below. The maximum values shown here are included as an illustration of the importance of refining the estimated water table location for paleoliquefaction studies. Based on regional water table characteristics, local site conditions, and stratigraphic relationships, it is felt that the actual maximum variation in the water table elevation is on the order of ± one to two feet rather than the five feet or more shown for this example. When the range in water table elevations is reduced to this level, even with a liberal estimate of the likely variation in the water table fluctuation, the uncertainty in the acceleration estimate is reduced to ± 0.02g. The maximum range will be maintained, however, for the remainder of this example for the sake of illustration.

When peak acceleration estimates have been made for each of the sample intervals within the liquefied deposit, the predicted blowcount found from the energy intensity function can be used to find the peak acceleration that would have been experienced at the site to induce the liquefaction evidence. For a **M**7.8 event at site HA (R=75.7km), the liquefaction suppression blowcount will be N_ℓ = 19.2. By comparing this value with the blowcount values through the soil profile it is possible to estimate a liquefied thickness as that where the average of the blowcount values approaches, but does not exceed this value. Examining the data in Table A.1 it can be seen that in boring B1, liquefaction is indicated for the uppermost sample only. In boring B2, the liquefaction prediction extends through four samples. A "best" estimate of the peak surface motion at this site due to a **M**7.8 Vincennes earthquake can be taken as the average of the values of acceleration predicted at each of the sample intervals in the two borings. The liquefied blowcount value in boring B1 most closely matches that of the prediction, and therefore the peak surface acceleration estimate is taken as $\mathbf{a}_p$ = 0.15g. The liquefied layer thickness is

indicated as the sum of the thicknesses of the layers associated with each sample interval predicted to be involved in the liquefaction.

This estimate of the peak surface motion assumes that the magnitude estimate is correct. By estimating the surface motion associated with other magnitudes it is possible to verify or refine this estimate. This has been done for this example in the same manner as shown in Table A.1 for three other magnitudes: **M**7.2, **M**7.5, and **M**8.0. The results for these magnitudes are presented in Tables A.2 through A.4 and are then presented graphically in Figure A.3. Figure A.3 presents the estimated surface motions required to induce liquefaction effects throughout the predicted liquefied thickness compared to the peak acceleration predicted by the Wabash Valley attenuation relationship.

The "best" estimate, as well as the maximum possible variation based on water table elevations are shown. Based on the "best" estimate curve, a **M**7.8 event is shown to provide good agreement between the two prediction techniques. Figure A.3 clearly illustrates the importance of having a well defined distribution of liquefaction sites associated with a given event when trying to estimate motions associated with paleoliquefaction evidence. The range of magnitudes and accelerations over which the "best" estimate and the attenuation predictions agree is very small, however, a small fluctuation in the water table elevation can have a significant impact on this result.

It can be seen here that if the estimated water table elevation is lowered, the site is predicted to not be susceptible to liquefaction at any magnitude. The in-situ stresses are increased significantly and greater accelerations are required to induce liquefaction. At the maximum water table depth, the two predictions do not intersect, and therefore liquefaction should not have occurred. Conversely, a higher water table would allow liquefaction to occur over a much greater range of magnitudes. This underscores the need to have a variety of sites in order to allow reasonable estimates of magnitude and peak ground motions to be made.

Table A.2. Liquefied thickness calculation for site HA experiencing a M7.2 Vincennes event

Site: **HA**

M = 7.2

$(N_1)_{60}$ < 13.7

Boring #	Cap (ft)	Best Est. Water Table Depth in ft. (range)		
1	10.5	4.75	0.25	10.5
2	11	4.5	0	10.25

Boring #: B1

layer thickness	Depth Below Cap	Total Depth	$(N_1)_{60}$	a (best)	a (min)	a (max)
1.25	0.5	11	**17.5**	**0.21**	0.15	0.30
3.00	2.0	12.5	30.2	0.61	0.45	0.83
6.25	4.0	14.5	26.4	0.43	0.33	0.56
11.00	8.5	19	27.1	0.44	0.36	0.54
6.75	13.5	24	40.1	1.30	1.11	1.55
1.3	<--liquefied	N_{avg}--->	**17.50**	**0.21**	0.15	0.30

Boring #: B2

layer thickness	Depth Below Cap	Total Depth	$(N_1)_{60}$	a (best)	a (min)	a (max)
1.25	0.5	11.5	16.8	0.20	0.14	0.27
1.75	2.0	13	**15.3**	**0.17**	0.12	0.23
2.00	4.0	15	16.3	0.18	0.14	0.23
2.50	6.0	17	19.1	0.22	0.18	0.28
4.00	9.0	20	36.2	0.94	0.77	1.15
5.00	14.0	25	34.3	0.78	0.67	0.93
1.8	<--liquefied	N_{avg}-->	**15.30**	**0.17**	0.12	0.23

Table A.3 Liquefied thickness calculation for site HA experiencing a M7.5 Vincennes event

Site: **HA**

M = 7.5

$(N_1)_{60}$ < 16.2

Boring #	Cap (ft)	Best Est. Water Table Depth in ft. (range)		
1	10.5	4.75	0.25	10.5
2	11	4.5	0	10.25

Boring #: 1

layer thickness	Depth Below Cap	Total Depth	$(N_1)_{60}$	a (best)	a (min)	a (max)
1.25	0.5	11	**17.5**	**0.18**	0.13	0.25
3.00	2.0	12.5	30.2	0.52	0.38	0.70
6.25	4.0	14.5	26.4	0.36	0.28	0.47
11.00	8.5	19	27.1	0.37	0.30	0.46
6.75	13.5	24	40.1	1.10	0.94	1.31
1.3	<--liquefied	Navg-->	**17.50**	**0.18**	0.13	0.25

Boring #: 2

layer thickness	Depth Below Cap	Total Depth	$(N_1)_{60}$	a (best)	a (min)	a (max)
1.25	0.5	11.5	**16.8**	**0.16**	0.12	0.23
1.75	2.0	13	**15.3**	**0.14**	0.10	0.19
2.00	4.0	15	**16.3**	**0.15**	0.12	0.20
2.50	6.0	17	19.1	0.19	0.15	0.24
4.00	9.0	20	36.2	0.79	0.65	0.97
5.00	14.0	25	34.3	0.66	0.57	0.79
5.0	<--liquefied	N_{avg}-->	**16.13**	**0.15**	0.11	0.21

Table A.4 Liquefied thickness calculation for site HA experiencing a M8.0 event

Site: **HA**

M = 8.0

$(N_1)_{60}$ < 21.5

Boring #	Cap (ft)	Best Est. Water Table Depth in ft. (range)		
1	10.5	4.75	0.25	10.5
2	11	4.5	0	10.25

Boring #: 1

layer thickness	Depth Below Cap	Total Depth	$(N_1)_{60}$	a (best)	a (min)	a (max)
1.25	0.5	11	**17.5**	**0.14**	0.10	0.20
3.00	2.0	12.5	30.2	0.40	0.29	0.54
6.25	4.0	14.5	26.4	0.28	0.22	0.37
11.00	8.5	19	27.1	0.28	0.23	0.35
6.75	13.5	24	40.1	0.85	0.72	1.01
1.3	<--liquefied	N_{avg}-->	**17.50**	**0.14**	0.10	0.20

Boring #: 2

layer thickness	Depth Below Cap	Total Depth	$(N_1)_{60}$	a (best)	a (min)	a (max)
1.25	0.5	11.5	**16.8**	**0.13**	0.09	0.18
1.75	2.0	13	**15.3**	**0.11**	0.08	0.15
2.00	4.0	15	**16.3**	**0.12**	0.09	0.15
2.50	6.0	17	**19.1**	**0.14**	0.11	0.18
4.00	9.0	20	**36.2**	**0.61**	0.50	0.75
5.00	14.0	25	34.3	0.51	0.44	0.61
11.5	<--liquefied	N_{avg}-->	**20.74**	**0.22**	0.18	0.28

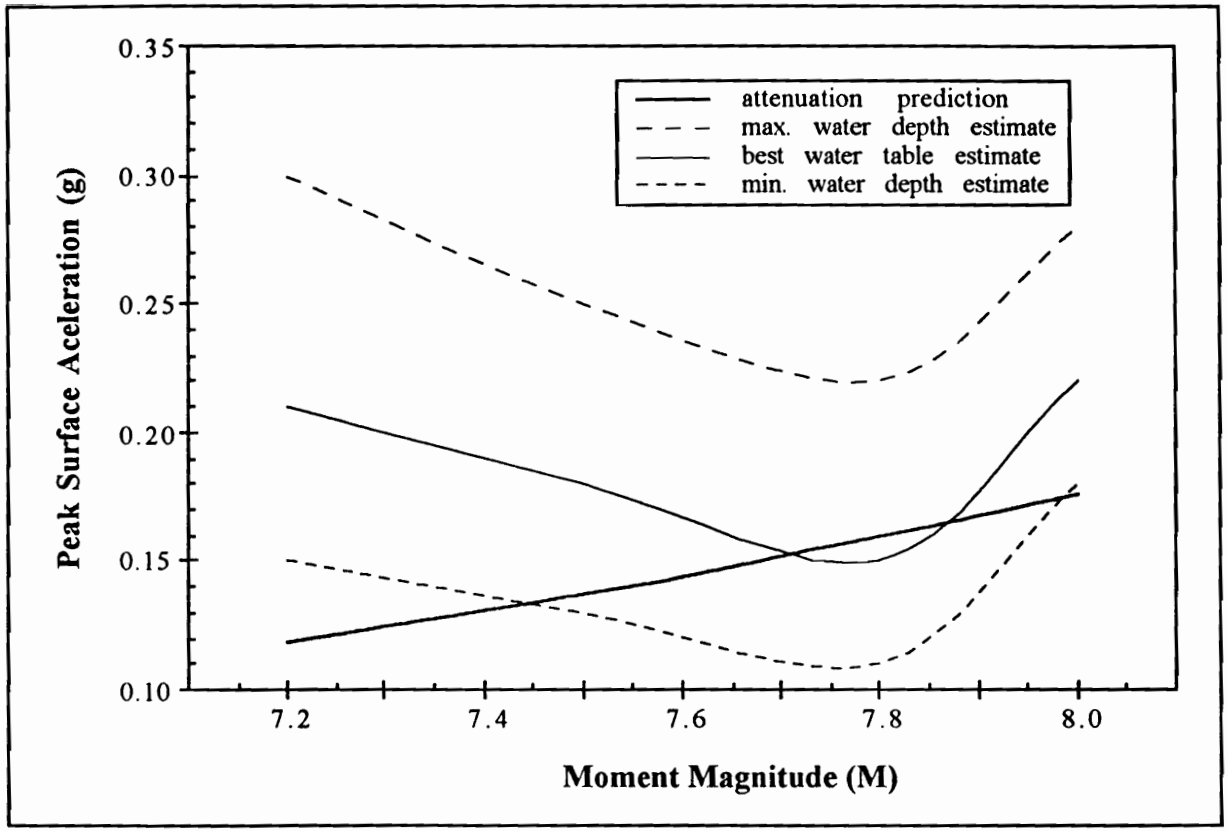

Figure A.3. Peak surface acceleration prediction based on energy intensity approach compared to the prediction of surface acceleration for site HA based on a CUS attenuation relationship.

Where paleoliquefaction sites have been identified over a reasonable distribution and have been associated with a given event, it is possible, however, to estimate seismic parameters based on the paleoliquefaction evidence with reasonable reliability. As noted previously, the possible variation in the water table elevation can be reduced based on the stratigraphic relationship between sites, and an assumption of relatively consistent regional water table elevations. Lateral spreading typically occurs near a river, and river levels and water table elevations are directly linked. Barring local thunderstorms or other flood-inducing events, this is therefore a reasonable assumption. Local site conditions can be used to estimate constraints on possible water table elevations that can then be extended to other locations based on stratigraphic relationships.

Once a reasonable range in the water table elevations has been estimated, the comparison of surface motion estimates for all paleoliquefaction sites associated with a given event, together with a regional attenuation relationship will tend to further reduce the uncertainty that will be associated with using a limited number of sites. Figures 6.22 through 6.25 show the results for each of the four earthquakes investigated for this study. It can be seen from these figures that as the magnitude estimate varies from a "best" estimate, the variation among sites increases. Additionally, the individual site estimates will diverge from the motions predicted based on the regional attenuation relationship. The result of the analysis is that a refined magnitude estimate can be obtained that is quite reliable. It is estimated that the resulting magnitude estimate is representative of the actual magnitude to within ± 0.25 to 0.5 magnitude units.

The energy intensity approach has been found to reliably predict the occurrence of liquefaction effects associated with historical earthquakes based on magnitude and distance alone. This technique has been extended here to provide a simple method to predict the liquefied thickness of a soil deposit at paleoliquefaction sites. This allows a "best" estimate of the surface motions associated with the causative event to be made for a

given site. This technique can be used to refine the magnitude estimate and estimate attenuation characteristics when a reasonable distribution of associated sites is available.

Appendix B:

Vincennes Event Boring Logs

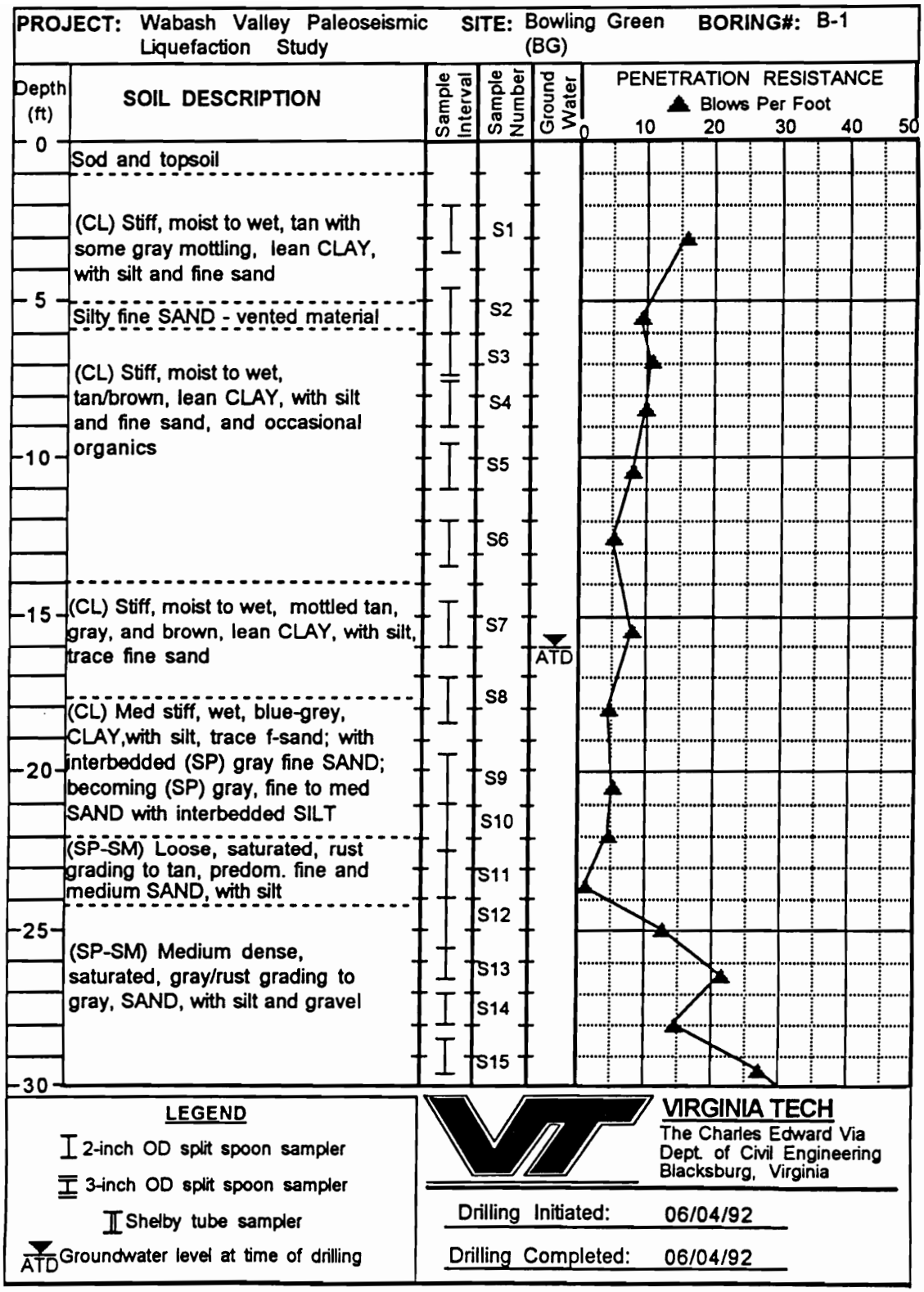
PROJECT: Wabash Valley Paleoseismic Liquefaction Study
SITE: Bowling Green (BG)
BORING#: B-1
Depth (ft)
SOIL DESCRIPTION
Sample Interval
Sample Number
Ground Water
PENETRATION RESISTANCE
Blows Per Foot
0
10
20
30
40
50
0
Sod and topsoil
(CL) Stiff, moist to wet, tan with some gray mottling, lean CLAY, with silt and fine sand
Silty fine SAND - vented material
(CL) Stiff, moist to wet, tan/brown, lean CLAY, with silt and fine sand, and occasional organics
(CL) Stiff, moist to wet, mottled tan, gray, and brown, lean CLAY, with silt, trace fine sand
(CL) Med stiff, wet, blue-grey, CLAY,with silt, trace f-sand; with interbedded (SP) gray fine SAND; becoming (SP) gray, fine to med SAND with interbedded SILT
(SP-SM) Loose, saturated, rust grading to tan, predom. fine and medium SAND, with silt
(SP-SM) Medium dense, saturated, gray/rust grading to gray, SAND, with silt and gravel
S1
S2
S3
S4
S5
S6
S7
S8
S9
S10
S11
S12
S13
S14
S15
ATD
5
10
15
20
25
30
LEGEND
2-inch OD split spoon sampler
3-inch OD split spoon sampler
Shelby tube sampler
ATD Groundwater level at time of drilling
VIRGINIA TECH
The Charles Edward Via Dept. of Civil Engineering Blacksburg, Virginia
Drilling Initiated: 06/04/92
Drilling Completed: 06/04/92

PROJECT: Wabash Valley Paleoseismic Liquefaction Study **SITE:** Bowling Green (BG) **BORING#:** B-1 (cont'd)

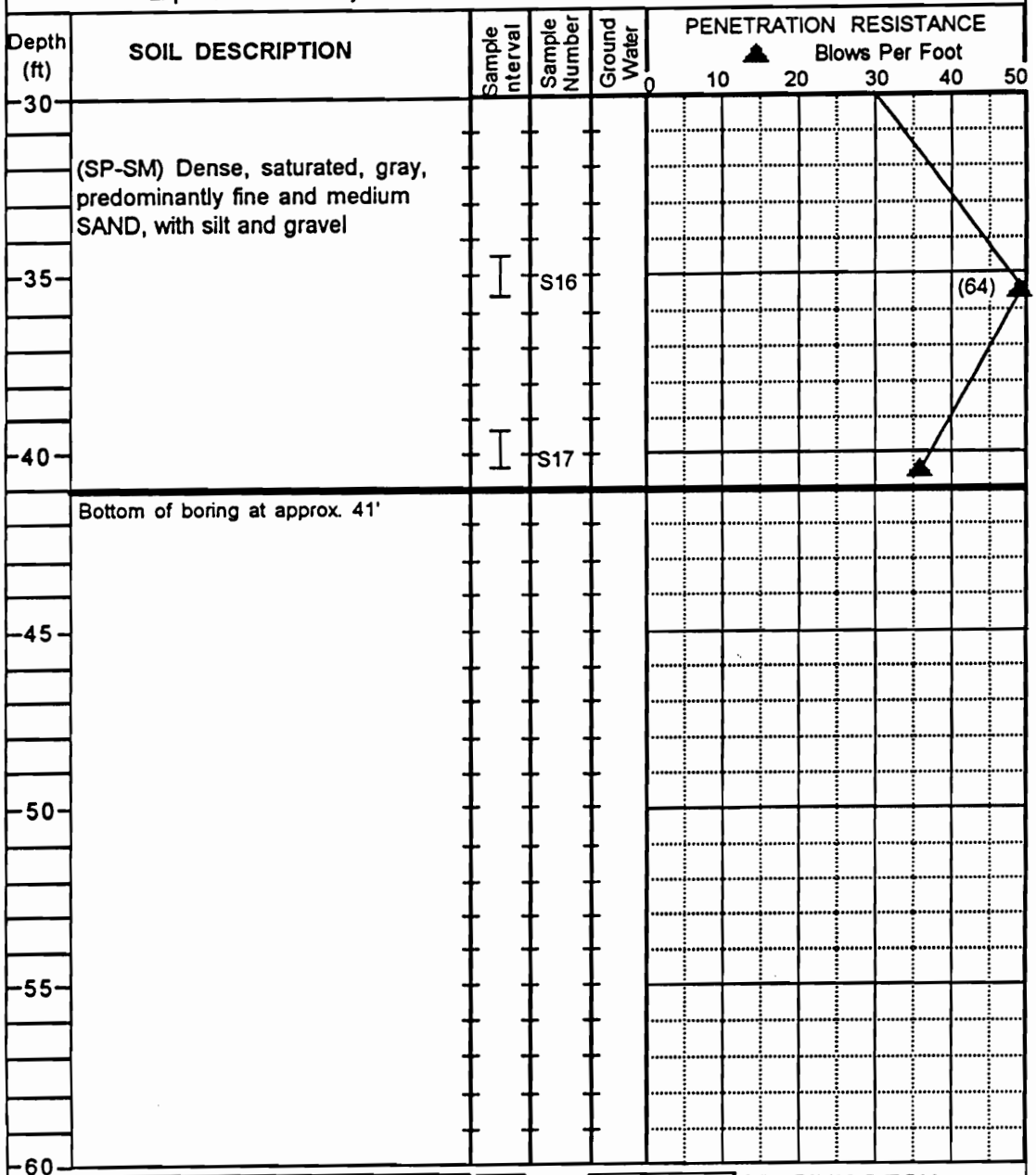

LEGEND

- 2-inch OD split spoon sampler
- 3-inch OD split spoon sampler
- Shelby tube sampler
- ATD Groundwater level at time of drilling

VIRGINIA TECH
The Charles Edward Via
Dept. of Civil Engineering
Blacksburg, Virginia

Drilling Initiated: 06/04/92

Drilling Completed: 06/04/92

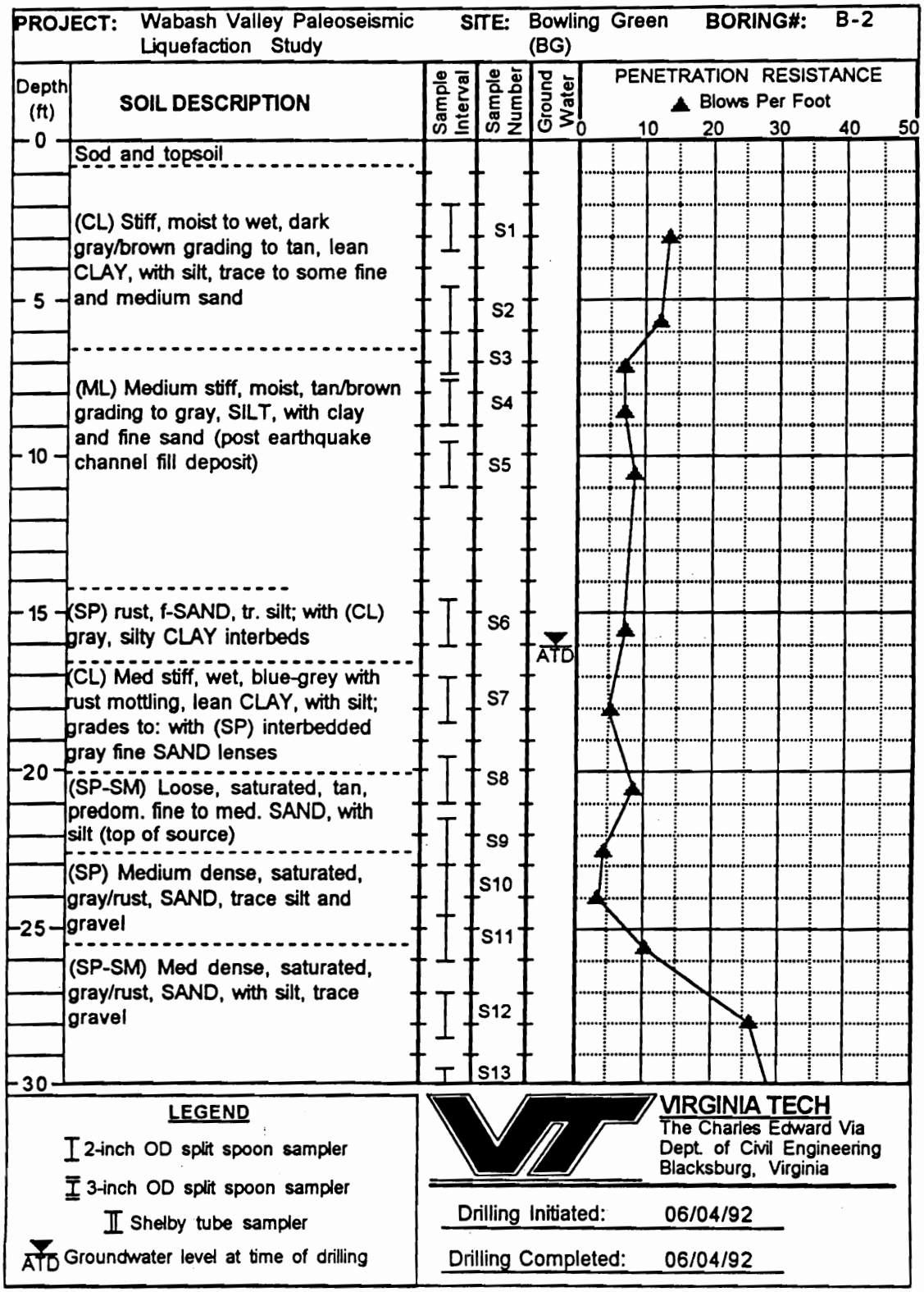
PROJECT: Wabash Valley Paleoseismic Liquefaction Study
SITE: Bowling Green (BG)
BORING#: B-2
Depth (ft)
SOIL DESCRIPTION
Sample Interval
Sample Number
Ground Water
PENETRATION RESISTANCE
Blows Per Foot
0
10
20
30
40
50
0
5
10
15
20
25
30
Sod and topsoil
(CL) Stiff, moist to wet, dark gray/brown grading to tan, lean CLAY, with silt, trace to some fine and medium sand
(ML) Medium stiff, moist, tan/brown grading to gray, SILT, with clay and fine sand (post earthquake channel fill deposit)
(SP) rust, f-SAND, tr. silt; with (CL) gray, silty CLAY interbeds
(CL) Med stiff, wet, blue-grey with rust mottling, lean CLAY, with silt; grades to: with (SP) interbedded gray fine SAND lenses
(SP-SM) Loose, saturated, tan, predom. fine to med. SAND, with silt (top of source)
(SP) Medium dense, saturated, gray/rust, SAND, trace silt and gravel
(SP-SM) Med dense, saturated, gray/rust, SAND, with silt, trace gravel
S1
S2
S3
S4
S5
S6
S7
S8
S9
S10
S11
S12
S13
ATD
LEGEND
2-inch OD split spoon sampler
3-inch OD split spoon sampler
Shelby tube sampler
ATD Groundwater level at time of drilling
VIRGINIA TECH
The Charles Edward Via Dept. of Civil Engineering Blacksburg, Virginia
Drilling Initiated: 06/04/92
Drilling Completed: 06/04/92

PROJECT: Wabash Valley Paleoseismic Liquefaction Study

SITE: Bowling Green (BG)

BORING#: B-2 (cont'd)

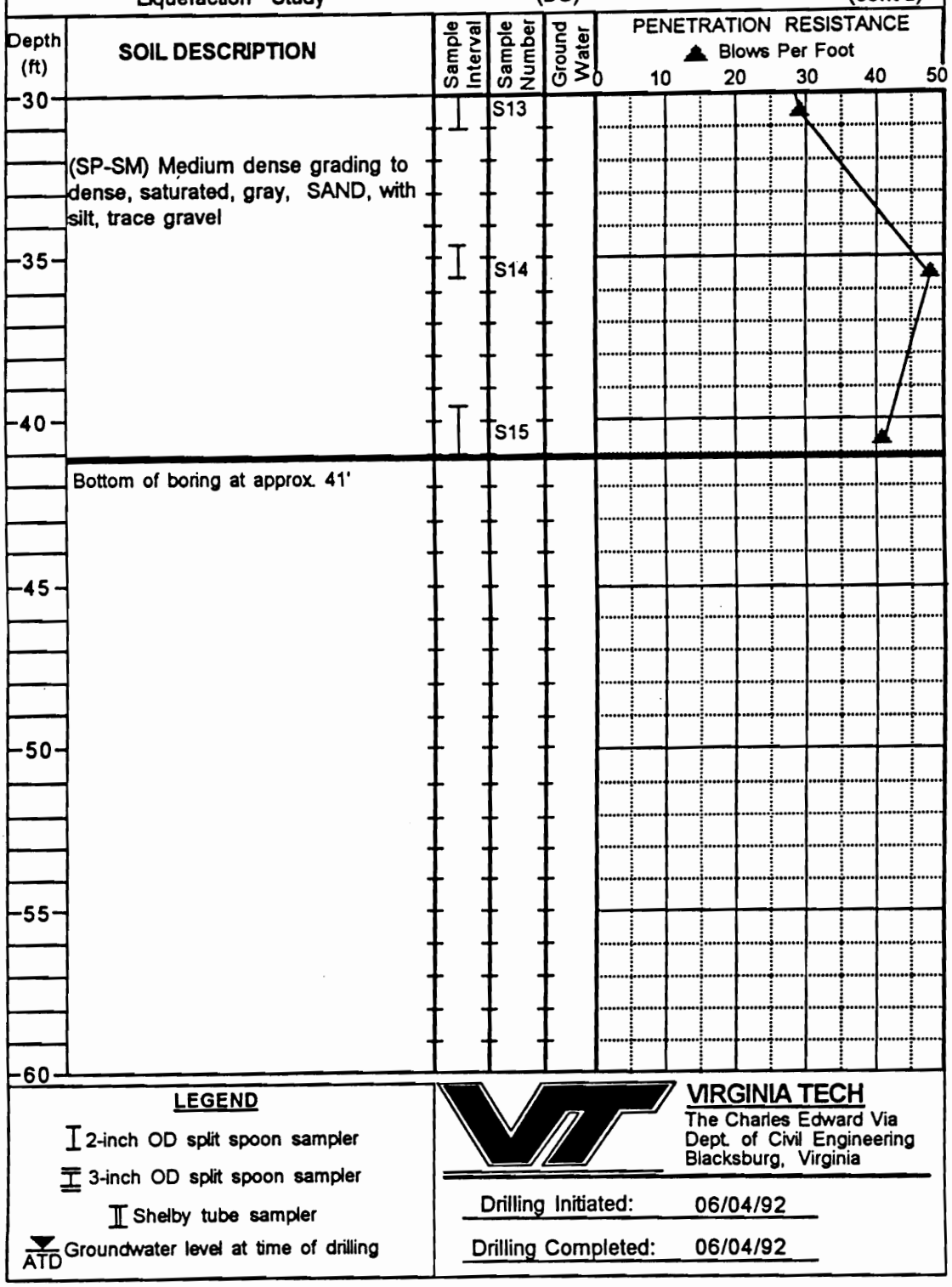

LEGEND

- 2-inch OD split spoon sampler
- 3-inch OD split spoon sampler
- Shelby tube sampler
- ATD Groundwater level at time of drilling

VIRGINIA TECH
The Charles Edward Via
Dept. of Civil Engineering
Blacksburg, Virginia

Drilling Initiated: 06/04/92

Drilling Completed: 06/04/92

PROJECT: Wabash Valley Paleoseismic Liquefaction Study **SITE:** Bowling Green (BG) **BORING#:** B-4

Depth (ft)	SOIL DESCRIPTION	Sample Interval	Sample Number	Ground Water
0	Sod and topsoil			
5	(CL) Stiff, moist to wet, dark gray/brown, lean CLAY, with silt, trace fine and med. sand (post earthquake channel fill)		S1	
10	(ML) Stiff, moist, brown grading to tan/brown, SILT, with clay and fine sand (post earthquake channel fill deposit)		S2	
15	(SP) Med. dense, wet to saturated, tan/brown fine SAND, trace silt; with (CL) lean CLAY, with silt and tr. fine sand, lenses		S3	
20	(SP) Loose grading to medium dense, wet to saturated, tan/brown, fine to medium SAND, trace silt		S4 S5	ATD
25	(SP-SM) Loose to med. dense, sat., tan/gray, predominantly fine and medium SAND, with silt		S6	
30	(SW-SM) Med dense, sat., gray/rust, SAND, with silt, some gravel		S7	
	(SP-SM) Loose to med. dense, sat., gray, predominantly fine and medium SAND, with silt		S8	

PENETRATION RESISTANCE
▲ Blows Per Foot
0 10 20 30 40 50

LEGEND

- 2-inch OD split spoon sampler
- 3-inch OD split spoon sampler
- Shelby tube sampler
- ATD Groundwater level at time of drilling

VIRGINIA TECH
The Charles Edward Via
Dept. of Civil Engineering
Blacksburg, Virginia

Drilling Initiated: 06/04/92

Drilling Completed: 06/05/92

PROJECT: Wabash Valley Paleoseismic Liquefaction Study

SITE: Bowling Green (BG)

BORING#: B-4 (cont'd)

Depth (ft)	SOIL DESCRIPTION	Sample Interval	Sample Number	Ground Water	PENETRATION RESISTANCE ▲ Blows Per Foot (0 10 20 30 40 50)
30	(SP-SM) Very dense, saturated, gray, SAND, with silt, and with gravel contents of up to 20%		S8		(54) ▲
35			S9		(67) ▲
40	(SP) Very dense, saturated, gray, predominantly fine and med. SAND, trace silt and gravel		S10		(65) ▲
	Bottom of boring at approx. 41'				
45					
50					
55					
60					

LEGEND

- 2-inch OD split spoon sampler
- 3-inch OD split spoon sampler
- Shelby tube sampler
- ATD Groundwater level at time of drilling

VIRGINIA TECH
The Charles Edward Via
Dept. of Civil Engineering
Blacksburg, Virginia

Drilling Initiated: 06/04/92

Drilling Completed: 06/05/92

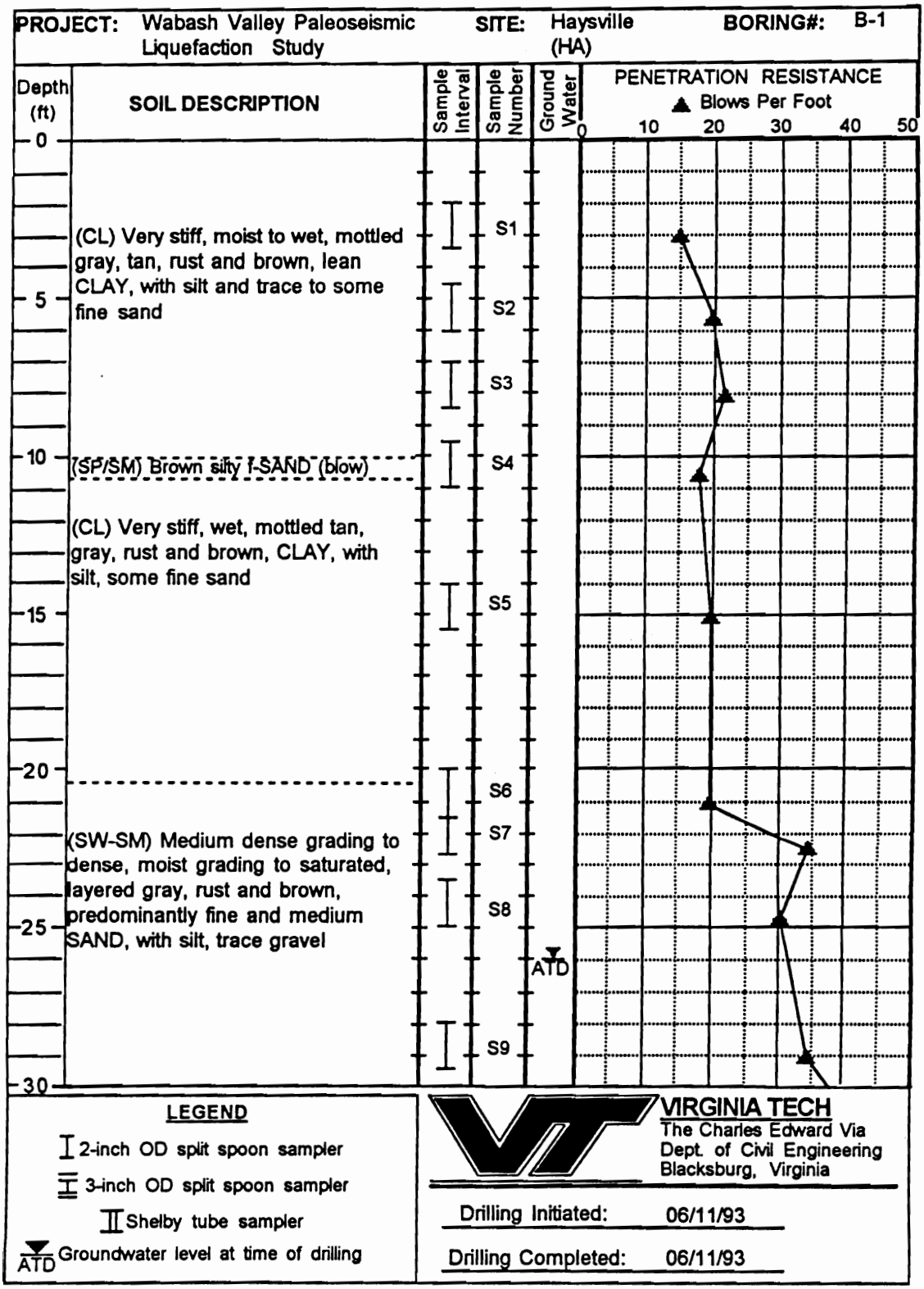
PROJECT: Wabash Valley Paleoseismic Liquefaction Study
SITE: Haysville (HA)
BORING#: B-1
Depth (ft)
SOIL DESCRIPTION
Sample Interval
Sample Number
Ground Water
PENETRATION RESISTANCE
Blows Per Foot
0
10
20
30
40
50
0
5
10
15
20
25
30
(CL) Very stiff, moist to wet, mottled gray, tan, rust and brown, lean CLAY, with silt and trace to some fine sand
(SP/SM) Brown silty f-SAND (blow)
(CL) Very stiff, wet, mottled tan, gray, rust and brown, CLAY, with silt, some fine sand
(SW-SM) Medium dense grading to dense, moist grading to saturated, layered gray, rust and brown, predominantly fine and medium SAND, with silt, trace gravel
S1
S2
S3
S4
S5
S6
S7
S8
S9
ATD
LEGEND
2-inch OD split spoon sampler
3-inch OD split spoon sampler
Shelby tube sampler
ATD Groundwater level at time of drilling
VIRGINIA TECH
The Charles Edward Via Dept. of Civil Engineering Blacksburg, Virginia
Drilling Initiated: 06/11/93
Drilling Completed: 06/11/93

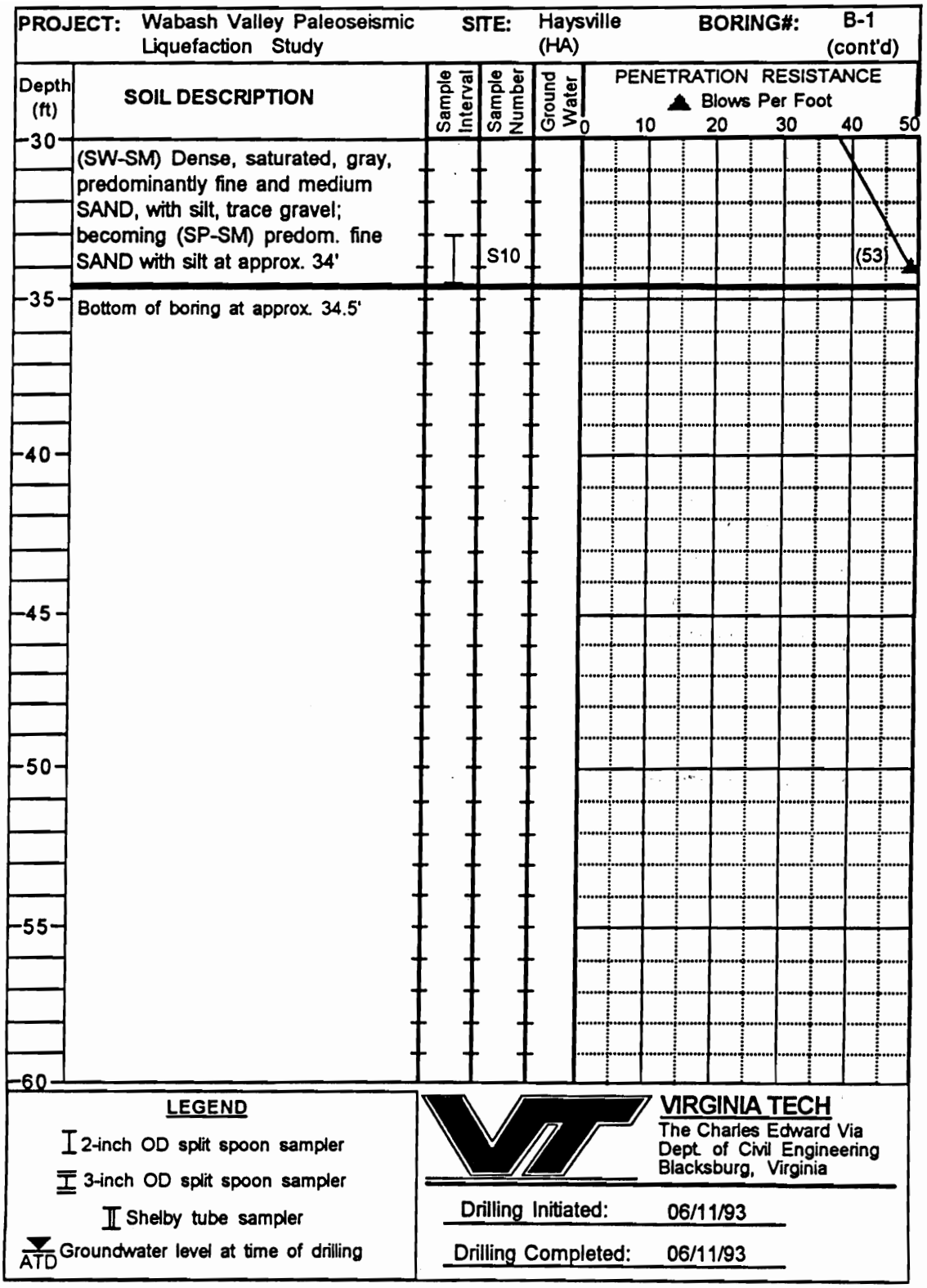
PROJECT: Wabash Valley Paleoseismic Liquefaction Study
SITE: Haysville (HA)
BORING#: B-1 (cont'd)
Depth (ft)
SOIL DESCRIPTION
Sample Interval
Sample Number
Ground Water
PENETRATION RESISTANCE
Blows Per Foot
0 10 20 30 40 50
30
(SW-SM) Dense, saturated, gray, predominantly fine and medium SAND, with silt, trace gravel; becoming (SP-SM) predom. fine SAND with silt at approx. 34'
S10
(53)
35
Bottom of boring at approx. 34.5'
40
45
50
55
60
LEGEND
2-inch OD split spoon sampler
3-inch OD split spoon sampler
Shelby tube sampler
ATD Groundwater level at time of drilling
VIRGINIA TECH
The Charles Edward Via Dept. of Civil Engineering Blacksburg, Virginia
Drilling Initiated: 06/11/93
Drilling Completed: 06/11/93

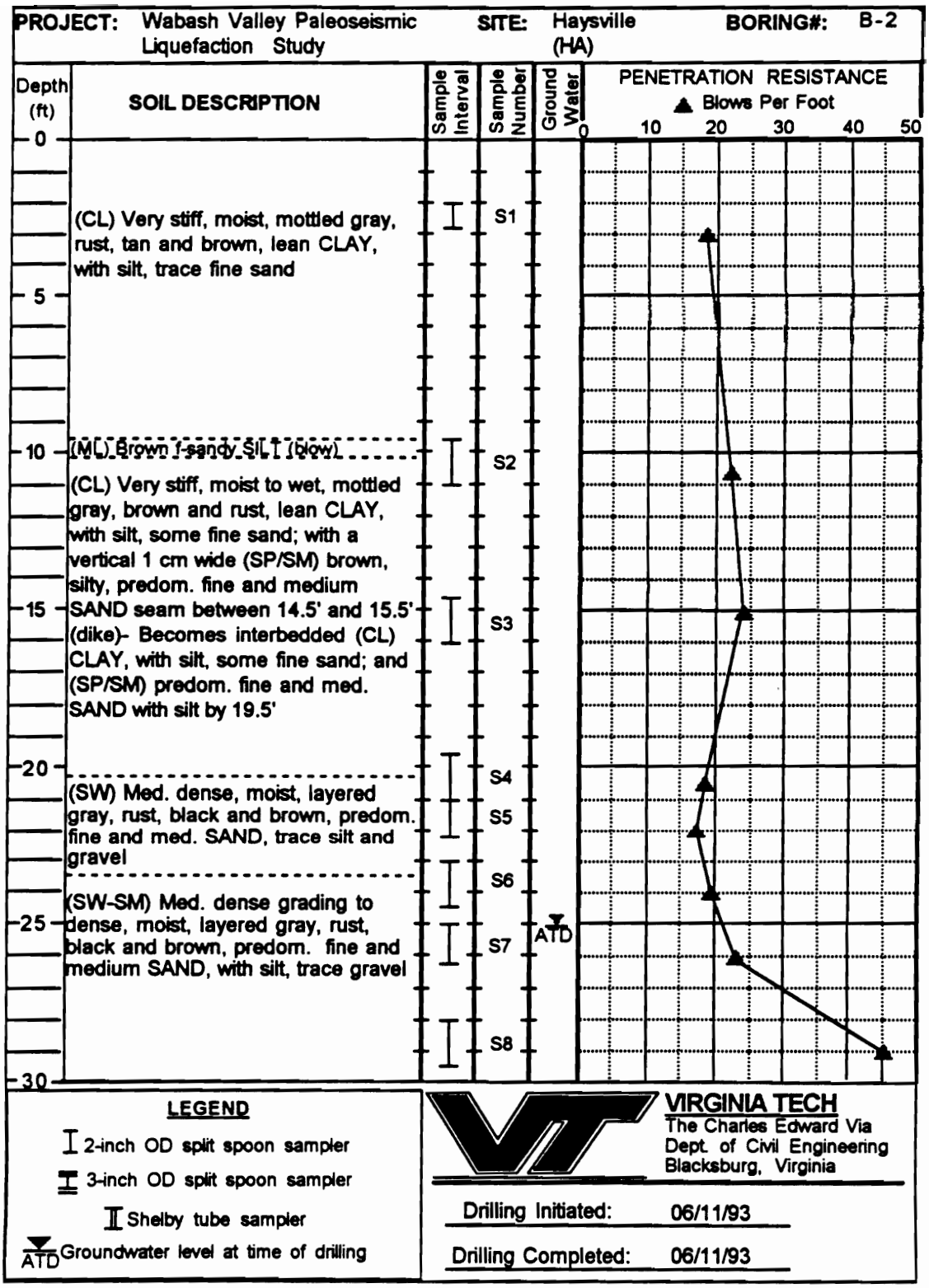
PROJECT: Wabash Valley Paleoseismic Liquefaction Study
SITE: Haysville (HA)
BORING#: B-2
Depth (ft)
SOIL DESCRIPTION
Sample Interval
Sample Number
Ground Water
PENETRATION RESISTANCE
Blows Per Foot
0
10
20
30
40
50
5
10
15
20
25
30
(CL) Very stiff, moist, mottled gray, rust, tan and brown, lean CLAY, with silt, trace fine sand
(ML) Brown f sandy SILT (blow)
(CL) Very stiff, moist to wet, mottled gray, brown and rust, lean CLAY, with silt, some fine sand; with a vertical 1 cm wide (SP/SM) brown, silty, predom. fine and medium SAND seam between 14.5' and 15.5' (dike)- Becomes interbedded (CL) CLAY, with silt, some fine sand; and (SP/SM) predom. fine and med. SAND with silt by 19.5'
(SW) Med. dense, moist, layered gray, rust, black and brown, predom. fine and med. SAND, trace silt and gravel
(SW-SM) Med. dense grading to dense, moist, layered gray, rust, black and brown, predom. fine and medium SAND, with silt, trace gravel
S1
S2
S3
S4
S5
S6
S7
S8
ATD
LEGEND
2-inch OD split spoon sampler
3-inch OD split spoon sampler
Shelby tube sampler
ATD Groundwater level at time of drilling
VIRGINIA TECH
The Charles Edward Via Dept. of Civil Engineering Blacksburg, Virginia
Drilling Initiated: 06/11/93
Drilling Completed: 06/11/93

PROJECT: Wabash Valley Paleoseismic Liquefaction Study **SITE:** Haysville (HA) **BORING#:** B-2 (cont'd)

Depth (ft)	SOIL DESCRIPTION	Sample Interval	Sample Number	Ground Water	PENETRATION RESISTANCE ▲ Blows Per Foot 0 10 20 30 40 50
30	(SW-SM) Dense, saturated, gray, predominantly fine and medium SAND, with silt, trace gravel; becoming (SP-SM) predom. fine SAND with silt at approx. 34.5'		S9		
35	Bottom of boring at approx. 34.5'				
40					
45					
50					
55					
60					

LEGEND

- 2-inch OD split spoon sampler
- 3-inch OD split spoon sampler
- Shelby tube sampler
- ATD Groundwater level at time of drilling

VIRGINIA TECH
The Charles Edward Via Dept. of Civil Engineering Blacksburg, Virginia

Drilling Initiated: 06/11/93

Drilling Completed: 06/11/93

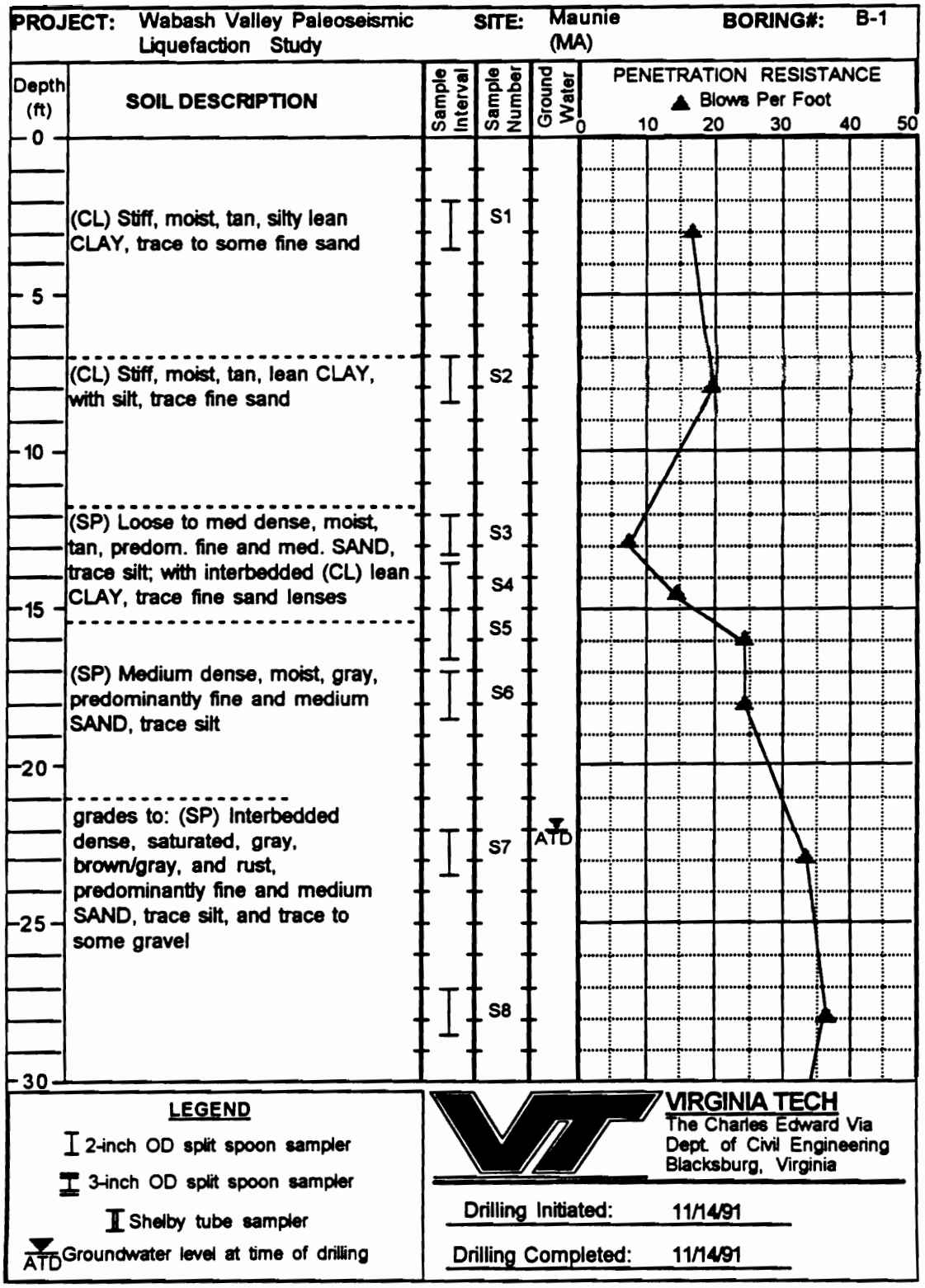
PROJECT: Wabash Valley Paleoseismic Liquefaction Study
SITE: Maunie (MA)
BORING#: B-1
Depth (ft)
SOIL DESCRIPTION
Sample Interval
Sample Number
Ground Water
PENETRATION RESISTANCE
Blows Per Foot
0
10
20
30
40
50
0
5
10
15
20
25
30
(CL) Stiff, moist, tan, silty lean CLAY, trace to some fine sand
S1
(CL) Stiff, moist, tan, lean CLAY, with silt, trace fine sand
S2
(SP) Loose to med dense, moist, tan, predom. fine and med. SAND, trace silt; with interbedded (CL) lean CLAY, trace fine sand lenses
S3
S4
S5
(SP) Medium dense, moist, gray, predominantly fine and medium SAND, trace silt
S6
grades to: (SP) Interbedded dense, saturated, gray, brown/gray, and rust, predominantly fine and medium SAND, trace silt, and trace to some gravel
ATD
S7
S8
LEGEND
2-inch OD split spoon sampler
3-inch OD split spoon sampler
Shelby tube sampler
ATD Groundwater level at time of drilling
VIRGINIA TECH
The Charles Edward Via Dept. of Civil Engineering Blacksburg, Virginia
Drilling Initiated: 11/14/91
Drilling Completed: 11/14/91

PROJECT: Wabash Valley Paleoseismic Liquefaction Study

SITE: Maunie (MA)

BORING#: B-1 (cont'd)

Depth (ft)	SOIL DESCRIPTION	Sample Interval	Sample Number	Ground Water	PENETRATION RESISTANCE ▲ Blows Per Foot 0 10 20 30 40 50
30	(SP) Dense, sat, tan/gray, predominantly fine and medium SAND, trace silt and trace to some gravel		S9		
35	Bottom of boring at approx. 33.5'				
40					
45					
50					
55					
60					

LEGEND

- 2-inch OD split spoon sampler
- 3-inch OD split spoon sampler
- Shelby tube sampler
- ATD Groundwater level at time of drilling

VIRGINIA TECH
The Charles Edward Via
Dept. of Civil Engineering
Blacksburg, Virginia

Drilling Initiated: 11/14/91

Drilling Completed: 11/14/91

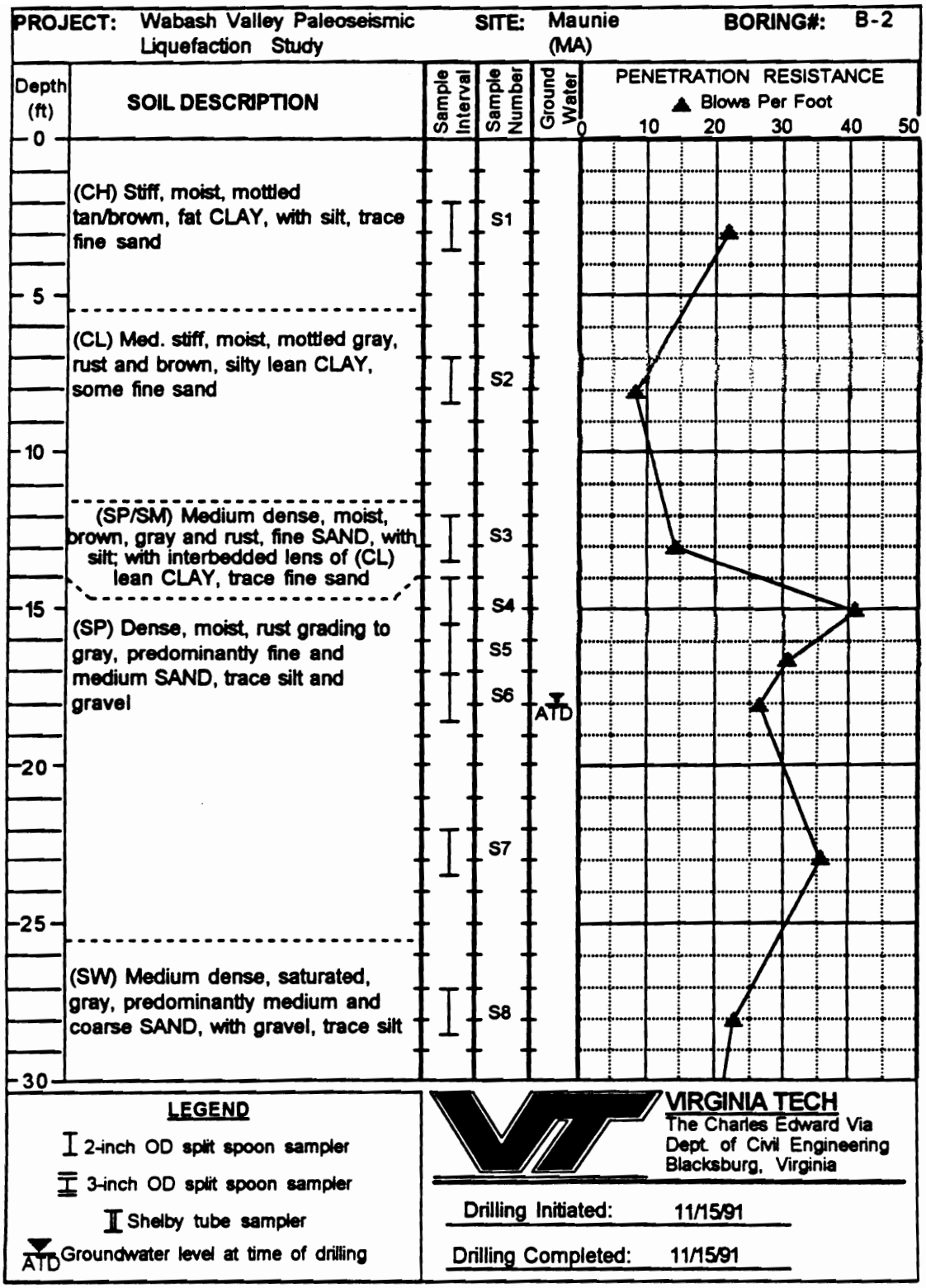
PROJECT: Wabash Valley Paleoseismic Liquefaction Study
SITE: Maunie (MA)
BORING#: B-2
Depth (ft)
SOIL DESCRIPTION
Sample Interval
Sample Number
Ground Water
PENETRATION RESISTANCE
Blows Per Foot
0
10
20
30
40
50
0
5
10
15
20
25
30
(CH) Stiff, moist, mottled tan/brown, fat CLAY, with silt, trace fine sand
(CL) Med. stiff, moist, mottled gray, rust and brown, silty lean CLAY, some fine sand
(SP/SM) Medium dense, moist, brown, gray and rust, fine SAND, with silt; with interbedded lens of (CL) lean CLAY, trace fine sand
(SP) Dense, moist, rust grading to gray, predominantly fine and medium SAND, trace silt and gravel
(SW) Medium dense, saturated, gray, predominantly medium and coarse SAND, with gravel, trace silt
S1
S2
S3
S4
S5
S6
S7
S8
ATD
LEGEND
2-inch OD split spoon sampler
3-inch OD split spoon sampler
Shelby tube sampler
Groundwater level at time of drilling
VIRGINIA TECH
The Charles Edward Via
Dept. of Civil Engineering
Blacksburg, Virginia
Drilling Initiated: 11/15/91
Drilling Completed: 11/15/91

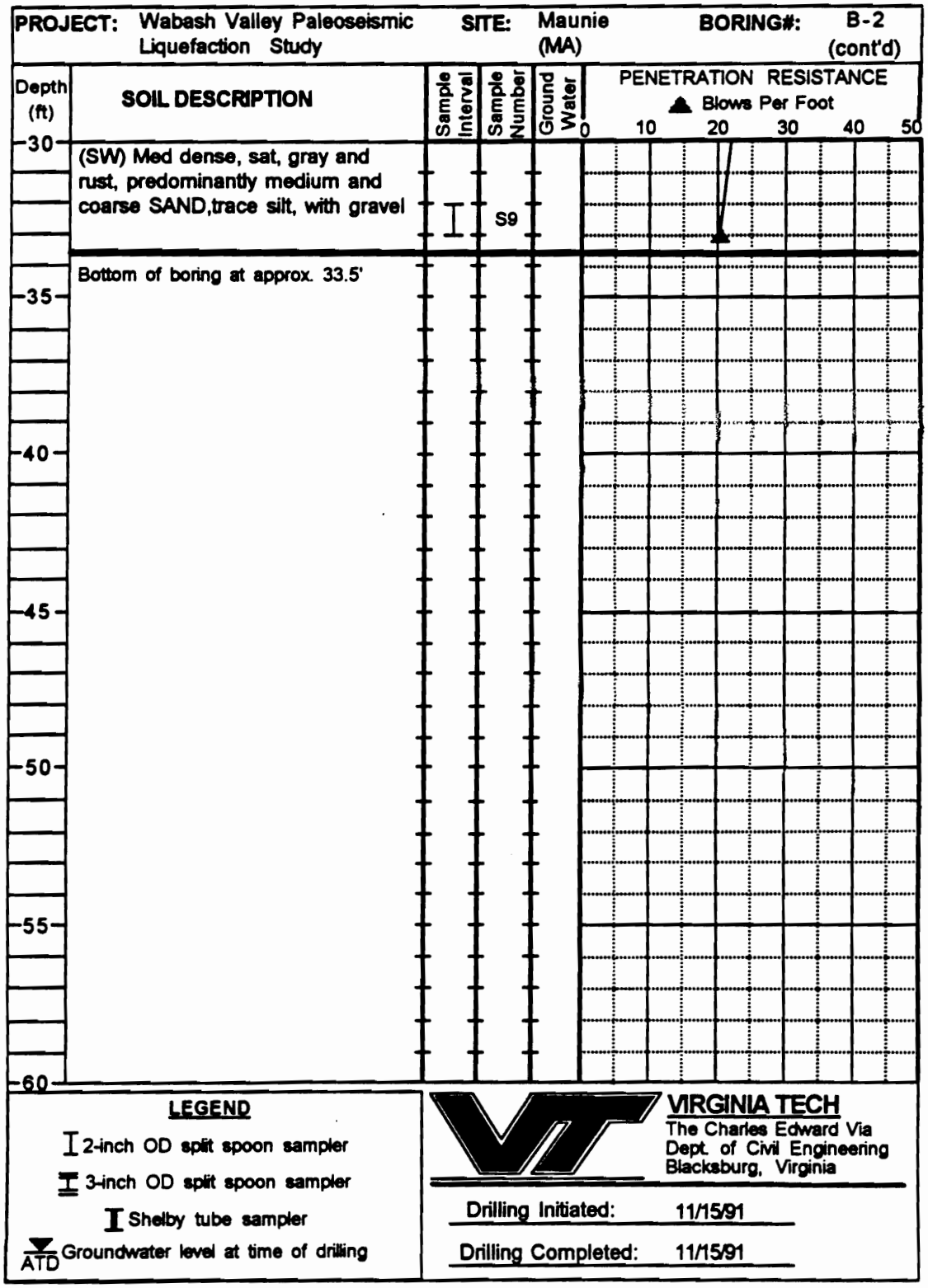
PROJECT: Wabash Valley Paleoseismic Liquefaction Study
SITE: Maunie (MA)
BORING#: B-2 (cont'd)
Depth (ft)
SOIL DESCRIPTION
Sample Interval
Sample Number
Ground Water
PENETRATION RESISTANCE
Blows Per Foot
0
10
20
30
40
50
-30
(SW) Med dense, sat, gray and rust, predominantly medium and coarse SAND,trace silt, with gravel
S9
Bottom of boring at approx. 33.5'
-35
-40
-45
-50
-55
-60
LEGEND
2-inch OD split spoon sampler
3-inch OD split spoon sampler
Shelby tube sampler
ATD Groundwater level at time of drilling
VIRGINIA TECH
The Charles Edward Via Dept. of Civil Engineering Blacksburg, Virginia
Drilling Initiated: 11/15/91
Drilling Completed: 11/15/91

PROJECT: Wabash Valley Paleoseismic Liquefaction Study

SITE: Maunie (MA)

BORING#: B-3

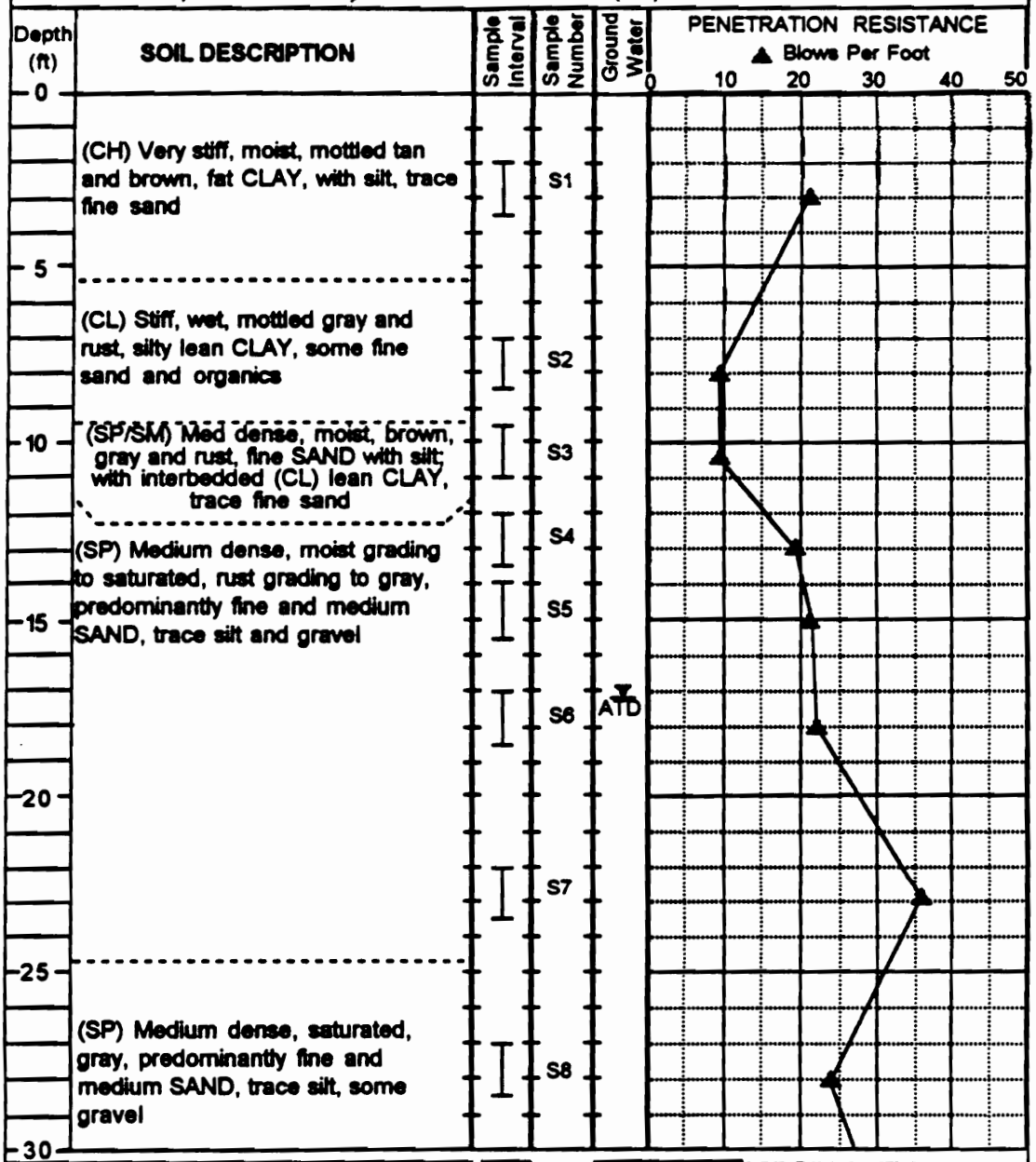

LEGEND

- 2-inch OD split spoon sampler
- 3-inch OD split spoon sampler
- Shelby tube sampler
- ATD Groundwater level at time of drilling

VIRGINIA TECH
The Charles Edward Via
Dept. of Civil Engineering
Blacksburg, Virginia

Drilling Initiated: 11/15/91

Drilling Completed: 11/15/91

PROJECT: Wabash Valley Paleoseismic Liquefaction Study

SITE: Maunie (MA)

BORING#: B-3 (cont'd)

Depth (ft)	SOIL DESCRIPTION	Sample Interval	Sample Number	Ground Water	PENETRATION RESISTANCE ▲ Blows Per Foot 0 10 20 30 40 50
30	(SP) Medium dense, sat, gray, predom. fine and medium SAND, trace silt, some gravel		S9		
	Bottom of boring at approx. 33.5'				
35					
40					
45					
50					
55					
60					

LEGEND

- 2-inch OD split spoon sampler
- 3-inch OD split spoon sampler
- Shelby tube sampler
- ATD Groundwater level at time of drilling

VIRGINIA TECH
The Charles Edward Via
Dept. of Civil Engineering
Blacksburg, Virginia

Drilling Initiated: 11/15/91

Drilling Completed: 11/15/91

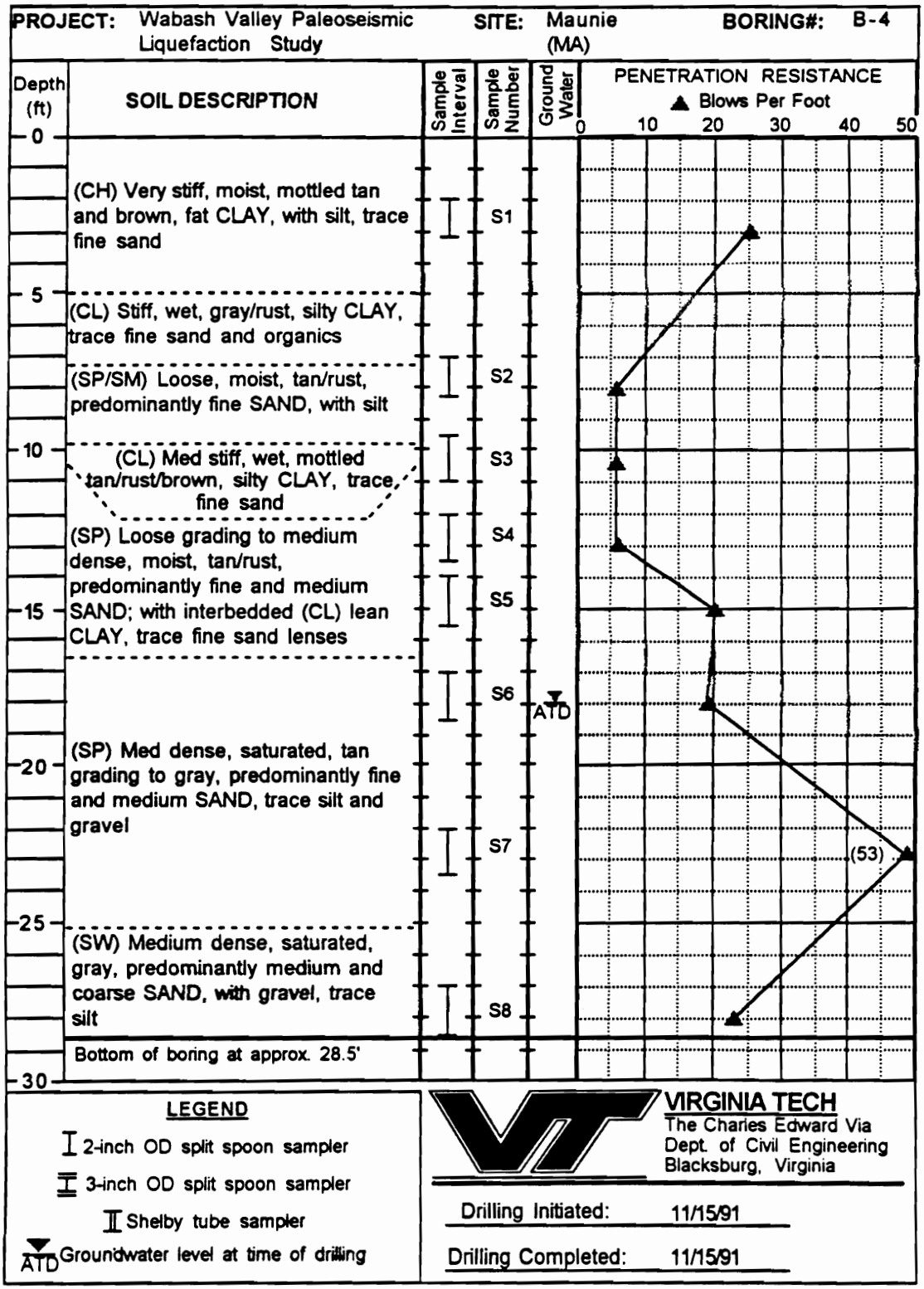
PROJECT: Wabash Valley Paleoseismic Liquefaction Study
SITE: Maunie (MA)
BORING#: B-4
Depth (ft)
SOIL DESCRIPTION
Sample Interval
Sample Number
Ground Water
PENETRATION RESISTANCE
Blows Per Foot
0
10
20
30
40
50
0
5
10
15
20
25
30
(CH) Very stiff, moist, mottled tan and brown, fat CLAY, with silt, trace fine sand
S1
(CL) Stiff, wet, gray/rust, silty CLAY, trace fine sand and organics
(SP/SM) Loose, moist, tan/rust, predominantly fine SAND, with silt
S2
(CL) Med stiff, wet, mottled tan/rust/brown, silty CLAY, trace fine sand
S3
(SP) Loose grading to medium dense, moist, tan/rust, predominantly fine and medium SAND; with interbedded (CL) lean CLAY, trace fine sand lenses
S4
S5
S6
ATD
(SP) Med dense, saturated, tan grading to gray, predominantly fine and medium SAND, trace silt and gravel
S7
(53)
(SW) Medium dense, saturated, gray, predominantly medium and coarse SAND, with gravel, trace silt
S8
Bottom of boring at approx. 28.5'
LEGEND
2-inch OD split spoon sampler
3-inch OD split spoon sampler
Shelby tube sampler
ATD Groundwater level at time of drilling
VIRGINIA TECH
The Charles Edward Via
Dept. of Civil Engineering
Blacksburg, Virginia
Drilling Initiated: 11/15/91
Drilling Completed: 11/15/91

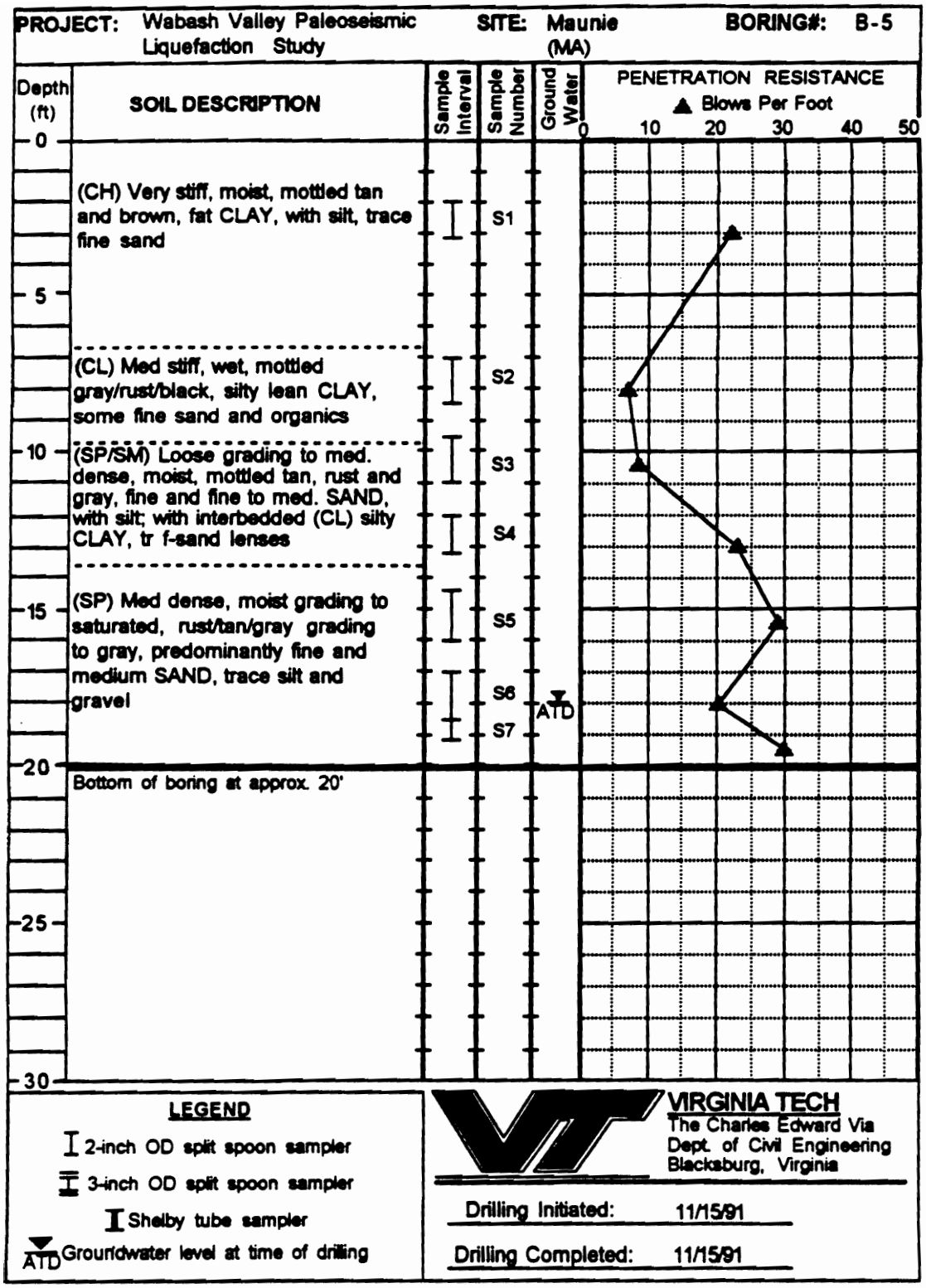
PROJECT: Wabash Valley Paleoseismic Liquefaction Study
SITE: Maunie (MA)
BORING#: B-5
Depth (ft)
SOIL DESCRIPTION
Sample Interval
Sample Number
Ground Water
PENETRATION RESISTANCE
Blows Per Foot
0
10
20
30
40
50
0
5
10
15
20
25
30
(CH) Very stiff, moist, mottled tan and brown, fat CLAY, with silt, trace fine sand
S1
(CL) Med stiff, wet, mottled gray/rust/black, silty lean CLAY, some fine sand and organics
S2
(SP/SM) Loose grading to med. dense, moist, mottled tan, rust and gray, fine and fine to med. SAND, with silt; with interbedded (CL) silty CLAY, tr f-sand lenses
S3
S4
(SP) Med dense, moist grading to saturated, rust/tan/gray grading to gray, predominantly fine and medium SAND, trace silt and gravel
S5
S6
S7
ATD
Bottom of boring at approx. 20'
LEGEND
2-inch OD split spoon sampler
3-inch OD split spoon sampler
Shelby tube sampler
ATD Groundwater level at time of drilling
VIRGINIA TECH
The Charles Edward Via Dept. of Civil Engineering Blacksburg, Virginia
Drilling Initiated: 11/15/91
Drilling Completed: 11/15/91

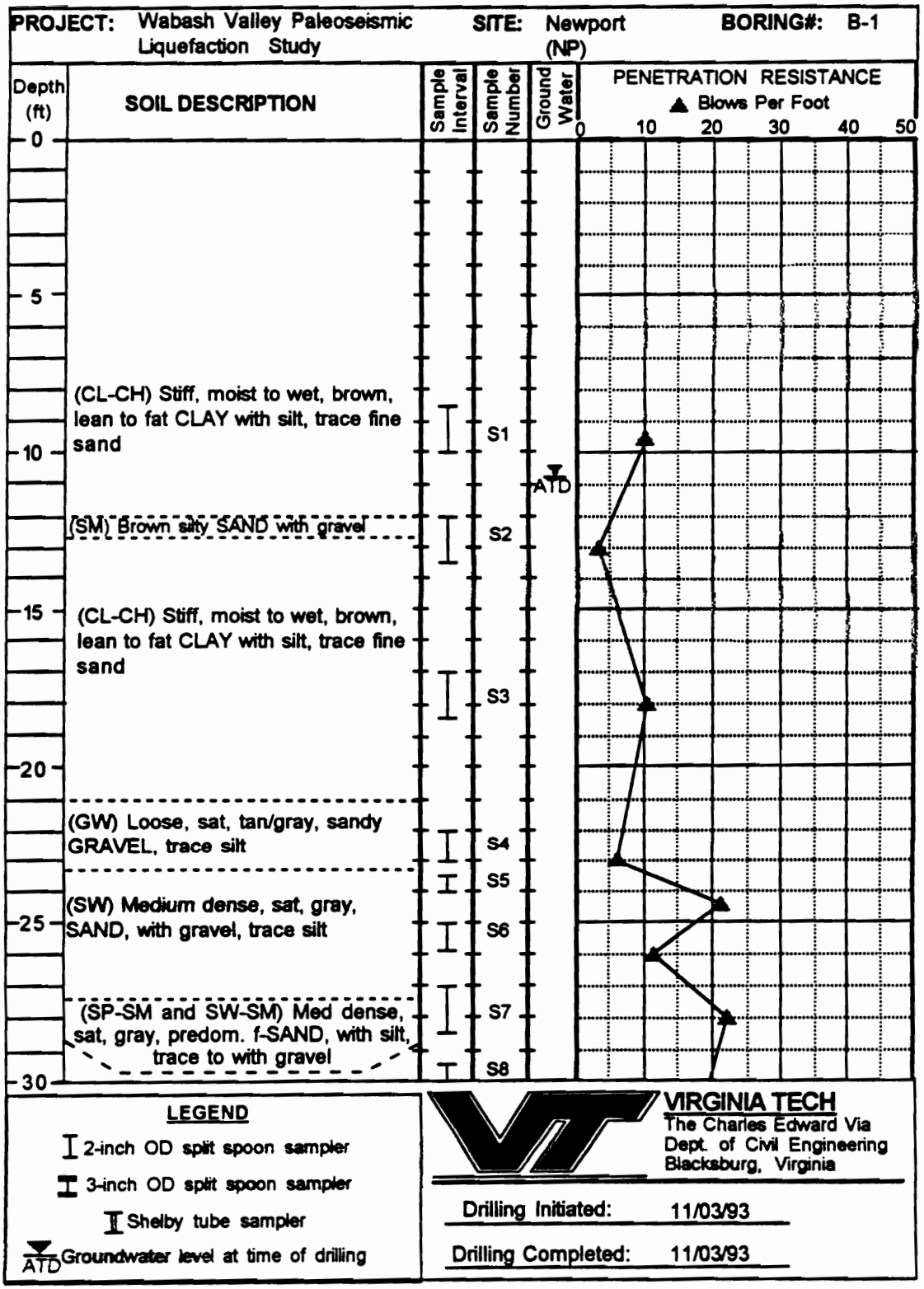
PROJECT: Wabash Valley Paleoseismic Liquefaction Study
SITE: Newport (NP)
BORING#: B-1
Depth (ft)
SOIL DESCRIPTION
Sample Interval
Sample Number
Ground Water
PENETRATION RESISTANCE
Blows Per Foot
0
10
20
30
40
50
5
10
15
20
25
30
(CL-CH) Stiff, moist to wet, brown, lean to fat CLAY with silt, trace fine sand
(SM) Brown silty SAND with gravel
(CL-CH) Stiff, moist to wet, brown, lean to fat CLAY with silt, trace fine sand
(GW) Loose, sat, tan/gray, sandy GRAVEL, trace silt
(SW) Medium dense, sat, gray, SAND, with gravel, trace silt
(SP-SM and SW-SM) Med dense, sat, gray, predom. f-SAND, with silt, trace to with gravel
S1
S2
S3
S4
S5
S6
S7
S8
ATD
LEGEND
2-inch OD split spoon sampler
3-inch OD split spoon sampler
Shelby tube sampler
ATD Groundwater level at time of drilling
VIRGINIA TECH
The Charles Edward Via Dept. of Civil Engineering Blacksburg, Virginia
Drilling Initiated: 11/03/93
Drilling Completed: 11/03/93

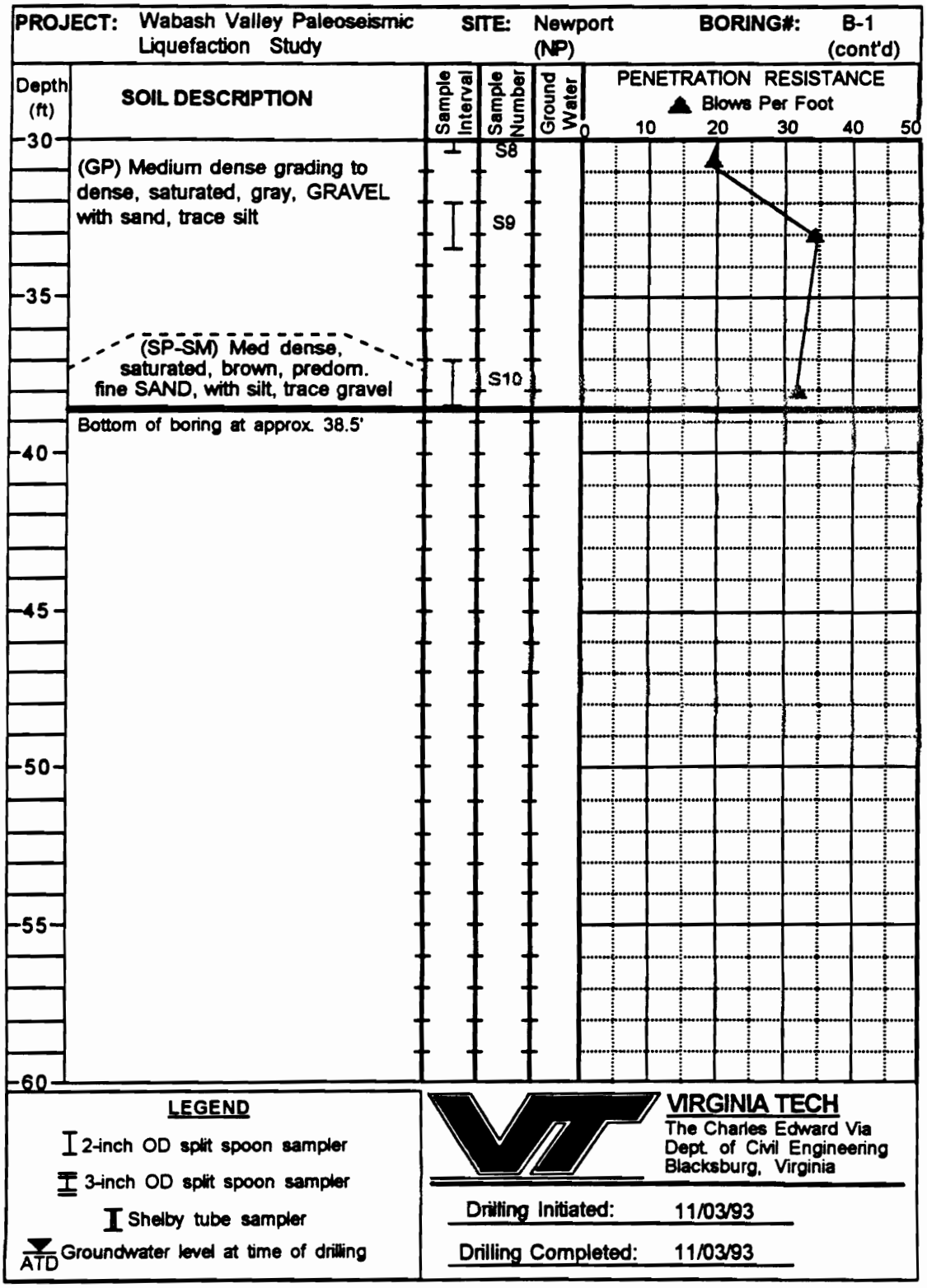
PROJECT: Wabash Valley Paleoseismic Liquefaction Study
SITE: Newport (NP)
BORING#: B-1 (cont'd)
Depth (ft)
SOIL DESCRIPTION
Sample Interval
Sample Number
Ground Water
PENETRATION RESISTANCE
Blows Per Foot
0
10
20
30
40
50
30
35
40
45
50
55
60
(GP) Medium dense grading to dense, saturated, gray, GRAVEL with sand, trace silt
S8
S9
(SP-SM) Med dense, saturated, brown, predom. fine SAND, with silt, trace gravel
S10
Bottom of boring at approx. 38.5'
LEGEND
2-inch OD split spoon sampler
3-inch OD split spoon sampler
Shelby tube sampler
ATD Groundwater level at time of drilling
VIRGINIA TECH
The Charles Edward Via Dept. of Civil Engineering Blacksburg, Virginia
Drilling Initiated: 11/03/93
Drilling Completed: 11/03/93

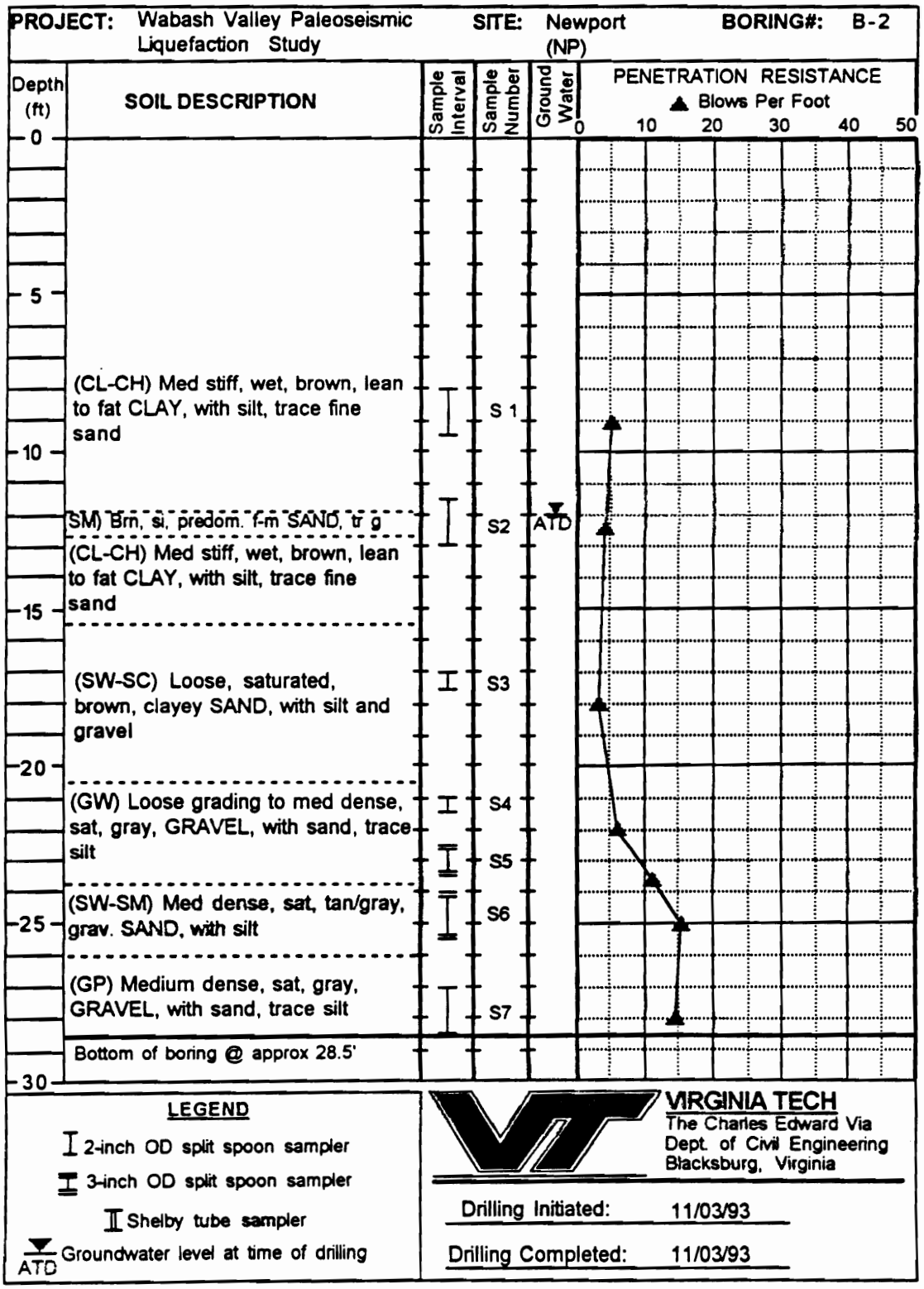
PROJECT: Wabash Valley Paleoseismic Liquefaction Study
SITE: Newport (NP)
BORING#: B-2
Depth (ft)
SOIL DESCRIPTION
Sample Interval
Sample Number
Ground Water
PENETRATION RESISTANCE
Blows Per Foot
0
10
20
30
40
50
0
5
10
15
20
25
30
(CL-CH) Med stiff, wet, brown, lean to fat CLAY, with silt, trace fine sand
S 1
SM) Brn, si, predom. f-m SAND, tr g
S2
ATD
(CL-CH) Med stiff, wet, brown, lean to fat CLAY, with silt, trace fine sand
(SW-SC) Loose, saturated, brown, clayey SAND, with silt and gravel
S3
(GW) Loose grading to med dense, sat, gray, GRAVEL, with sand, trace silt
S4
S5
(SW-SM) Med dense, sat, tan/gray, grav. SAND, with silt
S6
(GP) Medium dense, sat, gray, GRAVEL, with sand, trace silt
S7
Bottom of boring @ approx 28.5'
LEGEND
2-inch OD split spoon sampler
3-inch OD split spoon sampler
Shelby tube sampler
ATD Groundwater level at time of drilling
VIRGINIA TECH
The Charles Edward Via
Dept. of Civil Engineering
Blacksburg, Virginia
Drilling Initiated: 11/03/93
Drilling Completed: 11/03/93

PROJECT: Wabash Valley Paleoseismic Liquefaction Study **SITE:** Palestine (PA) **BORING#:** B-1

Depth (ft)	SOIL DESCRIPTION	Sample Interval	Sample Number	Ground Water
0	(SM) Loose, moist grading wetter with depth, tan, silty fine SAND, trace clay, and with occasional roots		S1	
5			S2	
	(CH) Stiff, moist grading to wet, brown, silty fat CLAY, trace fine to coarse sand		S3	
10			S4	
	(CL-CH) Stiff, moist grading to wet, mottled gray-brown and rust, silty lean to fat CLAY, trace fine to coarse sand		S5	ATD
15	(CL) Med stiff, wet, mottled tan and rust, silty lean CLAY, with fine sand		S6	
	(SM) Loose, wet, tan, silty fine SAND; with interbedded clean fine SAND and fine sandy SILT seams		S7	
20			S8	
	(SP) Med dense, sat, gray-black, gravelly, SAND, trace silt		S9	
	3" (CL) wet, brown, silty lean CLAY interbed at 22.5' overlies:		S10	
25	(GW) Med dense, dark gray, predominantly medium to coarse sandy GRAVEL, trace silt		NR	
			S11	
			S12	
30			S13	

PENETRATION RESISTANCE
▲ Blows Per Foot
0 10 20 30 40 50

LEGEND

- 2-inch OD split spoon sampler
- 3-inch OD split spoon sampler
- Shelby tube sampler
- ATD Groundwater level at time of drilling

VIRGINIA TECH
The Charles Edward Via
Dept. of Civil Engineering
Blacksburg, Virginia

Drilling Initiated: 05/26/92

Drilling Completed: 05/26/92

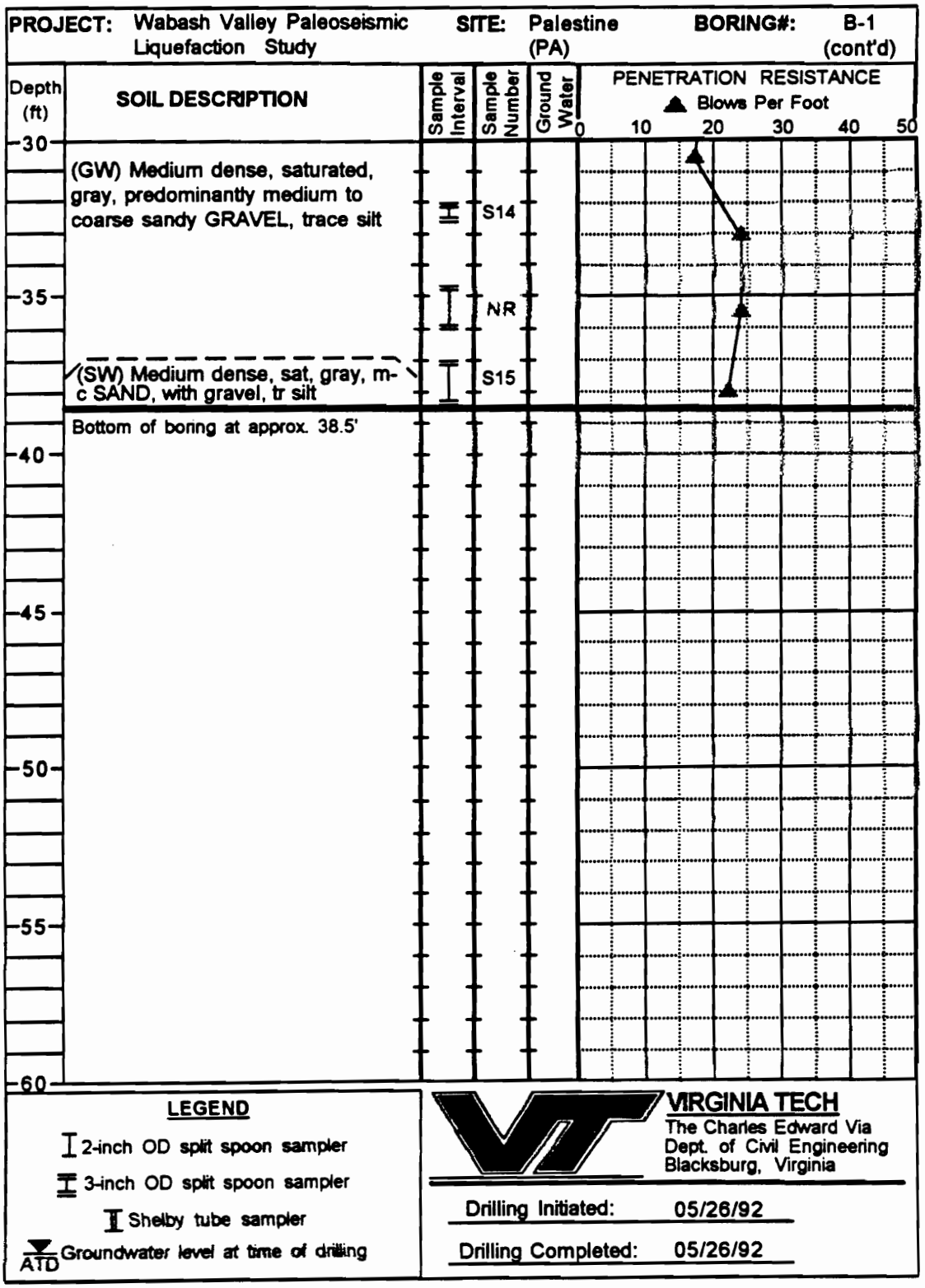
PROJECT: Wabash Valley Paleoseismic Liquefaction Study
SITE: Palestine (PA)
BORING#: B-1 (cont'd)
Depth (ft)
SOIL DESCRIPTION
Sample Interval
Sample Number
Ground Water
PENETRATION RESISTANCE
Blows Per Foot
0
10
20
30
40
50
-30
(GW) Medium dense, saturated, gray, predominantly medium to coarse sandy GRAVEL, trace silt
S14
-35
NR
(SW) Medium dense, sat, gray, m-c SAND, with gravel, tr silt
S15
Bottom of boring at approx. 38.5'
-40
-45
-50
-55
-60
LEGEND
2-inch OD split spoon sampler
3-inch OD split spoon sampler
Shelby tube sampler
ATD Groundwater level at time of drilling
VIRGINIA TECH
The Charles Edward Via Dept. of Civil Engineering Blacksburg, Virginia
Drilling Initiated: 05/26/92
Drilling Completed: 05/26/92

PROJECT: Wabash Valley Paleoseismic Liquefaction Study **SITE:** Palestine (PA) **BORING#:** B-2

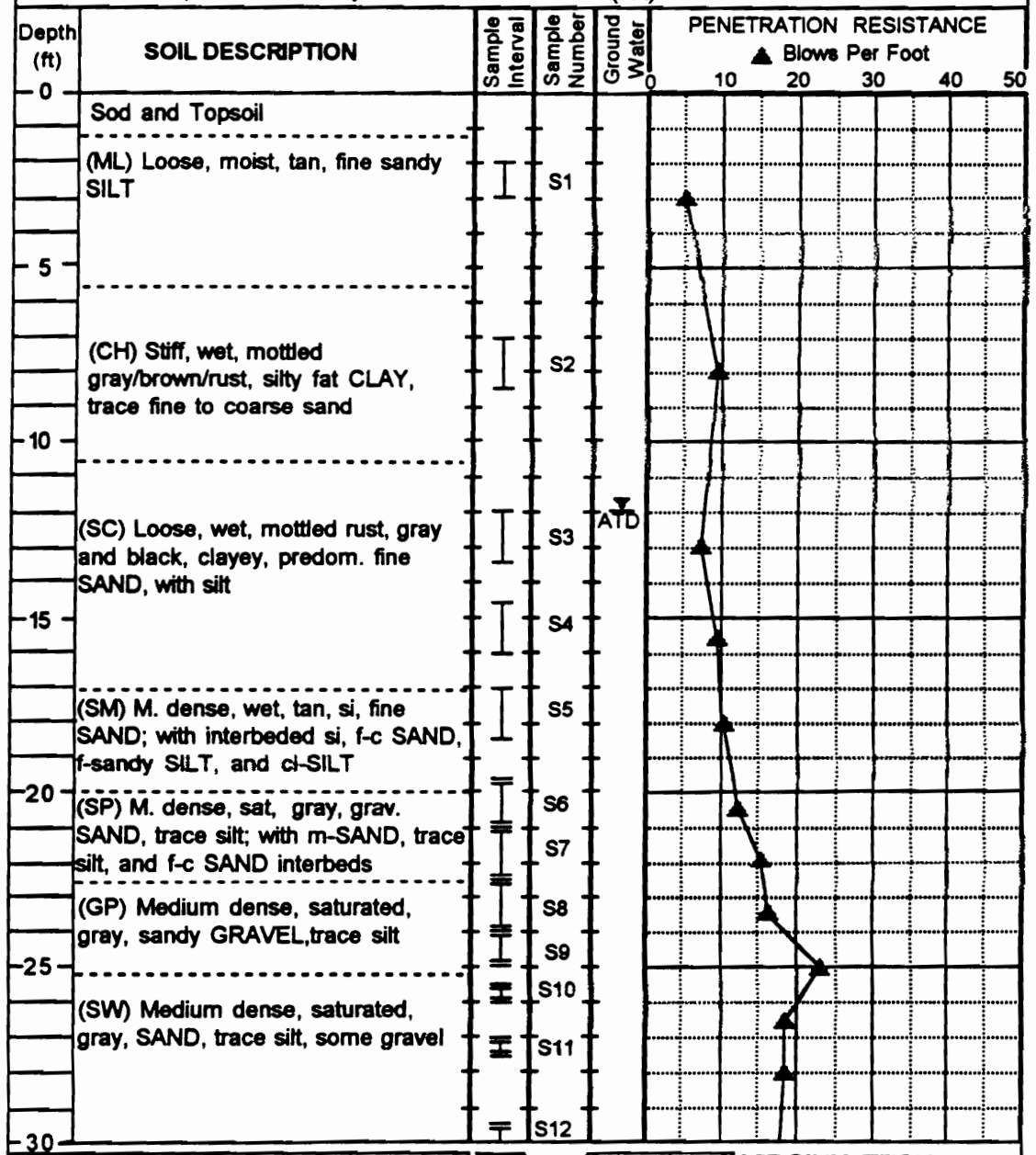

LEGEND

- 2-inch OD split spoon sampler
- 3-inch OD split spoon sampler
- Shelby tube sampler
- ATD Groundwater level at time of drilling

VIRGINIA TECH
The Charles Edward Via
Dept. of Civil Engineering
Blacksburg, Virginia

Drilling Initiated: 05/27/92

Drilling Completed: 05/27/92

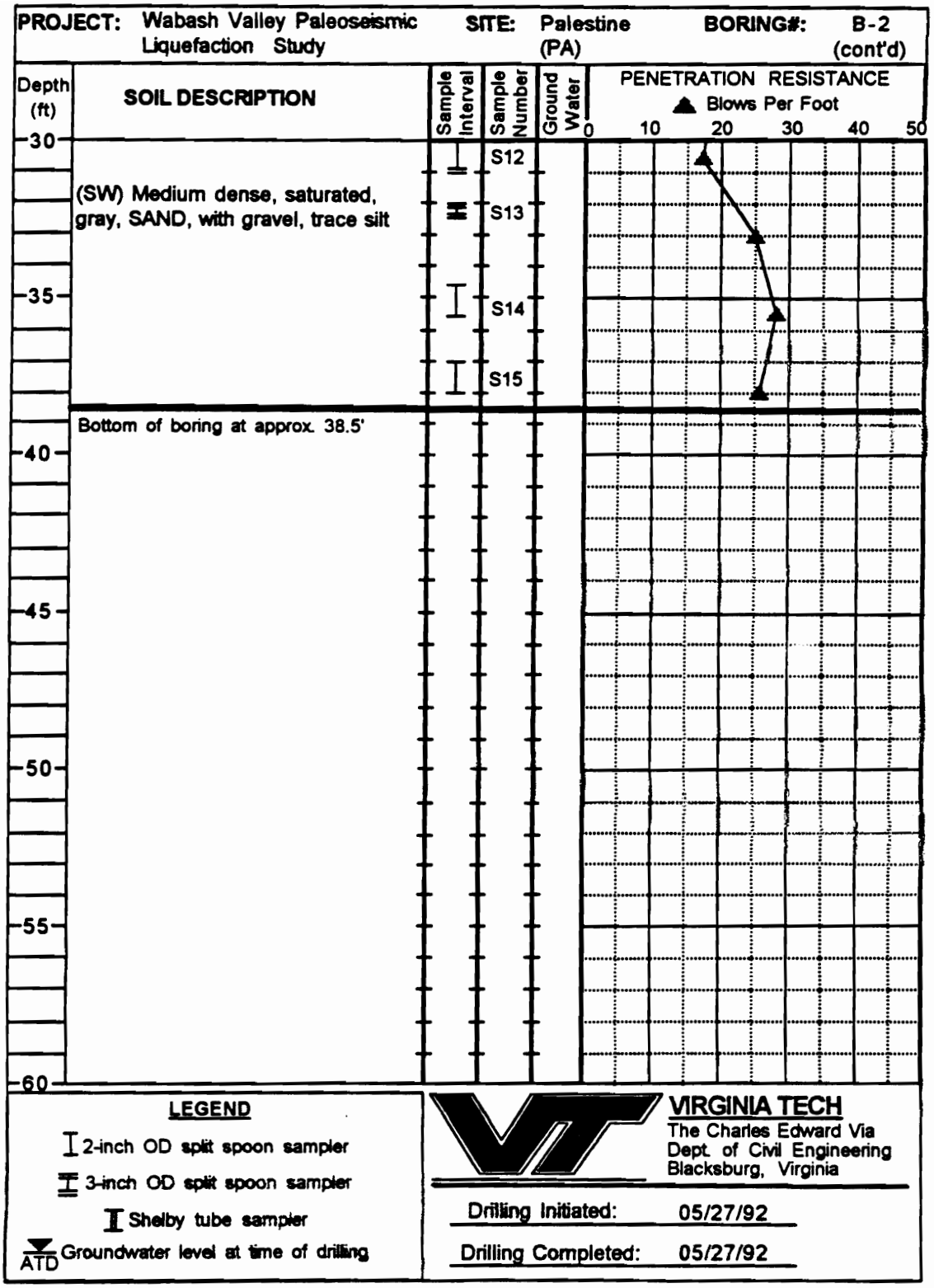
PROJECT: Wabash Valley Paleoseismic Liquefaction Study
SITE: Palestine (PA)
BORING#: B-2 (cont'd)
Depth (ft)
SOIL DESCRIPTION
Sample Interval
Sample Number
Ground Water
PENETRATION RESISTANCE
Blows Per Foot
0 10 20 30 40 50
30
35
40
45
50
55
60
S12
S13
S14
S15
(SW) Medium dense, saturated, gray, SAND, with gravel, trace silt
Bottom of boring at approx. 38.5'
LEGEND
2-inch OD split spoon sampler
3-inch OD split spoon sampler
Shelby tube sampler
ATD Groundwater level at time of drilling
VIRGINIA TECH
The Charles Edward Via Dept. of Civil Engineering Blacksburg, Virginia
Drilling Initiated: 05/27/92
Drilling Completed: 05/27/92

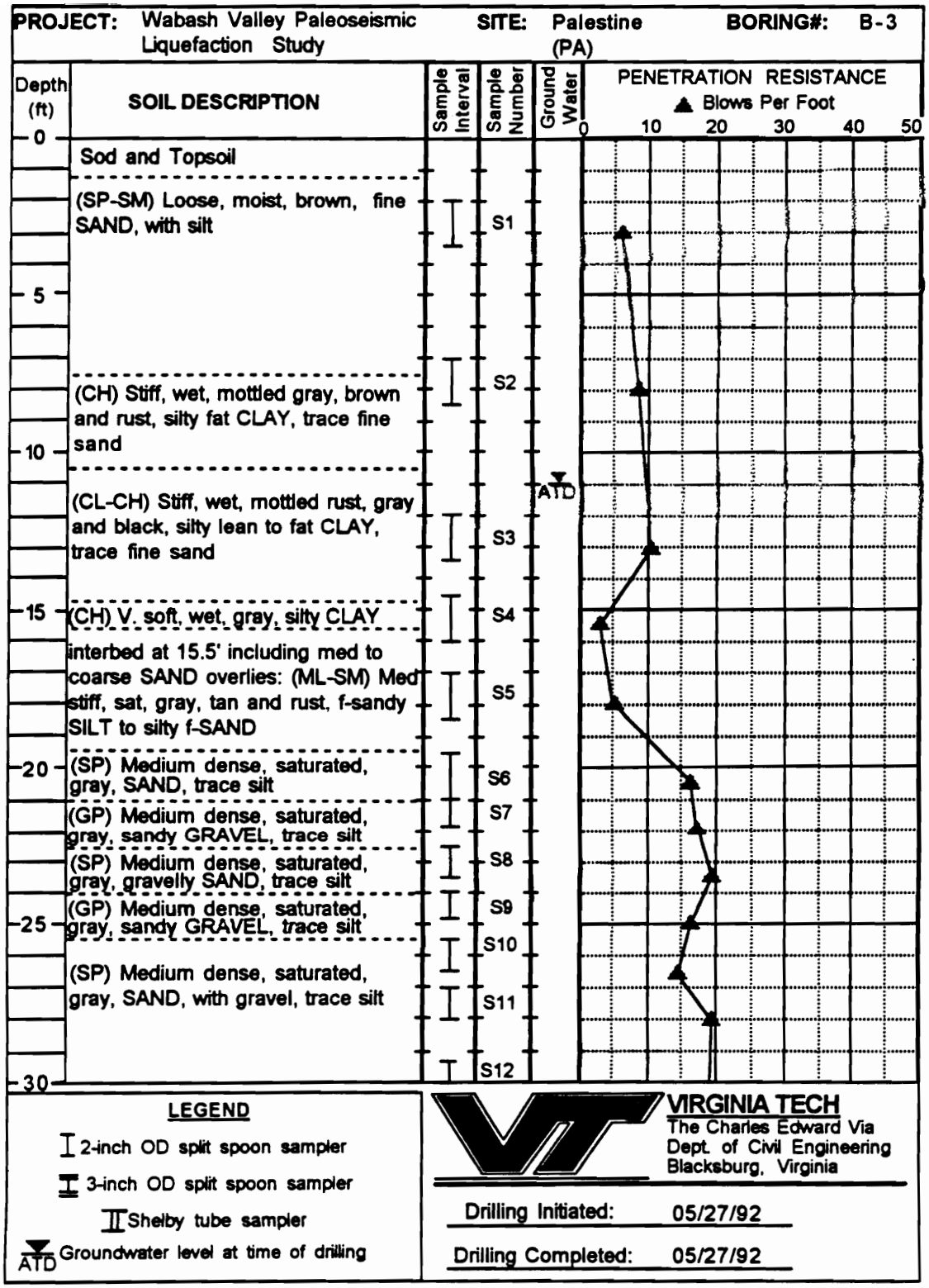
PROJECT: Wabash Valley Paleoseismic Liquefaction Study
SITE: Palestine (PA)
BORING#: B-3
Depth (ft)
SOIL DESCRIPTION
Sample Interval
Sample Number
Ground Water
PENETRATION RESISTANCE
Blows Per Foot
0
10
20
30
40
50
Sod and Topsoil
(SP-SM) Loose, moist, brown, fine SAND, with silt
S1
5
S2
(CH) Stiff, wet, mottled gray, brown and rust, silty fat CLAY, trace fine sand
10
ATD
(CL-CH) Stiff, wet, mottled rust, gray and black, silty lean to fat CLAY, trace fine sand
S3
15
(CH) V. soft, wet, gray, silty CLAY
S4
interbed at 15.5' including med to coarse SAND overlies: (ML-SM) Med stiff, sat, gray, tan and rust, f-sandy SILT to silty f-SAND
S5
20
(SP) Medium dense, saturated, gray, SAND, trace silt
S6
(GP) Medium dense, saturated, gray, sandy GRAVEL, trace silt
S7
(SP) Medium dense, saturated, gray, gravelly SAND, trace silt
S8
(GP) Medium dense, saturated, gray, sandy GRAVEL, trace silt
S9
25
S10
(SP) Medium dense, saturated, gray, SAND, with gravel, trace silt
S11
S12
30
LEGEND
2-inch OD split spoon sampler
3-inch OD split spoon sampler
Shelby tube sampler
ATD Groundwater level at time of drilling
VIRGINIA TECH
The Charles Edward Via Dept. of Civil Engineering Blacksburg, Virginia
Drilling Initiated: 05/27/92
Drilling Completed: 05/27/92

PROJECT: Wabash Valley Paleoseismic Liquefaction Study **SITE:** Palestine (PA) **BORING#:** B-3 (cont'd)

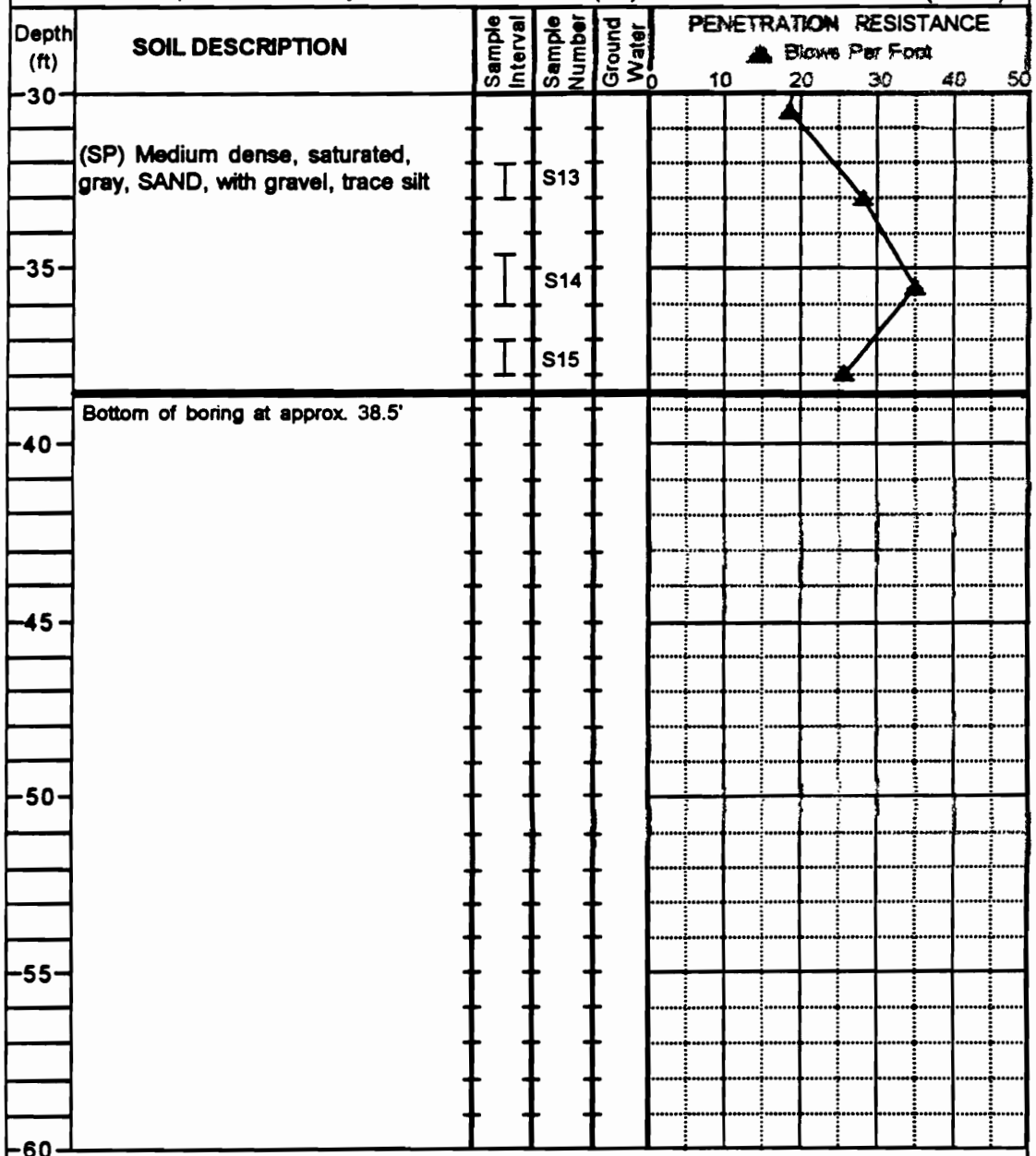

LEGEND

- 2-inch OD split spoon sampler
- 3-inch OD split spoon sampler
- Shelby tube sampler
- ATD Groundwater level at time of drilling

VIRGINIA TECH
The Charles Edward Via
Dept. of Civil Engineering
Blacksburg, Virginia

Drilling Initiated: 05/27/92

Drilling Completed: 05/27/92

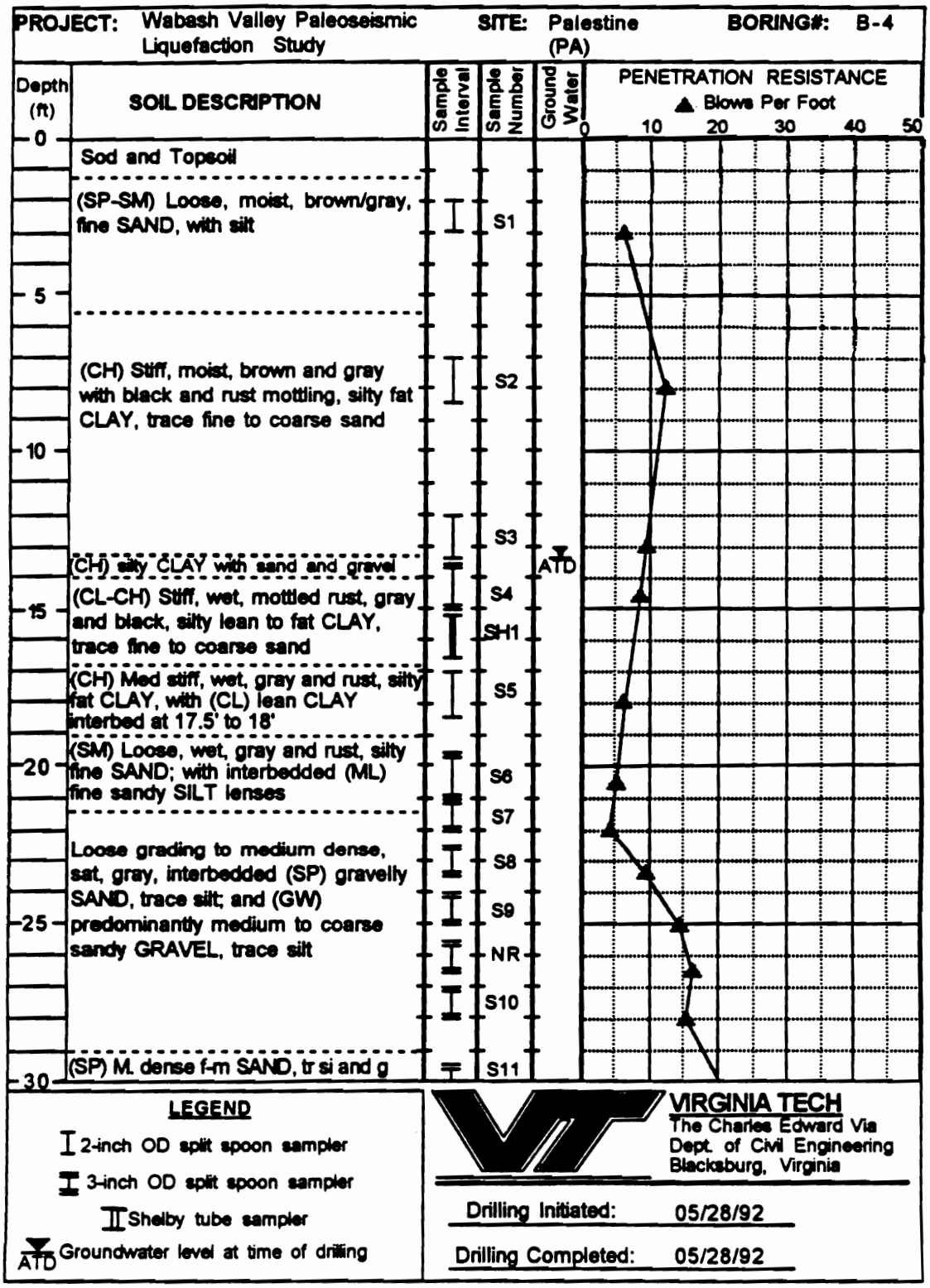
PROJECT: Wabash Valley Paleoseismic Liquefaction Study
SITE: Palestine (PA)
BORING#: B-4
Depth (ft)
SOIL DESCRIPTION
Sample Interval
Sample Number
Ground Water
PENETRATION RESISTANCE
Blows Per Foot
0
10
20
30
40
50
Sod and Topsoil
(SP-SM) Loose, moist, brown/gray, fine SAND, with silt
S1
5
(CH) Stiff, moist, brown and gray with black and rust mottling, silty fat CLAY, trace fine to coarse sand
S2
10
S3
(CH) silty CLAY with sand and gravel
ATD
(CL-CH) Stiff, wet, mottled rust, gray and black, silty lean to fat CLAY, trace fine to coarse sand
S4
15
SH1
(CH) Med stiff, wet, gray and rust, silty fat CLAY, with (CL) lean CLAY interbed at 17.5' to 18'
S5
(SM) Loose, wet, gray and rust, silty fine SAND; with interbedded (ML) fine sandy SILT lenses
20
S6
S7
Loose grading to medium dense, sat, gray, interbedded (SP) gravelly SAND, trace silt; and (GW) predominantly medium to coarse sandy GRAVEL, trace silt
S8
S9
25
NR
S10
(SP) M. dense f-m SAND, tr si and g
S11
30
LEGEND
2-inch OD split spoon sampler
3-inch OD split spoon sampler
Shelby tube sampler
ATD Groundwater level at time of drilling
VIRGINIA TECH
The Charles Edward Via Dept. of Civil Engineering Blacksburg, Virginia
Drilling Initiated: 05/28/92
Drilling Completed: 05/28/92

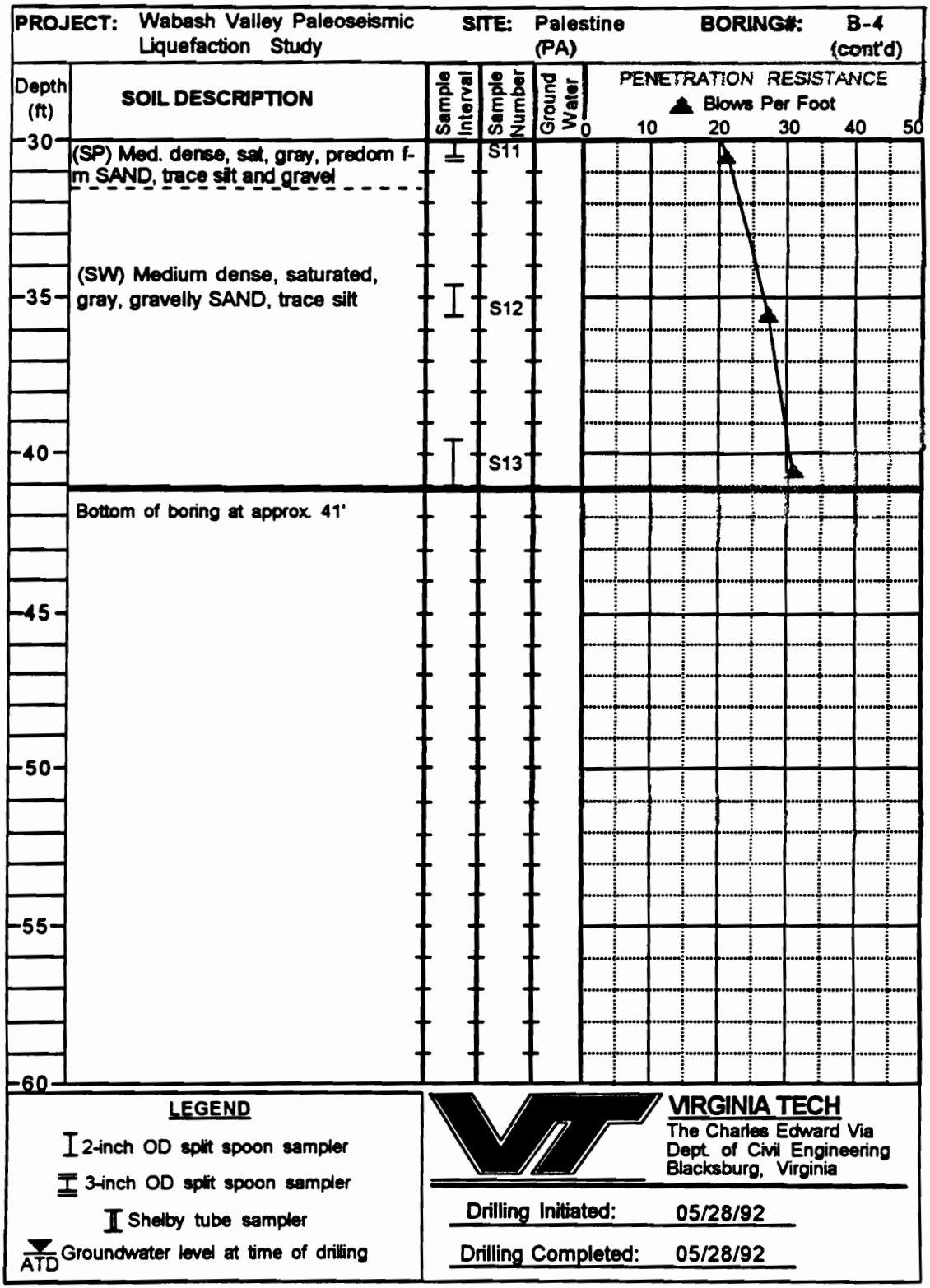
PROJECT: Wabash Valley Paleoseismic Liquefaction Study
SITE: Palestine (PA)
BORING#: B-4 (cont'd)
Depth (ft)
SOIL DESCRIPTION
Sample Interval
Sample Number
Ground Water
PENETRATION RESISTANCE
Blows Per Foot
0 10 20 30 40 50
30
(SP) Med. dense, sat, gray, predom f-m SAND, trace silt and gravel
S11
35
(SW) Medium dense, saturated, gray, gravelly SAND, trace silt
S12
40
S13
Bottom of boring at approx. 41'
45
50
55
60
LEGEND
2-inch OD split spoon sampler
3-inch OD split spoon sampler
Shelby tube sampler
ATD Groundwater level at time of drilling
VIRGINIA TECH
The Charles Edward Via Dept. of Civil Engineering Blacksburg, Virginia
Drilling Initiated: 05/28/92
Drilling Completed: 05/28/92

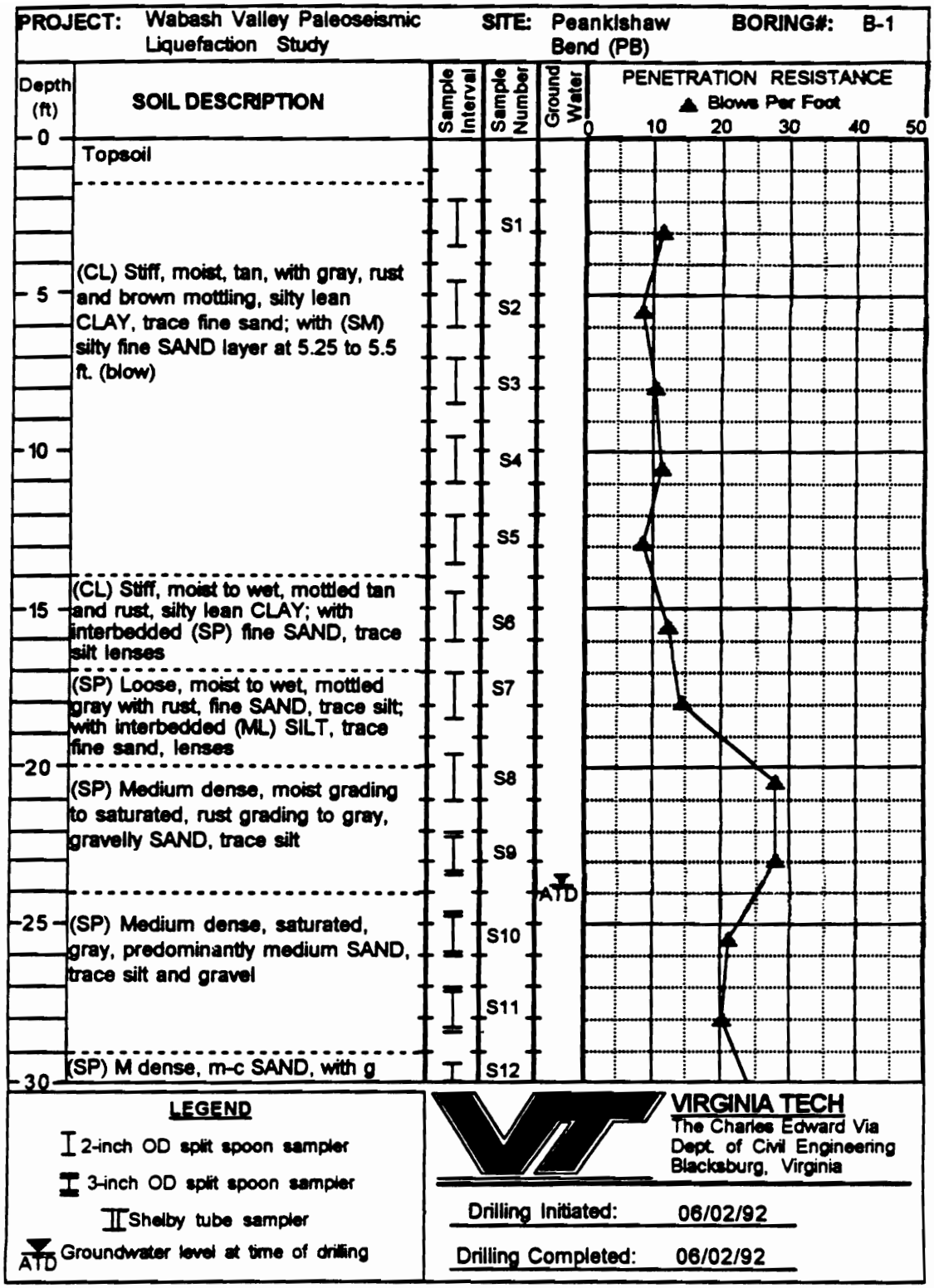
PROJECT: Wabash Valley Paleoseismic Liquefaction Study
SITE: Peankishaw Bend (PB)
BORING#: B-1
Depth (ft)
SOIL DESCRIPTION
Sample Interval
Sample Number
Ground Water
PENETRATION RESISTANCE
Blows Per Foot
0
10
20
30
40
50
Topsoil
(CL) Stiff, moist, tan, with gray, rust and brown mottling, silty lean CLAY, trace fine sand; with (SM) silty fine SAND layer at 5.25 to 5.5 ft. (blow)
(CL) Stiff, moist to wet, mottled tan and rust, silty lean CLAY; with interbedded (SP) fine SAND, trace silt lenses
(SP) Loose, moist to wet, mottled gray with rust, fine SAND, trace silt; with interbedded (ML) SILT, trace fine sand, lenses
(SP) Medium dense, moist grading to saturated, rust grading to gray, gravelly SAND, trace silt
(SP) Medium dense, saturated, gray, predominantly medium SAND, trace silt and gravel
(SP) M dense, m-c SAND, with g
S1
S2
S3
S4
S5
S6
S7
S8
S9
S10
S11
S12
ATD
5
10
15
20
25
30
LEGEND
2-inch OD split spoon sampler
3-inch OD split spoon sampler
Shelby tube sampler
Groundwater level at time of drilling
VIRGINIA TECH
The Charles Edward Via Dept. of Civil Engineering Blacksburg, Virginia
Drilling Initiated: 06/02/92
Drilling Completed: 06/02/92

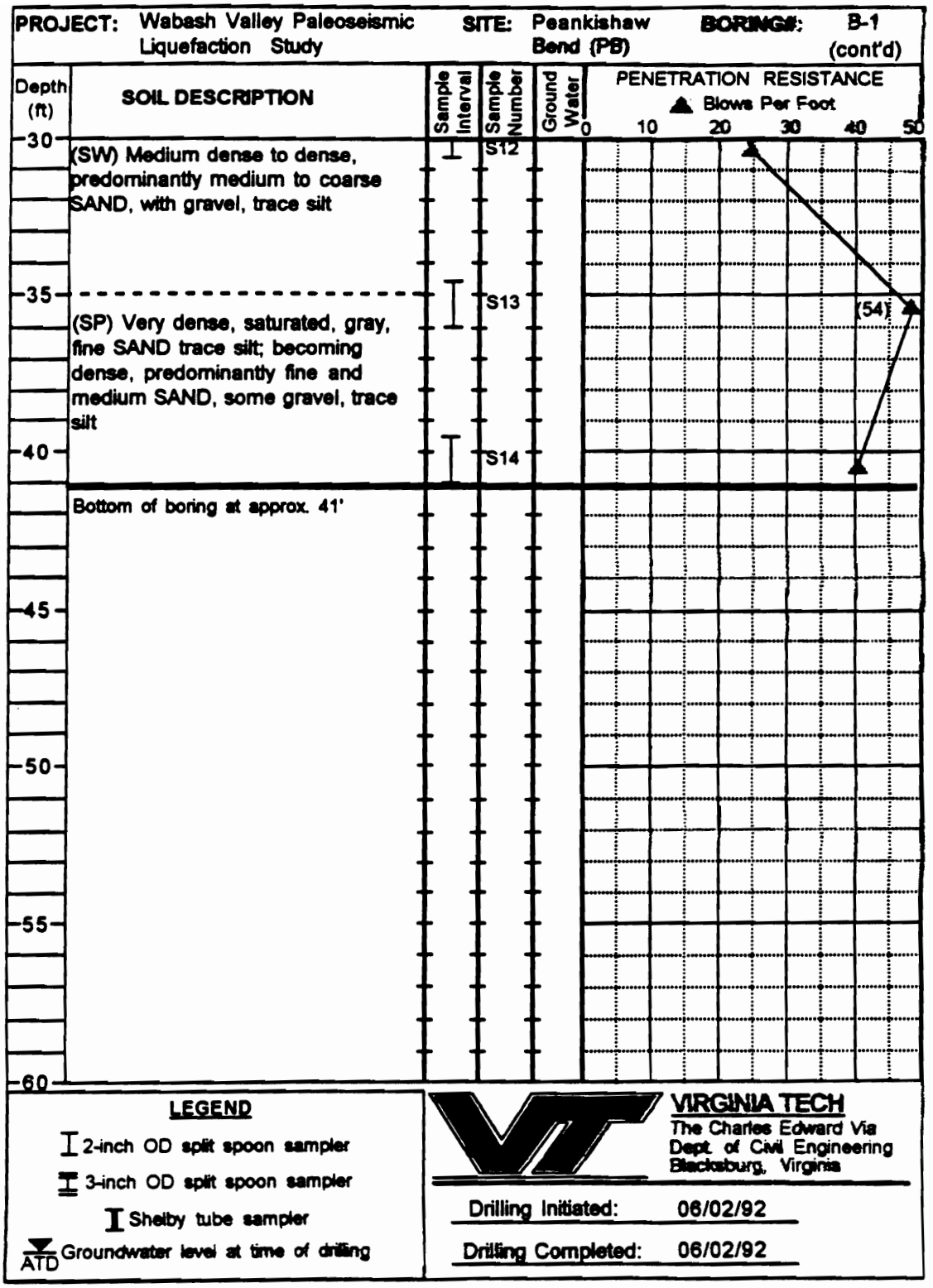
PROJECT: Wabash Valley Paleoseismic Liquefaction Study
SITE: Peankishaw Bend (PB)
BORING#: B-1 (cont'd)
Depth (ft)
SOIL DESCRIPTION
Sample Interval
Sample Number
Ground Water
PENETRATION RESISTANCE
Blows Per Foot
0 10 20 30 40 50
30
(SW) Medium dense to dense, predominantly medium to coarse SAND, with gravel, trace silt
S12
35
(SP) Very dense, saturated, gray, fine SAND trace silt; becoming dense, predominantly fine and medium SAND, some gravel, trace silt
S13
(54)
40
S14
Bottom of boring at approx. 41'
45
50
55
60
LEGEND
2-inch OD split spoon sampler
3-inch OD split spoon sampler
Shelby tube sampler
ATD Groundwater level at time of drilling
VIRGINIA TECH
The Charles Edward Via Dept. of Civil Engineering Blacksburg, Virginia
Drilling Initiated: 06/02/92
Drilling Completed: 06/02/92

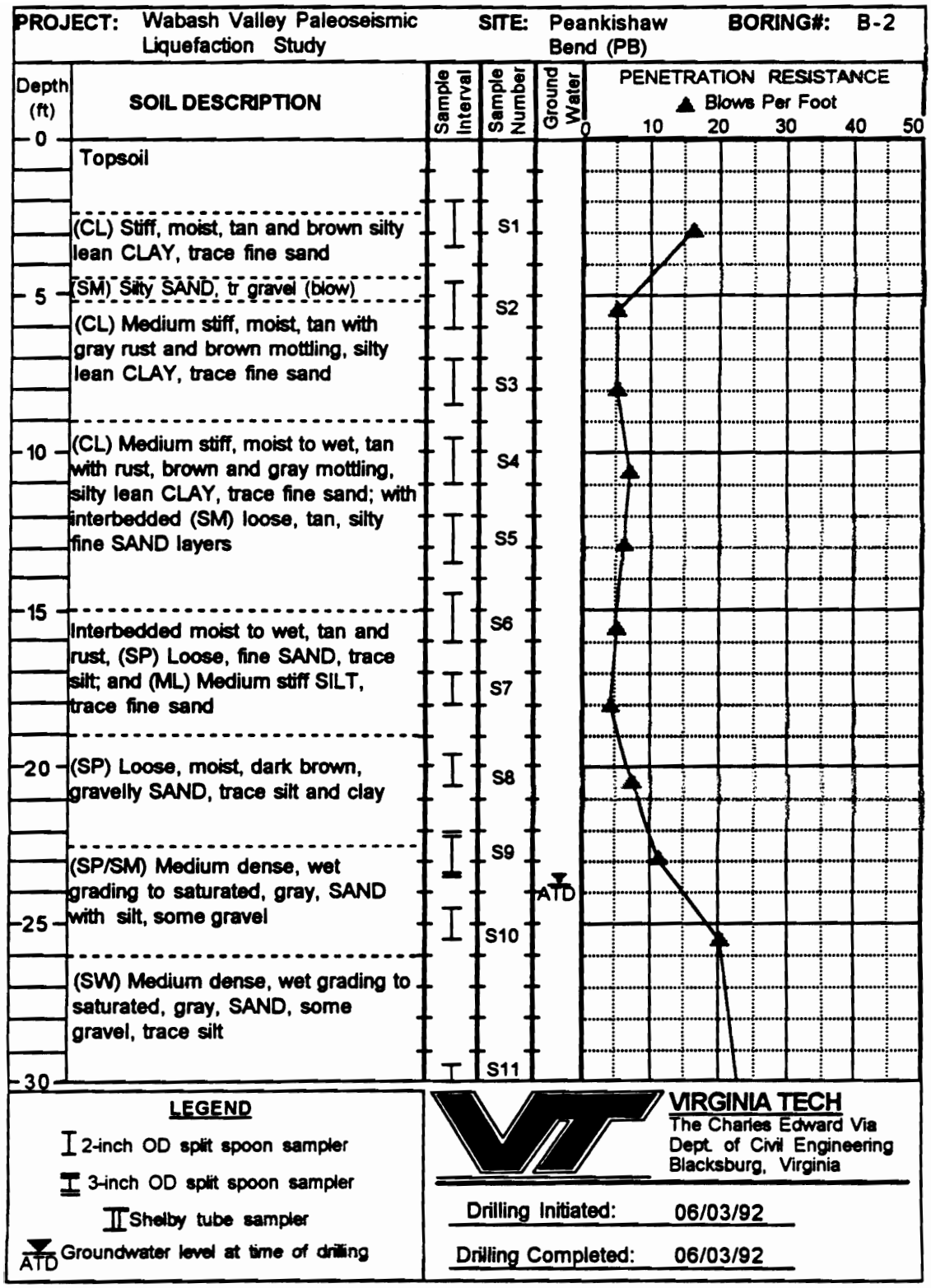
PROJECT: Wabash Valley Paleoseismic Liquefaction Study
SITE: Peankishaw Bend (PB)
BORING#: B-2
Depth (ft)
SOIL DESCRIPTION
Sample Interval
Sample Number
Ground Water
PENETRATION RESISTANCE
Blows Per Foot
0
10
20
30
40
50
0
Topsoil
(CL) Stiff, moist, tan and brown silty lean CLAY, trace fine sand
S1
5
(SM) Silty SAND, tr gravel (blow)
(CL) Medium stiff, moist, tan with gray rust and brown mottling, silty lean CLAY, trace fine sand
S2
S3
10
(CL) Medium stiff, moist to wet, tan with rust, brown and gray mottling, silty lean CLAY, trace fine sand; with interbedded (SM) loose, tan, silty fine SAND layers
S4
S5
15
Interbedded moist to wet, tan and rust, (SP) Loose, fine SAND, trace silt; and (ML) Medium stiff SILT, trace fine sand
S6
S7
20
(SP) Loose, moist, dark brown, gravelly SAND, trace silt and clay
S8
S9
(SP/SM) Medium dense, wet grading to saturated, gray, SAND with silt, some gravel
ATD
25
S10
(SW) Medium dense, wet grading to saturated, gray, SAND, some gravel, trace silt
S11
30
LEGEND
2-inch OD split spoon sampler
3-inch OD split spoon sampler
Shelby tube sampler
ATD Groundwater level at time of drilling
VIRGINIA TECH
The Charles Edward Via Dept. of Civil Engineering Blacksburg, Virginia
Drilling Initiated: 06/03/92
Drilling Completed: 06/03/92

PROJECT: Wabash Valley Paleoseismic Liquefaction Study **SITE:** Peankishaw Bend (PB) **BORING#:** B-2 (cont'd)

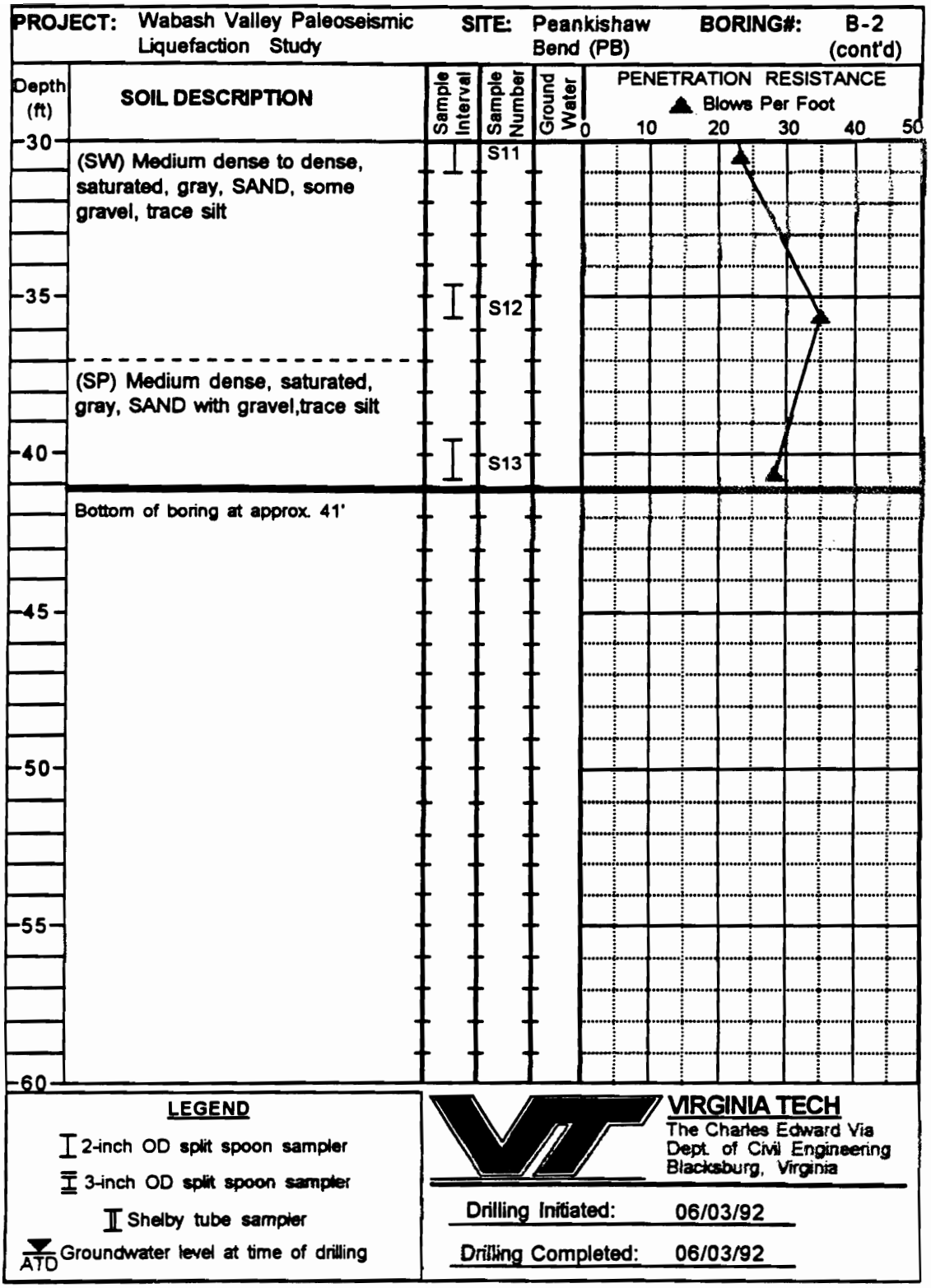

LEGEND

- 2-inch OD split spoon sampler
- 3-inch OD split spoon sampler
- Shelby tube sampler
- ATD Groundwater level at time of drilling

VIRGINIA TECH
The Charles Edward Via Dept. of Civil Engineering Blacksburg, Virginia

Drilling Initiated: 06/03/92

Drilling Completed: 06/03/92

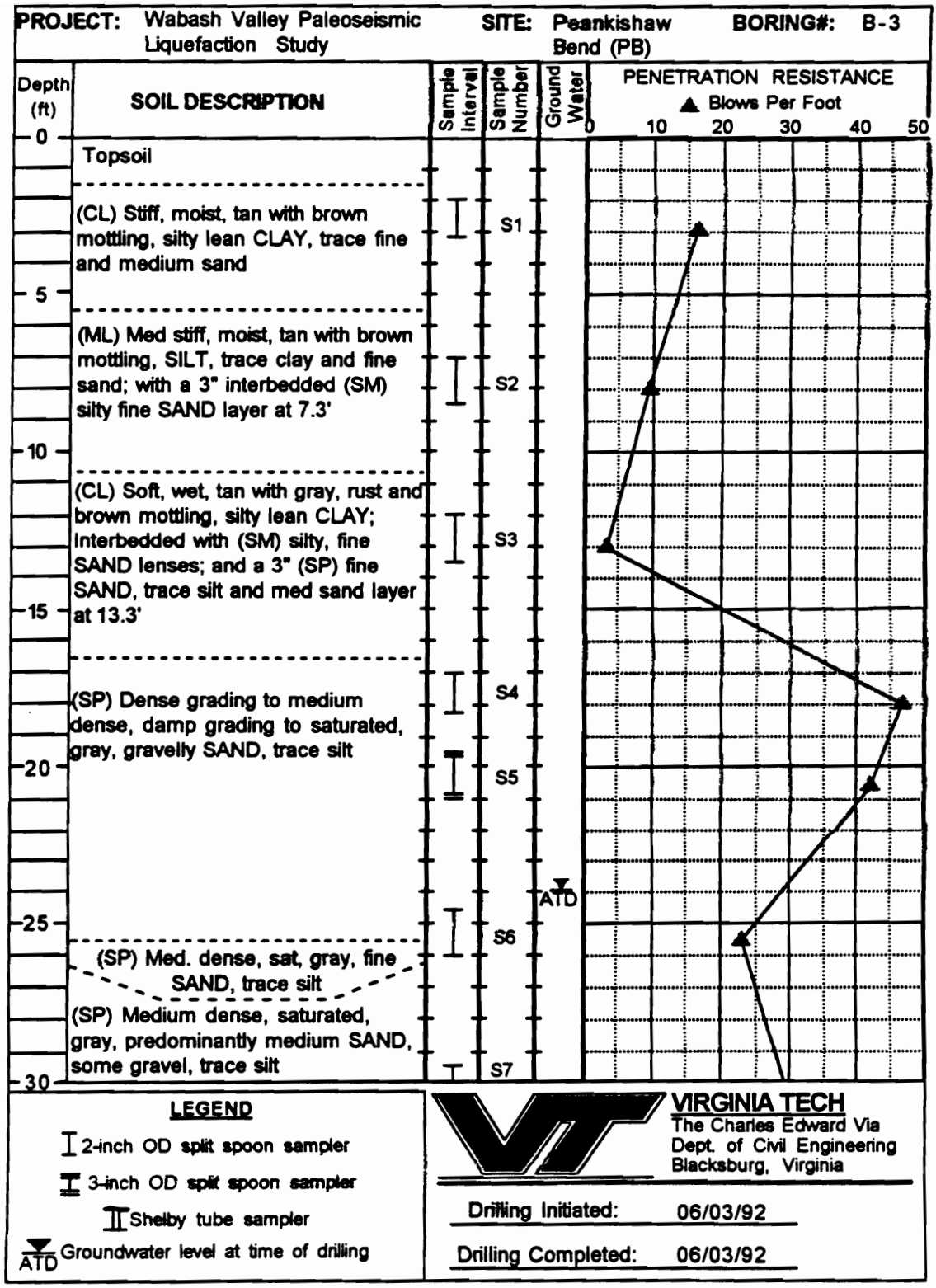
PROJECT: Wabash Valley Paleoseismic Liquefaction Study
SITE: Peankishaw Bend (PB)
BORING#: B-3
Depth (ft)
SOIL DESCRIPTION
Sample Interval
Sample Number
Ground Water
PENETRATION RESISTANCE
Blows Per Foot
0
10
20
30
40
50
0
5
10
15
20
25
30
Topsoil
(CL) Stiff, moist, tan with brown mottling, silty lean CLAY, trace fine and medium sand
(ML) Med stiff, moist, tan with brown mottling, SILT, trace clay and fine sand; with a 3" interbedded (SM) silty fine SAND layer at 7.3'
(CL) Soft, wet, tan with gray, rust and brown mottling, silty lean CLAY; interbedded with (SM) silty, fine SAND lenses; and a 3" (SP) fine SAND, trace silt and med sand layer at 13.3'
(SP) Dense grading to medium dense, damp grading to saturated, gray, gravelly SAND, trace silt
(SP) Med. dense, sat, gray, fine SAND, trace silt
(SP) Medium dense, saturated, gray, predominantly medium SAND, some gravel, trace silt
S1
S2
S3
S4
S5
S6
S7
ATD
LEGEND
2-inch OD split spoon sampler
3-inch OD split spoon sampler
Shelby tube sampler
ATD Groundwater level at time of drilling
VIRGINIA TECH
The Charles Edward Via Dept. of Civil Engineering Blacksburg, Virginia
Drilling Initiated: 06/03/92
Drilling Completed: 06/03/92

PROJECT: Wabash Valley Paleoseismic Liquefaction Study **SITE:** Peankishaw Bend (PB) **BORING#:** B-3 (cont'd)

Depth (ft)	SOIL DESCRIPTION	Sample Interval	Sample Number	Ground Water	PENETRATION RESISTANCE ▲ Blows Per Foot 0 10 20 30 40 50
30	(SP) Medium dense, saturated, gray, predominantly medium SAND, some gravel, trace silt		S7		
35			S8		
	Bottom of boring at approx. 36'				
40					
45					
50					
55					
60					

LEGEND

- 2-inch OD split spoon sampler
- 3-inch OD split spoon sampler
- Shelby tube sampler
- ATD Groundwater level at time of drilling

VIRGINIA TECH
The Charles Edward Via Dept. of Civil Engineering
Blacksburg, Virginia

Drilling Initiated: 06/03/92

Drilling Completed: 06/03/92

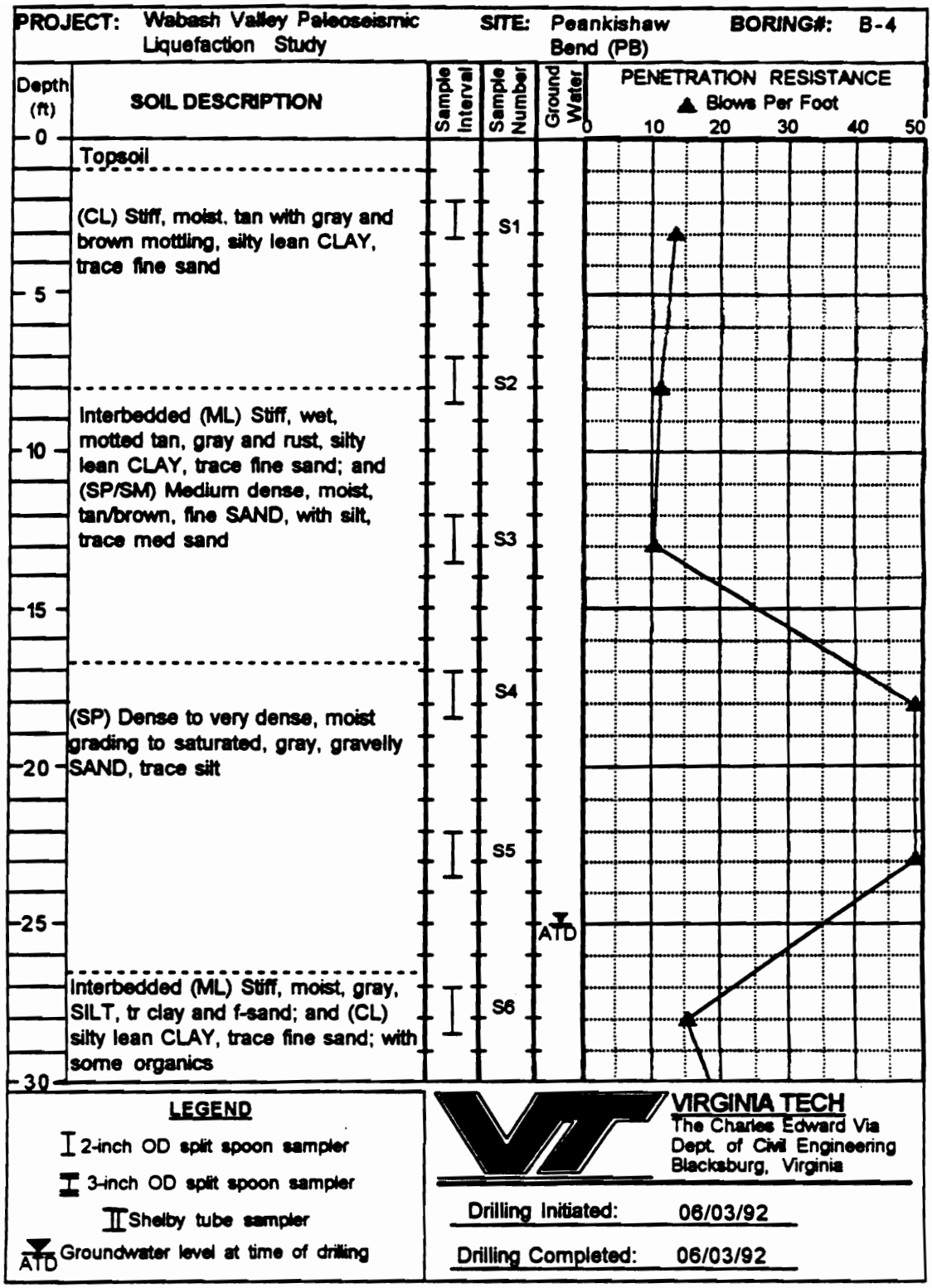
PROJECT: Wabash Valley Paleoseismic Liquefaction Study
SITE: Peankishaw Bend (PB)
BORING#: B-4
Depth (ft)
SOIL DESCRIPTION
Sample Interval
Sample Number
Ground Water
PENETRATION RESISTANCE
Blows Per Foot
0
10
20
30
40
50
0
5
10
15
20
25
30
Topsoil
(CL) Stiff, moist, tan with gray and brown mottling, silty lean CLAY, trace fine sand
Interbedded (ML) Stiff, wet, motted tan, gray and rust, silty lean CLAY, trace fine sand; and (SP/SM) Medium dense, moist, tan/brown, fine SAND, with silt, trace med sand
(SP) Dense to very dense, moist grading to saturated, gray, gravelly SAND, trace silt
Interbedded (ML) Stiff, moist, gray, SILT, tr clay and f-sand; and (CL) silty lean CLAY, trace fine sand; with some organics
S1
S2
S3
S4
S5
S6
ATD
LEGEND
2-inch OD split spoon sampler
3-inch OD split spoon sampler
Shelby tube sampler
Groundwater level at time of drilling
VIRGINIA TECH
The Charles Edward Via Dept. of Civil Engineering Blacksburg, Virginia
Drilling Initiated: 06/03/92
Drilling Completed: 06/03/92

PROJECT: Wabash Valley Paleoseismic Liquefaction Study

SITE: Peankishaw Bend (PB)

BORING#: B-4 (cont'd)

Depth (ft)	SOIL DESCRIPTION	Sample Interval	Sample Number	Ground Water	PENETRATION RESISTANCE ▲ Blows Per Foot 0 10 20 30 40 50
30	(SP) Medium dense, saturated, gray, fine SAND, trace silt; with interbedded, (ML) very stiff, laminated gray and rust, SILT, trace clay and fine sand		S7		
35	Bottom of boring at approx. 36'				
40					
45					
50					
55					
60					

LEGEND

- 2-inch OD split spoon sampler
- 3-inch OD split spoon sampler
- Shelby tube sampler
- ATD Groundwater level at time of drilling

VIRGINIA TECH
The Charles Edward Via
Dept. of Civil Engineering
Blacksburg, Virginia

Drilling Initiated: 06/03/92

Drilling Completed: 06/03/92

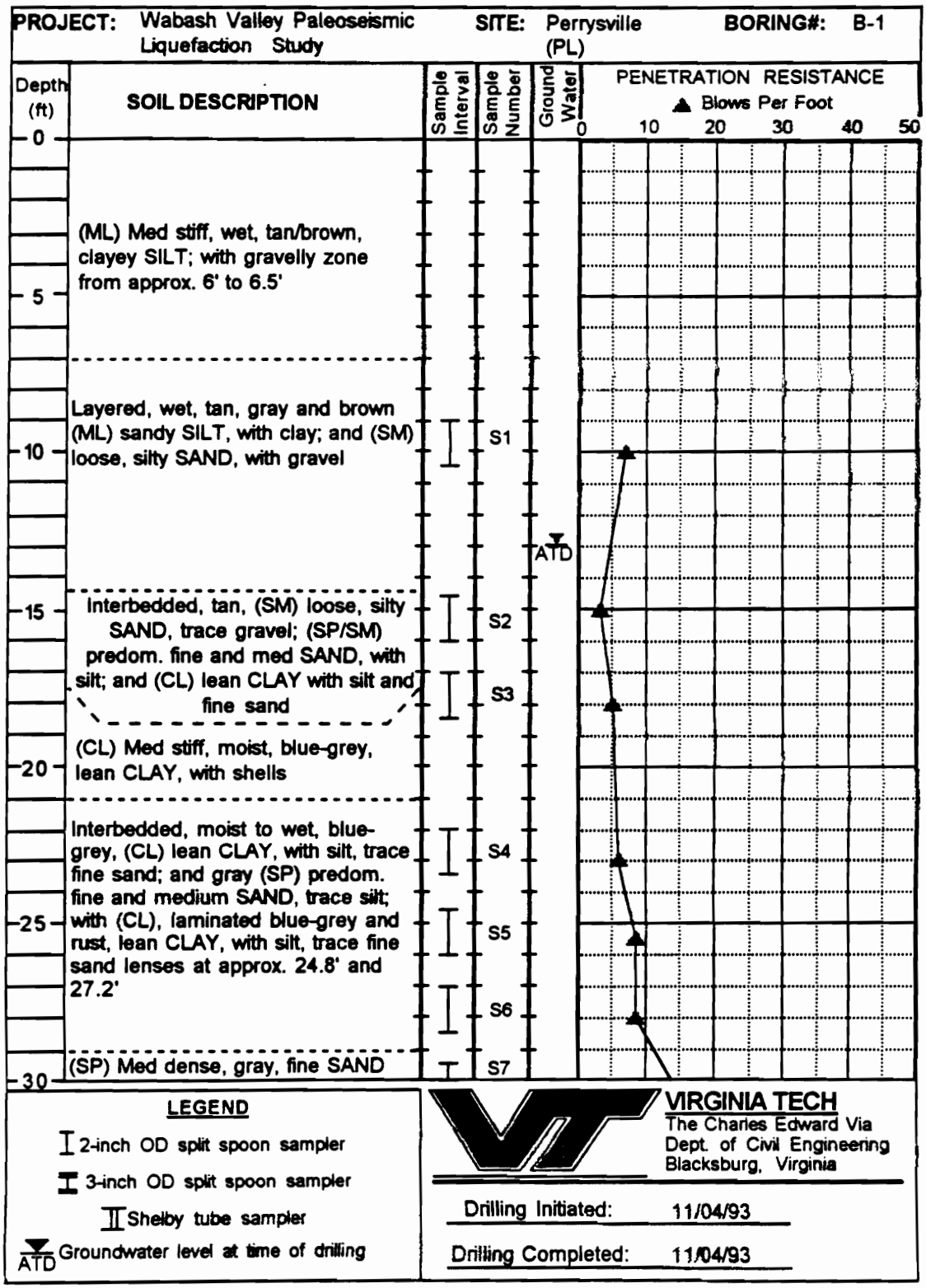
PROJECT: Wabash Valley Paleoseismic Liquefaction Study
SITE: Perrysville (PL)
BORING#: B-1
Depth (ft)
SOIL DESCRIPTION
Sample Interval
Sample Number
Ground Water
PENETRATION RESISTANCE
Blows Per Foot
0
10
20
30
40
50
0
5
10
15
20
25
30
(ML) Med stiff, wet, tan/brown, clayey SILT; with gravelly zone from approx. 6' to 6.5'
Layered, wet, tan, gray and brown (ML) sandy SILT, with clay; and (SM) loose, silty SAND, with gravel
S1
ATD
Interbedded, tan, (SM) loose, silty SAND, trace gravel; (SP/SM) predom. fine and med SAND, with silt; and (CL) lean CLAY with silt and fine sand
S2
S3
(CL) Med stiff, moist, blue-grey, lean CLAY, with shells
Interbedded, moist to wet, blue-grey, (CL) lean CLAY, with silt, trace fine sand; and gray (SP) predom. fine and medium SAND, trace silt; with (CL), laminated blue-grey and rust, lean CLAY, with silt, trace fine sand lenses at approx. 24.8' and 27.2'
S4
S5
S6
(SP) Med dense, gray, fine SAND
S7
LEGEND
2-inch OD split spoon sampler
3-inch OD split spoon sampler
Shelby tube sampler
ATD Groundwater level at time of drilling
VIRGINIA TECH
The Charles Edward Via
Dept. of Civil Engineering
Blacksburg, Virginia
Drilling Initiated: 11/04/93
Drilling Completed: 11/04/93

PROJECT: Wabash Valley Paleoseismic Liquefaction Study **SITE:** Perrysville (PL) **BORING#:** B-1 (cont'd)

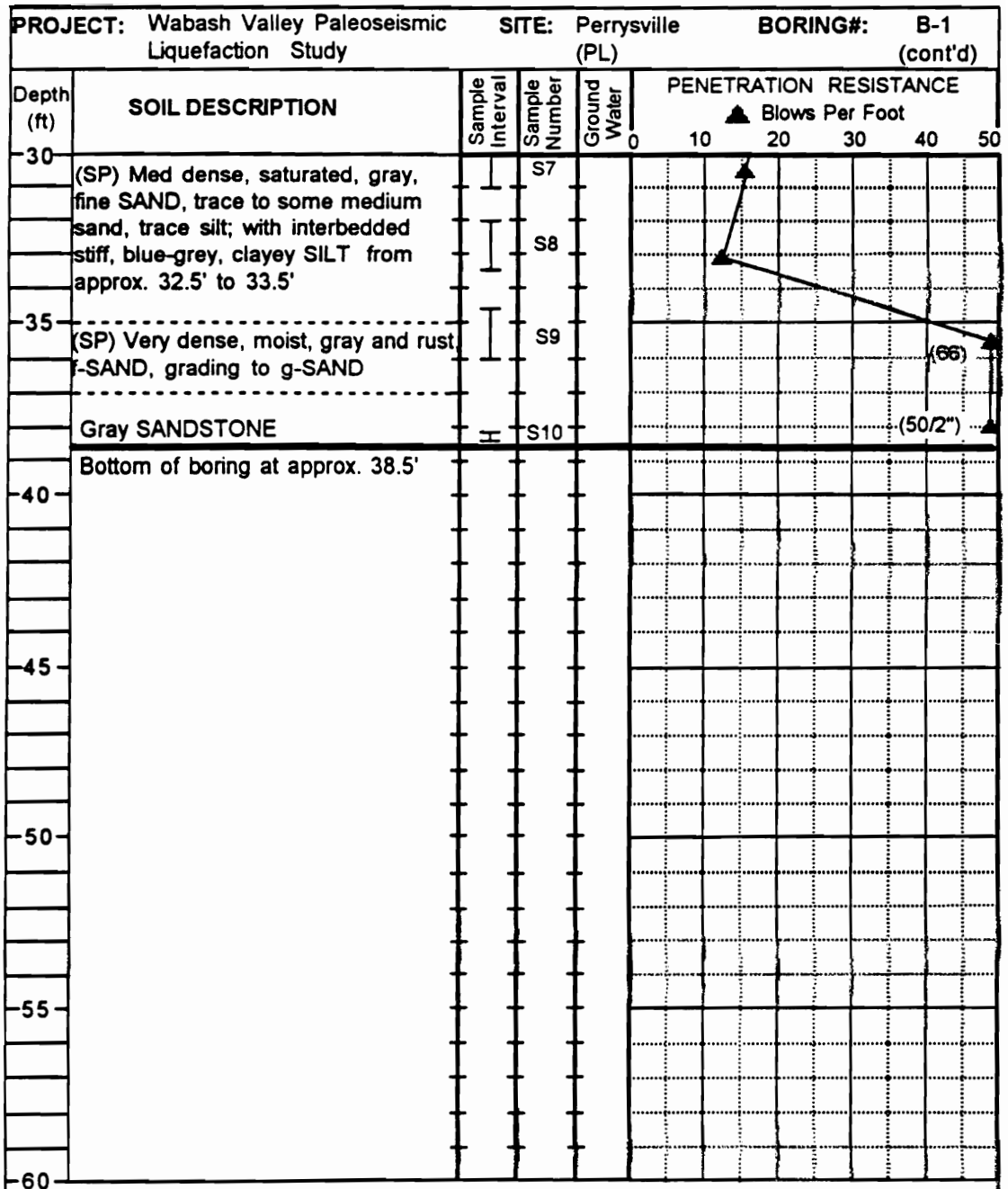

LEGEND

- 2-inch OD split spoon sampler
- 3-inch OD split spoon sampler
- Shelby tube sampler
- ATD Groundwater level at time of drilling

VIRGINIA TECH
The Charles Edward Via Dept. of Civil Engineering
Blacksburg, Virginia

Drilling Initiated: 11/04/93

Drilling Completed: 11/04/93

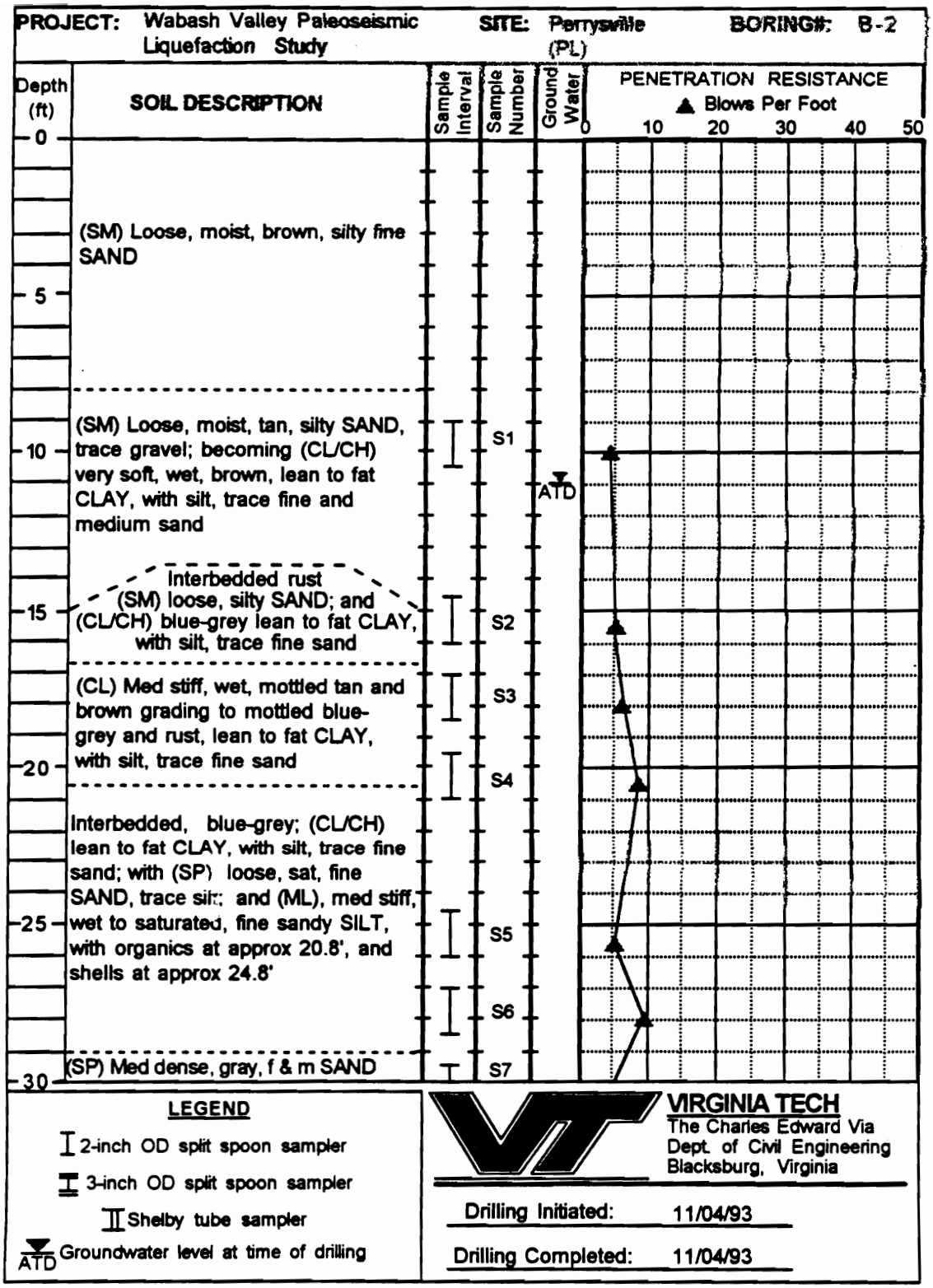
PROJECT: Wabash Valley Paleoseismic Liquefaction Study
SITE: Perrysville (PL)
BORING#: B-2
Depth (ft)
SOIL DESCRIPTION
Sample Interval
Sample Number
Ground Water
PENETRATION RESISTANCE
Blows Per Foot
0
10
20
30
40
50
5
10
15
20
25
30
(SM) Loose, moist, brown, silty fine SAND
(SM) Loose, moist, tan, silty SAND, trace gravel; becoming (CL/CH) very soft, wet, brown, lean to fat CLAY, with silt, trace fine and medium sand
ATD
Interbedded rust (SM) loose, silty SAND; and (CL/CH) blue-grey lean to fat CLAY, with silt, trace fine sand
(CL) Med stiff, wet, mottled tan and brown grading to mottled blue-grey and rust, lean to fat CLAY, with silt, trace fine sand
Interbedded, blue-grey; (CL/CH) lean to fat CLAY, with silt, trace fine sand; with (SP) loose, sat, fine SAND, trace silt; and (ML), med stiff, wet to saturated, fine sandy SILT, with organics at approx 20.8', and shells at approx 24.8'
(SP) Med dense, gray, f & m SAND
S1
S2
S3
S4
S5
S6
S7
LEGEND
2-inch OD split spoon sampler
3-inch OD split spoon sampler
Shelby tube sampler
ATD Groundwater level at time of drilling
VIRGINIA TECH
The Charles Edward Via Dept. of Civil Engineering Blacksburg, Virginia
Drilling Initiated: 11/04/93
Drilling Completed: 11/04/93

PROJECT: Wabash Valley Paleoseismic Liquefaction Study **SITE:** Perrysville (PL) **BORING#:** B-2 (cont'd)

Depth (ft)	SOIL DESCRIPTION	Sample Interval	Sample Number	Ground Water	PENETRATION RESISTANCE ▲ Blows Per Foot 0 10 20 30 40 50
30	(SP) Loose, fine SAND; grading to weathered and then fresh SANDSTONE		S7		(50/6")
			S8		
	Bottom of boring at approx. 32.5'				
35					
40					
45					
50					
55					
60					

LEGEND

- 2-inch OD split spoon sampler
- 3-inch OD split spoon sampler
- Shelby tube sampler
- ATD Groundwater level at time of drilling

VIRGINIA TECH
The Charles Edward Via Dept. of Civil Engineering
Blacksburg, Virginia

Drilling Initiated: 11/04/93

Drilling Completed: 11/04/93

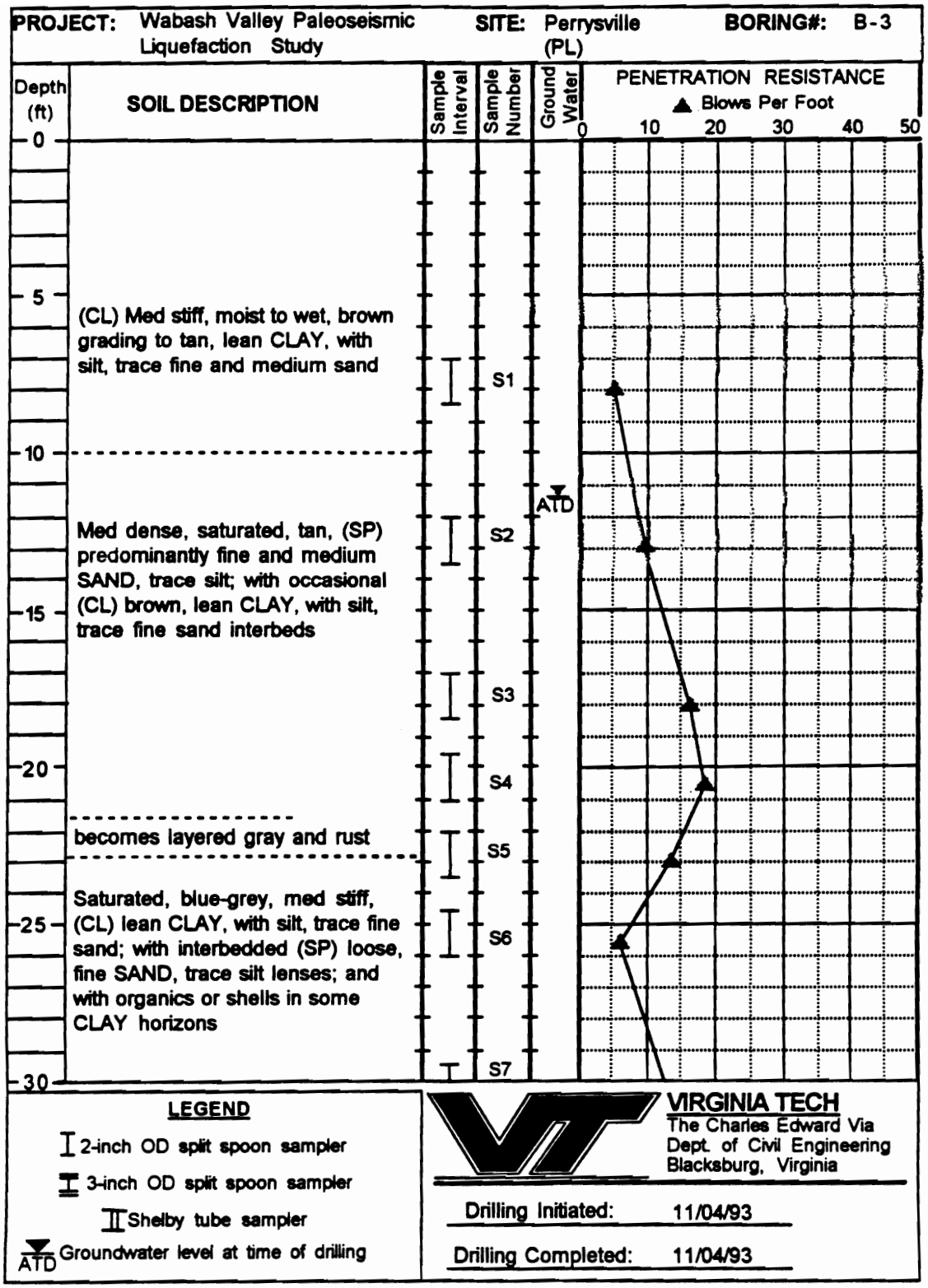
PROJECT: Wabash Valley Paleoseismic Liquefaction Study
SITE: Perrysville (PL)
BORING#: B-3
Depth (ft)
SOIL DESCRIPTION
Sample Interval
Sample Number
Ground Water
PENETRATION RESISTANCE
Blows Per Foot
0
10
20
30
40
50
0
5
10
15
20
25
30
(CL) Med stiff, moist to wet, brown grading to tan, lean CLAY, with silt, trace fine and medium sand
Med dense, saturated, tan, (SP) predominantly fine and medium SAND, trace silt; with occasional (CL) brown, lean CLAY, with silt, trace fine sand interbeds
becomes layered gray and rust
Saturated, blue-grey, med stiff, (CL) lean CLAY, with silt, trace fine sand; with interbedded (SP) loose, fine SAND, trace silt lenses; and with organics or shells in some CLAY horizons
S1
S2
S3
S4
S5
S6
S7
ATD
LEGEND
2-inch OD split spoon sampler
3-inch OD split spoon sampler
Shelby tube sampler
Groundwater level at time of drilling
VIRGINIA TECH
The Charles Edward Via
Dept. of Civil Engineering
Blacksburg, Virginia
Drilling Initiated: 11/04/93
Drilling Completed: 11/04/93

PROJECT: Wabash Valley Paleoseismic Liquefaction Study | SITE: Perrysville (PL) | BORING#: B-3 (cont'd)

Depth (ft)	SOIL DESCRIPTION	Sample Interval	Sample Number	Ground Water	PENETRATION RESISTANCE ▲ Blows Per Foot 0 10 20 30 40 50
30	(CL) Stiff, blue-grey CLAY, with shells and (SP) fine SAND lenses		S7		
	Weathered grading to fresh SANDSTONE		S8		(100/9")
	Bottom of boring at approx. 33.5'				
35					
40					
45					
50					
55					
60					

LEGEND

- 2-inch OD split spoon sampler
- 3-inch OD split spoon sampler
- Shelby tube sampler
- ATD Groundwater level at time of drilling

VIRGINIA TECH
The Charles Edward Via
Dept. of Civil Engineering
Blacksburg, Virginia

Drilling Initiated: 11/04/93

Drilling Completed: 11/04/93

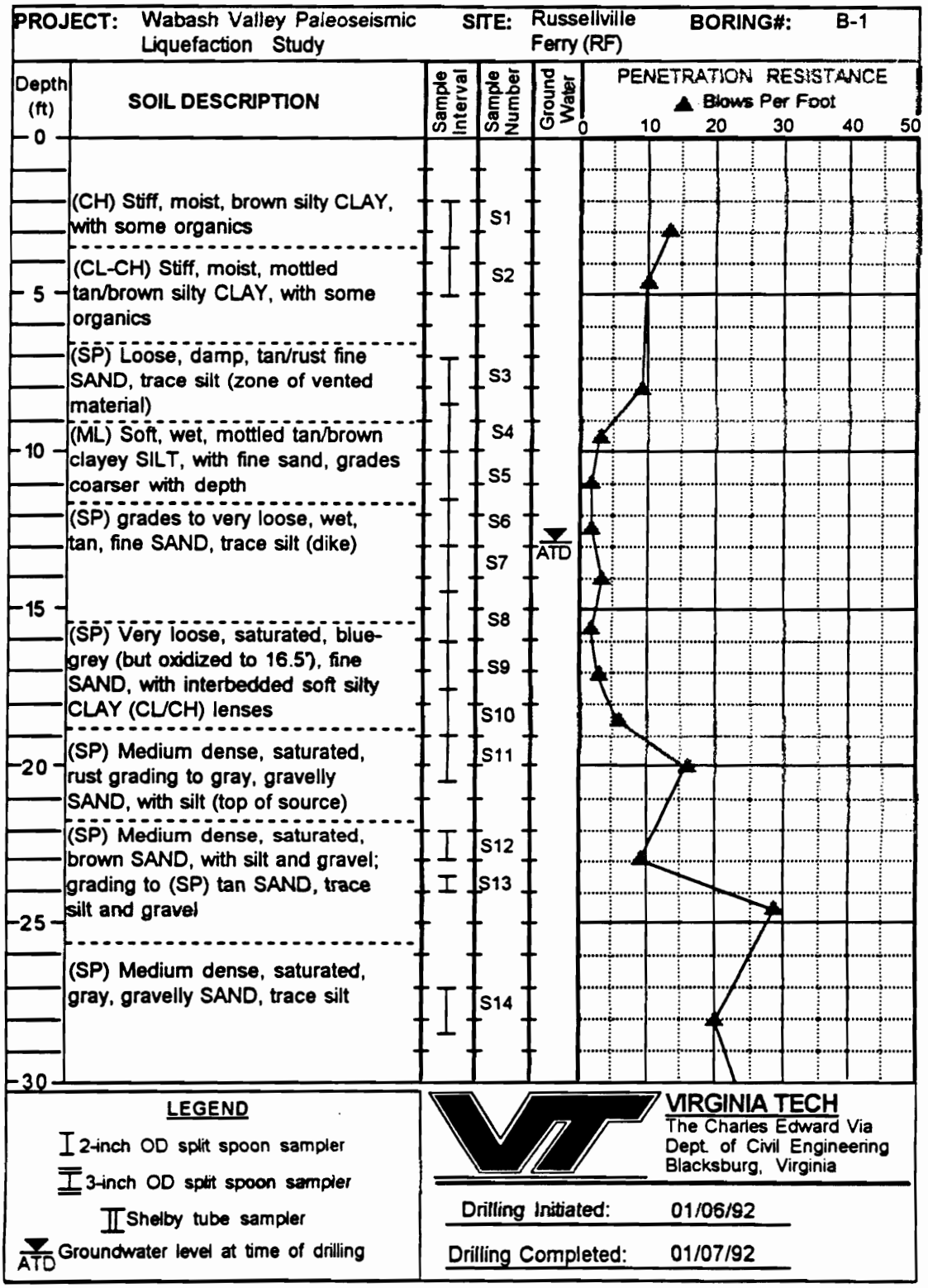
PROJECT: Wabash Valley Paleoseismic Liquefaction Study
SITE: Russellville Ferry (RF)
BORING#: B-1
Depth (ft)
SOIL DESCRIPTION
Sample Interval
Sample Number
Ground Water
PENETRATION RESISTANCE
Blows Per Foot
0
10
20
30
40
50
0
5
10
15
20
25
30
(CH) Stiff, moist, brown silty CLAY, with some organics
(CL-CH) Stiff, moist, mottled tan/brown silty CLAY, with some organics
(SP) Loose, damp, tan/rust fine SAND, trace silt (zone of vented material)
(ML) Soft, wet, mottled tan/brown clayey SILT, with fine sand, grades coarser with depth
(SP) grades to very loose, wet, tan, fine SAND, trace silt (dike)
(SP) Very loose, saturated, blue-grey (but oxidized to 16.5'), fine SAND, with interbedded soft silty CLAY (CL/CH) lenses
(SP) Medium dense, saturated, rust grading to gray, gravelly SAND, with silt (top of source)
(SP) Medium dense, saturated, brown SAND, with silt and gravel; grading to (SP) tan SAND, trace silt and gravel
(SP) Medium dense, saturated, gray, gravelly SAND, trace silt
S1
S2
S3
S4
S5
S6
S7
S8
S9
S10
S11
S12
S13
S14
ATD
LEGEND
2-inch OD split spoon sampler
3-inch OD split spoon sampler
Shelby tube sampler
Groundwater level at time of drilling
VIRGINIA TECH
The Charles Edward Via Dept. of Civil Engineering Blacksburg, Virginia
Drilling Initiated: 01/06/92
Drilling Completed: 01/07/92

PROJECT: Wabash Valley Paleoseismic Liquefaction Study

SITE: Russellville Ferry (RF)

BORING#: B-1 (cont'd)

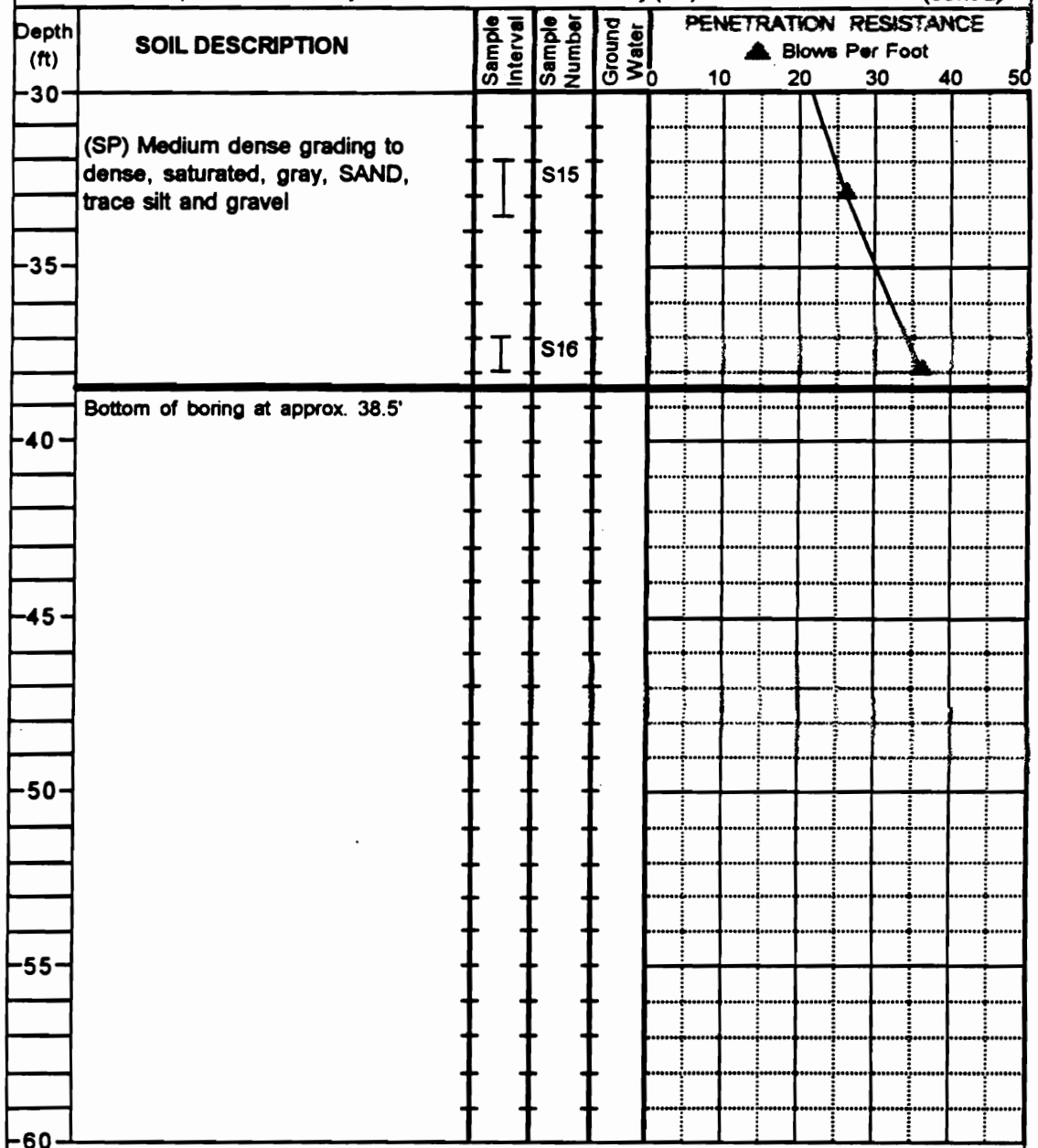

LEGEND

- 2-inch OD split spoon sampler
- 3-inch OD split spoon sampler
- Shelby tube sampler
- ATD Groundwater level at time of drilling

VIRGINIA TECH
The Charles Edward Via
Dept. of Civil Engineering
Blacksburg, Virginia

Drilling Initiated: 01/06/92

Drilling Completed: 01/07/92

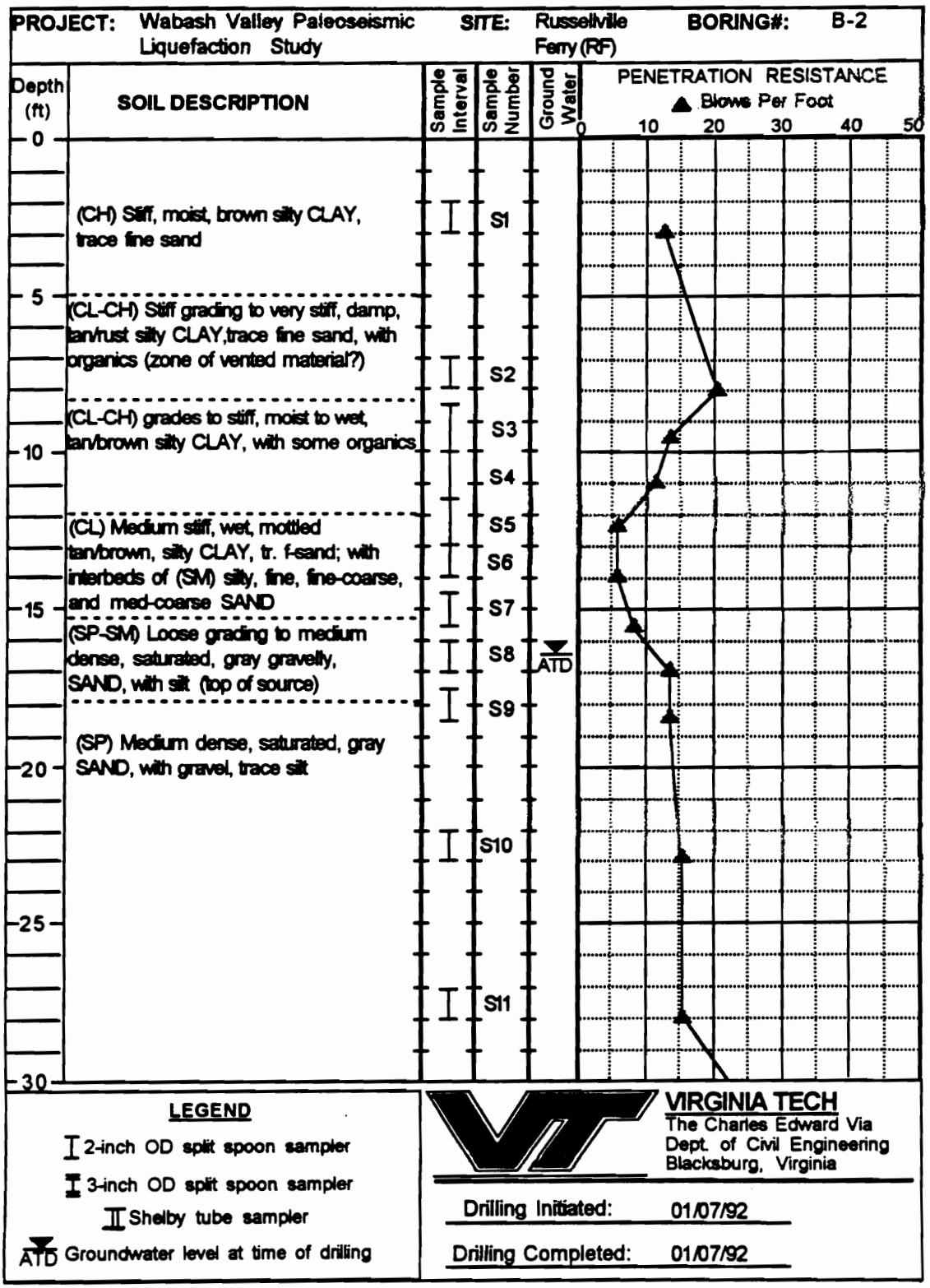
PROJECT: Wabash Valley Paleoseismic Liquefaction Study
SITE: Russellville Ferry (RF)
BORING#: B-2
Depth (ft)
SOIL DESCRIPTION
Sample Interval
Sample Number
Ground Water
PENETRATION RESISTANCE
Blows Per Foot
0
10
20
30
40
50
0
5
10
15
20
25
30
(CH) Stiff, moist, brown silty CLAY, trace fine sand
(CL-CH) Stiff grading to very stiff, damp, tan/rust silty CLAY,trace fine sand, with organics (zone of vented material?)
(CL-CH) grades to stiff, moist to wet, tan/brown silty CLAY, with some organics
(CL) Medium stiff, wet, mottled tan/brown, silty CLAY, tr. f-sand; with interbeds of (SM) silty, fine, fine-coarse, and med-coarse SAND
(SP-SM) Loose grading to medium dense, saturated, gray gravelly, SAND, with silt (top of source)
(SP) Medium dense, saturated, gray SAND, with gravel, trace silt
S1
S2
S3
S4
S5
S6
S7
S8
S9
S10
S11
ATD
LEGEND
2-inch OD split spoon sampler
3-inch OD split spoon sampler
Shelby tube sampler
Groundwater level at time of drilling
VIRGINIA TECH
The Charles Edward Via Dept. of Civil Engineering Blacksburg, Virginia
Drilling Initiated: 01/07/92
Drilling Completed: 01/07/92

PROJECT: Wabash Valley Paleoseismic Liquefaction Study

SITE: Russellville Ferry (RF)

BORING#: B-2 (cont'd)

Depth (ft)	SOIL DESCRIPTION	Sample Interval	Sample Number	Ground Water	PENETRATION RESISTANCE ▲ Blows Per Foot 0 10 20 30 40 50
30	(SP) Medium dense grading to dense, saturated, gray, SAND, with gravel, trace silt, with occasional fine sandy SILT lenses	I	S12		
35		I	S13		
	Bottom of boring at approx. 38.5'				
40					
45					
50					
55					
60					

LEGEND

I 2-inch OD split spoon sampler

I 3-inch OD split spoon sampler

I Shelby tube sampler

▼ ATD Groundwater level at time of drilling

VIRGINIA TECH
The Charles Edward Via
Dept. of Civil Engineering
Blacksburg, Virginia

Drilling Initiated: 01/07/92

Drilling Completed: 01/07/92

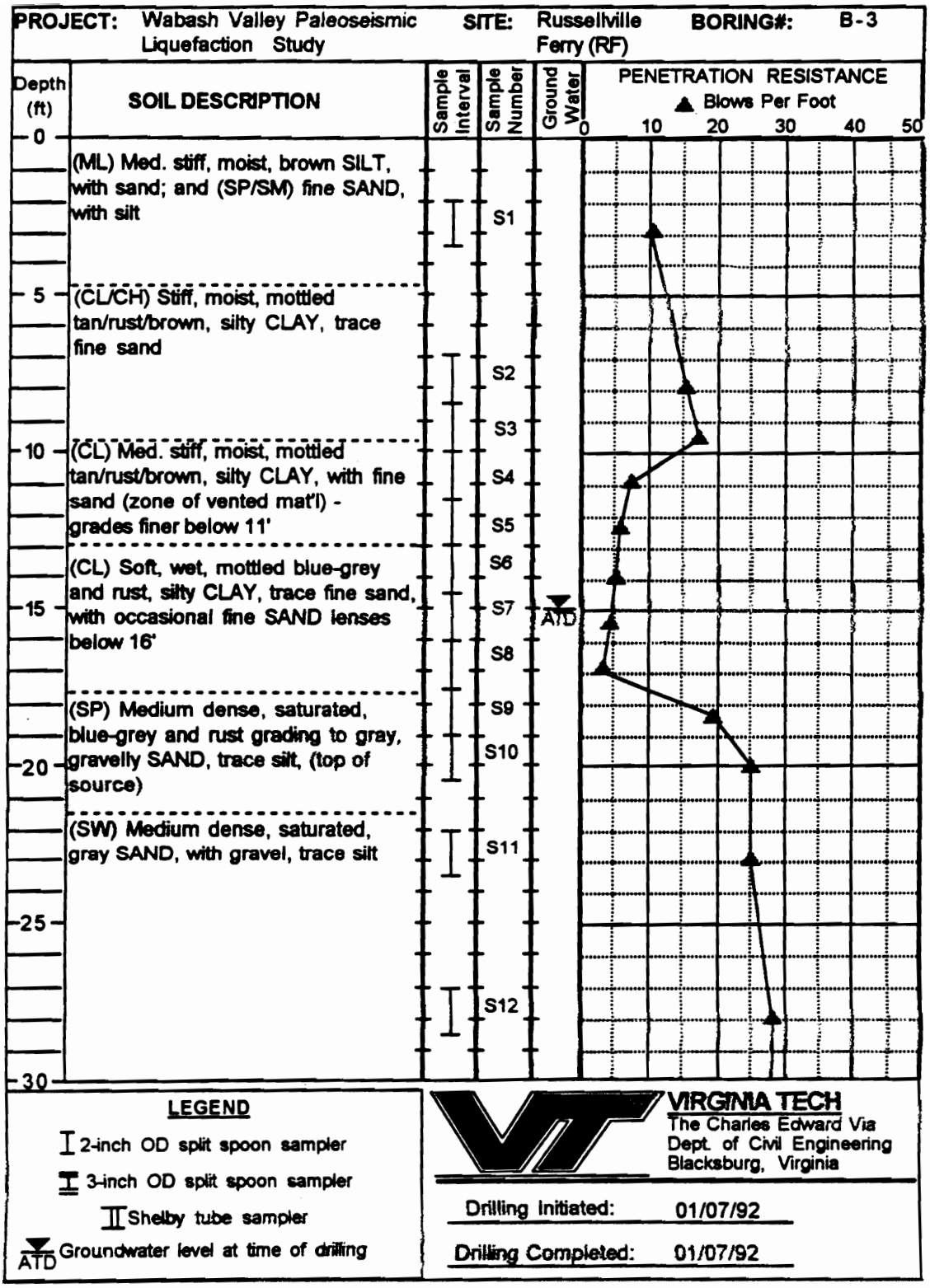
PROJECT: Wabash Valley Paleoseismic Liquefaction Study
SITE: Russellville Ferry (RF)
BORING#: B-3
Depth (ft)
SOIL DESCRIPTION
Sample Interval
Sample Number
Ground Water
PENETRATION RESISTANCE
Blows Per Foot
0
10
20
30
40
50
5
10
15
20
25
30
(ML) Med. stiff, moist, brown SILT, with sand; and (SP/SM) fine SAND, with silt
(CL/CH) Stiff, moist, mottled tan/rust/brown, silty CLAY, trace fine sand
(CL) Med. stiff, moist, mottled tan/rust/brown, silty CLAY, with fine sand (zone of vented mat'l) - grades finer below 11'
(CL) Soft, wet, mottled blue-grey and rust, silty CLAY, trace fine sand, with occasional fine SAND lenses below 16'
(SP) Medium dense, saturated, blue-grey and rust grading to gray, gravelly SAND, trace silt, (top of source)
(SW) Medium dense, saturated, gray SAND, with gravel, trace silt
S1
S2
S3
S4
S5
S6
S7
S8
S9
S10
S11
S12
ATD
LEGEND
2-inch OD split spoon sampler
3-inch OD split spoon sampler
Shelby tube sampler
ATD Groundwater level at time of drilling
VIRGINIA TECH
The Charles Edward Via Dept. of Civil Engineering Blacksburg, Virginia
Drilling Initiated: 01/07/92
Drilling Completed: 01/07/92

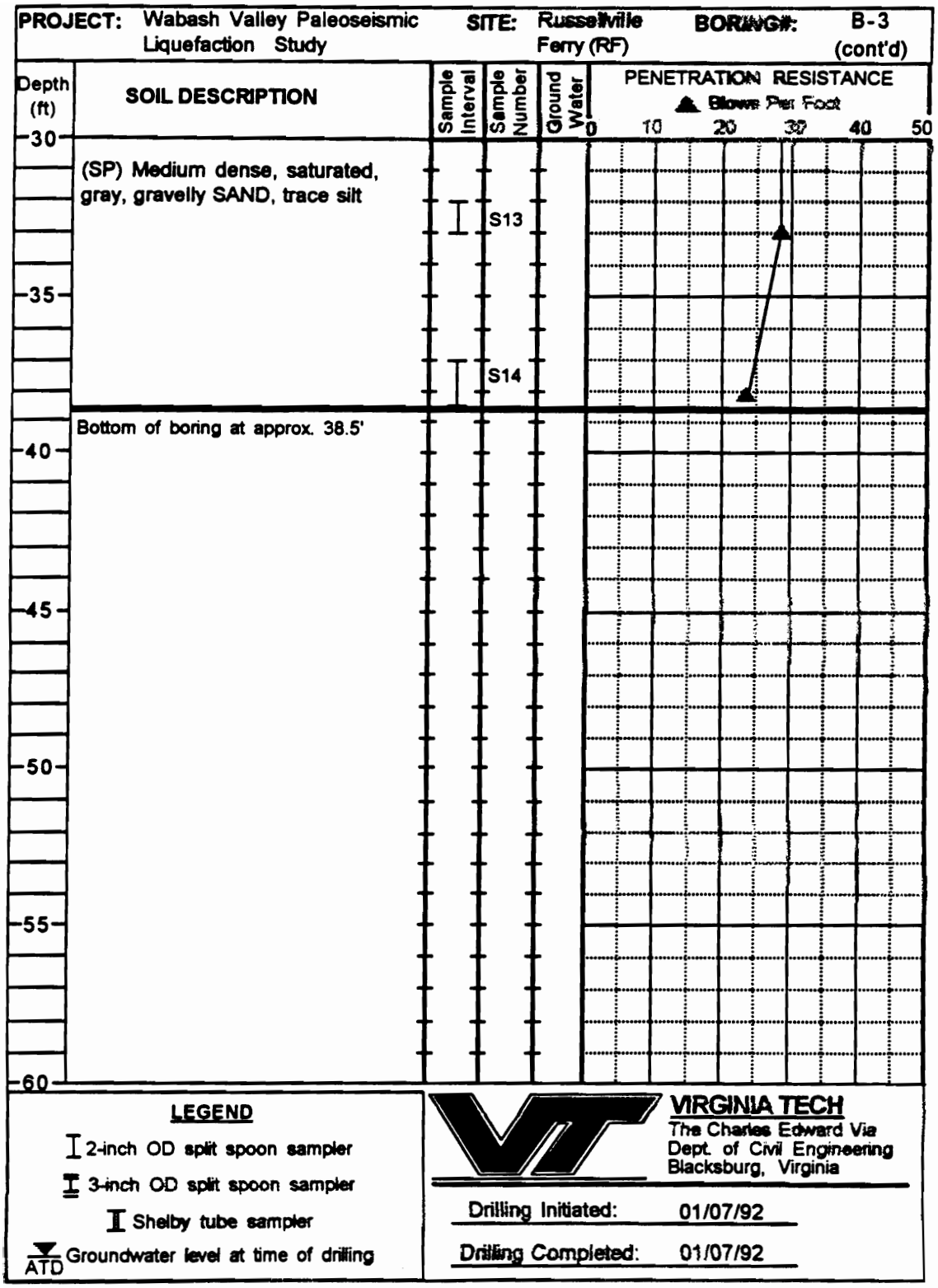
PROJECT: Wabash Valley Paleoseismic Liquefaction Study
SITE: Russellville Ferry (RF)
BORING#: B-3 (cont'd)
Depth (ft)
SOIL DESCRIPTION
Sample Interval
Sample Number
Ground Water
PENETRATION RESISTANCE
Blows Per Foot
0
10
20
30
40
50
30
35
40
45
50
55
60
(SP) Medium dense, saturated, gray, gravelly SAND, trace silt
S13
S14
Bottom of boring at approx. 38.5'
LEGEND
2-inch OD split spoon sampler
3-inch OD split spoon sampler
Shelby tube sampler
ATD Groundwater level at time of drilling
VIRGINIA TECH
The Charles Edward Via Dept. of Civil Engineering
Blacksburg, Virginia
Drilling Initiated: 01/07/92
Drilling Completed: 01/07/92

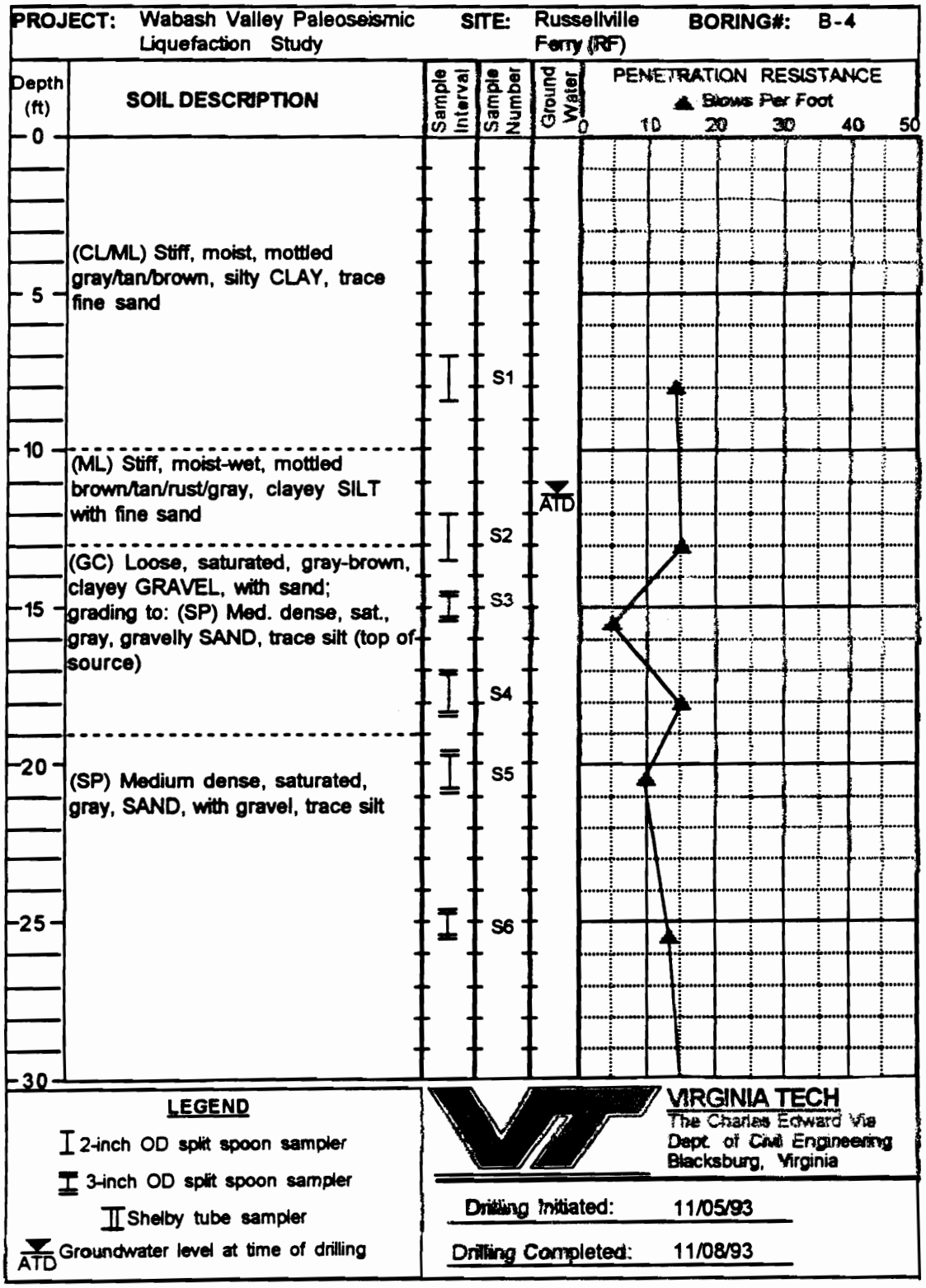
PROJECT: Wabash Valley Paleoseismic Liquefaction Study
SITE: Russellville Ferry (RF)
BORING#: B-4
Depth (ft)
SOIL DESCRIPTION
Sample Interval
Sample Number
Ground Water
PENETRATION RESISTANCE
Blows Per Foot
0
10
20
30
40
50
0
5
10
15
20
25
30
(CL/ML) Stiff, moist, mottled gray/tan/brown, silty CLAY, trace fine sand
(ML) Stiff, moist-wet, mottled brown/tan/rust/gray, clayey SILT with fine sand
(GC) Loose, saturated, gray-brown, clayey GRAVEL, with sand; grading to: (SP) Med. dense, sat., gray, gravelly SAND, trace silt (top of source)
(SP) Medium dense, saturated, gray, SAND, with gravel, trace silt
S1
S2
S3
S4
S5
S6
ATD
LEGEND
2-inch OD split spoon sampler
3-inch OD split spoon sampler
Shelby tube sampler
ATD Groundwater level at time of drilling
VIRGINIA TECH
The Charles Edward Via
Dept. of Civil Engineering
Blacksburg, Virginia
Drilling Initiated: 11/05/93
Drilling Completed: 11/08/93

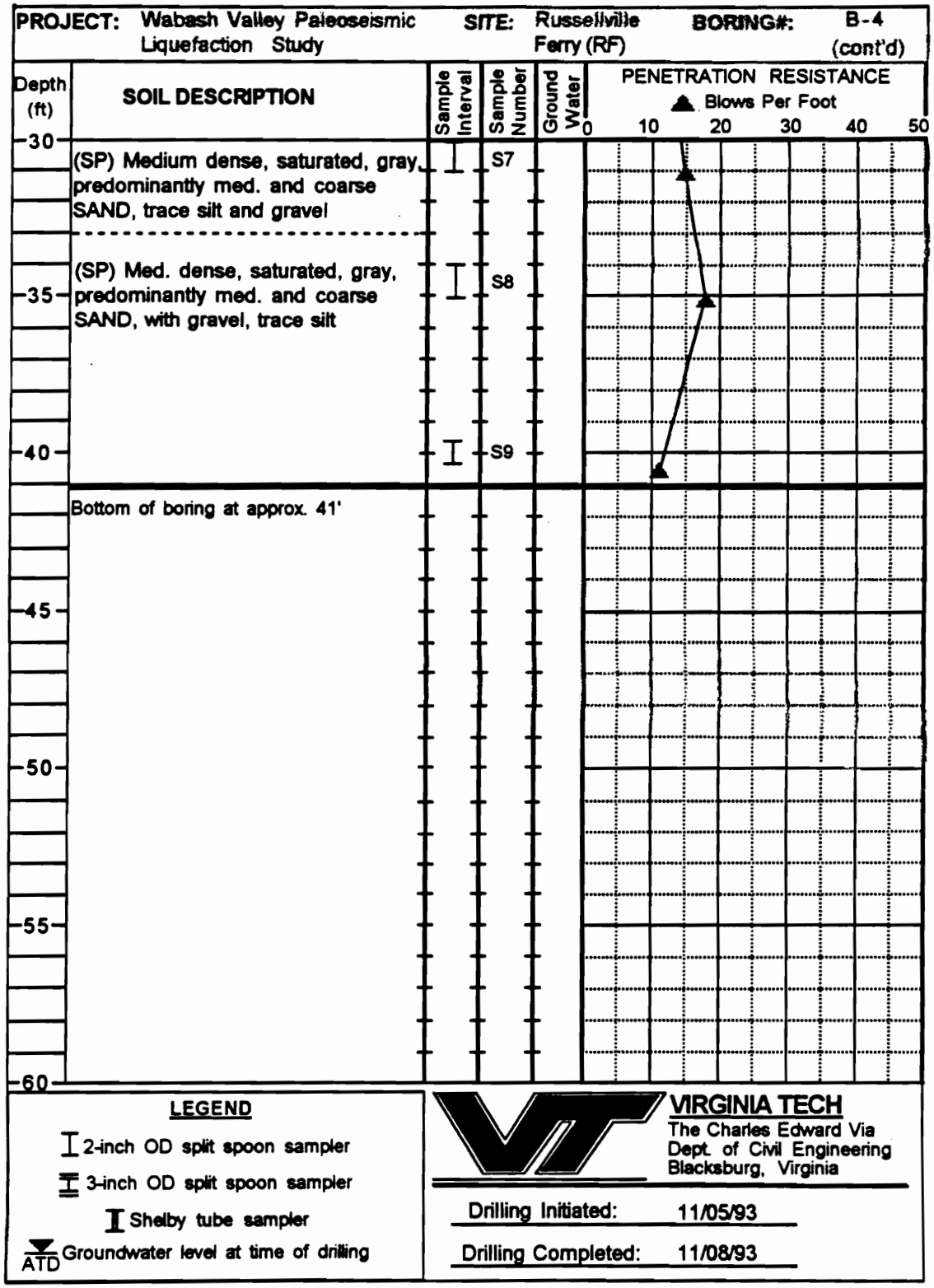
PROJECT: Wabash Valley Paleoseismic Liquefaction Study
SITE: Russellville Ferry (RF)
BORING#: B-4 (cont'd)
Depth (ft)
SOIL DESCRIPTION
Sample Interval
Sample Number
Ground Water
PENETRATION RESISTANCE
Blows Per Foot
0 10 20 30 40 50
30
(SP) Medium dense, saturated, gray, predominantly med. and coarse SAND, trace silt and gravel
S7
35
(SP) Med. dense, saturated, gray, predominantly med. and coarse SAND, with gravel, trace silt
S8
40
S9
Bottom of boring at approx. 41'
45
50
55
60
LEGEND
2-inch OD split spoon sampler
3-inch OD split spoon sampler
Shelby tube sampler
ATD Groundwater level at time of drilling
VIRGINIA TECH
The Charles Edward Via Dept. of Civil Engineering Blacksburg, Virginia
Drilling Initiated: 11/05/93
Drilling Completed: 11/08/93

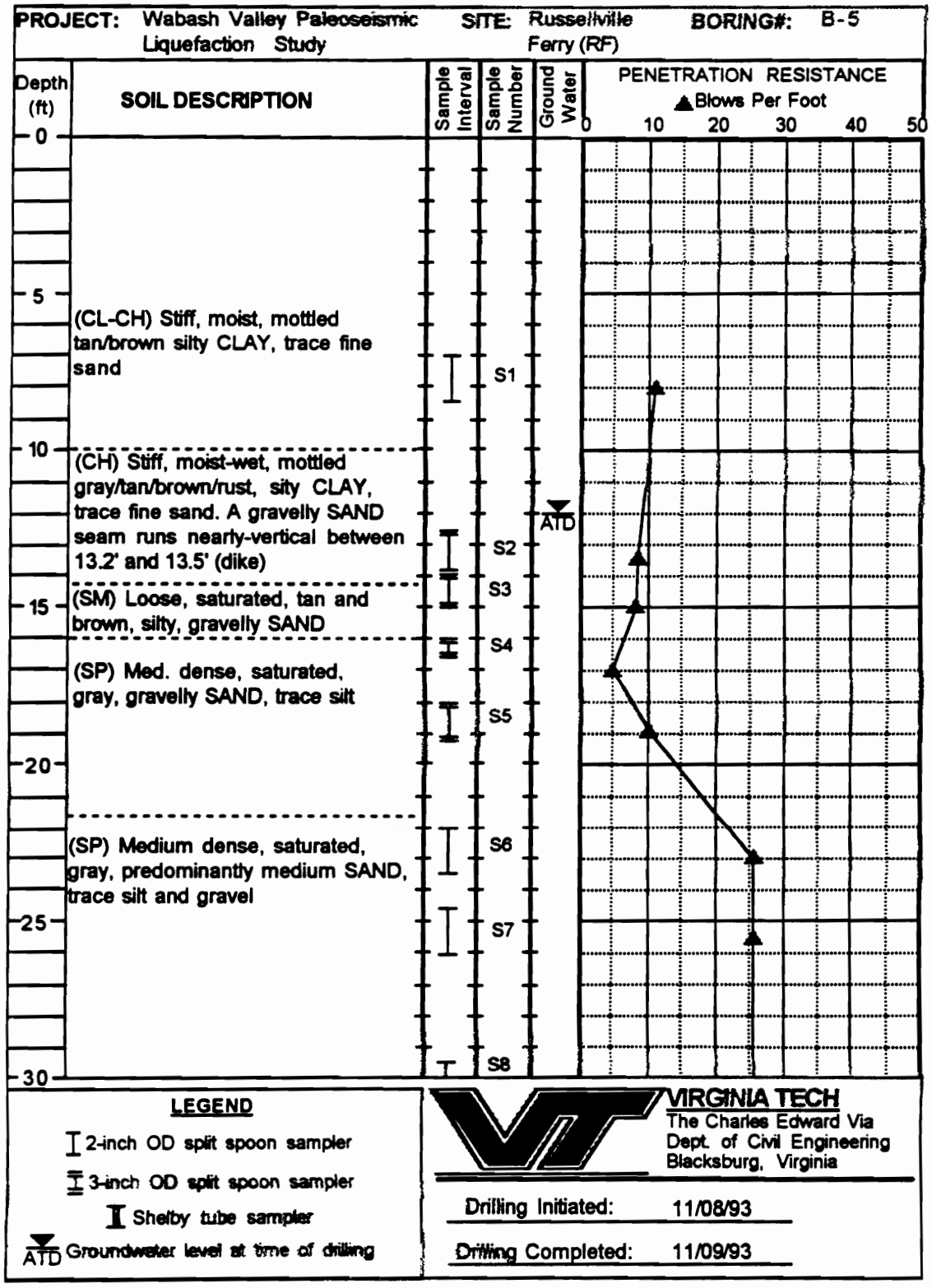
PROJECT: Wabash Valley Paleoseismic Liquefaction Study
SITE: Russellville Ferry (RF)
BORING#: B-5
Depth (ft)
SOIL DESCRIPTION
Sample Interval
Sample Number
Ground Water
PENETRATION RESISTANCE
Blows Per Foot
0
10
20
30
40
50
5
10
15
20
25
30
(CL-CH) Stiff, moist, mottled tan/brown silty CLAY, trace fine sand
(CH) Stiff, moist-wet, mottled gray/tan/brown/rust, silty CLAY, trace fine sand. A gravelly SAND seam runs nearly-vertical between 13.2' and 13.5' (dike)
(SM) Loose, saturated, tan and brown, silty, gravelly SAND
(SP) Med. dense, saturated, gray, gravelly SAND, trace silt
(SP) Medium dense, saturated, gray, predominantly medium SAND, trace silt and gravel
S1
S2
S3
S4
S5
S6
S7
S8
ATD
LEGEND
2-inch OD split spoon sampler
3-inch OD split spoon sampler
Shelby tube sampler
ATD Groundwater level at time of drilling
VIRGINIA TECH
The Charles Edward Via Dept. of Civil Engineering
Blacksburg, Virginia
Drilling Initiated: 11/08/93
Drilling Completed: 11/09/93

PROJECT: Wabash Valley Paleoseismic Liquefaction Study

SITE: Russellville Ferry (RF)

BORING#: B-5 (cont'd)

Depth (ft)	SOIL DESCRIPTION	Sample Interval	Sample Number	Ground Water
30	(SP) Medium dense, saturated, gray, predominantly medium SAND, trace silt and gravel		S8	
35			S9	
40	(SP) Med. dense, saturated, gray, predom. med to coarse SAND, with gravel, trace silt		S10	
	Bottom of boring at approx. 41'			
45				
50				
55				
60				

PENETRATION RESISTANCE
▲ Blows Per Foot
0 10 20 30 40 50

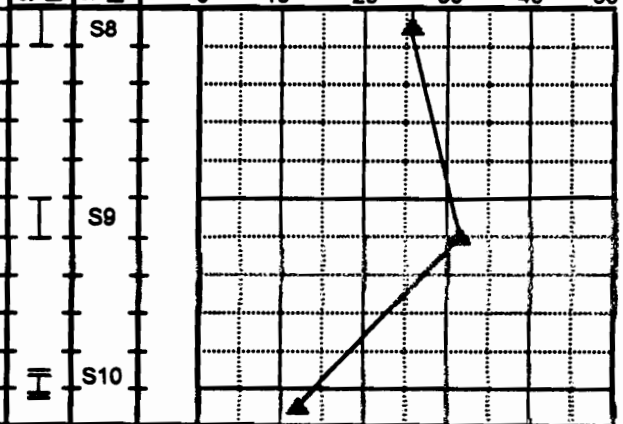

LEGEND

I 2-inch OD split spoon sampler

I 3-inch OD split spoon sampler

I Shelby tube sampler

ATD Groundwater level at time of drilling

VIRGINIA TECH
The Charles Edward Via
Dept. of Civil Engineering
Blacksburg, Virginia

Drilling Initiated: 11/08/93

Drilling Completed: 11/09/93

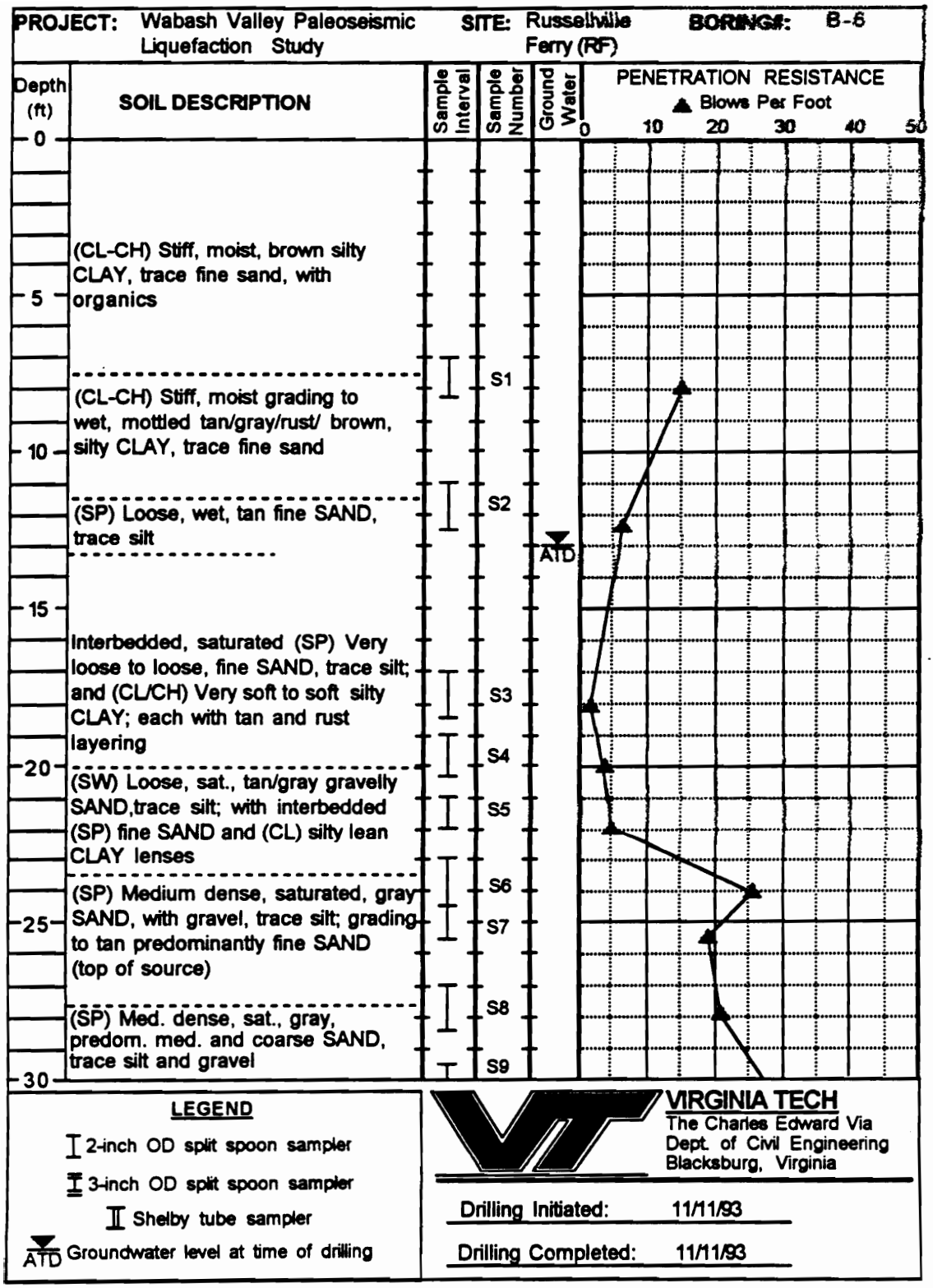
PROJECT: Wabash Valley Paleoseismic Liquefaction Study
SITE: Russellville Ferry (RF)
BORING#: B-6
Depth (ft)
SOIL DESCRIPTION
Sample Interval
Sample Number
Ground Water
PENETRATION RESISTANCE
Blows Per Foot
0
10
20
30
40
50
0
5
10
15
20
25
30
(CL-CH) Stiff, moist, brown silty CLAY, trace fine sand, with organics
(CL-CH) Stiff, moist grading to wet, mottled tan/gray/rust/ brown, silty CLAY, trace fine sand
(SP) Loose, wet, tan fine SAND, trace silt
Interbedded, saturated (SP) Very loose to loose, fine SAND, trace silt; and (CL/CH) Very soft to soft silty CLAY; each with tan and rust layering
(SW) Loose, sat., tan/gray gravelly SAND,trace silt; with interbedded (SP) fine SAND and (CL) silty lean CLAY lenses
(SP) Medium dense, saturated, gray SAND, with gravel, trace silt; grading to tan predominantly fine SAND (top of source)
(SP) Med. dense, sat., gray, predom. med. and coarse SAND, trace silt and gravel
S1
S2
S3
S4
S5
S6
S7
S8
S9
ATD
LEGEND
2-inch OD split spoon sampler
3-inch OD split spoon sampler
Shelby tube sampler
ATD Groundwater level at time of drilling
VIRGINIA TECH
The Charles Edward Via Dept. of Civil Engineering Blacksburg, Virginia
Drilling Initiated: 11/11/93
Drilling Completed: 11/11/93

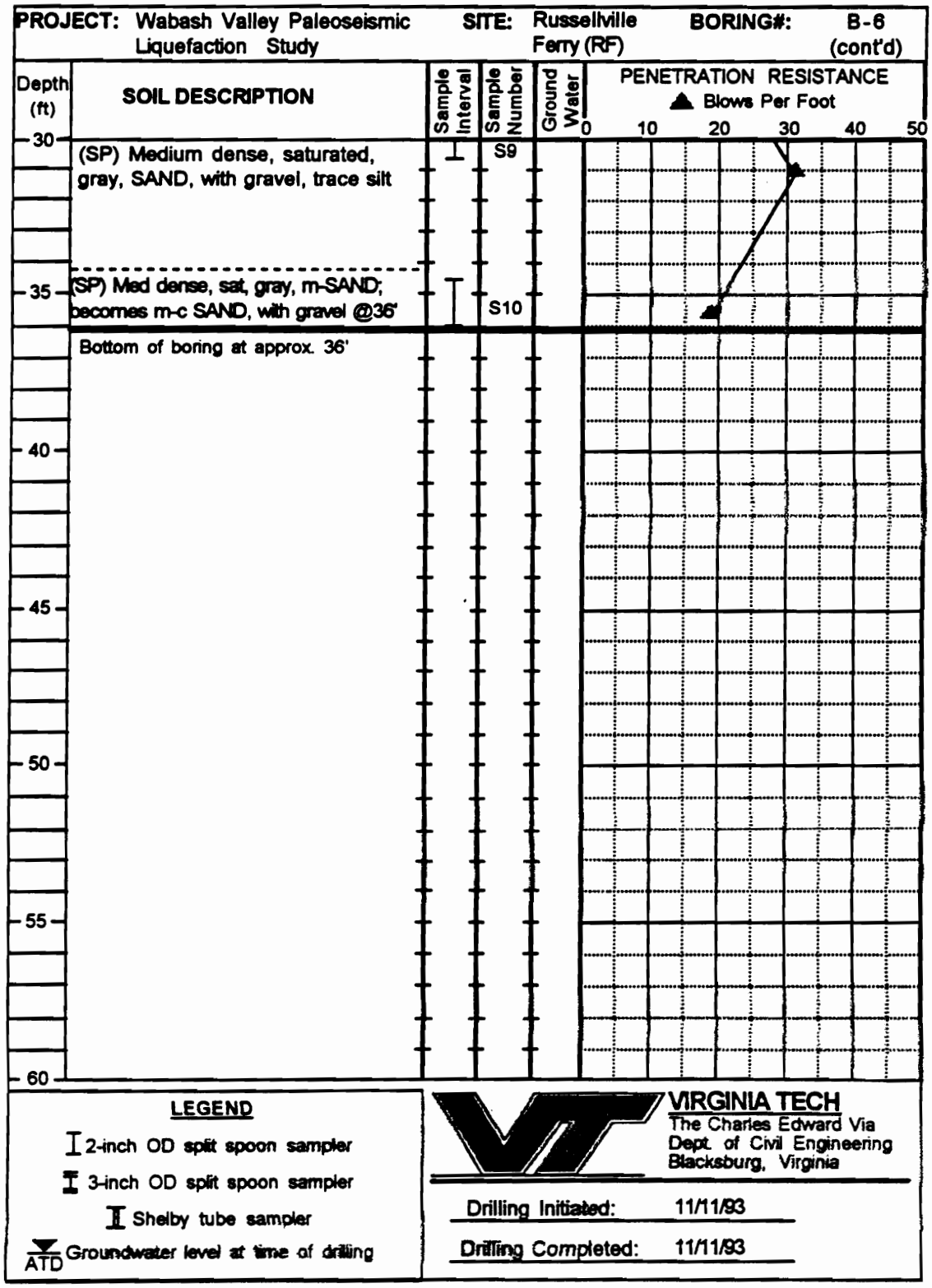
PROJECT: Wabash Valley Paleoseismic Liquefaction Study
SITE: Russellville Ferry (RF)
BORING#: B-6 (cont'd)
Depth (ft)
SOIL DESCRIPTION
Sample Interval
Sample Number
Ground Water
PENETRATION RESISTANCE
Blows Per Foot
0 10 20 30 40 50
30
(SP) Medium dense, saturated, gray, SAND, with gravel, trace silt
S9
35
(SP) Med dense, sat, gray, m-SAND; becomes m-c SAND, with gravel @36'
S10
Bottom of boring at approx. 36'
40
45
50
55
60
LEGEND
2-inch OD split spoon sampler
3-inch OD split spoon sampler
Shelby tube sampler
ATD Groundwater level at time of drilling
VIRGINIA TECH
The Charles Edward Via Dept. of Civil Engineering Blacksburg, Virginia
Drilling Initiated: 11/11/93
Drilling Completed: 11/11/93

PROJECT: Wabash Valley Paleoseismic Liquefaction Study **SITE:** Seven Mile Island (SM) **BORING#:** B-1

Depth (ft)	SOIL DESCRIPTION	Sample Interval	Sample Number	Ground Water
0	Sand and gravel over an old brick roadbed			
	(CL-CH) Med stiff, moist to wet, brown, silty, lean to fat CLAY, trace f-sand, with some organics		S1	
5	(CL) Stiff, moist, mottled tan, rust, brown and gray, silty lean CLAY, with fine sand, and organics		S2	
	(SP/SM) Loose, moist, gray with rust mottling, silty fine SAND; grading to (SP) gray fine SAND, trace silt		S3 S4	
10	(SP) Loose, moist, gray, becoming oxidized at 13.5', SAND, with gravel, trace silt		S5 S6	
15	Bottom of boring at approx. 14.5'			
20				
25				
30				

PENETRATION RESISTANCE
▲ Blows Per Foot
0 10 20 30 40 50

LEGEND

- 2-inch OD split spoon sampler
- 3-inch OD split spoon sampler
- Shelby tube sampler
- ATD Groundwater level at time of drilling

VIRGINIA TECH
The Charles Edward Via Dept. of Civil Engineering
Blacksburg, Virginia

Drilling Initiated: 01/08/92

Drilling Completed: 01/08/92

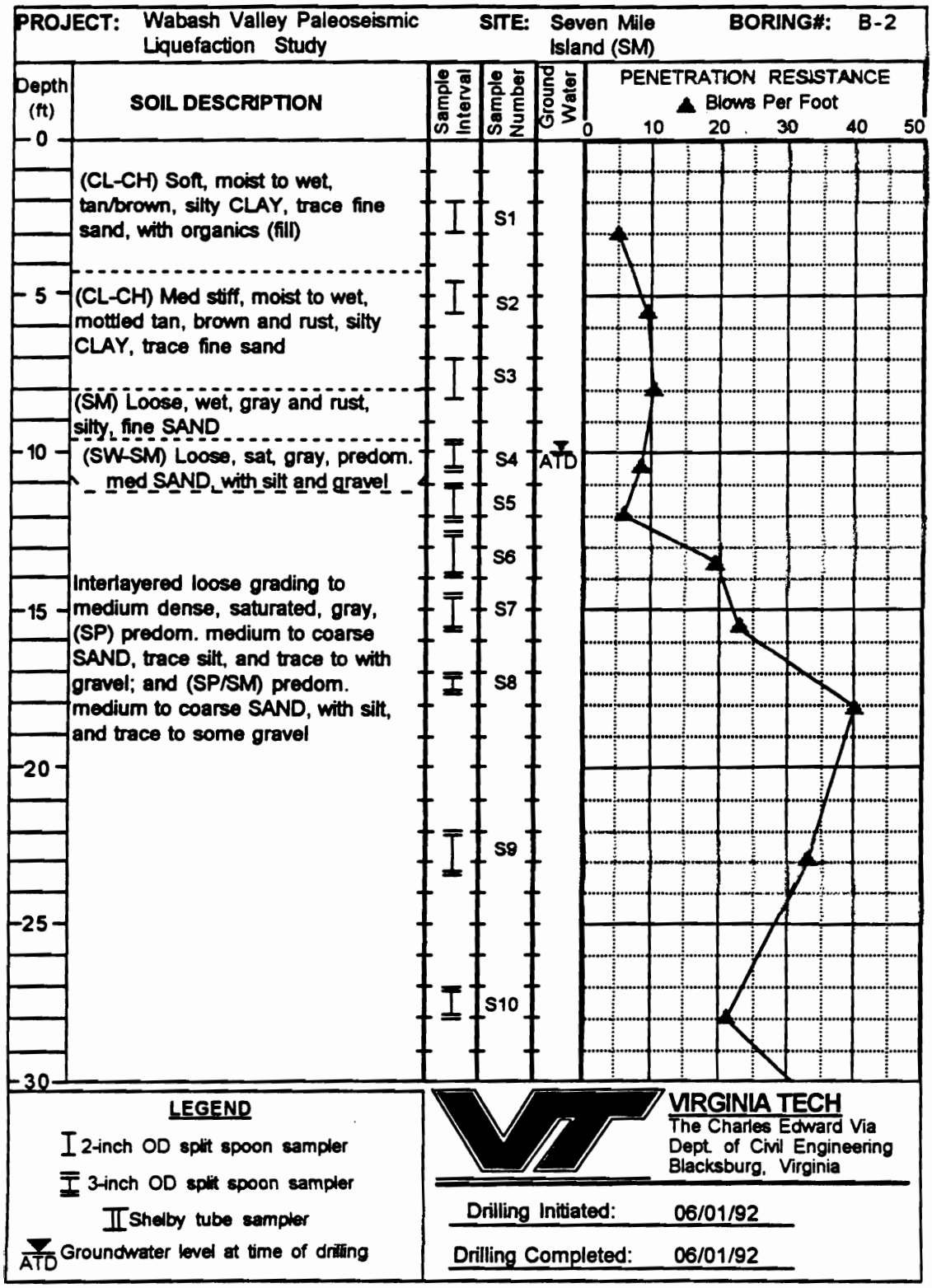
PROJECT: Wabash Valley Paleoseismic Liquefaction Study
SITE: Seven Mile Island (SM)
BORING#: B-2
Depth (ft)
SOIL DESCRIPTION
Sample Interval
Sample Number
Ground Water
PENETRATION RESISTANCE
Blows Per Foot
0
10
20
30
40
50
0
5
10
15
20
25
30
(CL-CH) Soft, moist to wet, tan/brown, silty CLAY, trace fine sand, with organics (fill)
(CL-CH) Med stiff, moist to wet, mottled tan, brown and rust, silty CLAY, trace fine sand
(SM) Loose, wet, gray and rust, silty, fine SAND
(SW-SM) Loose, sat, gray, predom. med SAND, with silt and gravel
Interlayered loose grading to medium dense, saturated, gray, (SP) predom. medium to coarse SAND, trace silt, and trace to with gravel; and (SP/SM) predom. medium to coarse SAND, with silt, and trace to some gravel
S1
S2
S3
S4
S5
S6
S7
S8
S9
S10
ATD
LEGEND
2-inch OD split spoon sampler
3-inch OD split spoon sampler
Shelby tube sampler
Groundwater level at time of drilling
VIRGINIA TECH
The Charles Edward Via
Dept. of Civil Engineering
Blacksburg, Virginia
Drilling Initiated: 06/01/92
Drilling Completed: 06/01/92

PROJECT: Wabash Valley Paleoseismic Liquefaction Study

SITE: Seven Mile Island (SM)

BORING#: B-2 (cont'd)

Depth (ft)	SOIL DESCRIPTION	Sample Interval	Sample Number	Ground Water	PENETRATION RESISTANCE ▲ Blows Per Foot 0 10 20 30 40 50
30	(SP) Dense, sat, gray, SAND, trace silt and gravel	3-inch OD split spoon	S11		
	Bottom of boring at approx. 33.5'				
35					
40					
45					
50					
55					
60					

LEGEND

- 2-inch OD split spoon sampler
- 3-inch OD split spoon sampler
- Shelby tube sampler
- ATD Groundwater level at time of drilling

VIRGINIA TECH
The Charles Edward Via
Dept. of Civil Engineering
Blacksburg, Virginia

Drilling Initiated: 06/01/92

Drilling Completed: 06/01/92

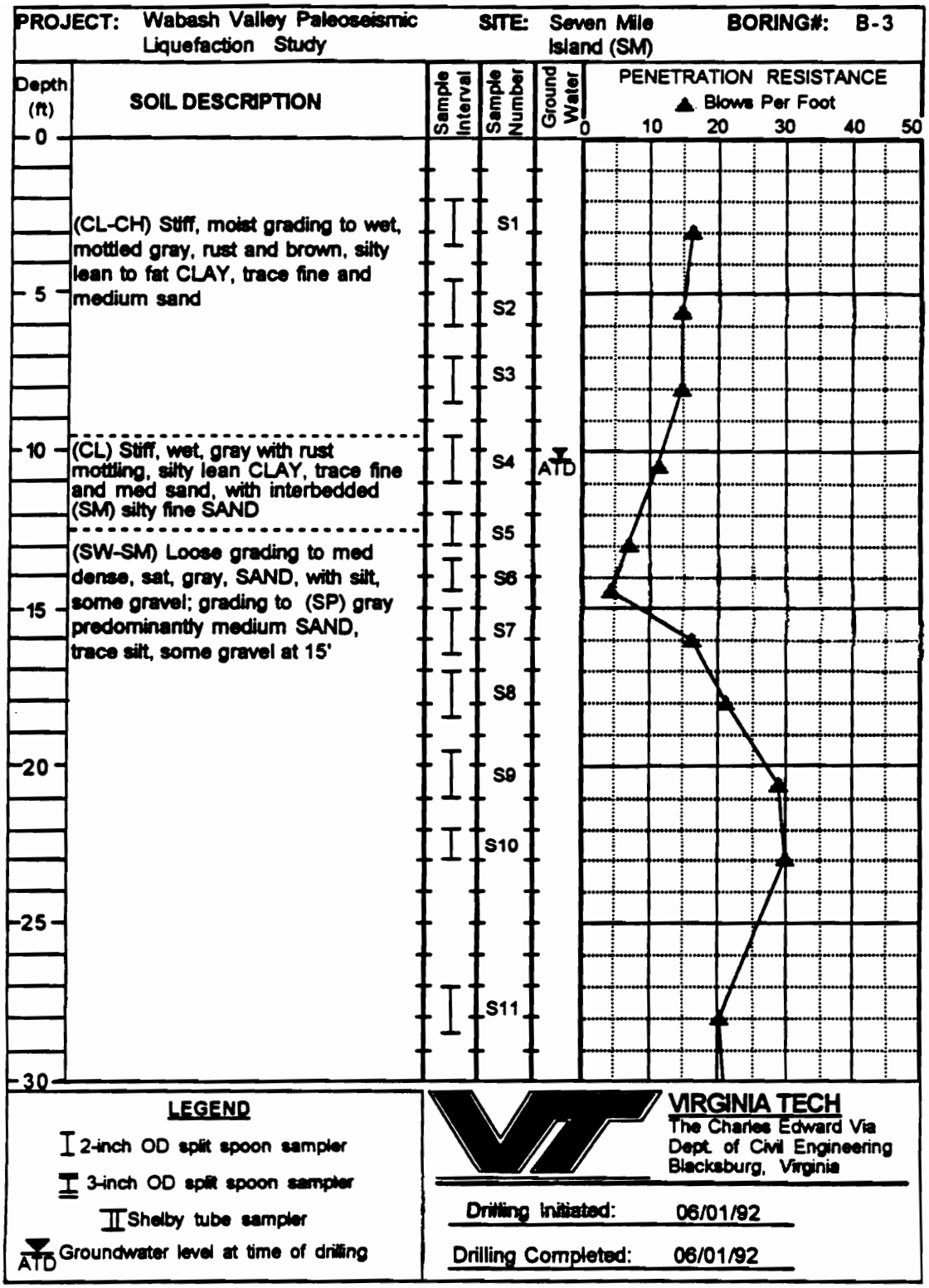
PROJECT: Wabash Valley Paleoseismic Liquefaction Study
SITE: Seven Mile Island (SM)
BORING#: B-3
Depth (ft)
SOIL DESCRIPTION
Sample Interval
Sample Number
Ground Water
PENETRATION RESISTANCE
Blows Per Foot
0
10
20
30
40
50
0
5
10
15
20
25
30
(CL-CH) Stiff, moist grading to wet, mottled gray, rust and brown, silty lean to fat CLAY, trace fine and medium sand
(CL) Stiff, wet, gray with rust mottling, silty lean CLAY, trace fine and med sand, with interbedded (SM) silty fine SAND
(SW-SM) Loose grading to med dense, sat, gray, SAND, with silt, some gravel; grading to (SP) gray predominantly medium SAND, trace silt, some gravel at 15'
S1
S2
S3
S4
S5
S6
S7
S8
S9
S10
S11
ATD
LEGEND
2-inch OD split spoon sampler
3-inch OD split spoon sampler
Shelby tube sampler
ATD Groundwater level at time of drilling
VIRGINIA TECH
The Charles Edward Via Dept. of Civil Engineering Blacksburg, Virginia
Drilling Initiated: 06/01/92
Drilling Completed: 06/01/92

PROJECT: Wabash Valley Paleoseismic Liquefaction Study **SITE:** Seven Mile Island (SM) **BORING#:** B-3 (cont'd)

Depth (ft)	SOIL DESCRIPTION	Sample Interval	Sample Number	Ground Water	PENETRATION RESISTANCE ▲ Blows Per Foot 0 10 20 30 40 50
30	(SP) Medium dense, saturated, gray, predominantly medium SAND, some gravel, trace silt	I	S12		
	Bottom of boring at approx. 33.5'				
35					
40					
45					
50					
55					
60					

LEGEND

- I 2-inch OD split spoon sampler
- I 3-inch OD split spoon sampler
- I Shelby tube sampler
- ATD Groundwater level at time of drilling

VIRGINIA TECH
The Charles Edward Via Dept. of Civil Engineering
Blacksburg, Virginia

Drilling Initiated: 06/01/92

Drilling Completed: 06/01/92

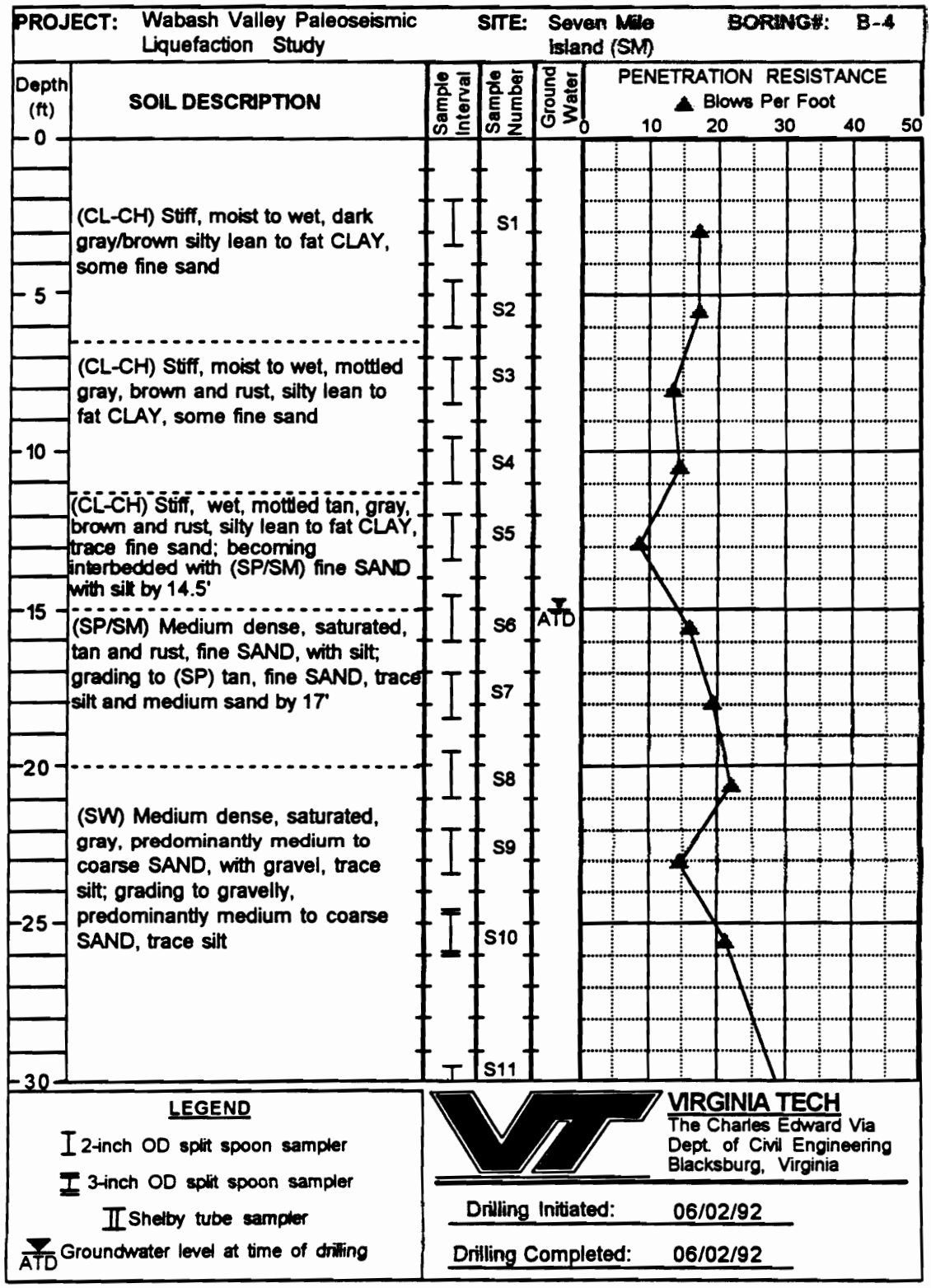
PROJECT: Wabash Valley Paleoseismic Liquefaction Study
SITE: Seven Mile Island (SM)
BORING#: B-4
Depth (ft)
SOIL DESCRIPTION
Sample Interval
Sample Number
Ground Water
PENETRATION RESISTANCE
Blows Per Foot
0
10
20
30
40
50
0
5
10
15
20
25
30
(CL-CH) Stiff, moist to wet, dark gray/brown silty lean to fat CLAY, some fine sand
(CL-CH) Stiff, moist to wet, mottled gray, brown and rust, silty lean to fat CLAY, some fine sand
(CL-CH) Stiff, wet, mottled tan, gray, brown and rust, silty lean to fat CLAY, trace fine sand; becoming interbedded with (SP/SM) fine SAND with silt by 14.5'
(SP/SM) Medium dense, saturated, tan and rust, fine SAND, with silt; grading to (SP) tan, fine SAND, trace silt and medium sand by 17'
(SW) Medium dense, saturated, gray, predominantly medium to coarse SAND, with gravel, trace silt; grading to gravelly, predominantly medium to coarse SAND, trace silt
S1
S2
S3
S4
S5
S6
S7
S8
S9
S10
S11
ATD
LEGEND
2-inch OD split spoon sampler
3-inch OD split spoon sampler
Shelby tube sampler
Groundwater level at time of drilling
VIRGINIA TECH
The Charles Edward Via Dept. of Civil Engineering Blacksburg, Virginia
Drilling Initiated: 06/02/92
Drilling Completed: 06/02/92

PROJECT: Wabash Valley Paleoseismic Liquefaction Study

SITE: Seven Mile Island (SM)

BORING#: B-4 (cont'd)

Depth (ft)	SOIL DESCRIPTION	Sample Interval	Sample Number	Ground Water	PENETRATION RESISTANCE ▲ Blows Per Foot 0 10 20 30 40 50
30	(SW) Medium dense, saturated, gray, gravelly, predominantly medium to coarse SAND, trace silt	I	S11		
35		I	S12		
	Bottom of boring at approx. 36'				
40					
45					
50					
55					
60					

LEGEND

- I 2-inch OD split spoon sampler
- I 3-inch OD split spoon sampler
- I Shelby tube sampler
- ATD Groundwater level at time of drilling

VIRGINIA TECH
The Charles Edward Via Dept. of Civil Engineering
Blacksburg, Virginia

Drilling Initiated: 06/02/92

Drilling Completed: 06/02/92

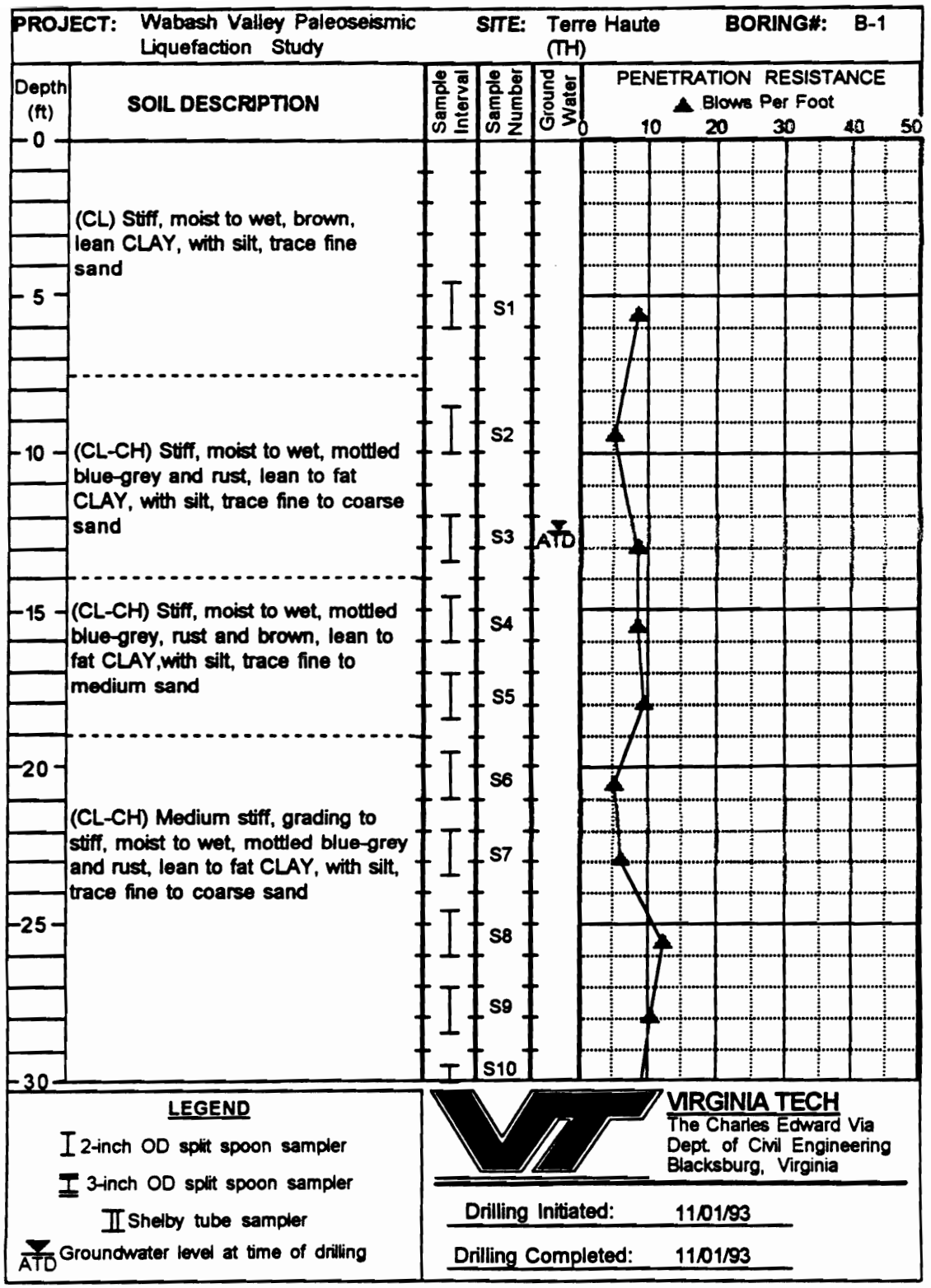
PROJECT: Wabash Valley Paleoseismic Liquefaction Study
SITE: Terre Haute (TH)
BORING#: B-1
Depth (ft)
SOIL DESCRIPTION
Sample Interval
Sample Number
Ground Water
PENETRATION RESISTANCE
Blows Per Foot
0
10
20
30
40
50
5
10
15
20
25
30
(CL) Stiff, moist to wet, brown, lean CLAY, with silt, trace fine sand
(CL-CH) Stiff, moist to wet, mottled blue-grey and rust, lean to fat CLAY, with silt, trace fine to coarse sand
(CL-CH) Stiff, moist to wet, mottled blue-grey, rust and brown, lean to fat CLAY,with silt, trace fine to medium sand
(CL-CH) Medium stiff, grading to stiff, moist to wet, mottled blue-grey and rust, lean to fat CLAY, with silt, trace fine to coarse sand
S1
S2
S3
S4
S5
S6
S7
S8
S9
S10
ATD
LEGEND
2-inch OD split spoon sampler
3-inch OD split spoon sampler
Shelby tube sampler
Groundwater level at time of drilling
VIRGINIA TECH
The Charles Edward Via Dept. of Civil Engineering Blacksburg, Virginia
Drilling Initiated: 11/01/93
Drilling Completed: 11/01/93

PROJECT: Wabash Valley Paleoseismic Liquefaction Study

SITE: Terre Haute (TH)

BORING#: B-1 (cont'd)

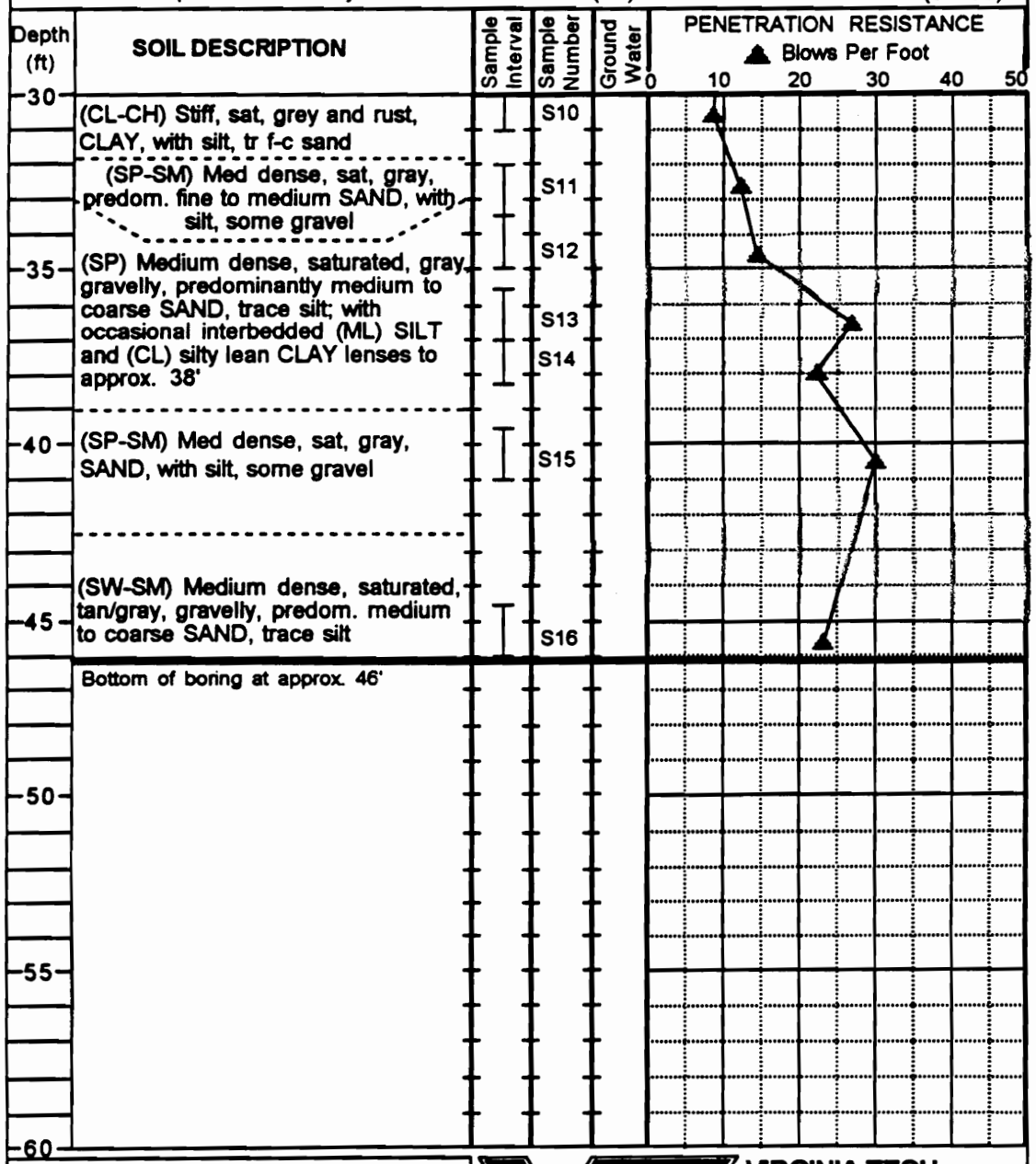

LEGEND

- 2-inch OD split spoon sampler
- 3-inch OD split spoon sampler
- Shelby tube sampler
- ATD Groundwater level at time of drilling

VIRGINIA TECH
The Charles Edward Via
Dept. of Civil Engineering
Blacksburg, Virginia

Drilling Initiated: 11/01/93

Drilling Completed: 11/01/93

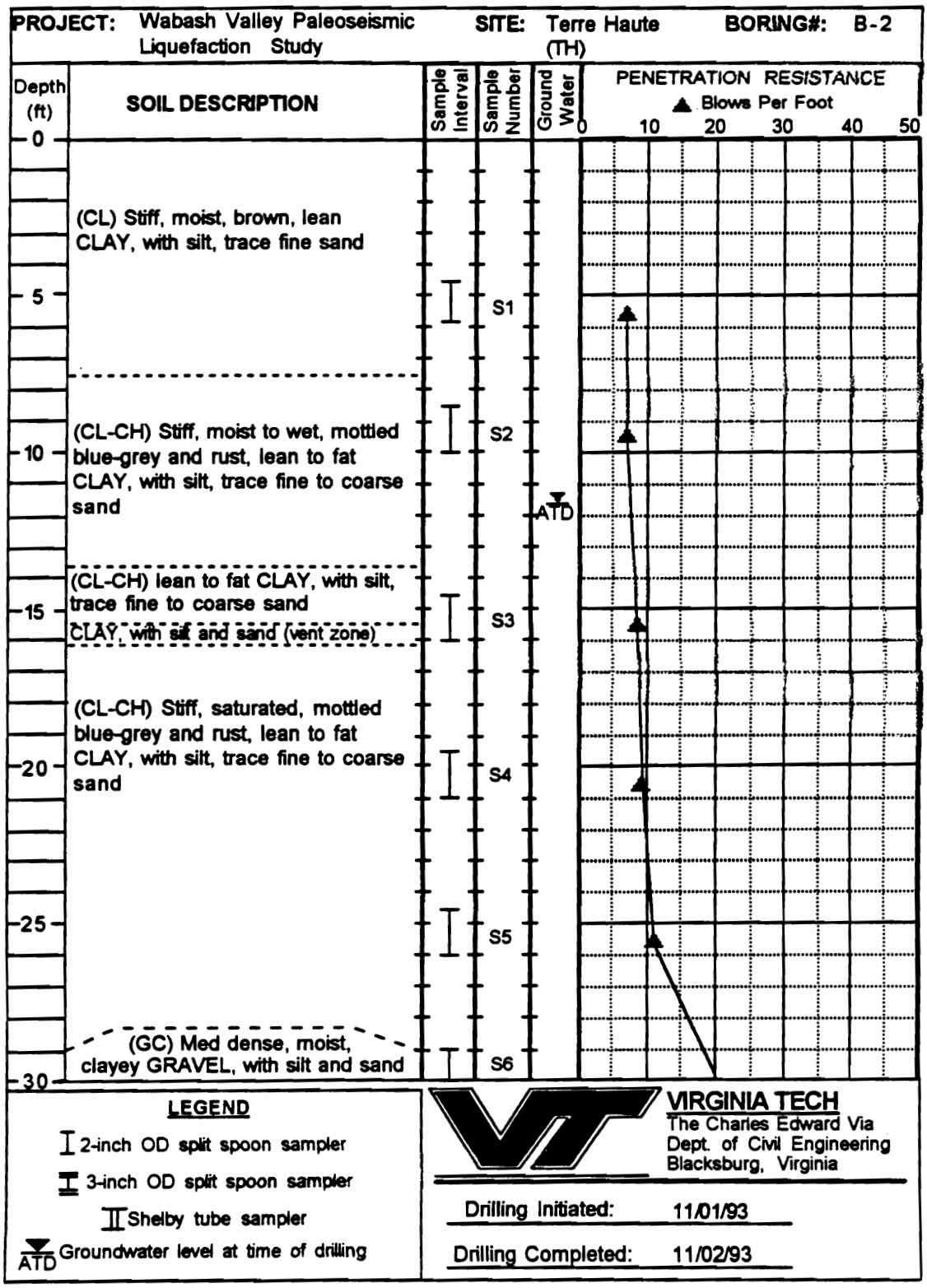
PROJECT: Wabash Valley Paleoseismic Liquefaction Study
SITE: Terre Haute (TH)
BORING#: B-2
Depth (ft)
SOIL DESCRIPTION
Sample Interval
Sample Number
Ground Water
PENETRATION RESISTANCE
Blows Per Foot
0
10
20
30
40
50
0
5
10
15
20
25
30
(CL) Stiff, moist, brown, lean CLAY, with silt, trace fine sand
S1
(CL-CH) Stiff, moist to wet, mottled blue-grey and rust, lean to fat CLAY, with silt, trace fine to coarse sand
S2
ATD
(CL-CH) lean to fat CLAY, with silt, trace fine to coarse sand
CLAY, with silt and sand (vent zone)
S3
(CL-CH) Stiff, saturated, mottled blue-grey and rust, lean to fat CLAY, with silt, trace fine to coarse sand
S4
S5
(GC) Med dense, moist, clayey GRAVEL, with silt and sand
S6
LEGEND
2-inch OD split spoon sampler
3-inch OD split spoon sampler
Shelby tube sampler
ATD Groundwater level at time of drilling
VIRGINIA TECH
The Charles Edward Via Dept. of Civil Engineering Blacksburg, Virginia
Drilling Initiated: 11/01/93
Drilling Completed: 11/02/93

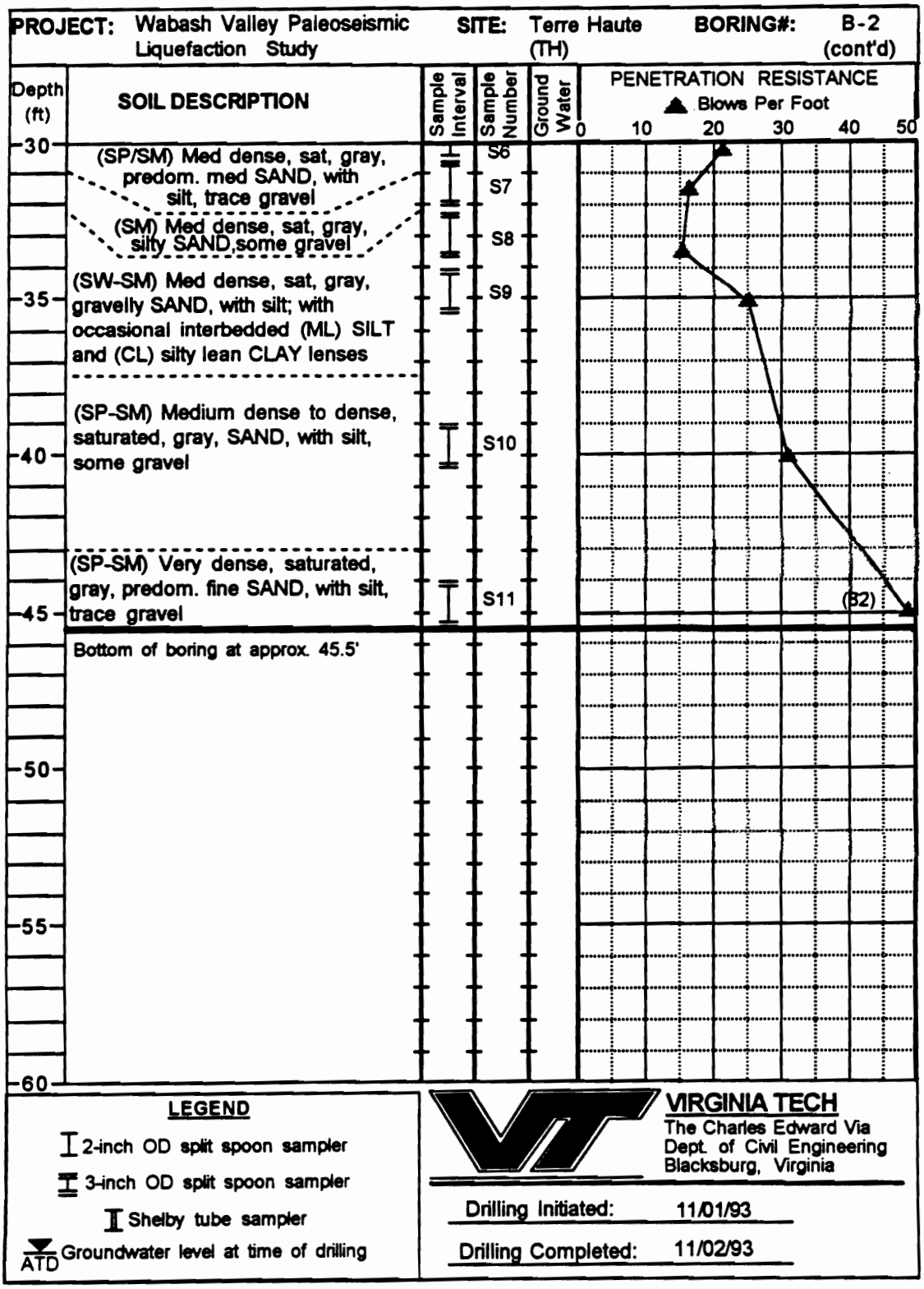
PROJECT: Wabash Valley Paleoseismic Liquefaction Study
SITE: Terre Haute (TH)
BORING#: B-2 (cont'd)
Depth (ft)
SOIL DESCRIPTION
Sample Interval
Sample Number
Ground Water
PENETRATION RESISTANCE
Blows Per Foot
0 10 20 30 40 50
-30
(SP/SM) Med dense, sat, gray, predom. med SAND, with silt, trace gravel
(SM) Med dense, sat, gray, silty SAND,some gravel
S6
S7
S8
-35
(SW-SM) Med dense, sat, gray, gravelly SAND, with silt; with occasional interbedded (ML) SILT and (CL) silty lean CLAY lenses
S9
(SP-SM) Medium dense to dense, saturated, gray, SAND, with silt, some gravel
-40
S10
(SP-SM) Very dense, saturated, gray, predom. fine SAND, with silt, trace gravel
-45
S11
(82)
Bottom of boring at approx. 45.5'
-50
-55
-60
LEGEND
2-inch OD split spoon sampler
3-inch OD split spoon sampler
Shelby tube sampler
ATD Groundwater level at time of drilling
VIRGINIA TECH
The Charles Edward Via Dept. of Civil Engineering Blacksburg, Virginia
Drilling Initiated: 11/01/93
Drilling Completed: 11/02/93

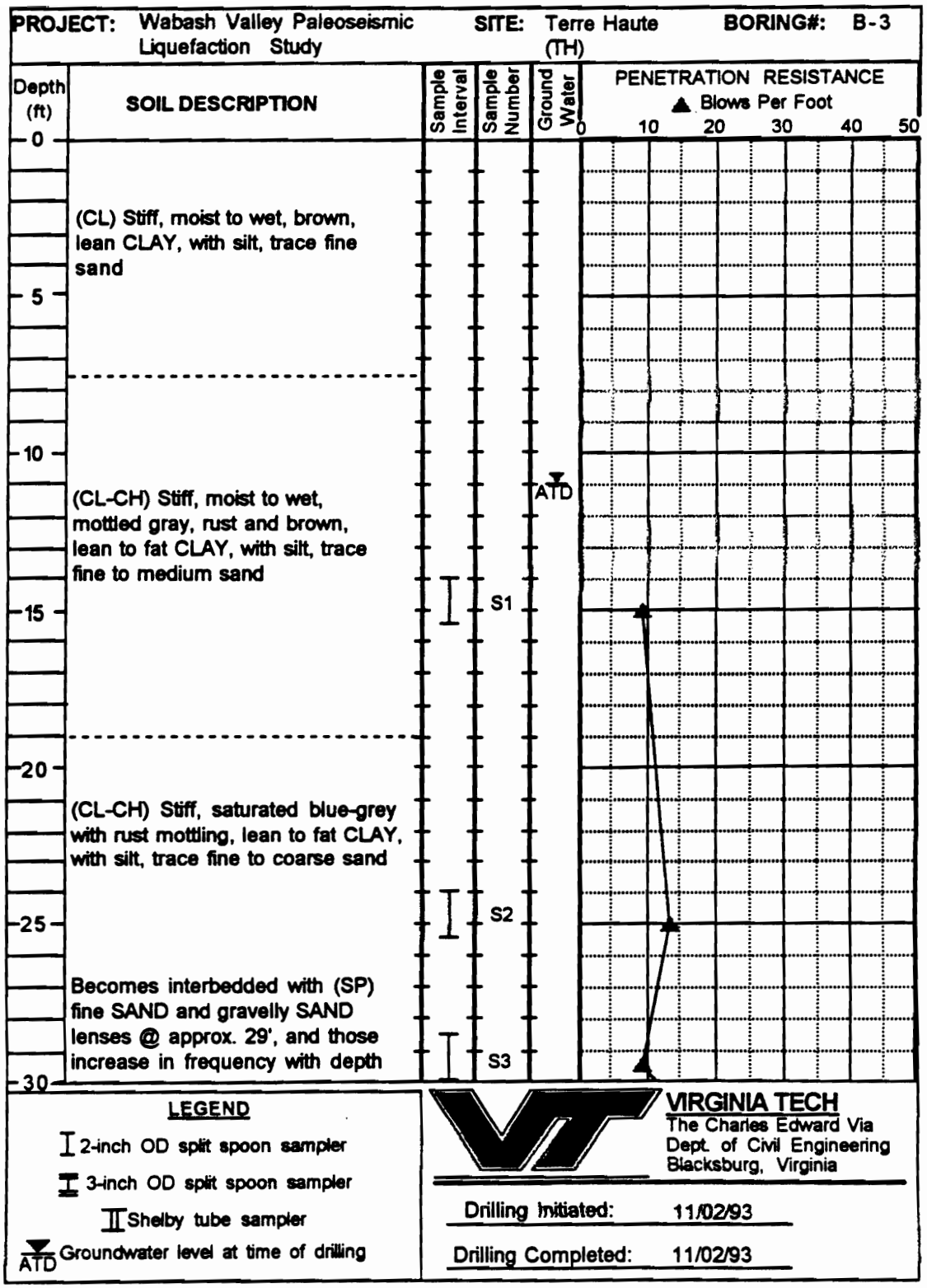
PROJECT: Wabash Valley Paleoseismic Liquefaction Study
SITE: Terre Haute (TH)
BORING#: B-3
Depth (ft)
SOIL DESCRIPTION
Sample Interval
Sample Number
Ground Water
PENETRATION RESISTANCE
▲ Blows Per Foot
0
10
20
30
40
50
0
5
10
15
20
25
30
(CL) Stiff, moist to wet, brown, lean CLAY, with silt, trace fine sand
(CL-CH) Stiff, moist to wet, mottled gray, rust and brown, lean to fat CLAY, with silt, trace fine to medium sand
ATD
S1
(CL-CH) Stiff, saturated blue-grey with rust mottling, lean to fat CLAY, with silt, trace fine to coarse sand
S2
Becomes interbedded with (SP) fine SAND and gravelly SAND lenses @ approx. 29', and those increase in frequency with depth
S3
LEGEND
2-inch OD split spoon sampler
3-inch OD split spoon sampler
Shelby tube sampler
ATD Groundwater level at time of drilling
VIRGINIA TECH
The Charles Edward Via Dept. of Civil Engineering Blacksburg, Virginia
Drilling Initiated: 11/02/93
Drilling Completed: 11/02/93

PROJECT: Wabash Valley Paleoseismic Liquefaction Study

SITE: Terre Haute (TH)

BORING#: B-3 (cont'd)

Depth (ft)	SOIL DESCRIPTION	Sample Interval	Sample Number	Ground Water
30	(GC) Stiff, sat, blue-grey and rust, clayey GRAVEL; with (SP) Med dense, sat, gray, predom. f-m SAND layer @ 31' to 32.5'		S4	
			S5	
35	(GP-GM) Medium dense, saturated, tan/gray, GRAVEL, with silt and sand		S6	
	(SP-SM) Med. dense, sat, gray, predom. f-m SAND, with silt, tr g		S7	
40	Bottom of boring at approx. 40'			
45				
50				
55				
60				

PENETRATION RESISTANCE
▲ Blows Per Foot
0 10 20 30 40 50

LEGEND

- 2-inch OD split spoon sampler
- 3-inch OD split spoon sampler
- Shelby tube sampler
- ATD Groundwater level at time of drilling

VIRGINIA TECH
The Charles Edward Via
Dept. of Civil Engineering
Blacksburg, Virginia

Drilling Initiated: 11/02/93

Drilling Completed: 11/02/93

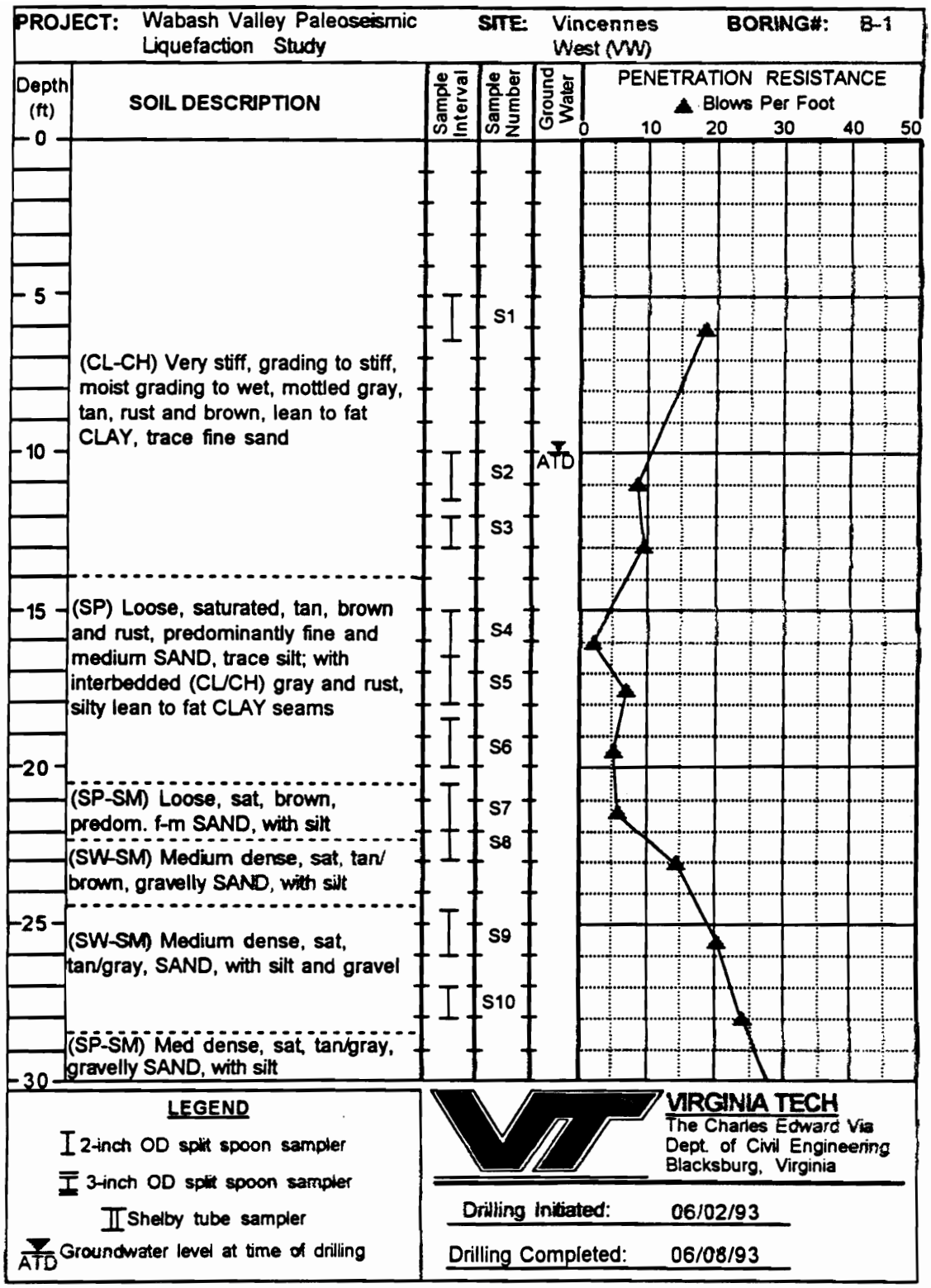
PROJECT: Wabash Valley Paleoseismic Liquefaction Study
SITE: Vincennes West (VW)
BORING#: B-1
Depth (ft)
SOIL DESCRIPTION
Sample Interval
Sample Number
Ground Water
PENETRATION RESISTANCE
Blows Per Foot
0
10
20
30
40
50
5
10
15
20
25
30
S1
S2
S3
S4
S5
S6
S7
S8
S9
S10
ATD
(CL-CH) Very stiff, grading to stiff, moist grading to wet, mottled gray, tan, rust and brown, lean to fat CLAY, trace fine sand
(SP) Loose, saturated, tan, brown and rust, predominantly fine and medium SAND, trace silt; with interbedded (CL/CH) gray and rust, silty lean to fat CLAY seams
(SP-SM) Loose, sat, brown, predom. f-m SAND, with silt
(SW-SM) Medium dense, sat, tan/brown, gravelly SAND, with silt
(SW-SM) Medium dense, sat, tan/gray, SAND, with silt and gravel
(SP-SM) Med dense, sat, tan/gray, gravelly SAND, with silt
LEGEND
2-inch OD split spoon sampler
3-inch OD split spoon sampler
Shelby tube sampler
ATD Groundwater level at time of drilling
VIRGINIA TECH
The Charles Edward Via Dept. of Civil Engineering Blacksburg, Virginia
Drilling Initiated: 06/02/93
Drilling Completed: 06/08/93

PROJECT: Wabash Valley Paleoseismic Liquefaction Study **SITE:** Vincennes West (VW) **BORING#:** B-1 (cont'd)

Depth (ft)	SOIL DESCRIPTION	Sample Interval	Sample Number	Ground Water	PENETRATION RESISTANCE ▲ Blows Per Foot 0 10 20 30 40 50
30	(SP-SM) Medium dense, saturated, gray, gravelly SAND, with silt	I	S11		
	Bottom of boring at approx. 33.5'				
35					
40					
45					
50					
55					
60					

LEGEND

I 2-inch OD split spoon sampler

I 3-inch OD split spoon sampler

I Shelby tube sampler

ATD Groundwater level at time of drilling

VIRGINIA TECH
The Charles Edward Via
Dept. of Civil Engineering
Blacksburg, Virginia

Drilling Initiated: 06/02/93

Drilling Completed: 06/08/93

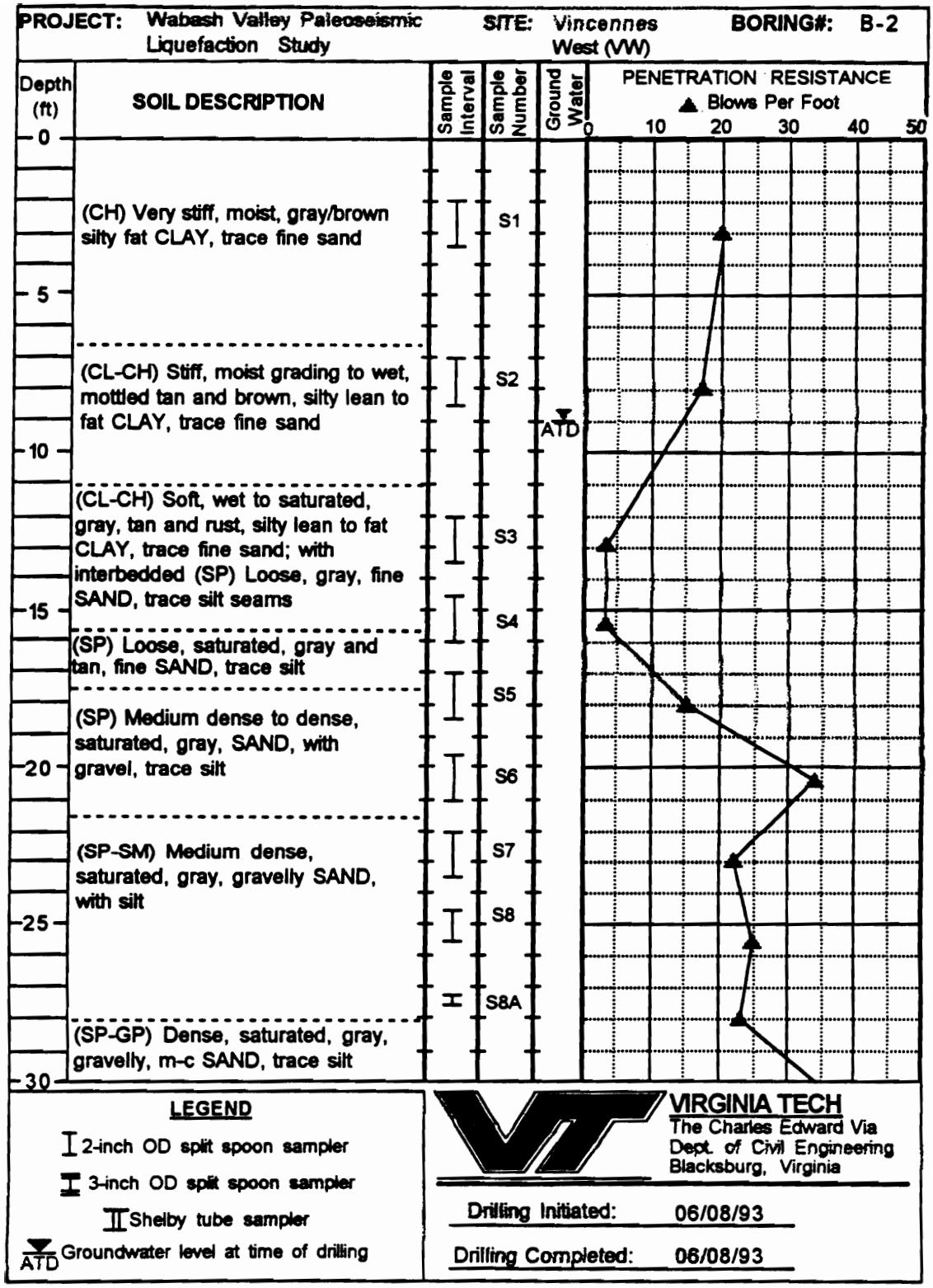
PROJECT: Wabash Valley Paleoseismic Liquefaction Study
SITE: Vincennes West (VW)
BORING#: B-2
Depth (ft)
SOIL DESCRIPTION
Sample Interval
Sample Number
Ground Water
PENETRATION RESISTANCE
Blows Per Foot
0
10
20
30
40
50
0
5
10
15
20
25
30
(CH) Very stiff, moist, gray/brown silty fat CLAY, trace fine sand
(CL-CH) Stiff, moist grading to wet, mottled tan and brown, silty lean to fat CLAY, trace fine sand
(CL-CH) Soft, wet to saturated, gray, tan and rust, silty lean to fat CLAY, trace fine sand; with interbedded (SP) Loose, gray, fine SAND, trace silt seams
(SP) Loose, saturated, gray and tan, fine SAND, trace silt
(SP) Medium dense to dense, saturated, gray, SAND, with gravel, trace silt
(SP-SM) Medium dense, saturated, gray, gravelly SAND, with silt
(SP-GP) Dense, saturated, gray, gravelly, m-c SAND, trace silt
S1
S2
S3
S4
S5
S6
S7
S8
S8A
ATD
LEGEND
2-inch OD split spoon sampler
3-inch OD split spoon sampler
Shelby tube sampler
Groundwater level at time of drilling
VIRGINIA TECH
The Charles Edward Via
Dept. of Civil Engineering
Blacksburg, Virginia
Drilling Initiated: 06/08/93
Drilling Completed: 06/08/93

PROJECT: Wabash Valley Paleoseismic Liquefaction Study

SITE: Vincennes West (VW)

BORING#: B-2 (cont'd)

Depth (ft)	SOIL DESCRIPTION	Sample Interval	Sample Number	Ground Water	PENETRATION RESISTANCE ▲ Blows Per Foot 0 10 20 30 40 50
30	(SP-GP) Dense, saturated, gray, gravelly, predominantly medium to coarse SAND, trace silt	I	S9		
	Bottom of boring at approx. 33.5'				
35					
40					
45					
50					
55					
60					

LEGEND

- I 2-inch OD split spoon sampler
- I 3-inch OD split spoon sampler
- I Shelby tube sampler
- ATD Groundwater level at time of drilling

VIRGINIA TECH
The Charles Edward Via Dept. of Civil Engineering
Blacksburg, Virginia

Drilling Initiated: 06/08/93

Drilling Completed: 06/08/93

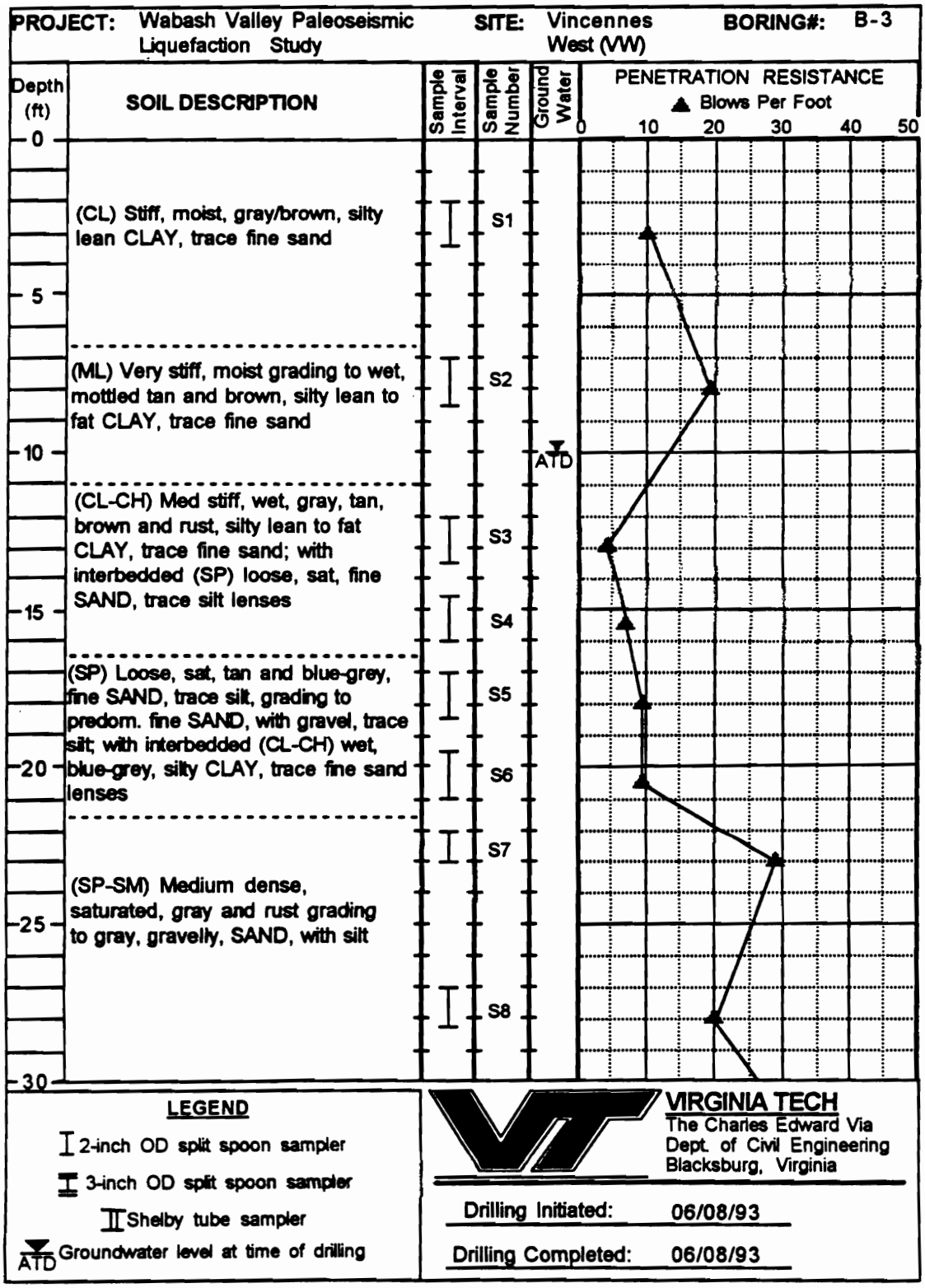
PROJECT: Wabash Valley Paleoseismic Liquefaction Study
SITE: Vincennes West (VW)
BORING#: B-3
Depth (ft)
SOIL DESCRIPTION
Sample Interval
Sample Number
Ground Water
PENETRATION RESISTANCE
Blows Per Foot
0
10
20
30
40
50
0
5
10
15
20
25
30
(CL) Stiff, moist, gray/brown, silty lean CLAY, trace fine sand
(ML) Very stiff, moist grading to wet, mottled tan and brown, silty lean to fat CLAY, trace fine sand
(CL-CH) Med stiff, wet, gray, tan, brown and rust, silty lean to fat CLAY, trace fine sand; with interbedded (SP) loose, sat, fine SAND, trace silt lenses
(SP) Loose, sat, tan and blue-grey, fine SAND, trace silt, grading to predom. fine SAND, with gravel, trace silt; with interbedded (CL-CH) wet, blue-grey, silty CLAY, trace fine sand lenses
(SP-SM) Medium dense, saturated, gray and rust grading to gray, gravelly, SAND, with silt
S1
S2
S3
S4
S5
S6
S7
S8
ATD
LEGEND
2-inch OD split spoon sampler
3-inch OD split spoon sampler
Shelby tube sampler
ATD Groundwater level at time of drilling
VIRGINIA TECH
The Charles Edward Via Dept. of Civil Engineering Blacksburg, Virginia
Drilling Initiated: 06/08/93
Drilling Completed: 06/08/93

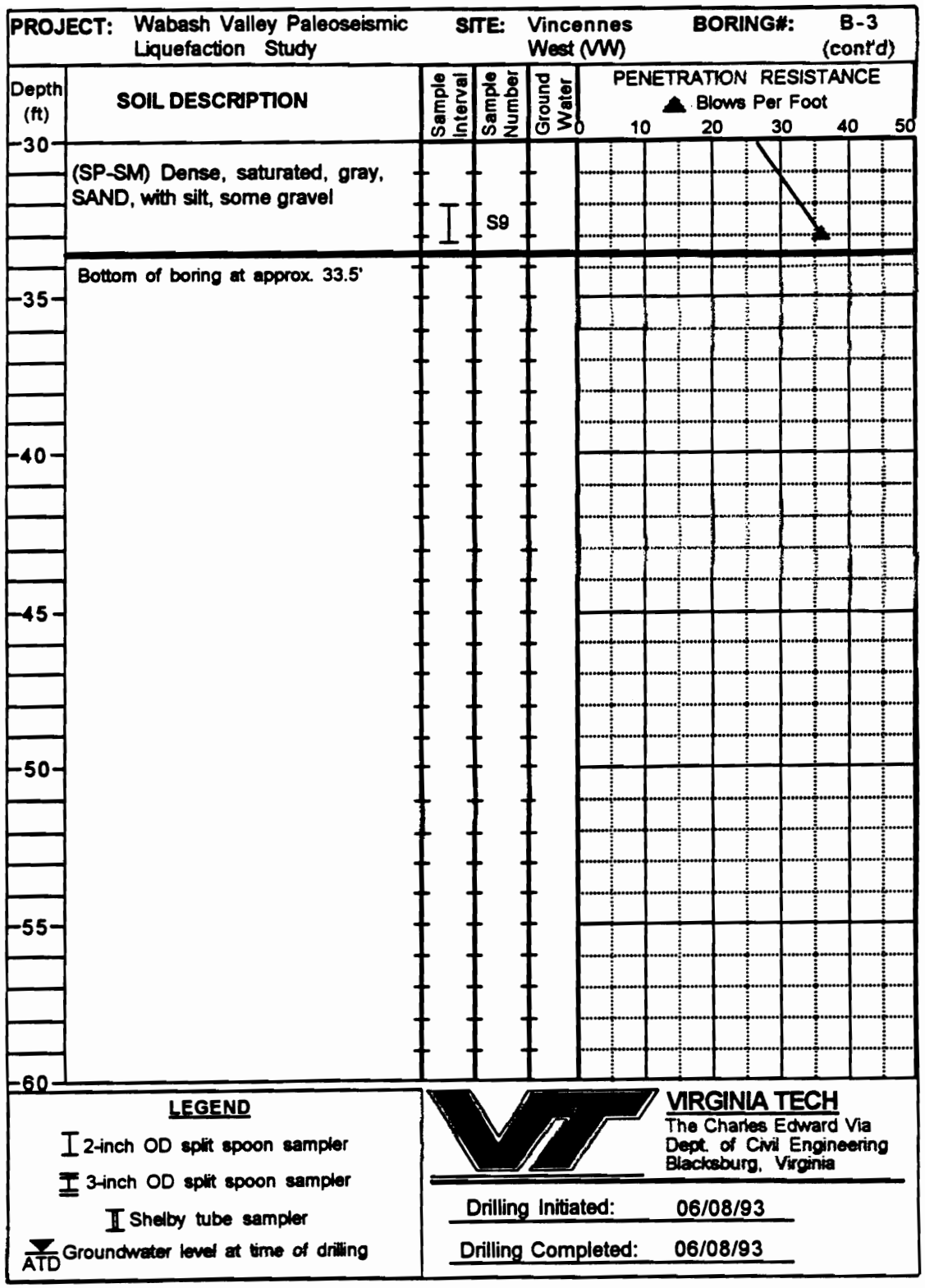
PROJECT: Wabash Valley Paleoseismic Liquefaction Study
SITE: Vincennes West (VW)
BORING#: B-3 (cont'd)
Depth (ft)
SOIL DESCRIPTION
Sample Interval
Sample Number
Ground Water
PENETRATION RESISTANCE
Blows Per Foot
0
10
20
30
40
50
30
(SP-SM) Dense, saturated, gray, SAND, with silt, some gravel
S9
Bottom of boring at approx. 33.5'
35
40
45
50
55
60
LEGEND
2-inch OD split spoon sampler
3-inch OD split spoon sampler
Shelby tube sampler
ATD Groundwater level at time of drilling
VIRGINIA TECH
The Charles Edward Via
Dept. of Civil Engineering
Blacksburg, Virginia
Drilling Initiated: 06/08/93
Drilling Completed: 06/08/93

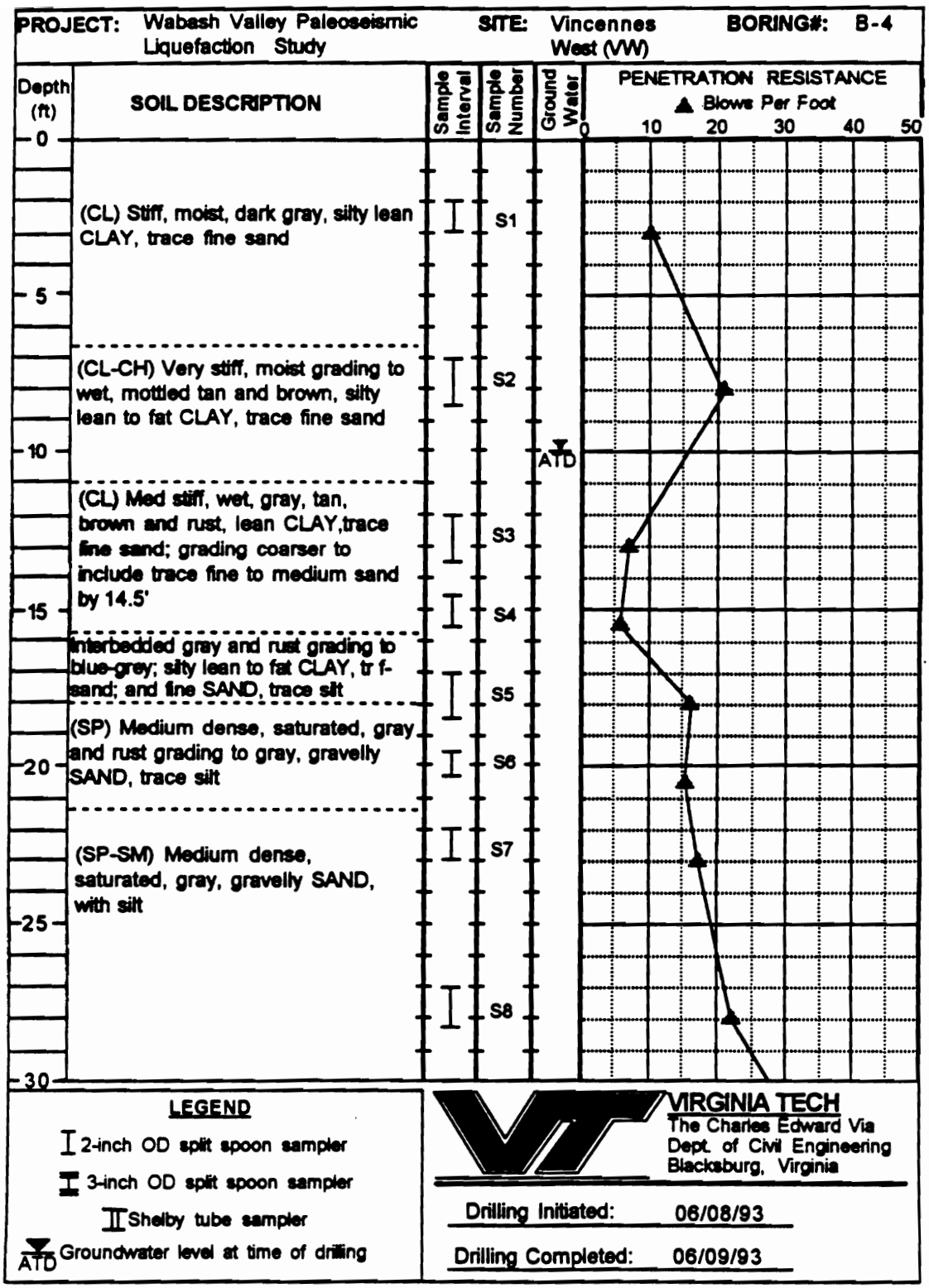
PROJECT: Wabash Valley Paleoseismic Liquefaction Study
SITE: Vincennes West (VW)
BORING#: B-4
Depth (ft)
SOIL DESCRIPTION
Sample Interval
Sample Number
Ground Water
PENETRATION RESISTANCE
Blows Per Foot
0
10
20
30
40
50
0
5
10
15
20
25
30
(CL) Stiff, moist, dark gray, silty lean CLAY, trace fine sand
(CL-CH) Very stiff, moist grading to wet, mottled tan and brown, silty lean to fat CLAY, trace fine sand
(CL) Med stiff, wet, gray, tan, brown and rust, lean CLAY,trace fine sand; grading coarser to include trace fine to medium sand by 14.5'
Interbedded gray and rust grading to blue-grey; silty lean to fat CLAY, tr f-sand; and fine SAND, trace silt
(SP) Medium dense, saturated, gray and rust grading to gray, gravelly SAND, trace silt
(SP-SM) Medium dense, saturated, gray, gravelly SAND, with silt
S1
S2
S3
S4
S5
S6
S7
S8
ATD
LEGEND
2-inch OD split spoon sampler
3-inch OD split spoon sampler
Shelby tube sampler
Groundwater level at time of drilling
VIRGINIA TECH
The Charles Edward Via Dept. of Civil Engineering Blacksburg, Virginia
Drilling Initiated: 06/08/93
Drilling Completed: 06/09/93

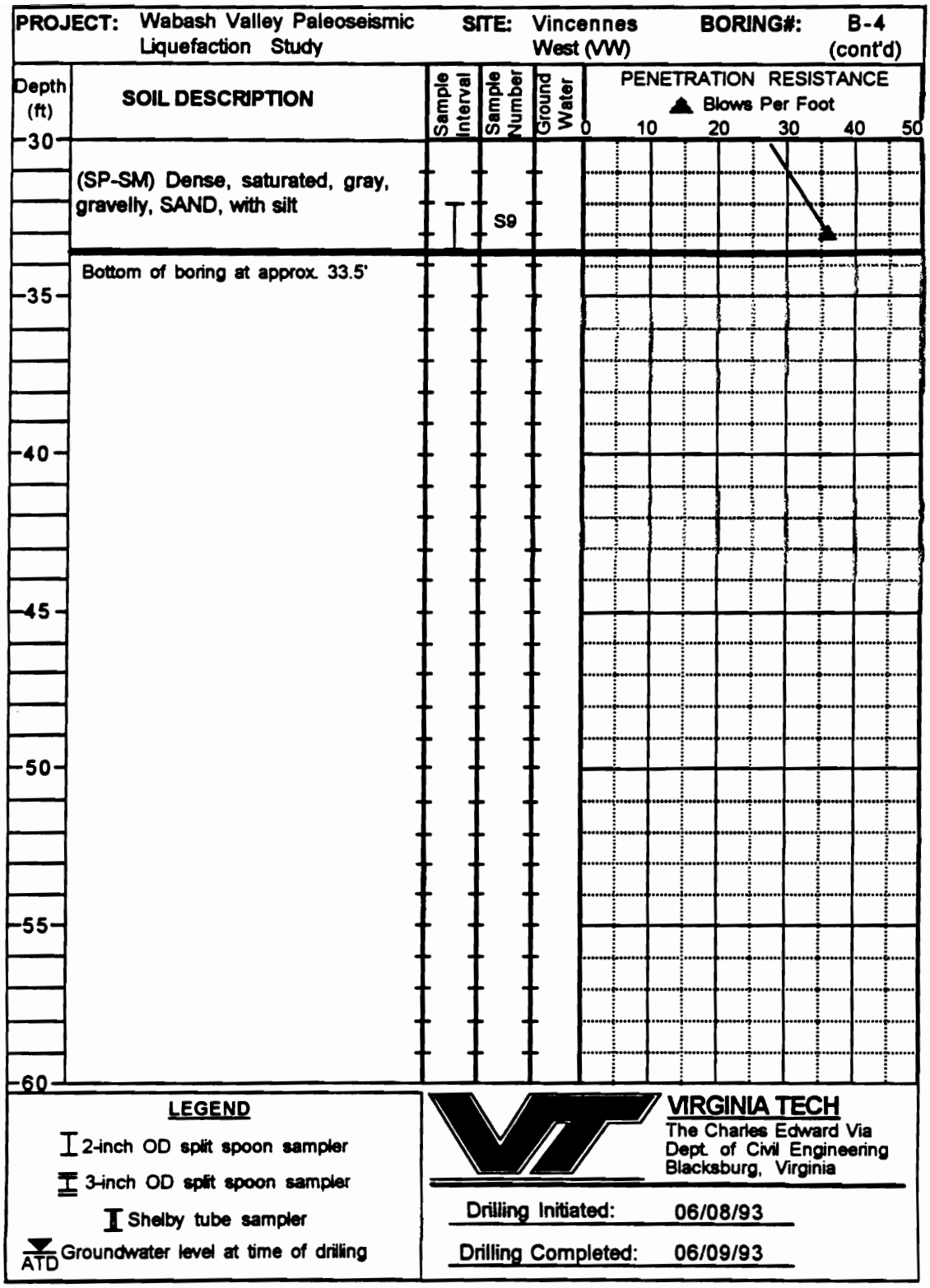
PROJECT: Wabash Valley Paleoseismic Liquefaction Study
SITE: Vincennes West (VW)
BORING#: B-4 (cont'd)
Depth (ft)
SOIL DESCRIPTION
Sample Interval
Sample Number
Ground Water
PENETRATION RESISTANCE
Blows Per Foot
0
10
20
30
40
50
30
(SP-SM) Dense, saturated, gray, gravelly, SAND, with silt
S9
Bottom of boring at approx. 33.5'
35
40
45
50
55
60
LEGEND
2-inch OD split spoon sampler
3-inch OD split spoon sampler
Shelby tube sampler
ATD Groundwater level at time of drilling
VIRGINIA TECH
The Charles Edward Via Dept. of Civil Engineering Blacksburg, Virginia
Drilling Initiated: 06/08/93
Drilling Completed: 06/09/93

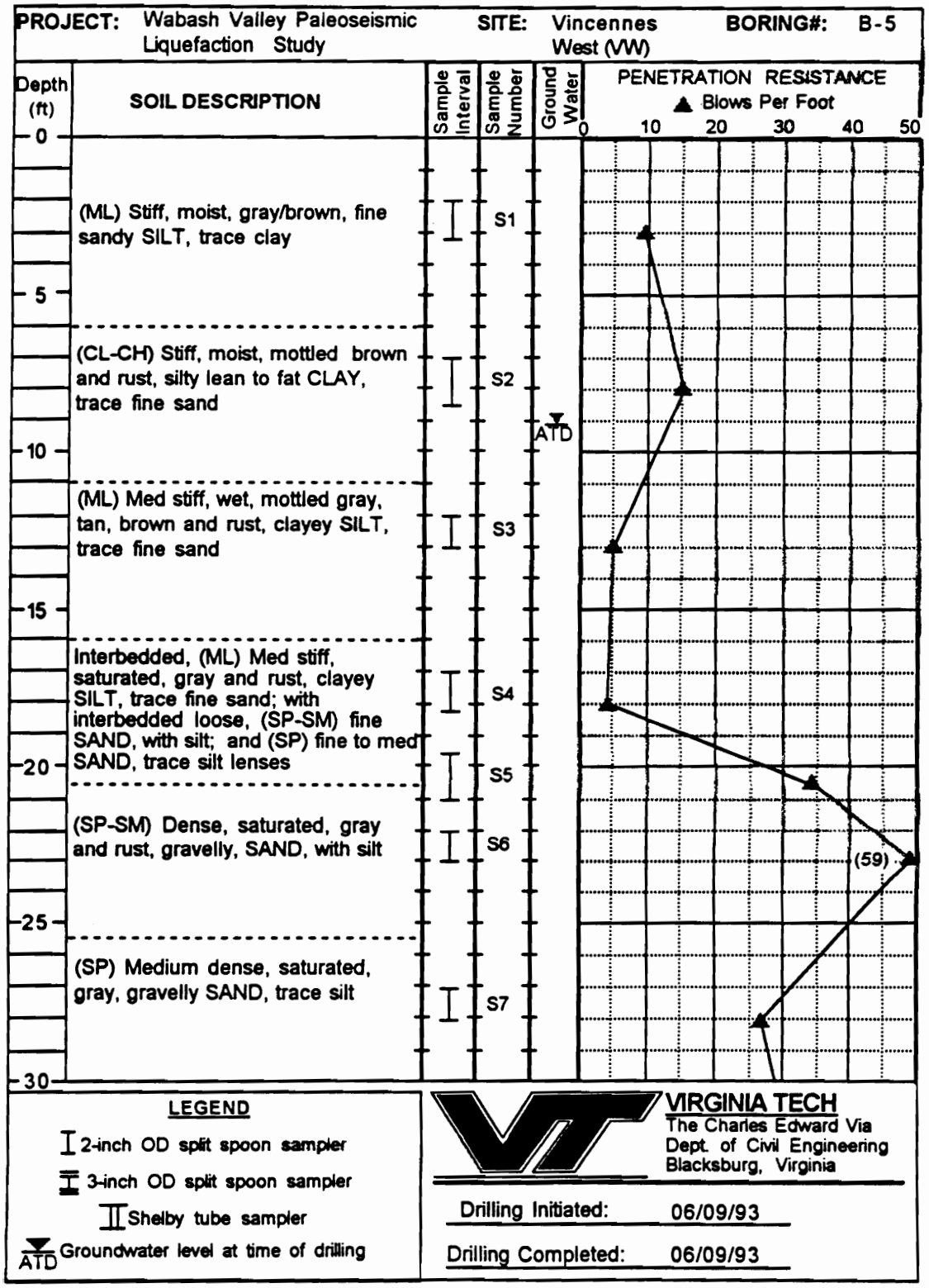
PROJECT: Wabash Valley Paleoseismic Liquefaction Study
SITE: Vincennes West (VW)
BORING#: B-5
Depth (ft)
SOIL DESCRIPTION
Sample Interval
Sample Number
Ground Water
PENETRATION RESISTANCE
Blows Per Foot
0
10
20
30
40
50
0
5
10
15
20
25
30
(ML) Stiff, moist, gray/brown, fine sandy SILT, trace clay
S1
(CL-CH) Stiff, moist, mottled brown and rust, silty lean to fat CLAY, trace fine sand
S2
ATD
(ML) Med stiff, wet, mottled gray, tan, brown and rust, clayey SILT, trace fine sand
S3
Interbedded, (ML) Med stiff, saturated, gray and rust, clayey SILT, trace fine sand; with interbedded loose, (SP-SM) fine SAND, with silt; and (SP) fine to med SAND, trace silt lenses
S4
S5
(SP-SM) Dense, saturated, gray and rust, gravelly, SAND, with silt
S6
(59)
(SP) Medium dense, saturated, gray, gravelly SAND, trace silt
S7
LEGEND
2-inch OD split spoon sampler
3-inch OD split spoon sampler
Shelby tube sampler
ATD Groundwater level at time of drilling
VIRGINIA TECH
The Charles Edward Via Dept. of Civil Engineering
Blacksburg, Virginia
Drilling Initiated: 06/09/93
Drilling Completed: 06/09/93

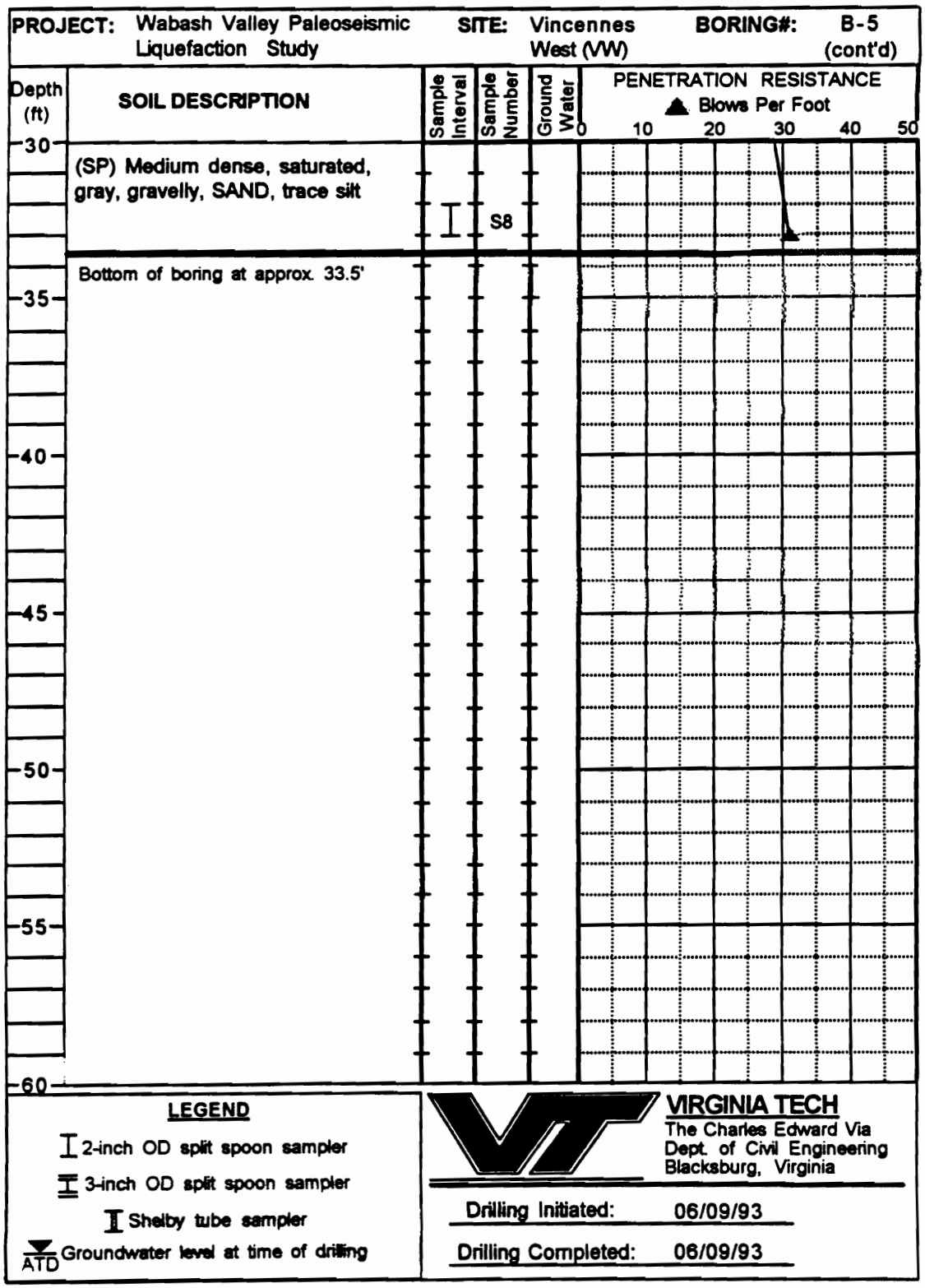
PROJECT: Wabash Valley Paleoseismic Liquefaction Study
SITE: Vincennes West (VW)
BORING#: B-5 (cont'd)
Depth (ft)
SOIL DESCRIPTION
Sample Interval
Sample Number
Ground Water
PENETRATION RESISTANCE
Blows Per Foot
0
10
20
30
40
50
30
(SP) Medium dense, saturated, gray, gravelly, SAND, trace silt
S8
Bottom of boring at approx. 33.5'
35
40
45
50
55
60
LEGEND
2-inch OD split spoon sampler
3-inch OD split spoon sampler
Shelby tube sampler
ATD Groundwater level at time of drilling
VIRGINIA TECH
The Charles Edward Via Dept. of Civil Engineering Blacksburg, Virginia
Drilling Initiated: 06/09/93
Drilling Completed: 06/09/93

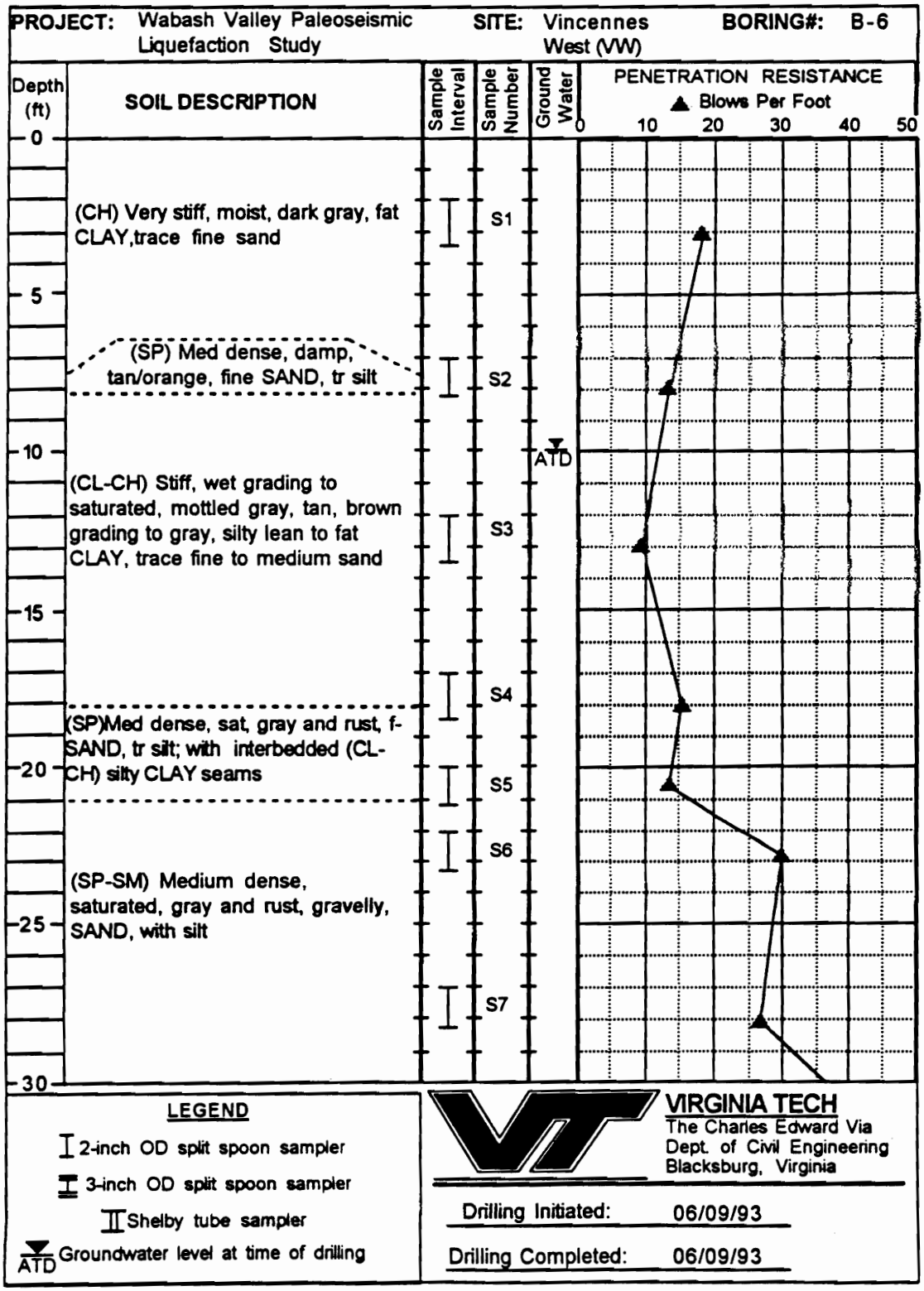
PROJECT: Wabash Valley Paleoseismic Liquefaction Study
SITE: Vincennes West (VW)
BORING#: B-6
Depth (ft)
SOIL DESCRIPTION
Sample Interval
Sample Number
Ground Water
PENETRATION RESISTANCE
Blows Per Foot
0
10
20
30
40
50
0
5
10
15
20
25
30
(CH) Very stiff, moist, dark gray, fat CLAY,trace fine sand
(SP) Med dense, damp, tan/orange, fine SAND, tr silt
(CL-CH) Stiff, wet grading to saturated, mottled gray, tan, brown grading to gray, silty lean to fat CLAY, trace fine to medium sand
(SP)Med dense, sat, gray and rust, f-SAND, tr silt; with interbedded (CL-CH) silty CLAY seams
(SP-SM) Medium dense, saturated, gray and rust, gravelly, SAND, with silt
S1
S2
S3
S4
S5
S6
S7
ATD
LEGEND
2-inch OD split spoon sampler
3-inch OD split spoon sampler
Shelby tube sampler
ATD Groundwater level at time of drilling
VIRGINIA TECH
The Charles Edward Via Dept. of Civil Engineering Blacksburg, Virginia
Drilling Initiated: 06/09/93
Drilling Completed: 06/09/93

PROJECT: Wabash Valley Paleoseismic Liquefaction Study **SITE:** Vincennes West (VW) **BORING#:** B-6 (cont'd)

Depth (ft)	SOIL DESCRIPTION	Sample Interval	Sample Number	Ground Water	PENETRATION RESISTANCE ▲ Blows Per Foot 0 10 20 30 40 50
30	(SP) Dense, saturated, gray, SAND, with gravel, trace silt	I	S8		(60)
	Bottom of boring at approx. 33.5'				
35					
40					
45					
50					
55					
60					

LEGEND

- I 2-inch OD split spoon sampler
- I 3-inch OD split spoon sampler
- I Shelby tube sampler
- ATD Groundwater level at time of drilling

VIRGINIA TECH
The Charles Edward Via
Dept. of Civil Engineering
Blacksburg, Virginia

Drilling Initiated: 06/09/93

Drilling Completed: 06/09/93

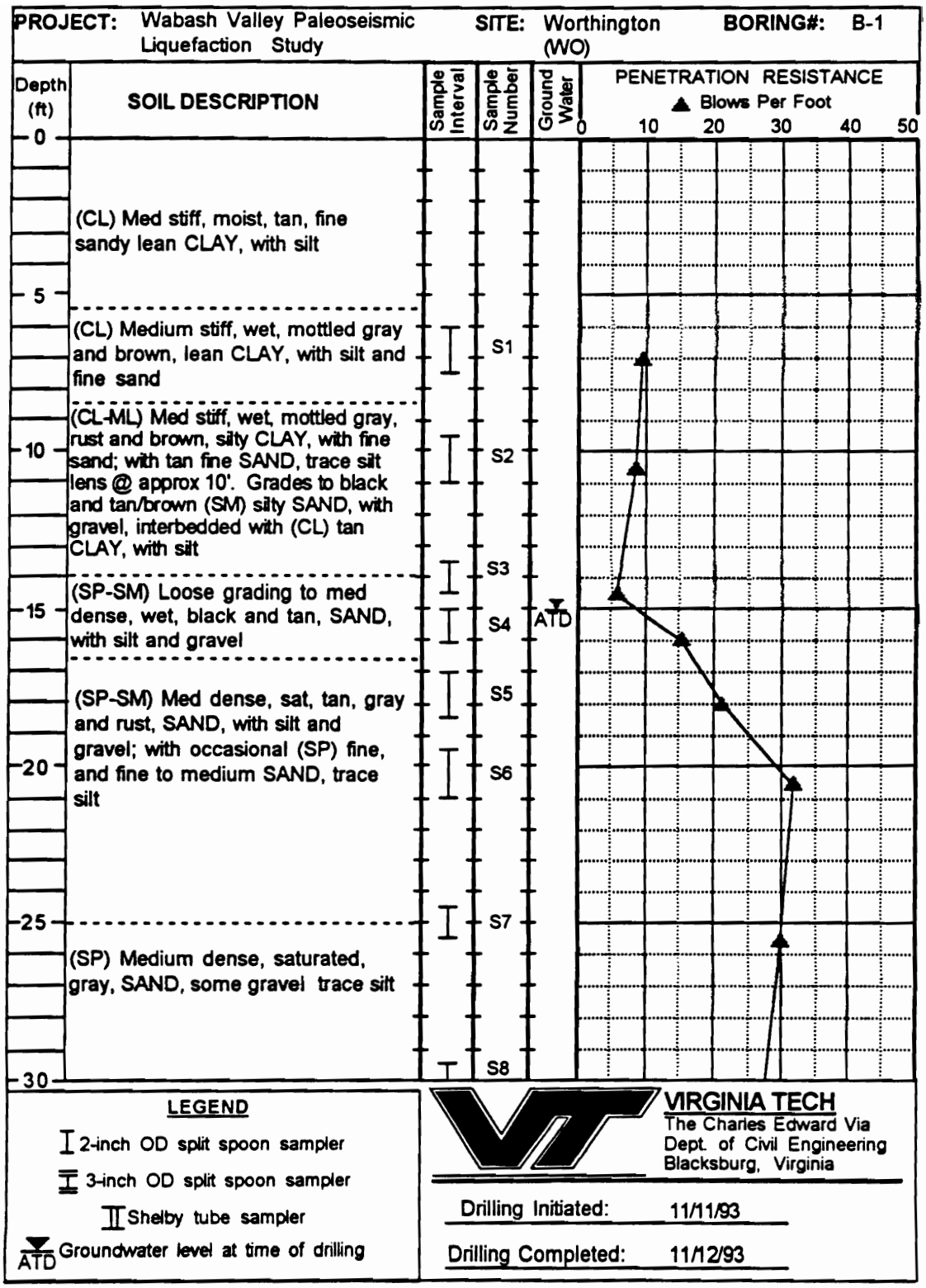
PROJECT: Wabash Valley Paleoseismic Liquefaction Study
SITE: Worthington (WO)
BORING#: B-1
Depth (ft)
SOIL DESCRIPTION
Sample Interval
Sample Number
Ground Water
PENETRATION RESISTANCE
Blows Per Foot
0
10
20
30
40
50
0
5
10
15
20
25
30
(CL) Med stiff, moist, tan, fine sandy lean CLAY, with silt
(CL) Medium stiff, wet, mottled gray and brown, lean CLAY, with silt and fine sand
(CL-ML) Med stiff, wet, mottled gray, rust and brown, silty CLAY, with fine sand; with tan fine SAND, trace silt lens @ approx 10'. Grades to black and tan/brown (SM) silty SAND, with gravel, interbedded with (CL) tan CLAY, with silt
(SP-SM) Loose grading to med dense, wet, black and tan, SAND, with silt and gravel
(SP-SM) Med dense, sat, tan, gray and rust, SAND, with silt and gravel; with occasional (SP) fine, and fine to medium SAND, trace silt
(SP) Medium dense, saturated, gray, SAND, some gravel trace silt
S1
S2
S3
S4
S5
S6
S7
S8
ATD
LEGEND
2-inch OD split spoon sampler
3-inch OD split spoon sampler
Shelby tube sampler
ATD Groundwater level at time of drilling
VIRGINIA TECH
The Charles Edward Via Dept. of Civil Engineering
Blacksburg, Virginia
Drilling Initiated: 11/11/93
Drilling Completed: 11/12/93

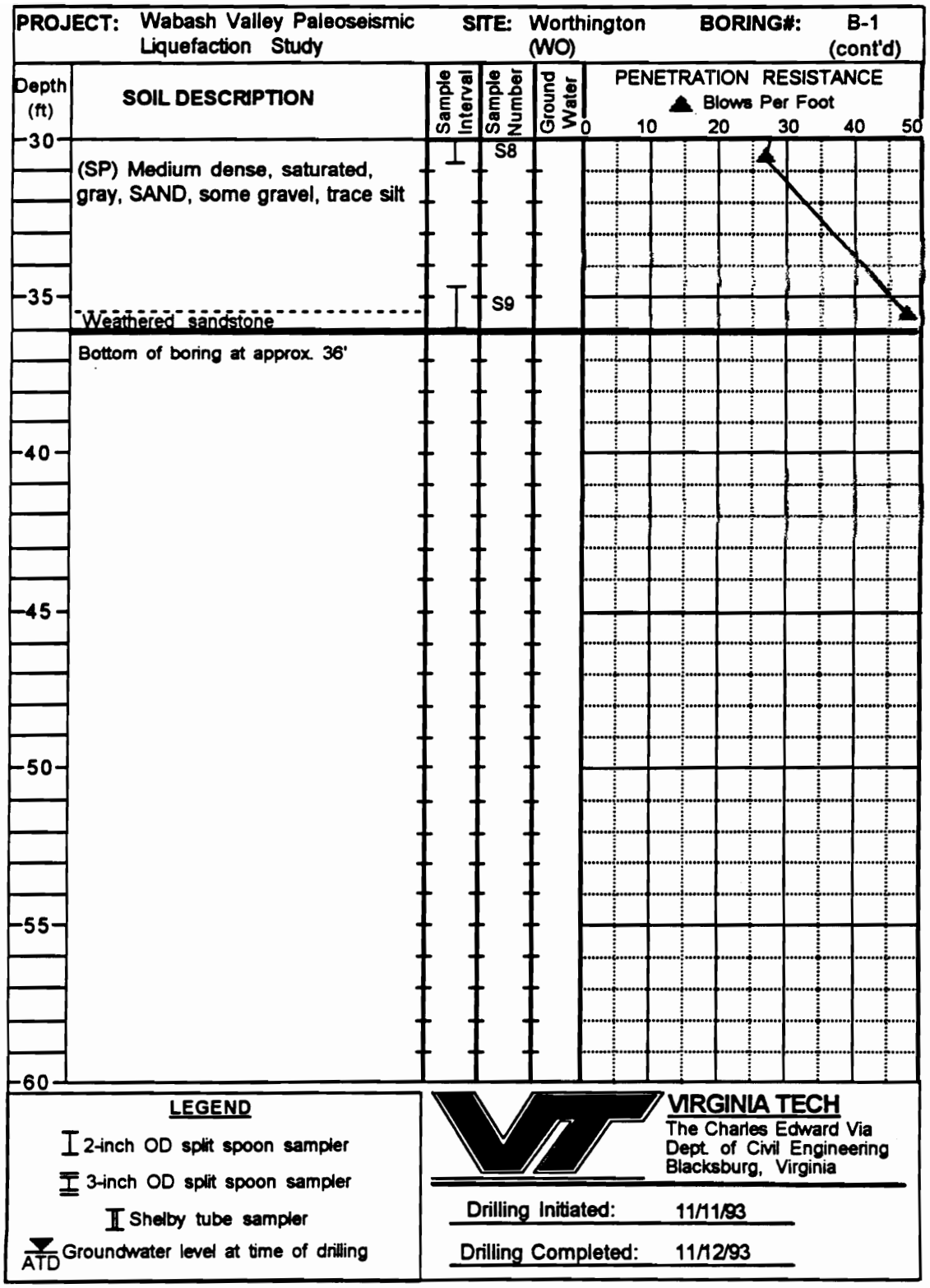
PROJECT: Wabash Valley Paleoseismic Liquefaction Study
SITE: Worthington (WO)
BORING#: B-1 (cont'd)
Depth (ft)
SOIL DESCRIPTION
Sample Interval
Sample Number
Ground Water
PENETRATION RESISTANCE
Blows Per Foot
0
10
20
30
40
50
30
35
40
45
50
55
60
(SP) Medium dense, saturated, gray, SAND, some gravel, trace silt
S8
S9
Weathered sandstone
Bottom of boring at approx. 36'
LEGEND
2-inch OD split spoon sampler
3-inch OD split spoon sampler
Shelby tube sampler
ATD Groundwater level at time of drilling
VIRGINIA TECH
The Charles Edward Via Dept. of Civil Engineering Blacksburg, Virginia
Drilling Initiated: 11/11/93
Drilling Completed: 11/12/93

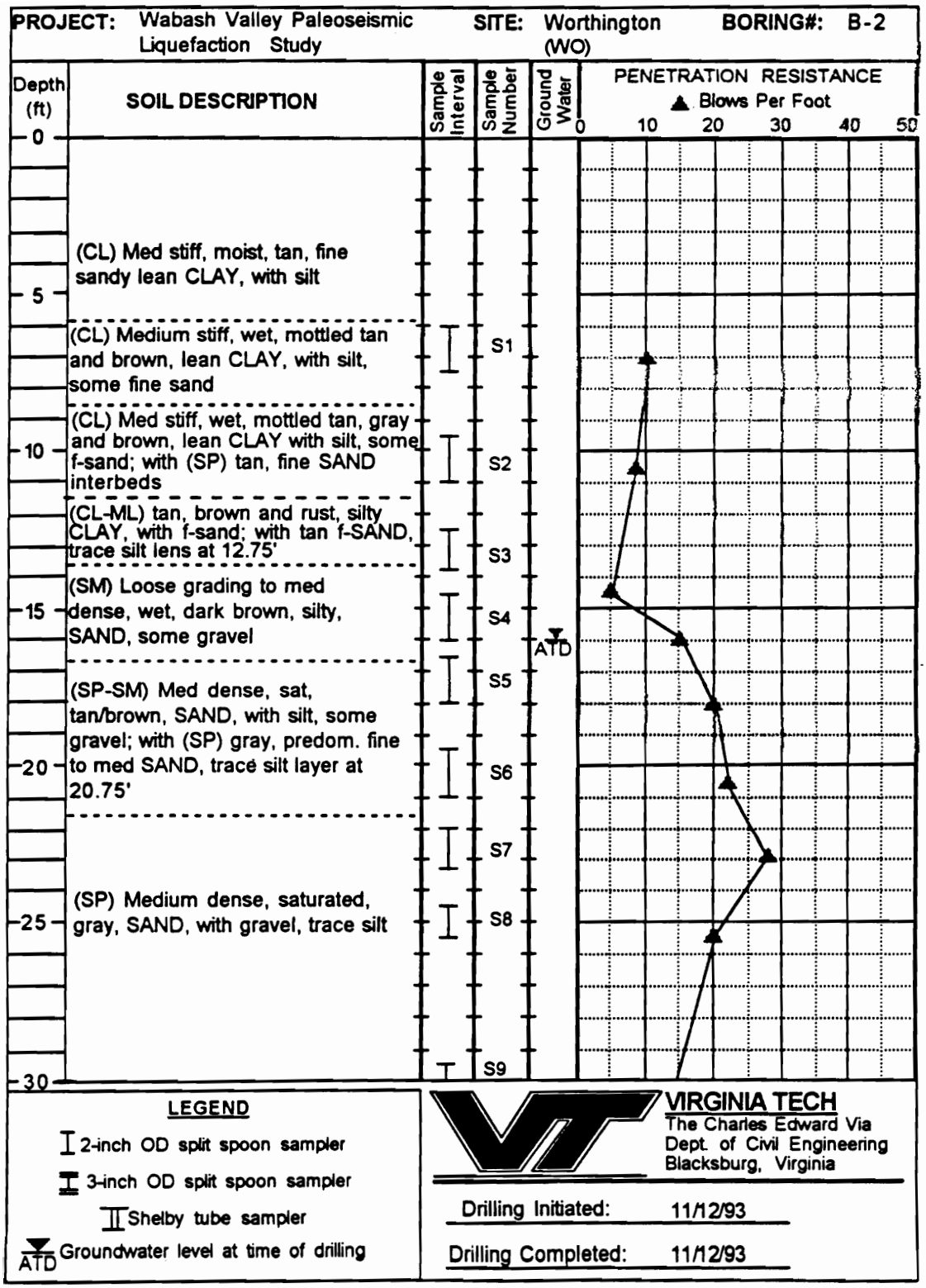
PROJECT: Wabash Valley Paleoseismic Liquefaction Study
SITE: Worthington (WO)
BORING#: B-2
Depth (ft)
SOIL DESCRIPTION
Sample Interval
Sample Number
Ground Water
PENETRATION RESISTANCE
Blows Per Foot
0
10
20
30
40
50
0
5
10
15
20
25
30
(CL) Med stiff, moist, tan, fine sandy lean CLAY, with silt
(CL) Medium stiff, wet, mottled tan and brown, lean CLAY, with silt, some fine sand
(CL) Med stiff, wet, mottled tan, gray and brown, lean CLAY with silt, some f-sand; with (SP) tan, fine SAND interbeds
(CL-ML) tan, brown and rust, silty CLAY, with f-sand; with tan f-SAND, trace silt lens at 12.75'
(SM) Loose grading to med dense, wet, dark brown, silty, SAND, some gravel
(SP-SM) Med dense, sat, tan/brown, SAND, with silt, some gravel; with (SP) gray, predom. fine to med SAND, trace silt layer at 20.75'
(SP) Medium dense, saturated, gray, SAND, with gravel, trace silt
S1
S2
S3
S4
S5
S6
S7
S8
S9
ATD
LEGEND
2-inch OD split spoon sampler
3-inch OD split spoon sampler
Shelby tube sampler
ATD Groundwater level at time of drilling
VIRGINIA TECH
The Charles Edward Via Dept. of Civil Engineering Blacksburg, Virginia
Drilling Initiated: 11/12/93
Drilling Completed: 11/12/93

PROJECT: Wabash Valley Paleoseismic Liquefaction Study **SITE:** Worthington (WO) **BORING#:** B-2 (cont'd)

Depth (ft)	SOIL DESCRIPTION	Sample Interval	Sample Number	Ground Water	PENETRATION RESISTANCE ▲ Blows Per Foot 0 10 20 30 40 50
30	(SP) Medium dense, saturated, gray, SAND, some gravel, trace silt		S9		
35			S10		
40	Weathered grading to fresh sandstone		S11		(68)
	Bottom of boring at approx. 41.5'				
45					
50					
55					
60					

LEGEND

- 2-inch OD split spoon sampler
- 3-inch OD split spoon sampler
- Shelby tube sampler
- ATD Groundwater level at time of drilling

VIRGINIA TECH
The Charles Edward Via
Dept. of Civil Engineering
Blacksburg, Virginia

Drilling Initiated: 11/12/93

Drilling Completed: 11/12/93

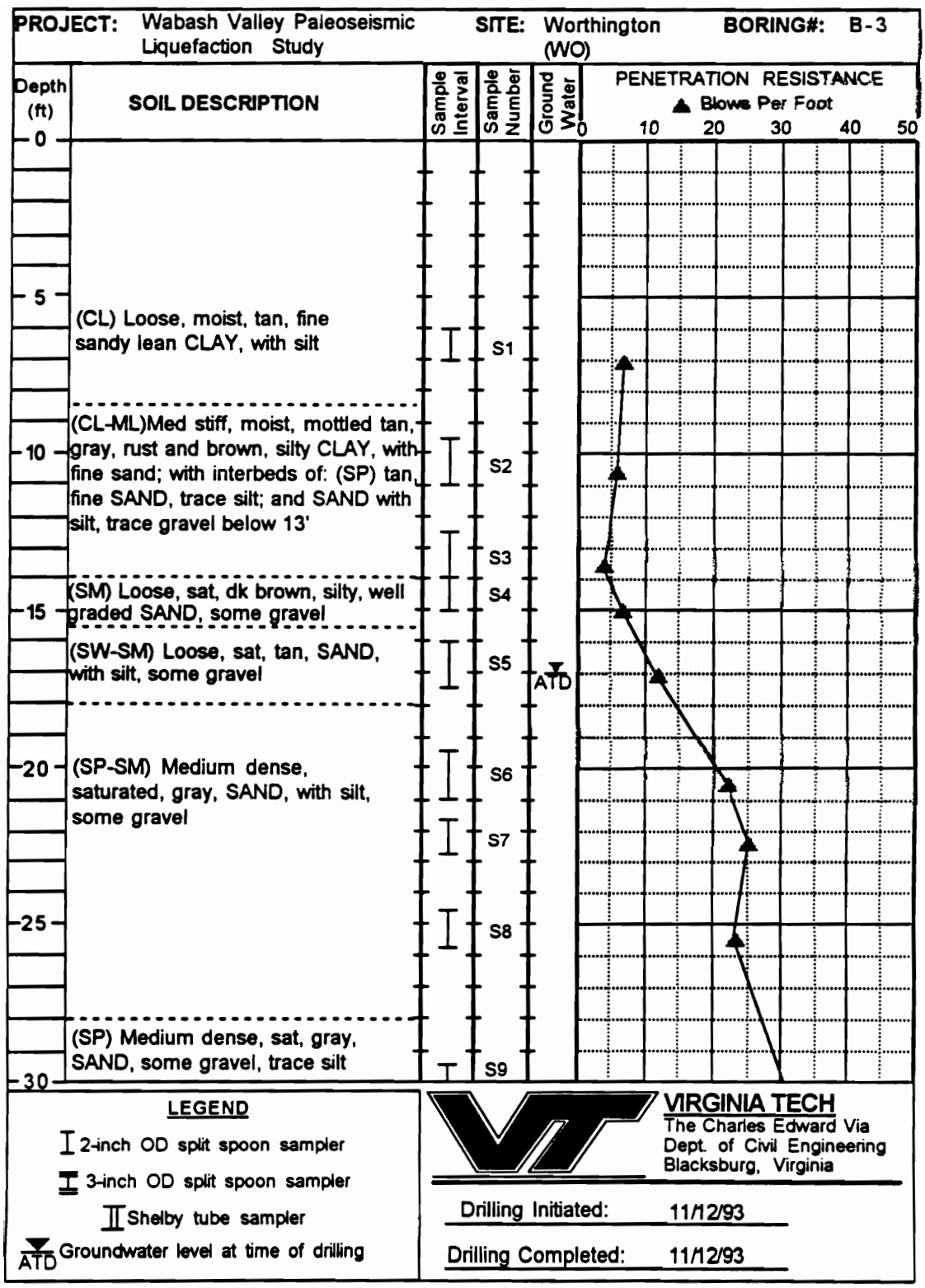
PROJECT: Wabash Valley Paleoseismic Liquefaction Study
SITE: Worthington (WO)
BORING#: B-3
Depth (ft)
SOIL DESCRIPTION
Sample Interval
Sample Number
Ground Water
PENETRATION RESISTANCE
Blows Per Foot
0
10
20
30
40
50
5
10
15
20
25
30
(CL) Loose, moist, tan, fine sandy lean CLAY, with silt
(CL-ML)Med stiff, moist, mottled tan, gray, rust and brown, silty CLAY, with fine sand; with interbeds of: (SP) tan, fine SAND, trace silt; and SAND with silt, trace gravel below 13'
(SM) Loose, sat, dk brown, silty, well graded SAND, some gravel
(SW-SM) Loose, sat, tan, SAND, with silt, some gravel
(SP-SM) Medium dense, saturated, gray, SAND, with silt, some gravel
(SP) Medium dense, sat, gray, SAND, some gravel, trace silt
S1
S2
S3
S4
S5
S6
S7
S8
S9
ATD
LEGEND
2-inch OD split spoon sampler
3-inch OD split spoon sampler
Shelby tube sampler
Groundwater level at time of drilling
VIRGINIA TECH
The Charles Edward Via
Dept. of Civil Engineering
Blacksburg, Virginia
Drilling Initiated: 11/12/93
Drilling Completed: 11/12/93

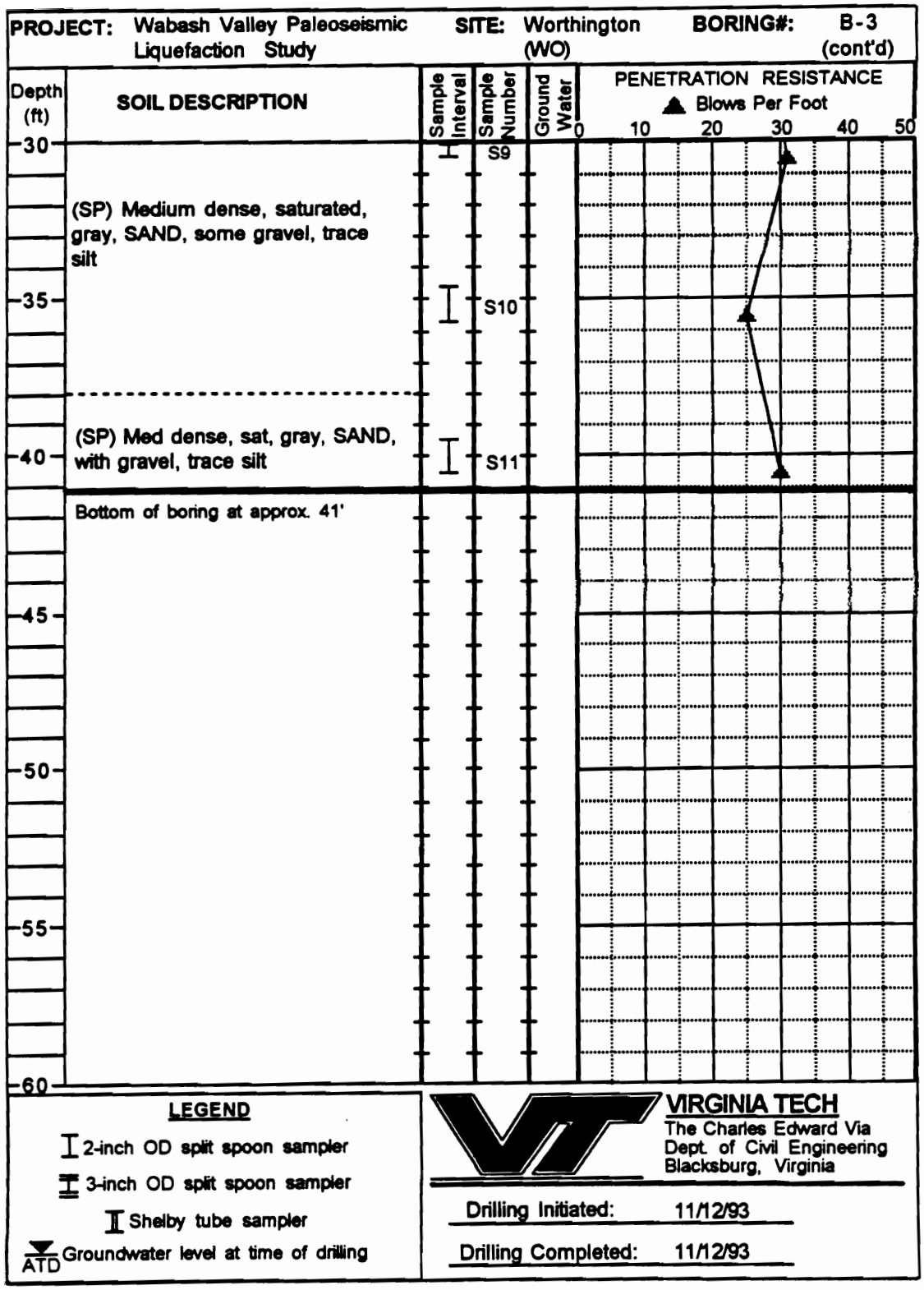
PROJECT: Wabash Valley Paleoseismic Liquefaction Study
SITE: Worthington (WO)
BORING#: B-3 (cont'd)
Depth (ft)
SOIL DESCRIPTION
Sample Interval
Sample Number
Ground Water
PENETRATION RESISTANCE
Blows Per Foot
0
10
20
30
40
50
30
35
40
45
50
55
60
S9
S10
S11
(SP) Medium dense, saturated, gray, SAND, some gravel, trace silt
(SP) Med dense, sat, gray, SAND, with gravel, trace silt
Bottom of boring at approx. 41'
LEGEND
2-inch OD split spoon sampler
3-inch OD split spoon sampler
Shelby tube sampler
ATD Groundwater level at time of drilling
VIRGINIA TECH
The Charles Edward Via Dept. of Civil Engineering Blacksburg, Virginia
Drilling Initiated: 11/12/93
Drilling Completed: 11/12/93

PROJECT: Wabash Valley Paleoseismic Liquefaction Study **SITE:** York (YO) **BORING#:** B-1

Depth (ft)	SOIL DESCRIPTION	Sample Interval	Sample Number	Ground Water
0	Sod and Topsoil			
	(CL) Med stiff, moist, tan, lean CLAY, with silt, some fine sand		S1	
5	(CL-CH) Stiff, moist, dark brown, lean to fat CLAY, with silt, trace fine sand		S2	
			S3	
10	(CH) Stiff, moist, mottled tan, brown and rust, fat CLAY, with silt; with interbedded (ML) gray, SILT seams cotaining free water between 12' and 14'.		S4	
			S5	
15			S6	ATD
	(CL-CH) Med stiff, wet, mottled gray, tan and rust, lean to fat CLAY, with silt		S7	
20	(CL) Soft, wet, mottled gray, rust and brown, lean CLAY, with silt, trace fine sand		S8	
	Interbedded sat, tan, gray, rust and black; (CL/CH) soft, lean to fat CLAY with silt, and (SP/SM) loose, silty fine SAND; grading to (SP/SM) loose, f-m SAND, trace silt and gravel, with interbedded (CL) lean CLAY, with silt lenses		S9	
			S10	
25			S11	
			S12	
	(SP) Med dense, sat, gray/tan, predom. fine to med SAND, trace silt and gravel (top of source)		S13	
30			S14	

PENETRATION RESISTANCE
▲ Blows Per Foot
0 10 20 30 40 50

LEGEND

- I 2-inch OD split spoon sampler
- I 3-inch OD split spoon sampler
- II Shelby tube sampler
- ATD Groundwater level at time of drilling

VIRGINIA TECH
The Charles Edward Via Dept. of Civil Engineering
Blacksburg, Virginia

Drilling Initiated: 05/28/92

Drilling Completed: 05/28/92

PROJECT: Wabash Valley Paleoseismic Liquefaction Study **SITE:** York (YO) **BORING#:** B-1 (cont'd)

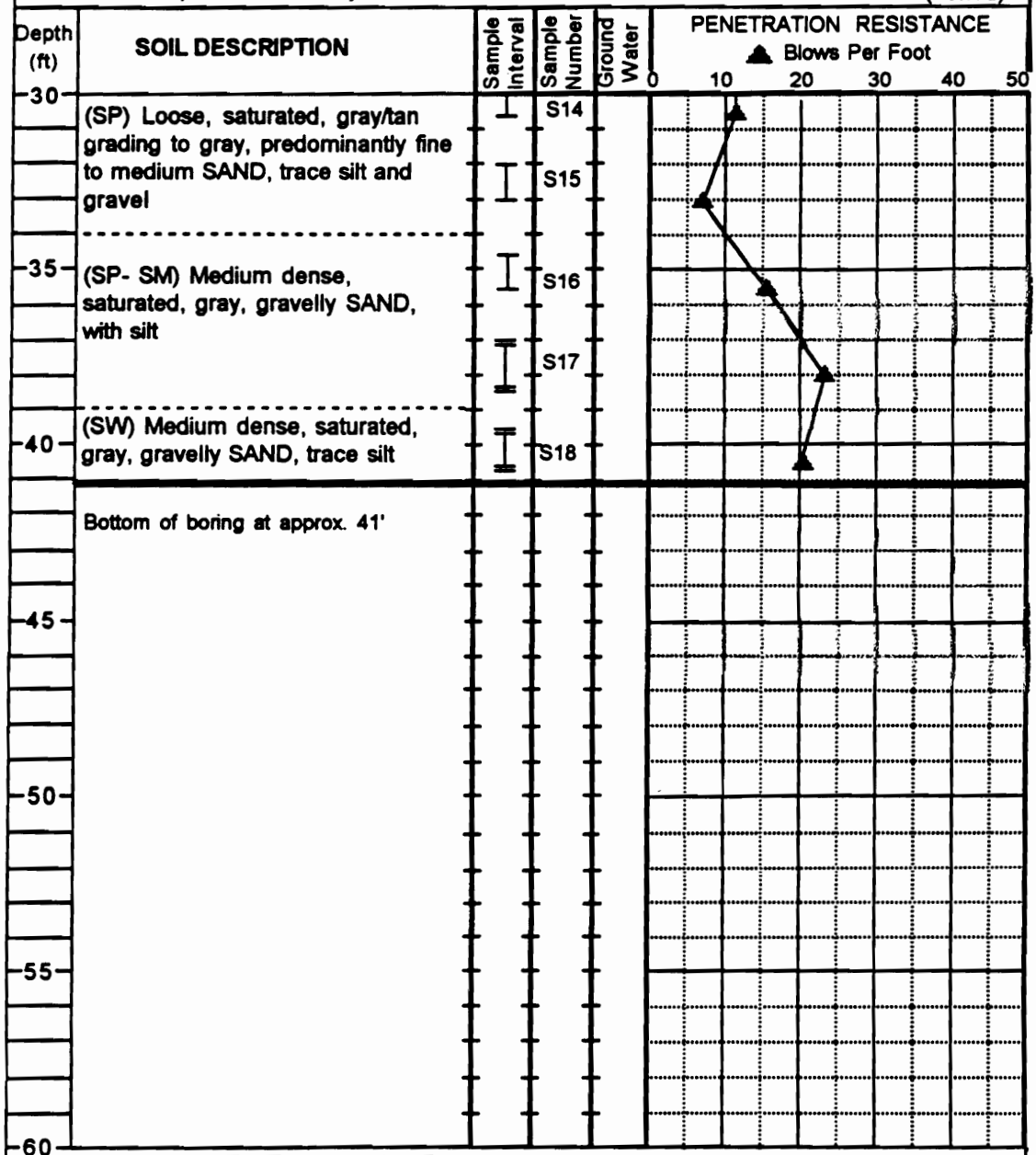

LEGEND

- 2-inch OD split spoon sampler
- 3-inch OD split spoon sampler
- Shelby tube sampler
- ATD Groundwater level at time of drilling

VIRGINIA TECH
The Charles Edward Via Dept. of Civil Engineering
Blacksburg, Virginia

Drilling Initiated: 05/28/92

Drilling Completed: 05/28/92

PROJECT: Wabash Valley Paleoseismic Liquefaction Study **SITE:** York (YO) **BORING#:** B-2

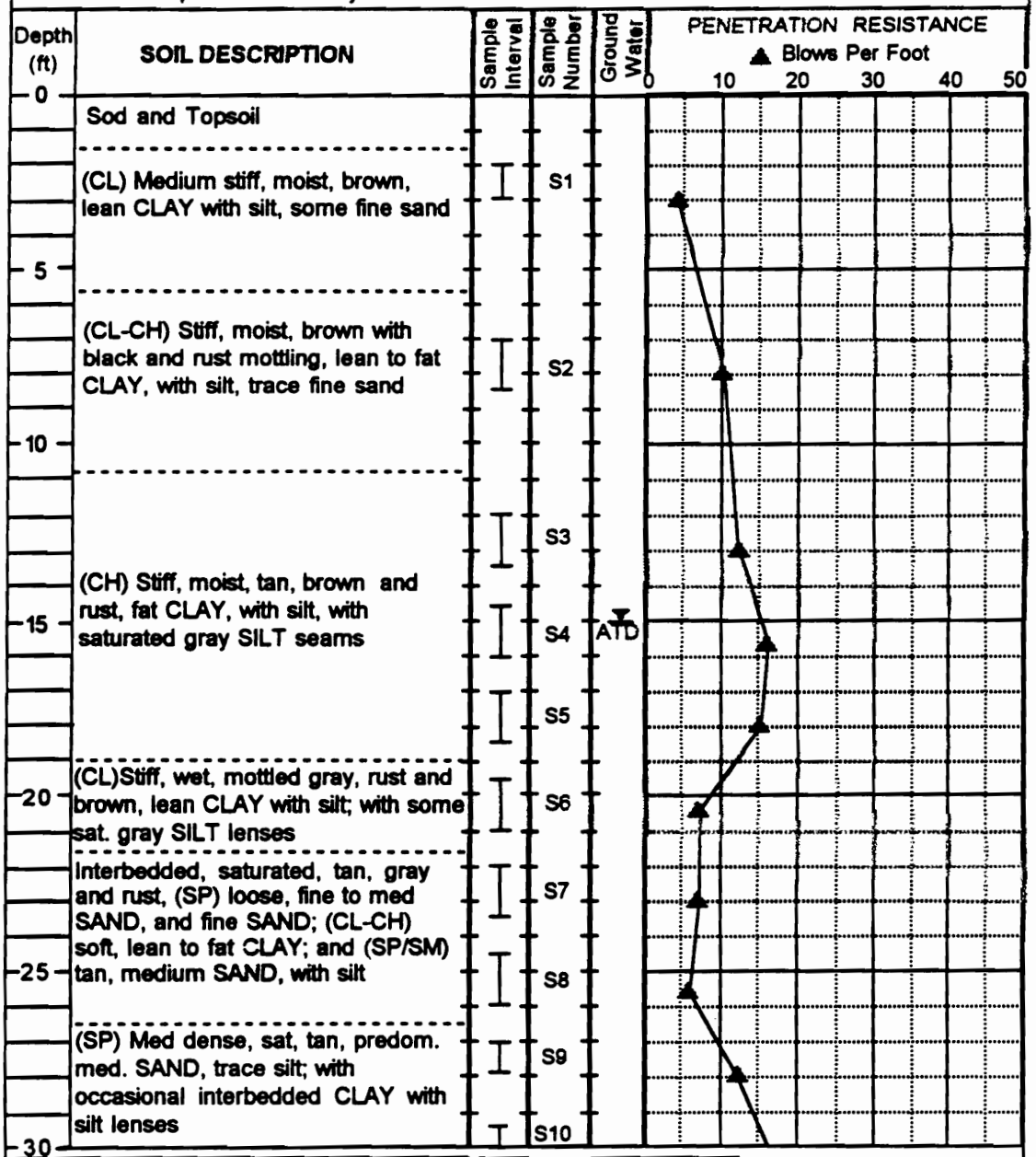

LEGEND

- 2-inch OD split spoon sampler
- 3-inch OD split spoon sampler
- Shelby tube sampler
- ATD Groundwater level at time of drilling

VIRGINIA TECH
The Charles Edward Via
Dept. of Civil Engineering
Blacksburg, Virginia

Drilling Initiated: 05/28/92

Drilling Completed: 05/29/92

PROJECT: Wabash Valley Paleoseismic Liquefaction Study **SITE:** York (YO) **BORING#:** B-2 (cont'd)

Depth (ft)	SOIL DESCRIPTION	Sample Interval	Sample Number	Ground Water
30	(SP) Medium dense, sat., tan, predom. fine to med. SAND, trace silt; with occasional interbedded (CL/CH) CLAY, with silt seams		S10	
			S11	
35	(SP) Medium dense, saturated, gray/tan, SAND, some gravel, trace silt		S12	
			S13	
40			S14	
	Bottom of boring at approx. 41'			
45				
50				
55				
60				

PENETRATION RESISTANCE
▲ Blows Per Foot
0 10 20 30 40 50

LEGEND

- 2-inch OD split spoon sampler
- 3-inch OD split spoon sampler
- Shelby tube sampler
- ATD Groundwater level at time of drilling

VIRGINIA TECH
The Charles Edward Via Dept. of Civil Engineering
Blacksburg, Virginia

Drilling Initiated: 05/28/92

Drilling Completed: 05/29/92

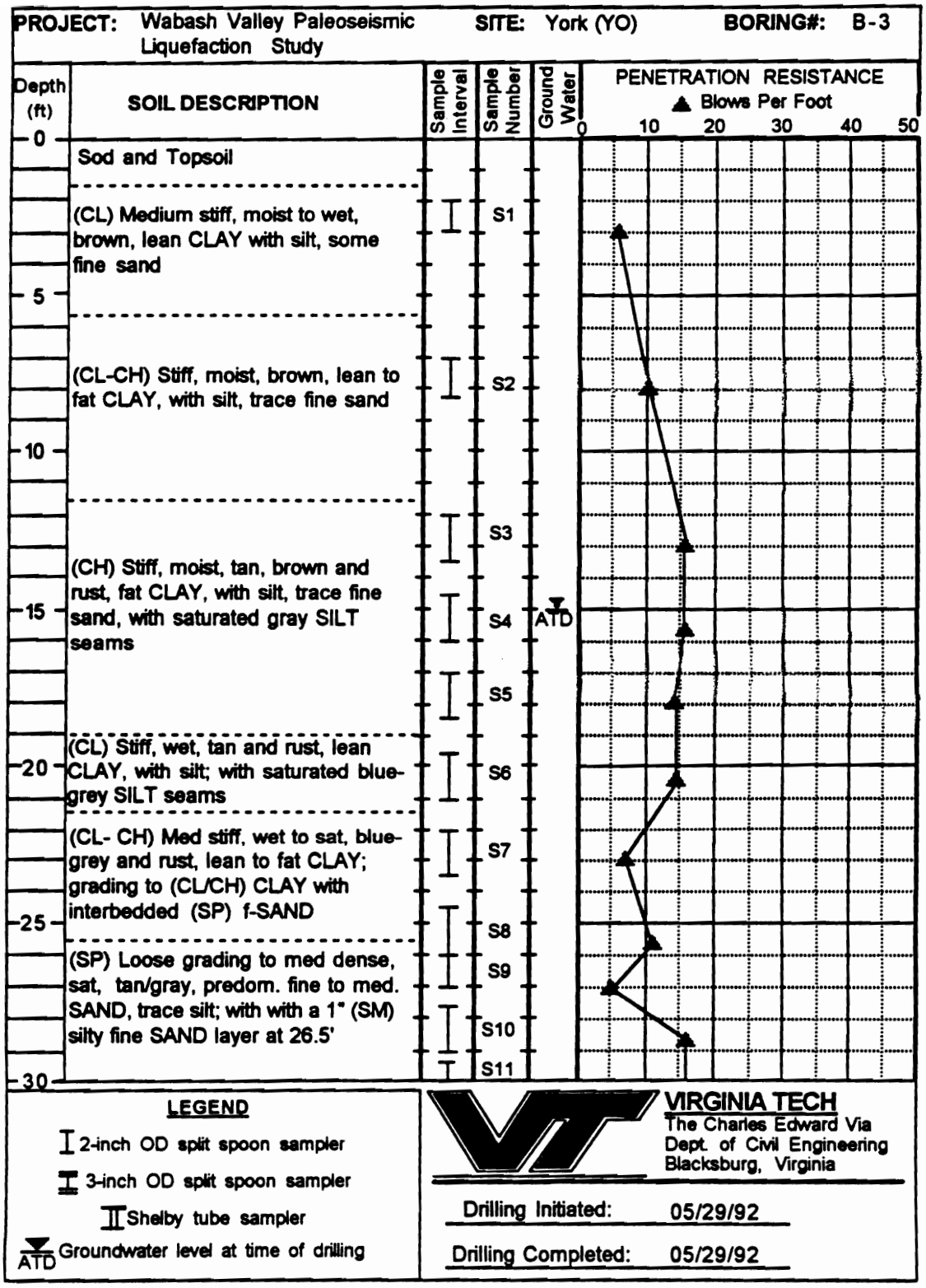
PROJECT: Wabash Valley Paleoseismic Liquefaction Study
SITE: York (YO)
BORING#: B-3
Depth (ft)
SOIL DESCRIPTION
Sample Interval
Sample Number
Ground Water
PENETRATION RESISTANCE
Blows Per Foot
0
10
20
30
40
50
0
5
10
15
20
25
30
Sod and Topsoil
(CL) Medium stiff, moist to wet, brown, lean CLAY with silt, some fine sand
(CL-CH) Stiff, moist, brown, lean to fat CLAY, with silt, trace fine sand
(CH) Stiff, moist, tan, brown and rust, fat CLAY, with silt, trace fine sand, with saturated gray SILT seams
(CL) Stiff, wet, tan and rust, lean CLAY, with silt; with saturated blue-grey SILT seams
(CL- CH) Med stiff, wet to sat, blue-grey and rust, lean to fat CLAY; grading to (CL/CH) CLAY with interbedded (SP) f-SAND
(SP) Loose grading to med dense, sat, tan/gray, predom. fine to med. SAND, trace silt; with with a 1" (SM) silty fine SAND layer at 26.5'
S1
S2
S3
S4
S5
S6
S7
S8
S9
S10
S11
ATD
LEGEND
2-inch OD split spoon sampler
3-inch OD split spoon sampler
Shelby tube sampler
ATD Groundwater level at time of drilling
VIRGINIA TECH
The Charles Edward Via
Dept. of Civil Engineering
Blacksburg, Virginia
Drilling Initiated: 05/29/92
Drilling Completed: 05/29/92

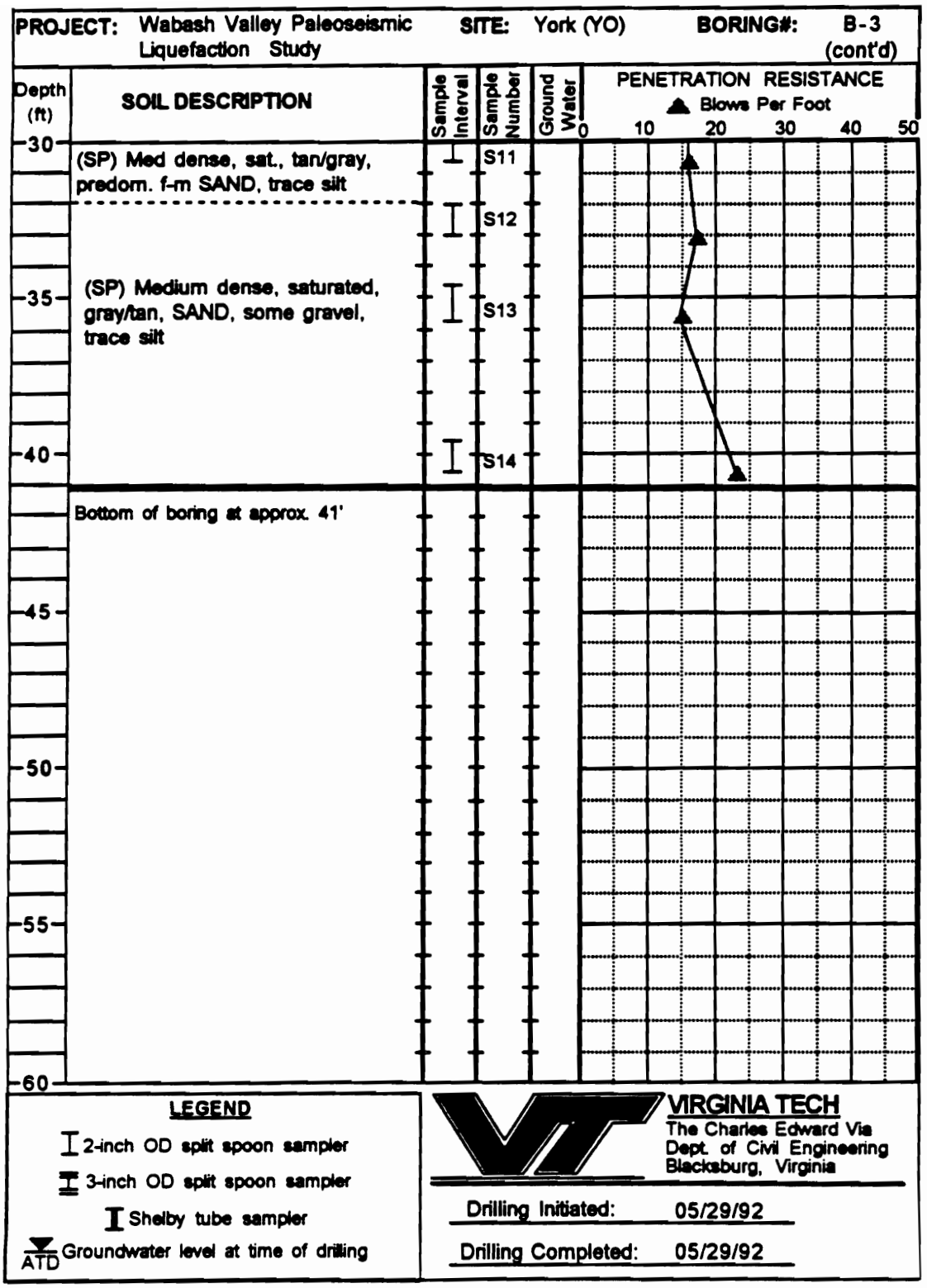
PROJECT: Wabash Valley Paleoseismic Liquefaction Study
SITE: York (YO)
BORING#: B-3 (cont'd)
Depth (ft)
SOIL DESCRIPTION
Sample Interval
Sample Number
Ground Water
PENETRATION RESISTANCE
Blows Per Foot
0
10
20
30
40
50
30
(SP) Med dense, sat., tan/gray, predom. f-m SAND, trace silt
S11
S12
35
(SP) Medium dense, saturated, gray/tan, SAND, some gravel, trace silt
S13
40
S14
Bottom of boring at approx. 41'
45
50
55
60
LEGEND
2-inch OD split spoon sampler
3-inch OD split spoon sampler
Shelby tube sampler
ATD Groundwater level at time of drilling
VIRGINIA TECH
The Charles Edward Via Dept. of Civil Engineering Blacksburg, Virginia
Drilling Initiated: 05/29/92
Drilling Completed: 05/29/92

Appendix C:

Skelton Event Boring Logs

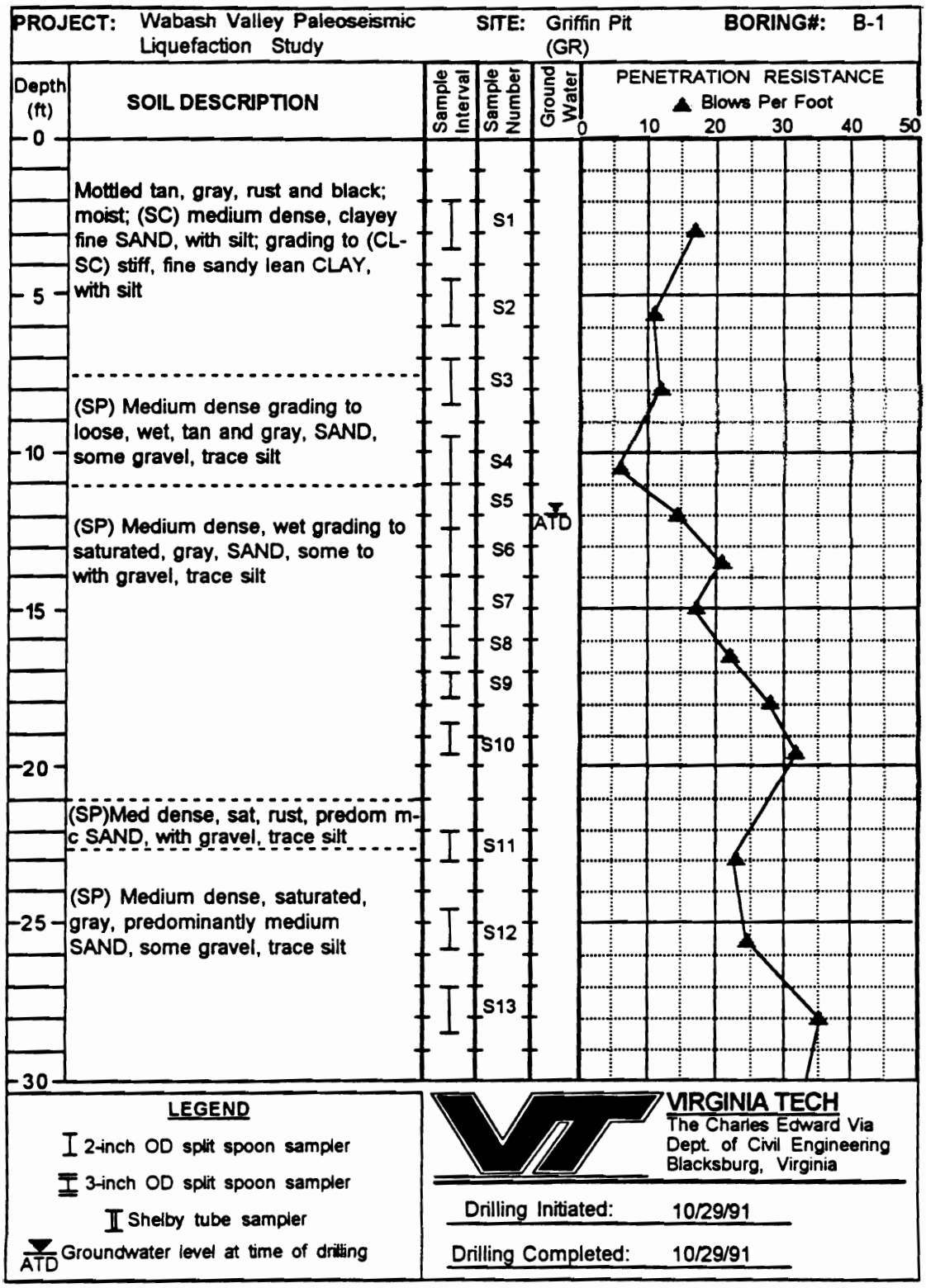
PROJECT: Wabash Valley Paleoseismic Liquefaction Study
SITE: Griffin Pit (GR)
BORING#: B-1
Depth (ft)
SOIL DESCRIPTION
Sample Interval
Sample Number
Ground Water
PENETRATION RESISTANCE
Blows Per Foot
0
10
20
30
40
50
0
5
10
15
20
25
30
Mottled tan, gray, rust and black; moist; (SC) medium dense, clayey fine SAND, with silt; grading to (CL-SC) stiff, fine sandy lean CLAY, with silt
(SP) Medium dense grading to loose, wet, tan and gray, SAND, some gravel, trace silt
(SP) Medium dense, wet grading to saturated, gray, SAND, some to with gravel, trace silt
(SP)Med dense, sat, rust, predom m-c SAND, with gravel, trace silt
(SP) Medium dense, saturated, gray, predominantly medium SAND, some gravel, trace silt
S1
S2
S3
S4
S5
S6
S7
S8
S9
S10
S11
S12
S13
ATD
LEGEND
2-inch OD split spoon sampler
3-inch OD split spoon sampler
Shelby tube sampler
ATD Groundwater level at time of drilling
VIRGINIA TECH
The Charles Edward Via Dept. of Civil Engineering
Blacksburg, Virginia
Drilling Initiated: 10/29/91
Drilling Completed: 10/29/91

PROJECT: Wabash Valley Paleoseismic Liquefaction Study | SITE: Griffin Pit (GR) | BORING#: B-1 (cont'd)

Depth (ft)	SOIL DESCRIPTION	Sample Interval	Sample Number	Ground Water	PENETRATION RESISTANCE ▲ Blows Per Foot (0 10 20 30 40 50)
30	(SP) Medium dense, saturated, gray, predominantly medium SAND, some gravel, trace silt				
	(SP) Dense, sat, gray, predom. fine SAND, trace silt	I	S14		
35	(SP) Medium dense, sat, gray, predominantly medium to coarse SAND, with gravel, trace silt	I	S15		
	Bottom of boring at approx. 38.5'				
40					
45					
50					
55					
60					

LEGEND

- I 2-inch OD split spoon sampler
- I 3-inch OD split spoon sampler
- I Shelby tube sampler
- ATD Groundwater level at time of drilling

VIRGINIA TECH
The Charles Edward Via
Dept. of Civil Engineering
Blacksburg, Virginia

Drilling Initiated: 10/29/91

Drilling Completed: 10/29/91

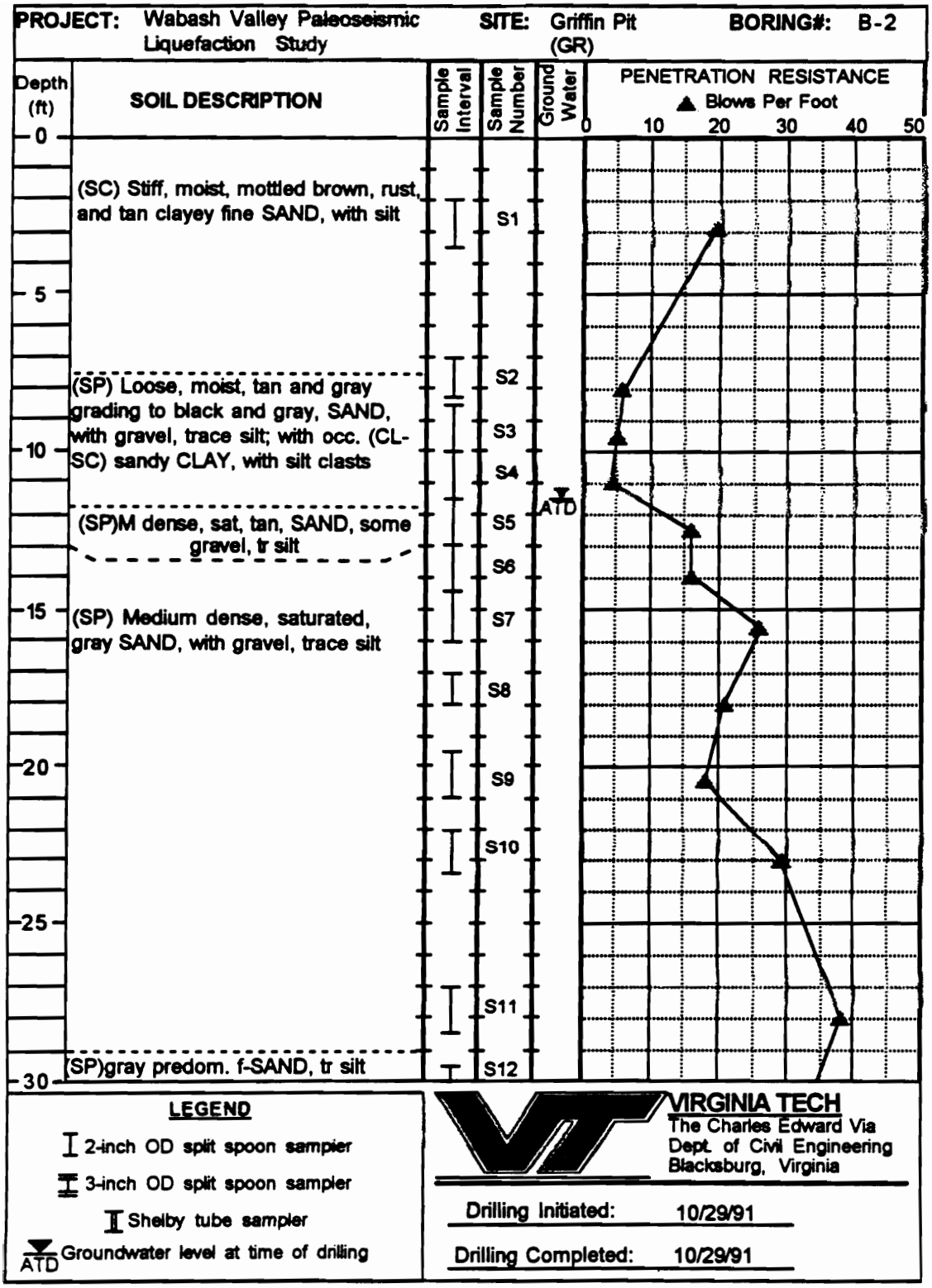
PROJECT: Wabash Valley Paleoseismic Liquefaction Study
SITE: Griffin Pit (GR)
BORING#: B-2
Depth (ft)
SOIL DESCRIPTION
Sample Interval
Sample Number
Ground Water
PENETRATION RESISTANCE
Blows Per Foot
0
10
20
30
40
50
0
5
10
15
20
25
30
(SC) Stiff, moist, mottled brown, rust, and tan clayey fine SAND, with silt
(SP) Loose, moist, tan and gray grading to black and gray, SAND, with gravel, trace silt; with occ. (CL-SC) sandy CLAY, with silt clasts
(SP)M dense, sat, tan, SAND, some gravel, tr silt
(SP) Medium dense, saturated, gray SAND, with gravel, trace silt
(SP)gray predom. f-SAND, tr silt
S1
S2
S3
S4
S5
S6
S7
S8
S9
S10
S11
S12
ATD
LEGEND
2-inch OD split spoon sampler
3-inch OD split spoon sampler
Shelby tube sampler
ATD Groundwater level at time of drilling
VIRGINIA TECH
The Charles Edward Via Dept. of Civil Engineering Blacksburg, Virginia
Drilling Initiated: 10/29/91
Drilling Completed: 10/29/91

PROJECT: Wabash Valley Paleoseismic Liquefaction Study **SITE:** Griffin Pit (GR) **BORING#:** B-2 (cont'd)

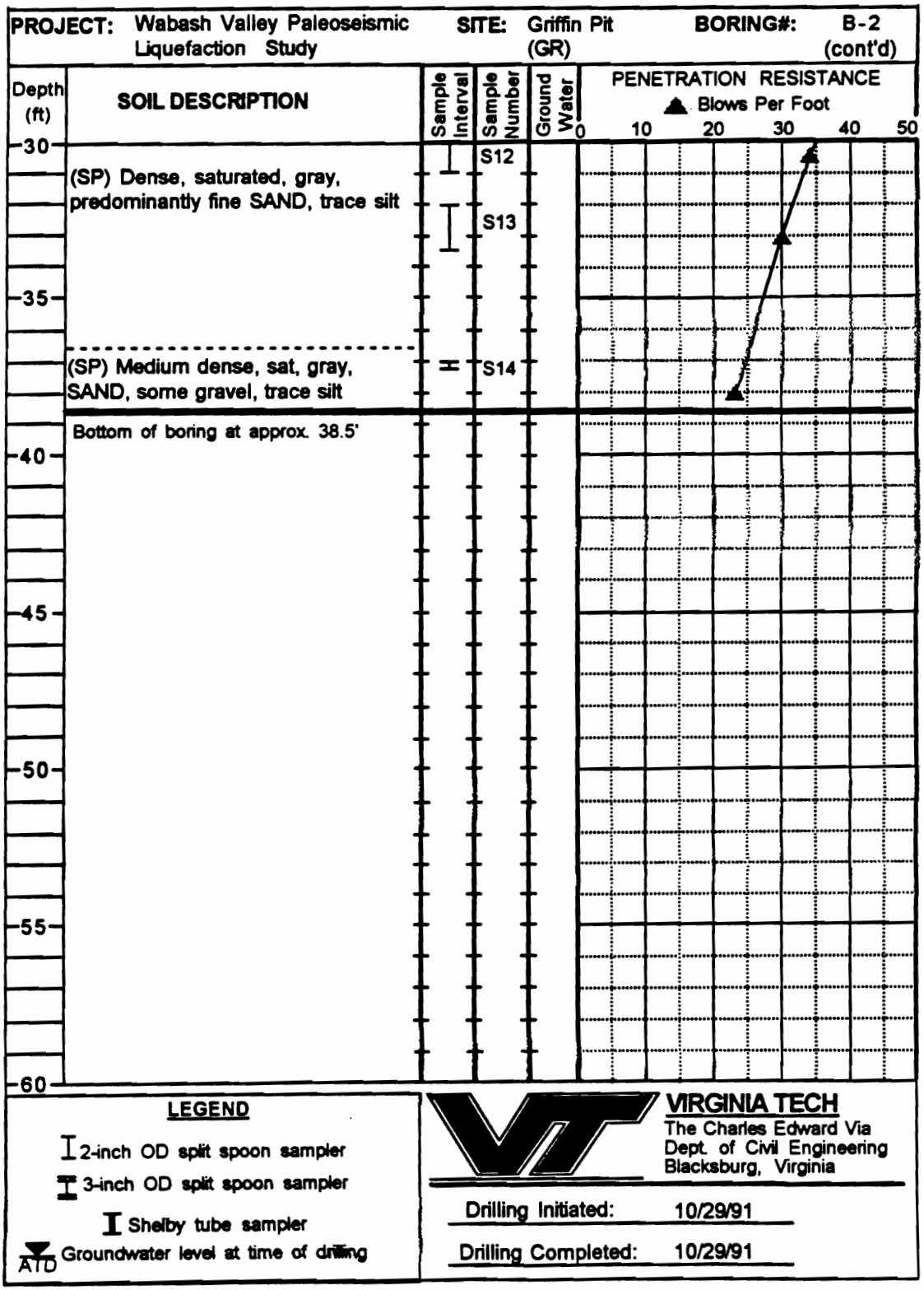

LEGEND

- 2-inch OD split spoon sampler
- 3-inch OD split spoon sampler
- Shelby tube sampler
- ATD Groundwater level at time of drilling

VIRGINIA TECH
The Charles Edward Via Dept. of Civil Engineering Blacksburg, Virginia

Drilling Initiated: 10/29/91

Drilling Completed: 10/29/91

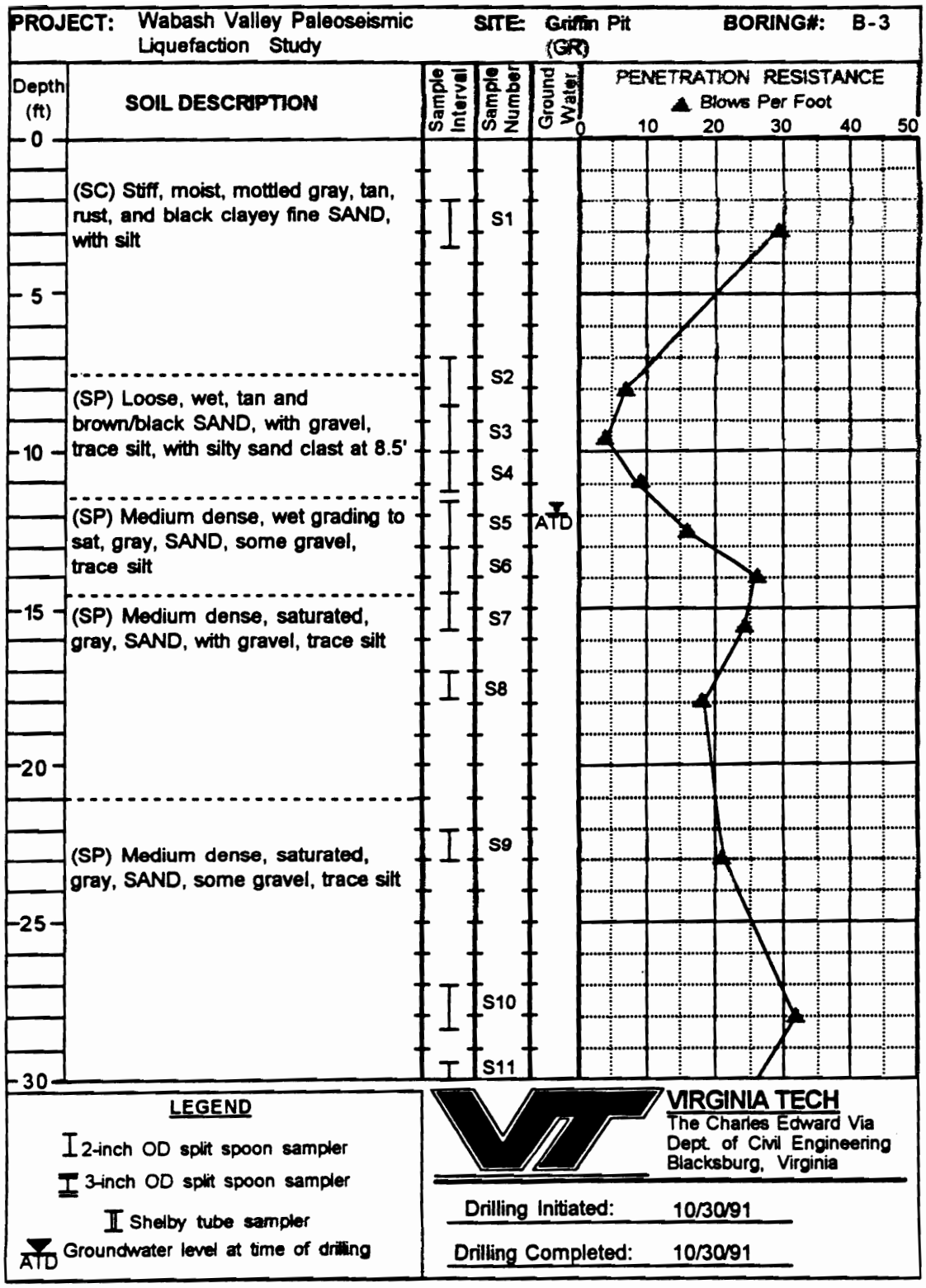
PROJECT: Wabash Valley Paleoseismic Liquefaction Study
SITE: Griffin Pit (GR)
BORING#: B-3
Depth (ft)
SOIL DESCRIPTION
Sample Interval
Sample Number
Ground Water
PENETRATION RESISTANCE
Blows Per Foot
0
10
20
30
40
50
0
5
10
15
20
25
30
(SC) Stiff, moist, mottled gray, tan, rust, and black clayey fine SAND, with silt
(SP) Loose, wet, tan and brown/black SAND, with gravel, trace silt, with silty sand clast at 8.5'
(SP) Medium dense, wet grading to sat, gray, SAND, some gravel, trace silt
(SP) Medium dense, saturated, gray, SAND, with gravel, trace silt
(SP) Medium dense, saturated, gray, SAND, some gravel, trace silt
S1
S2
S3
S4
S5
S6
S7
S8
S9
S10
S11
ATD
LEGEND
2-inch OD split spoon sampler
3-inch OD split spoon sampler
Shelby tube sampler
ATD Groundwater level at time of drilling
VIRGINIA TECH
The Charles Edward Via Dept. of Civil Engineering Blacksburg, Virginia
Drilling Initiated: 10/30/91
Drilling Completed: 10/30/91

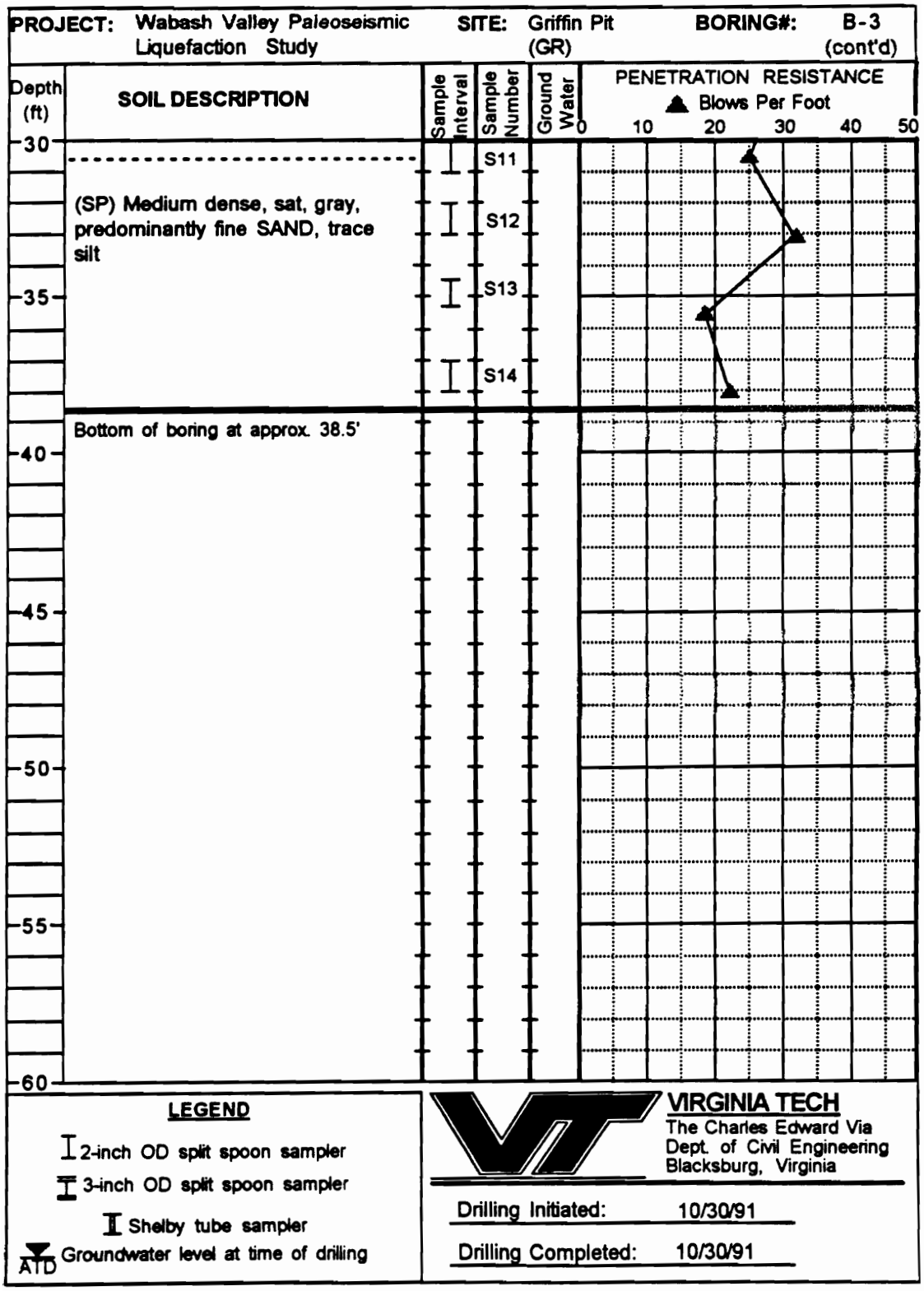
PROJECT: Wabash Valley Paleoseismic Liquefaction Study
SITE: Griffin Pit (GR)
BORING#: B-3 (cont'd)
Depth (ft)
SOIL DESCRIPTION
Sample Interval
Sample Number
Ground Water
PENETRATION RESISTANCE
Blows Per Foot
0
10
20
30
40
50
30
35
40
45
50
55
60
S11
S12
S13
S14
(SP) Medium dense, sat, gray, predominantly fine SAND, trace silt
Bottom of boring at approx. 38.5'
LEGEND
2-inch OD split spoon sampler
3-inch OD split spoon sampler
Shelby tube sampler
ATD Groundwater level at time of drilling
VIRGINIA TECH
The Charles Edward Via
Dept. of Civil Engineering
Blacksburg, Virginia
Drilling Initiated: 10/30/91
Drilling Completed: 10/30/91

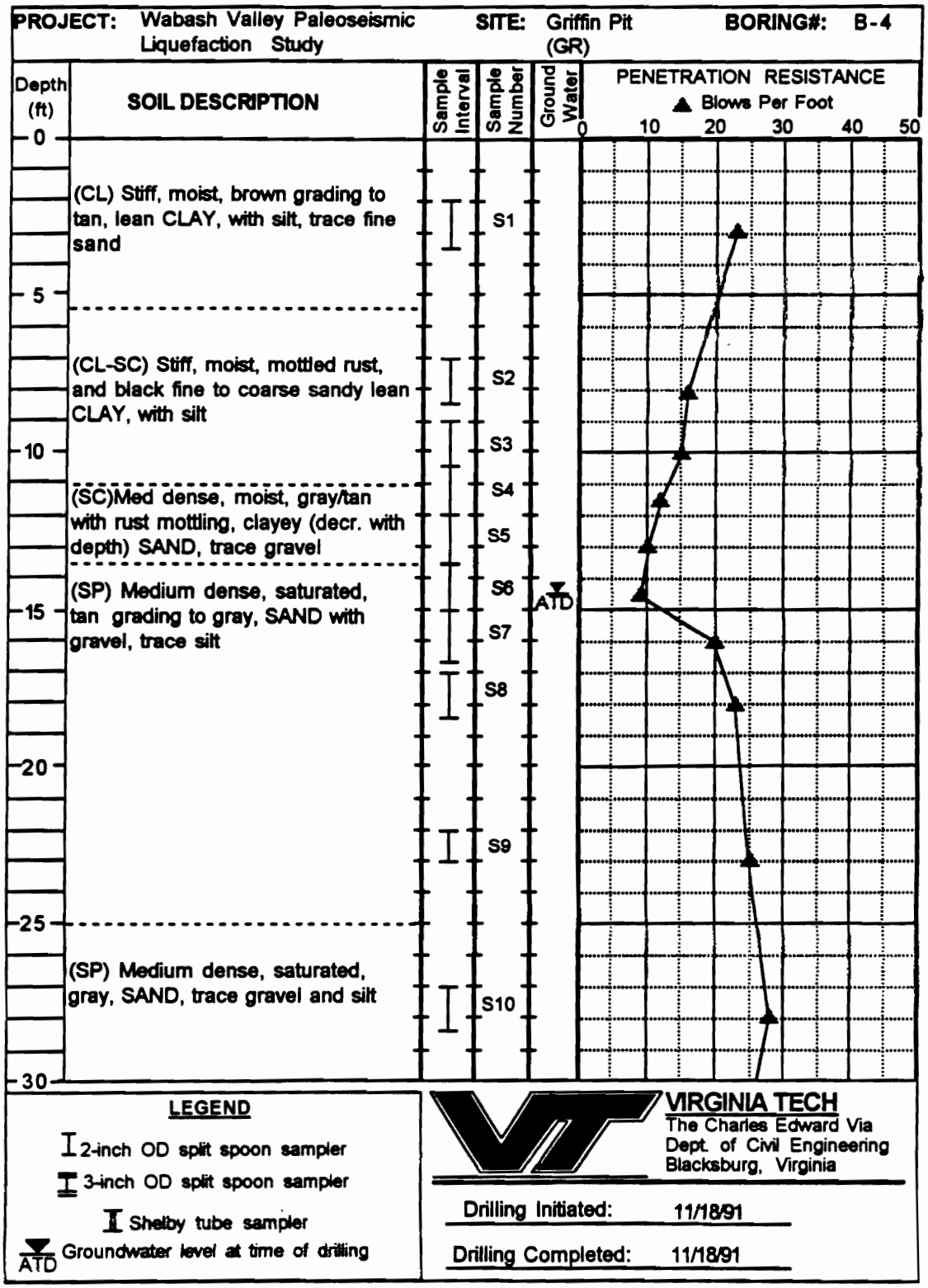
PROJECT: Wabash Valley Paleoseismic Liquefaction Study
SITE: Griffin Pit (GR)
BORING#: B-4
Depth (ft)
SOIL DESCRIPTION
Sample Interval
Sample Number
Ground Water
PENETRATION RESISTANCE
Blows Per Foot
0
10
20
30
40
50
0
5
10
15
20
25
30
(CL) Stiff, moist, brown grading to tan, lean CLAY, with silt, trace fine sand
(CL-SC) Stiff, moist, mottled rust, and black fine to coarse sandy lean CLAY, with silt
(SC)Med dense, moist, gray/tan with rust mottling, clayey (decr. with depth) SAND, trace gravel
(SP) Medium dense, saturated, tan grading to gray, SAND with gravel, trace silt
(SP) Medium dense, saturated, gray, SAND, trace gravel and silt
S1
S2
S3
S4
S5
S6
S7
S8
S9
S10
ATD
LEGEND
2-inch OD split spoon sampler
3-inch OD split spoon sampler
Shelby tube sampler
ATD Groundwater level at time of drilling
VIRGINIA TECH
The Charles Edward Via Dept. of Civil Engineering Blacksburg, Virginia
Drilling Initiated: 11/18/91
Drilling Completed: 11/18/91

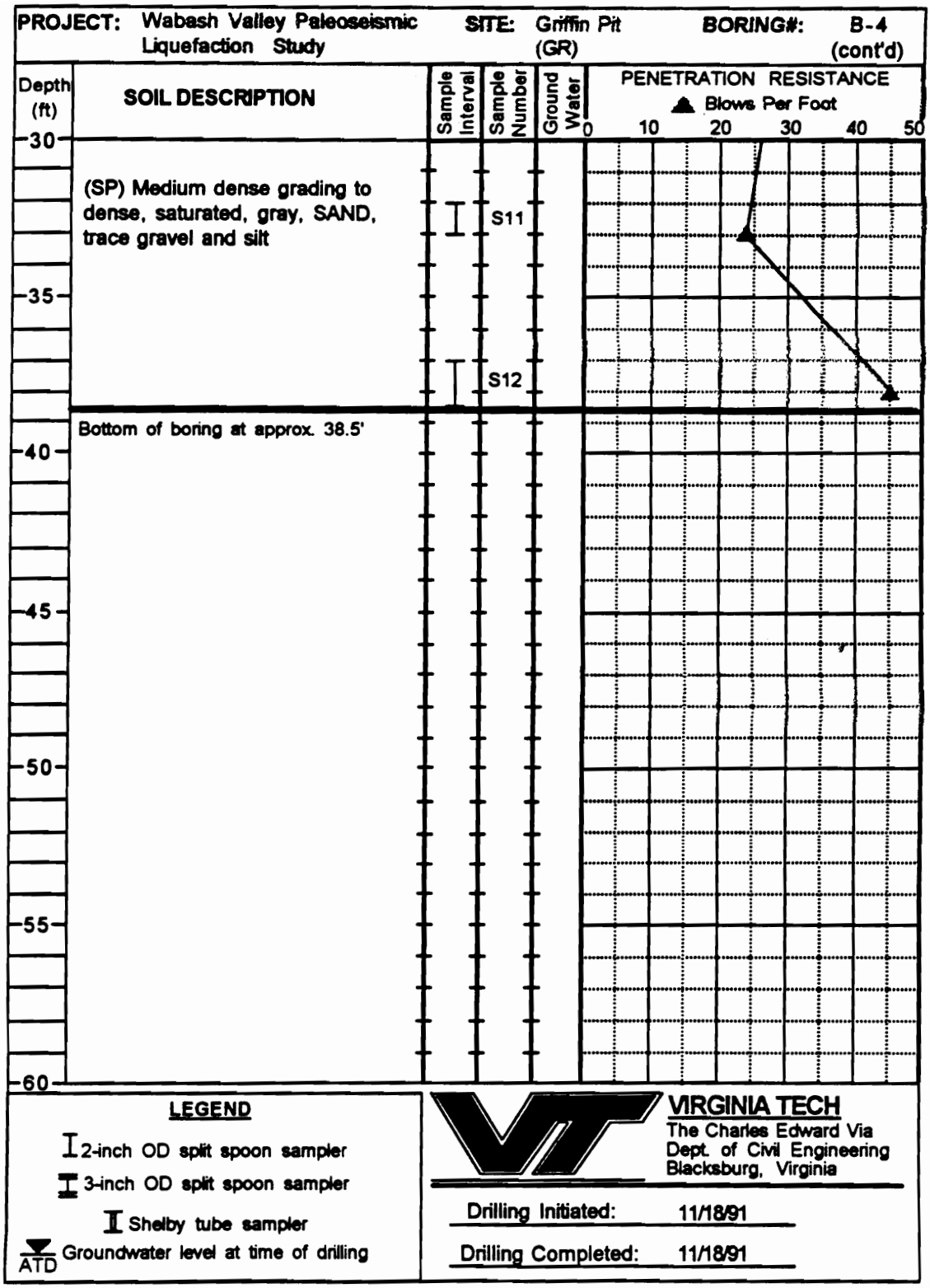
PROJECT: Wabash Valley Paleoseismic Liquefaction Study
SITE: Griffin Pit (GR)
BORING#: B-4 (cont'd)
Depth (ft)
SOIL DESCRIPTION
Sample Interval
Sample Number
Ground Water
PENETRATION RESISTANCE
Blows Per Foot
0
10
20
30
40
50
30
35
40
45
50
55
60
(SP) Medium dense grading to dense, saturated, gray, SAND, trace gravel and silt
S11
S12
Bottom of boring at approx. 38.5'
LEGEND
2-inch OD split spoon sampler
3-inch OD split spoon sampler
Shelby tube sampler
ATD
Groundwater level at time of drilling
VIRGINIA TECH
The Charles Edward Via Dept. of Civil Engineering Blacksburg, Virginia
Drilling Initiated: 11/18/91
Drilling Completed: 11/18/91

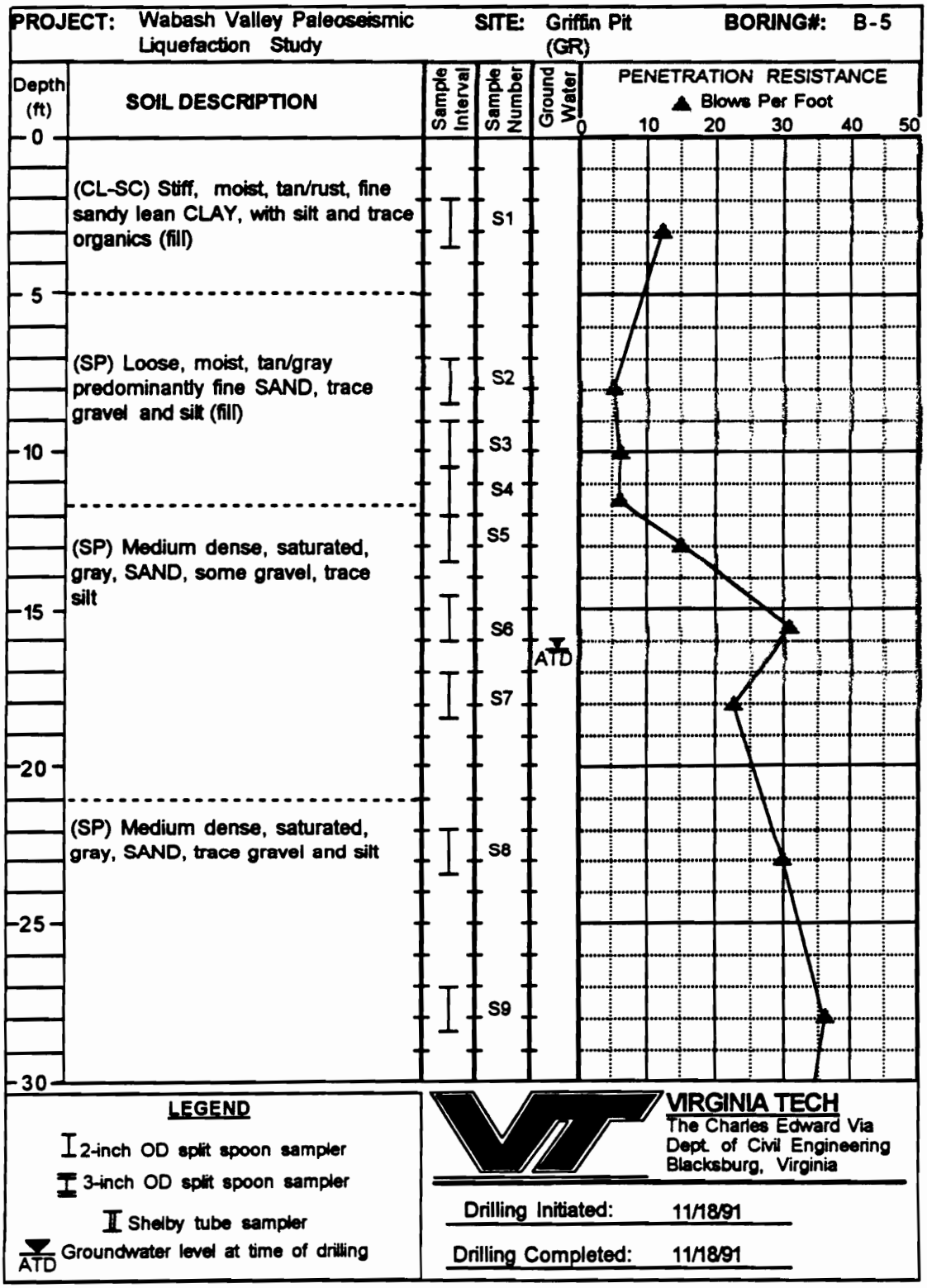
PROJECT: Wabash Valley Paleoseismic Liquefaction Study
SITE: Griffin Pit (GR)
BORING#: B-5
Depth (ft)
SOIL DESCRIPTION
Sample Interval
Sample Number
Ground Water
PENETRATION RESISTANCE
Blows Per Foot
0
10
20
30
40
50
0
5
10
15
20
25
30
(CL-SC) Stiff, moist, tan/rust, fine sandy lean CLAY, with silt and trace organics (fill)
(SP) Loose, moist, tan/gray predominantly fine SAND, trace gravel and silt (fill)
(SP) Medium dense, saturated, gray, SAND, some gravel, trace silt
(SP) Medium dense, saturated, gray, SAND, trace gravel and silt
S1
S2
S3
S4
S5
S6
S7
S8
S9
ATD
LEGEND
2-inch OD split spoon sampler
3-inch OD split spoon sampler
Shelby tube sampler
ATD Groundwater level at time of drilling
VIRGINIA TECH
The Charles Edward Via Dept. of Civil Engineering Blacksburg, Virginia
Drilling Initiated: 11/18/91
Drilling Completed: 11/18/91

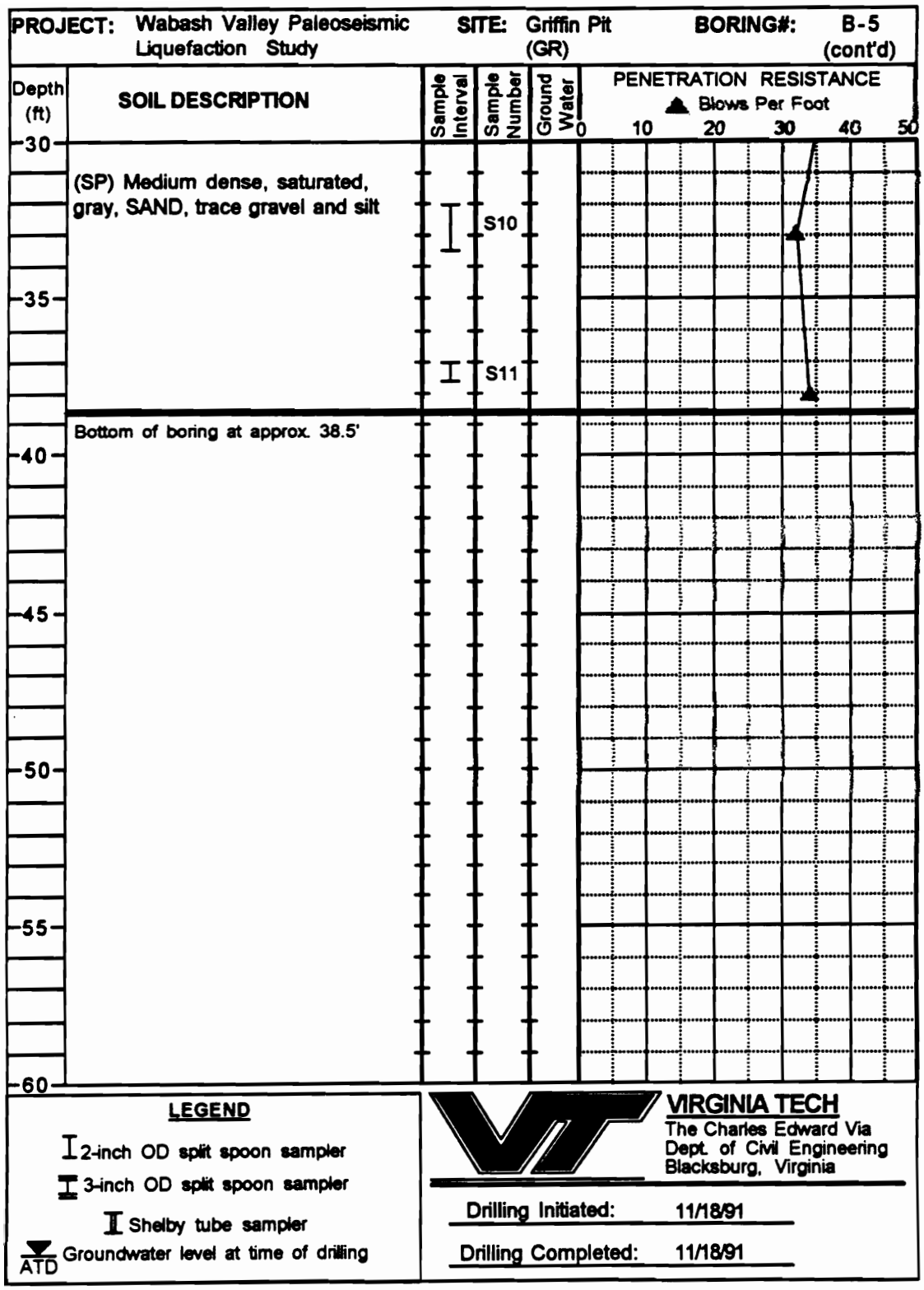
PROJECT: Wabash Valley Paleoseismic Liquefaction Study
SITE: Griffin Pit (GR)
BORING#: B-5 (cont'd)
Depth (ft)
SOIL DESCRIPTION
Sample Interval
Sample Number
Ground Water
PENETRATION RESISTANCE
Blows Per Foot
0
10
20
30
40
50
30
35
40
45
50
55
60
(SP) Medium dense, saturated, gray, SAND, trace gravel and silt
S10
S11
Bottom of boring at approx. 38.5'
LEGEND
2-inch OD split spoon sampler
3-inch OD split spoon sampler
Shelby tube sampler
ATD
Groundwater level at time of drilling
VIRGINIA TECH
The Charles Edward Via Dept. of Civil Engineering
Blacksburg, Virginia
Drilling Initiated: 11/18/91
Drilling Completed: 11/18/91

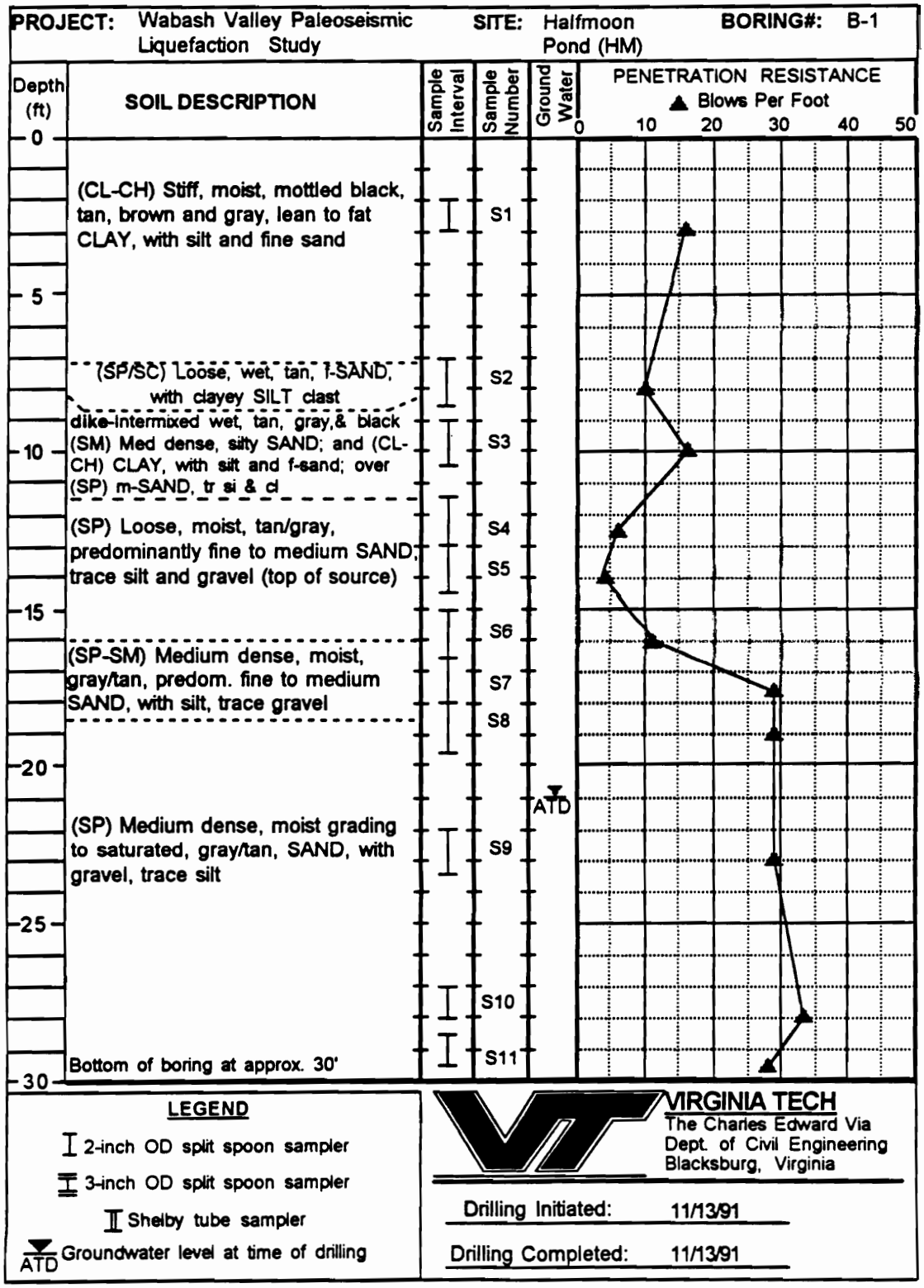
PROJECT: Wabash Valley Paleoseismic Liquefaction Study
SITE: Halfmoon Pond (HM)
BORING#: B-1
Depth (ft)
SOIL DESCRIPTION
Sample Interval
Sample Number
Ground Water
PENETRATION RESISTANCE
Blows Per Foot
0
10
20
30
40
50
0
5
10
15
20
25
30
(CL-CH) Stiff, moist, mottled black, tan, brown and gray, lean to fat CLAY, with silt and fine sand
S1
(SP/SC) Loose, wet, tan, f-SAND, with clayey SILT clast
S2
dike-intermixed wet, tan, gray,& black (SM) Med dense, silty SAND; and (CL-CH) CLAY, with silt and f-sand; over (SP) m-SAND, tr si & cl
S3
(SP) Loose, moist, tan/gray, predominantly fine to medium SAND, trace silt and gravel (top of source)
S4
S5
S6
(SP-SM) Medium dense, moist, gray/tan, predom. fine to medium SAND, with silt, trace gravel
S7
S8
ATD
(SP) Medium dense, moist grading to saturated, gray/tan, SAND, with gravel, trace silt
S9
S10
Bottom of boring at approx. 30'
S11
LEGEND
2-inch OD split spoon sampler
3-inch OD split spoon sampler
Shelby tube sampler
ATD Groundwater level at time of drilling
VIRGINIA TECH
The Charles Edward Via
Dept. of Civil Engineering
Blacksburg, Virginia
Drilling Initiated: 11/13/91
Drilling Completed: 11/13/91

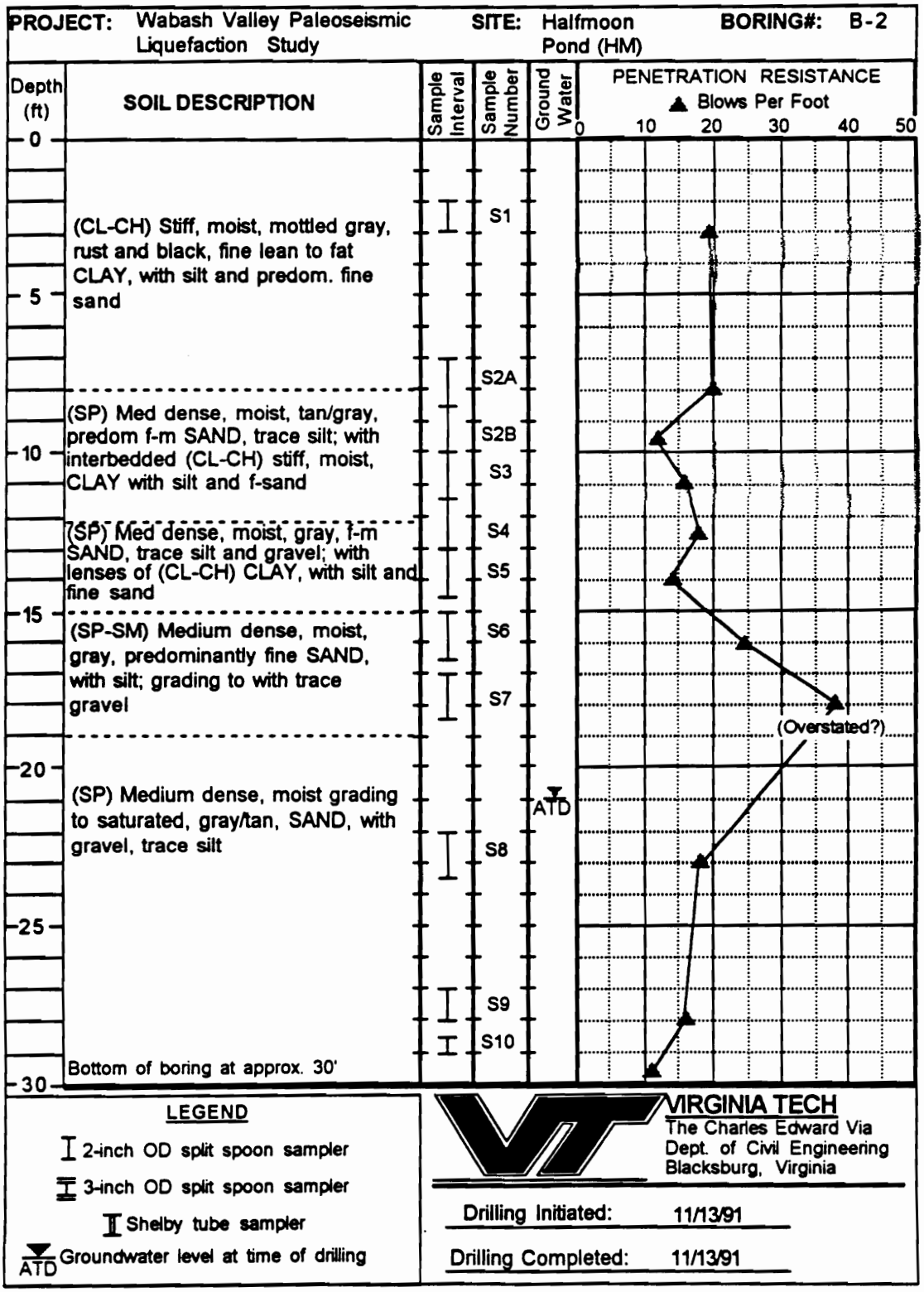
PROJECT: Wabash Valley Paleoseismic Liquefaction Study
SITE: Halfmoon Pond (HM)
BORING#: B-2
Depth (ft)
SOIL DESCRIPTION
Sample Interval
Sample Number
Ground Water
PENETRATION RESISTANCE
Blows Per Foot
0
10
20
30
40
50
5
10
15
20
25
30
(CL-CH) Stiff, moist, mottled gray, rust and black, fine lean to fat CLAY, with silt and predom. fine sand
(SP) Med dense, moist, tan/gray, predom f-m SAND, trace silt; with interbedded (CL-CH) stiff, moist, CLAY with silt and f-sand
(SP) Med dense, moist, gray, f-m SAND, trace silt and gravel; with lenses of (CL-CH) CLAY, with silt and fine sand
(SP-SM) Medium dense, moist, gray, predominantly fine SAND, with silt; grading to with trace gravel
(SP) Medium dense, moist grading to saturated, gray/tan, SAND, with gravel, trace silt
Bottom of boring at approx. 30'
S1
S2A
S2B
S3
S4
S5
S6
S7
S8
S9
S10
ATD
(Overstated?)
LEGEND
2-inch OD split spoon sampler
3-inch OD split spoon sampler
Shelby tube sampler
ATD Groundwater level at time of drilling
VIRGINIA TECH
The Charles Edward Via Dept. of Civil Engineering Blacksburg, Virginia
Drilling Initiated: 11/13/91
Drilling Completed: 11/13/91

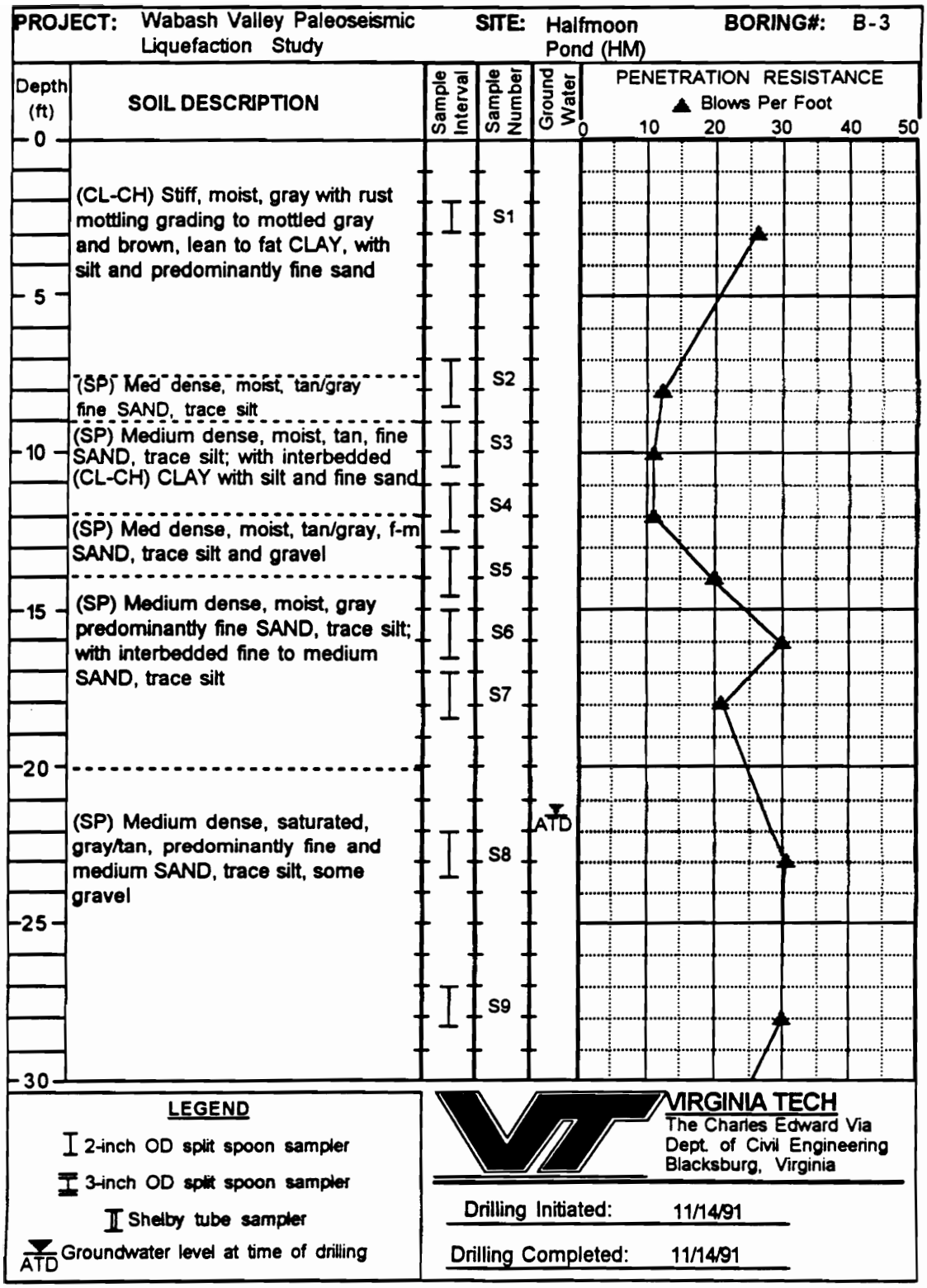
PROJECT: Wabash Valley Paleoseismic Liquefaction Study
SITE: Halfmoon Pond (HM)
BORING#: B-3
Depth (ft)
SOIL DESCRIPTION
Sample Interval
Sample Number
Ground Water
PENETRATION RESISTANCE
Blows Per Foot
0
10
20
30
40
50
0
5
10
15
20
25
30
(CL-CH) Stiff, moist, gray with rust mottling grading to mottled gray and brown, lean to fat CLAY, with silt and predominantly fine sand
S1
(SP) Med dense, moist, tan/gray fine SAND, trace silt
S2
(SP) Medium dense, moist, tan, fine SAND, trace silt; with interbedded (CL-CH) CLAY with silt and fine sand
S3
S4
(SP) Med dense, moist, tan/gray, f-m SAND, trace silt and gravel
S5
(SP) Medium dense, moist, gray predominantly fine SAND, trace silt; with interbedded fine to medium SAND, trace silt
S6
S7
ATD
(SP) Medium dense, saturated, gray/tan, predominantly fine and medium SAND, trace silt, some gravel
S8
S9
LEGEND
2-inch OD split spoon sampler
3-inch OD split spoon sampler
Shelby tube sampler
ATD Groundwater level at time of drilling
VIRGINIA TECH
The Charles Edward Via
Dept. of Civil Engineering
Blacksburg, Virginia
Drilling Initiated: 11/14/91
Drilling Completed: 11/14/91

PROJECT: Wabash Valley Paleoseismic Liquefaction Study **SITE:** Halfmoon Pond (HM) **BORING#:** B-3 (cont'd)

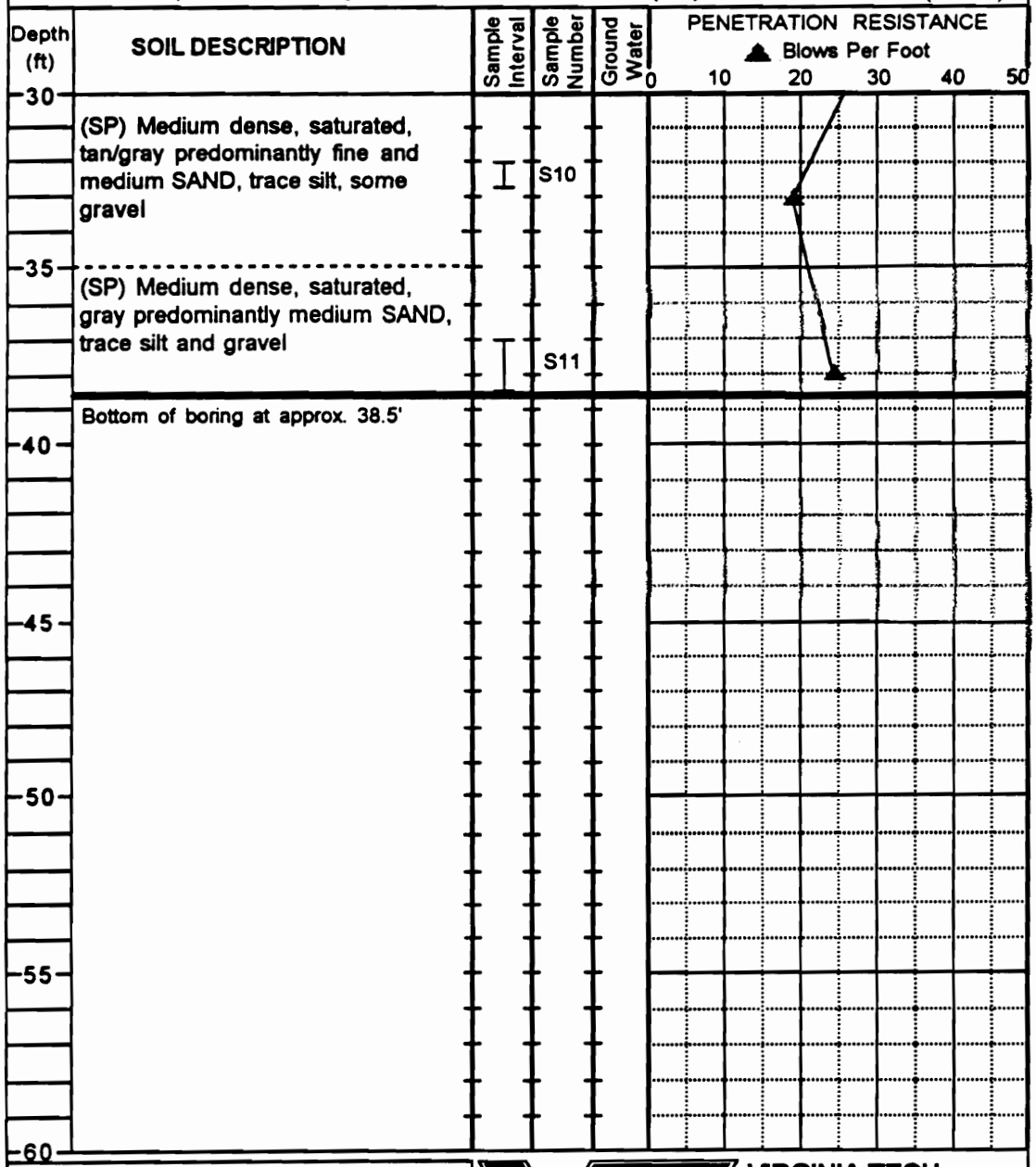

LEGEND

- 2-inch OD split spoon sampler
- 3-inch OD split spoon sampler
- Shelby tube sampler
- ATD Groundwater level at time of drilling

VIRGINIA TECH
The Charles Edward Via
Dept. of Civil Engineering
Blacksburg, Virginia

Drilling Initiated: 11/14/91

Drilling Completed: 11/14/91

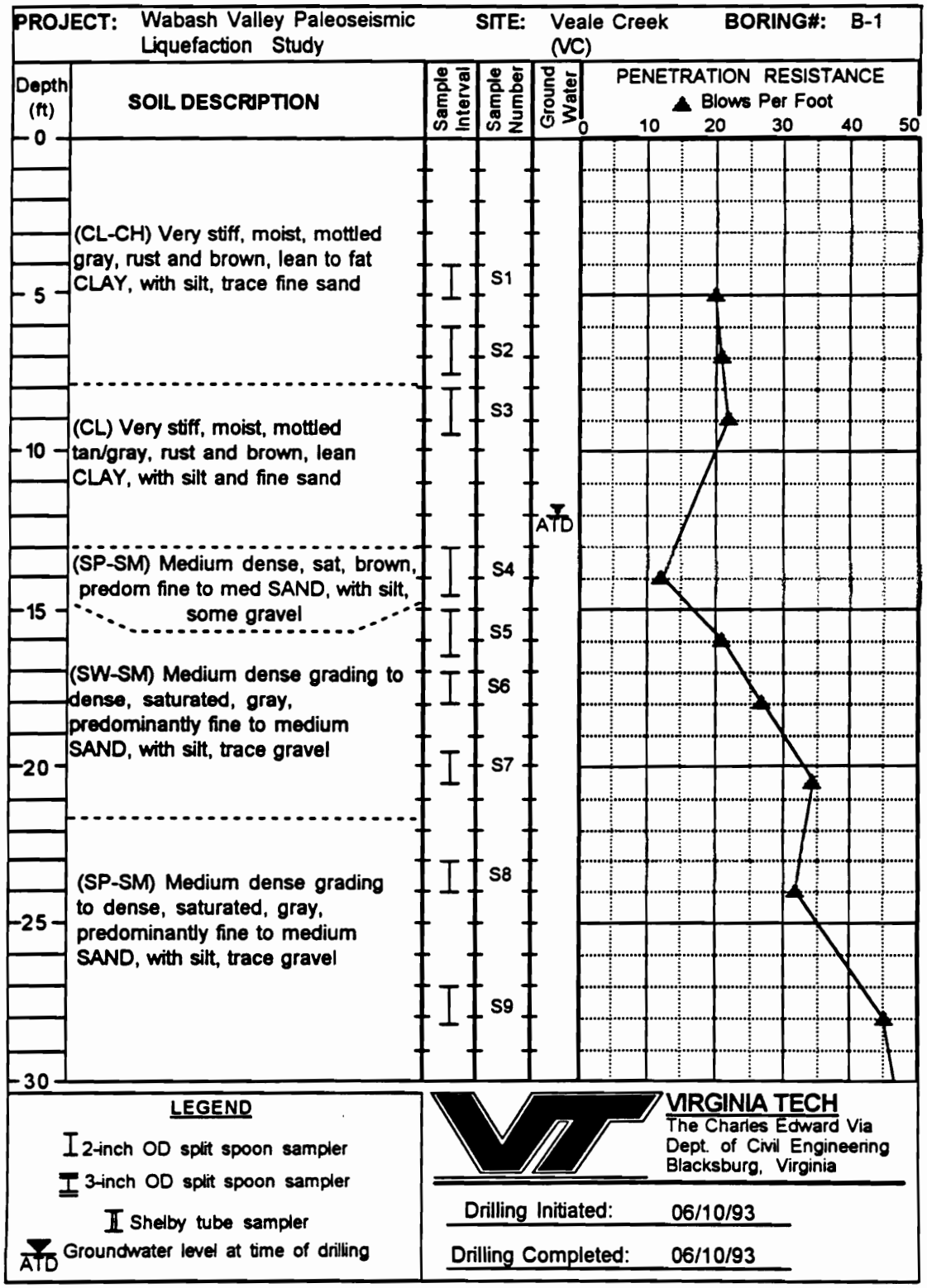
PROJECT: Wabash Valley Paleoseismic Liquefaction Study
SITE: Veale Creek (VC)
BORING#: B-1
Depth (ft)
SOIL DESCRIPTION
Sample Interval
Sample Number
Ground Water
PENETRATION RESISTANCE
Blows Per Foot
0
10
20
30
40
50
0
5
10
15
20
25
30
(CL-CH) Very stiff, moist, mottled gray, rust and brown, lean to fat CLAY, with silt, trace fine sand
(CL) Very stiff, moist, mottled tan/gray, rust and brown, lean CLAY, with silt and fine sand
(SP-SM) Medium dense, sat, brown, predom fine to med SAND, with silt, some gravel
(SW-SM) Medium dense grading to dense, saturated, gray, predominantly fine to medium SAND, with silt, trace gravel
(SP-SM) Medium dense grading to dense, saturated, gray, predominantly fine to medium SAND, with silt, trace gravel
S1
S2
S3
S4
S5
S6
S7
S8
S9
ATD
LEGEND
2-inch OD split spoon sampler
3-inch OD split spoon sampler
Shelby tube sampler
ATD Groundwater level at time of drilling
VIRGINIA TECH
The Charles Edward Via
Dept. of Civil Engineering
Blacksburg, Virginia
Drilling Initiated: 06/10/93
Drilling Completed: 06/10/93

PROJECT: Wabash Valley Paleoseismic Liquefaction Study **SITE:** Veale Creek (VC) **BORING#:** B-1 (cont'd)

Depth (ft)	SOIL DESCRIPTION	Sample Interval	Sample Number	Ground Water	PENETRATION RESISTANCE ▲ Blows Per Foot 0 10 20 30 40 50
30	(SP-SM) Dense, saturated, gray, predominantly fine to medium SAND, with silt, trace gravel		S10		(67)
	Bottom of boring at approx. 33.5'				
35					
40					
45					
50					
55					
60					

LEGEND

- 2-inch OD split spoon sampler
- 3-inch OD split spoon sampler
- Shelby tube sampler
- ATD Groundwater level at time of drilling

VIRGINIA TECH
The Charles Edward Via
Dept. of Civil Engineering
Blacksburg, Virginia

Drilling Initiated: 06/10/93

Drilling Completed: 06/10/93

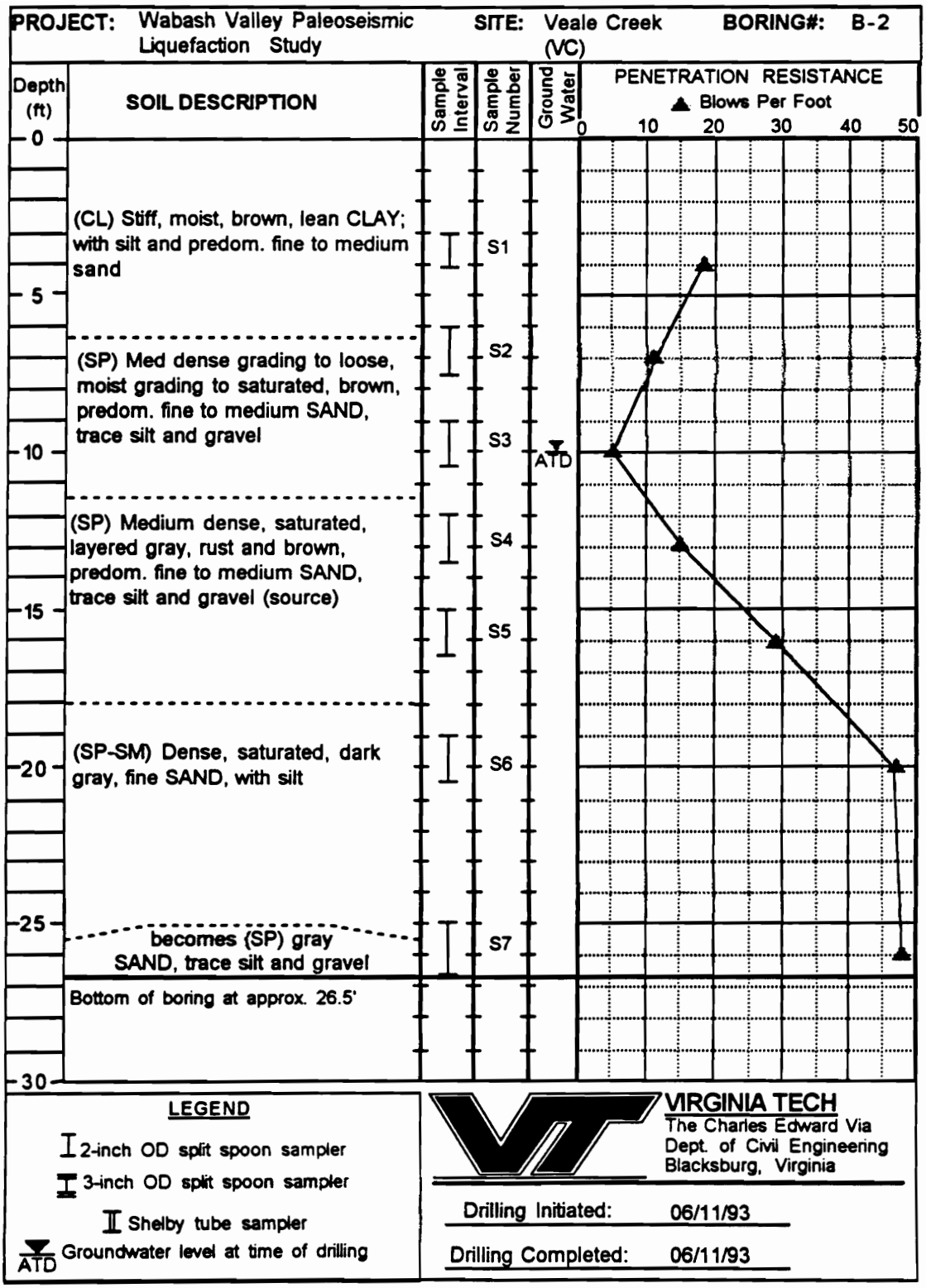
PROJECT: Wabash Valley Paleoseismic Liquefaction Study
SITE: Veale Creek (VC)
BORING#: B-2
Depth (ft)
SOIL DESCRIPTION
Sample Interval
Sample Number
Ground Water
PENETRATION RESISTANCE
Blows Per Foot
0
10
20
30
40
50
0
5
10
15
20
25
30
(CL) Stiff, moist, brown, lean CLAY; with silt and predom. fine to medium sand
S1
(SP) Med dense grading to loose, moist grading to saturated, brown, predom. fine to medium SAND, trace silt and gravel
S2
S3
ATD
(SP) Medium dense, saturated, layered gray, rust and brown, predom. fine to medium SAND, trace silt and gravel (source)
S4
S5
(SP-SM) Dense, saturated, dark gray, fine SAND, with silt
S6
becomes (SP) gray SAND, trace silt and gravel
S7
Bottom of boring at approx. 26.5'
LEGEND
2-inch OD split spoon sampler
3-inch OD split spoon sampler
Shelby tube sampler
ATD Groundwater level at time of drilling
VIRGINIA TECH
The Charles Edward Via Dept. of Civil Engineering Blacksburg, Virginia
Drilling Initiated: 06/11/93
Drilling Completed: 06/11/93

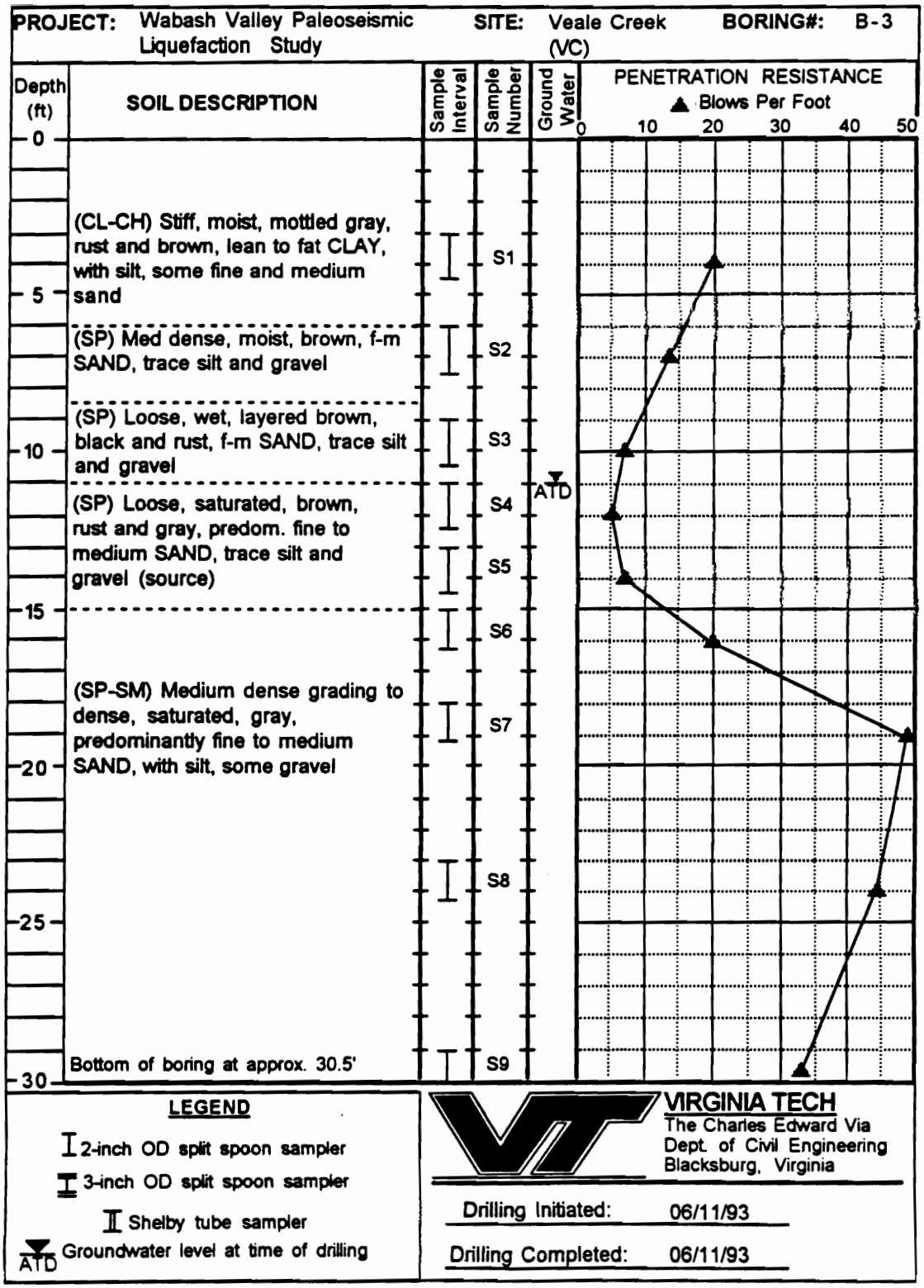
PROJECT: Wabash Valley Paleoseismic Liquefaction Study
SITE: Veale Creek (VC)
BORING#: B-3
Depth (ft)
SOIL DESCRIPTION
Sample Interval
Sample Number
Ground Water
PENETRATION RESISTANCE
Blows Per Foot
0
10
20
30
40
50
0
5
10
15
20
25
30
(CL-CH) Stiff, moist, mottled gray, rust and brown, lean to fat CLAY, with silt, some fine and medium sand
(SP) Med dense, moist, brown, f-m SAND, trace silt and gravel
(SP) Loose, wet, layered brown, black and rust, f-m SAND, trace silt and gravel
(SP) Loose, saturated, brown, rust and gray, predom. fine to medium SAND, trace silt and gravel (source)
(SP-SM) Medium dense grading to dense, saturated, gray, predominantly fine to medium SAND, with silt, some gravel
Bottom of boring at approx. 30.5'
S1
S2
S3
S4
S5
S6
S7
S8
S9
ATD
LEGEND
2-inch OD split spoon sampler
3-inch OD split spoon sampler
Shelby tube sampler
Groundwater level at time of drilling
VIRGINIA TECH
The Charles Edward Via Dept. of Civil Engineering Blacksburg, Virginia
Drilling Initiated: 06/11/93
Drilling Completed: 06/11/93

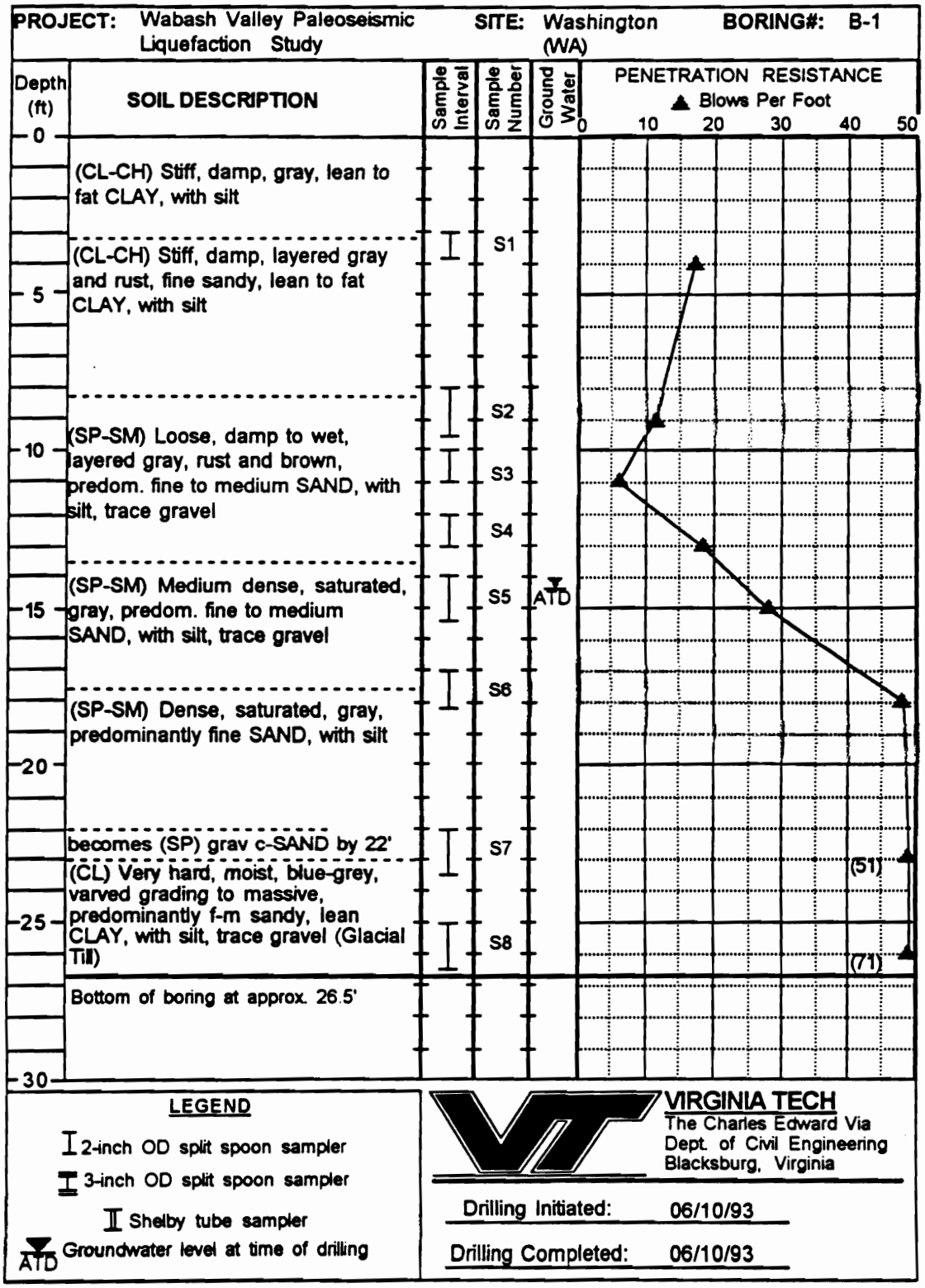
PROJECT: Wabash Valley Paleoseismic Liquefaction Study
SITE: Washington (WA)
BORING#: B-1
Depth (ft)
SOIL DESCRIPTION
Sample Interval
Sample Number
Ground Water
PENETRATION RESISTANCE
Blows Per Foot
0
10
20
30
40
50
0
5
10
15
20
25
30
(CL-CH) Stiff, damp, gray, lean to fat CLAY, with silt
(CL-CH) Stiff, damp, layered gray and rust, fine sandy, lean to fat CLAY, with silt
(SP-SM) Loose, damp to wet, layered gray, rust and brown, predom. fine to medium SAND, with silt, trace gravel
(SP-SM) Medium dense, saturated, gray, predom. fine to medium SAND, with silt, trace gravel
(SP-SM) Dense, saturated, gray, predominantly fine SAND, with silt
becomes (SP) grav c-SAND by 22'
(CL) Very hard, moist, blue-grey, varved grading to massive, predominantly f-m sandy, lean CLAY, with silt, trace gravel (Glacial Till)
Bottom of boring at approx. 26.5'
S1
S2
S3
S4
S5
S6
S7
S8
ATD
(51)
(71)
LEGEND
2-inch OD split spoon sampler
3-inch OD split spoon sampler
Shelby tube sampler
Groundwater level at time of drilling
VIRGINIA TECH
The Charles Edward Via
Dept. of Civil Engineering
Blacksburg, Virginia
Drilling Initiated: 06/10/93
Drilling Completed: 06/10/93

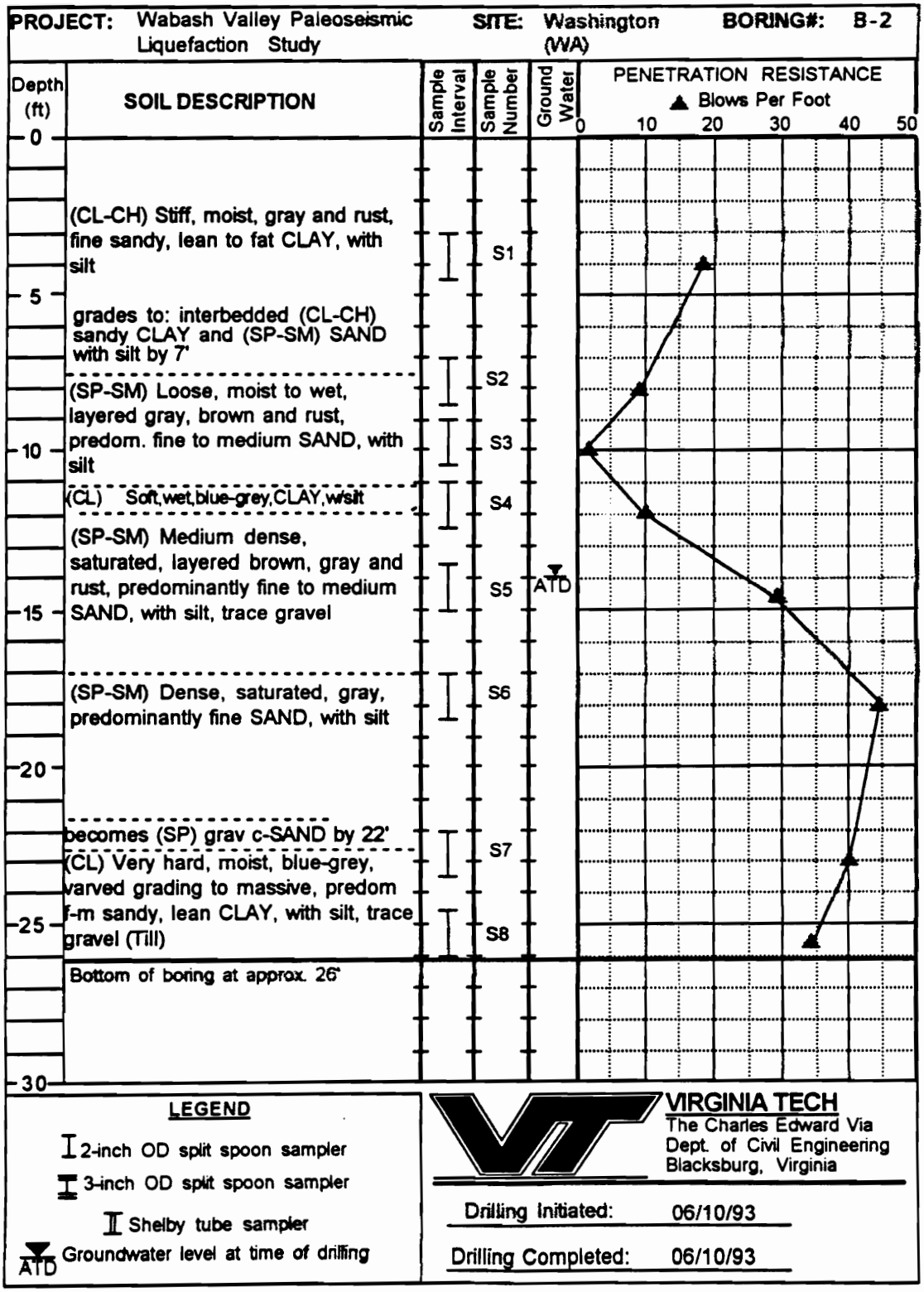
PROJECT: Wabash Valley Paleoseismic Liquefaction Study
SITE: Washington (WA)
BORING#: B-2
Depth (ft)
SOIL DESCRIPTION
Sample Interval
Sample Number
Ground Water
PENETRATION RESISTANCE
Blows Per Foot
0
10
20
30
40
50
0
5
10
15
20
25
30
(CL-CH) Stiff, moist, gray and rust, fine sandy, lean to fat CLAY, with silt
grades to: interbedded (CL-CH) sandy CLAY and (SP-SM) SAND with silt by 7'
(SP-SM) Loose, moist to wet, layered gray, brown and rust, predom. fine to medium SAND, with silt
(CL) Soft,wet,blue-grey,CLAY,w/silt
(SP-SM) Medium dense, saturated, layered brown, gray and rust, predominantly fine to medium SAND, with silt, trace gravel
(SP-SM) Dense, saturated, gray, predominantly fine SAND, with silt
becomes (SP) grav c-SAND by 22'
(CL) Very hard, moist, blue-grey, varved grading to massive, predom f-m sandy, lean CLAY, with silt, trace gravel (Till)
Bottom of boring at approx. 26'
S1
S2
S3
S4
S5
S6
S7
S8
ATD
LEGEND
2-inch OD split spoon sampler
3-inch OD split spoon sampler
Shelby tube sampler
Groundwater level at time of drilling
VIRGINIA TECH
The Charles Edward Via
Dept. of Civil Engineering
Blacksburg, Virginia
Drilling Initiated: 06/10/93
Drilling Completed: 06/10/93

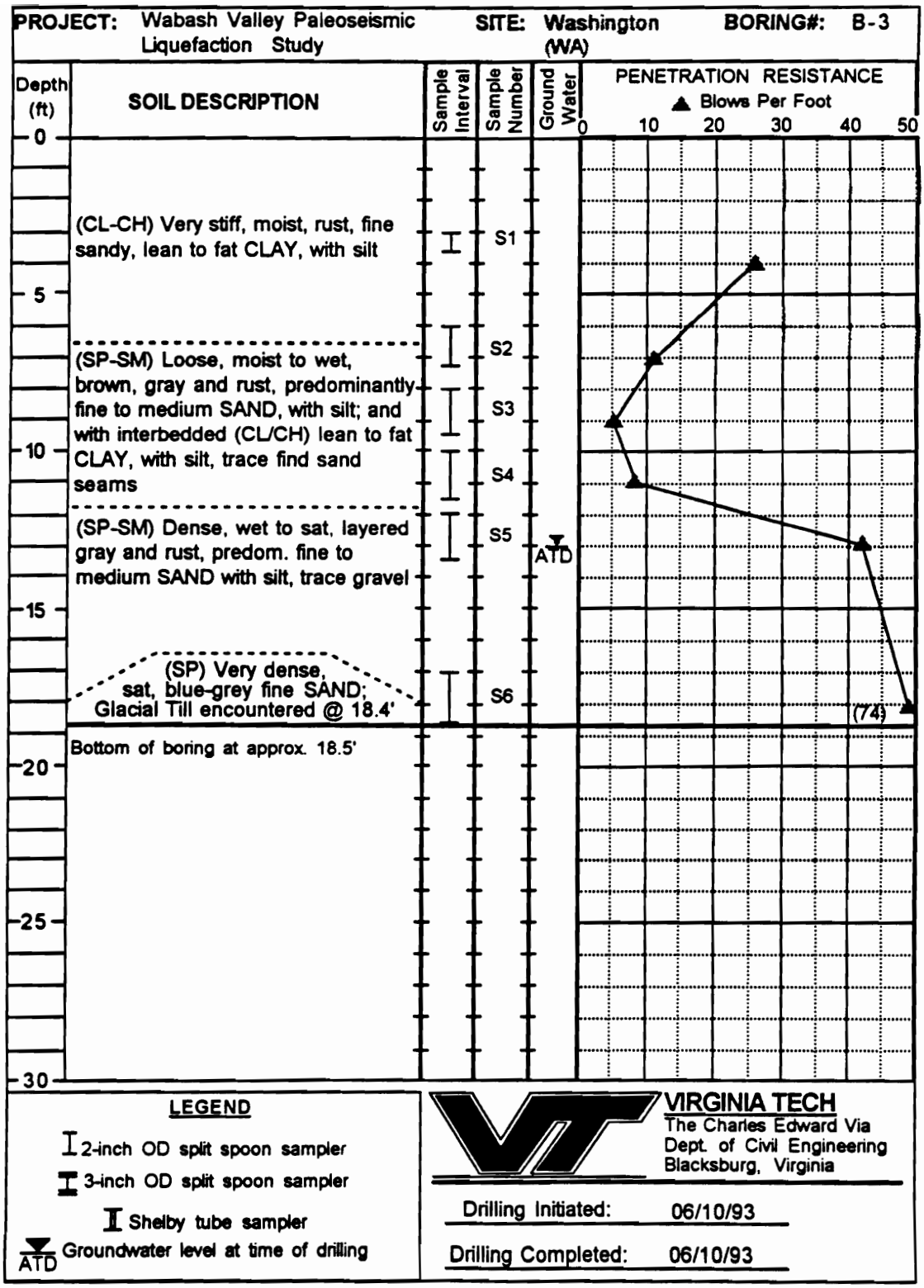
PROJECT: Wabash Valley Paleoseismic Liquefaction Study
SITE: Washington (WA)
BORING#: B-3
Depth (ft)
SOIL DESCRIPTION
Sample Interval
Sample Number
Ground Water
PENETRATION RESISTANCE
Blows Per Foot
0
10
20
30
40
50
0
5
10
15
20
25
30
(CL-CH) Very stiff, moist, rust, fine sandy, lean to fat CLAY, with silt
S1
S2
(SP-SM) Loose, moist to wet, brown, gray and rust, predominantly fine to medium SAND, with silt; and with interbedded (CL/CH) lean to fat CLAY, with silt, trace find sand seams
S3
S4
(SP-SM) Dense, wet to sat, layered gray and rust, predom. fine to medium SAND with silt, trace gravel
S5
ATD
(SP) Very dense, sat, blue-grey fine SAND; Glacial Till encountered @ 18.4'
S6
(74)
Bottom of boring at approx. 18.5'
LEGEND
2-inch OD split spoon sampler
3-inch OD split spoon sampler
Shelby tube sampler
ATD Groundwater level at time of drilling
VIRGINIA TECH
The Charles Edward Via
Dept. of Civil Engineering
Blacksburg, Virginia
Drilling Initiated: 06/10/93
Drilling Completed: 06/10/93

Appendix D:

Vallonia Event Boring Logs

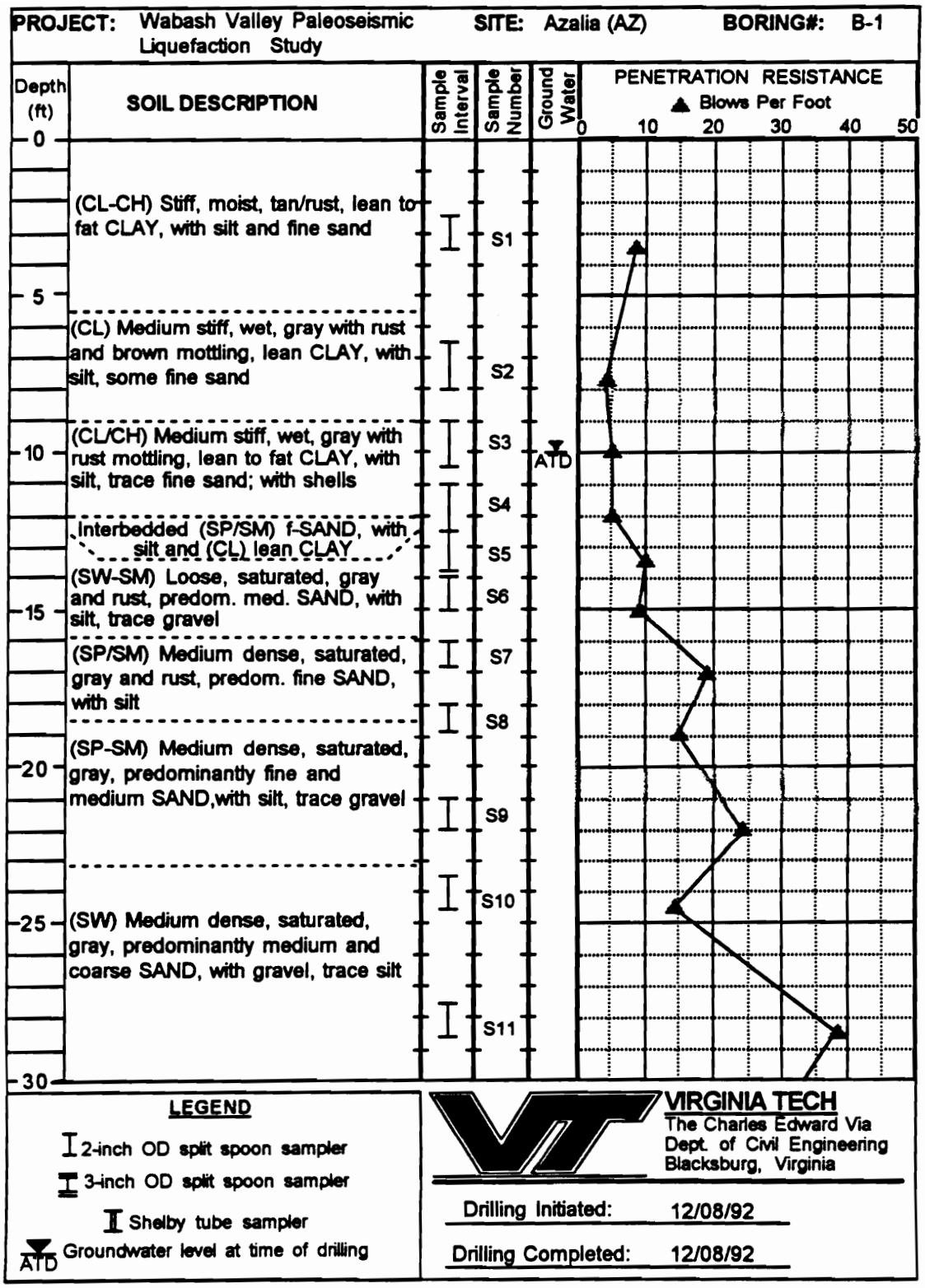
PROJECT: Wabash Valley Paleoseismic Liquefaction Study
SITE: Azalia (AZ)
BORING#: B-1
Depth (ft)
SOIL DESCRIPTION
Sample Interval
Sample Number
Ground Water
PENETRATION RESISTANCE
Blows Per Foot
0
10
20
30
40
50
0
5
10
15
20
25
30
(CL-CH) Stiff, moist, tan/rust, lean to fat CLAY, with silt and fine sand
S1
(CL) Medium stiff, wet, gray with rust and brown mottling, lean CLAY, with silt, some fine sand
S2
(CL/CH) Medium stiff, wet, gray with rust mottling, lean to fat CLAY, with silt, trace fine sand; with shells
S3
ATD
S4
Interbedded (SP/SM) f-SAND, with silt and (CL) lean CLAY
S5
(SW-SM) Loose, saturated, gray and rust, predom. med. SAND, with silt, trace gravel
S6
(SP/SM) Medium dense, saturated, gray and rust, predom. fine SAND, with silt
S7
S8
(SP-SM) Medium dense, saturated, gray, predominantly fine and medium SAND,with silt, trace gravel
S9
S10
(SW) Medium dense, saturated, gray, predominantly medium and coarse SAND, with gravel, trace silt
S11
LEGEND
2-inch OD split spoon sampler
3-inch OD split spoon sampler
Shelby tube sampler
ATD Groundwater level at time of drilling
VIRGINIA TECH
The Charles Edward Via
Dept. of Civil Engineering
Blacksburg, Virginia
Drilling Initiated: 12/08/92
Drilling Completed: 12/08/92

PROJECT: Wabash Valley Paleoseismic Liquefaction Study **SITE:** Azalia (AZ) **BORING#:** B-1 (cont'd)

Depth (ft)	SOIL DESCRIPTION	Sample Interval	Sample Number	Ground Water	PENETRATION RESISTANCE ▲ Blows Per Foot 0 10 20 30 40 50
30	(SW-SM) Medium dense, saturated, light gray, predominantly fine to medium SAND, with silt, some gravel	I	S12		
35	Bottom of boring at approx. 34'				
40					
45					
50					
55					
60					

LEGEND

I 2-inch OD split spoon sampler

I 3-inch OD split spoon sampler

I Shelby tube sampler

ATD Groundwater level at time of drilling

VIRGINIA TECH
The Charles Edward Via
Dept. of Civil Engineering
Blacksburg, Virginia

Drilling Initiated: 12/08/92

Drilling Completed: 12/08/92

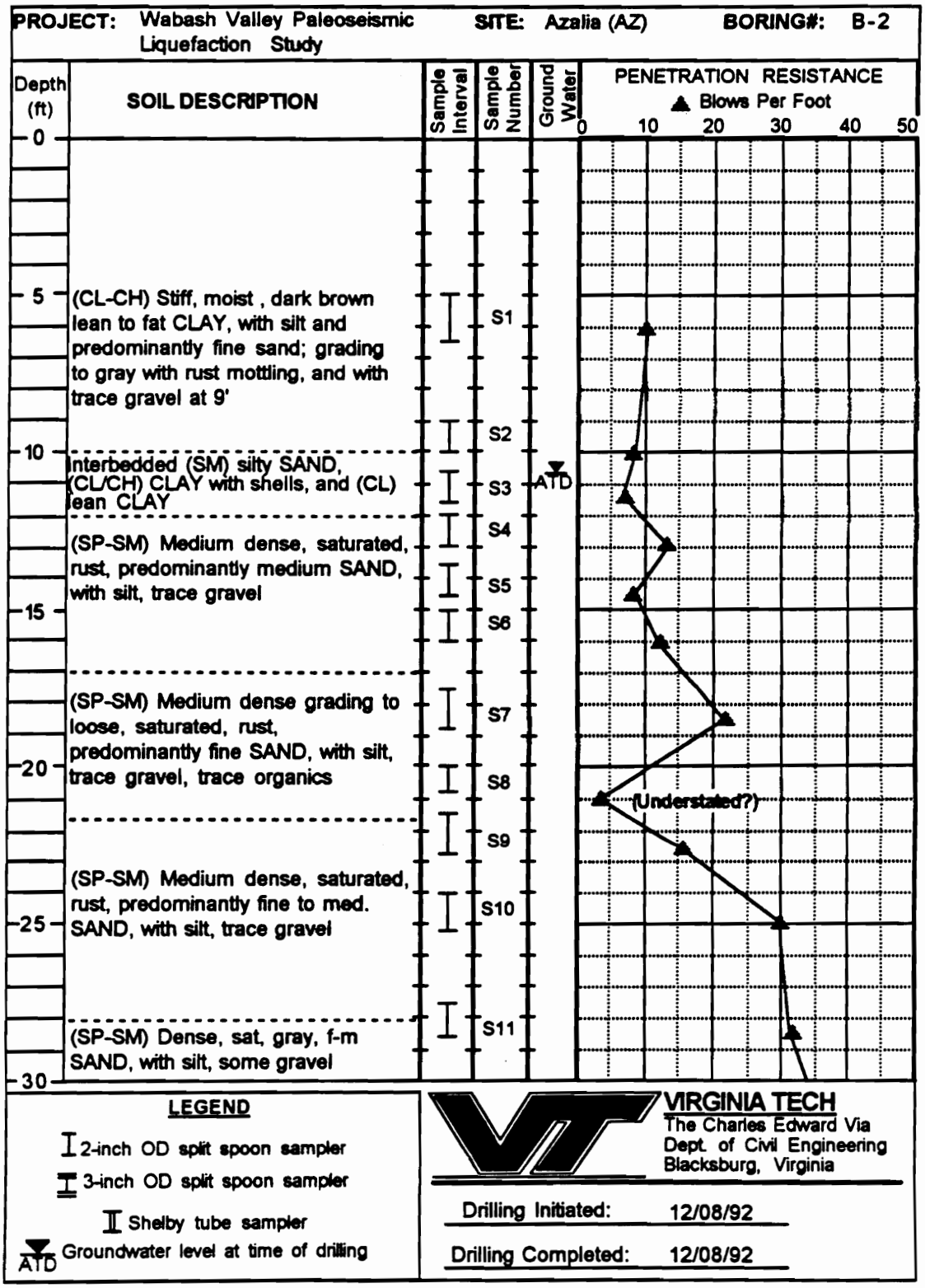
PROJECT: Wabash Valley Paleoseismic Liquefaction Study
SITE: Azalia (AZ)
BORING#: B-2
Depth (ft)
SOIL DESCRIPTION
Sample Interval
Sample Number
Ground Water
PENETRATION RESISTANCE
Blows Per Foot
0
10
20
30
40
50
0
5
10
15
20
25
30
(CL-CH) Stiff, moist , dark brown lean to fat CLAY, with silt and predominantly fine sand; grading to gray with rust mottling, and with trace gravel at 9'
Interbedded (SM) silty SAND, (CL/CH) CLAY with shells, and (CL) lean CLAY
(SP-SM) Medium dense, saturated, rust, predominantly medium SAND, with silt, trace gravel
(SP-SM) Medium dense grading to loose, saturated, rust, predominantly fine SAND, with silt, trace gravel, trace organics
(SP-SM) Medium dense, saturated, rust, predominantly fine to med. SAND, with silt, trace gravel
(SP-SM) Dense, sat, gray, f-m SAND, with silt, some gravel
S1
S2
S3
S4
S5
S6
S7
S8
S9
S10
S11
ATD
(Understated?)
LEGEND
2-inch OD split spoon sampler
3-inch OD split spoon sampler
Shelby tube sampler
Groundwater level at time of drilling
VIRGINIA TECH
The Charles Edward Via
Dept. of Civil Engineering
Blacksburg, Virginia
Drilling Initiated: 12/08/92
Drilling Completed: 12/08/92

PROJECT: Wabash Valley Paleoseismic Liquefaction Study **SITE:** Azalia (AZ) **BORING#:** B-2 (cont'd)

Depth (ft)	SOIL DESCRIPTION	Sample Interval	Sample Number	Ground Water	PENETRATION RESISTANCE ▲ Blows Per Foot 0 10 20 30 40 50
30	(SW-SM) Dense, saturated, light gray, predominantly fine to medium SAND, with silt, some gravel	I	S12		
35	Bottom of boring at approx. 34'				
40					
45					
50					
55					
60					

LEGEND

I 2-inch OD split spoon sampler

I 3-inch OD split spoon sampler

I Shelby tube sampler

▼ ATD Groundwater level at time of drilling

VIRGINIA TECH
The Charles Edward Via
Dept. of Civil Engineering
Blacksburg, Virginia

Drilling Initiated: 12/08/92

Drilling Completed: 12/08/92

PROJECT: Wabash Valley Paleoseismic Liquefaction Study **SITE:** Azalia (AZ) **BORING#:** B-3

Depth (ft)	SOIL DESCRIPTION	Sample Interval	Sample Number	Ground Water
0	(CL-CH) Stiff, moist, dark brown, lean to fat CLAY, with silt, trace fine sand			
	(CL-CH) Stiff, moist, rust with brown mottling, lean to fat CLAY, with silt, some fine sand		S1	
5	(SC) Loose, tan/rust grading to brown clayey predom. fine SAND		S2	
	(SM) Medium dense, saturated, interbedded gray/brown/rust, silty predom. med. SAND, some gravel		S3	
10			S4	ATD
	(SP/SM) Medium dense, sat, gray, predom. fine SAND, with silt, tr gravel; with interbeded rust and gray predom. c-SAND, with silt, tr gravel at 13'-13.5'		S5	
15				
	(SP) Medium dense, saturated, gray, predominantly medium and coarse SAND, with gravel, trace silt		S6	
20			S7	
25				
	(SW-SM) Medium dense, saturated, gray, SAND, with silt, some gravel		S8	
30	Bottom of Boring at approx. 29'			

PENETRATION RESISTANCE
▲ Blows Per Foot
0 10 20 30 40 50

LEGEND

- 2-inch OD split spoon sampler
- 3-inch OD split spoon sampler
- Shelby tube sampler
- ATD Groundwater level at time of drilling

VIRGINIA TECH
The Charles Edward Via
Dept. of Civil Engineering
Blacksburg, Virginia

Drilling Initiated: 12/08/92

Drilling Completed: 12/08/92

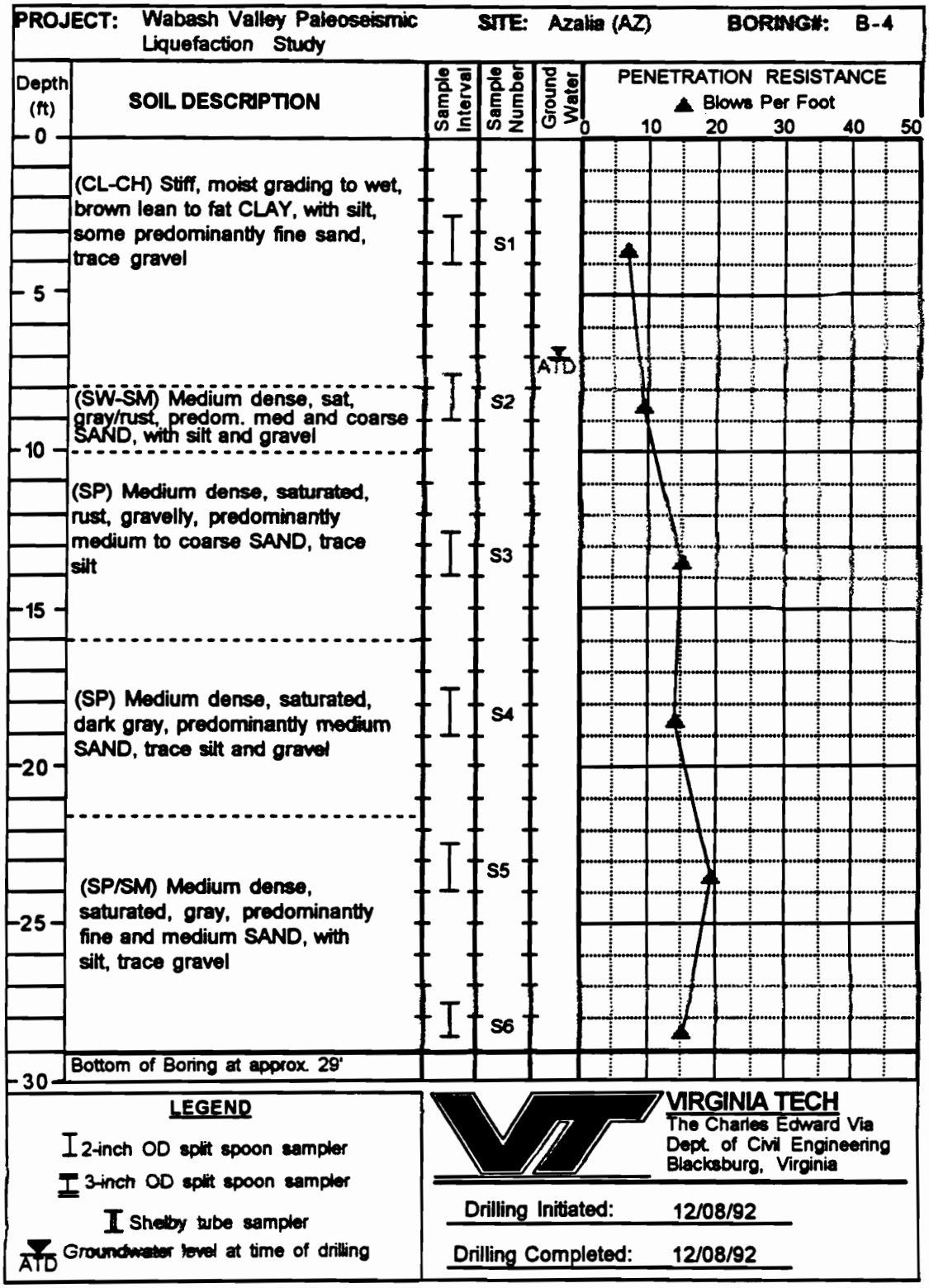
PROJECT: Wabash Valley Paleoseismic Liquefaction Study
SITE: Azalia (AZ)
BORING#: B-4
Depth (ft)
SOIL DESCRIPTION
Sample Interval
Sample Number
Ground Water
PENETRATION RESISTANCE
Blows Per Foot
0
10
20
30
40
50
0
5
10
15
20
25
30
(CL-CH) Stiff, moist grading to wet, brown lean to fat CLAY, with silt, some predominantly fine sand, trace gravel
S1
ATD
(SW-SM) Medium dense, sat, gray/rust, predom. med and coarse SAND, with silt and gravel
S2
(SP) Medium dense, saturated, rust, gravelly, predominantly medium to coarse SAND, trace silt
S3
(SP) Medium dense, saturated, dark gray, predominantly medium SAND, trace silt and gravel
S4
(SP/SM) Medium dense, saturated, gray, predominantly fine and medium SAND, with silt, trace gravel
S5
S6
Bottom of Boring at approx. 29'
LEGEND
2-inch OD split spoon sampler
3-inch OD split spoon sampler
Shelby tube sampler
ATD Groundwater level at time of drilling
VIRGINIA TECH
The Charles Edward Via Dept. of Civil Engineering
Blacksburg, Virginia
Drilling Initiated: 12/08/92
Drilling Completed: 12/08/92

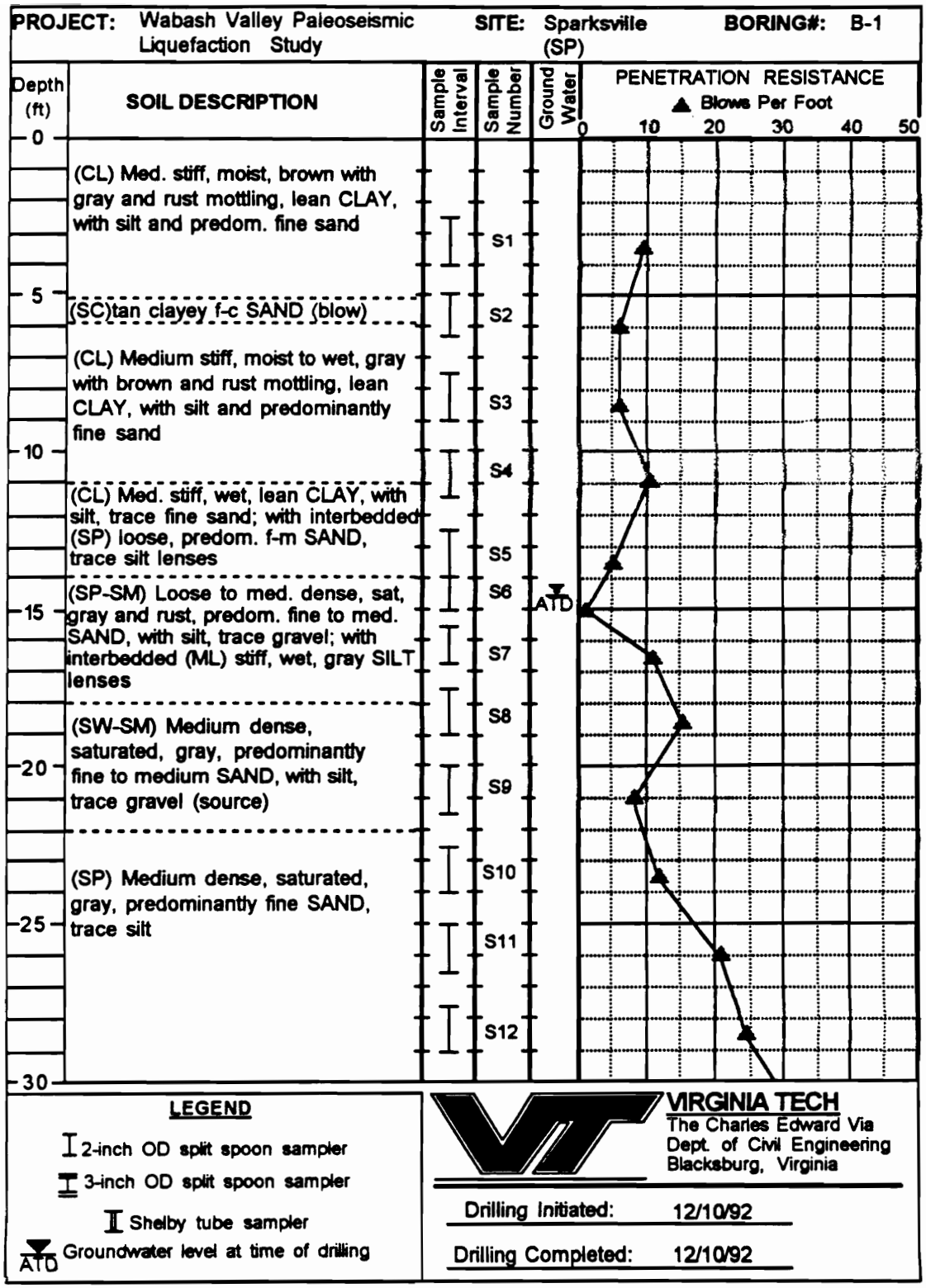
PROJECT: Wabash Valley Paleoseismic Liquefaction Study
SITE: Sparksville (SP)
BORING#: B-1
Depth (ft)
SOIL DESCRIPTION
Sample Interval
Sample Number
Ground Water
PENETRATION RESISTANCE
Blows Per Foot
0
10
20
30
40
50
0
5
10
15
20
25
30
(CL) Med. stiff, moist, brown with gray and rust mottling, lean CLAY, with silt and predom. fine sand
(SC)tan clayey f-c SAND (blow)
(CL) Medium stiff, moist to wet, gray with brown and rust mottling, lean CLAY, with silt and predominantly fine sand
(CL) Med. stiff, wet, lean CLAY, with silt, trace fine sand; with interbedded (SP) loose, predom. f-m SAND, trace silt lenses
(SP-SM) Loose to med. dense, sat, gray and rust, predom. fine to med. SAND, with silt, trace gravel; with interbedded (ML) stiff, wet, gray SILT lenses
(SW-SM) Medium dense, saturated, gray, predominantly fine to medium SAND, with silt, trace gravel (source)
(SP) Medium dense, saturated, gray, predominantly fine SAND, trace silt
S1
S2
S3
S4
S5
S6
S7
S8
S9
S10
S11
S12
ATD
LEGEND
2-inch OD split spoon sampler
3-inch OD split spoon sampler
Shelby tube sampler
Groundwater level at time of drilling
VIRGINIA TECH
The Charles Edward Via
Dept. of Civil Engineering
Blacksburg, Virginia
Drilling Initiated: 12/10/92
Drilling Completed: 12/10/92

PROJECT: Wabash Valley Paleoseismic Liquefaction Study

SITE: Sparksville (SP)

BORING#: B-1 (cont'd)

Depth (ft)	SOIL DESCRIPTION	Sample Interval	Sample Number	Ground Water	PENETRATION RESISTANCE ▲ Blows Per Foot 0 10 20 30 40 50
30	(SP-SM) Medium dense, saturated, gray, predominantly fine to medium SAND, with silt, some gravel		S13		
35			S14		
40	Bottom of boring at approx. 39'				
45					
50					
55					
60					

VIRGINIA TECH
The Charles Edward Via
Dept. of Civil Engineering
Blacksburg, Virginia

LEGEND

- 2-inch OD split spoon sampler
- 3-inch OD split spoon sampler
- Shelby tube sampler
- ATD Groundwater level at time of drilling

Drilling Initiated: 12/10/92

Drilling Completed: 12/10/92

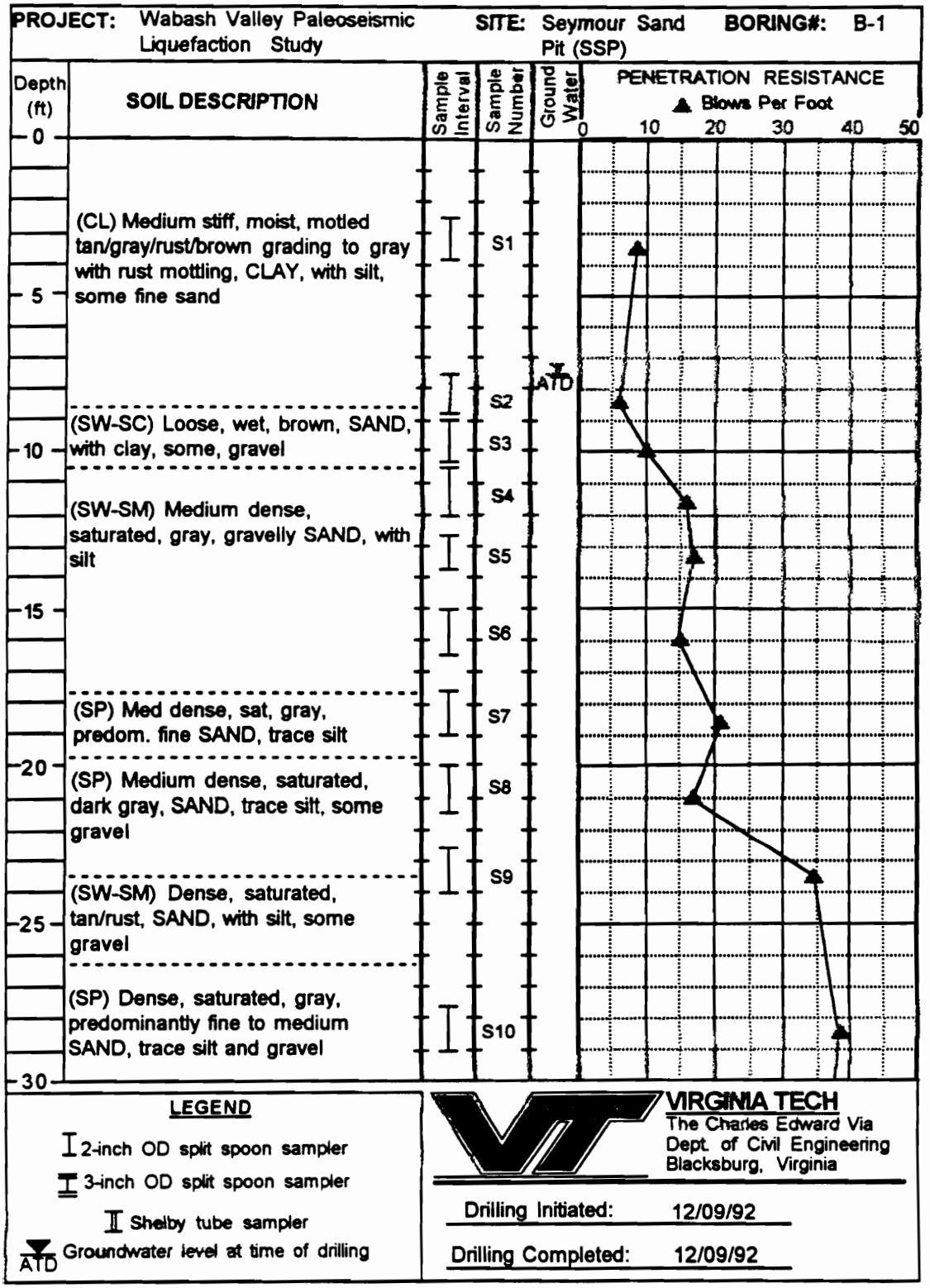
PROJECT: Wabash Valley Paleoseismic Liquefaction Study
SITE: Seymour Sand Pit (SSP)
BORING#: B-1
Depth (ft)
SOIL DESCRIPTION
Sample Interval
Sample Number
Ground Water
PENETRATION RESISTANCE
Blows Per Foot
0
10
20
30
40
50
0
5
10
15
20
25
30
(CL) Medium stiff, moist, motled tan/gray/rust/brown grading to gray with rust mottling, CLAY, with silt, some fine sand
(SW-SC) Loose, wet, brown, SAND, with clay, some, gravel
(SW-SM) Medium dense, saturated, gray, gravelly SAND, with silt
(SP) Med dense, sat, gray, predom. fine SAND, trace silt
(SP) Medium dense, saturated, dark gray, SAND, trace silt, some gravel
(SW-SM) Dense, saturated, tan/rust, SAND, with silt, some gravel
(SP) Dense, saturated, gray, predominantly fine to medium SAND, trace silt and gravel
S1
S2
S3
S4
S5
S6
S7
S8
S9
S10
ATD
LEGEND
2-inch OD split spoon sampler
3-inch OD split spoon sampler
Shelby tube sampler
ATD Groundwater level at time of drilling
VIRGINIA TECH
The Charles Edward Via Dept. of Civil Engineering Blacksburg, Virginia
Drilling Initiated: 12/09/92
Drilling Completed: 12/09/92

PROJECT: Wabash Valley Paleoseismic Liquefaction Study **SITE:** Seymour Sand Pit (SSP) **BORING#:** B-1 (cont'd)

Depth (ft)	SOIL DESCRIPTION	Sample Interval	Sample Number	Ground Water	PENETRATION RESISTANCE ▲ Blows Per Foot 0 10 20 30 40 50
30	(SP) Dense, sat, gray, predom. m-c SAND, trace silt, some gravel; becoming predom. f-m SAND, trace silt and gravel at 33.5'	I	S11		
35	Bottom of boring at approx. 34'				
40					
45					
50					
55					
60					

LEGEND

I 2-inch OD split spoon sampler

I 3-inch OD split spoon sampler

I Shelby tube sampler

ATD Groundwater level at time of drilling

VIRGINIA TECH
The Charles Edward Via
Dept. of Civil Engineering
Blacksburg, Virginia

Drilling Initiated: 12/09/92

Drilling Completed: 12/09/92

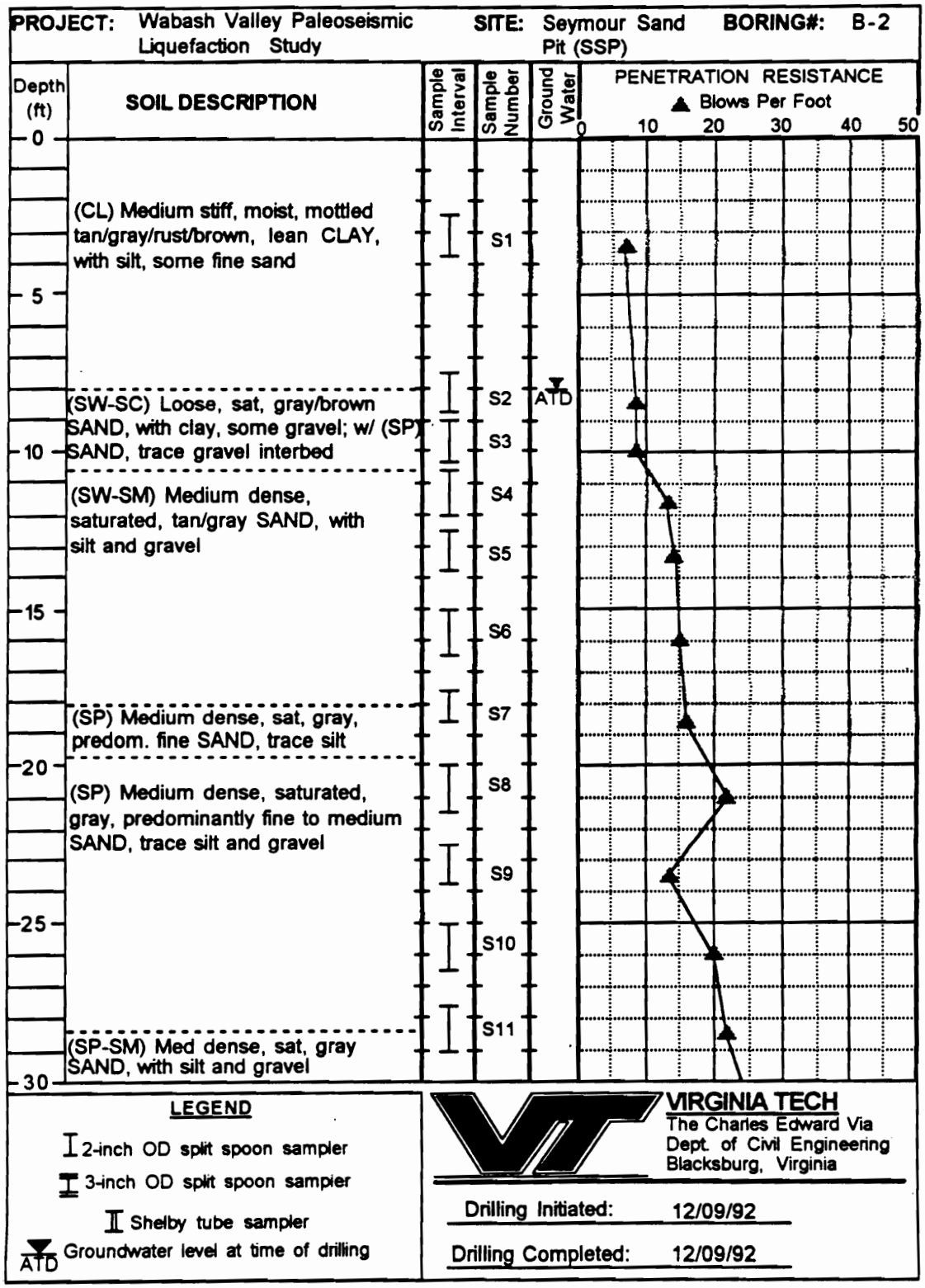
PROJECT: Wabash Valley Paleoseismic Liquefaction Study
SITE: Seymour Sand Pit (SSP)
BORING#: B-2
Depth (ft)
SOIL DESCRIPTION
Sample Interval
Sample Number
Ground Water
PENETRATION RESISTANCE
Blows Per Foot
0
10
20
30
40
50
0
5
10
15
20
25
30
(CL) Medium stiff, moist, mottled tan/gray/rust/brown, lean CLAY, with silt, some fine sand
(SW-SC) Loose, sat, gray/brown SAND, with clay, some gravel; w/ (SP) SAND, trace gravel interbed
(SW-SM) Medium dense, saturated, tan/gray SAND, with silt and gravel
(SP) Medium dense, sat, gray, predom. fine SAND, trace silt
(SP) Medium dense, saturated, gray, predominantly fine to medium SAND, trace silt and gravel
(SP-SM) Med dense, sat, gray SAND, with silt and gravel
S1
S2
S3
S4
S5
S6
S7
S8
S9
S10
S11
ATD
LEGEND
2-inch OD split spoon sampler
3-inch OD split spoon sampler
Shelby tube sampler
Groundwater level at time of drilling
VIRGINIA TECH
The Charles Edward Via
Dept. of Civil Engineering
Blacksburg, Virginia
Drilling Initiated: 12/09/92
Drilling Completed: 12/09/92

PROJECT: Wabash Valley Paleoseismic Liquefaction Study

SITE: Seymour Sand Pit (SSP)

BORING#: B-2 (cont'd)

Depth (ft)	SOIL DESCRIPTION	Sample Interval	Sample Number	Ground Water
30	(SP-SM) Medium dense, saturated, gray, SAND, with silt and gravel	I	S12	
35	(SP) Dense, saturated, gray, predominantly fine to medium SAND, trace silt and gravel	I	S13	
40	Bottom of boring at approx. 39'			
45				
50				
55				
60				

PENETRATION RESISTANCE
▲ Blows Per Foot
0 10 20 30 40 50

LEGEND

I 2-inch OD split spoon sampler

I 3-inch OD split spoon sampler

I Shelby tube sampler

ATD Groundwater level at time of drilling

VIRGINIA TECH
The Charles Edward Via Dept. of Civil Engineering
Blacksburg, Virginia

Drilling Initiated: 12/09/92

Drilling Completed: 12/09/92

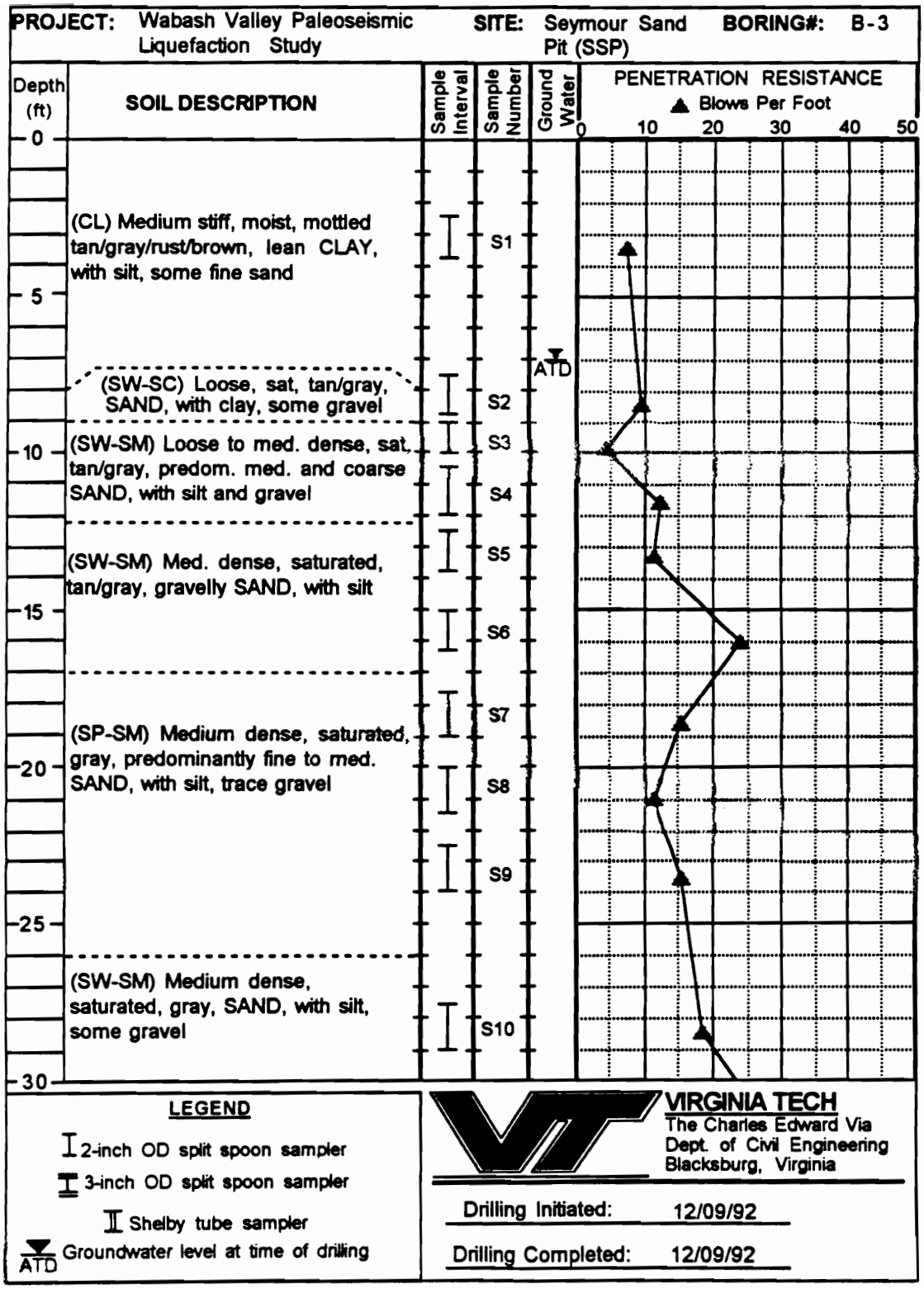
PROJECT: Wabash Valley Paleoseismic Liquefaction Study
SITE: Seymour Sand Pit (SSP)
BORING#: B-3
Depth (ft)
SOIL DESCRIPTION
Sample Interval
Sample Number
Ground Water
PENETRATION RESISTANCE
Blows Per Foot
0
10
20
30
40
50
0
5
10
15
20
25
30
(CL) Medium stiff, moist, mottled tan/gray/rust/brown, lean CLAY, with silt, some fine sand
S1
ATD
(SW-SC) Loose, sat, tan/gray, SAND, with clay, some gravel
S2
(SW-SM) Loose to med. dense, sat. tan/gray, predom. med. and coarse SAND, with silt and gravel
S3
S4
(SW-SM) Med. dense, saturated, tan/gray, gravelly SAND, with silt
S5
S6
(SP-SM) Medium dense, saturated, gray, predominantly fine to med. SAND, with silt, trace gravel
S7
S8
S9
(SW-SM) Medium dense, saturated, gray, SAND, with silt, some gravel
S10
LEGEND
2-inch OD split spoon sampler
3-inch OD split spoon sampler
Shelby tube sampler
ATD Groundwater level at time of drilling
VIRGINIA TECH
The Charles Edward Via Dept. of Civil Engineering Blacksburg, Virginia
Drilling Initiated: 12/09/92
Drilling Completed: 12/09/92

PROJECT: Wabash Valley Paleoseismic Liquefaction Study **SITE:** Seymour Sand Pit (SSP) **BORING #:** B-3 (cont'd)

Depth (ft)	SOIL DESCRIPTION	Sample Interval	Sample Number	Ground Water	PENETRATION RESISTANCE ▲ Blows per foot 0 10 20 30 40 50
30	(SP) Dense, saturated, gray, fine to medium SAND, trace coarse sand and gravel	I	S11		
35	Bottom of boring at approx. 34'				
40					
45					
50					
55					
60					

LEGEND

I 2-inch OD split spoon sampler

I 3-inch OD split spoon sampler

I Shelby tube sampler

ATD Groundwater level at time of drilling

VIRGINIA TECH
The Charles Edward Via
Dept. of Civil Engineering
Blacksburg, Virginia

Drilling Initiated: 12/09/92

Drilling Completed: 12/09/92

Appendix E:

Waverly Event Boring Logs

PROJECT: Wabash Valley Paleoseismic Liquefaction Study **SITE:** Martinsville (MV) **BORING#:** B-1

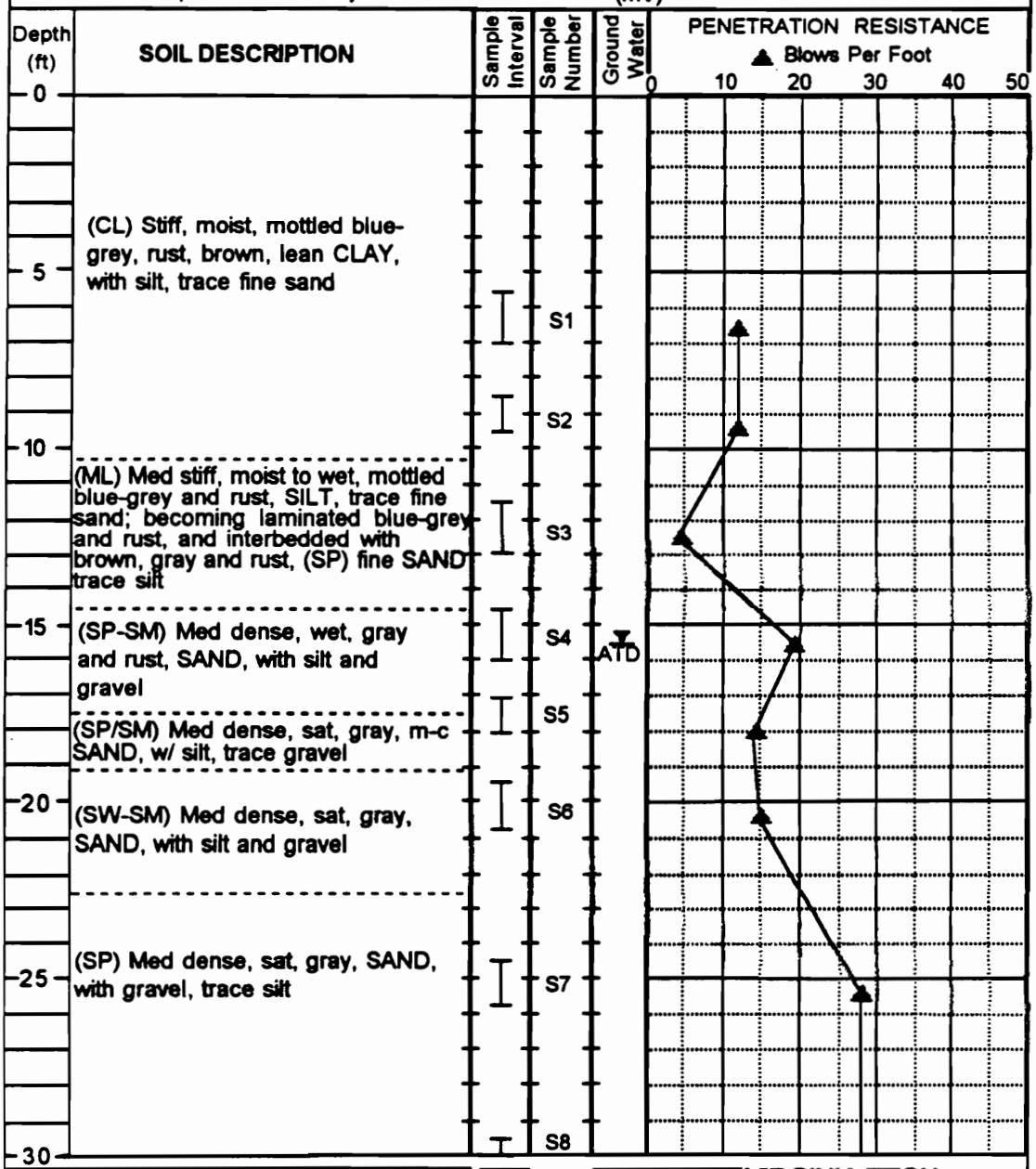

LEGEND

- 2-inch OD split spoon sampler
- 3-inch OD split spoon sampler
- Shelby tube sampler
- ATD Groundwater level at time of drilling

VIRGINIA TECH
The Charles Edward Via
Dept. of Civil Engineering
Blacksburg, Virginia

Drilling Initiated: 11/12/93

Drilling Completed: 11/12/93

PROJECT: Wabash Valley Paleoseismic Liquefaction Study

SITE: Martinsville (MV)

BORING#: B-1 (cont'd)

Depth (ft)	SOIL DESCRIPTION	Sample Interval	Sample Number	Ground Water	PENETRATION RESISTANCE ▲ Blows Per Foot (0 10 20 30 40 50)
30	(SP) Medium dense, saturated, gray and rust, gravelly, SAND, trace silt	I	S8		
35	c-gravel or cobble broken up at 35'	I	S9		(Overstated)
	Bottom of boring at approx. 36'				
40					
45					
50					
55					
60					

LEGEND

I 2-inch OD split spoon sampler

I 3-inch OD split spoon sampler

I Shelby tube sampler

▼ ATD Groundwater level at time of drilling

VIRGINIA TECH
The Charles Edward Via
Dept. of Civil Engineering
Blacksburg, Virginia

Drilling Initiated: 11/12/93

Drilling Completed: 11/12/93

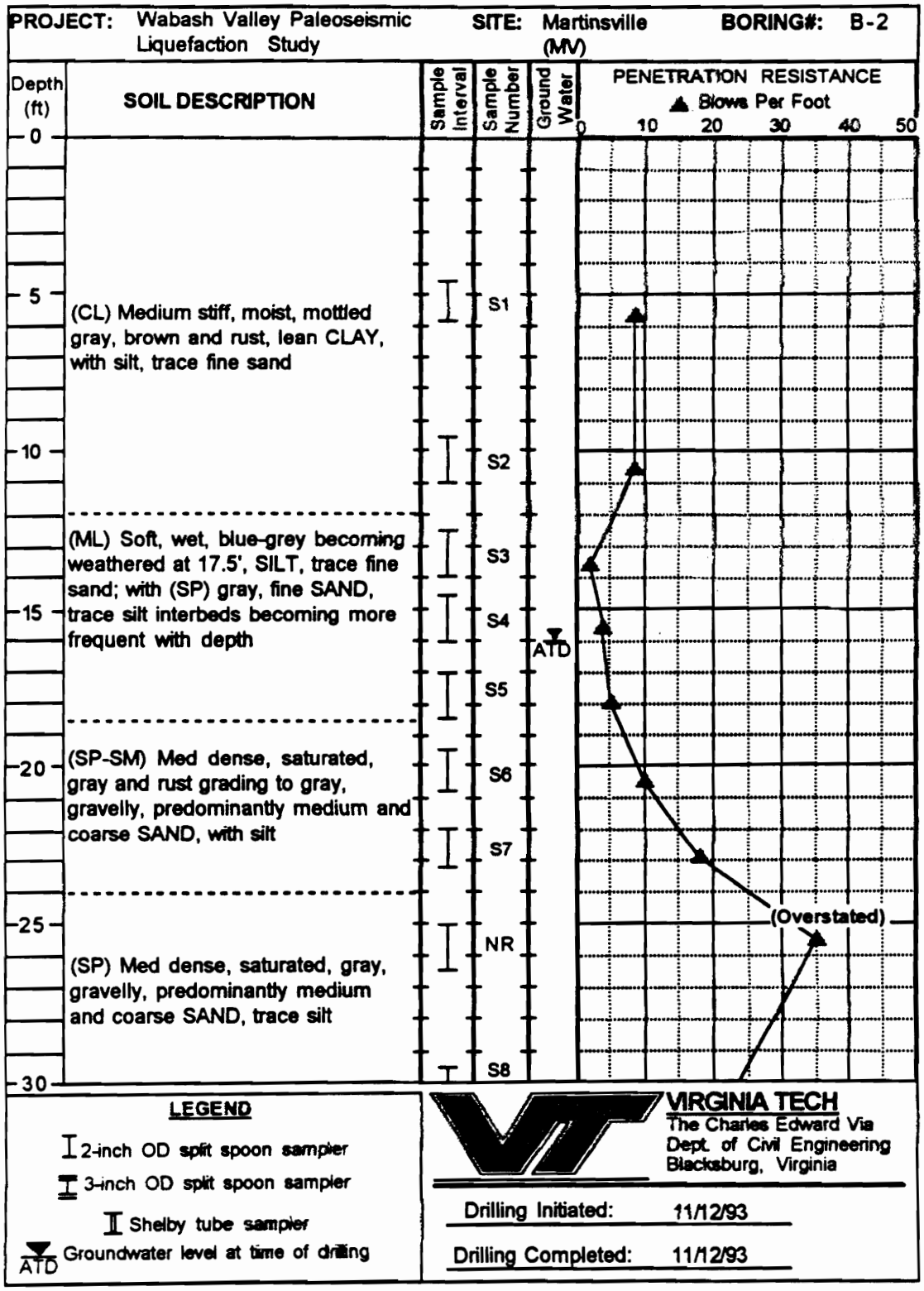
PROJECT: Wabash Valley Paleoseismic Liquefaction Study
SITE: Martinsville (MV)
BORING#: B-2
Depth (ft)
SOIL DESCRIPTION
Sample Interval
Sample Number
Ground Water
PENETRATION RESISTANCE
Blows Per Foot
0
10
20
30
40
50
5
10
15
20
25
30
(CL) Medium stiff, moist, mottled gray, brown and rust, lean CLAY, with silt, trace fine sand
(ML) Soft, wet, blue-grey becoming weathered at 17.5', SILT, trace fine sand; with (SP) gray, fine SAND, trace silt interbeds becoming more frequent with depth
(SP-SM) Med dense, saturated, gray and rust grading to gray, gravelly, predominantly medium and coarse SAND, with silt
(SP) Med dense, saturated, gray, gravelly, predominantly medium and coarse SAND, trace silt
S1
S2
S3
S4
S5
S6
S7
NR
S8
ATD
(Overstated)
LEGEND
2-inch OD split spoon sampler
3-inch OD split spoon sampler
Shelby tube sampler
Groundwater level at time of drilling
VIRGINIA TECH
The Charles Edward Via Dept. of Civil Engineering
Blacksburg, Virginia
Drilling Initiated: 11/12/93
Drilling Completed: 11/12/93

PROJECT: Wabash Valley Paleoseismic Liquefaction Study

SITE: Martinsville (MV)

BORING#: B-2 (cont'd)

Depth (ft)	SOIL DESCRIPTION	Sample Interval	Sample Number	Ground Water	PENETRATION RESISTANCE ▲ Blows Per Foot 0 10 20 30 40 50
30	(SP) Medium dense, saturated, gray, gravelly, predominantly medium to coarse SAND, trace silt		S8		
35			S9		
40	(SP) Medium dense, saturated, gray, predom. fine to medium SAND, trace silt and gravel		S10		
	Bottom of boring at approx. 41'				
45					
50					
55					
60					

LEGEND

- 2-inch OD split spoon sampler
- 3-inch OD split spoon sampler
- Shelby tube sampler
- ATD Groundwater level at time of drilling

VIRGINIA TECH
The Charles Edward Via Dept. of Civil Engineering
Blacksburg, Virginia

Drilling Initiated: 11/12/93

Drilling Completed: 11/12/93

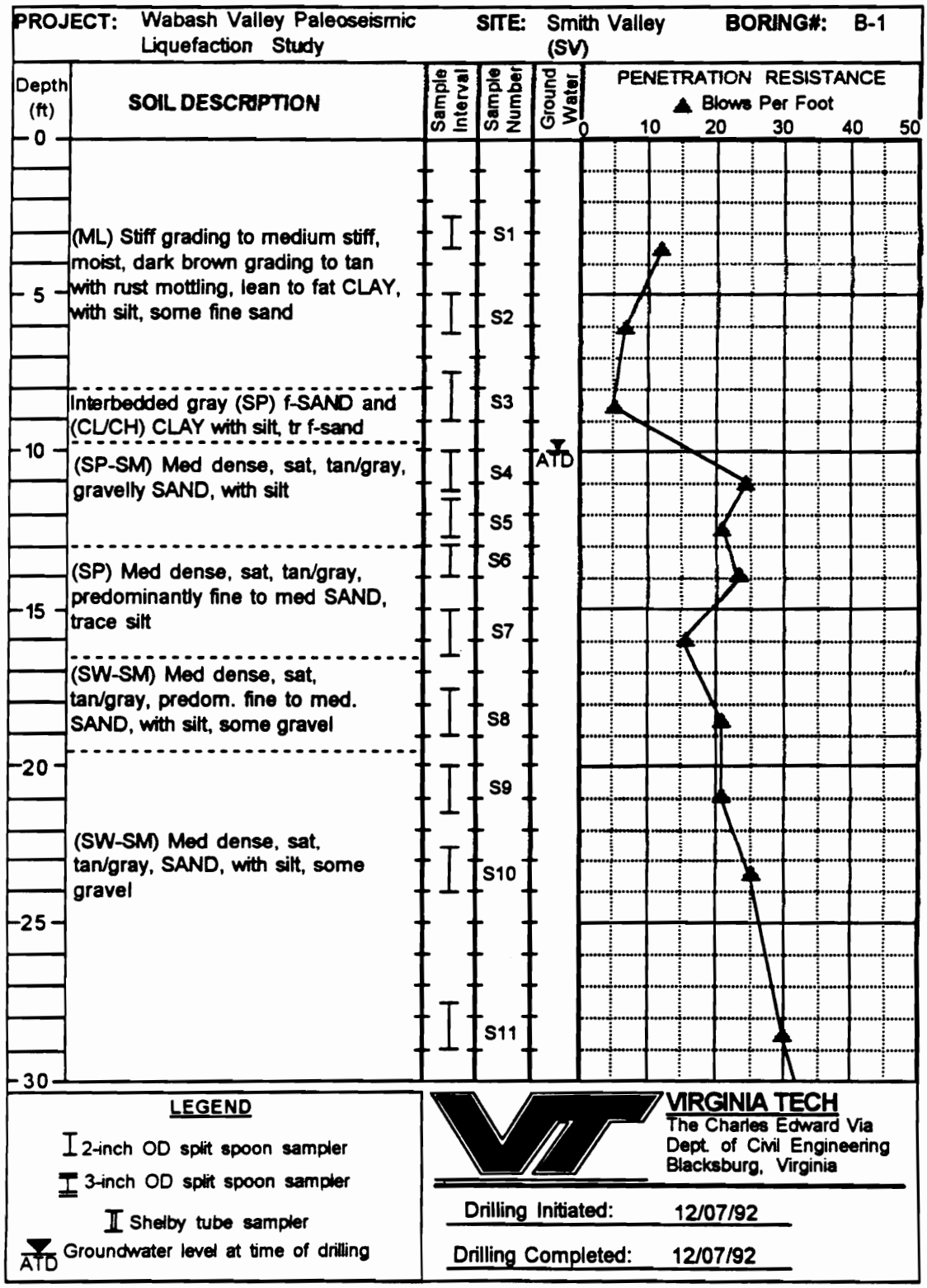
PROJECT: Wabash Valley Paleoseismic Liquefaction Study
SITE: Smith Valley (SV)
BORING#: B-1
Depth (ft)
SOIL DESCRIPTION
Sample Interval
Sample Number
Ground Water
PENETRATION RESISTANCE
Blows Per Foot
0
10
20
30
40
50
0
5
10
15
20
25
30
(ML) Stiff grading to medium stiff, moist, dark brown grading to tan with rust mottling, lean to fat CLAY, with silt, some fine sand
Interbedded gray (SP) f-SAND and (CL/CH) CLAY with silt, tr f-sand
(SP-SM) Med dense, sat, tan/gray, gravelly SAND, with silt
(SP) Med dense, sat, tan/gray, predominantly fine to med SAND, trace silt
(SW-SM) Med dense, sat, tan/gray, predom. fine to med. SAND, with silt, some gravel
(SW-SM) Med dense, sat, tan/gray, SAND, with silt, some gravel
S1
S2
S3
S4
S5
S6
S7
S8
S9
S10
S11
ATD
LEGEND
2-inch OD split spoon sampler
3-inch OD split spoon sampler
Shelby tube sampler
Groundwater level at time of drilling
VIRGINIA TECH
The Charles Edward Via
Dept. of Civil Engineering
Blacksburg, Virginia
Drilling Initiated: 12/07/92
Drilling Completed: 12/07/92

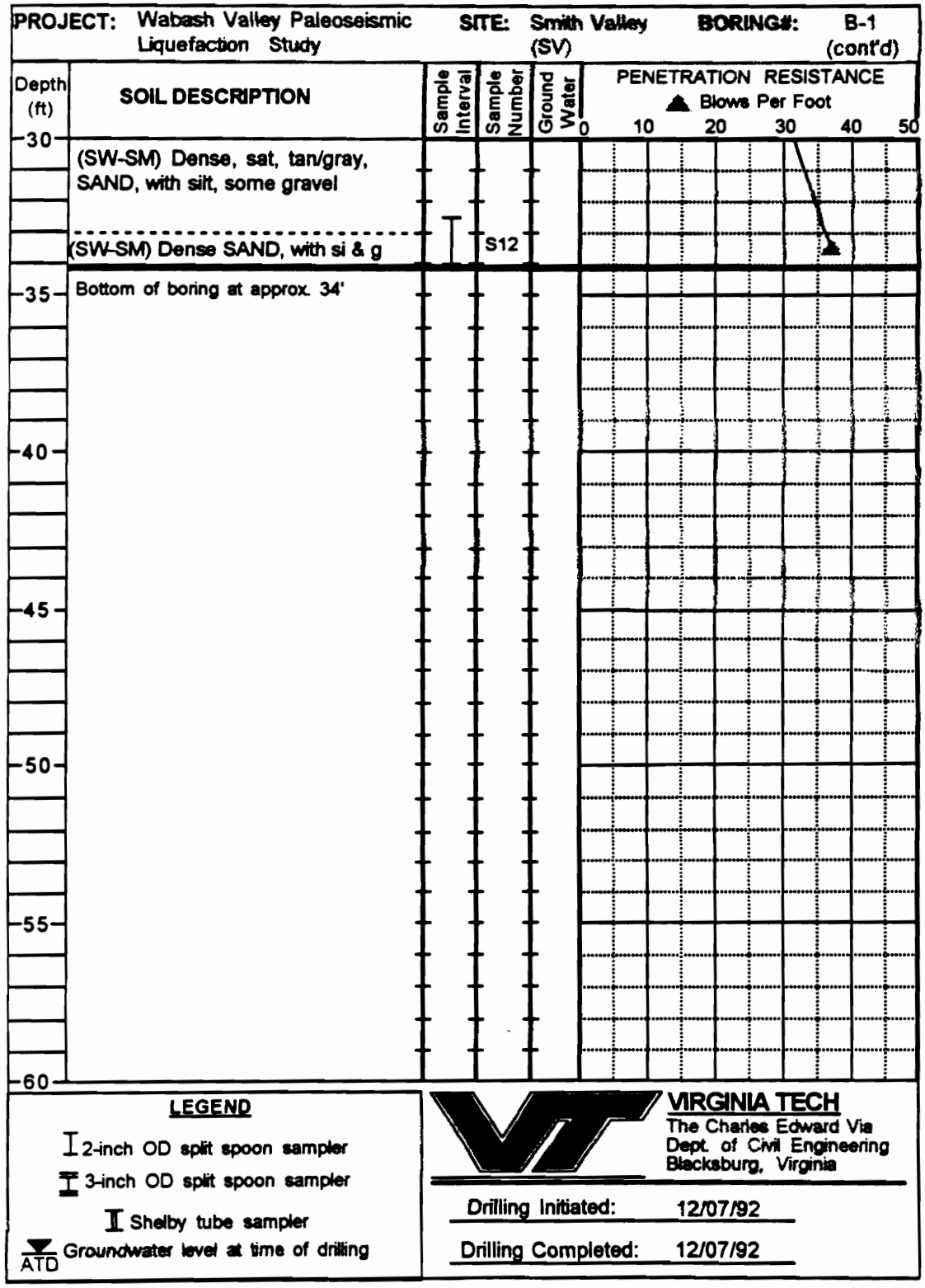
PROJECT: Wabash Valley Paleoseismic Liquefaction Study
SITE: Smith Valley (SV)
BORING#: B-1 (cont'd)
Depth (ft)
SOIL DESCRIPTION
Sample Interval
Sample Number
Ground Water
PENETRATION RESISTANCE
Blows Per Foot
0 10 20 30 40 50
30
(SW-SM) Dense, sat, tan/gray, SAND, with silt, some gravel
(SW-SM) Dense SAND, with si & g
S12
35
Bottom of boring at approx. 34'
40
45
50
55
60
LEGEND
2-inch OD split spoon sampler
3-inch OD split spoon sampler
Shelby tube sampler
ATD Groundwater level at time of drilling
VIRGINIA TECH
The Charles Edward Via Dept. of Civil Engineering Blacksburg, Virginia
Drilling Initiated: 12/07/92
Drilling Completed: 12/07/92

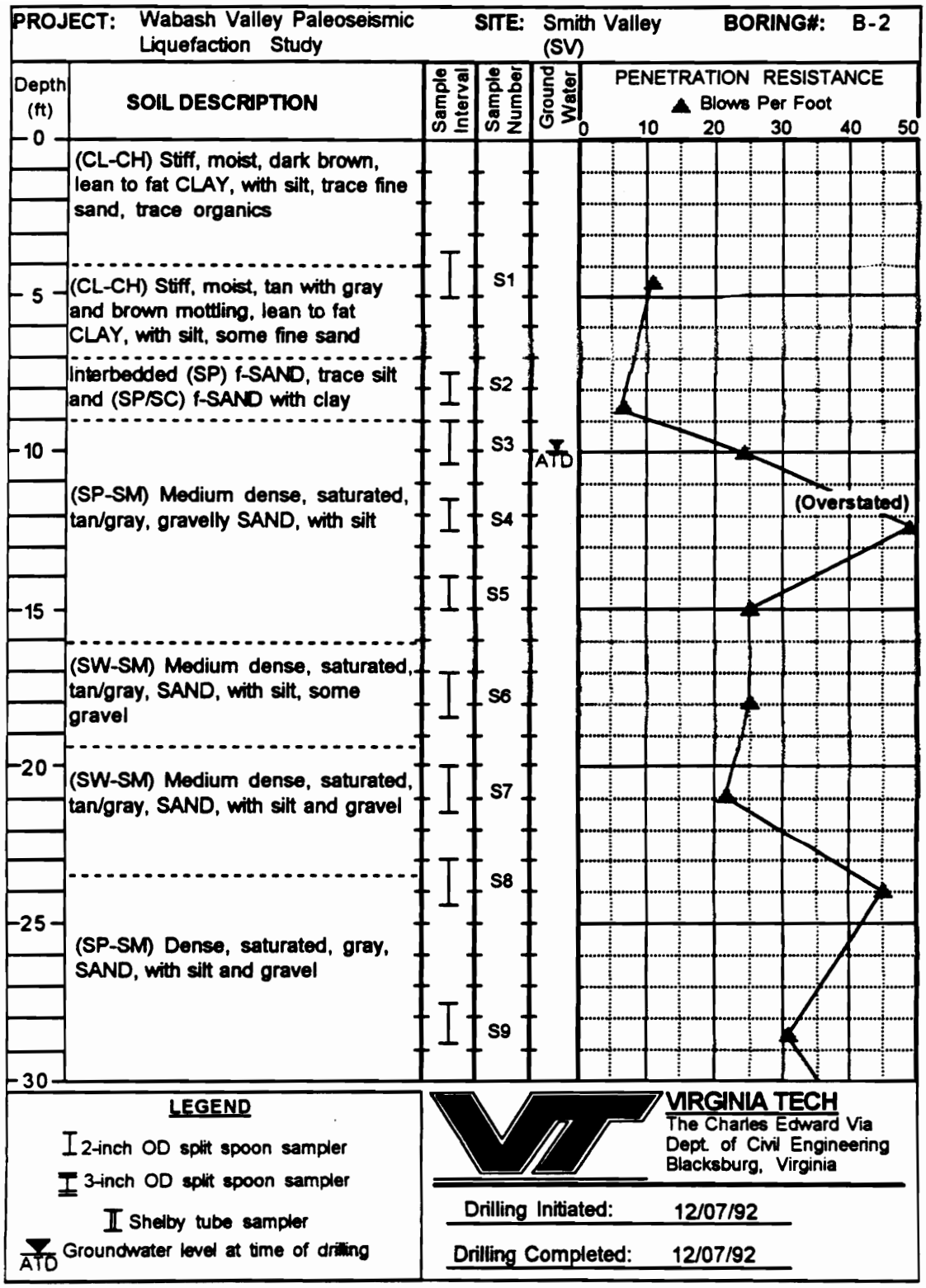
PROJECT: Wabash Valley Paleoseismic Liquefaction Study
SITE: Smith Valley (SV)
BORING#: B-2
Depth (ft)
SOIL DESCRIPTION
Sample Interval
Sample Number
Ground Water
PENETRATION RESISTANCE
Blows Per Foot
0
10
20
30
40
50
(CL-CH) Stiff, moist, dark brown, lean to fat CLAY, with silt, trace fine sand, trace organics
(CL-CH) Stiff, moist, tan with gray and brown mottling, lean to fat CLAY, with silt, some fine sand
S1
Interbedded (SP) f-SAND, trace silt and (SP/SC) f-SAND with clay
S2
S3
ATD
(SP-SM) Medium dense, saturated, tan/gray, gravelly SAND, with silt
(Overstated)
S4
S5
(SW-SM) Medium dense, saturated, tan/gray, SAND, with silt, some gravel
S6
(SW-SM) Medium dense, saturated, tan/gray, SAND, with silt and gravel
S7
S8
(SP-SM) Dense, saturated, gray, SAND, with silt and gravel
S9
5
10
15
20
25
30
LEGEND
2-inch OD split spoon sampler
3-inch OD split spoon sampler
Shelby tube sampler
ATD Groundwater level at time of drilling
VIRGINIA TECH
The Charles Edward Via Dept. of Civil Engineering Blacksburg, Virginia
Drilling Initiated: 12/07/92
Drilling Completed: 12/07/92

PROJECT: Wabash Valley Paleoseismic Liquefaction Study

SITE: Smith Valley (SV)

BORING#: B-2 (cont'd)

Depth (ft)	SOIL DESCRIPTION	Sample Interval	Sample Number	Ground Water	PENETRATION RESISTANCE ▲ Blows Per Foot 0 10 20 30 40 50
30	(SP-SM) Dense, saturated, gray, SAND, with silt and gravel	I	S10		
35	Bottom of boring at approx. 34'				
40					
45					
50					
55					
60					

LEGEND

I 2-inch OD split spoon sampler

I 3-inch OD split spoon sampler

I Shelby tube sampler

▼ ATD Groundwater level at time of drilling

VIRGINIA TECH
The Charles Edward Via
Dept. of Civil Engineering
Blacksburg, Virginia

Drilling Initiated: 12/07/92

Drilling Completed: 12/07/92

Appendix F:

Laboratory Test Results

Vincennes Event Grainsize Curves

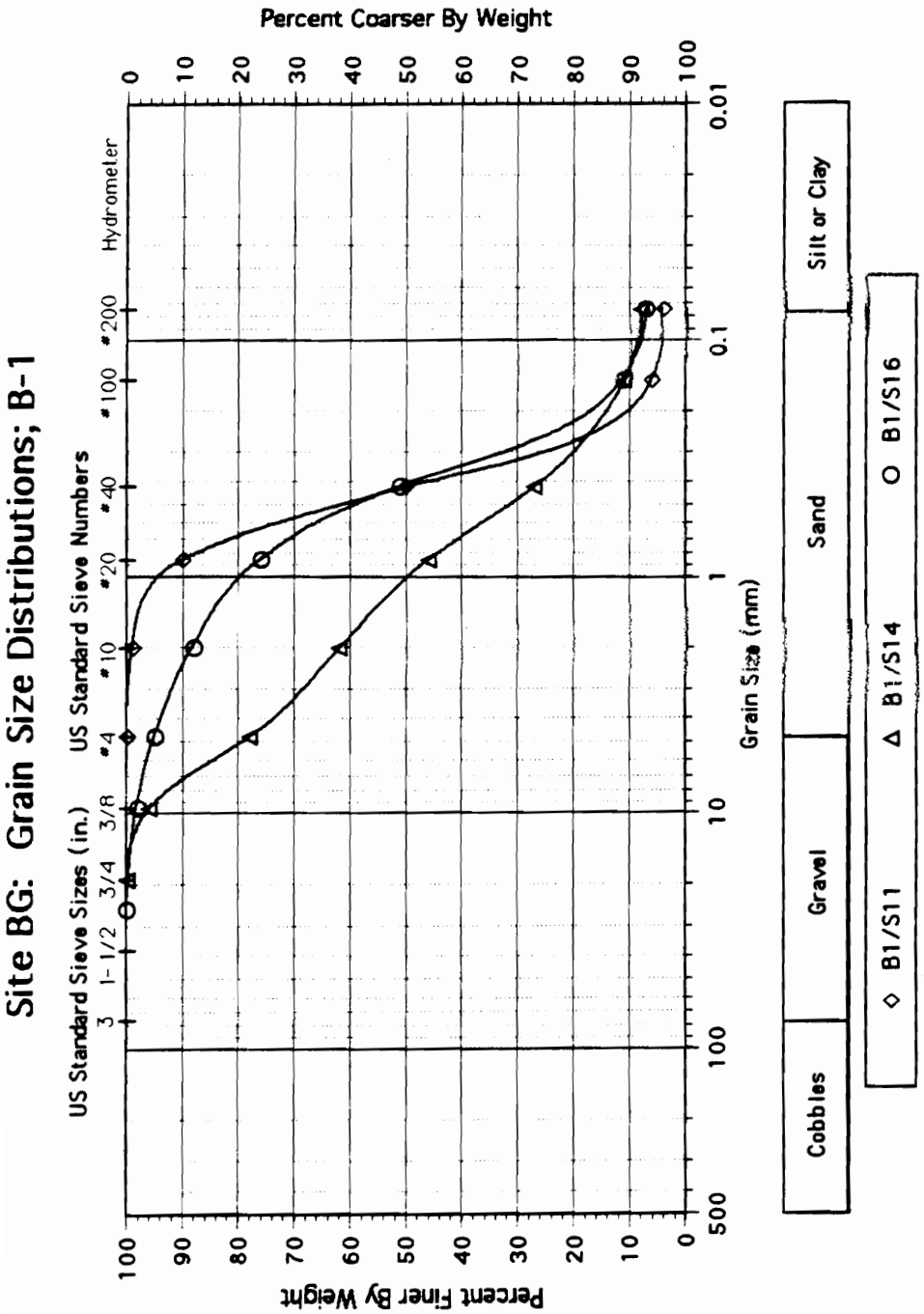
Site BG: Grain Size Distributions; B-1
Percent Coarser By Weight
Percent Finer By Weight
US Standard Sieve Sizes (in.)
US Standard Sieve Numbers
Hydrometer
Grain Size (mm)
Cobbles
Gravel
Sand
Silt or Clay
◇ B1/S11
△ B1/S14
○ B1/S16

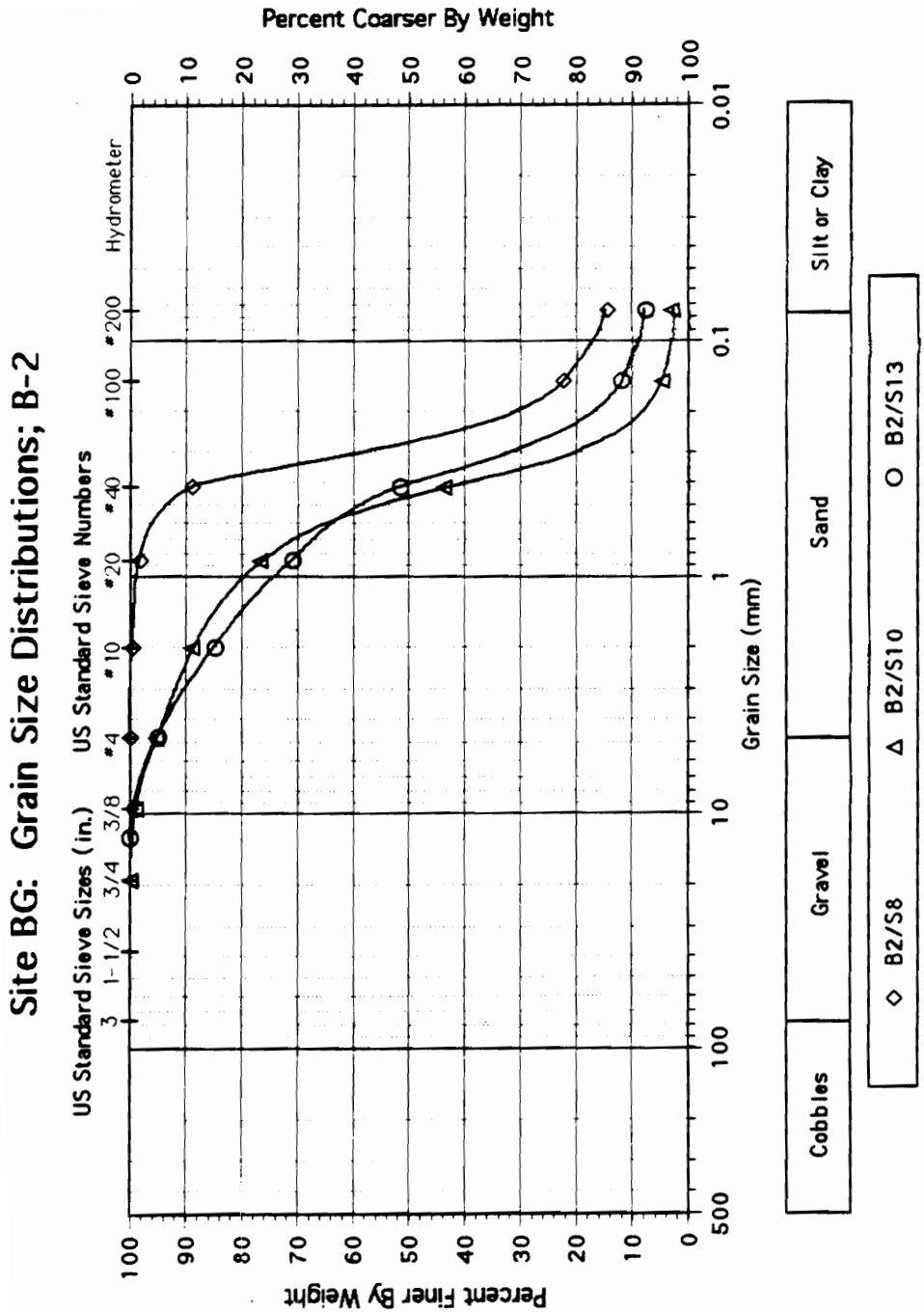
Site BG: Grain Size Distributions; B-2
Percent Coarser By Weight
Percent Finer By Weight
US Standard Sieve Sizes (in.)
US Standard Sieve Numbers
Hydrometer
Grain Size (mm)
Cobbles
Gravel
Sand
Silt or Clay
◇ B2/S8
△ B2/S10
○ B2/S13

Site BG: Grain Size Distributions; B-4

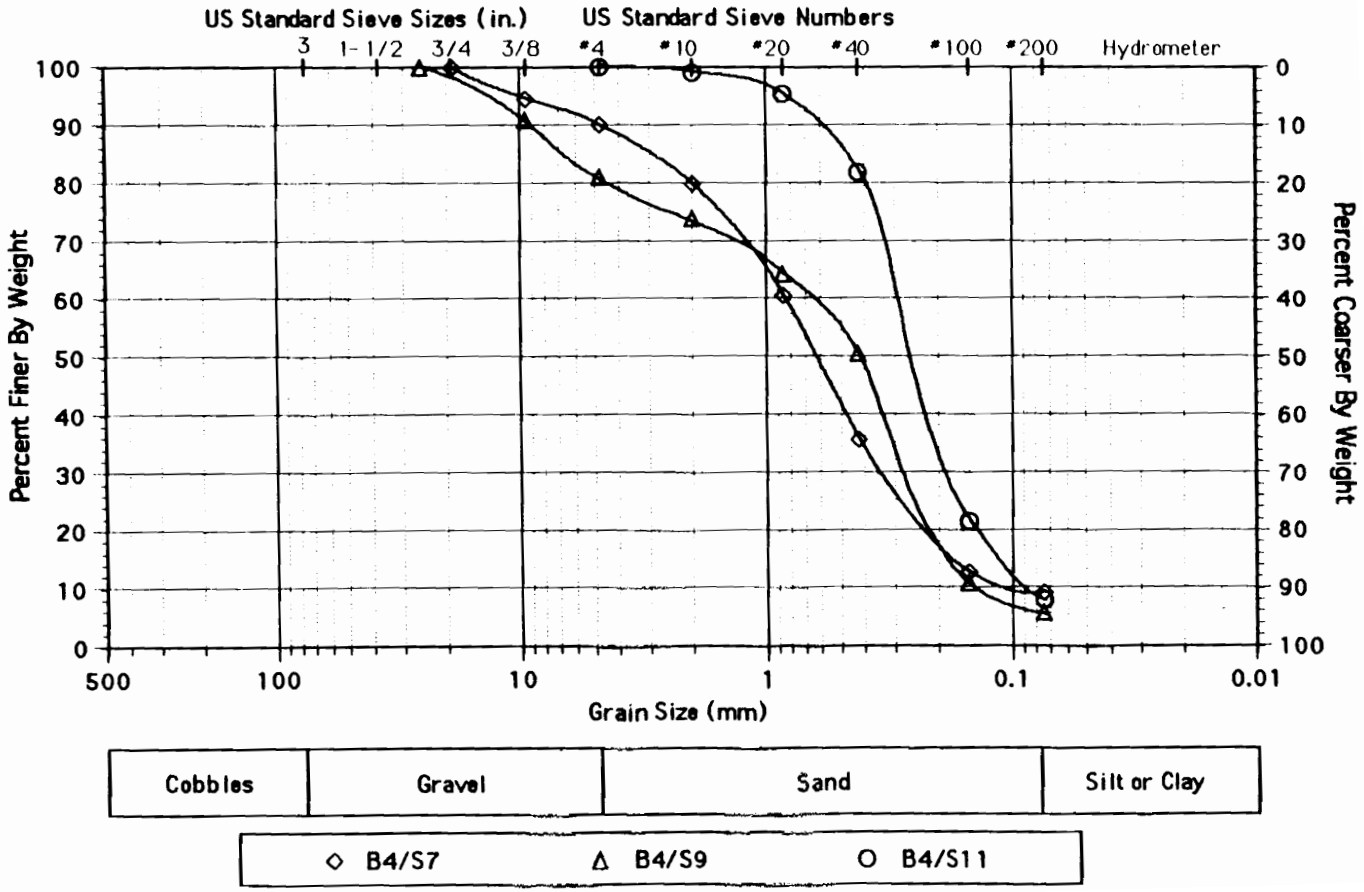

Site HA: Grainsize Distributions; B-1

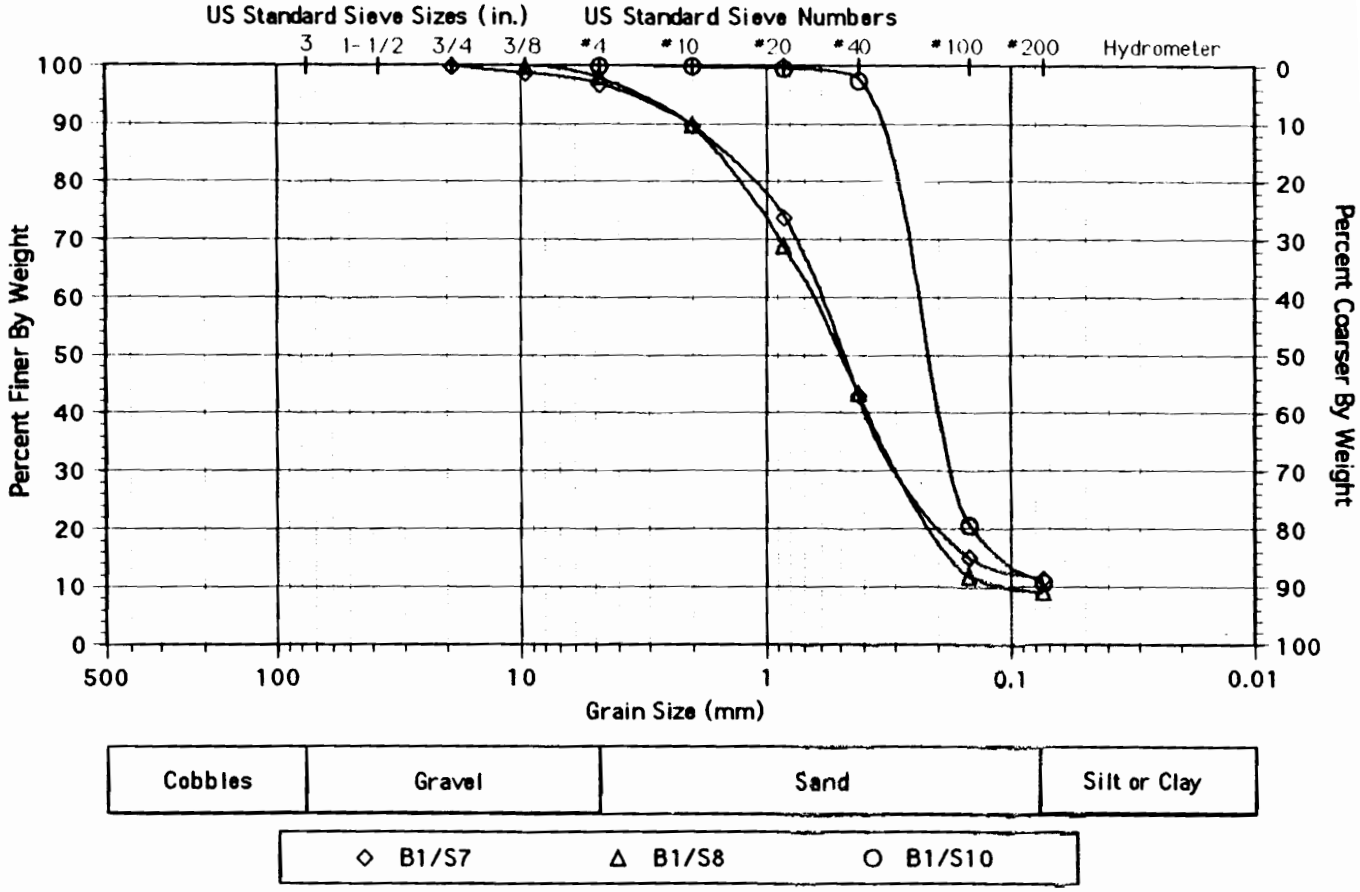

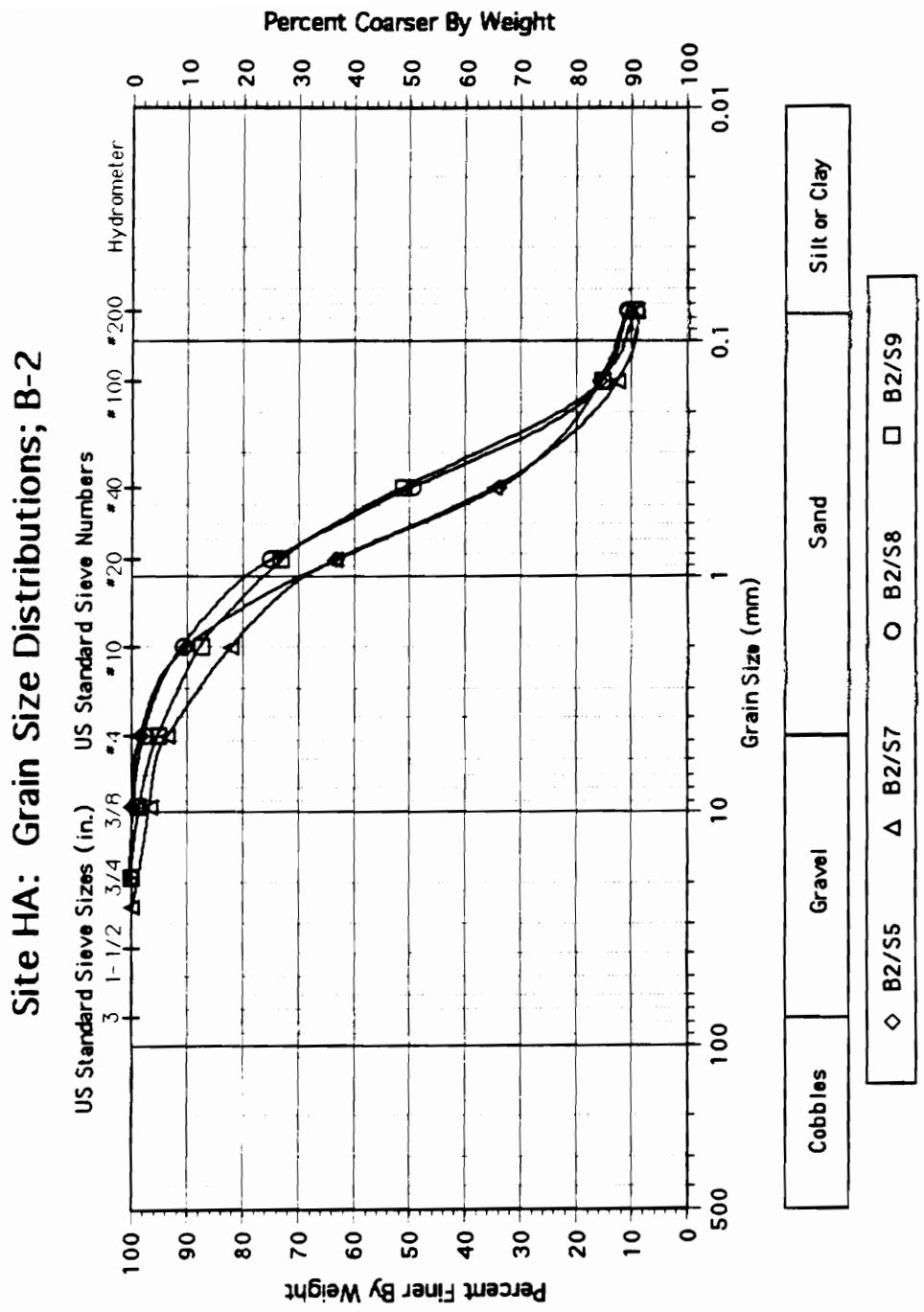
Site HA: Grain Size Distributions; B-2
Percent Coarser By Weight
Percent Finer By Weight
US Standard Sieve Sizes (in.)
US Standard Sieve Numbers
Hydrometer
Grain Size (mm)
Cobbles
Gravel
Sand
Silt or Clay
◇ B2/S5
△ B2/S7
○ B2/S8
□ B2/S9

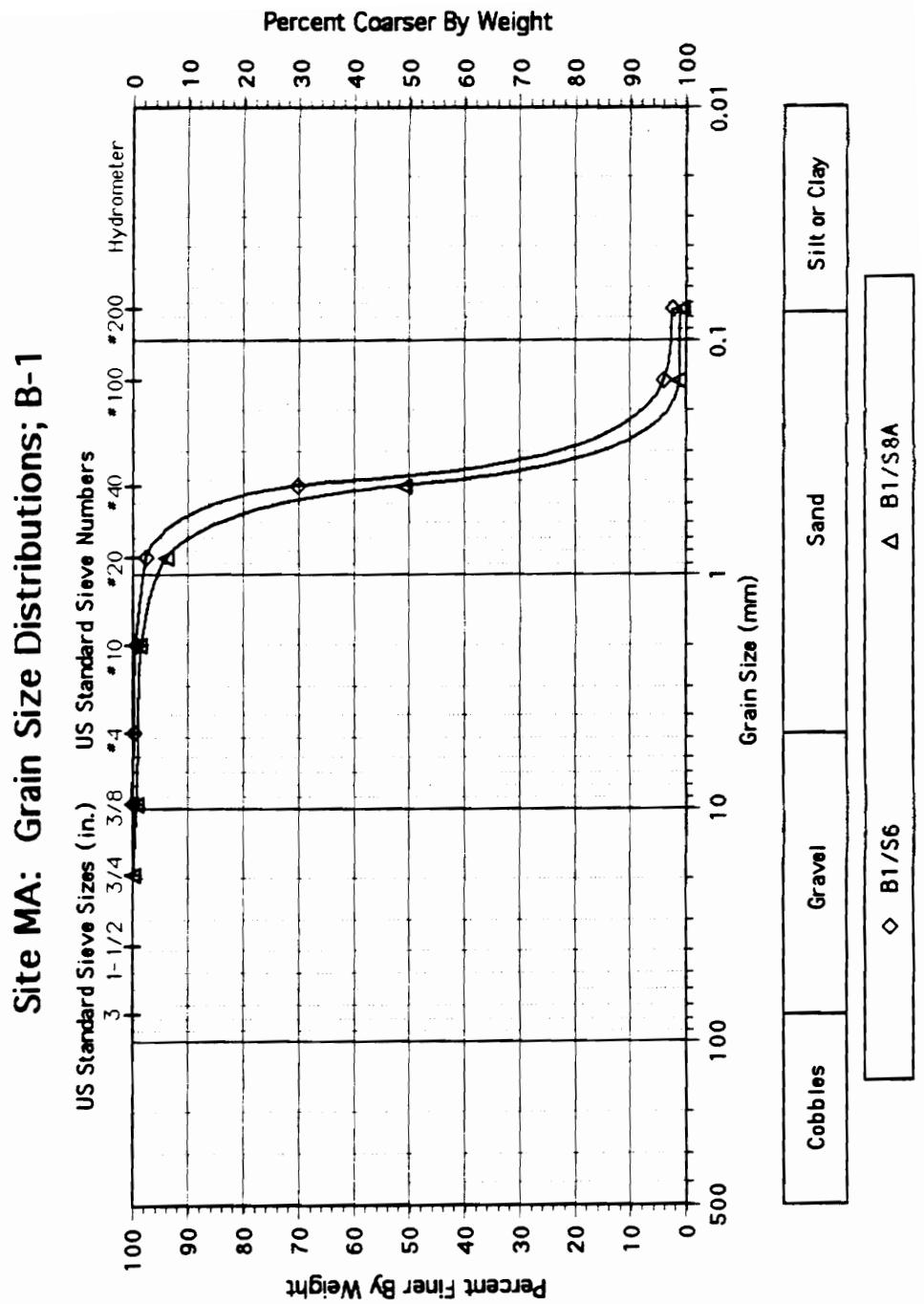
Site MA: Grain Size Distributions; B-1
Percent Coarser By Weight
US Standard Sieve Sizes (in.)
US Standard Sieve Numbers
Hydrometer
Percent Finer By Weight
Grain Size (mm)
Cobbles
Gravel
Sand
Silt or Clay
◇ B1/S6
△ B1/S8A

Site MA: Grain Size Distributions; B-2

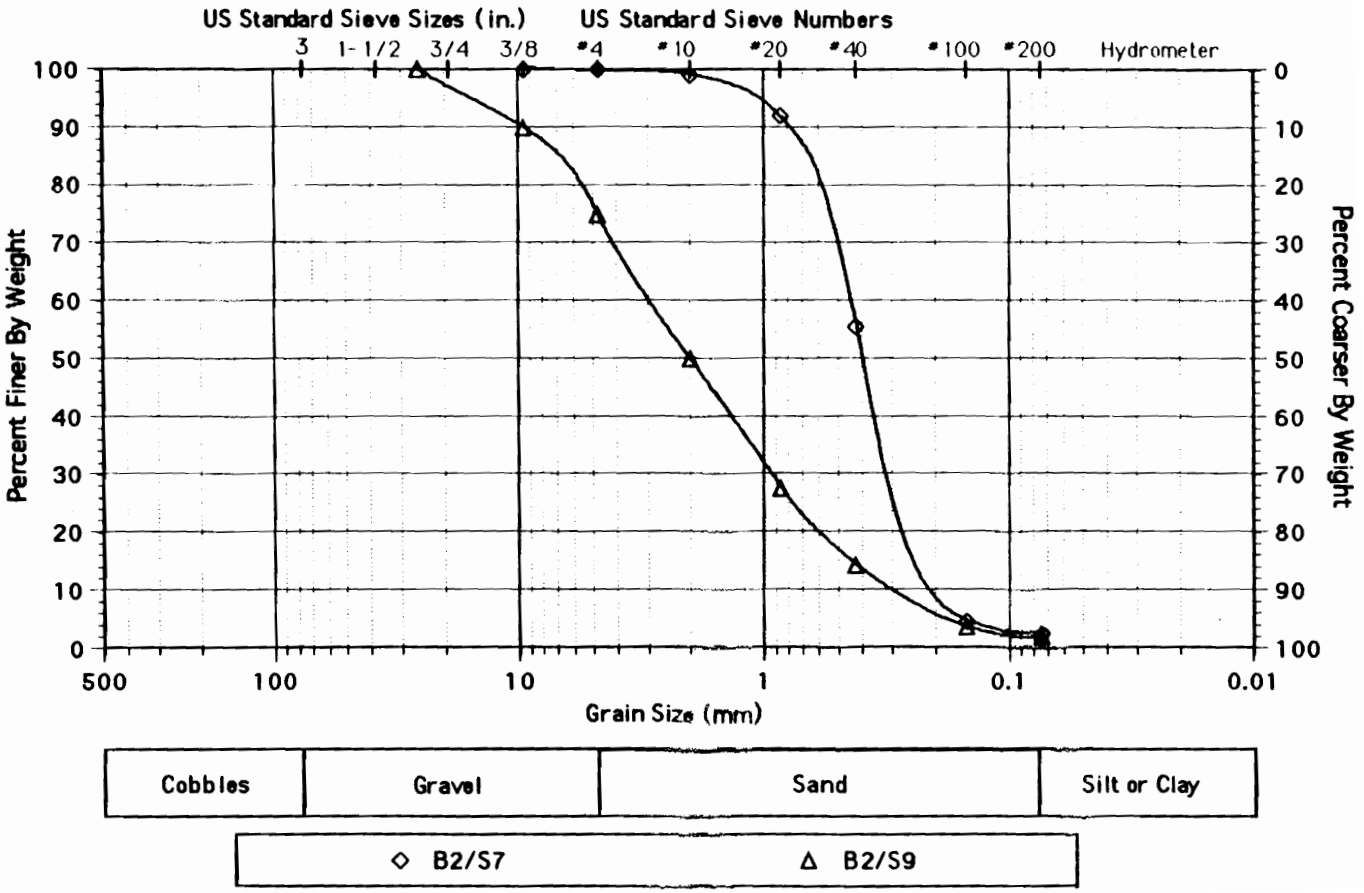

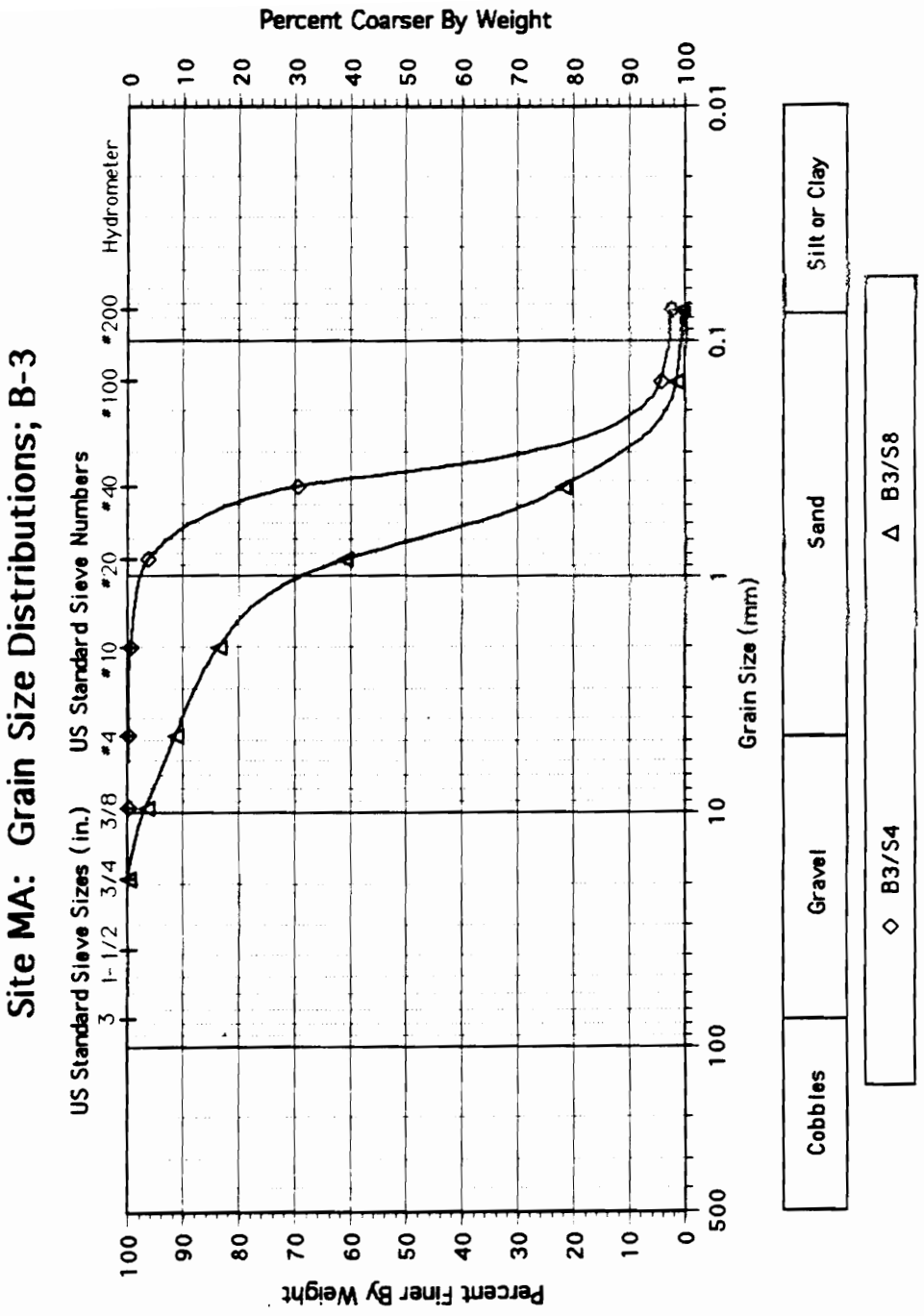
Site MA: Grain Size Distributions; B-3
Percent Coarser By Weight
Percent Finer By Weight
US Standard Sieve Sizes (in.)
US Standard Sieve Numbers
Hydrometer
Grain Size (mm)
Cobbles
Gravel
Sand
Silt or Clay
◇ B3/S4
△ B3/S8

Site MA: Grain Size Distributions; B-4

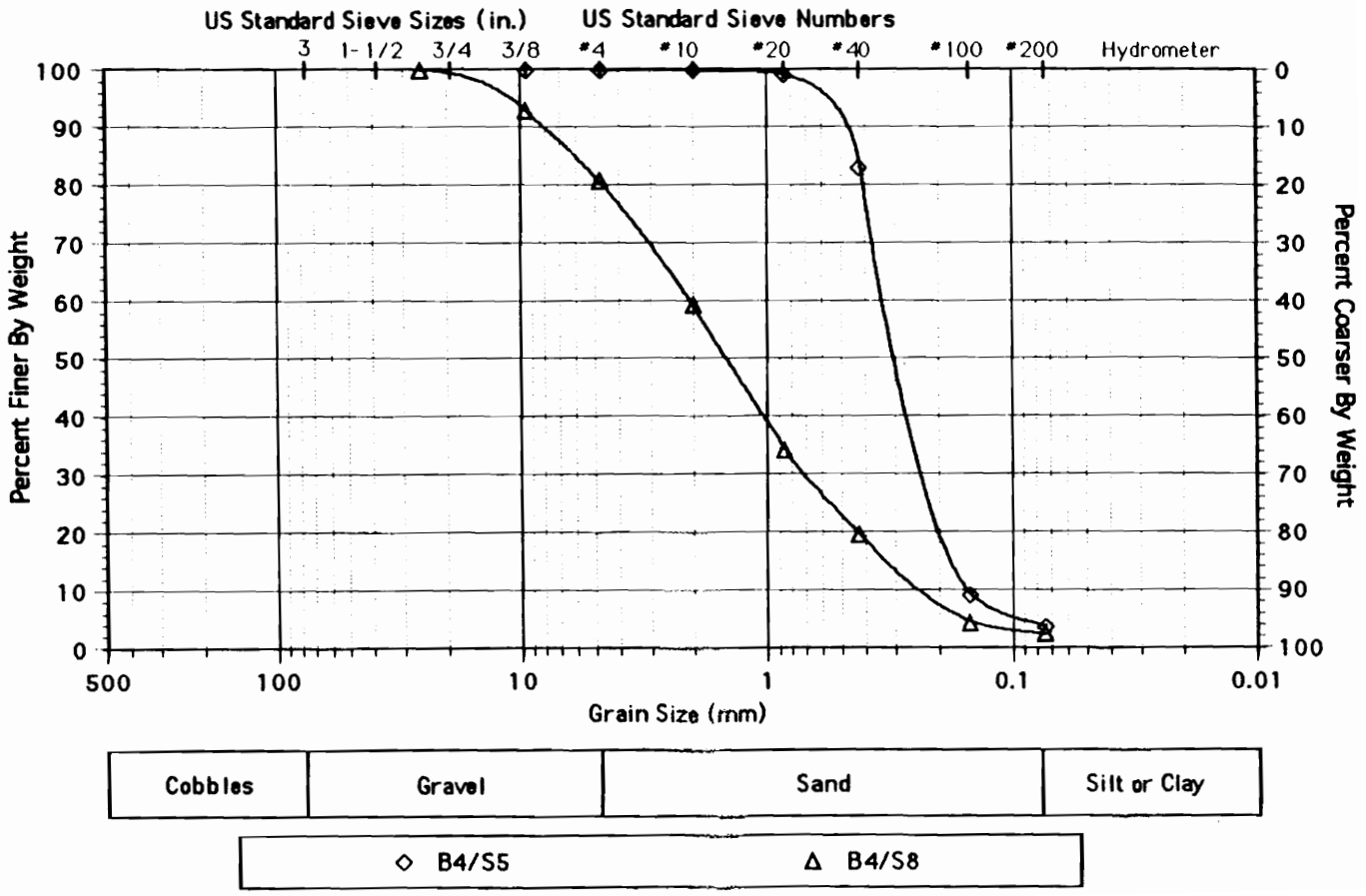

Site MA: Grain Size Distributions; B-5

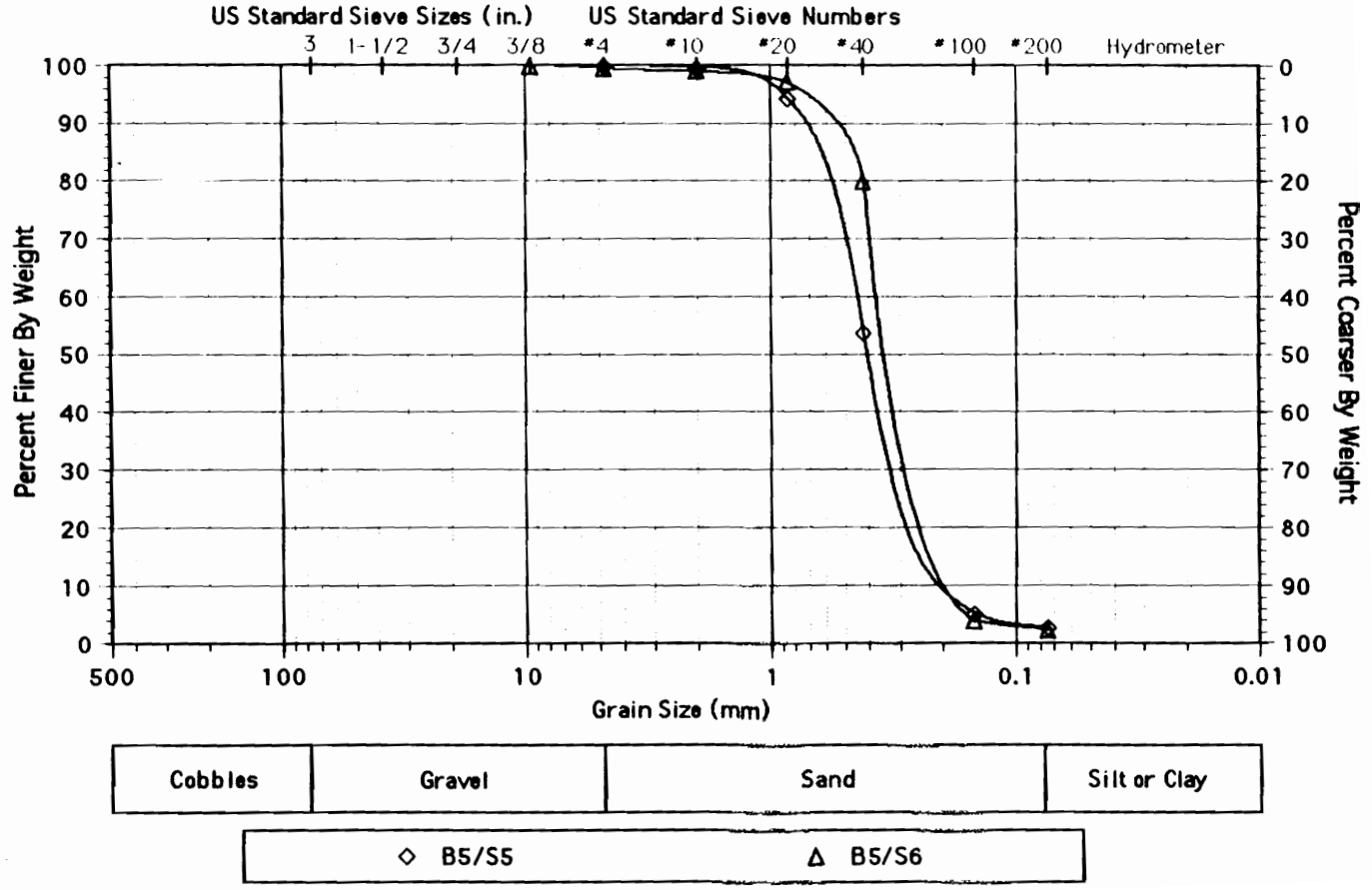

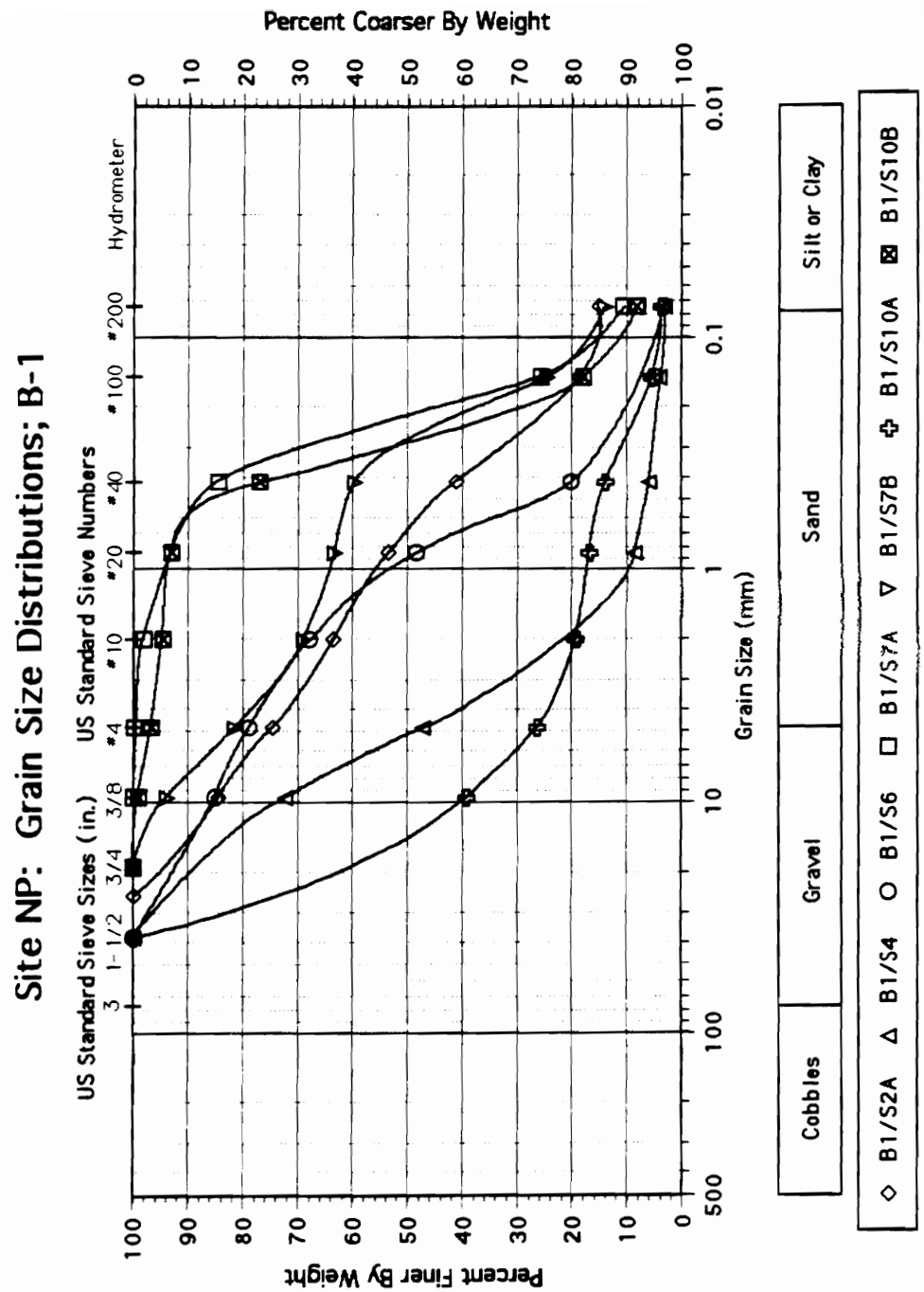
Site NP: Grain Size Distributions; B-1
Percent Coarser By Weight
Percent Finer By Weight
US Standard Sieve Sizes (in.)
US Standard Sieve Numbers
Hydrometer
Grain Size (mm)
Cobbles
Gravel
Sand
Silt or Clay
B1/S2A
B1/S4
B1/S6
B1/S7A
B1/S7B
B1/S10A
B1/S10B

Site NP: Grain Size Distributions; B-2

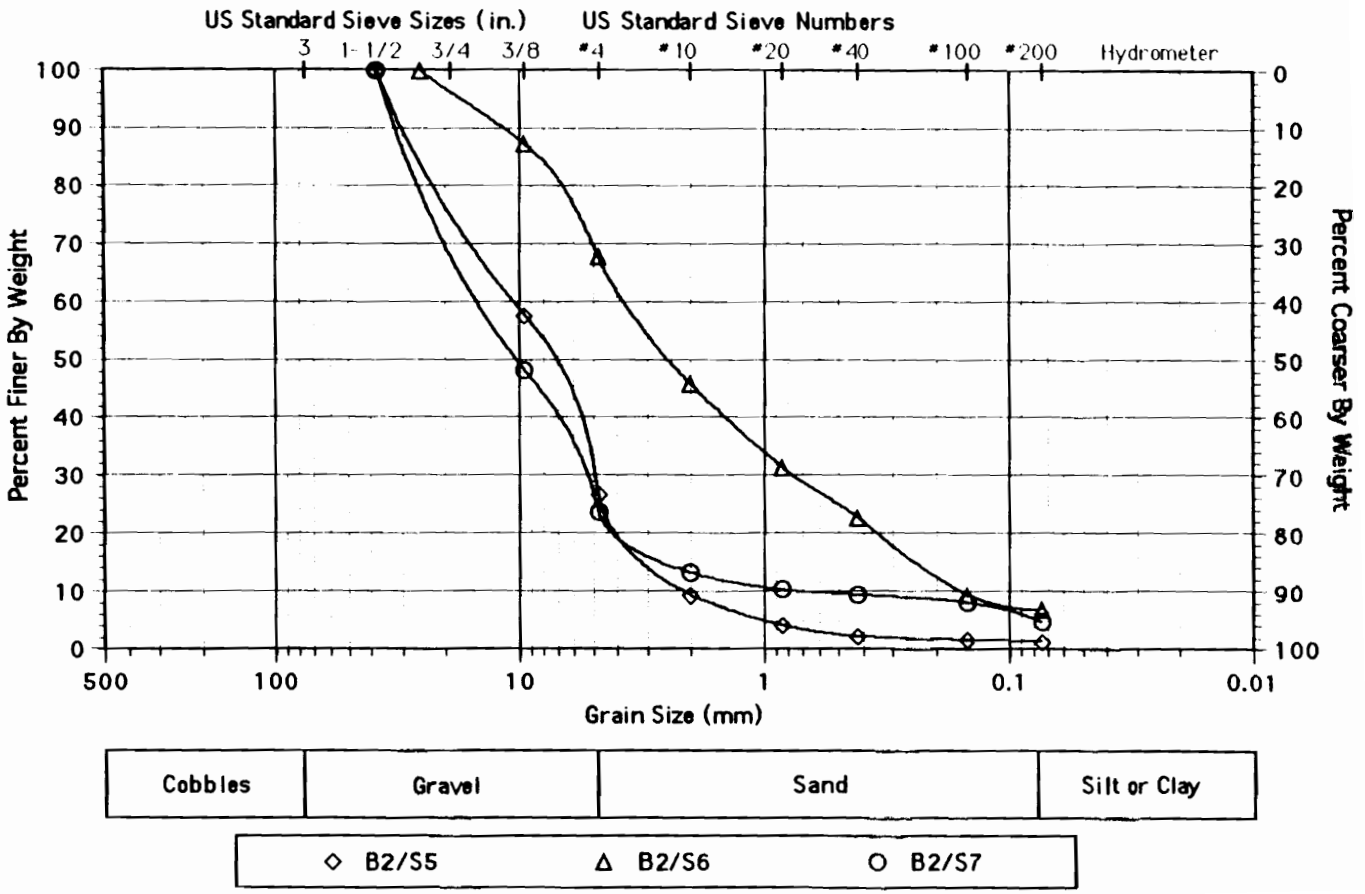

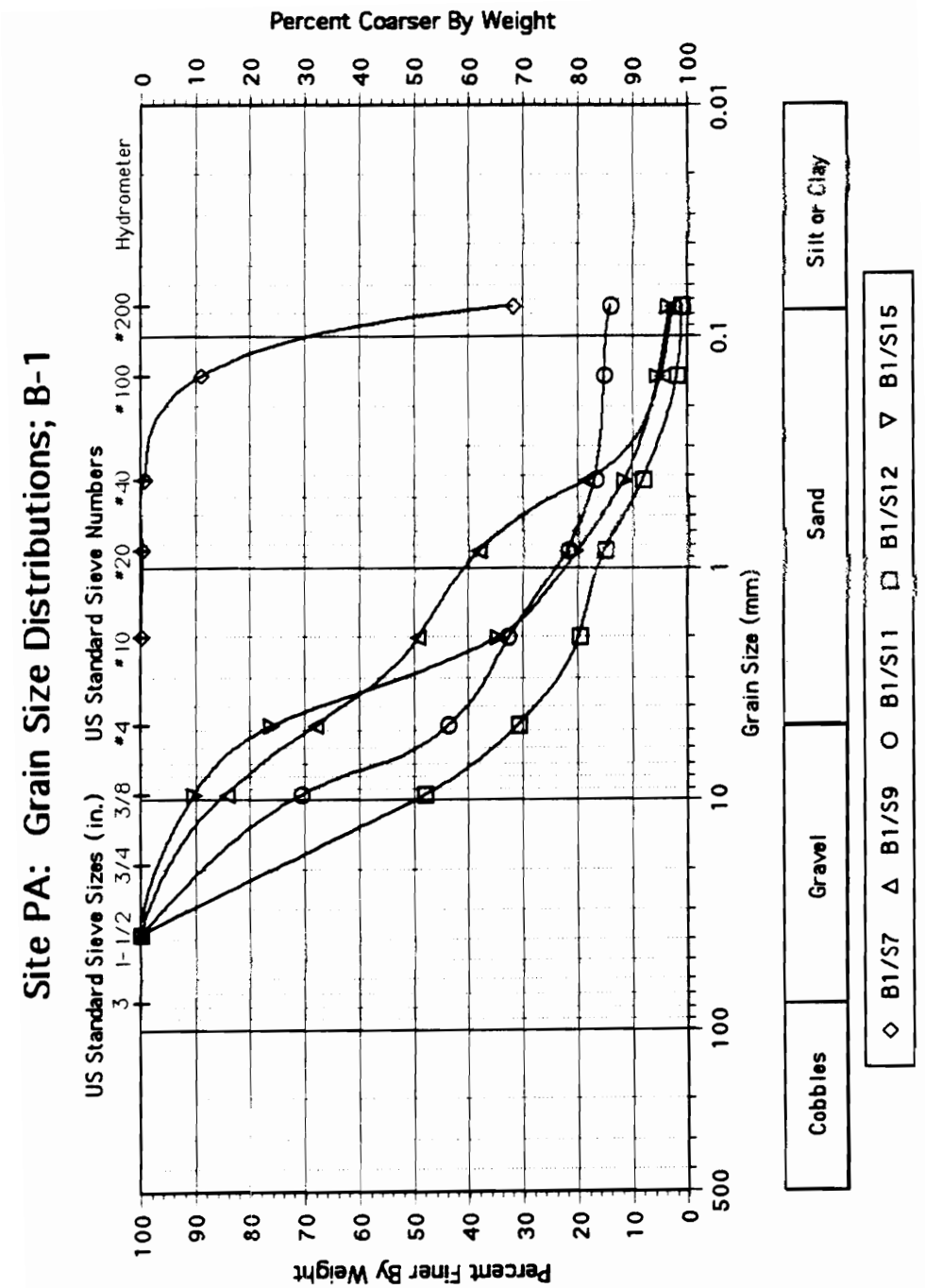
Site PA: Grain Size Distributions; B-1
Percent Coarser By Weight
Percent Finer By Weight
US Standard Sieve Sizes (in.)
US Standard Sieve Numbers
Hydrometer
Grain Size (mm)
Cobbles
Gravel
Sand
Silt or Clay
◇ B1/S7
△ B1/S9
○ B1/S11
□ B1/S12
▽ B1/S15

Site PA: Grain Size Distributions; B-2

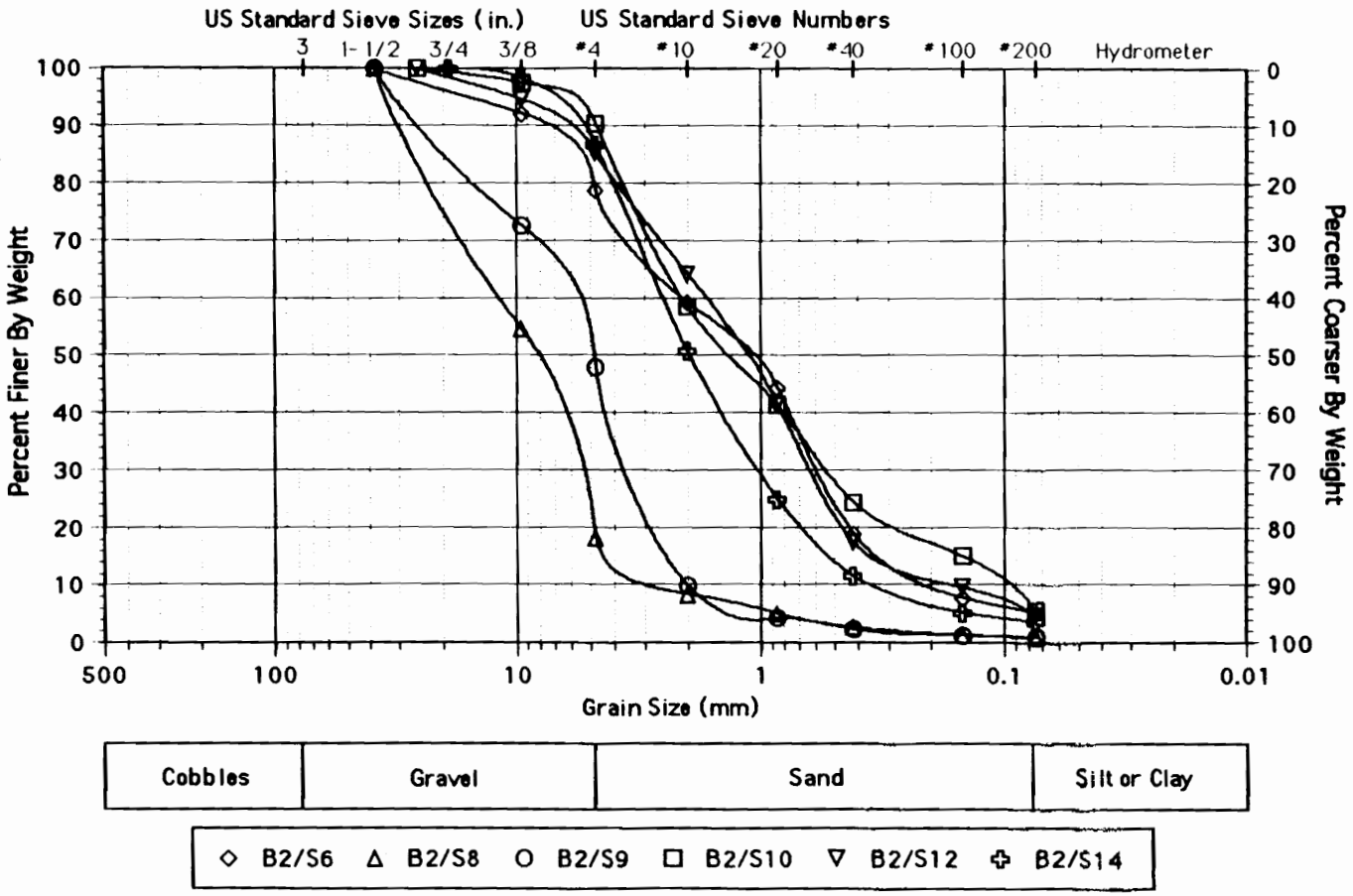

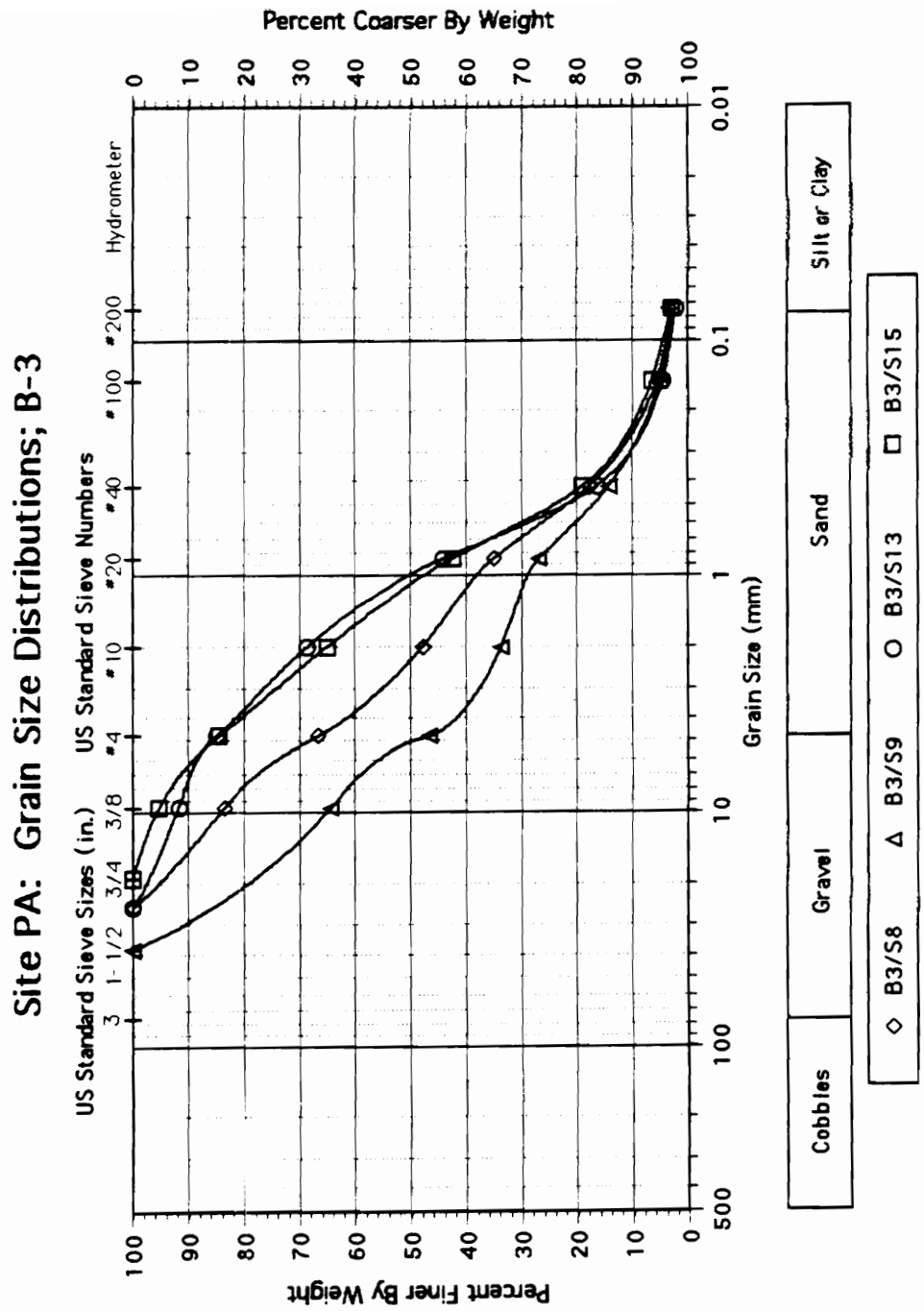
Site PA: Grain Size Distributions; B-3
Percent Coarser By Weight
Percent Finer By Weight
US Standard Sieve Sizes (in.)
US Standard Sieve Numbers
Hydrometer
Grain Size (mm)
Cobbles
Gravel
Sand
Silt or Clay
B3/S8
B3/S9
B3/S13
B3/S15

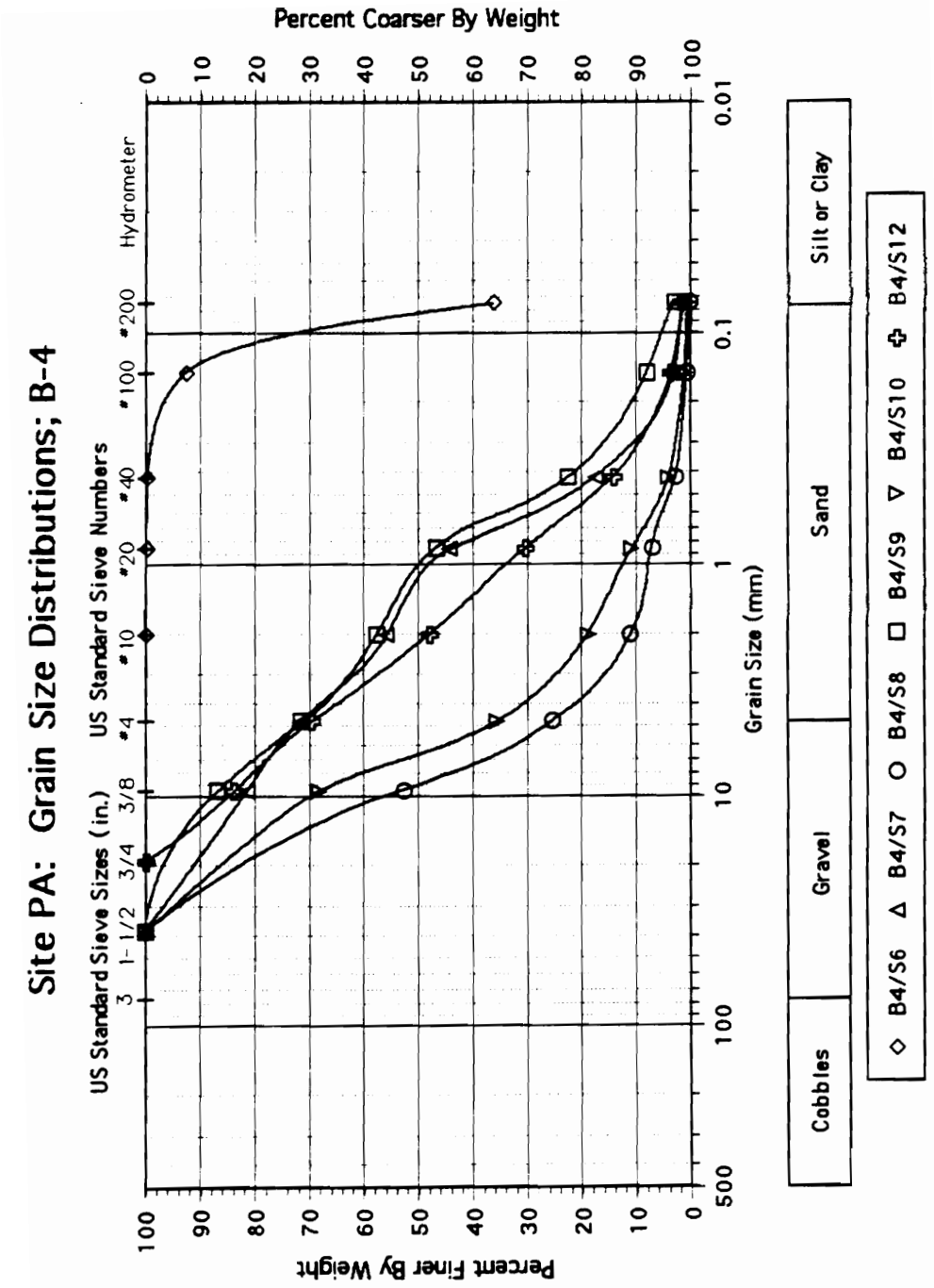
Site PA: Grain Size Distributions; B-4
Percent Coarser By Weight
Percent Finer By Weight
US Standard Sieve Sizes (in.)
US Standard Sieve Numbers
Hydrometer
Grain Size (mm)
Cobbles
Gravel
Sand
Silt or Clay
B4/S6
B4/S7
B4/S8
B4/S9
B4/S10
B4/S12

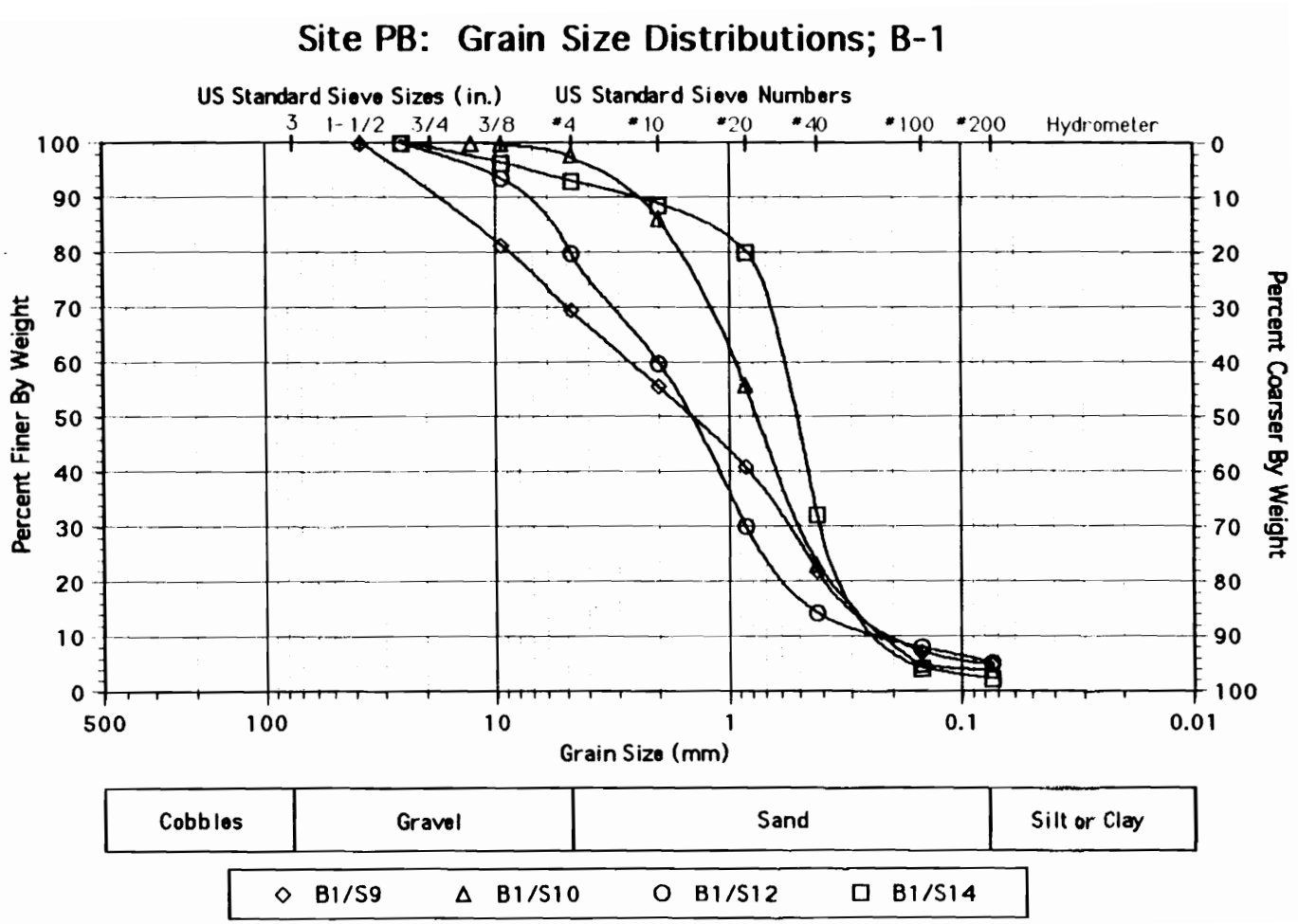
Site PB: Grain Size Distributions; B-1
US Standard Sieve Sizes (in.)
US Standard Sieve Numbers
3
1-1/2
3/4
3/8
#4
#10
#20
#40
#100
#200
Hydrometer
Percent Finer By Weight
Percent Coarser By Weight
100
90
80
70
60
50
40
30
20
10
0
500
100
10
1
0.1
0.01
Grain Size (mm)
Cobbles
Gravel
Sand
Silt or Clay
B1/S9
B1/S10
B1/S12
B1/S14

Site PB: Grain Size Distributions; B-2

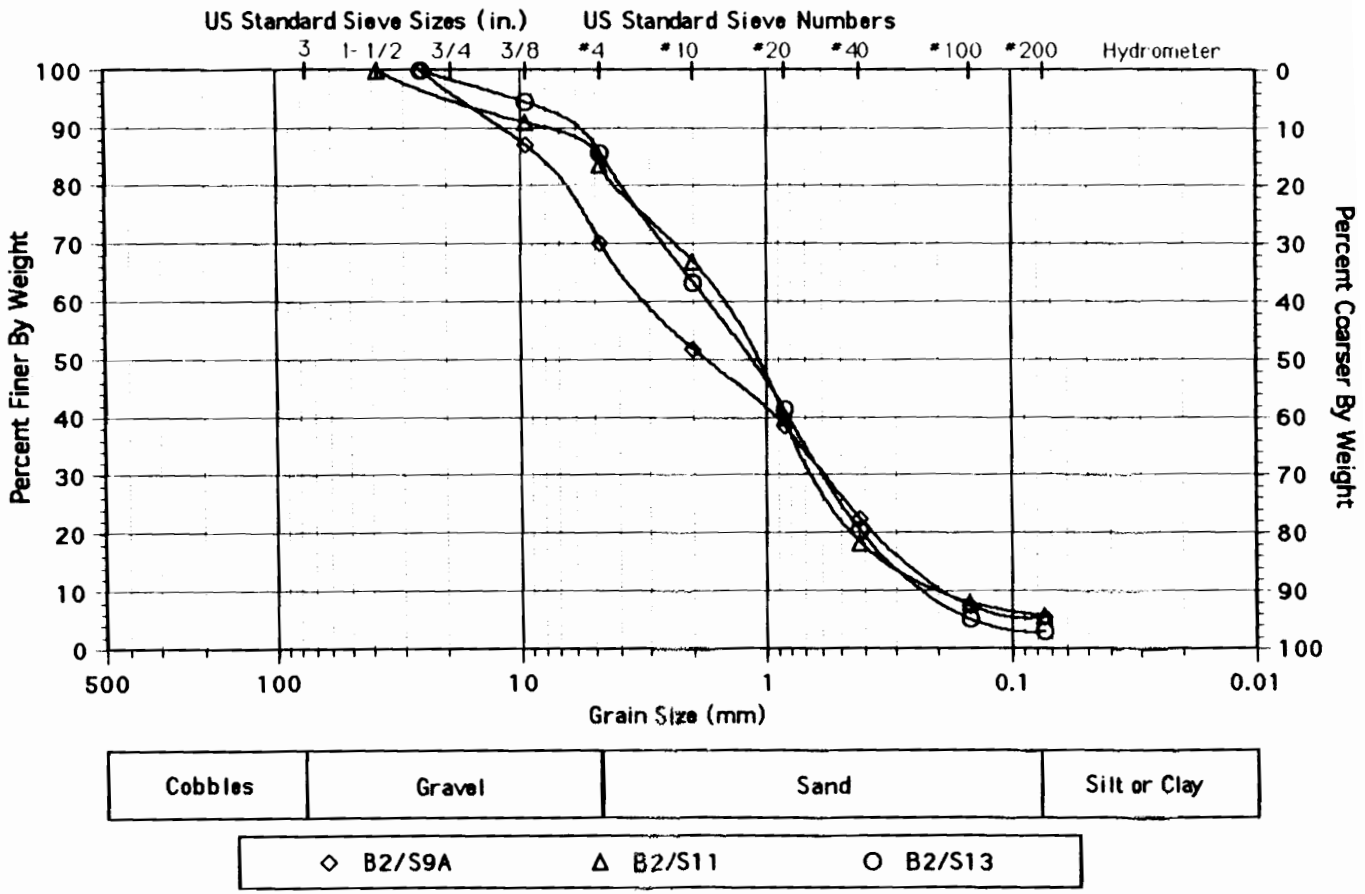

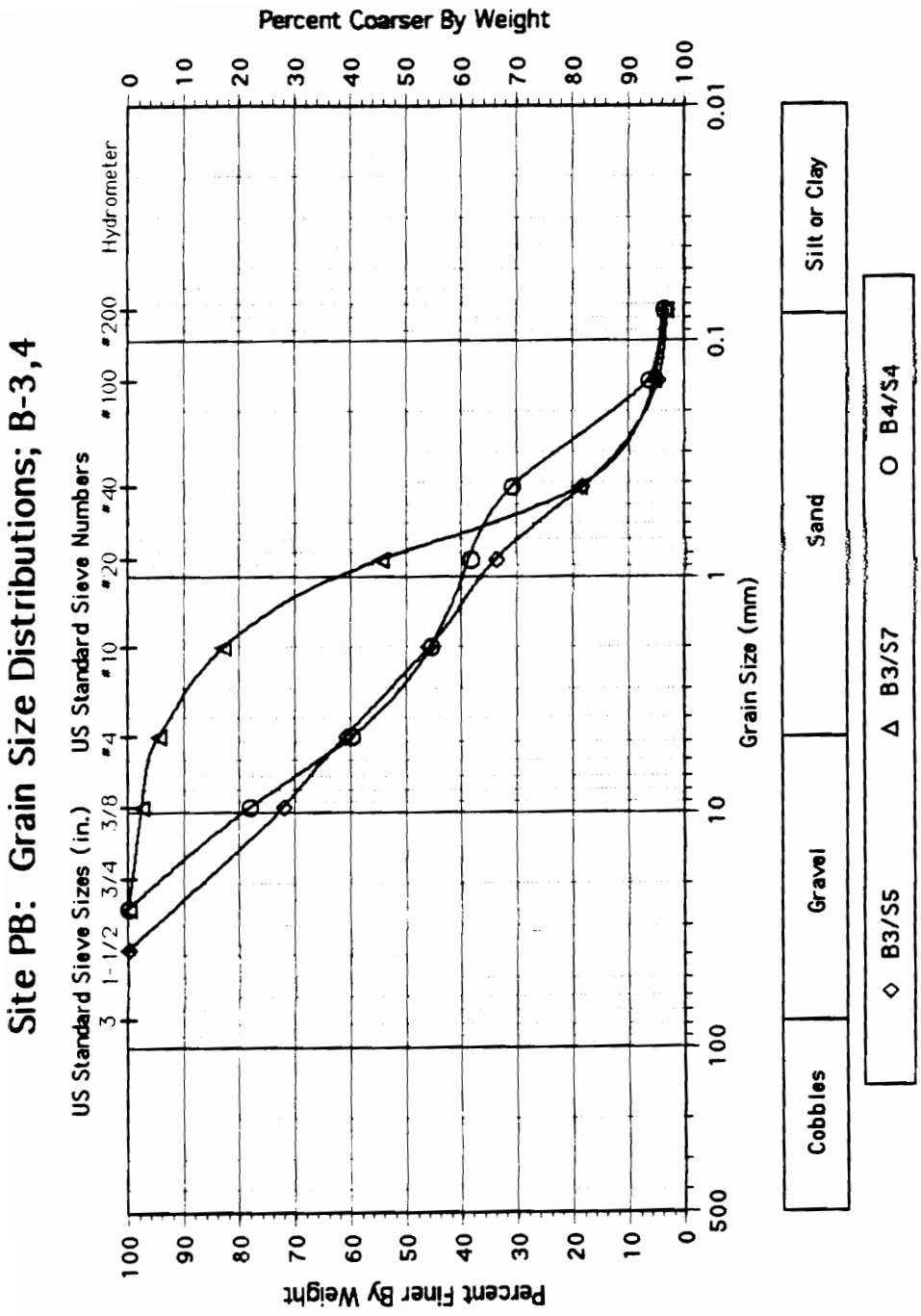
Site PB: Grain Size Distributions; B-3,4
Percent Coarser By Weight
Percent Finer By Weight
US Standard Sieve Sizes (in.)
US Standard Sieve Numbers
Hydrometer
Grain Size (mm)
Cobbles
Gravel
Sand
Silt or Clay
◇ B3/S5
△ B3/S7
○ B4/S4

Site PL: Grain Size Distributions; B-1

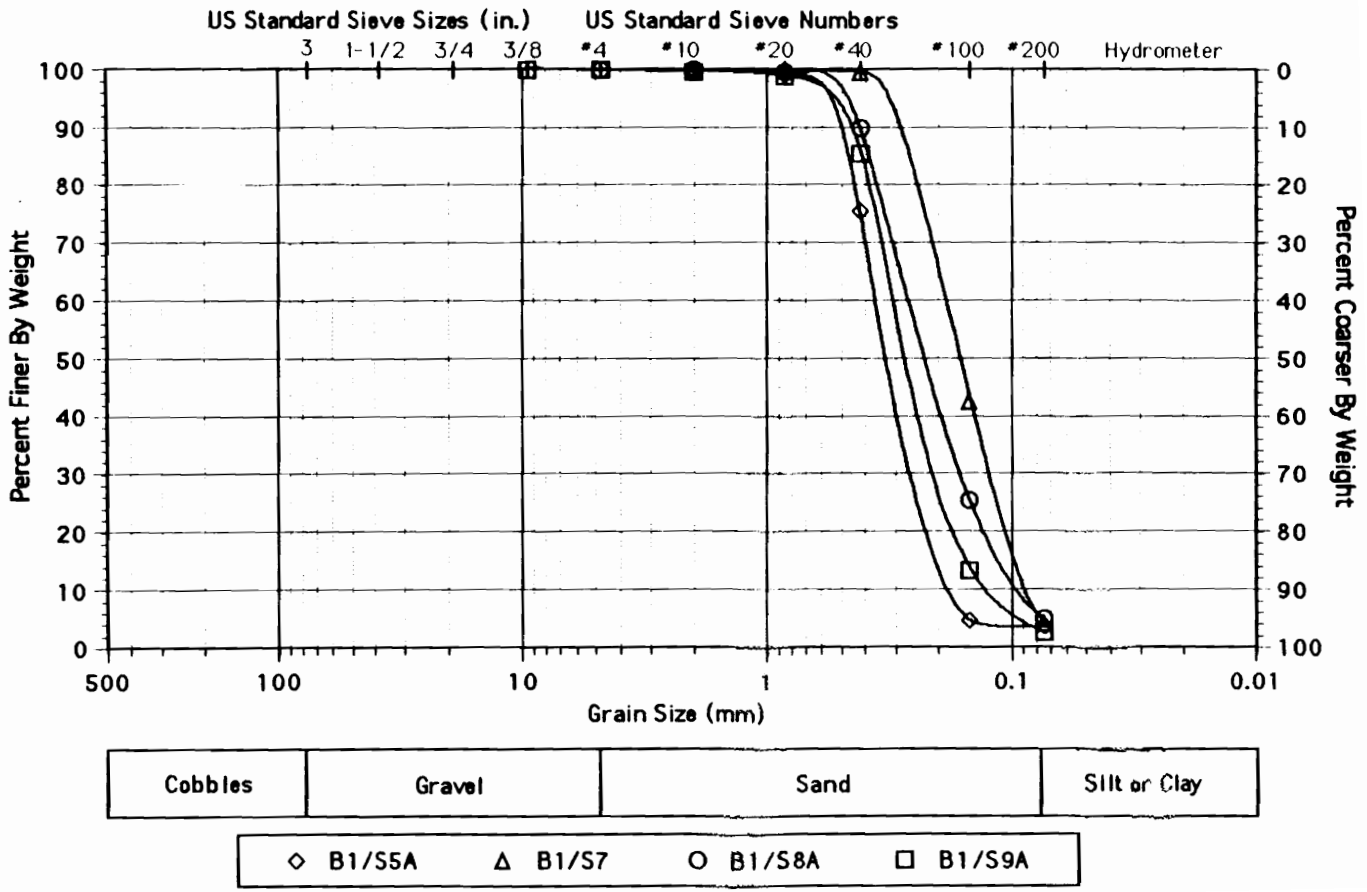

Site PL: Grain Size Distributions; B-2

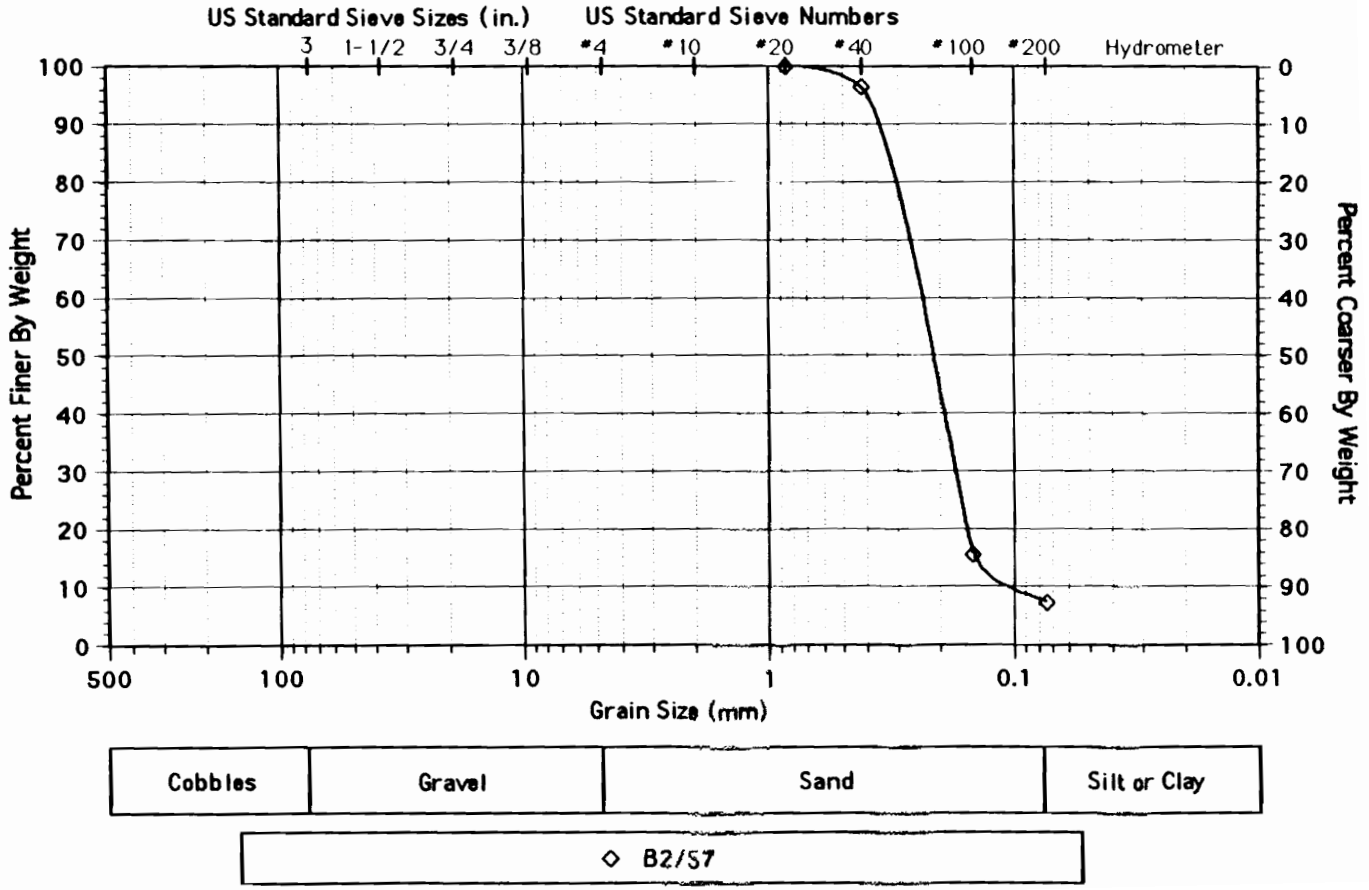

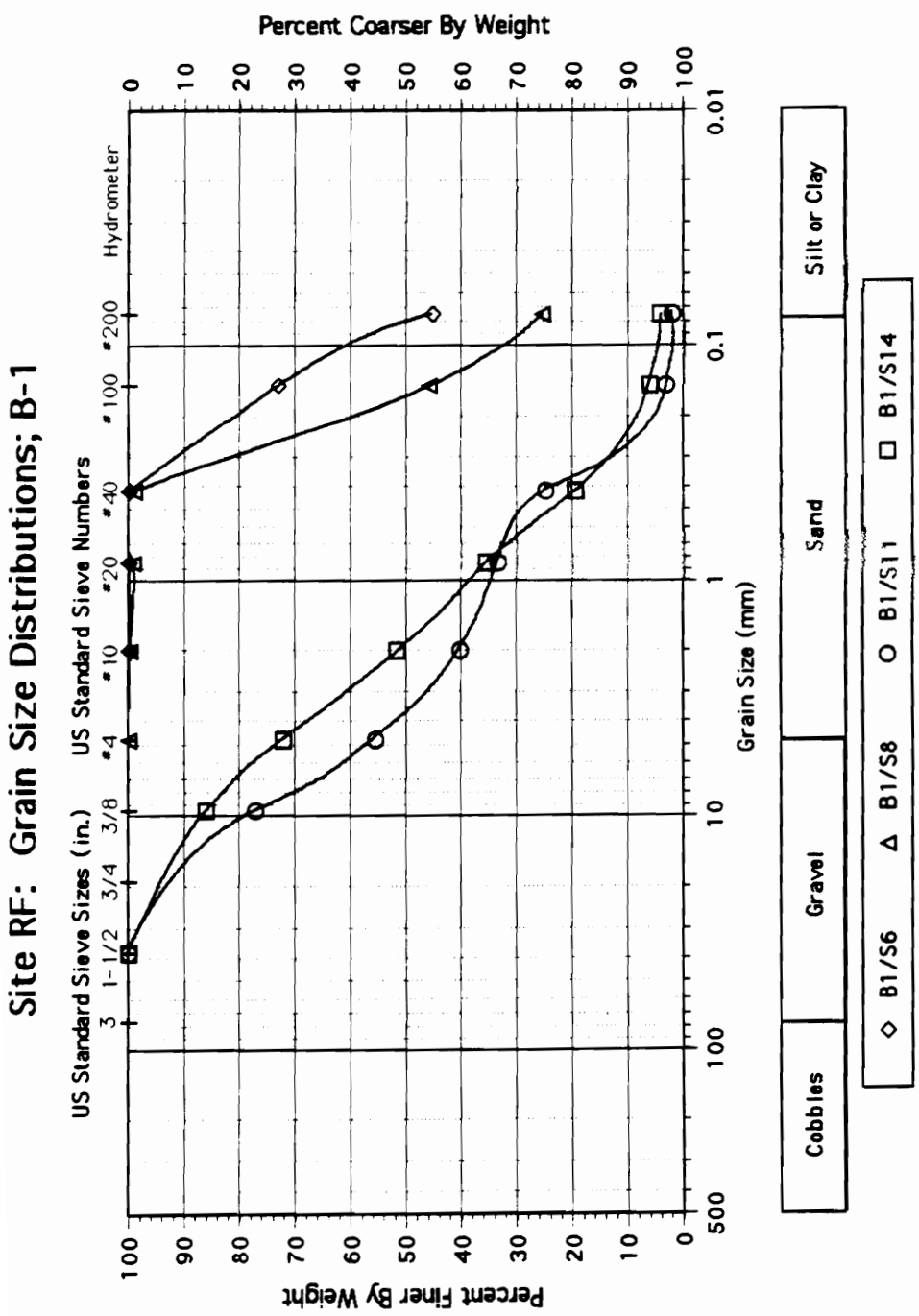
Site RF: Grain Size Distributions; B-1
Percent Coarser By Weight
Percent Finer By Weight
US Standard Sieve Sizes (in.)
US Standard Sieve Numbers
Hydrometer
3
1-1/2
3/4
3/8
#4
#10
#20
#40
#100
#200
Grain Size (mm)
Cobbles
Gravel
Sand
Silt or Clay
B1/S6
B1/S8
B1/S11
B1/S14

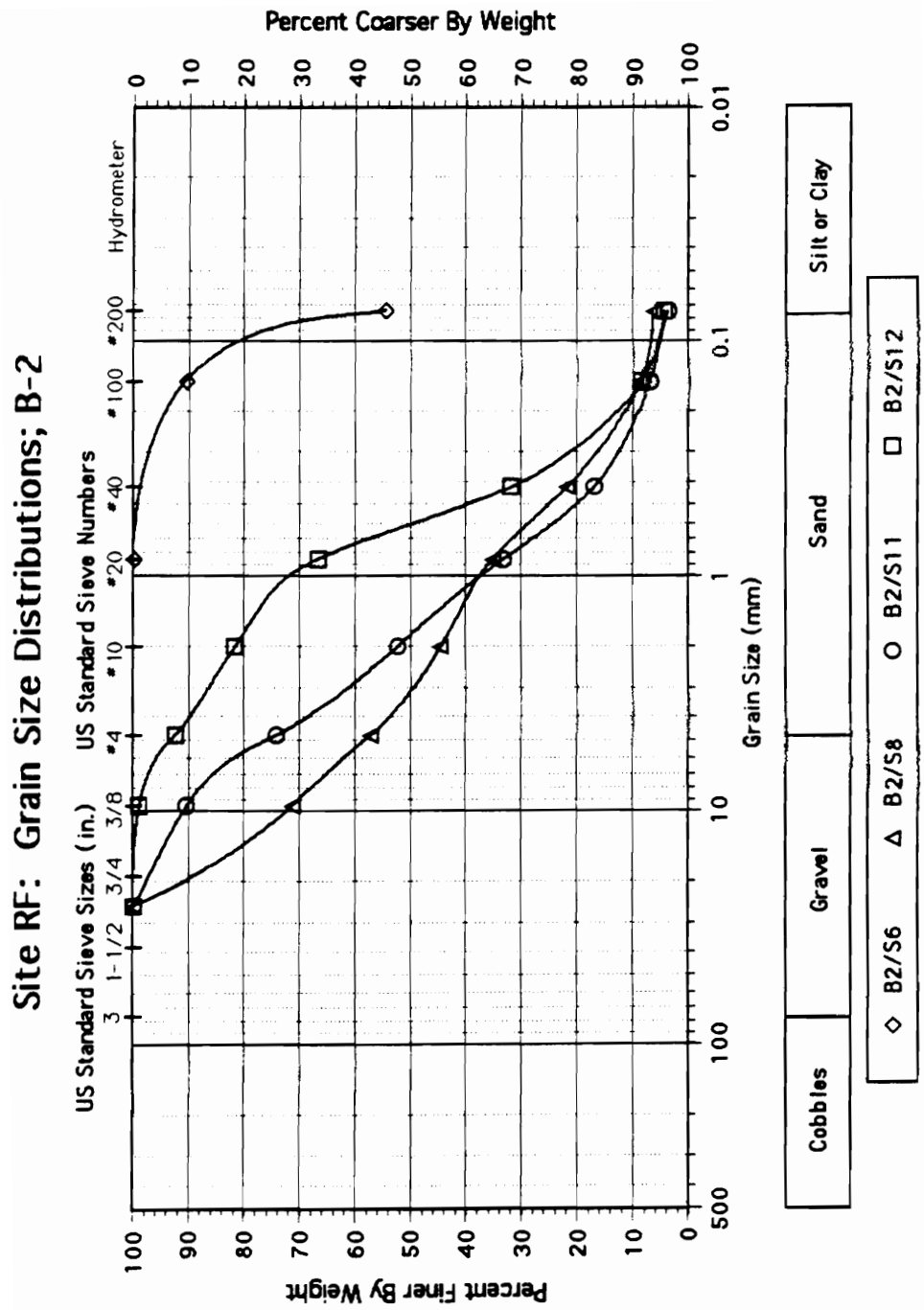
Site RF: Grain Size Distributions; B-2
Percent Coarser By Weight
Percent Finer By Weight
US Standard Sieve Sizes (in.)
US Standard Sieve Numbers
Hydrometer
Grain Size (mm)
Cobbles
Gravel
Sand
Silt or Clay
B2/S6
B2/S8
B2/S11
B2/S12

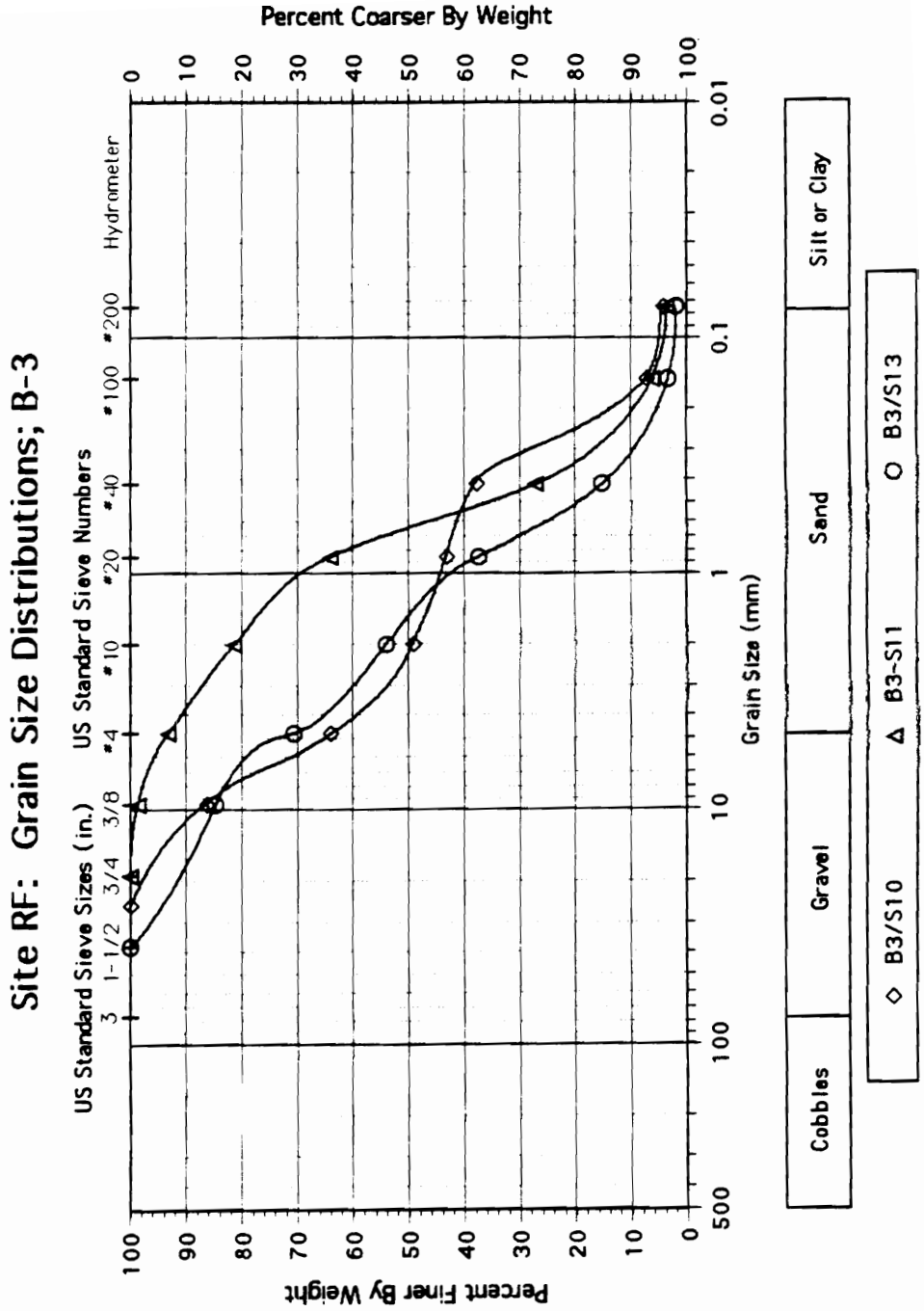
Site RF: Grain Size Distributions; B-3
Percent Coarser By Weight
Percent Finer By Weight
US Standard Sieve Sizes (in.)
US Standard Sieve Numbers
Hydrometer
Grain Size (mm)
Cobbles
Gravel
Sand
Silt or Clay
◇ B3/S10
△ B3-S11
○ B3/S13

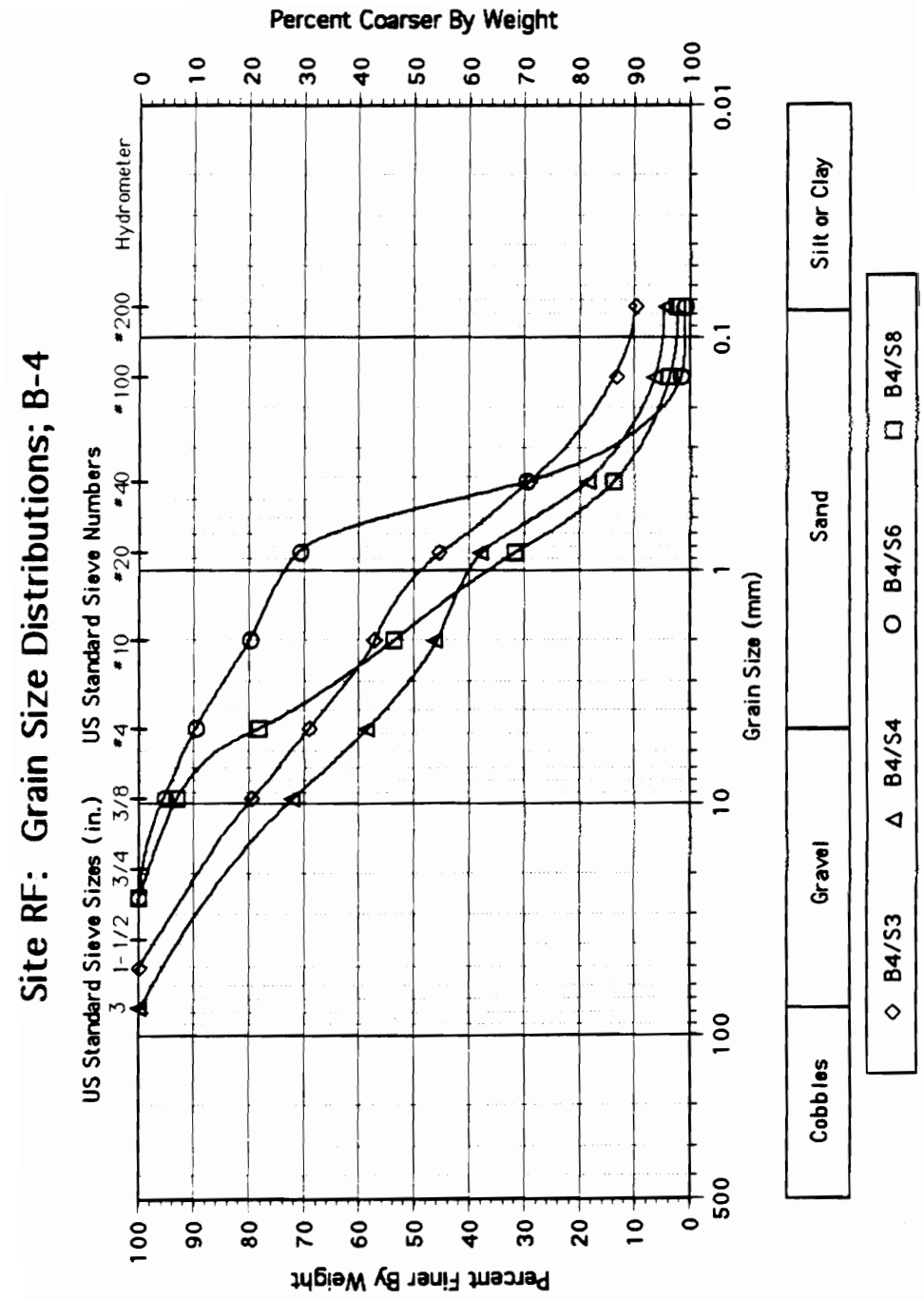
Site RF: Grain Size Distributions; B-4
Percent Coarser By Weight
Percent Finer By Weight
US Standard Sieve Sizes (in.)
US Standard Sieve Numbers
Hydrometer
Grain Size (mm)
Cobbles
Gravel
Sand
Silt or Clay
B4/S3
B4/S4
B4/S6
B4/S8

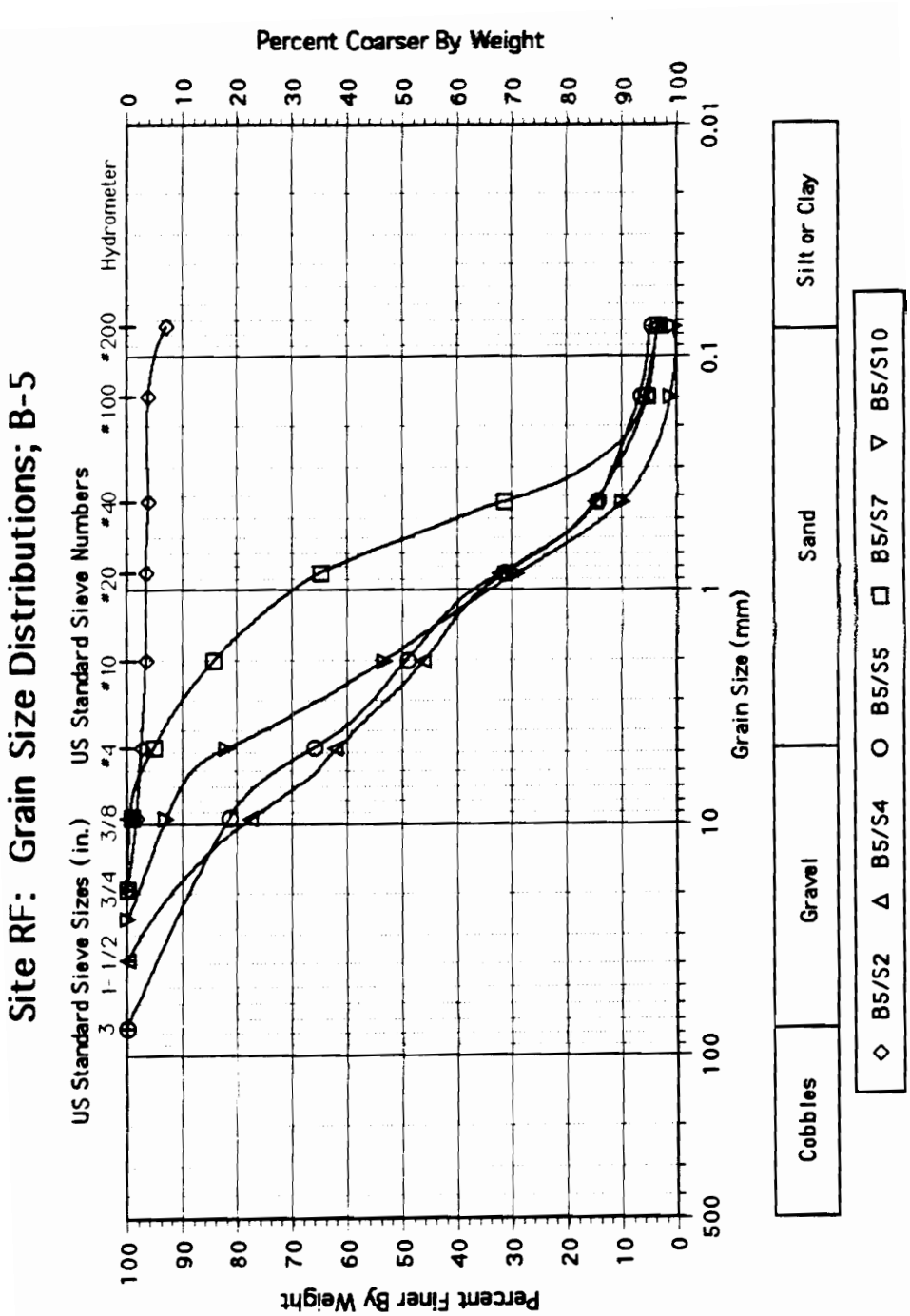
Site RF: Grain Size Distributions; B-5
Percent Coarser By Weight
Percent Finer By Weight
US Standard Sieve Sizes (in.)
US Standard Sieve Numbers
Hydrometer
Grain Size (mm)
Cobbles
Gravel
Sand
Silt or Clay
B5/S2
B5/S4
B5/S5
B5/S7
B5/S10

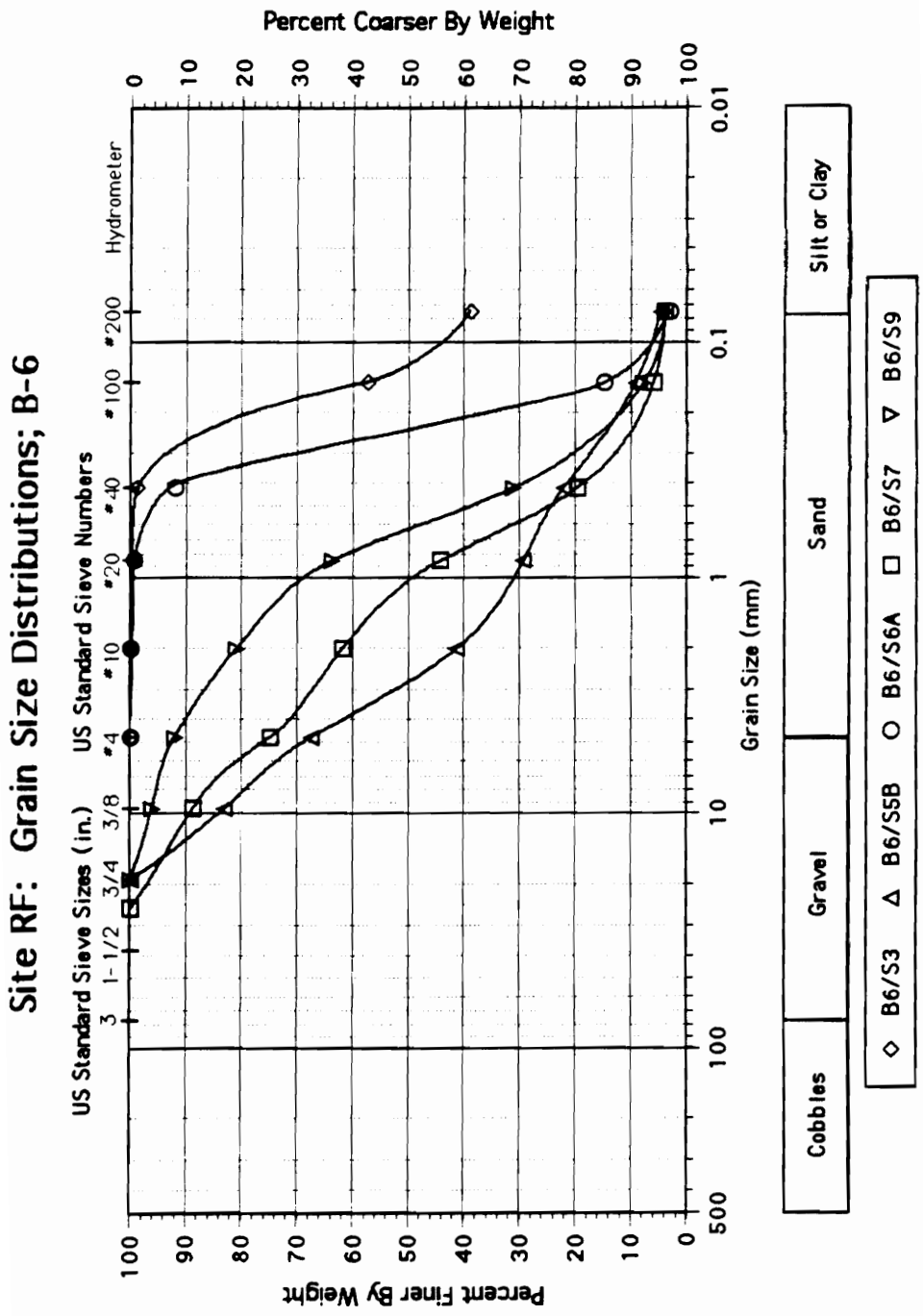
Site RF: Grain Size Distributions; B-6
Percent Coarser By Weight
Percent Finer By Weight
US Standard Sieve Sizes (in.)
US Standard Sieve Numbers
Hydrometer
Grain Size (mm)
Cobbles
Gravel
Sand
Silt or Clay
B6/S3
B6/S5B
B6/S6A
B6/S7
B6/S9

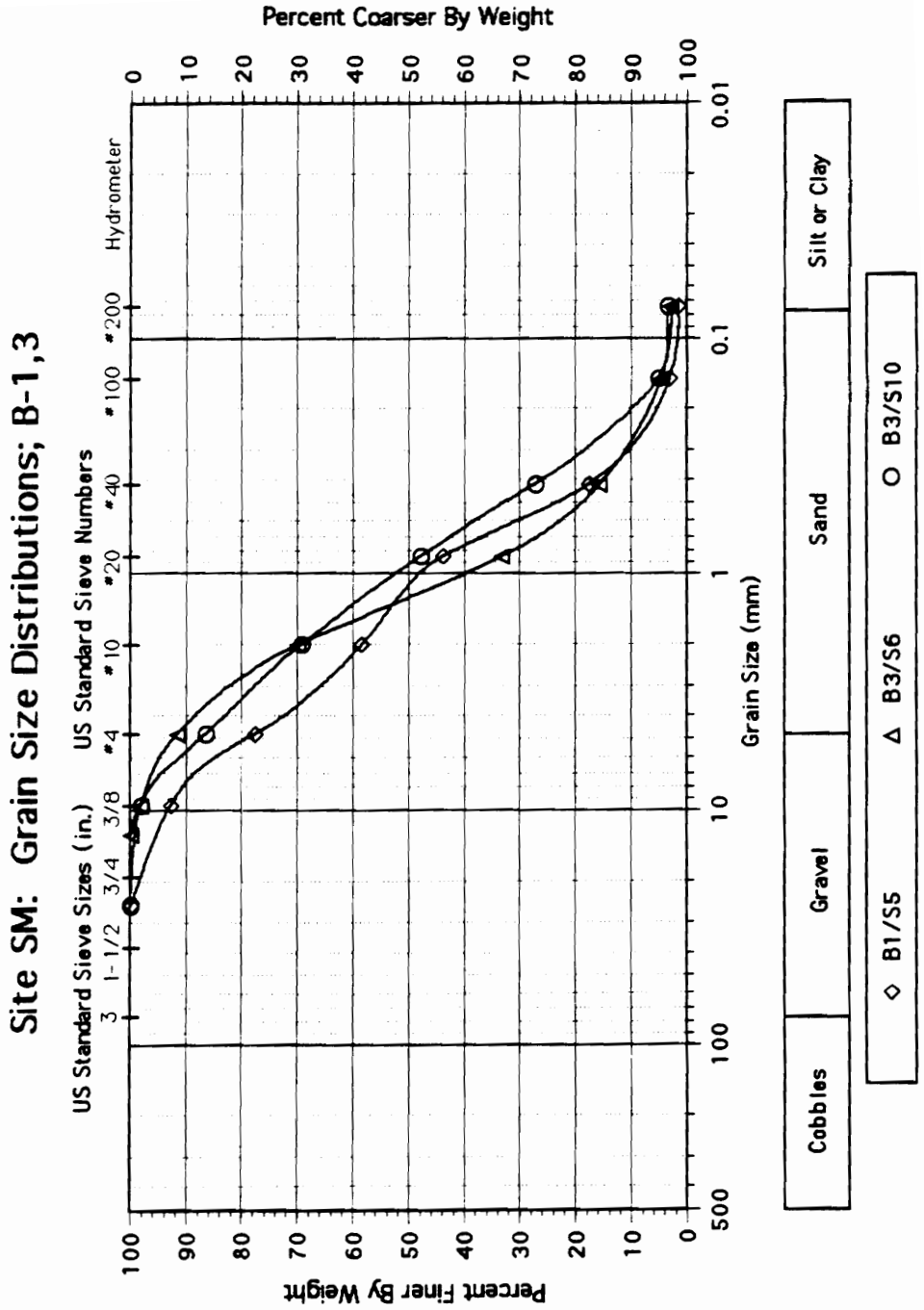
Site SM: Grain Size Distributions; B-1,3
Percent Coarser By Weight
Percent Finer By Weight
US Standard Sieve Sizes (in.)
US Standard Sieve Numbers
Hydrometer
Grain Size (mm)
Cobbles
Gravel
Sand
Silt or Clay
◇ B1/S5
△ B3/S6
○ B3/S10

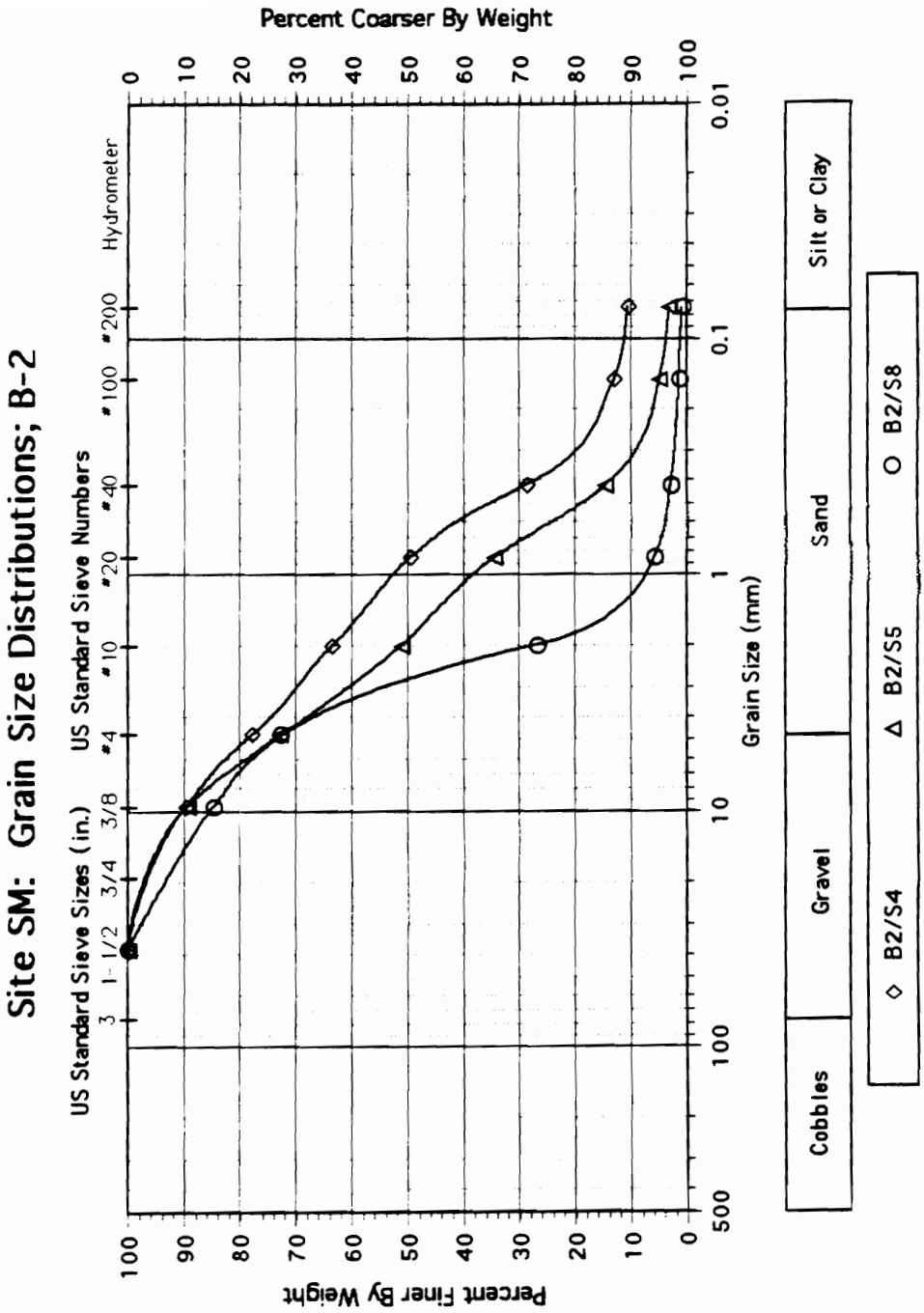
Site SM: Grain Size Distributions; B-2
Percent Coarser By Weight
Percent Finer By Weight
US Standard Sieve Sizes (in.)
3
1-1/2
3/4
3/8
US Standard Sieve Numbers
#4
#10
#20
#40
#100
#200
Hydrometer
Grain Size (mm)
Cobbles
Gravel
Sand
Silt or Clay
◇ B2/S4
△ B2/S5
○ B2/S8

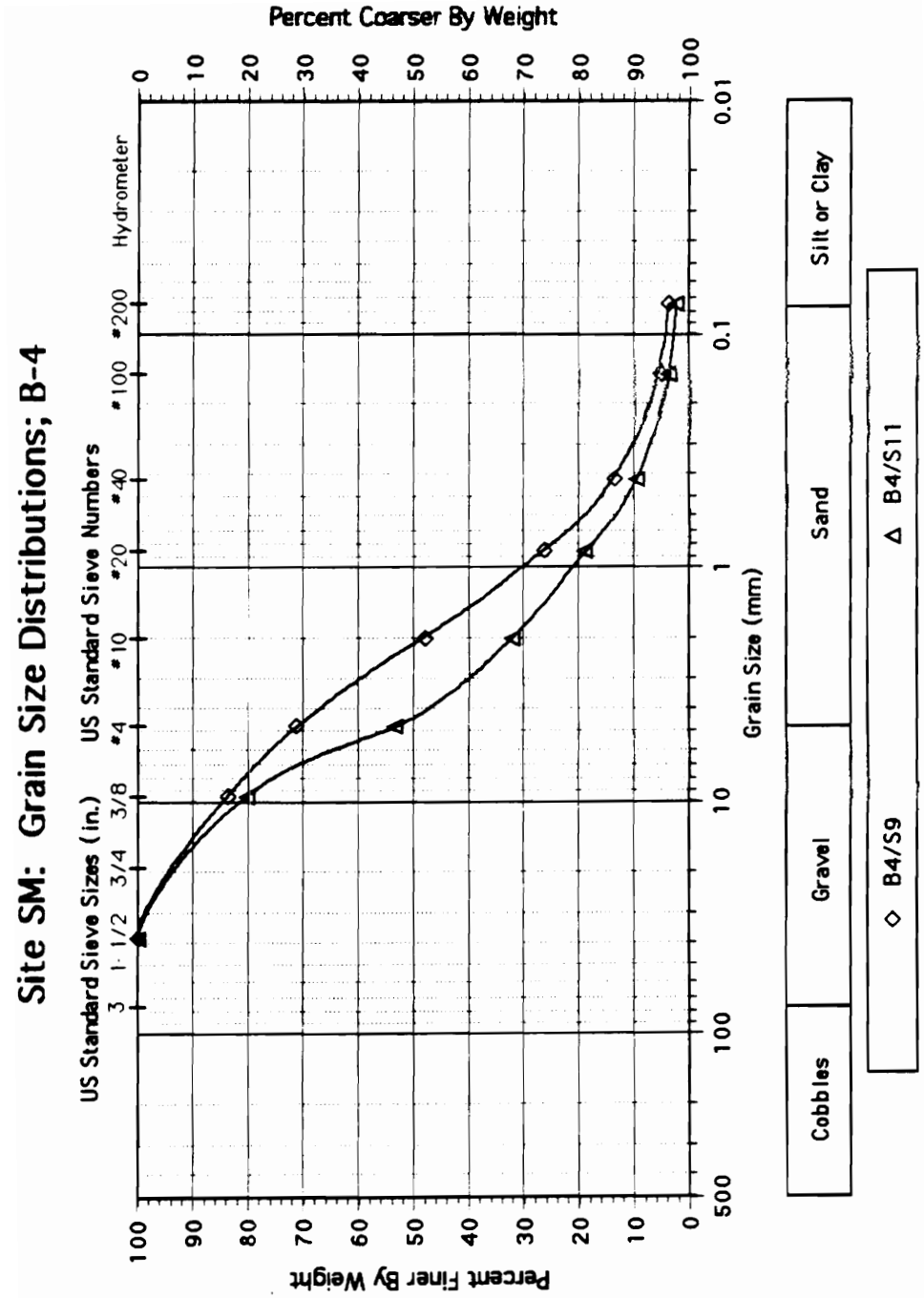
Site SM: Grain Size Distributions; B-4
Percent Coarser By Weight
Percent Finer By Weight
US Standard Sieve Sizes (in.)
US Standard Sieve Numbers
Hydrometer
Grain Size (mm)
Cobbles
Gravel
Sand
Silt or Clay
◇ B4/S9
△ B4/S11

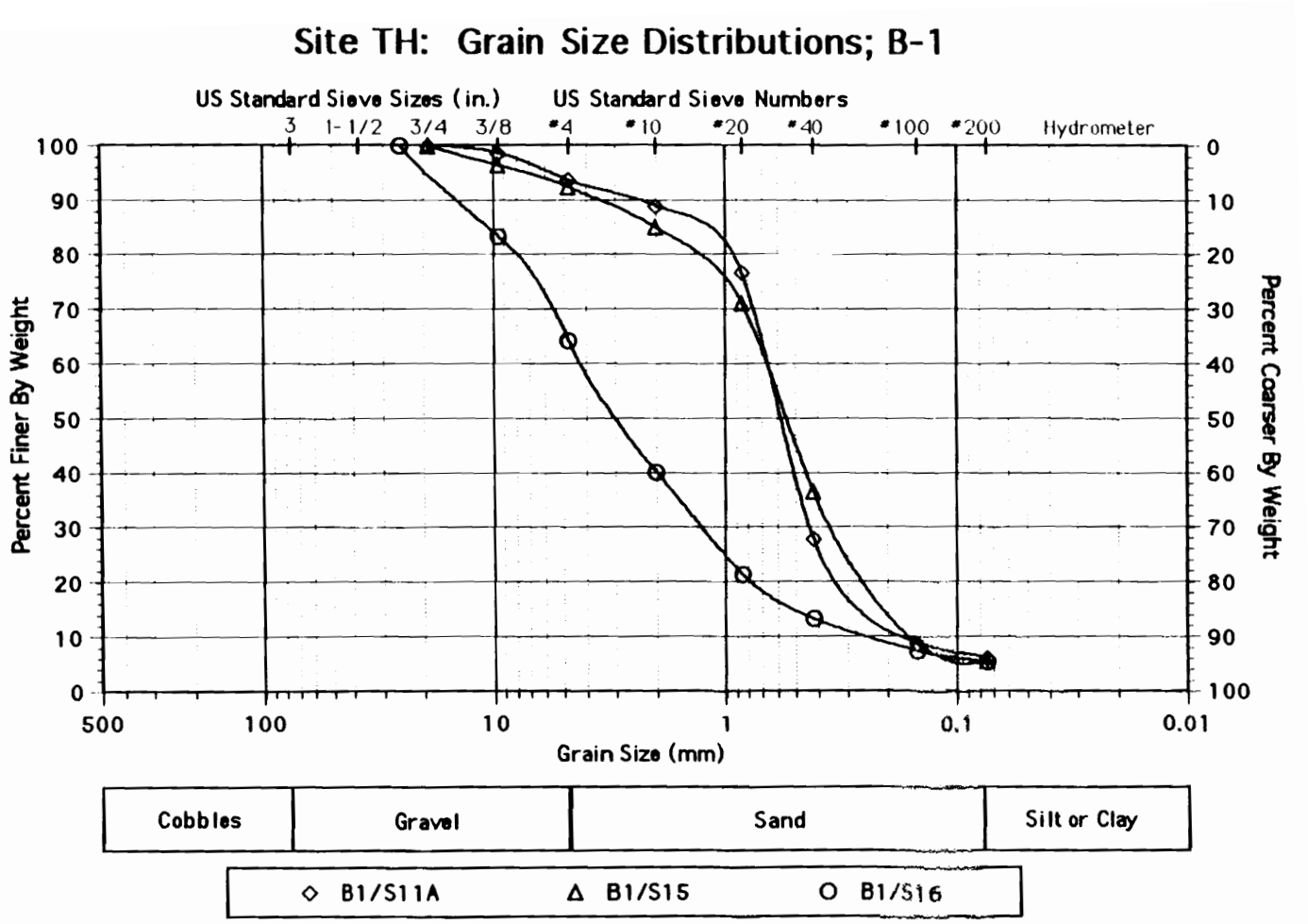
Site TH: Grain Size Distributions; B-1
US Standard Sieve Sizes (in.)
US Standard Sieve Numbers
3
1-1/2
3/4
3/8
#4
#10
#20
#40
#100
#200
Hydrometer
Percent Finer By Weight
Percent Coarser By Weight
100
90
80
70
60
50
40
30
20
10
0
500
100
10
1
0.1
0.01
Grain Size (mm)
Cobbles
Gravel
Sand
Silt or Clay
◇ B1/S11A
△ B1/S15
○ B1/S16

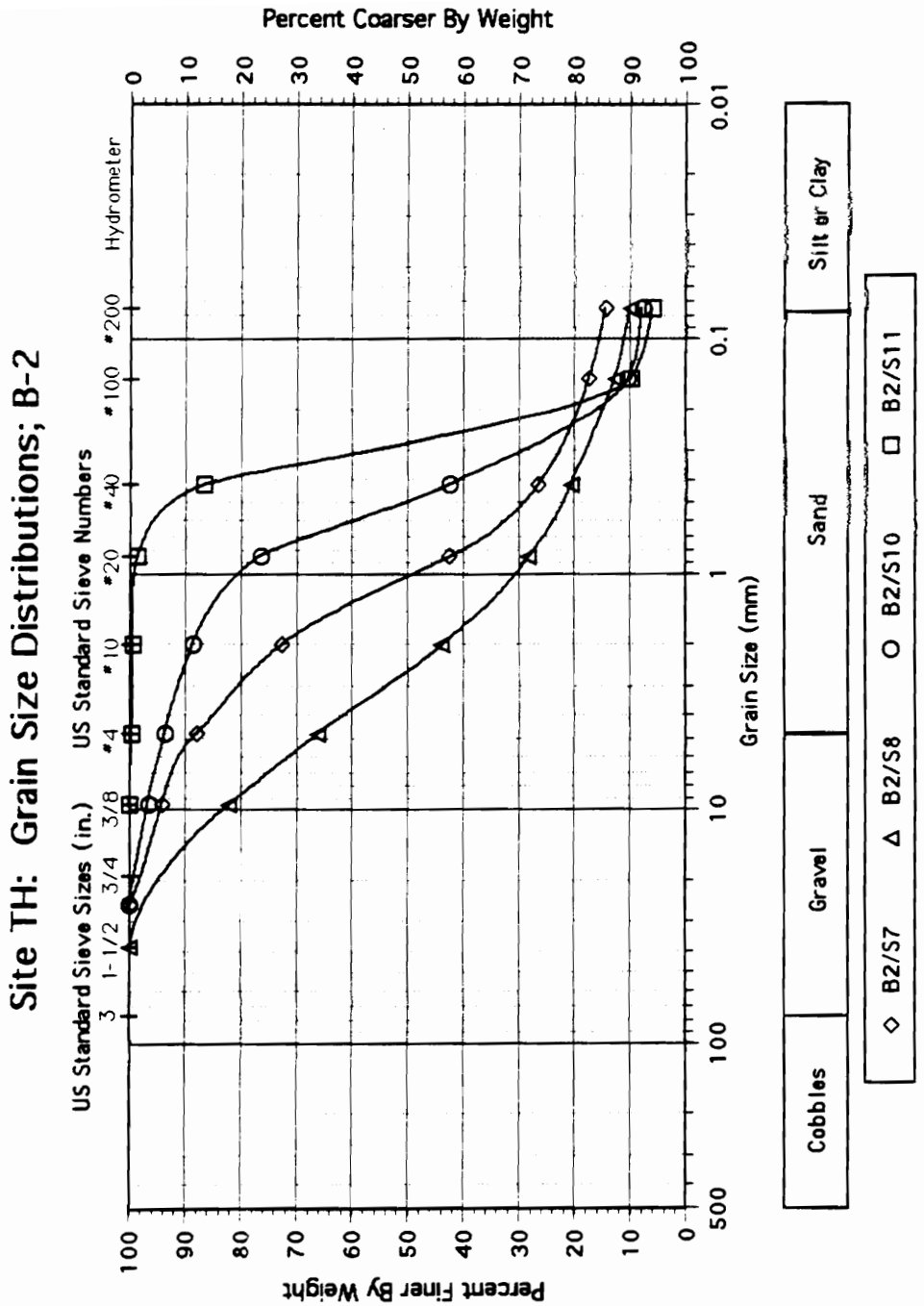
Site TH: Grain Size Distributions; B-2
Percent Coarser By Weight
Percent Finer By Weight
US Standard Sieve Sizes (in.)
US Standard Sieve Numbers
Hydrometer
Grain Size (mm)
Cobbles
Gravel
Sand
Silt or Clay
B2/S7
B2/S8
B2/S10
B2/S11

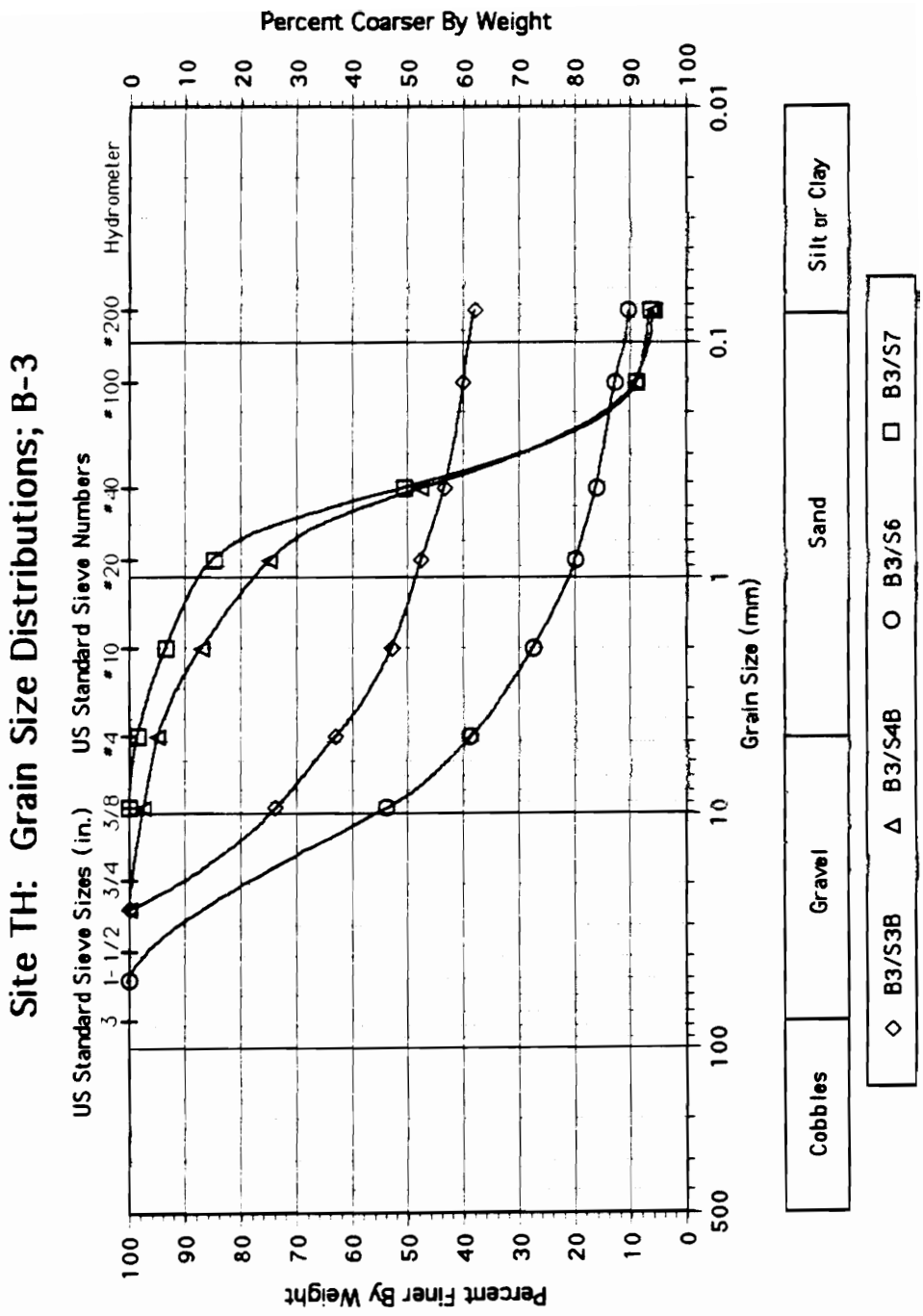
Site TH: Grain Size Distributions; B-3
Percent Coarser By Weight
Percent Finer By Weight
US Standard Sieve Sizes (in.)
US Standard Sieve Numbers
Hydrometer
Grain Size (mm)
Cobbles
Gravel
Sand
Silt or Clay
B3/S3B
B3/S4B
B3/S6
B3/S7

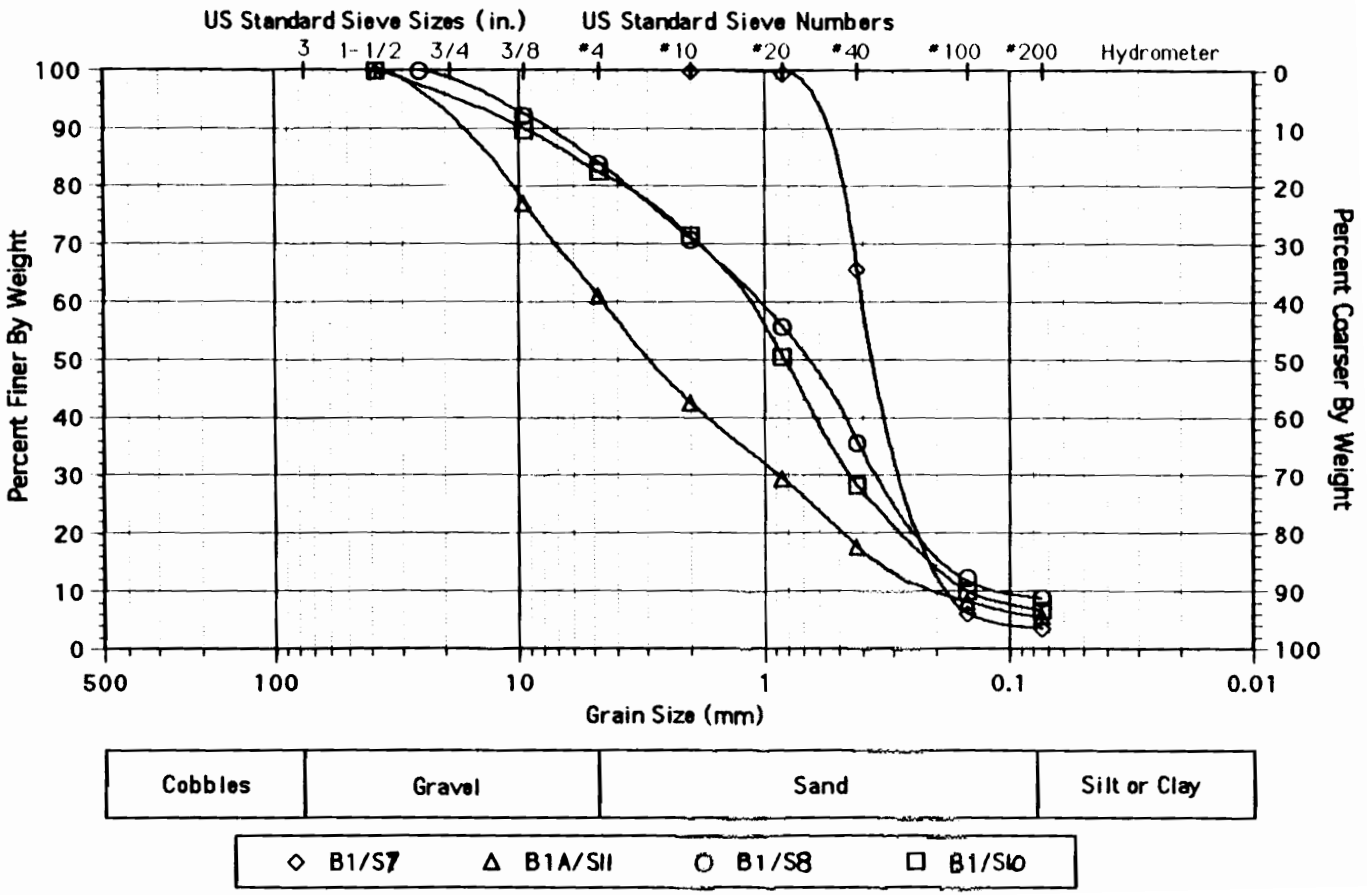
Site VW: Grain Size Distributions; B-1
US Standard Sieve Sizes (in.)
US Standard Sieve Numbers
3
1-1/2
3/4
3/8
#4
#10
#20
#40
#100
#200
Hydrometer
Percent Finer By Weight
Percent Coarser By Weight
100
90
80
70
60
50
40
30
20
10
0
500
100
10
1
0.1
0.01
Grain Size (mm)
Cobbles
Gravel
Sand
Silt or Clay
B1/S7
B1A/S11
B1/S8
B1/S10

Site VW: Grain Size Distributions; B-2

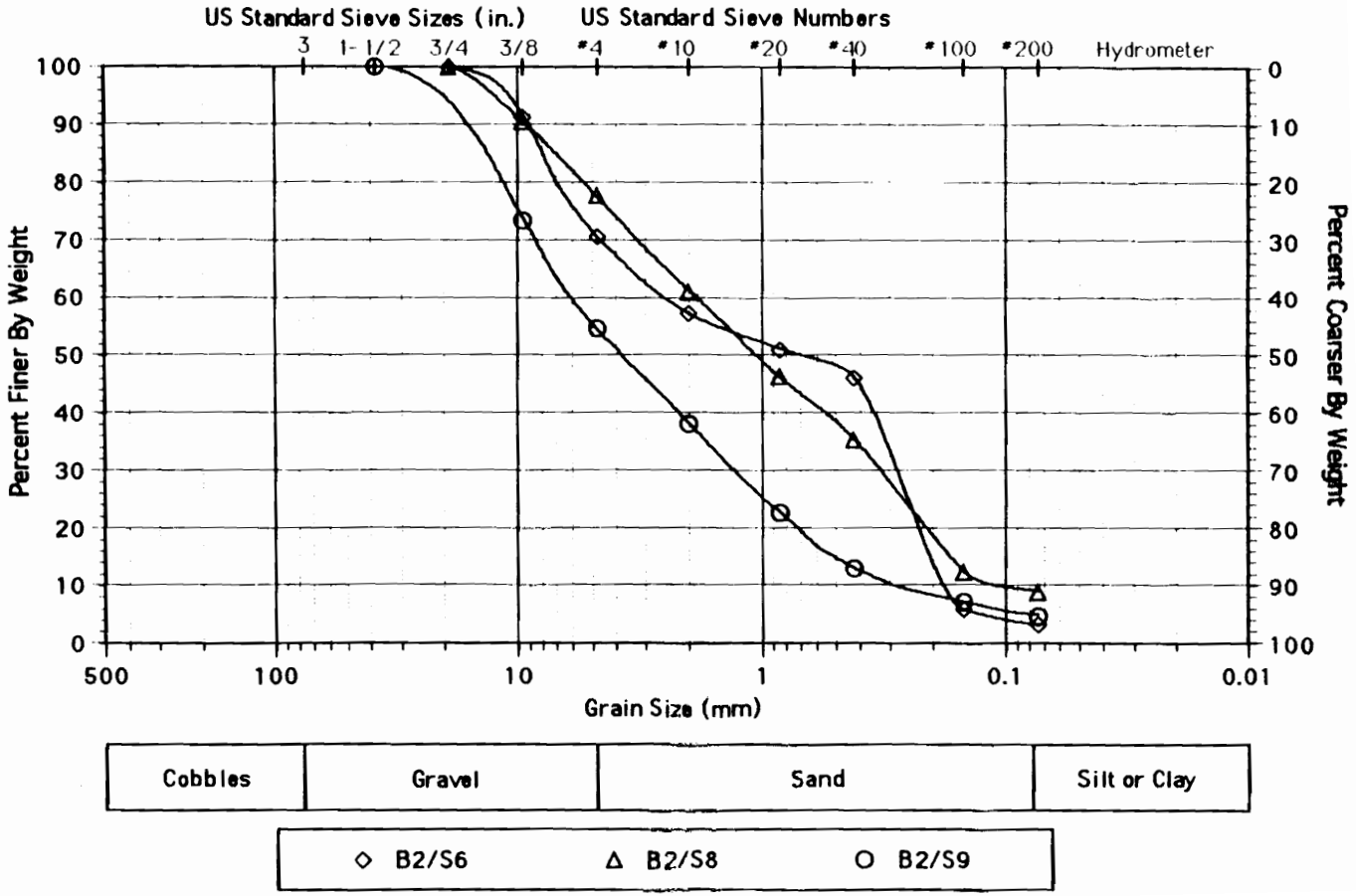

Site VW: Grain Size Distributions; B-3

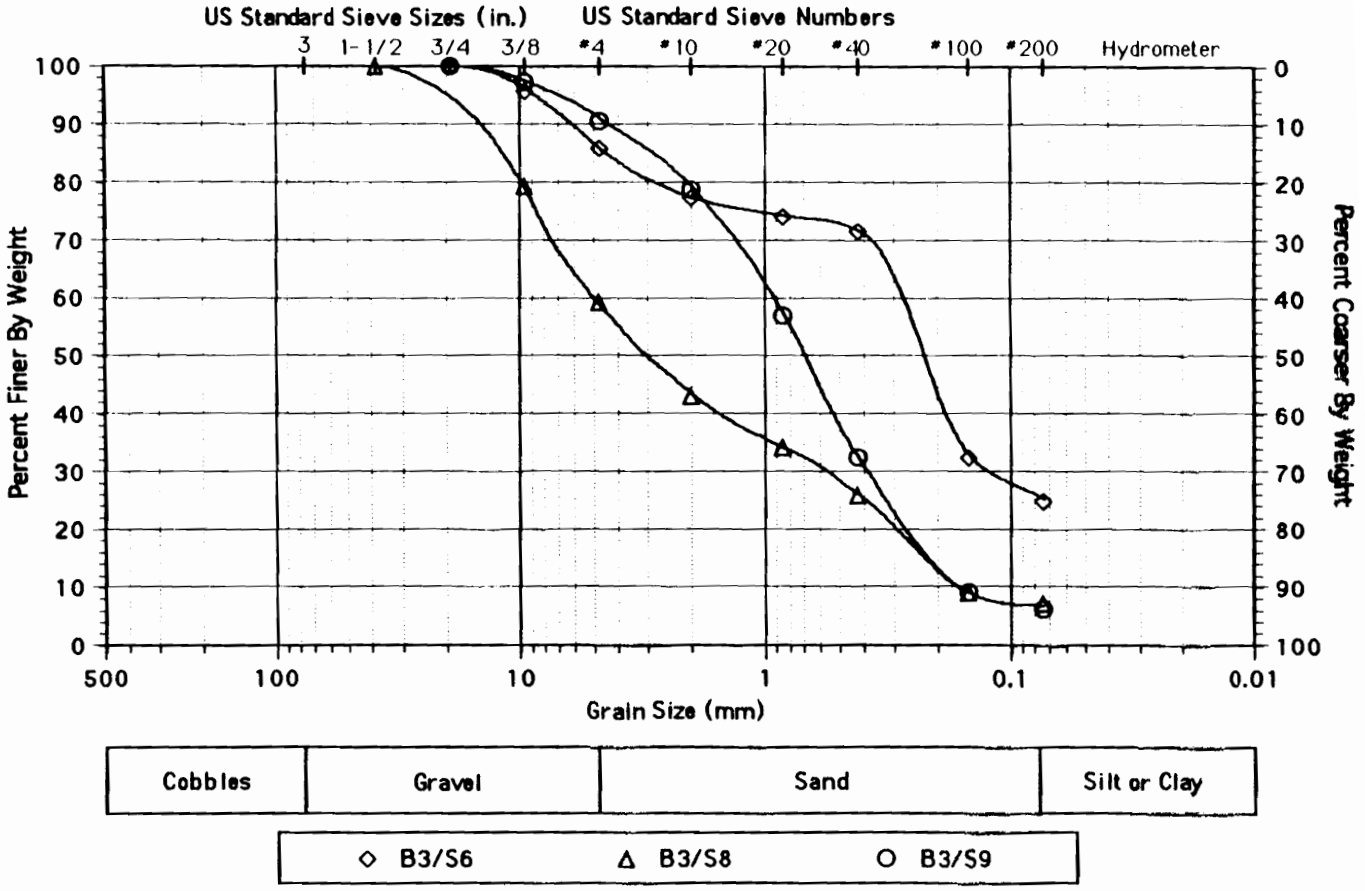

Site VW: Grain Size Distributions; B-4

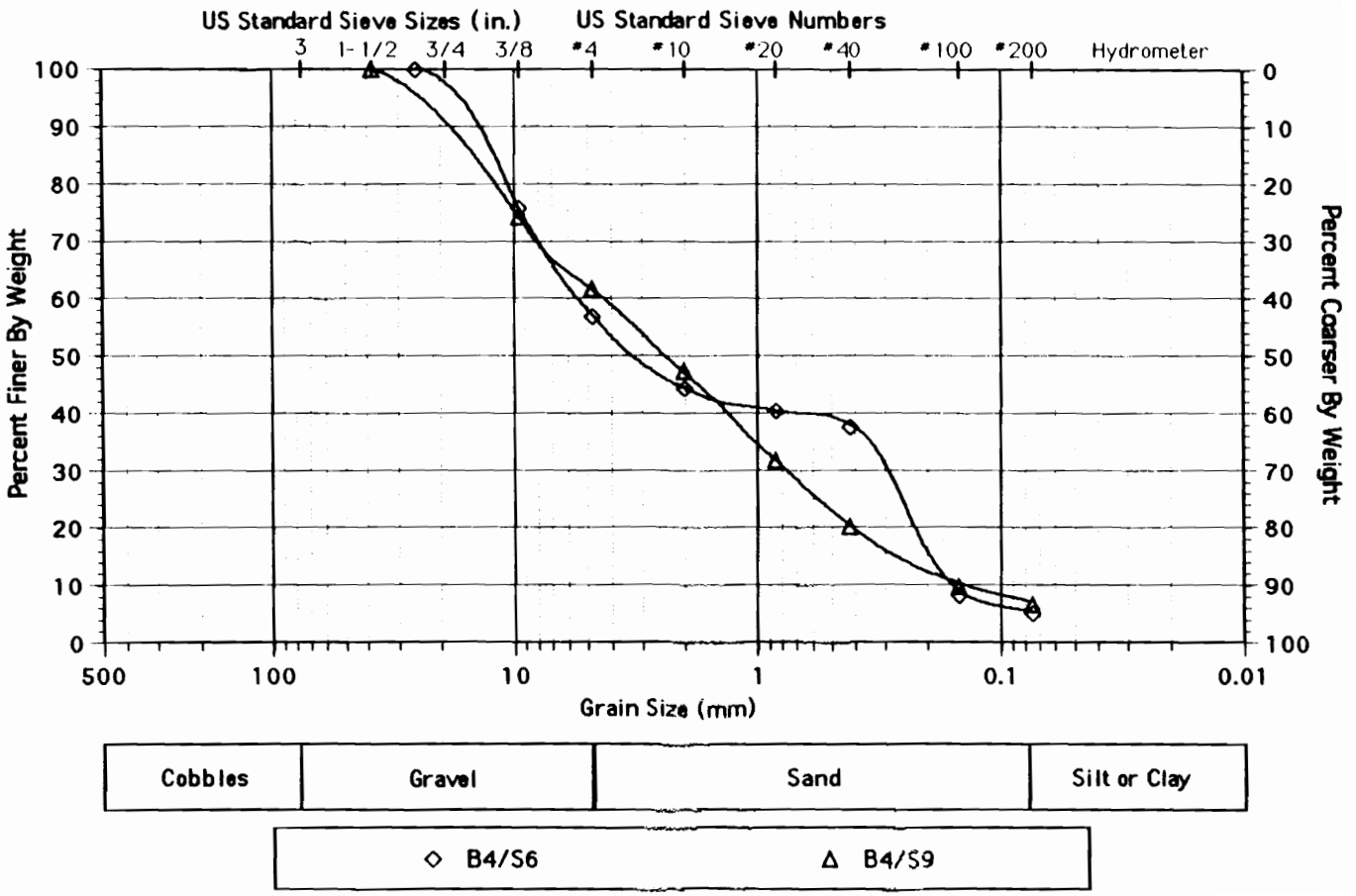

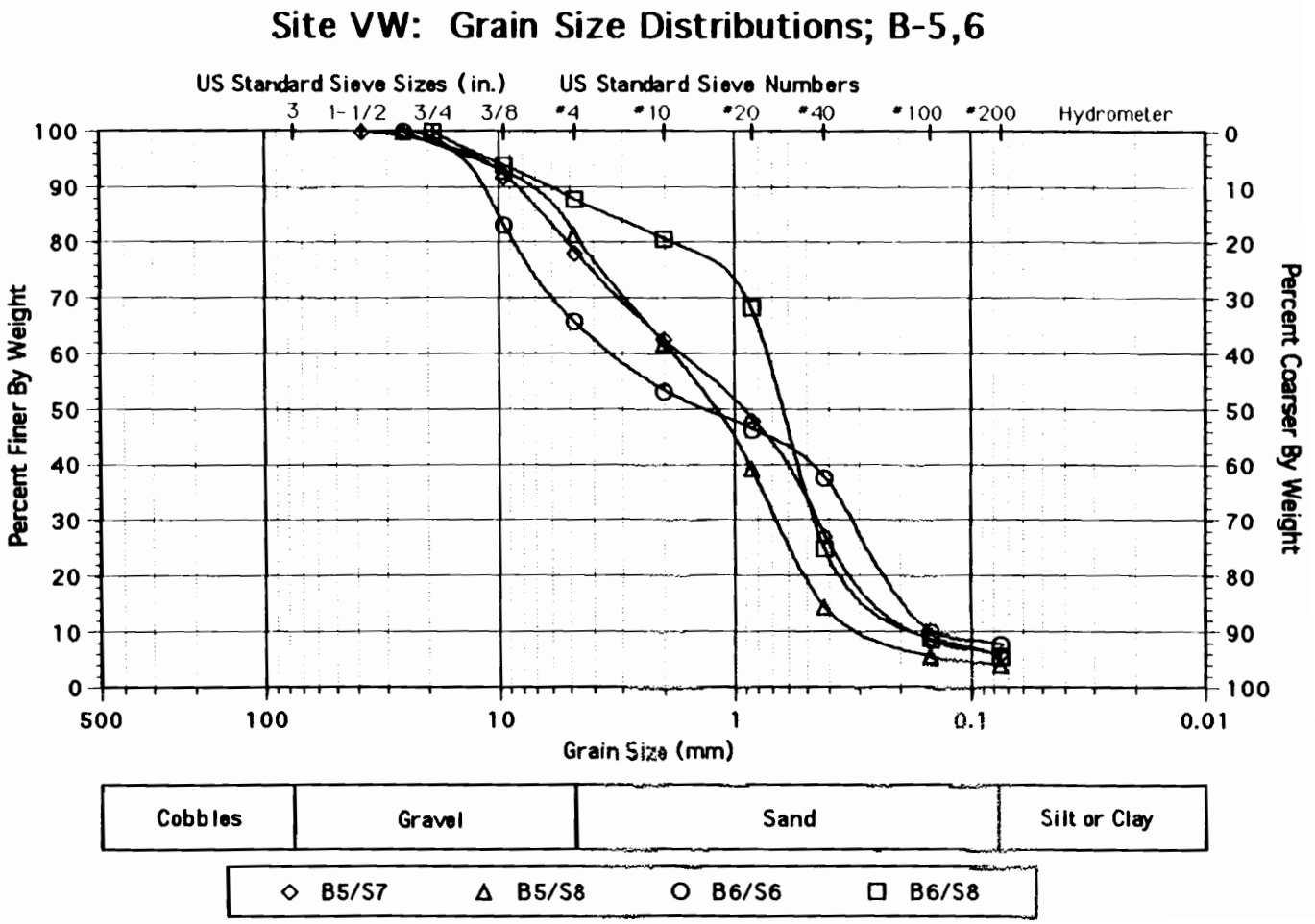
Site VW: Grain Size Distributions; B-5,6
US Standard Sieve Sizes (in.)
US Standard Sieve Numbers
3
1-1/2
3/4
3/8
#4
#10
#20
#40
#100
#200
Hydrometer
Percent Finer By Weight
Percent Coarser By Weight
100
90
80
70
60
50
40
30
20
10
0
500
100
10
1
0.1
0.01
Grain Size (mm)
Cobbles
Gravel
Sand
Silt or Clay
B5/S7
B5/S8
B6/S6
B6/S8

Site WO: Grain Size Distributions; B-1

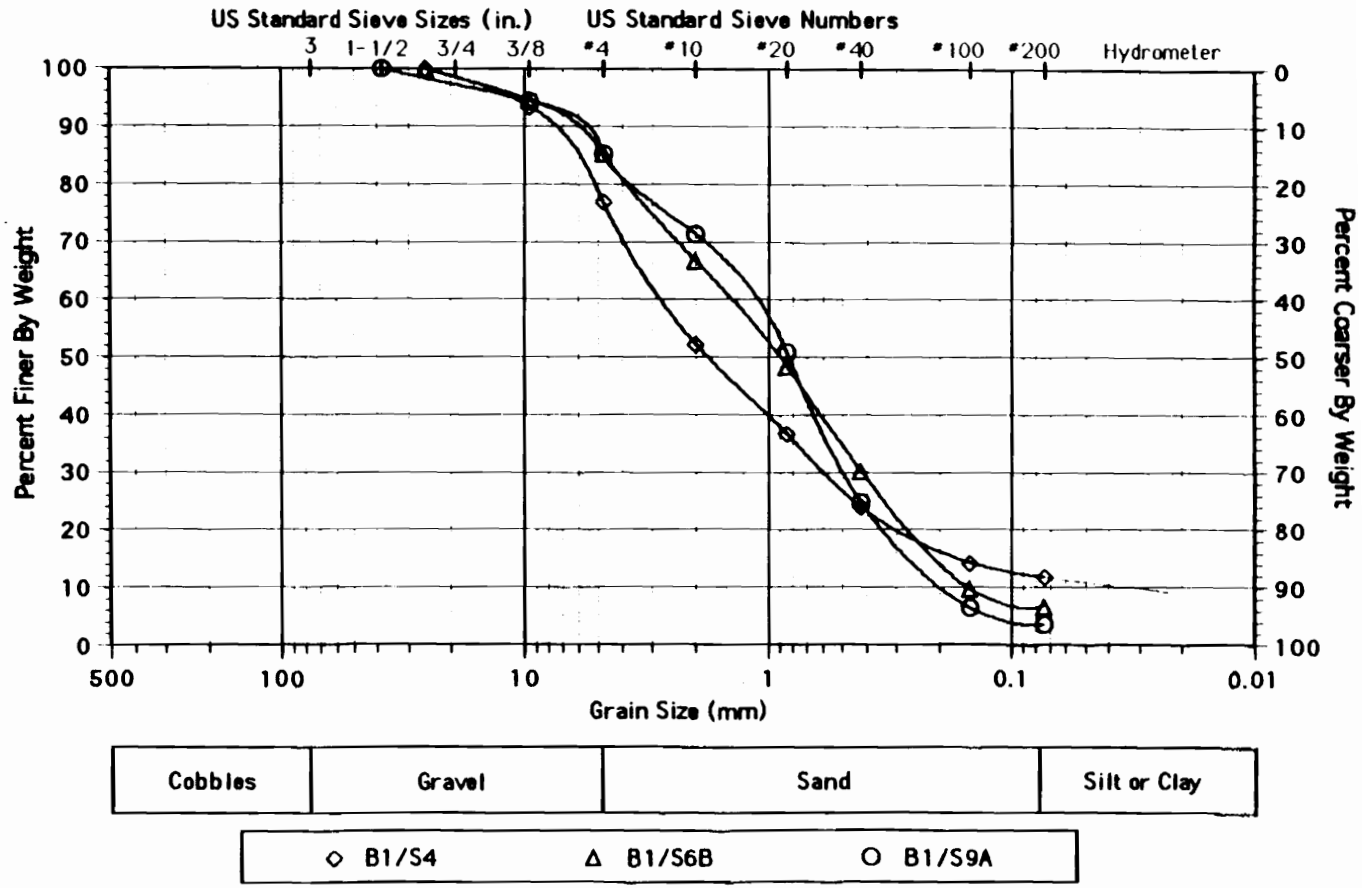

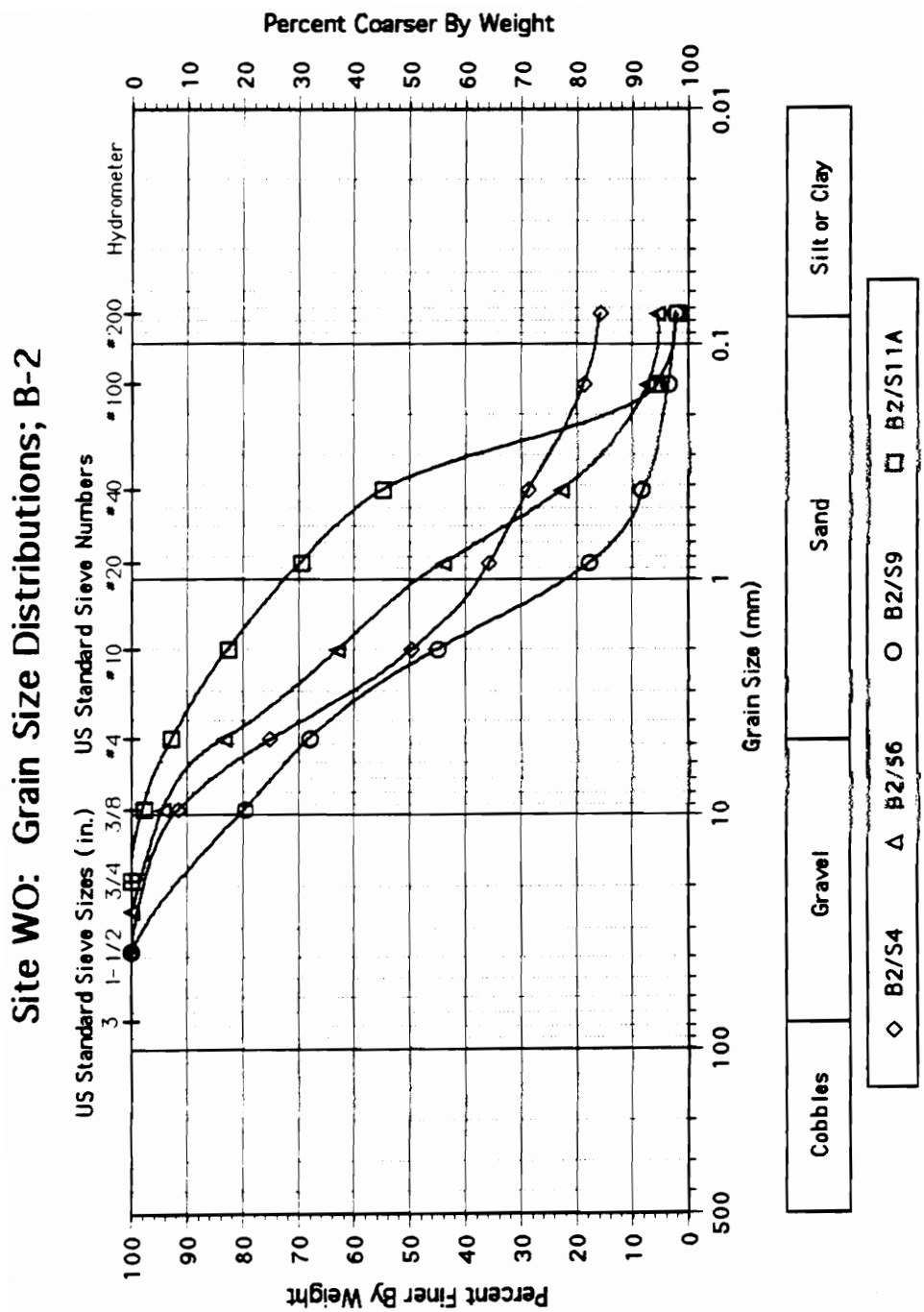
Site WO: Grain Size Distributions; B-2
Percent Coarser By Weight
US Standard Sieve Sizes (in.)
US Standard Sieve Numbers
Hydrometer
Percent Finer By Weight
Grain Size (mm)
Cobbles
Gravel
Sand
Silt or Clay
B2/S4
B2/S6
B2/S9
B2/S11A

Site WO: Grain Size Distributions; B-3

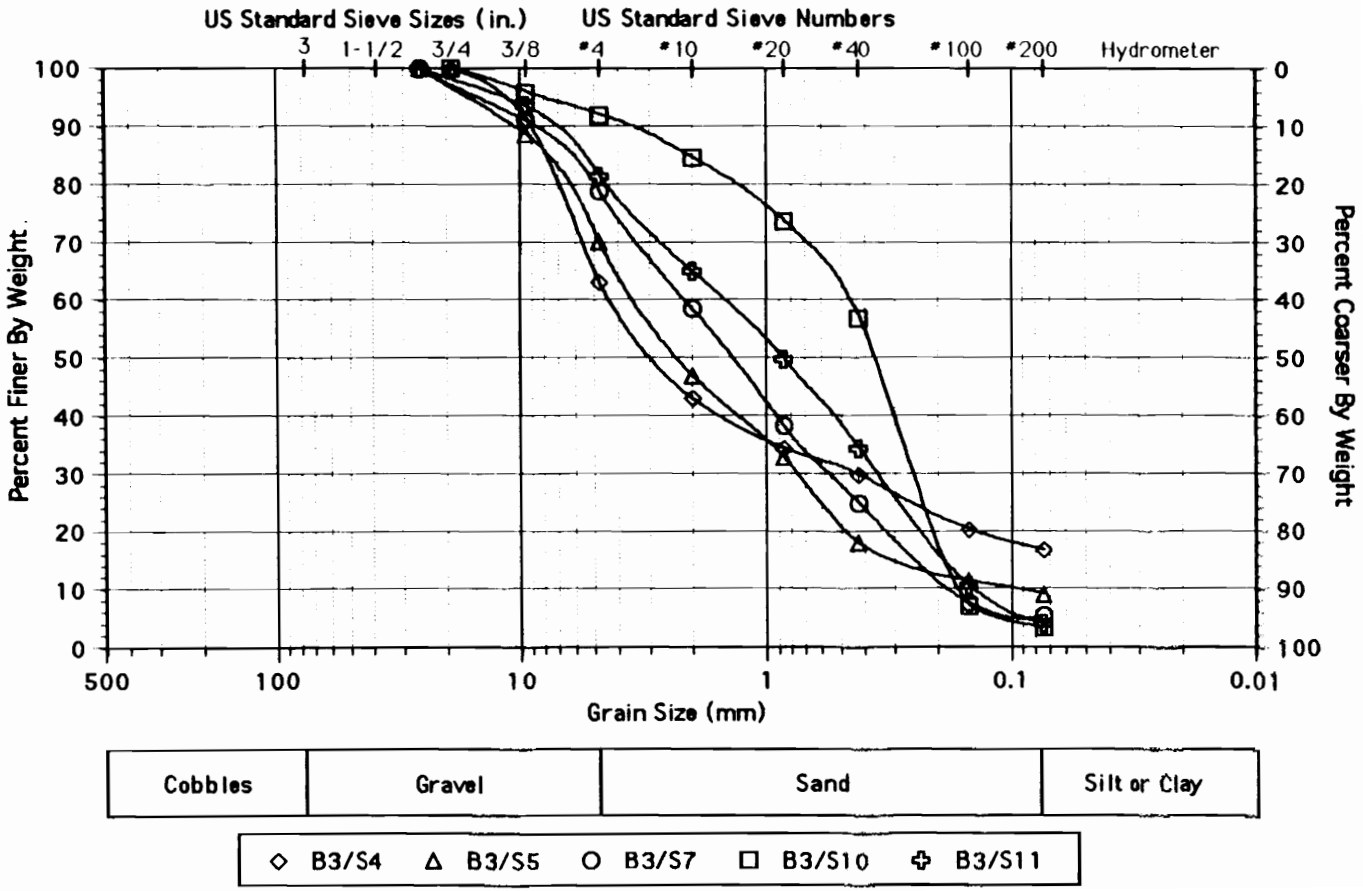

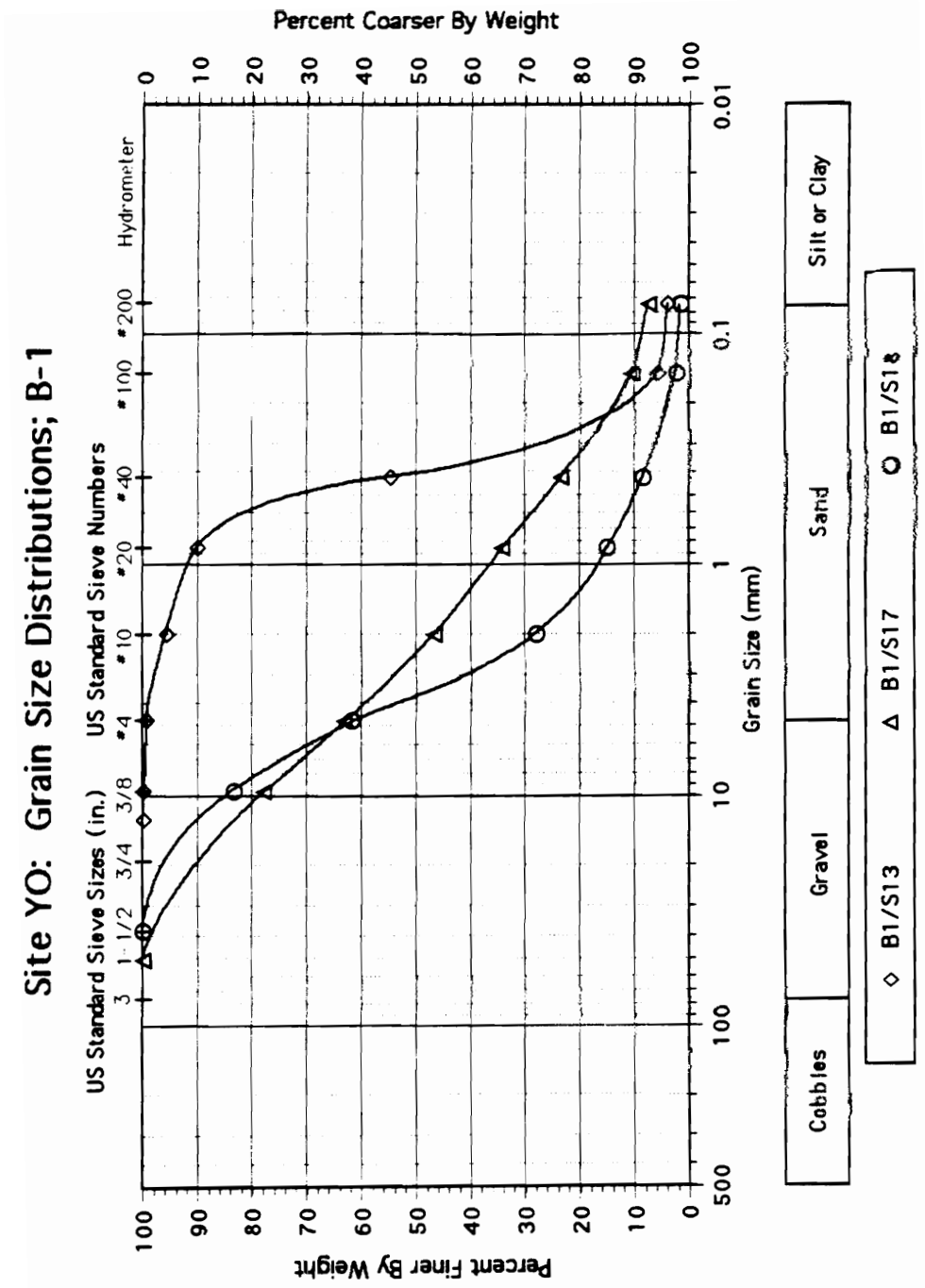
Site YO: Grain Size Distributions; B-1
Percent Coarser By Weight
Percent Finer By Weight
US Standard Sieve Sizes (in.)
US Standard Sieve Numbers
Hydrometer
Grain Size (mm)
Cobbles
Gravel
Sand
Silt or Clay
◇ B1/S13
△ B1/S17
○ B1/S18

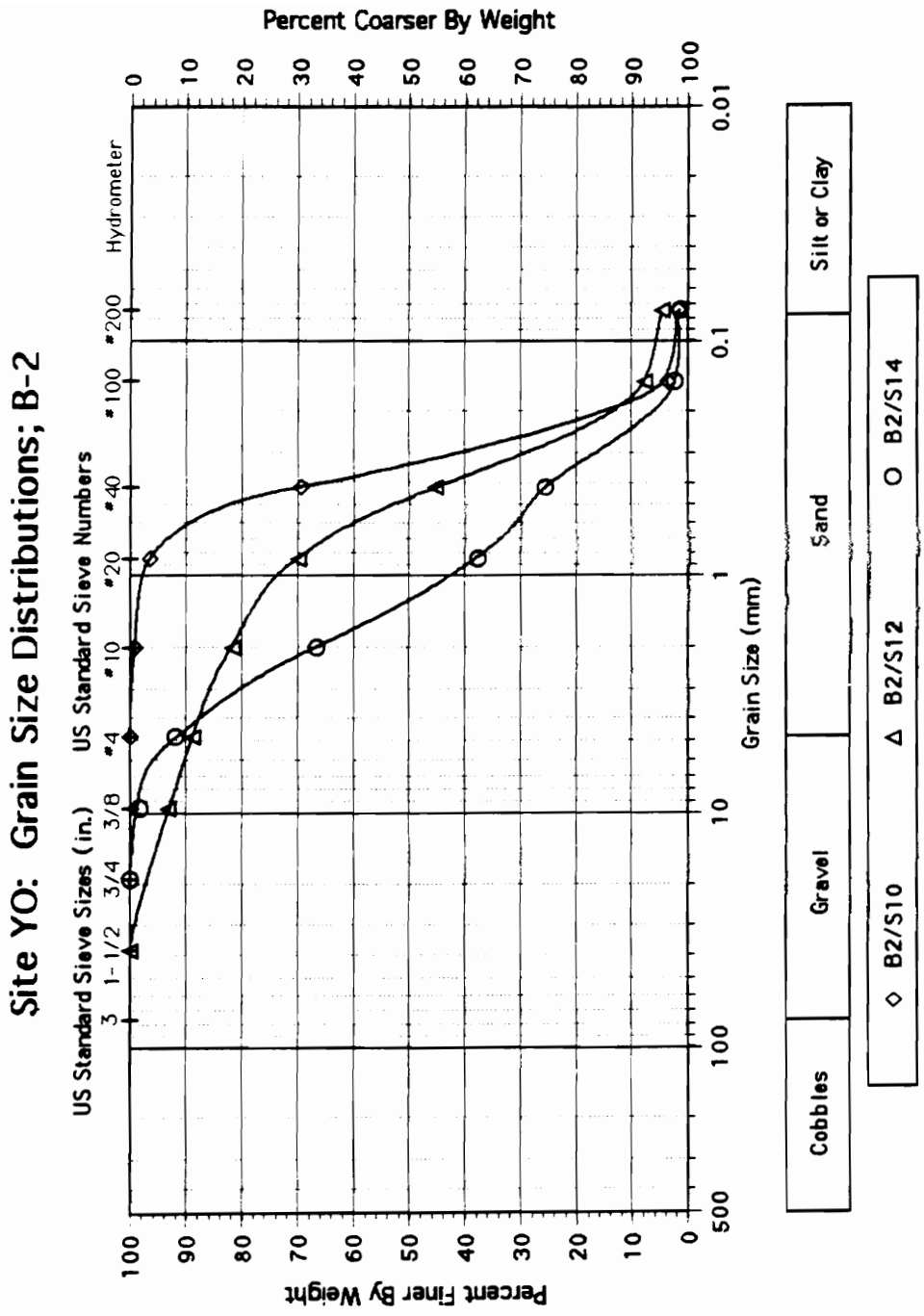
Site YO: Grain Size Distributions; B-2
Percent Coarser By Weight
Percent Finer By Weight
US Standard Sieve Sizes (in.)
US Standard Sieve Numbers
Hydrometer
Grain Size (mm)
Cobbles
Gravel
Sand
Silt or Clay
◇ B2/S10
△ B2/S12
○ B2/S14

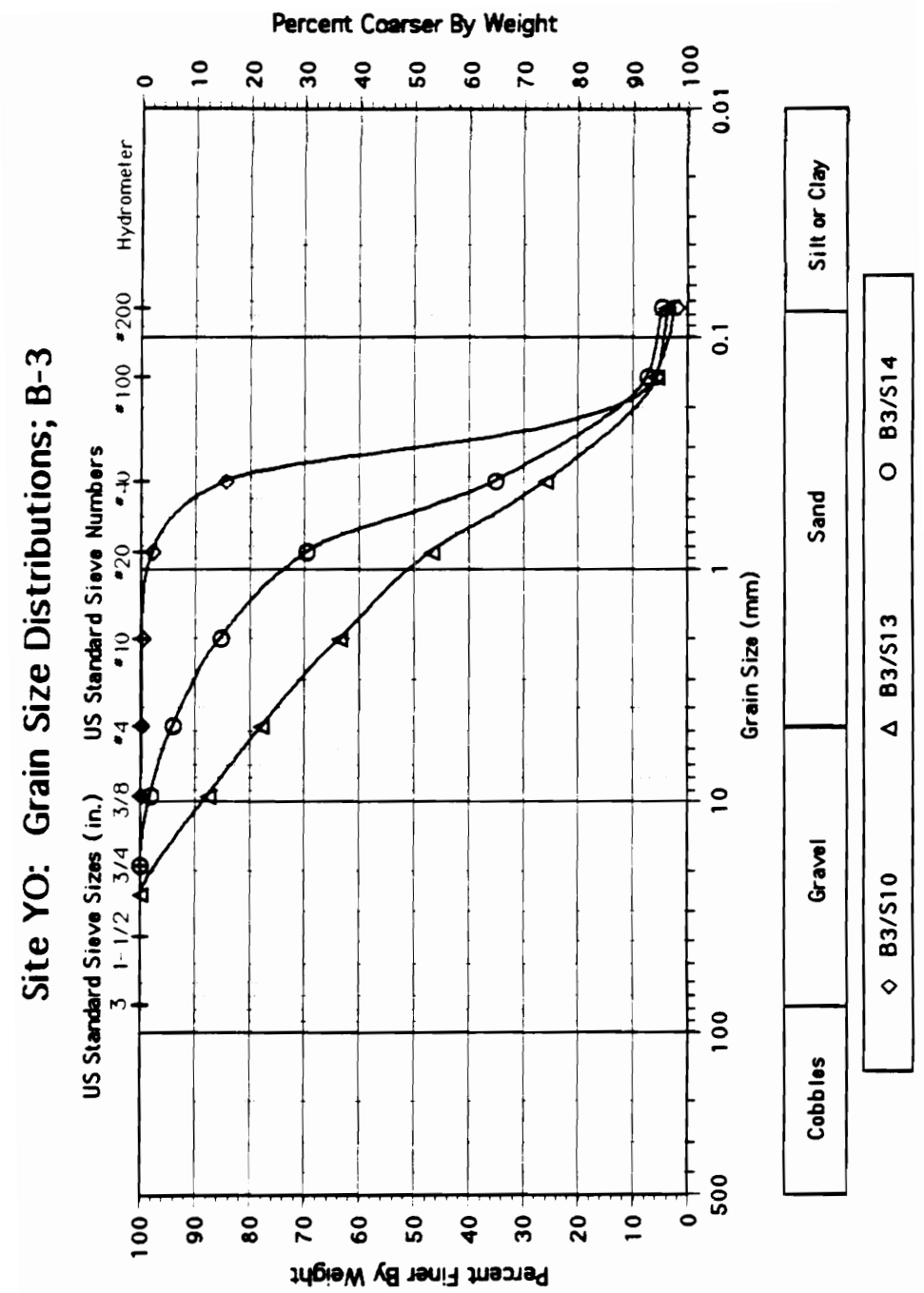
Site YO: Grain Size Distributions; B-3
Percent Coarser By Weight
Percent Finer By Weight
US Standard Sieve Sizes (in.)
US Standard Sieve Numbers
Hydrometer
Grain Size (mm)
Cobbles
Gravel
Sand
Silt or Clay
◇ B3/S10
△ B3/S13
○ B3/S14

Skelton Event Grainsize Curves

Site GR: Grain Size Distributions; B-1

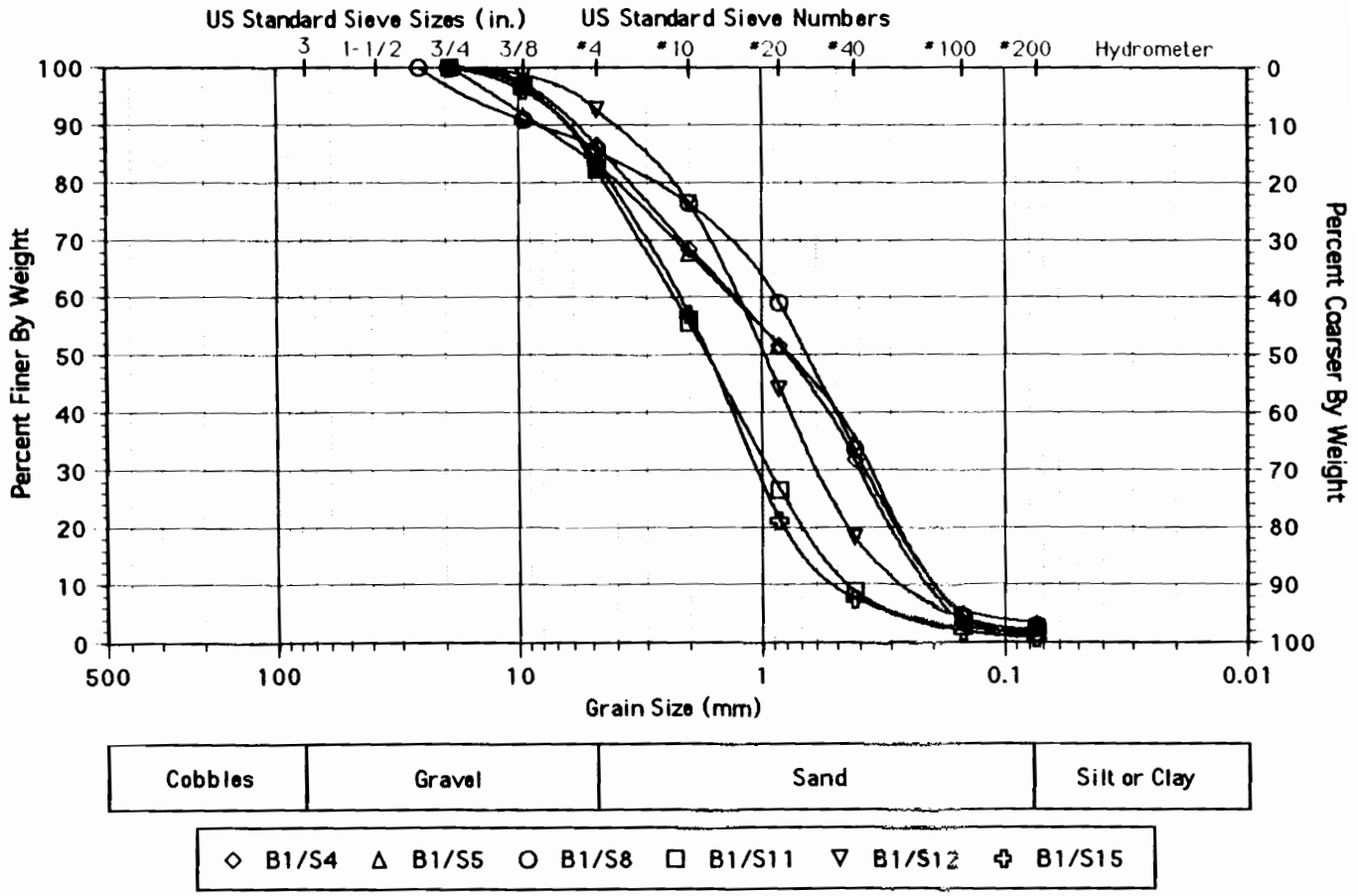

Site GR: Grain Size Distributions; B-2

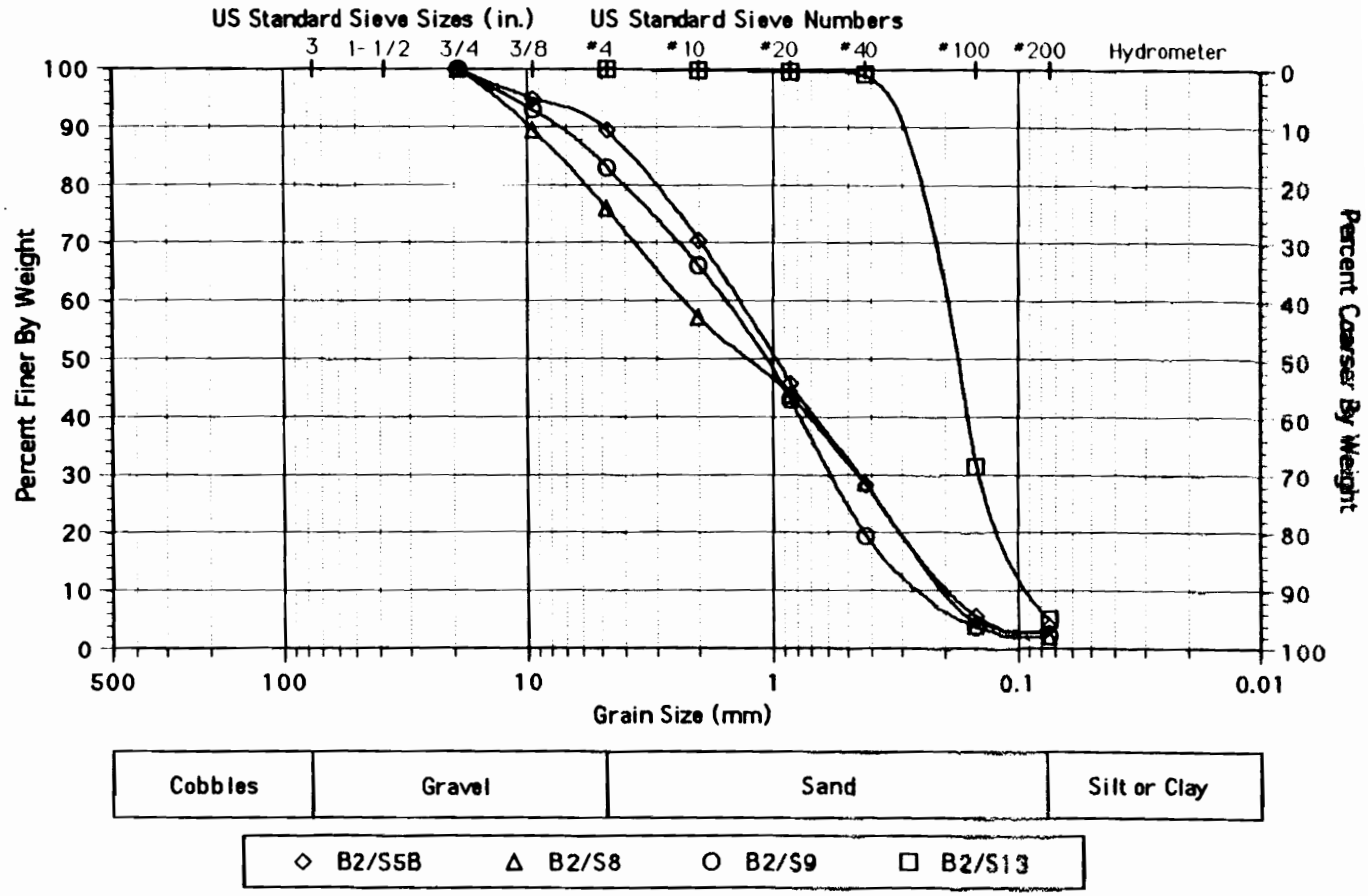

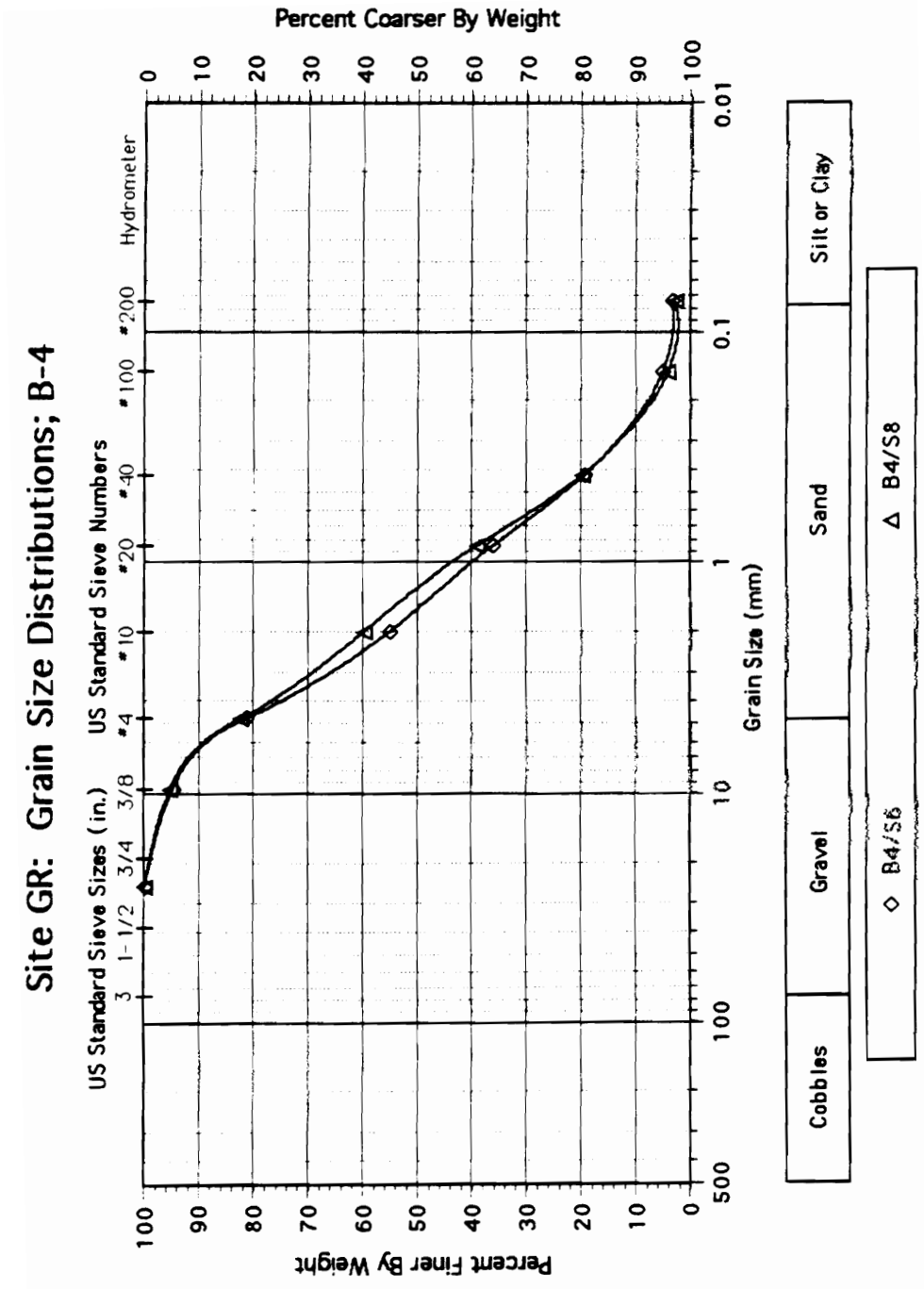
Site GR: Grain Size Distributions; B-4
Percent Coarser By Weight
US Standard Sieve Sizes (in.)
US Standard Sieve Numbers
Hydrometer
Percent Finer By Weight
Grain Size (mm)
Cobbles
Gravel
Sand
Silt or Clay
◇ B4/S6
△ B4/S8

Site HM: Grain Size Distributions; B-1

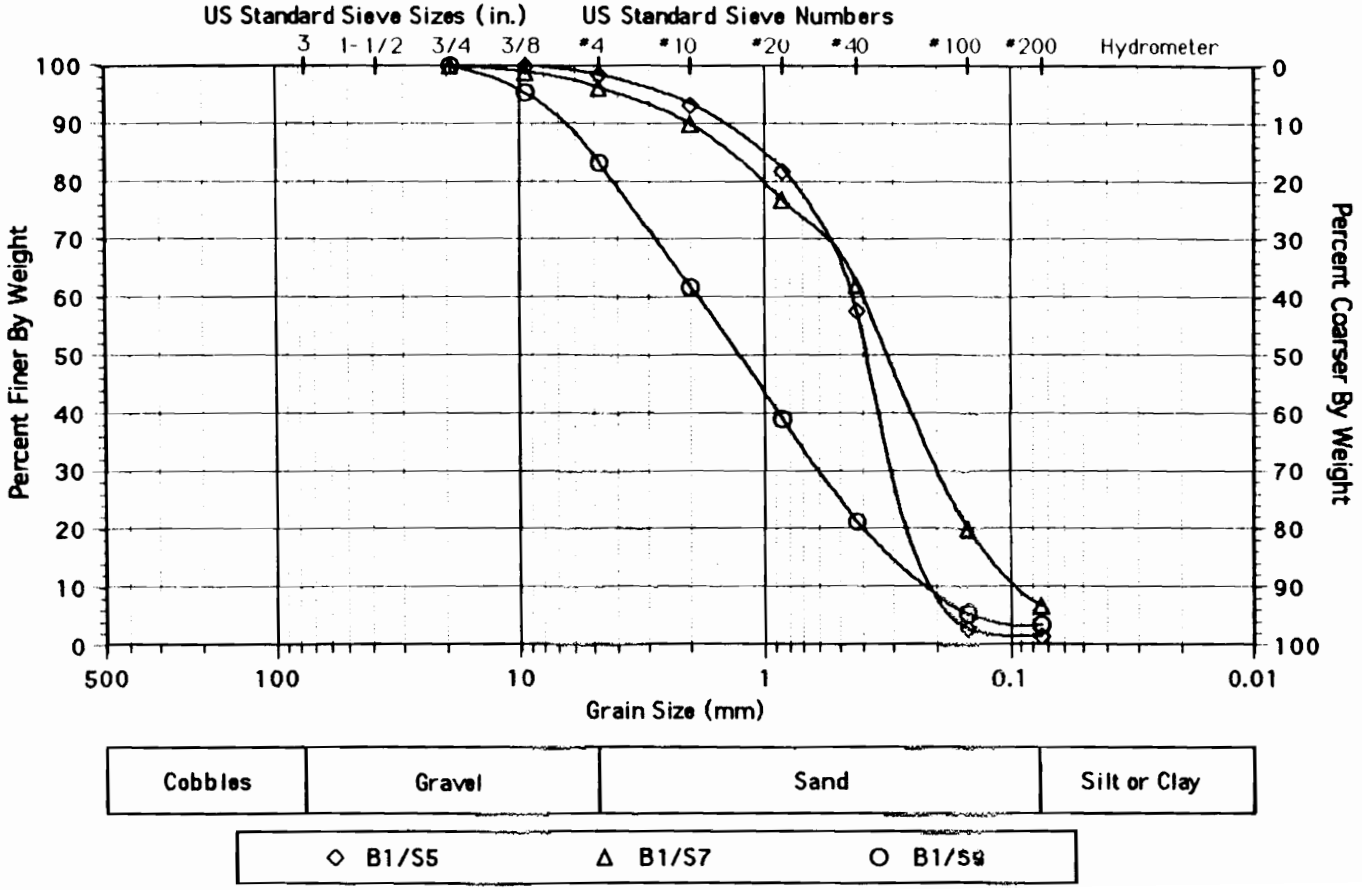

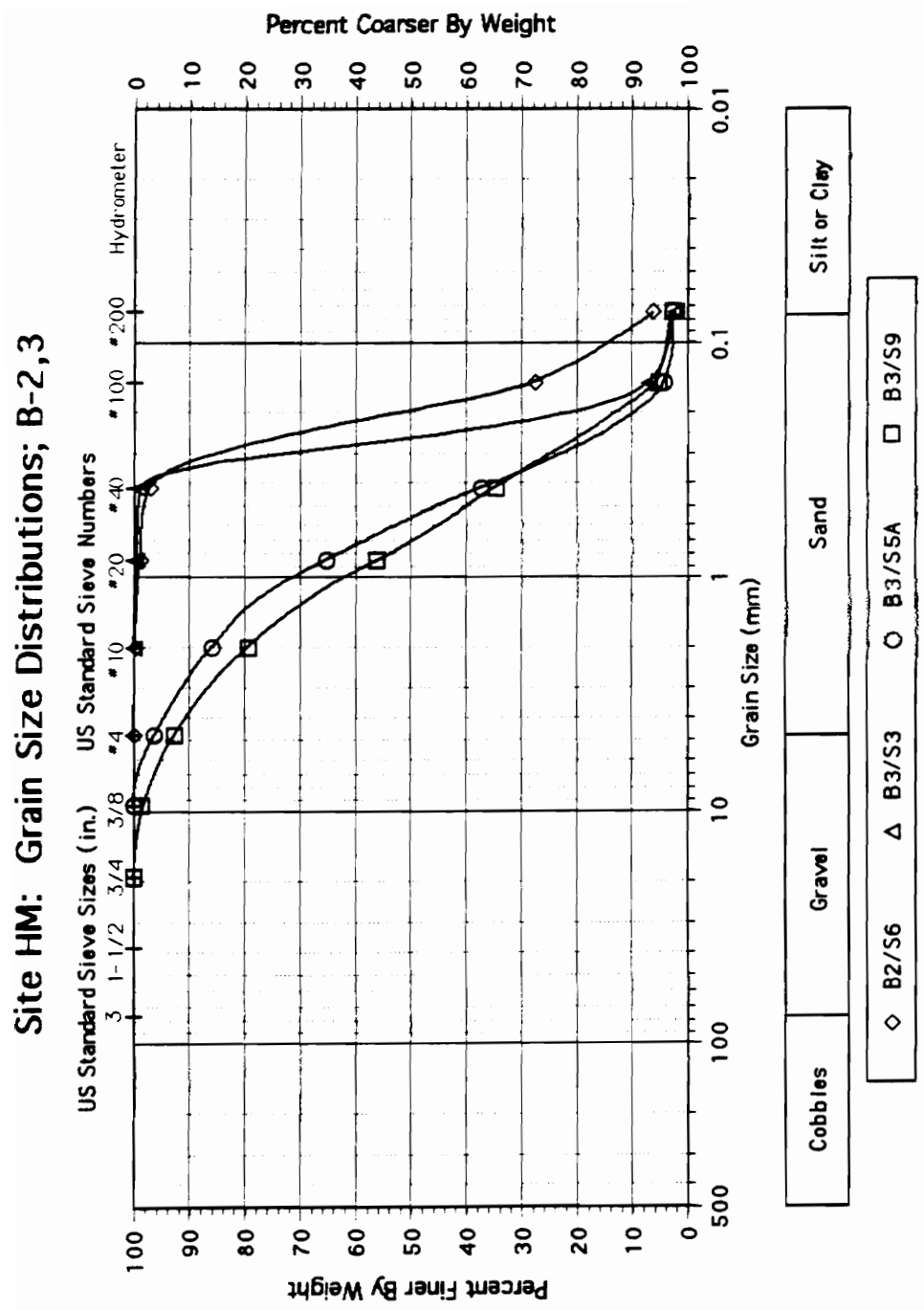
Site HM: Grain Size Distributions; B-2,3
Percent Coarser By Weight
Percent Finer By Weight
US Standard Sieve Sizes (in.)
US Standard Sieve Numbers
Hydrometer
Grain Size (mm)
Cobbles
Gravel
Sand
Silt or Clay
B2/S6
B3/S3
B3/S5A
B3/S9

Site VC: Grain Size Distributions; B-1

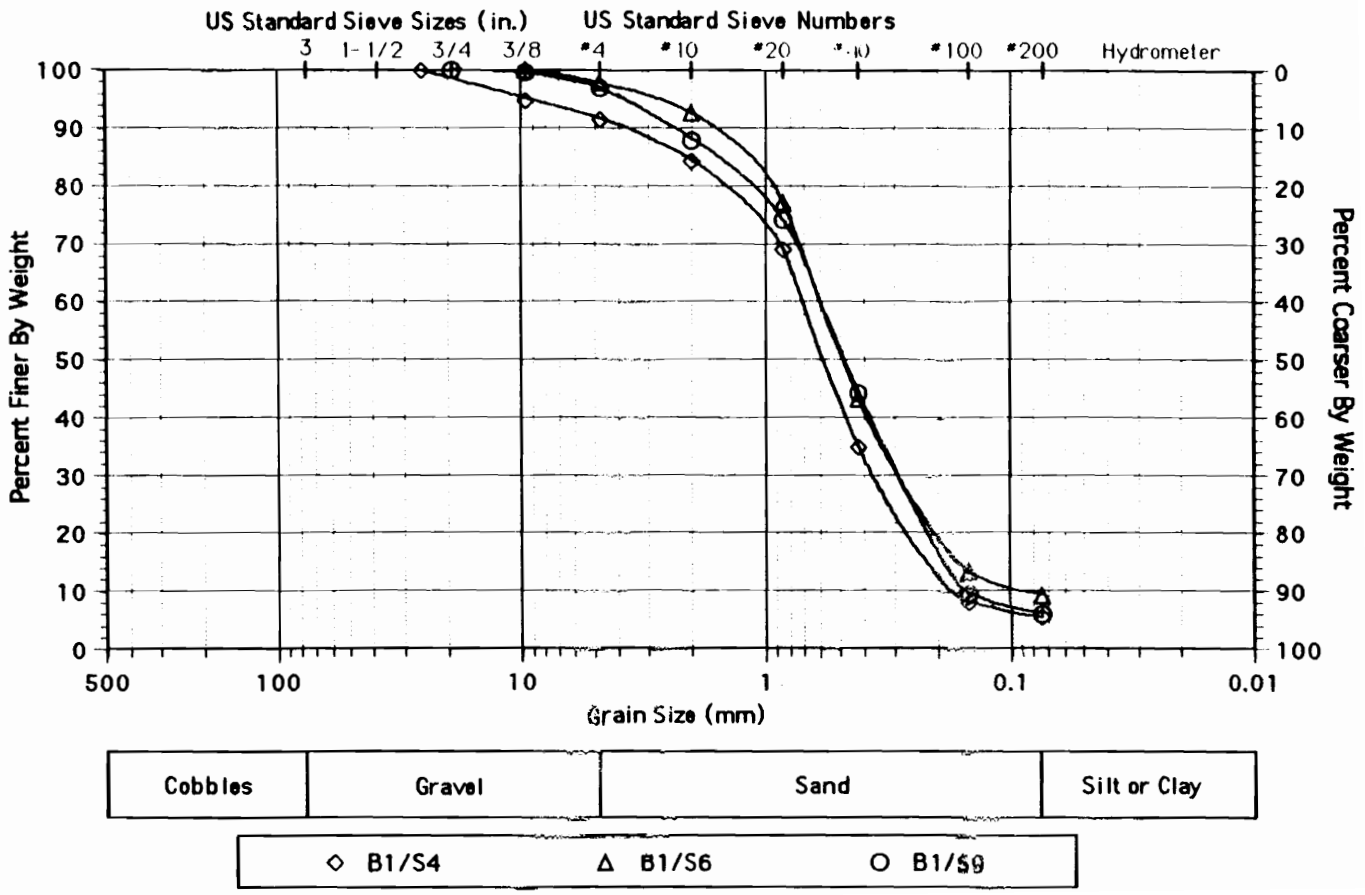

Site VC: Grain Size Distributions; B-2

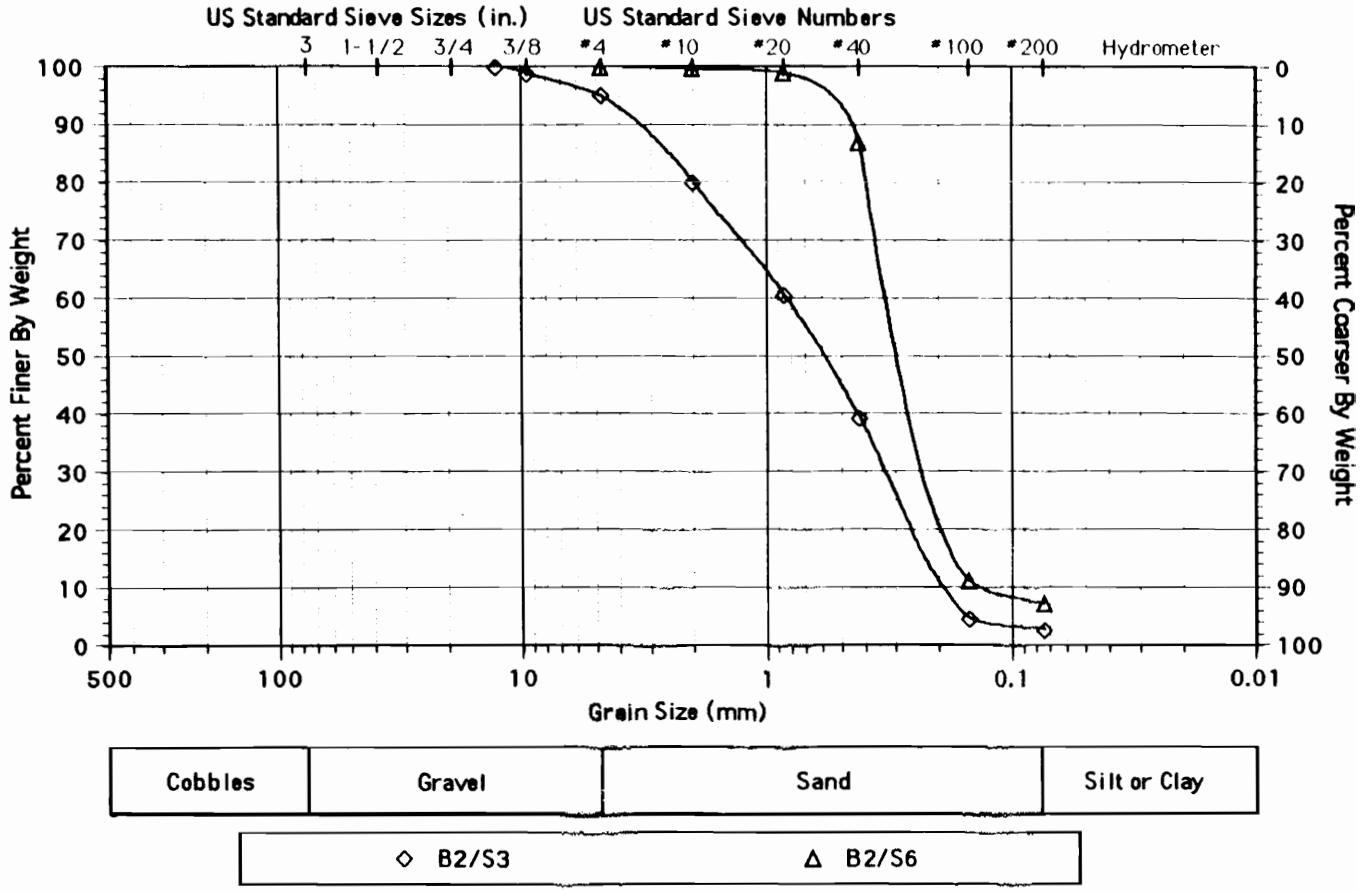

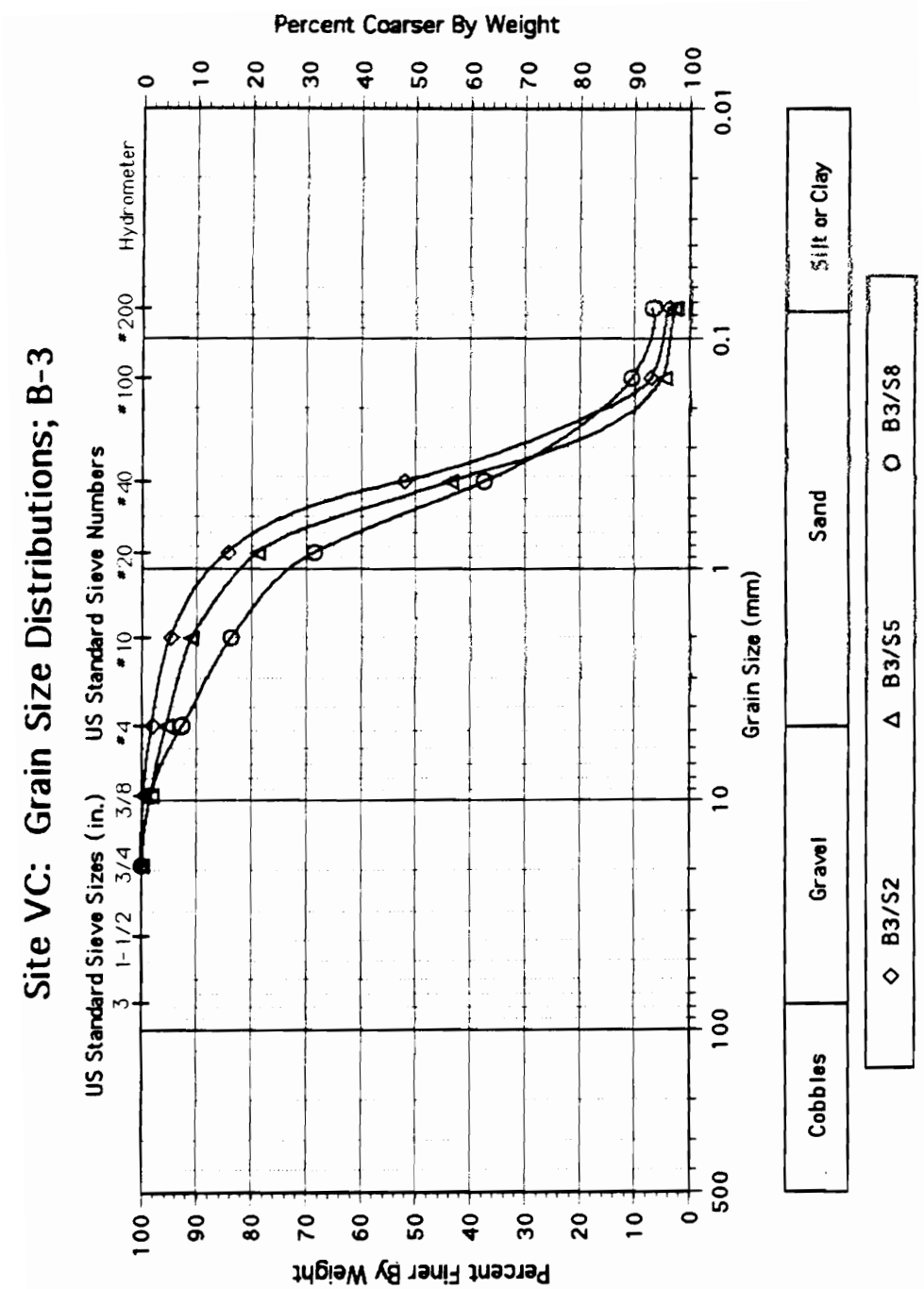
Site VC: Grain Size Distributions; B-3
Percent Coarser By Weight
US Standard Sieve Sizes (in.)
US Standard Sieve Numbers
Hydrometer
Percent Finer By Weight
Grain Size (mm)
Cobbles
Gravel
Sand
Silt or Clay
◇ B3/S2
△ B3/S5
○ B3/S8

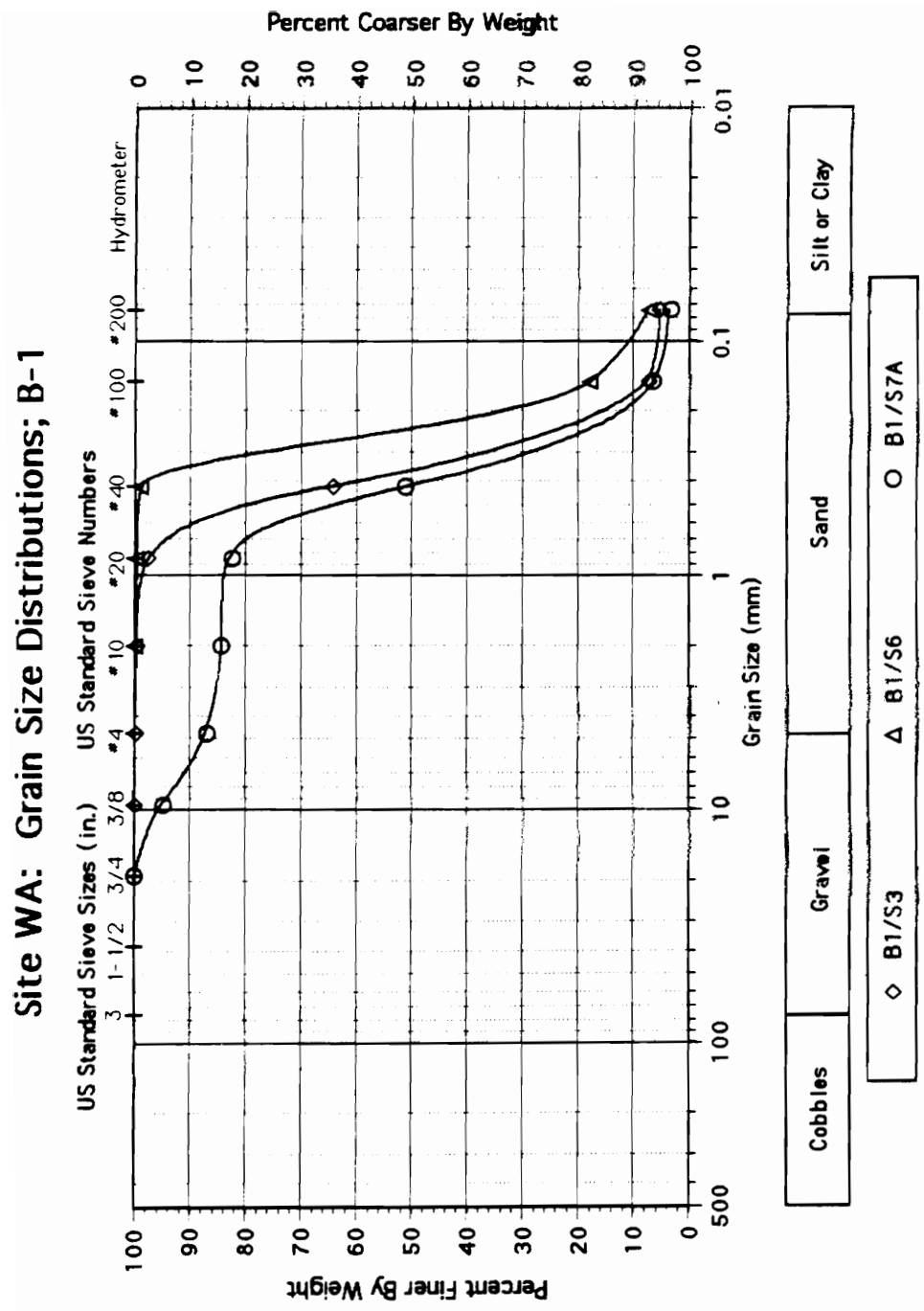
Site WA: Grain Size Distributions; B-1
Percent Coarser By Weight
Percent Finer By Weight
US Standard Sieve Sizes (in.)
US Standard Sieve Numbers
Hydrometer
Grain Size (mm)
Cobbles
Gravel
Sand
Silt or Clay
◇ B1/S3
△ B1/S6
○ B1/S7A

Site WA: Grain Size Distributions; B-2

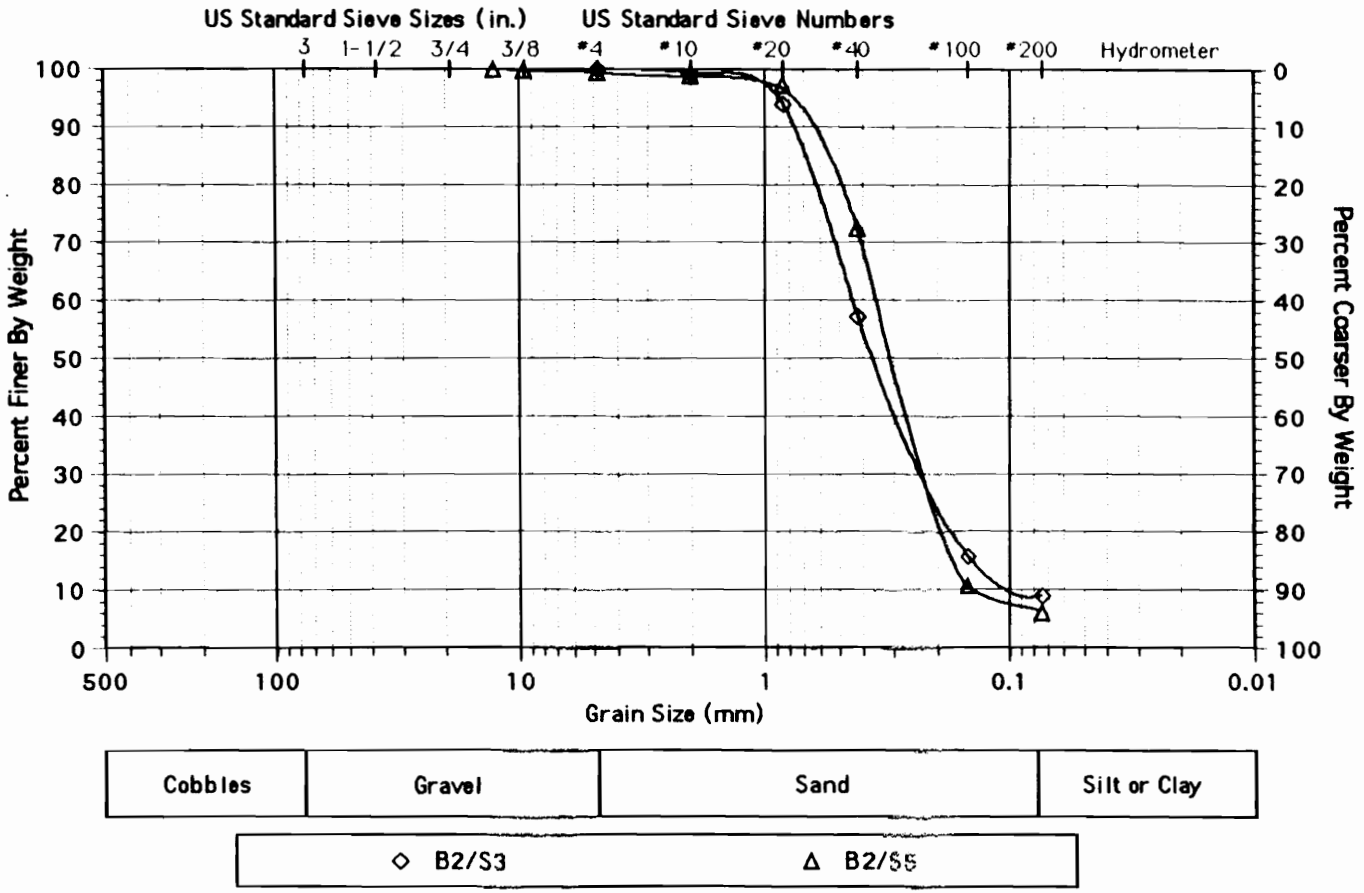

Vallonia Event Grainsize Curves

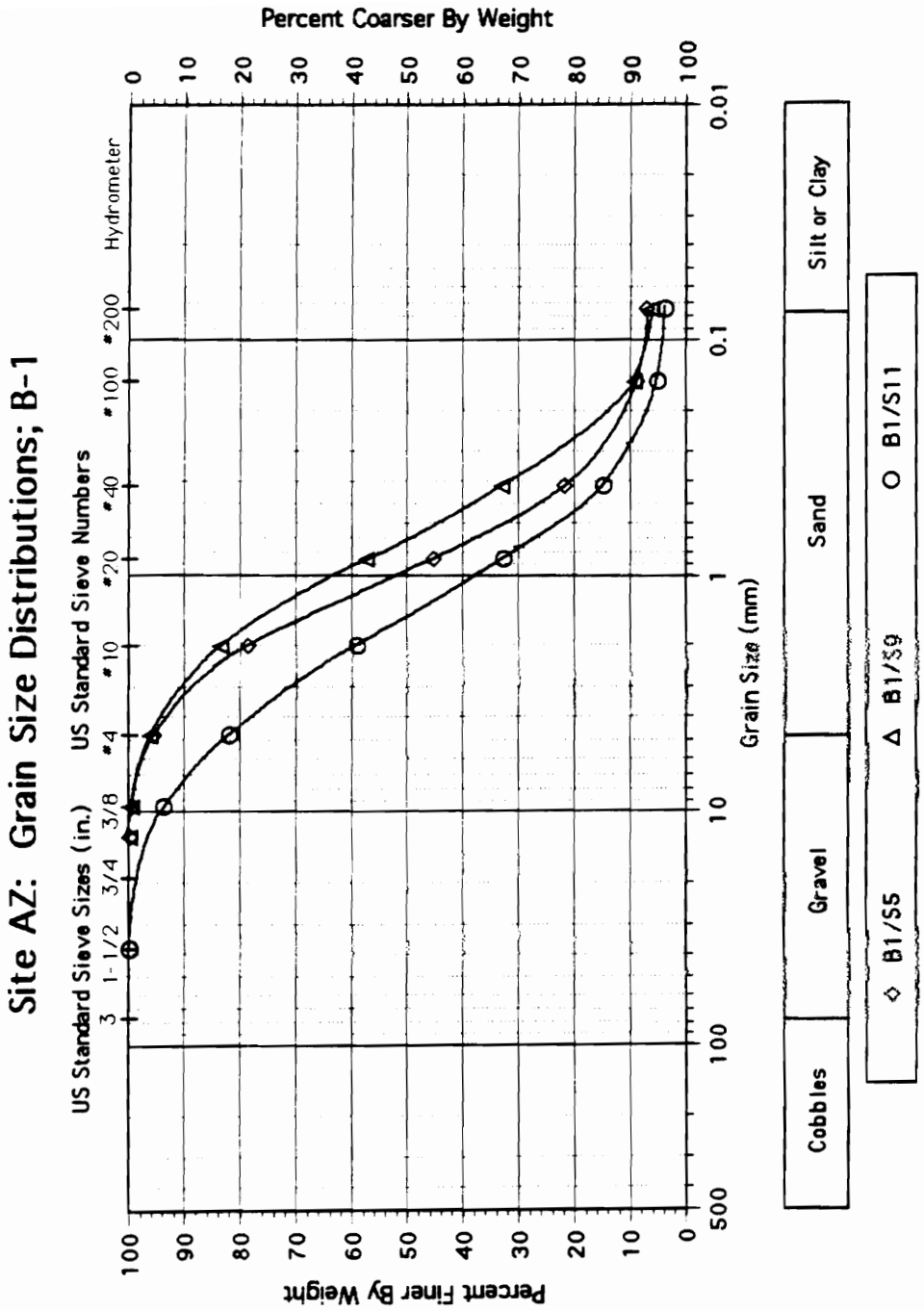
Site AZ: Grain Size Distributions; B-1
Percent Coarser By Weight
Percent Finer By Weight
US Standard Sieve Sizes (in.)
US Standard Sieve Numbers
Hydrometer
Grain Size (mm)
Cobbles
Gravel
Sand
Silt or Clay
◇ B1/S5
△ B1/S9
○ B1/S11

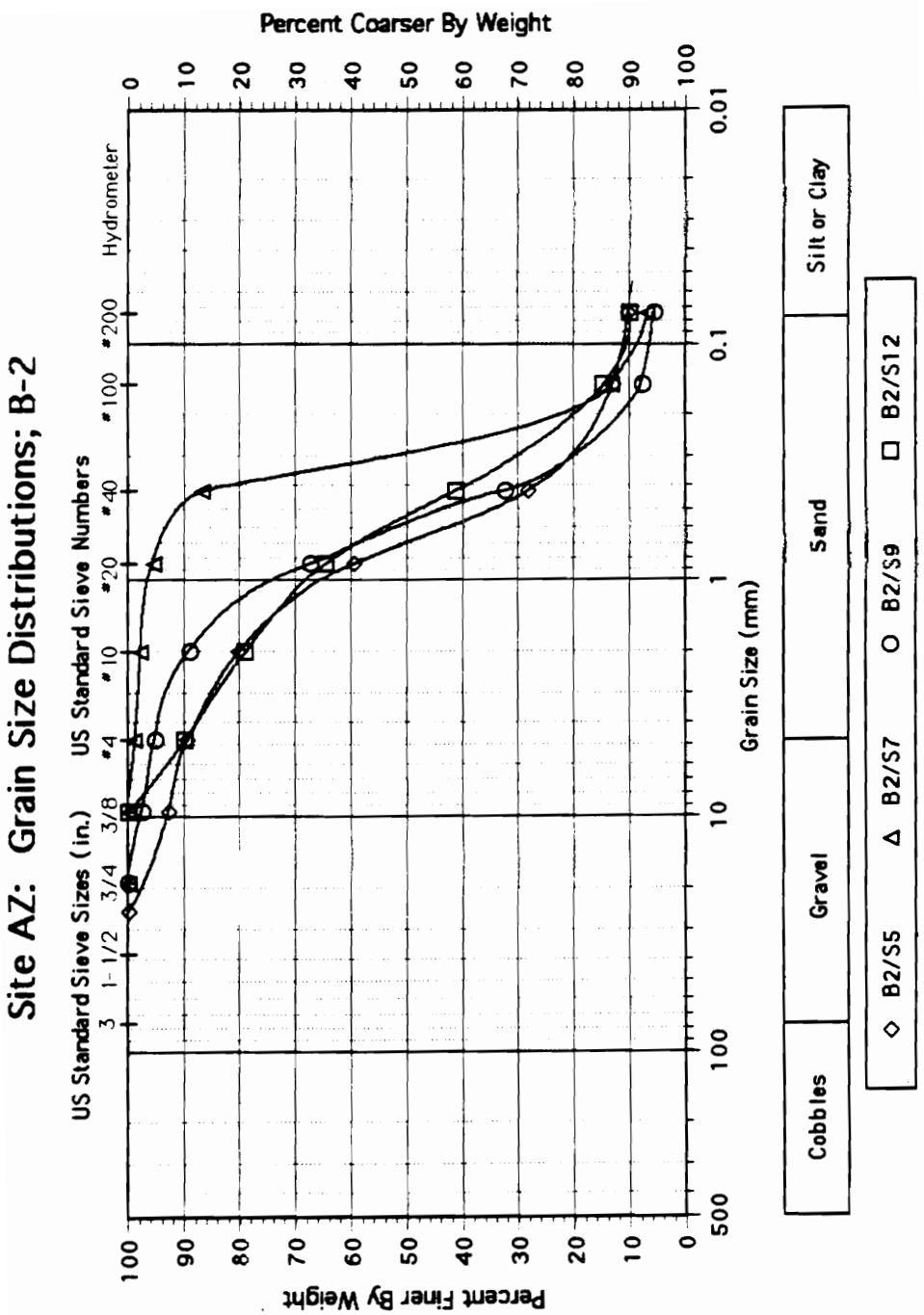
Site AZ: Grain Size Distributions; B-2
Percent Coarser By Weight
Percent Finer By Weight
US Standard Sieve Sizes (in.)
US Standard Sieve Numbers
3
1-1/2
3/4
3/8
#4
#10
#20
#40
#100
#200
Hydrometer
Grain Size (mm)
Cobbles
Gravel
Sand
Silt or Clay
B2/S5
B2/S7
B2/S9
B2/S12

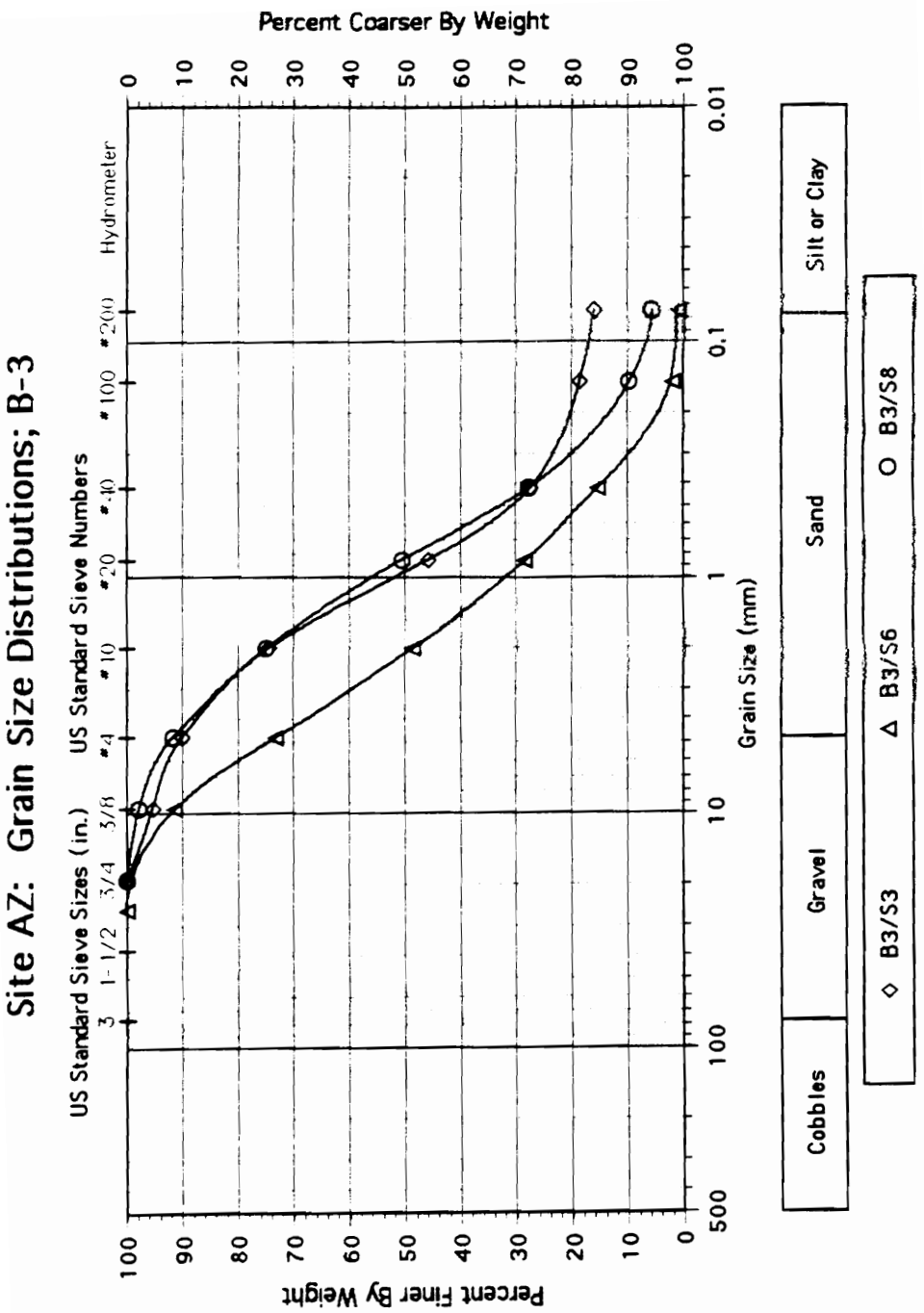
Site AZ: Grain Size Distributions; B-3
Percent Coarser By Weight
Percent Finer By Weight
US Standard Sieve Sizes (in.)
US Standard Sieve Numbers
Hydrometer
Grain Size (mm)
Cobbles
Gravel
Sand
Silt or Clay
◇ B3/S3
△ B3/S6
○ B3/S8

Site AZ: Grain Size Distributions; B-4

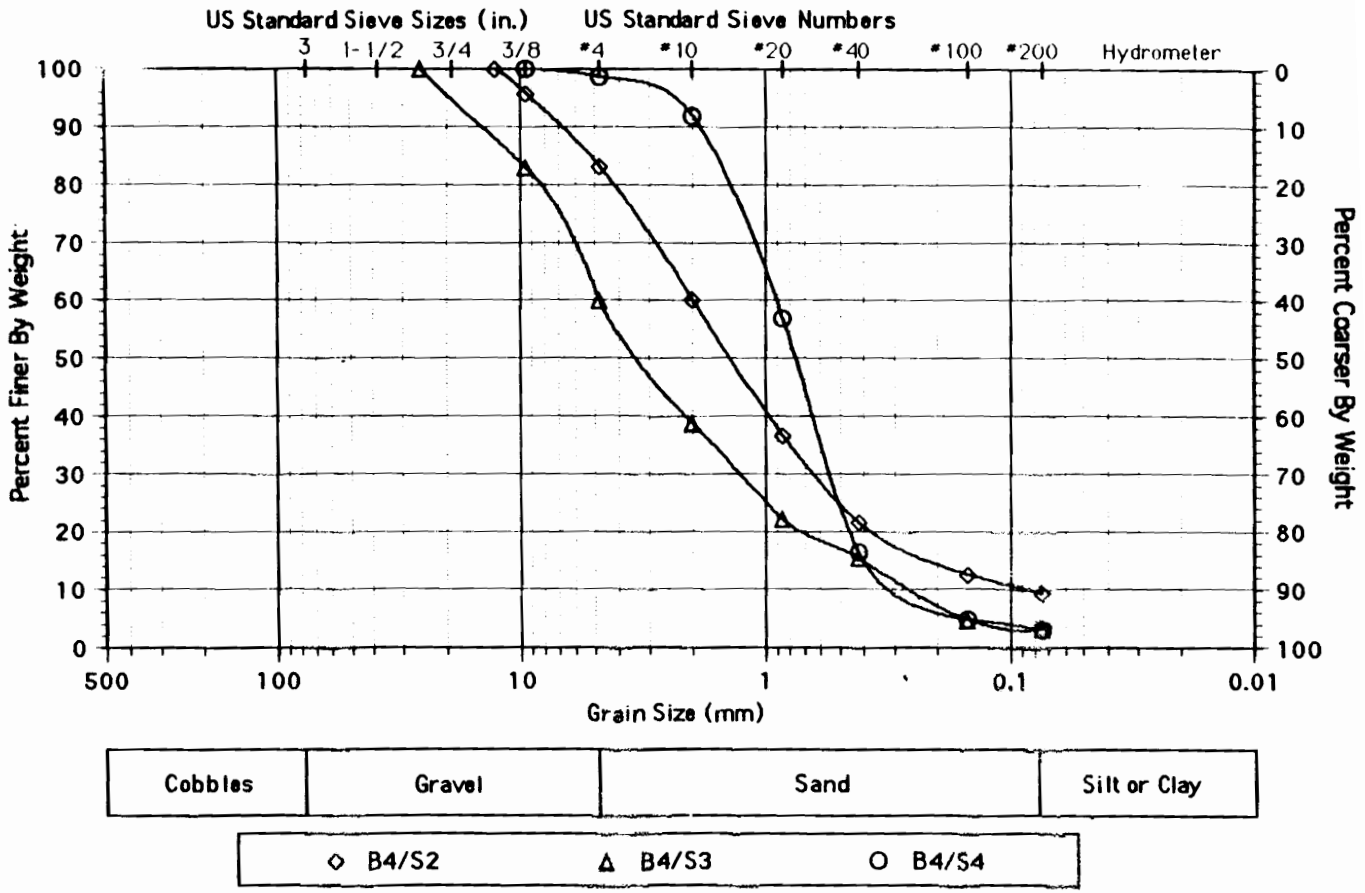

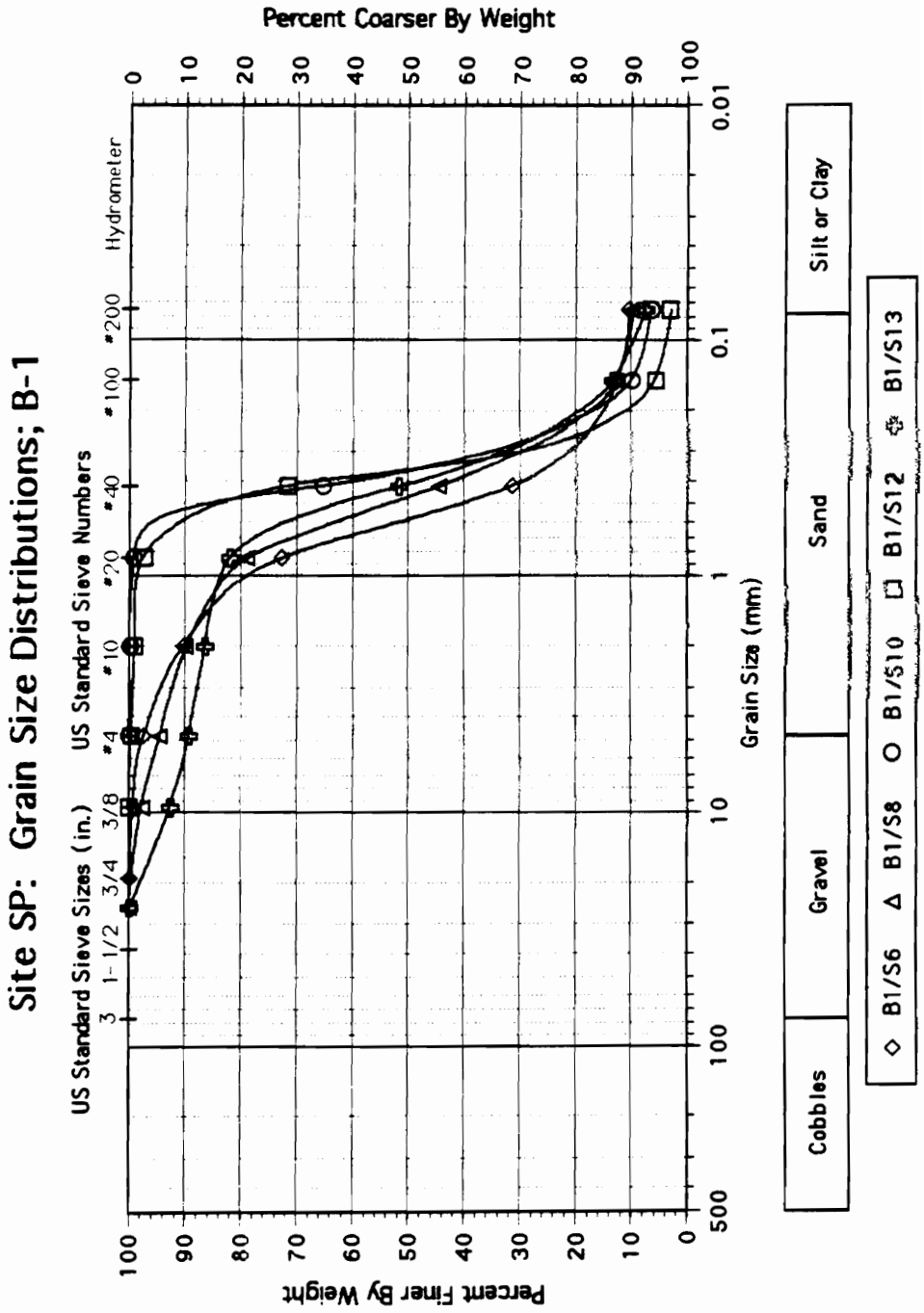
Site SP: Grain Size Distributions; B-1
Percent Coarser By Weight
US Standard Sieve Sizes (in.)
US Standard Sieve Numbers
Hydrometer
Percent Finer By Weight
Grain Size (mm)
Cobbles
Gravel
Sand
Silt or Clay
◇ B1/S6
△ B1/S8
○ B1/S10
□ B1/S12
B1/S13

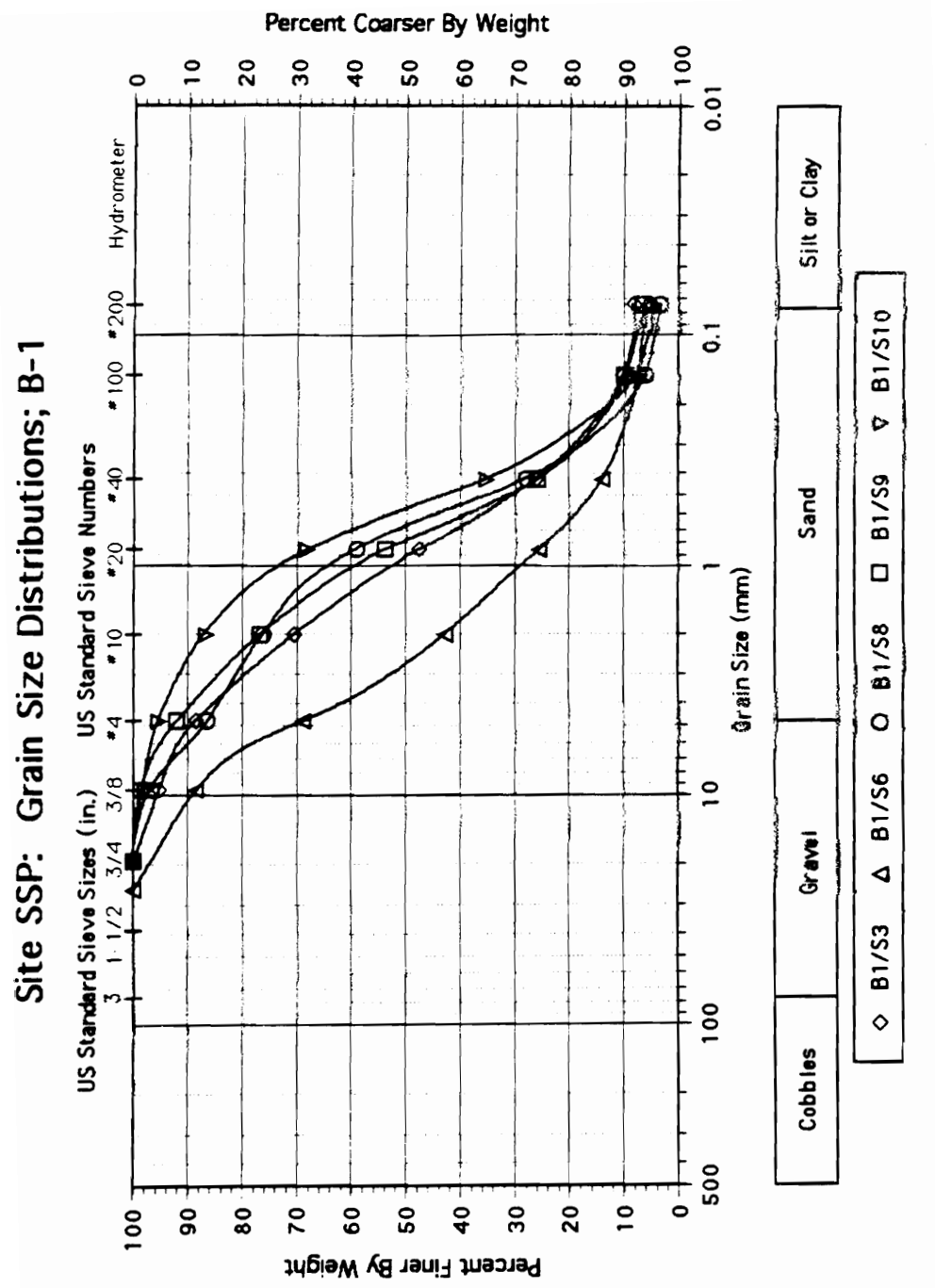
Site SSP: Grain Size Distributions; B-1
Percent Coarser By Weight
Percent Finer By Weight
US Standard Sieve Sizes (in.)
US Standard Sieve Numbers
Hydrometer
Grain Size (mm)
Cobbles
Gravel
Sand
Silt or Clay
B1/S3
B1/S6
B1/S8
B1/S9
B1/S10

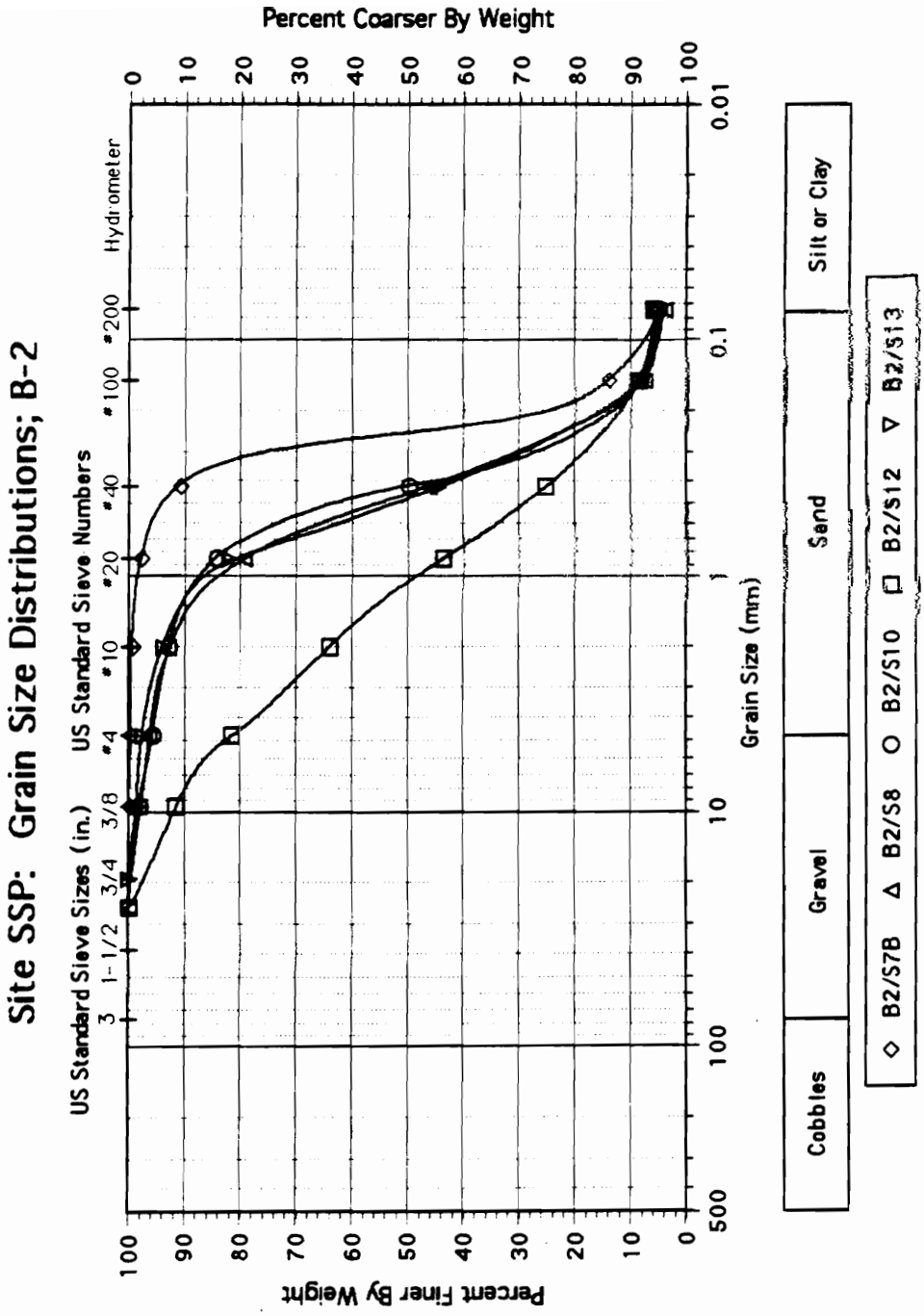
Site SSP: Grain Size Distributions; B-2
Percent Coarser By Weight
Percent Finer By Weight
US Standard Sieve Sizes (in.)
US Standard Sieve Numbers
Hydrometer
Grain Size (mm)
Cobbles
Gravel
Sand
Silt or Clay
◇ B2/S7B △ B2/S8 ○ B2/S10 □ B2/S12 ▽ B2/S13

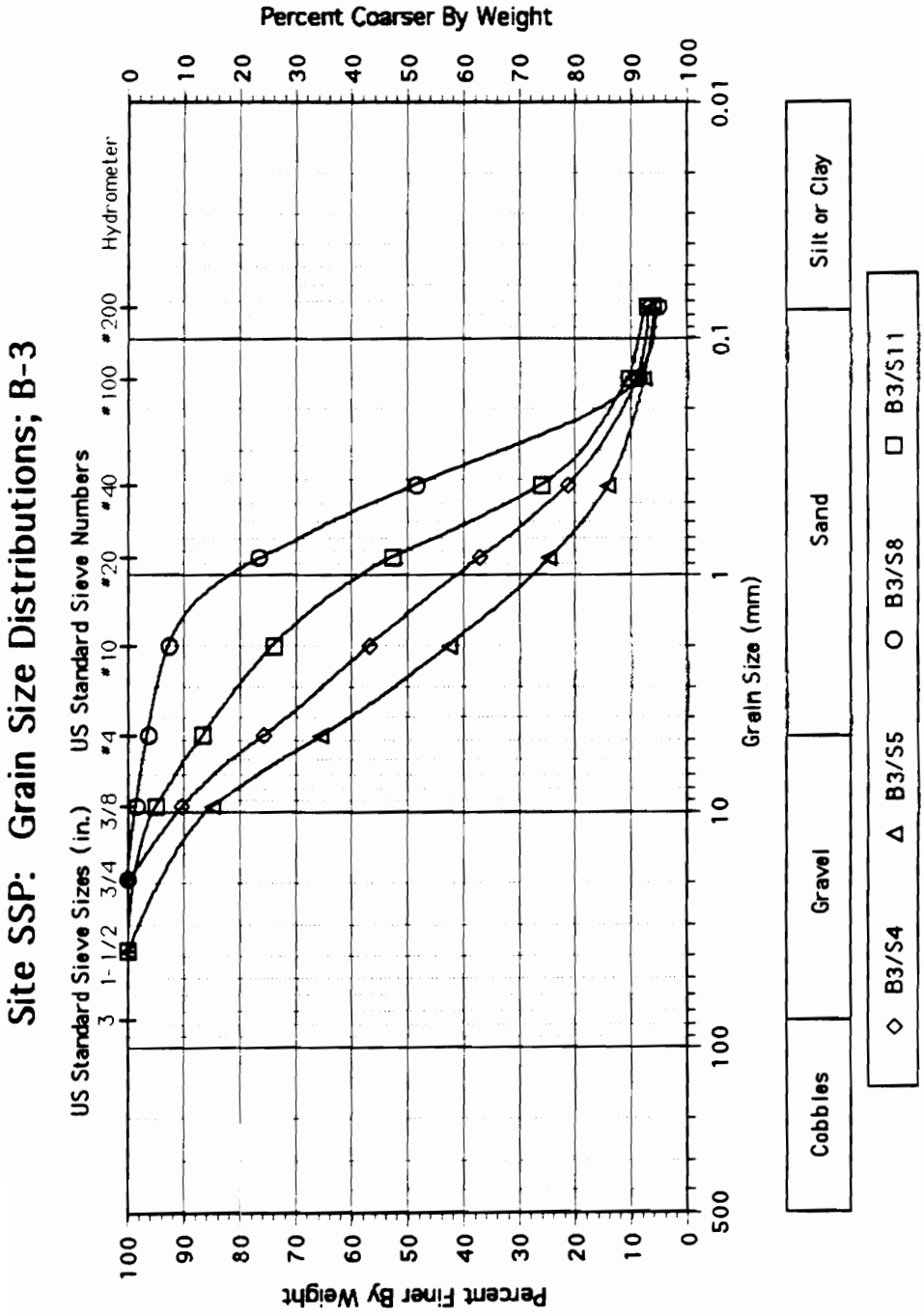
Site SSP: Grain Size Distributions; B-3
Percent Coarser By Weight
Percent Finer By Weight
US Standard Sieve Sizes (in.)
US Standard Sieve Numbers
Hydrometer
Grain Size (mm)
Cobbles
Gravel
Sand
Silt or Clay
B3/S4
B3/S5
B3/S8
B3/S11

Waverly Event Grainsize Curves

Site MV: Grain Size Distributions; B-1

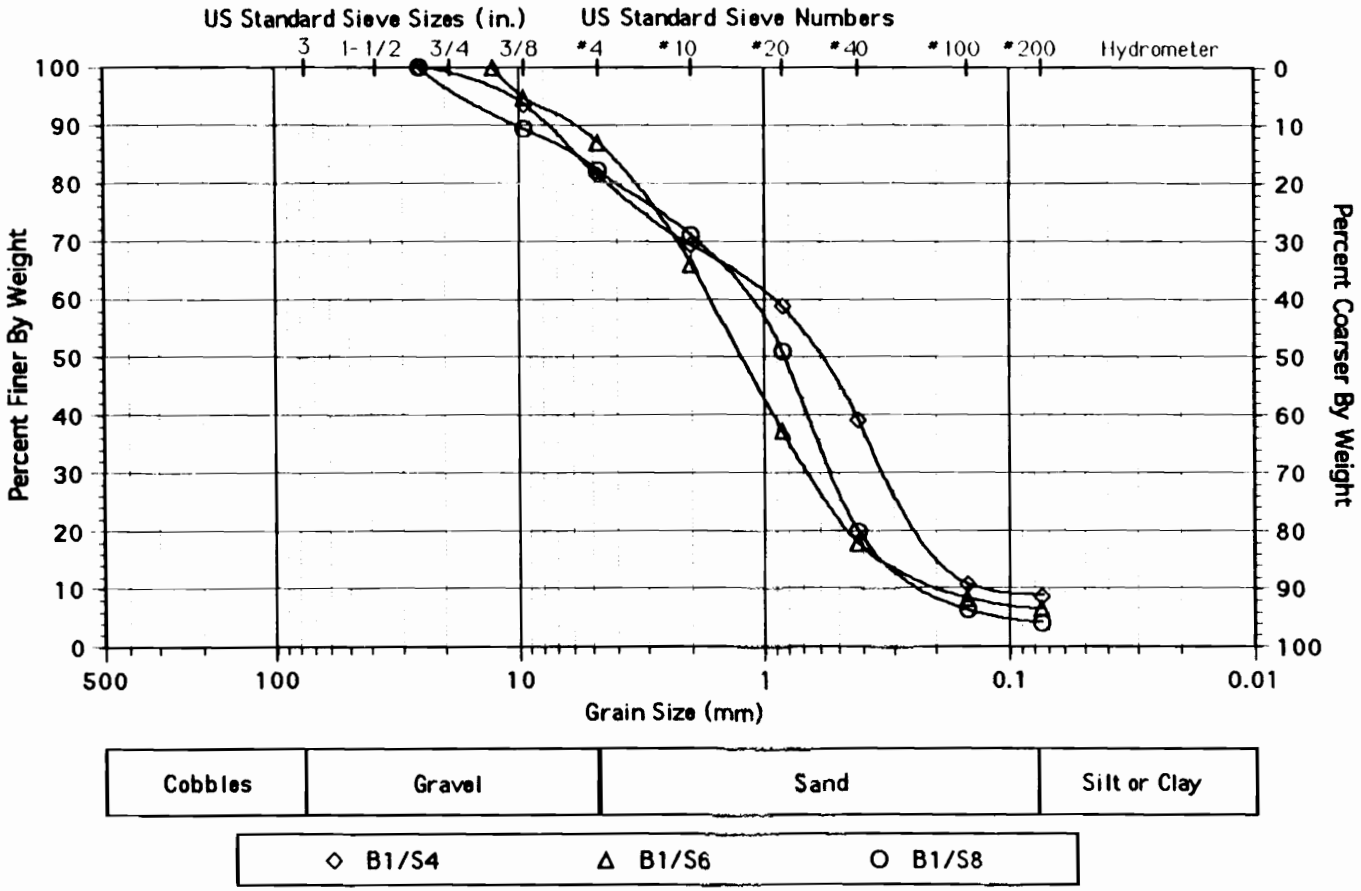

Site MV: Grain Size Distributions; B-2

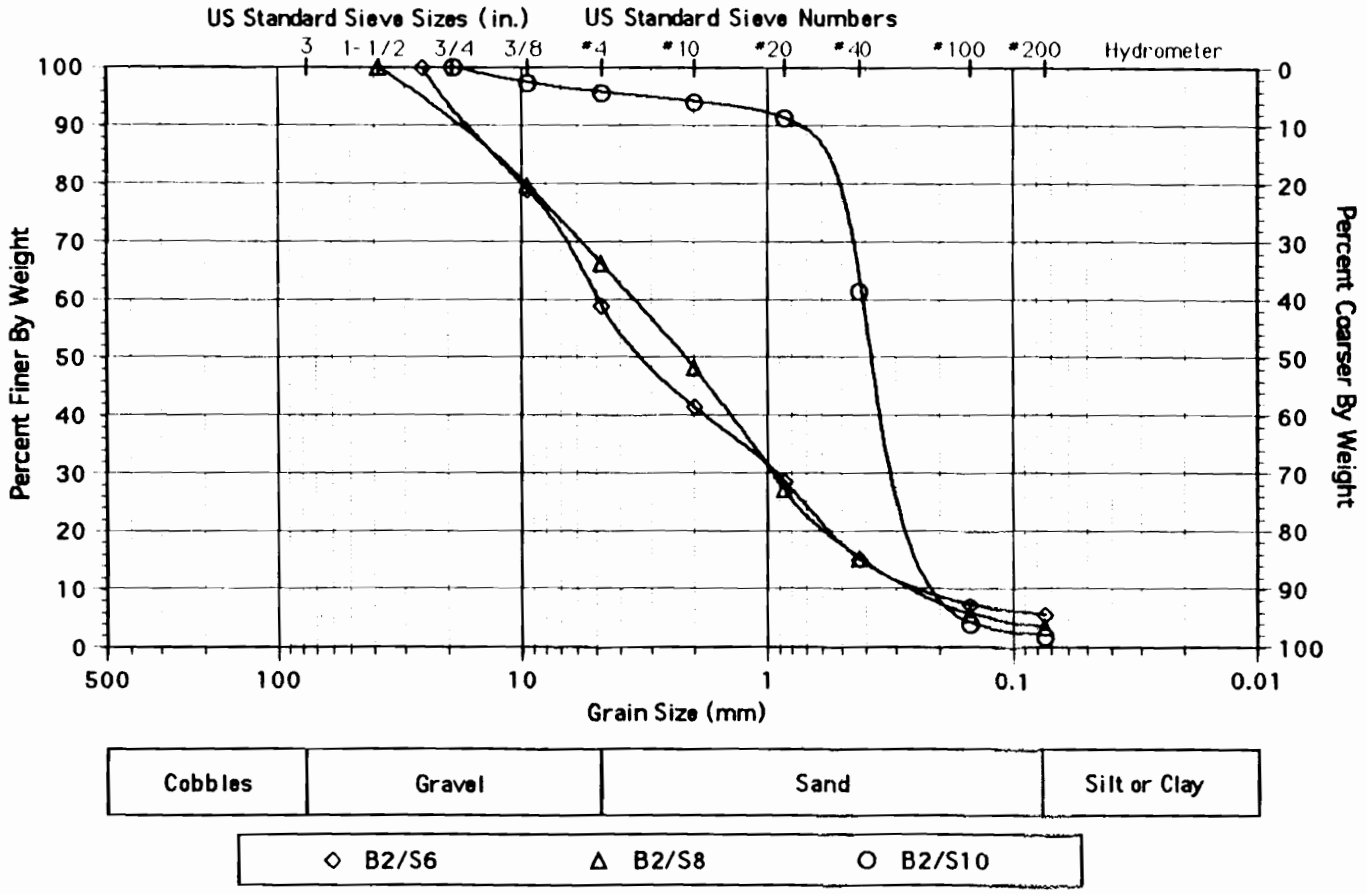

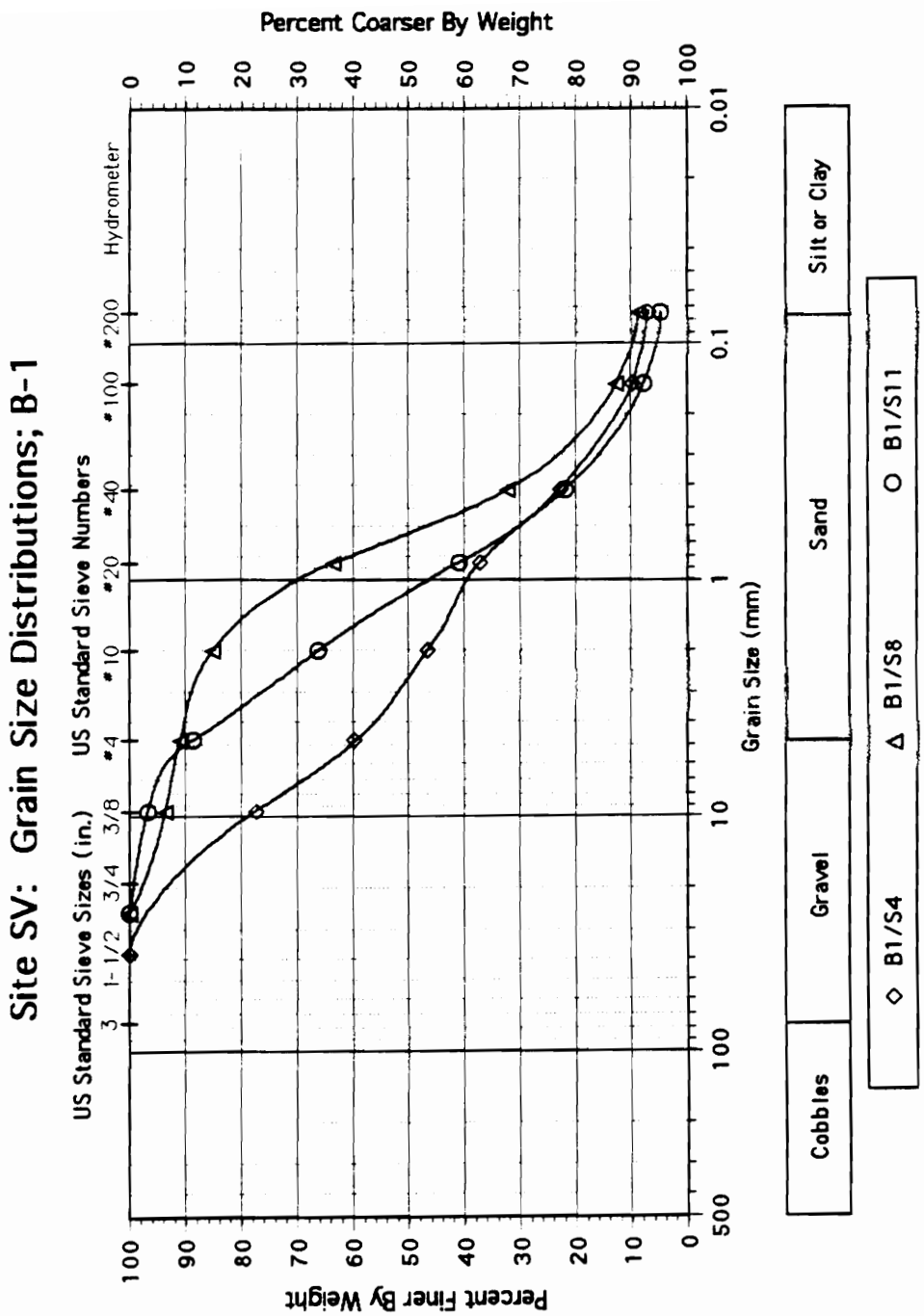
Site SV: Grain Size Distributions; B-1
Percent Coarser By Weight
US Standard Sieve Sizes (in.)
US Standard Sieve Numbers
Hydrometer
Percent Finer By Weight
Grain Size (mm)
Cobbles
Gravel
Sand
Silt or Clay
◇ B1/S4
△ B1/S8
○ B1/S11

Site SV: Grain Size Distributions; B-2

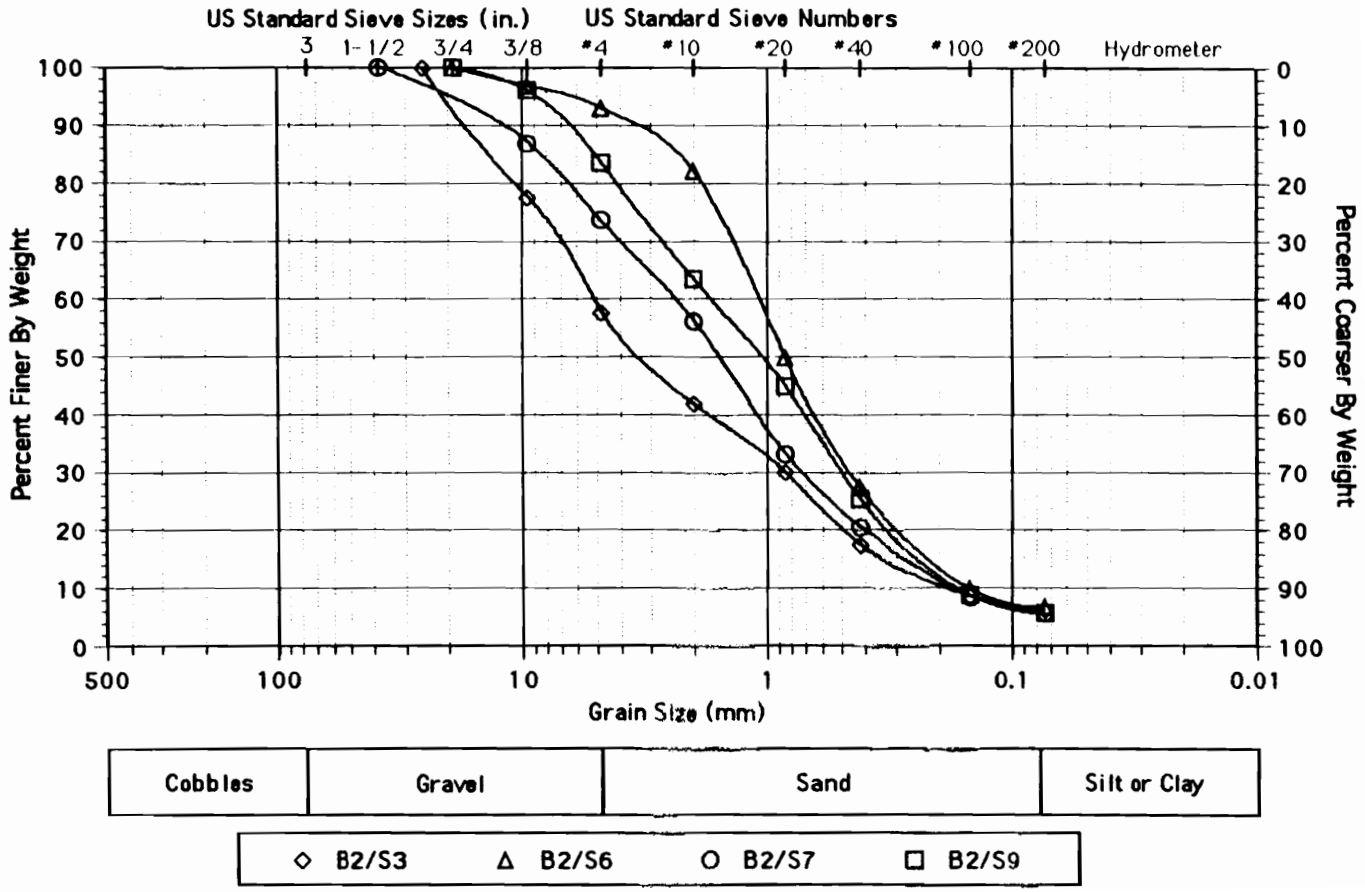

Grainsize Curves for Vincennes Event

Index Density and Specific Gravity Test Specimens

Site MA: In-Situ Density Test # 1 and Dr Specimen

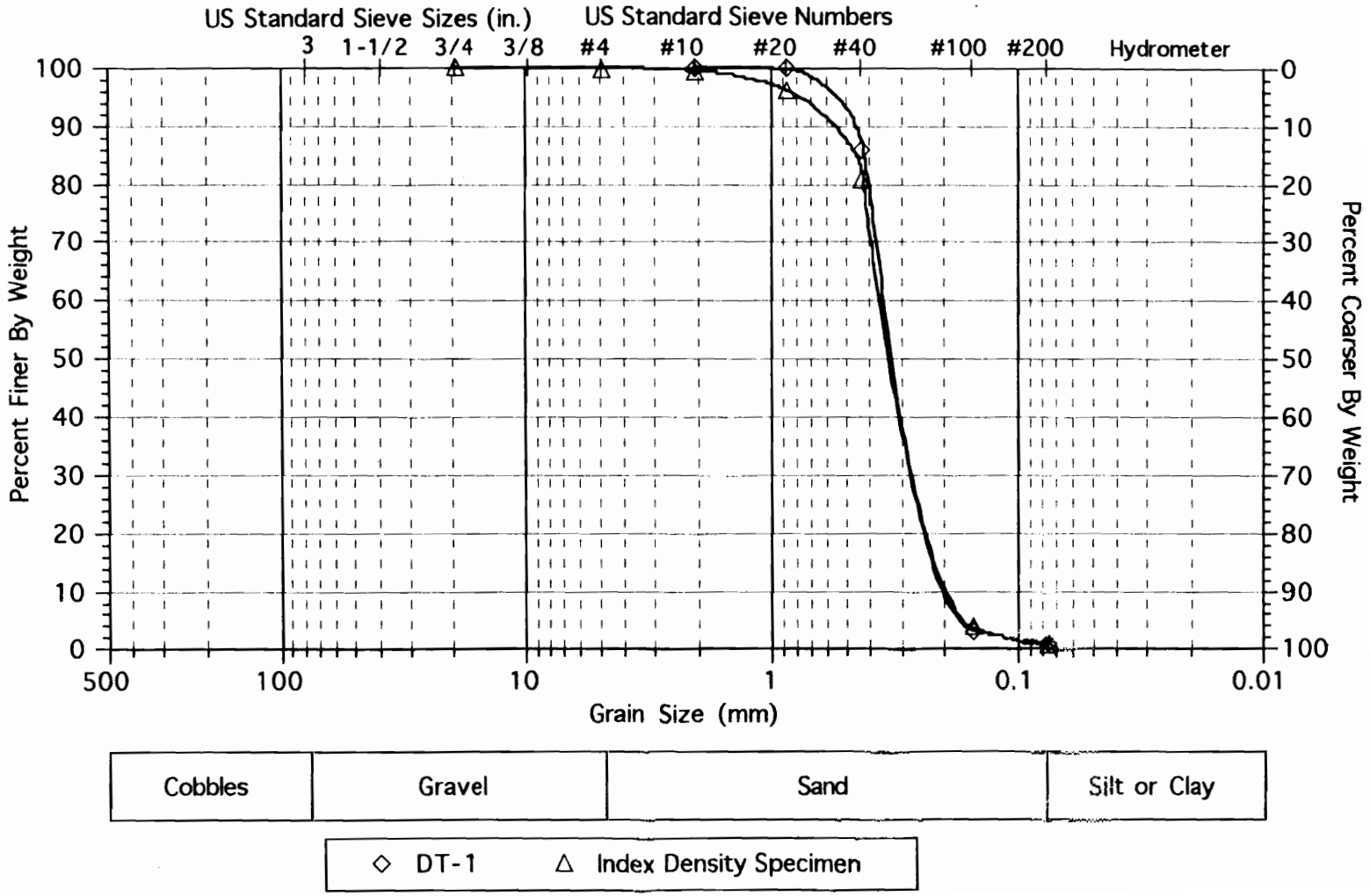

Site MA: In-Situ Density Test #'s 2,3,4 and Dr Specimen

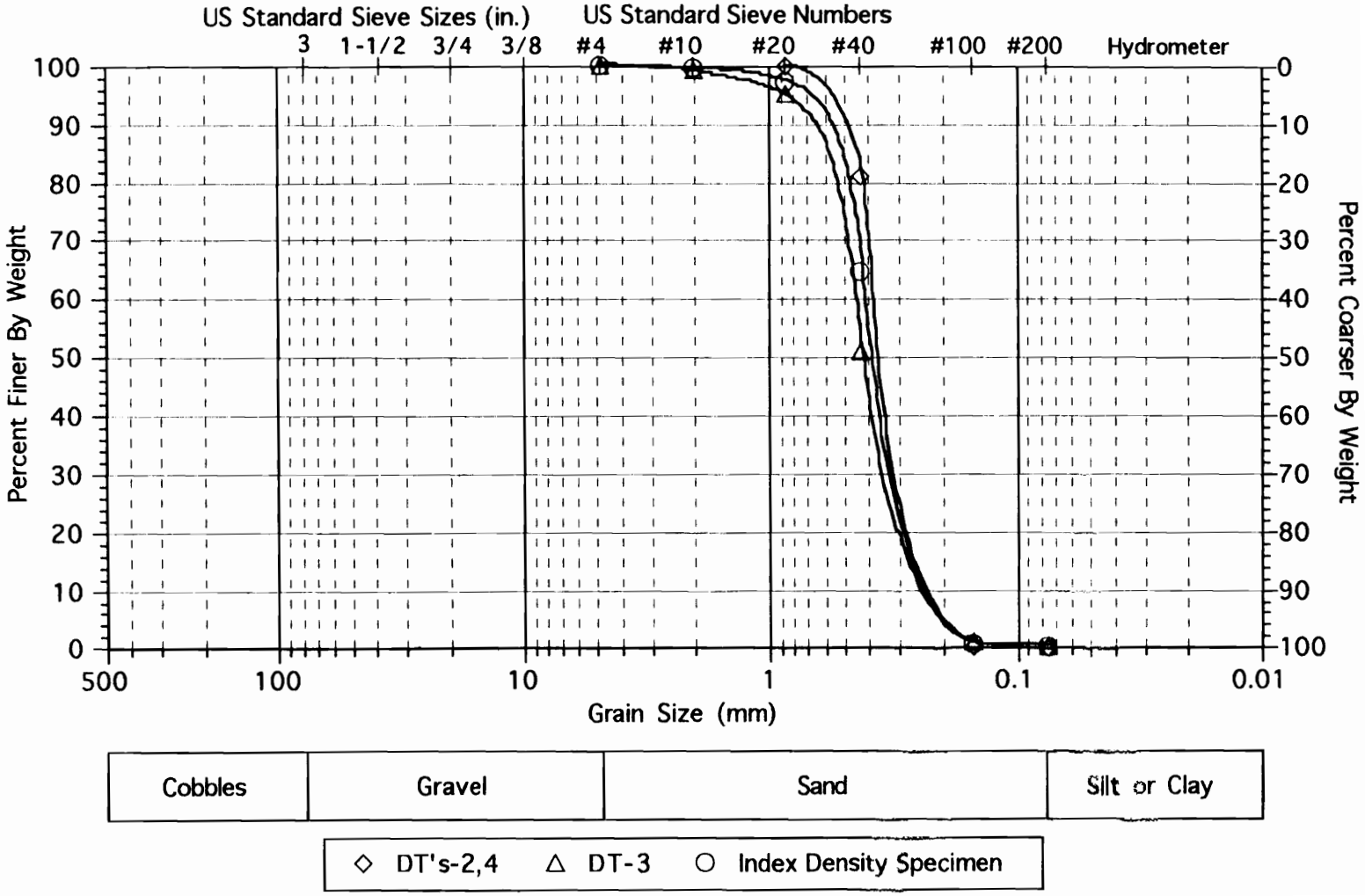

Site PB: In-Situ Density Tests #'s 1,2,3A and Dr Specimen

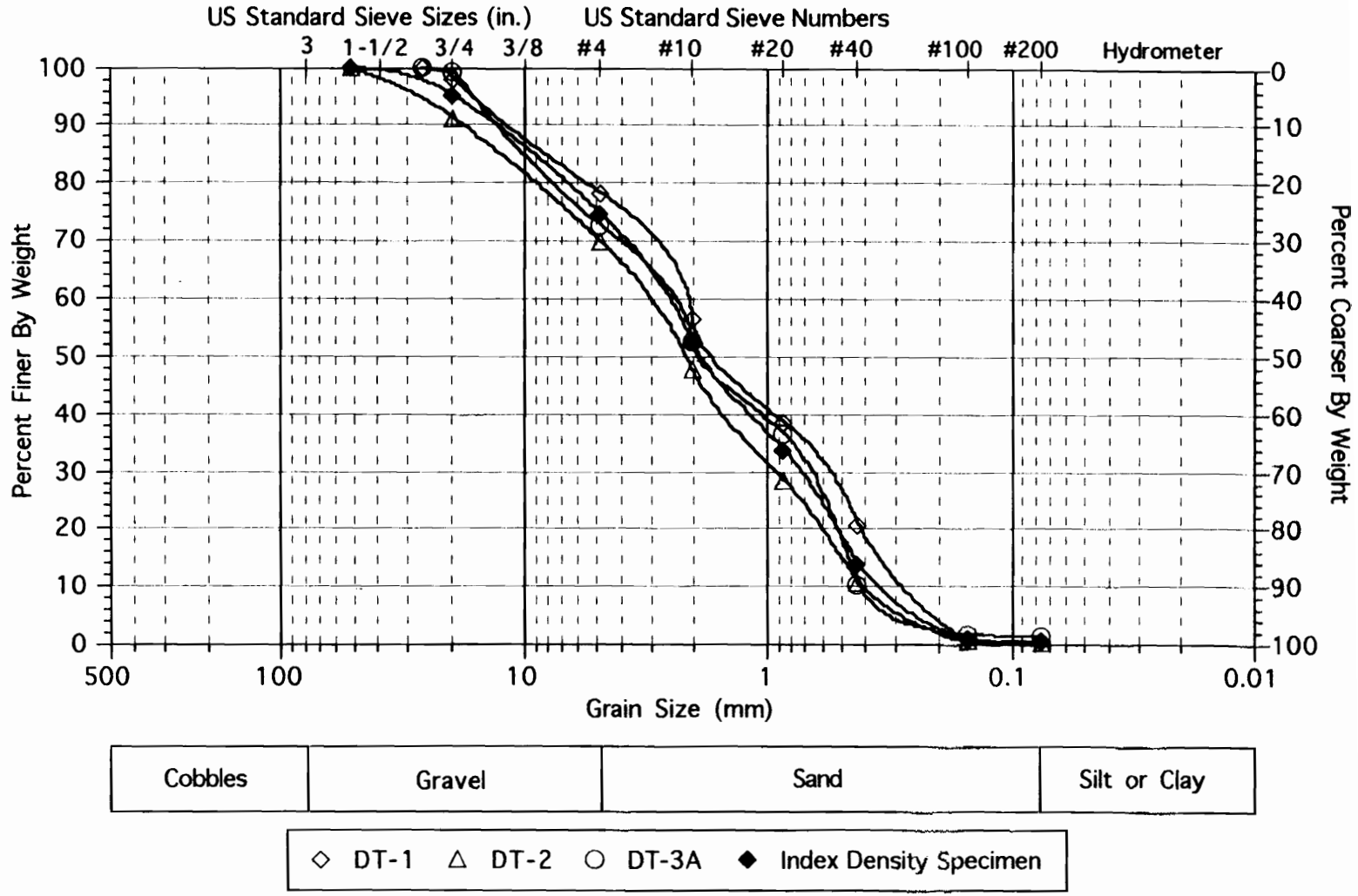

Site PB: In-Situ Density Tests #'s 3,6 and Dr Specimen

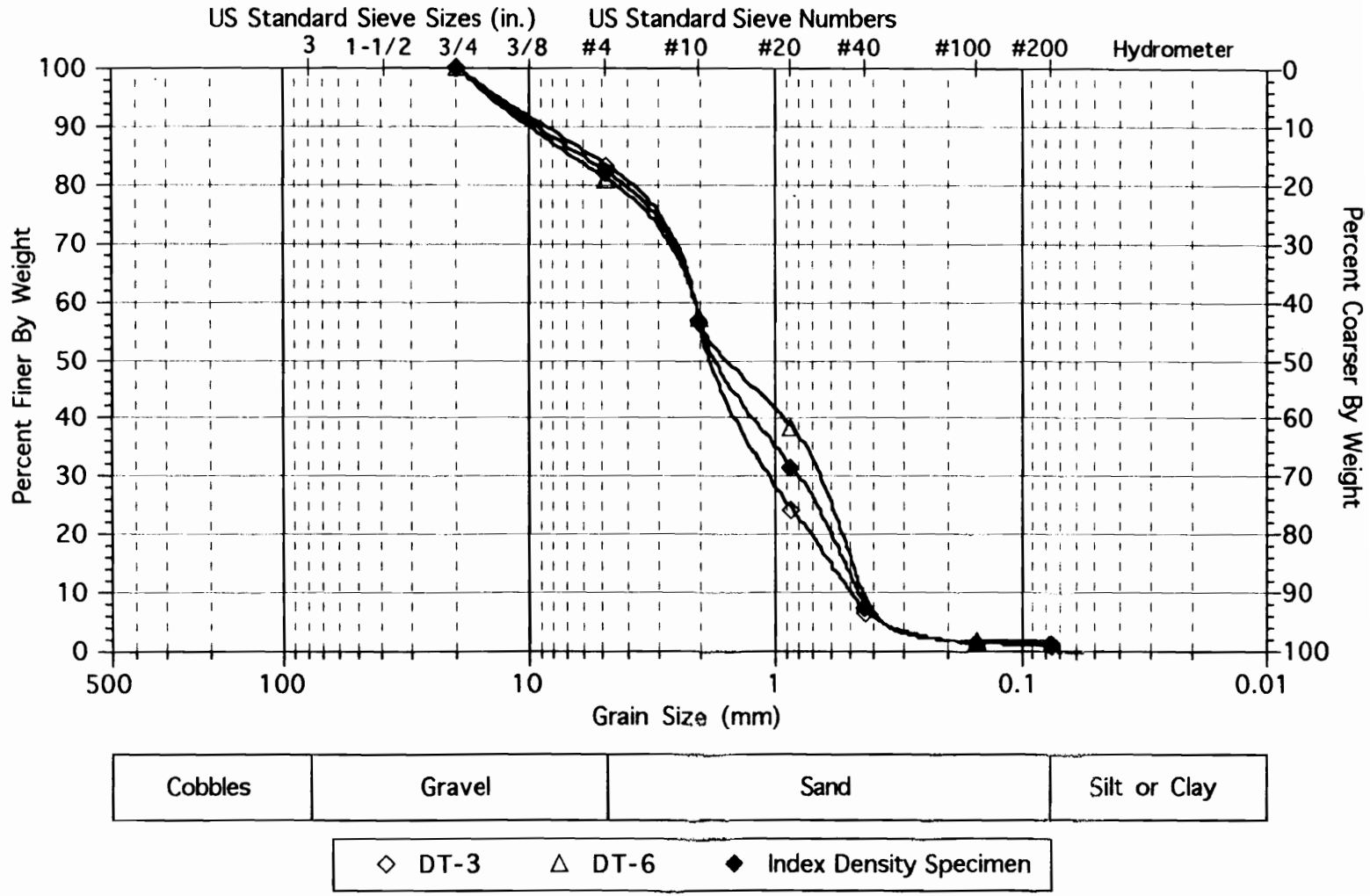

Site PB: In-Situ Density Tests #'s 4,5 and Dr Specimen

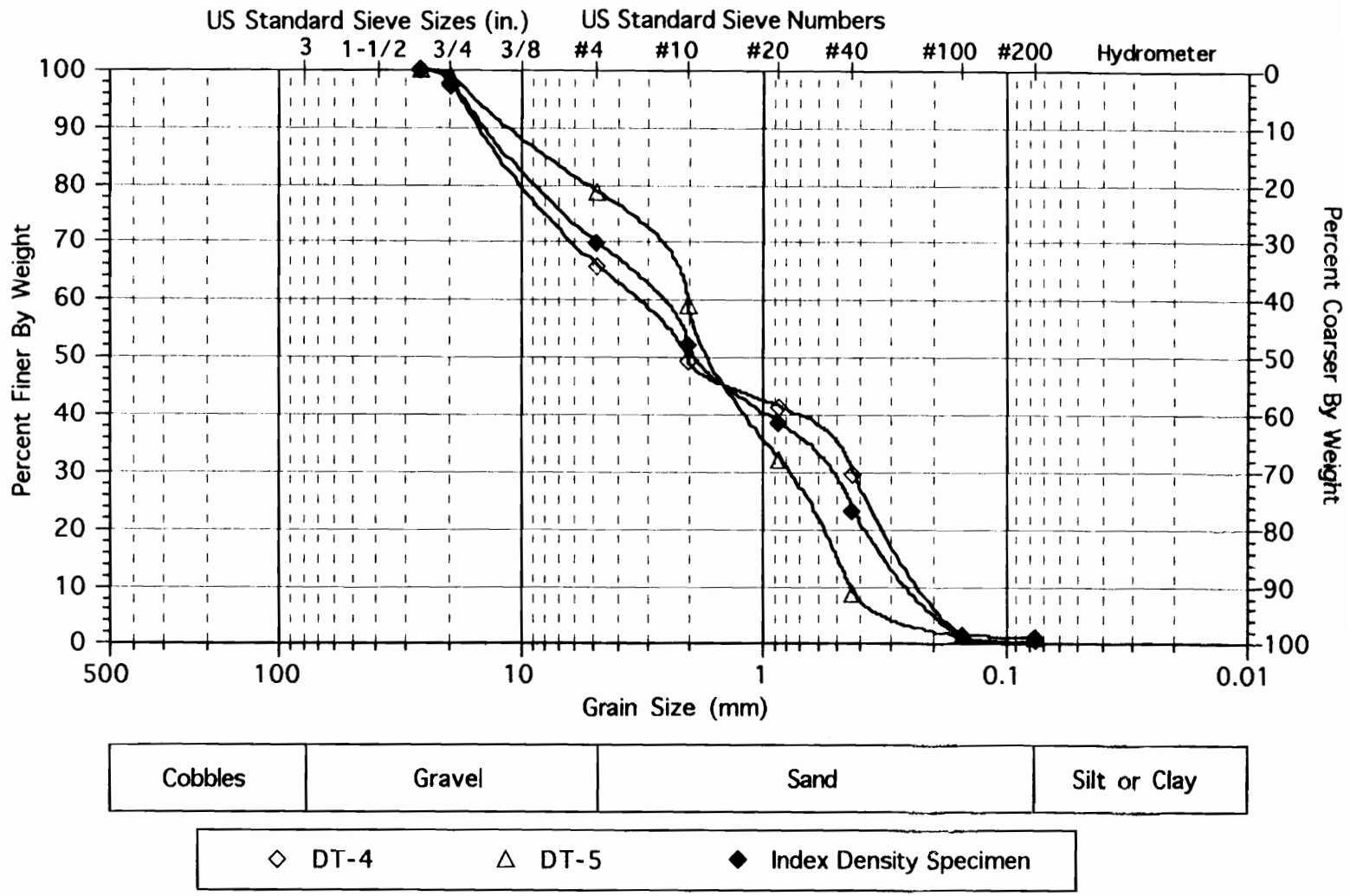

Site PB: Index Density Specimen, DT #'s 7,7A

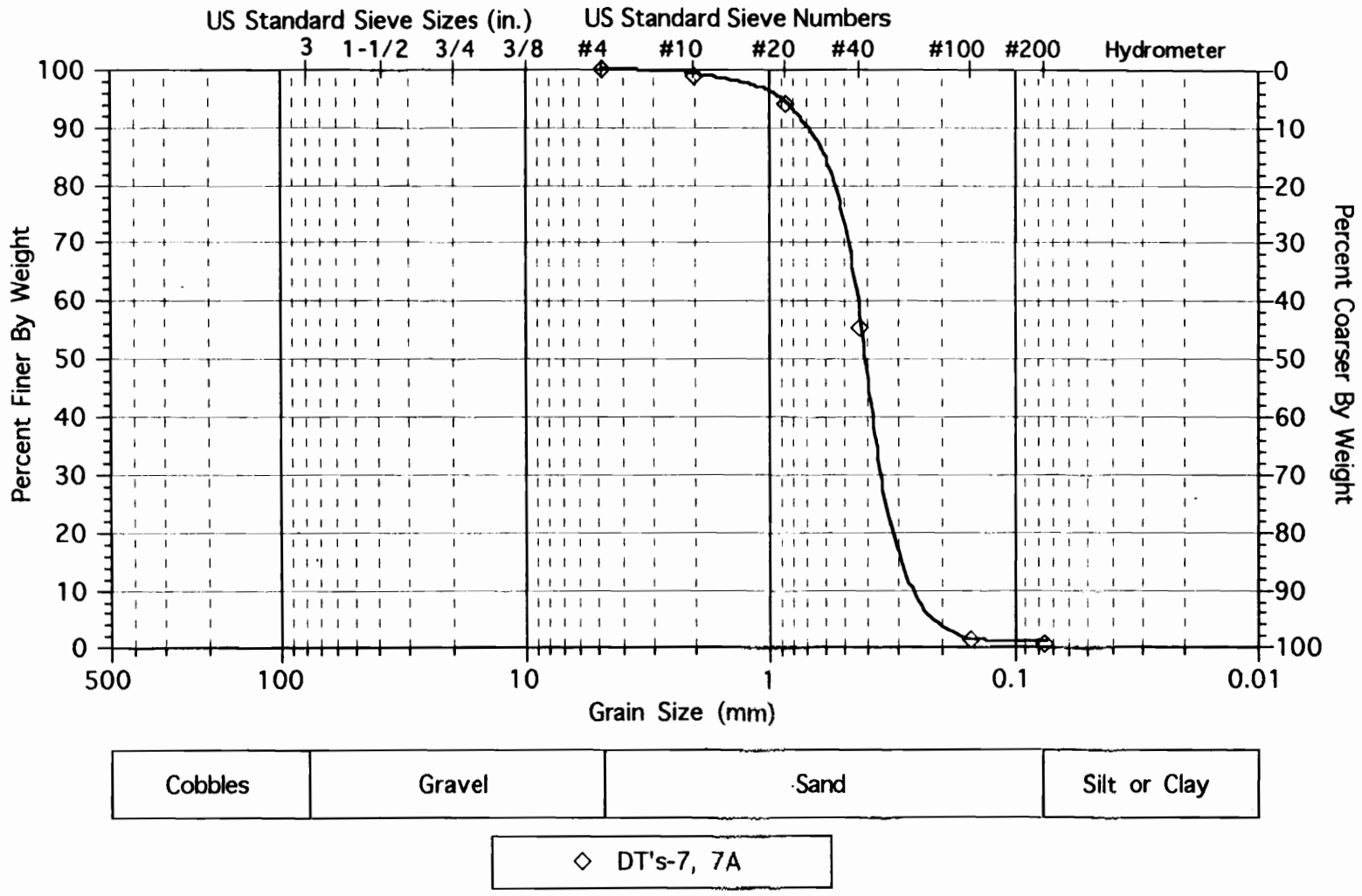

Site PB: Grain Size Distributions; All Density Test Samples

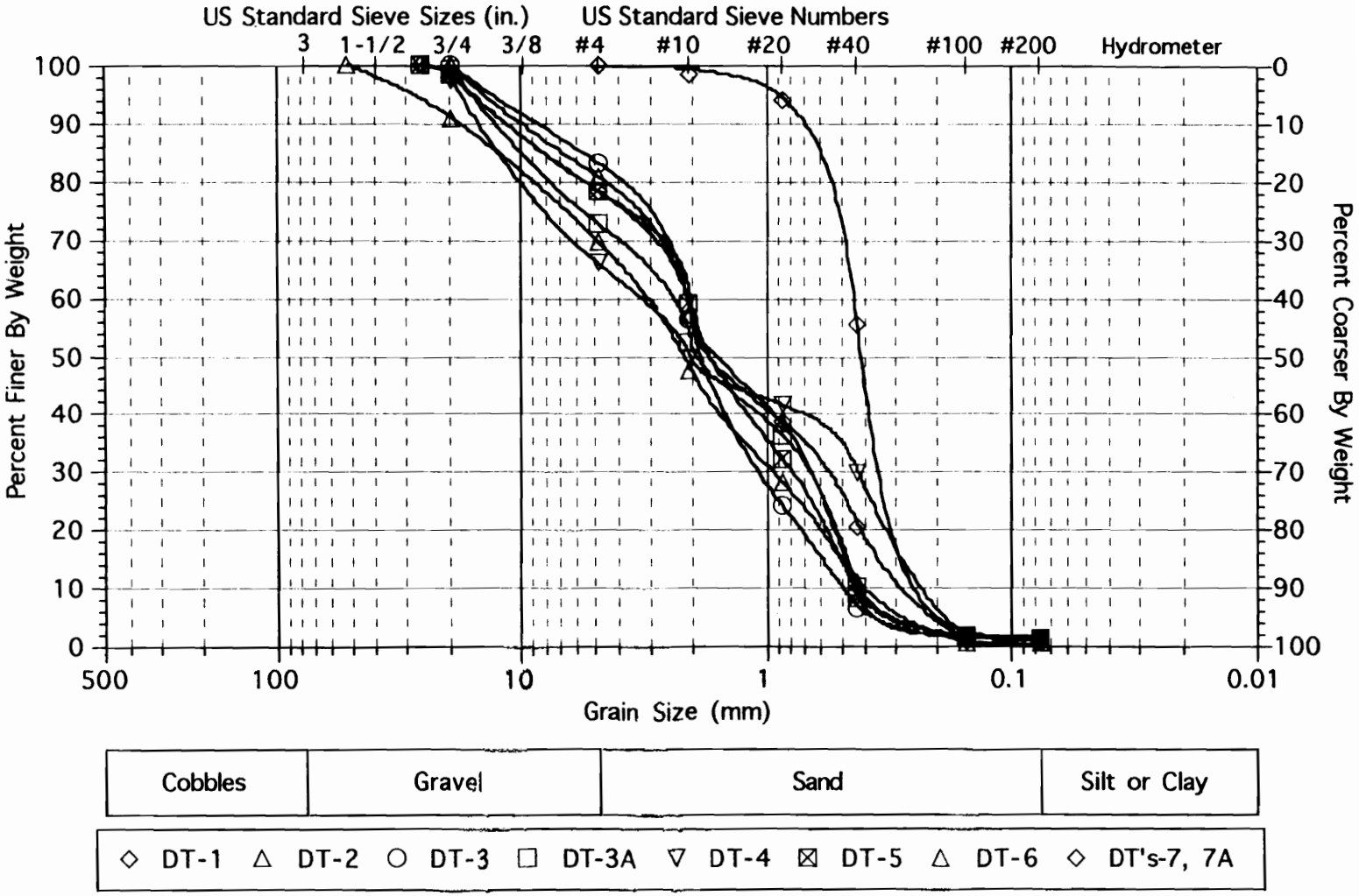

Site RF: In-Situ Density Tests #'s 1-3 and Index Density Specimen

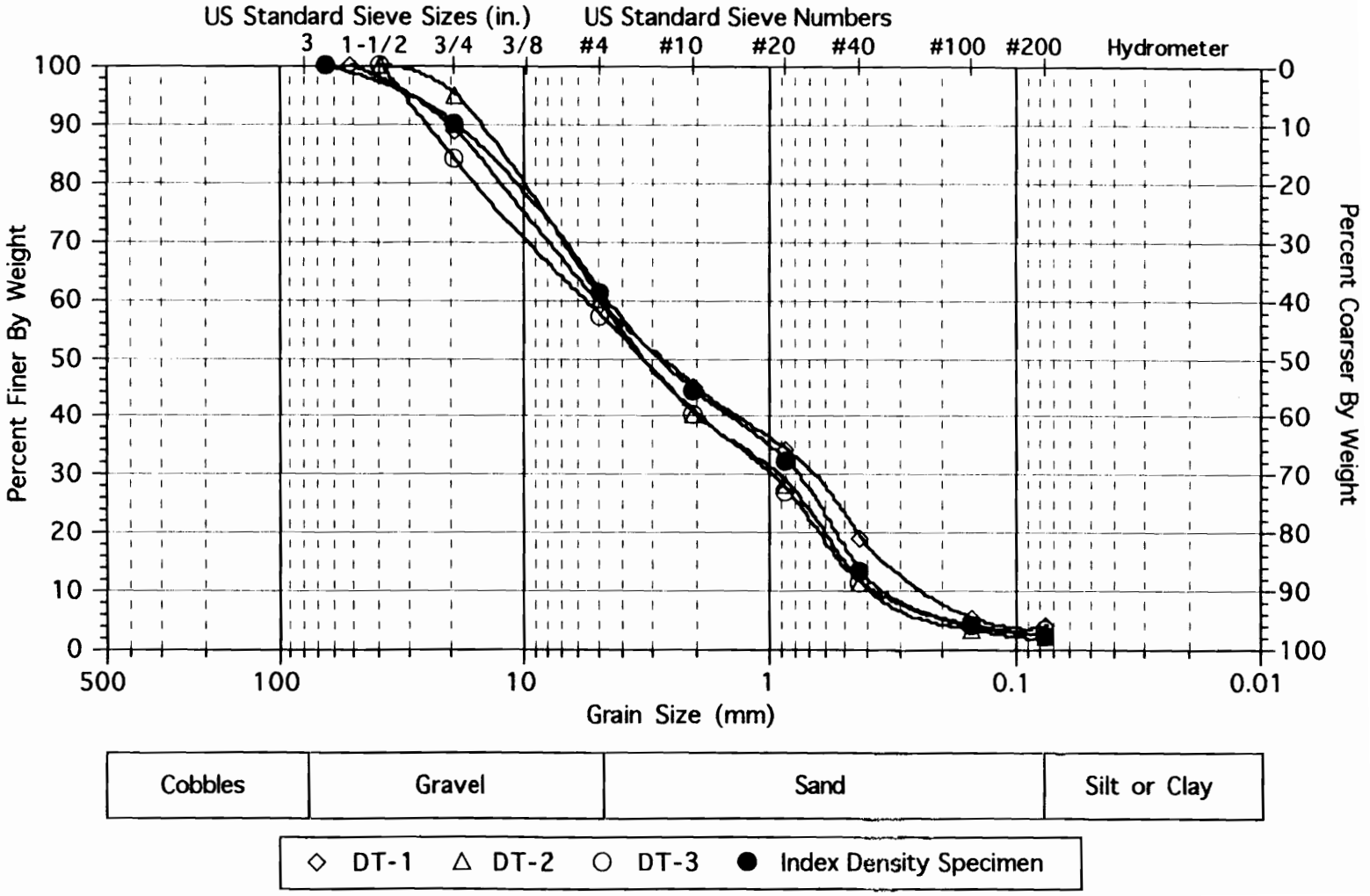

Site RF: In-Situ Density Test # 4 and Index Density Specimen

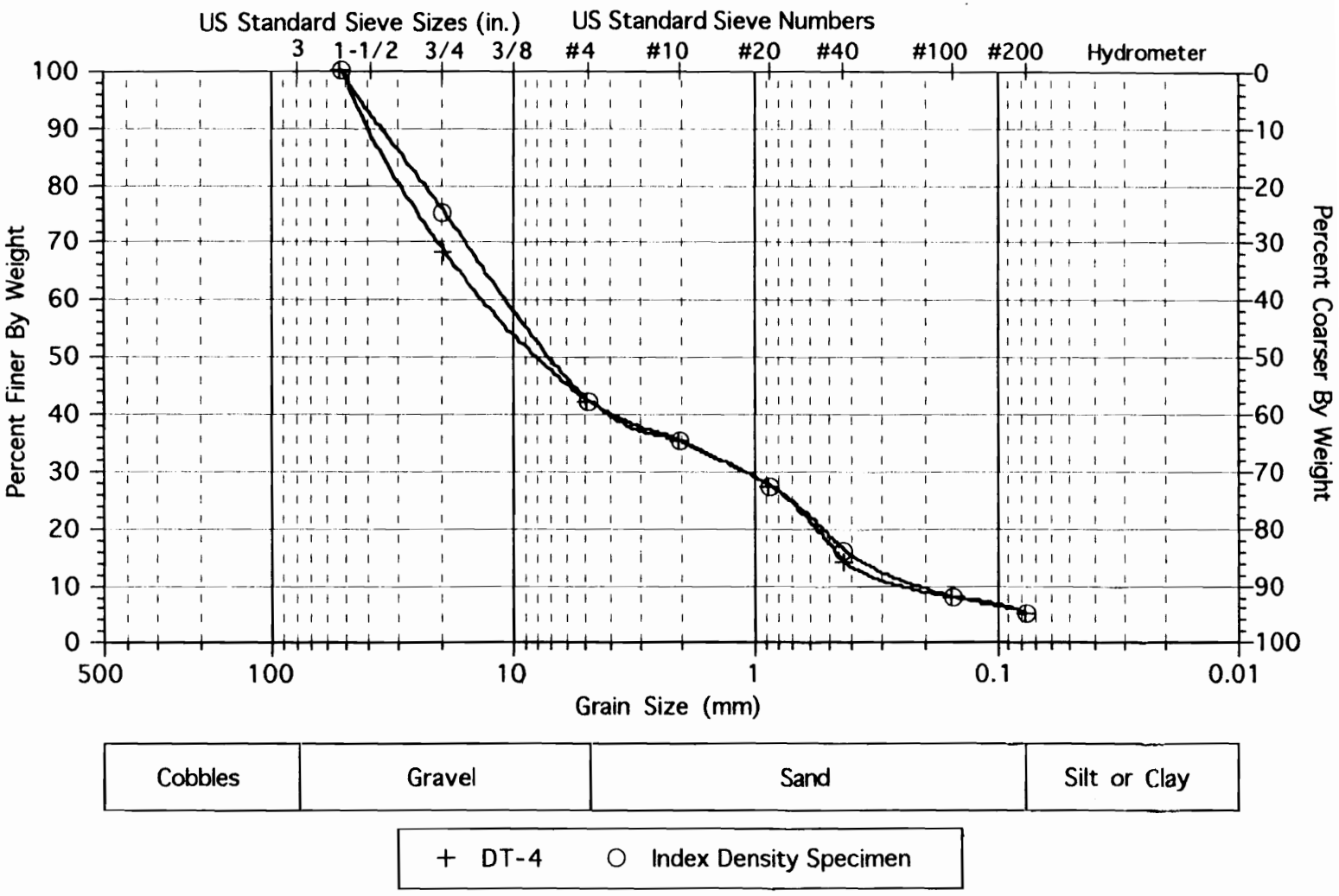

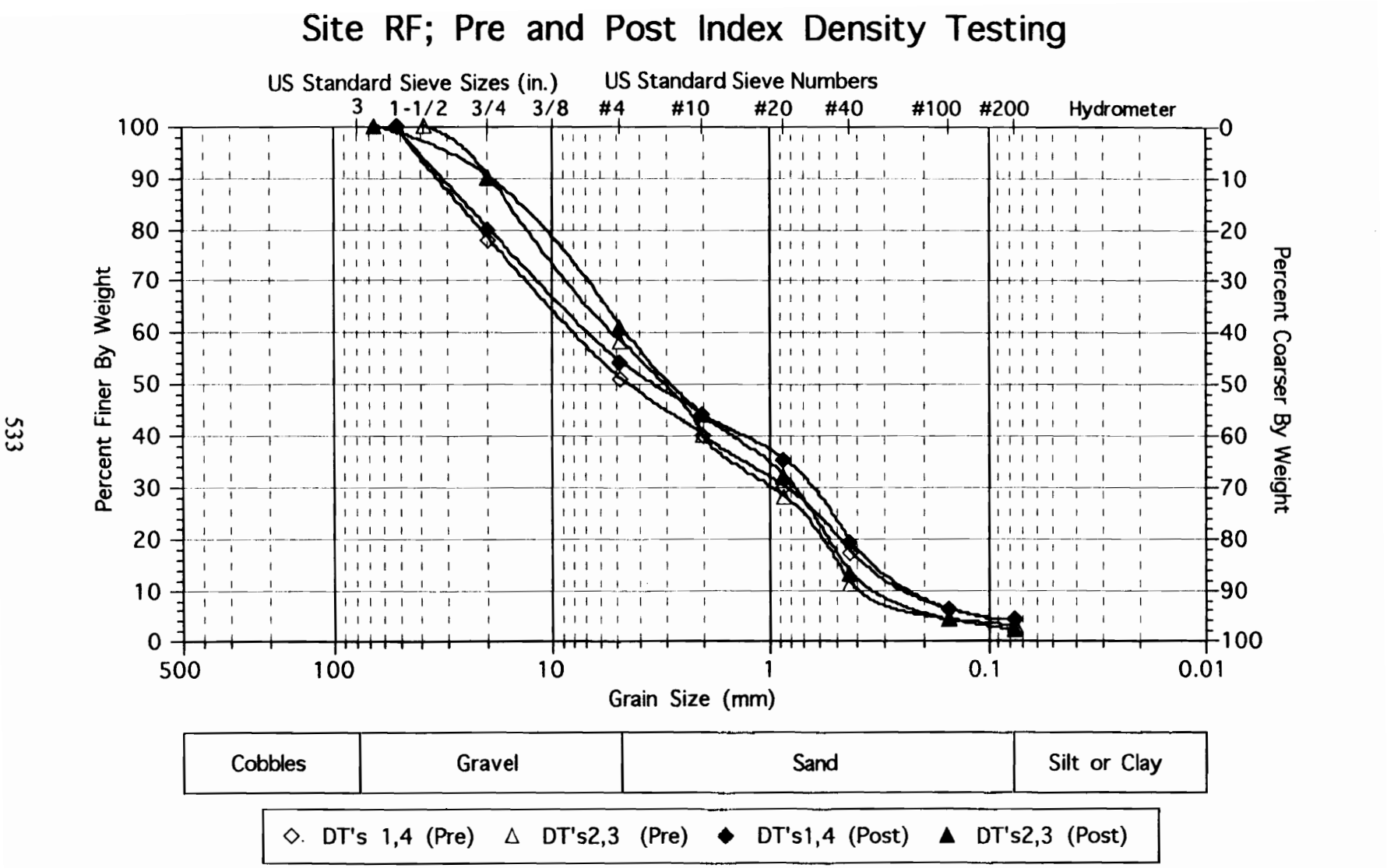
Site RF; Pre and Post Index Density Testing
US Standard Sieve Sizes (in.)
US Standard Sieve Numbers
3
1-1/2
3/4
3/8
#4
#10
#20
#40
#100
#200
Hydrometer
Percent Finer By Weight
Percent Coarser By Weight
100
90
80
70
60
50
40
30
20
10
0
500
100
10
1
0.1
0.01
Grain Size (mm)
Cobbles
Gravel
Sand
Silt or Clay
◇ DT's 1,4 (Pre)
△ DT's2,3 (Pre)
◆ DT's1,4 (Post)
▲ DT's2,3 (Post)

Site SM: In-Situ Density Test #'s 1,4 and Dr Specimen

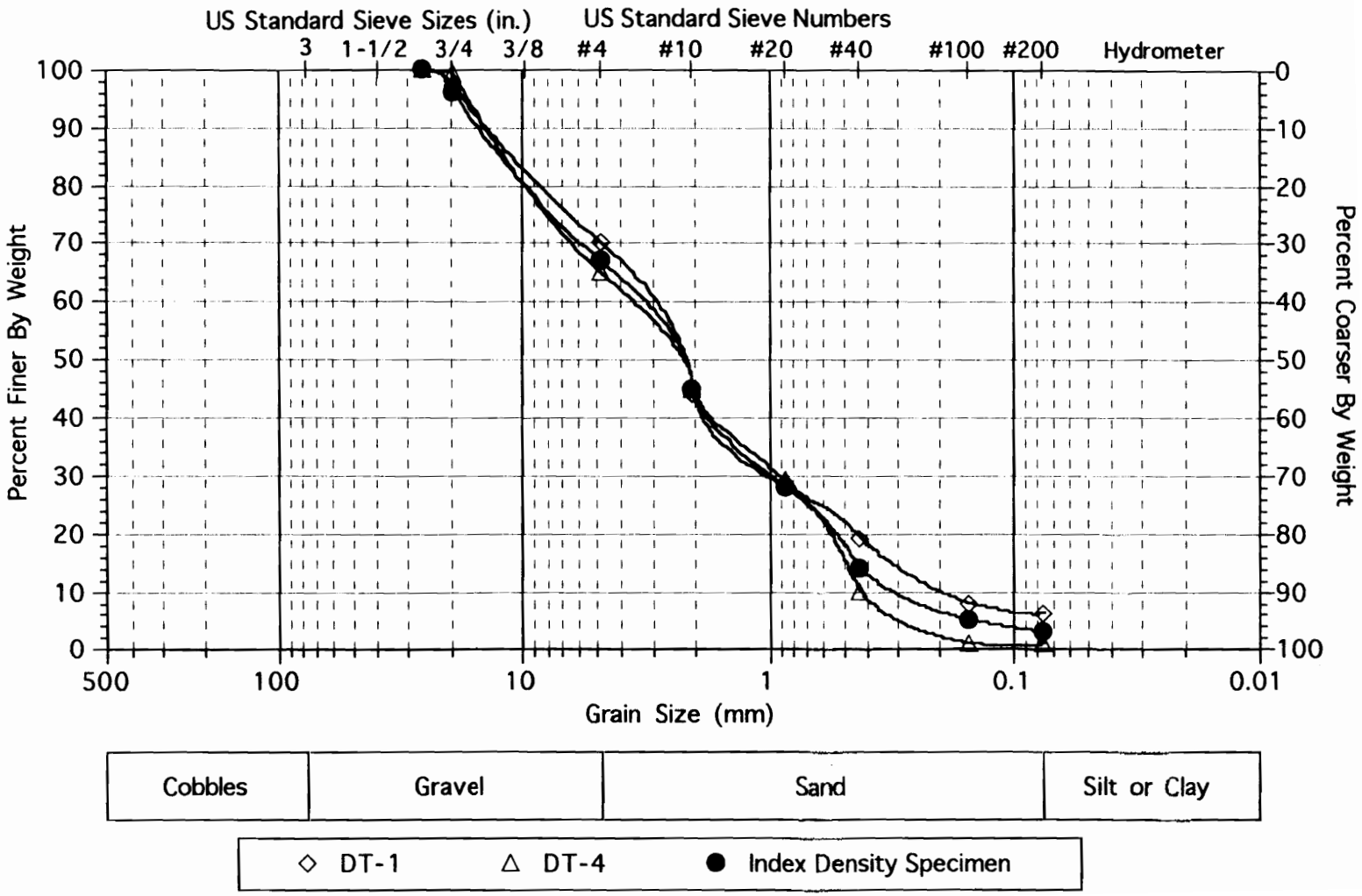

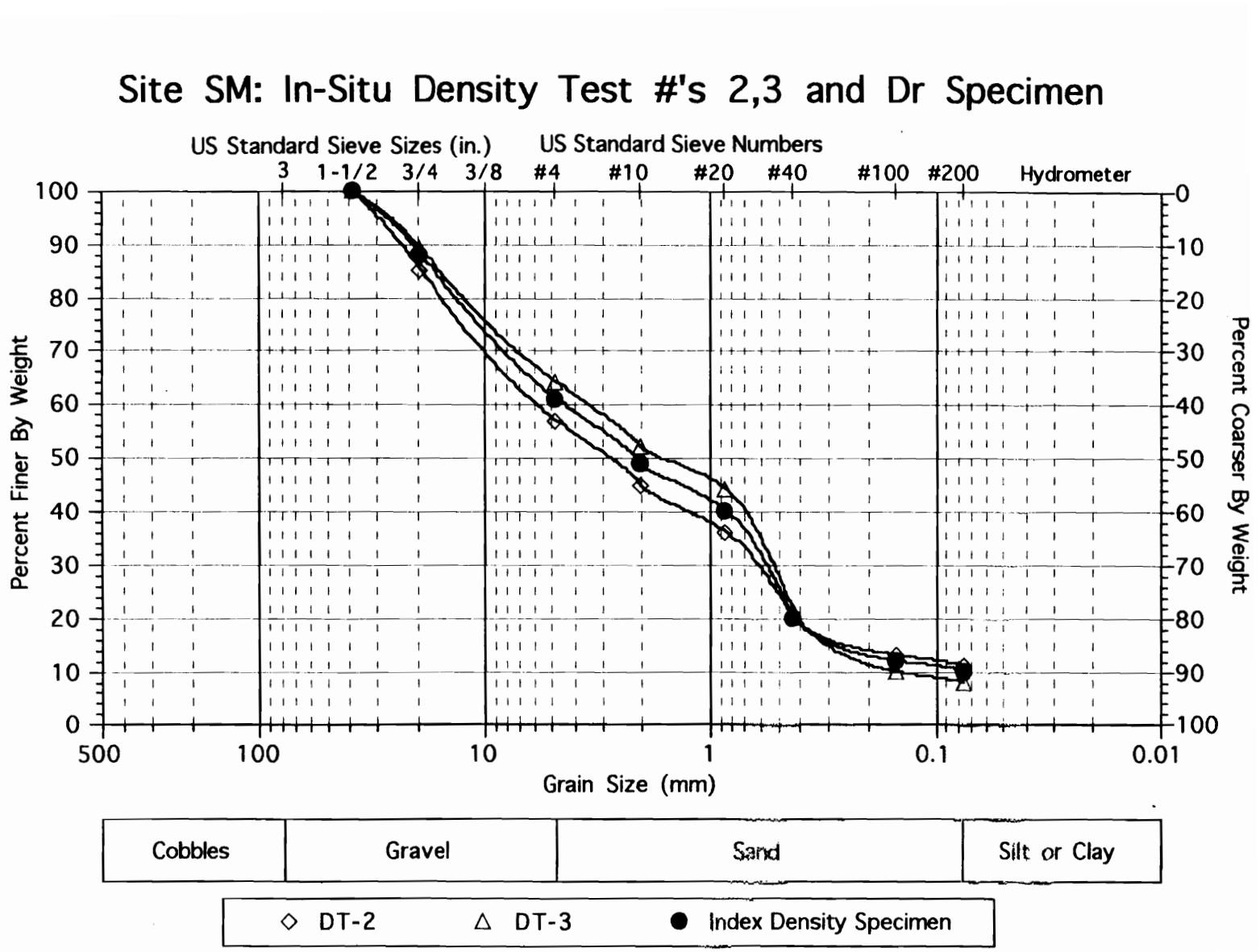
Site SM: In-Situ Density Test #'s 2,3 and Dr Specimen
US Standard Sieve Sizes (in.)
US Standard Sieve Numbers
3
1-1/2
3/4
3/8
#4
#10
#20
#40
#100
#200
Hydrometer
Percent Finer By Weight
Percent Coarser By Weight
100
90
80
70
60
50
40
30
20
10
0
500
100
10
1
0.1
0.01
Grain Size (mm)
Cobbles
Gravel
Sand
Silt or Clay
◇ DT-2
△ DT-3
● Index Density Specimen

Site SM: In-Situ Density Test #'s 5,6 and Dr Specimen

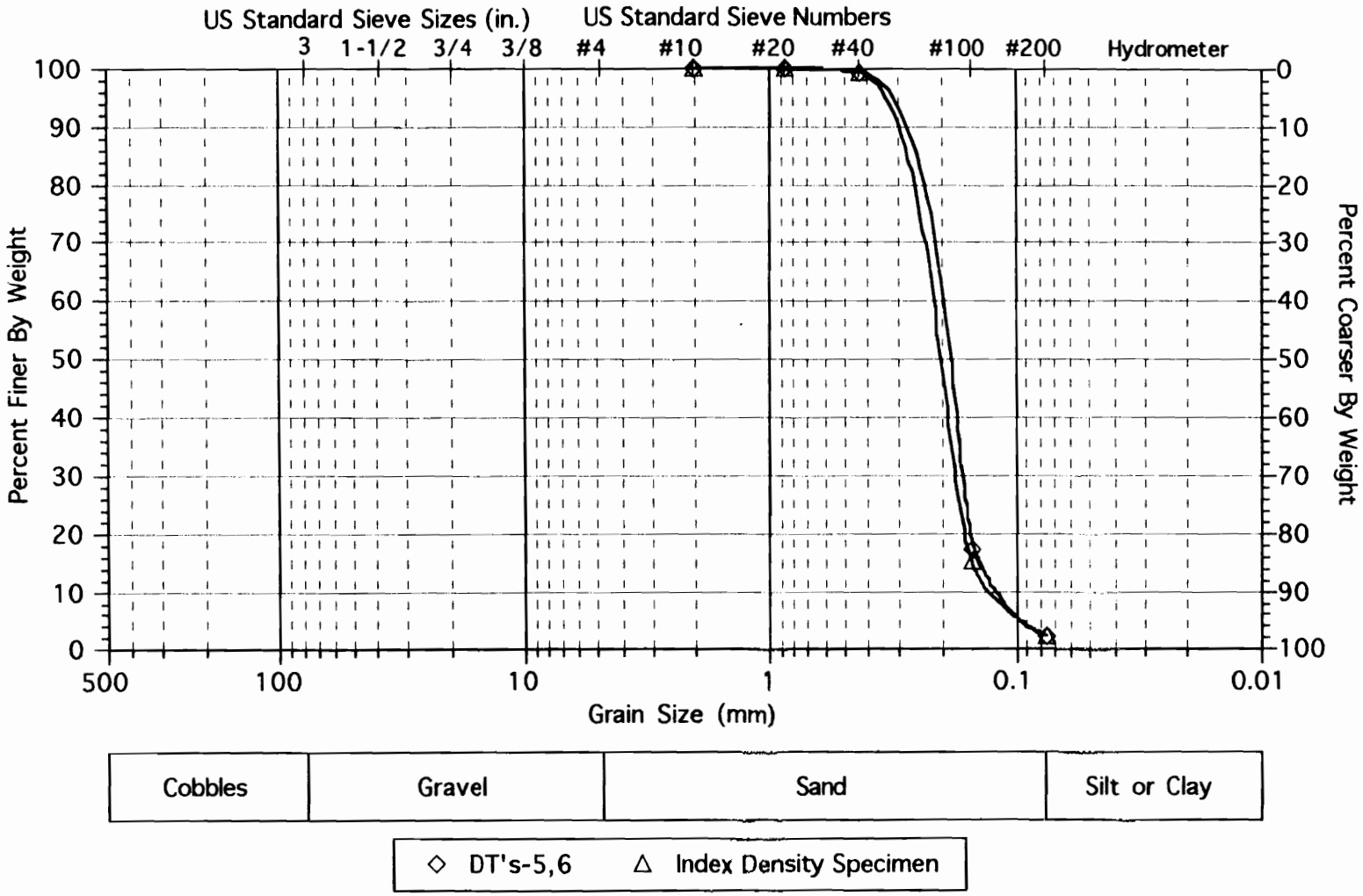

Site SM: DT's-1,4; Pre & Post Index Testing, and Gs Specimen

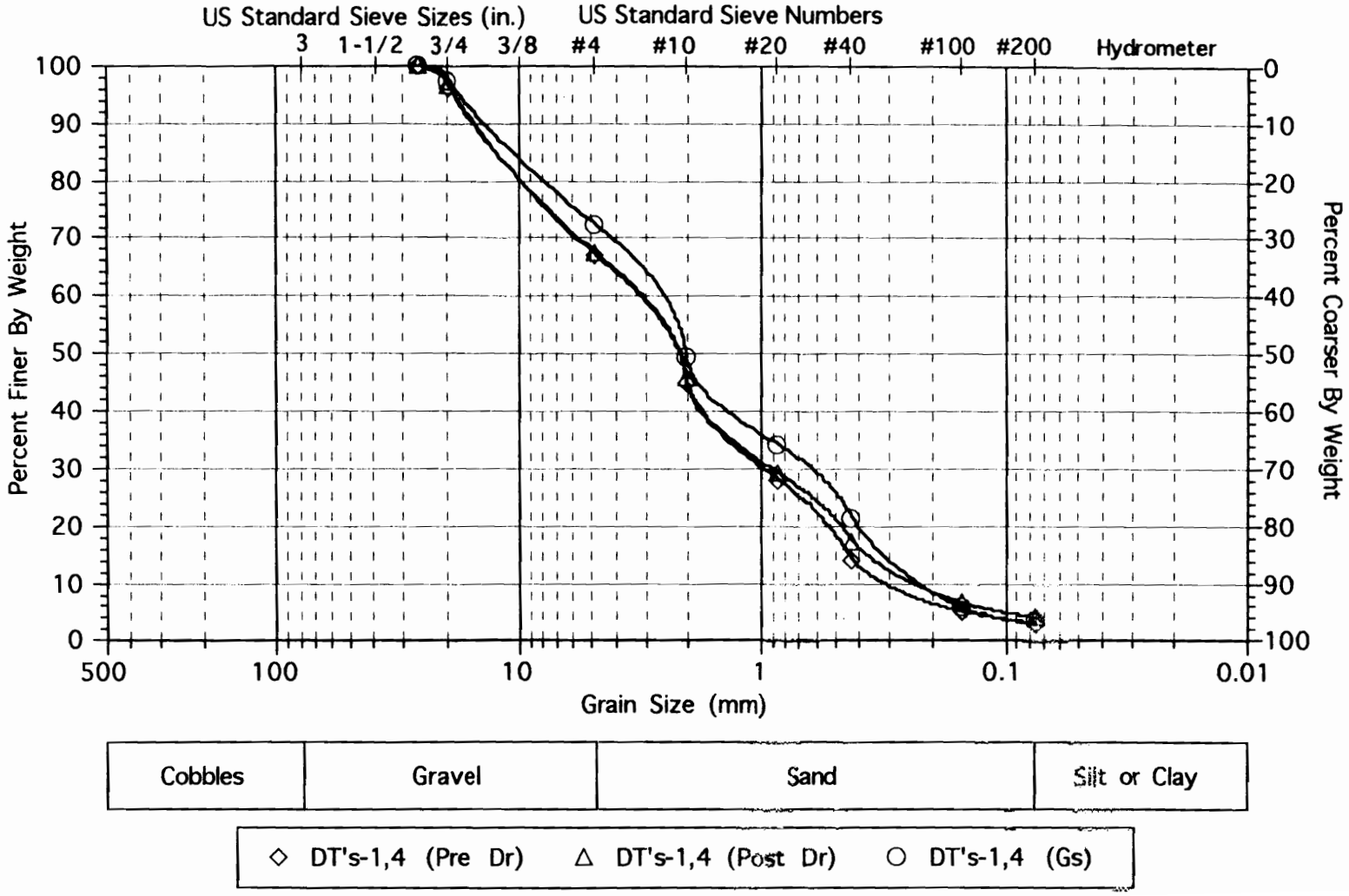

Site SM: DT's-2,3; Pre & Post Index Testing, and Gs Specimen

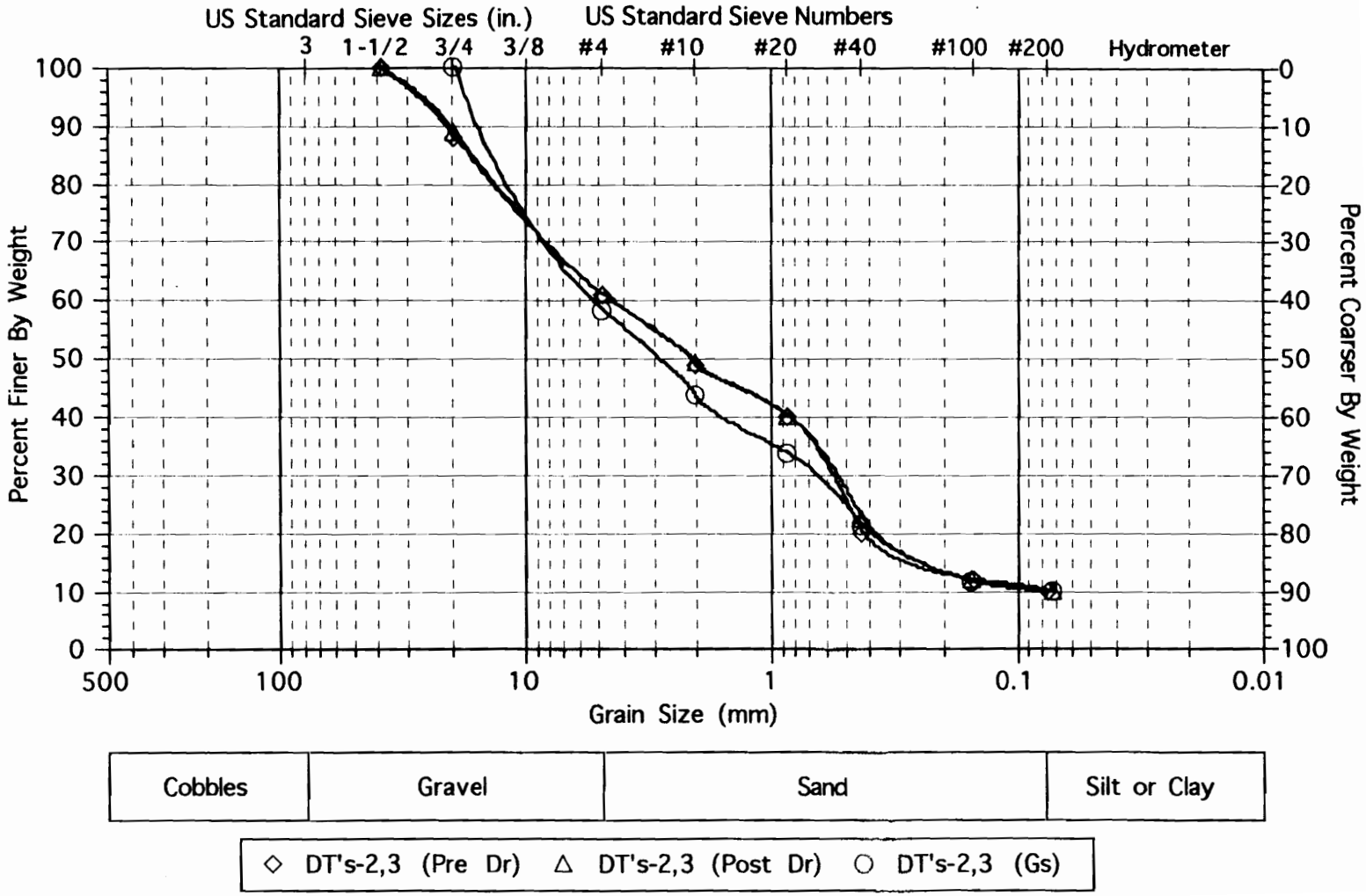

Grainsize Curves for Skelton Event

Index Density and Specific Gravity Test Specimens

Site GR: In-Situ Density Test #'s 1,5,9

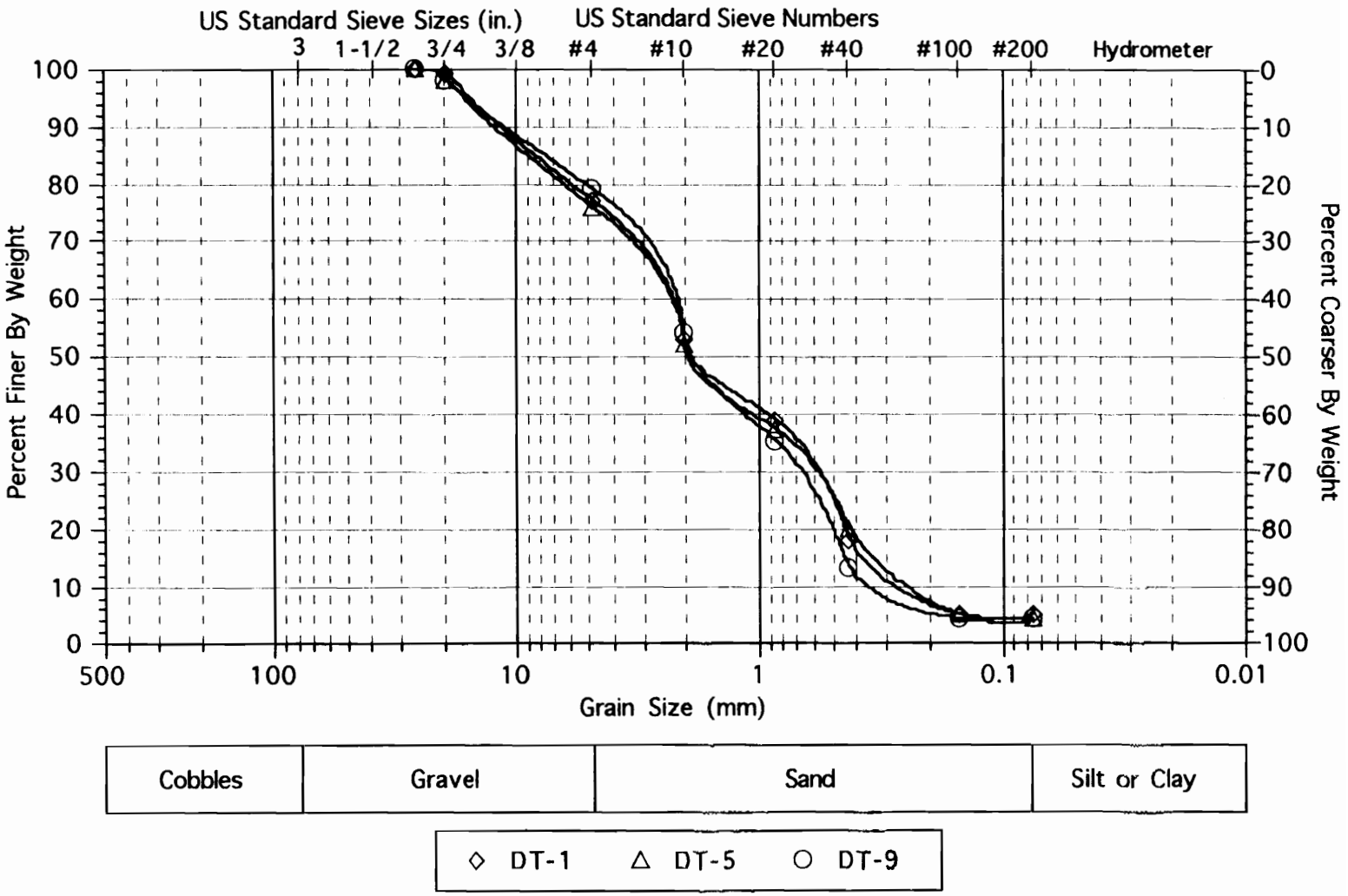

Site GR: In-Situ Density Test #'s 2, 2A, 3, 3A

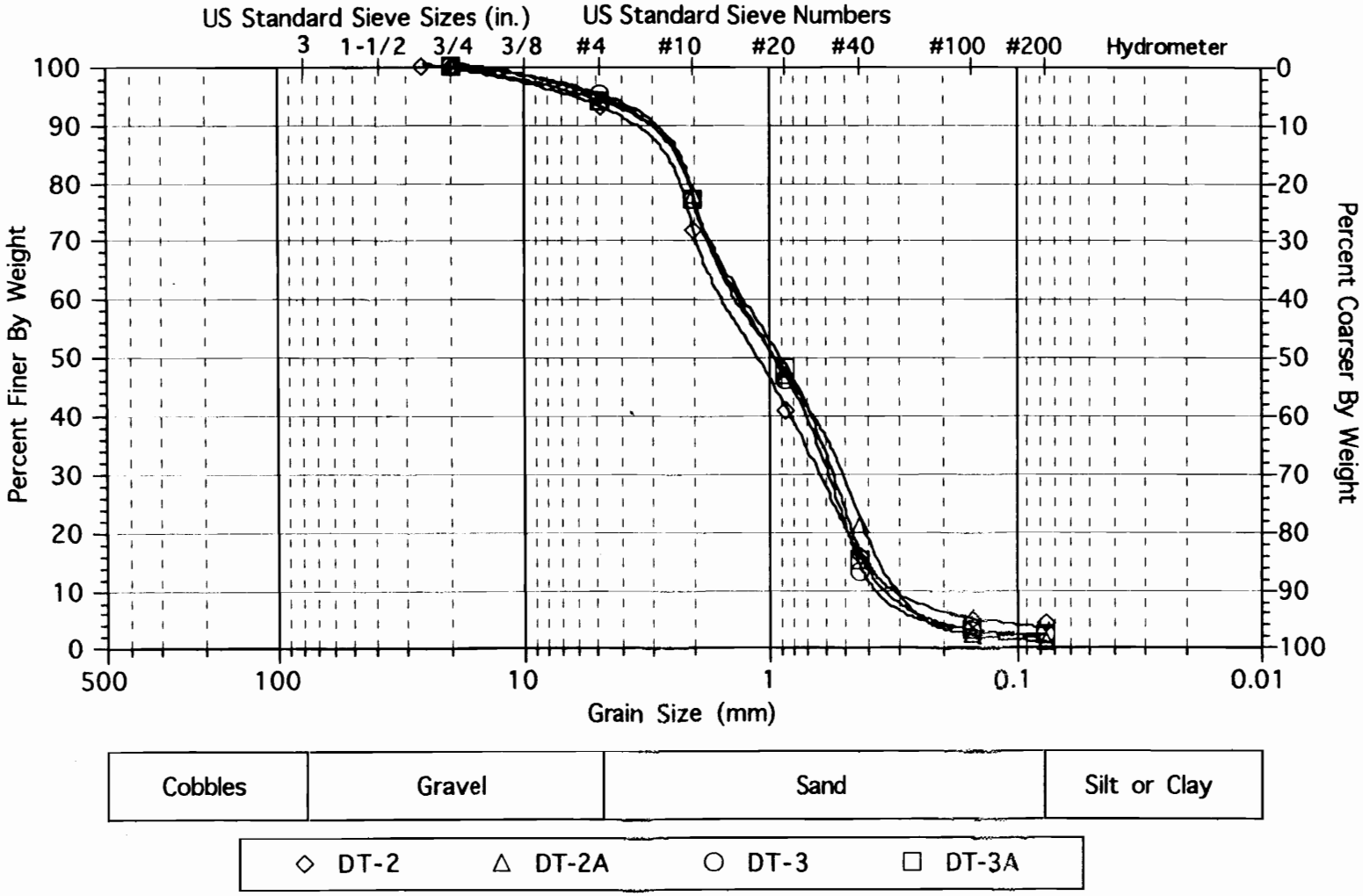

Site GR: In-Situ Density Test #'s 4,6,7; Dr and Gs Samples

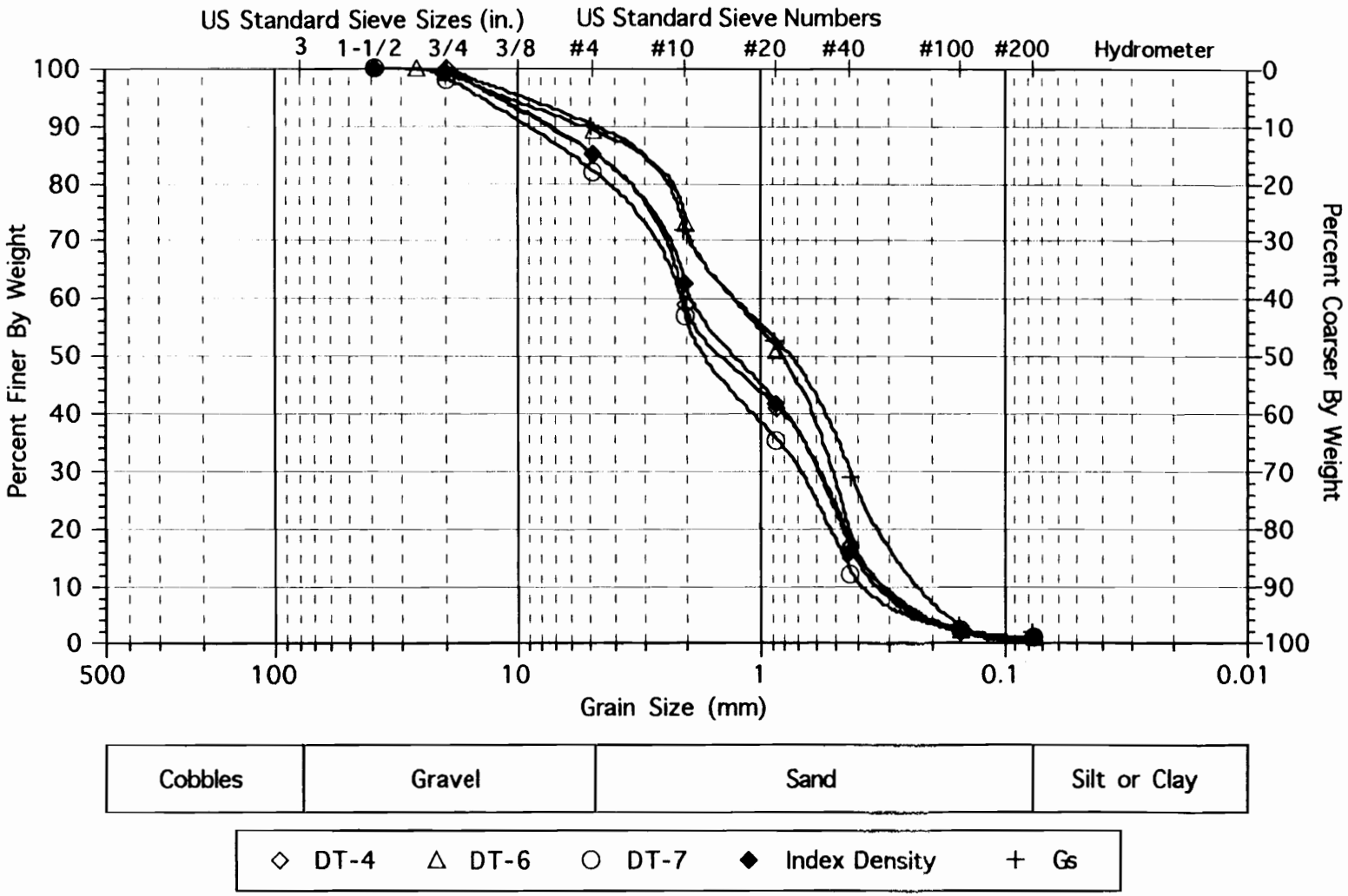

Site GR: In-Situ Density Test # 8

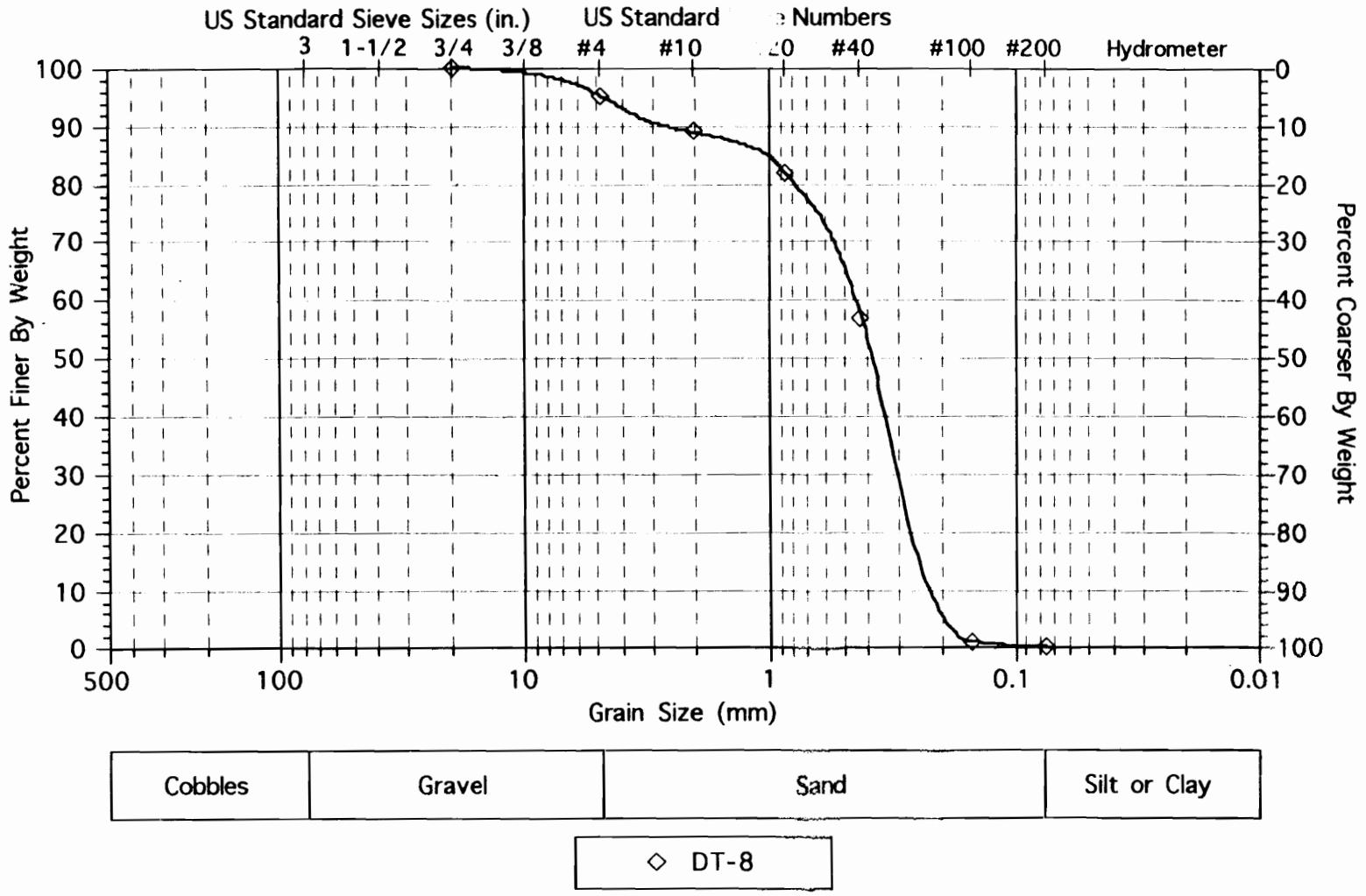

Site HM: In-Situ Density Test #'s 1,5

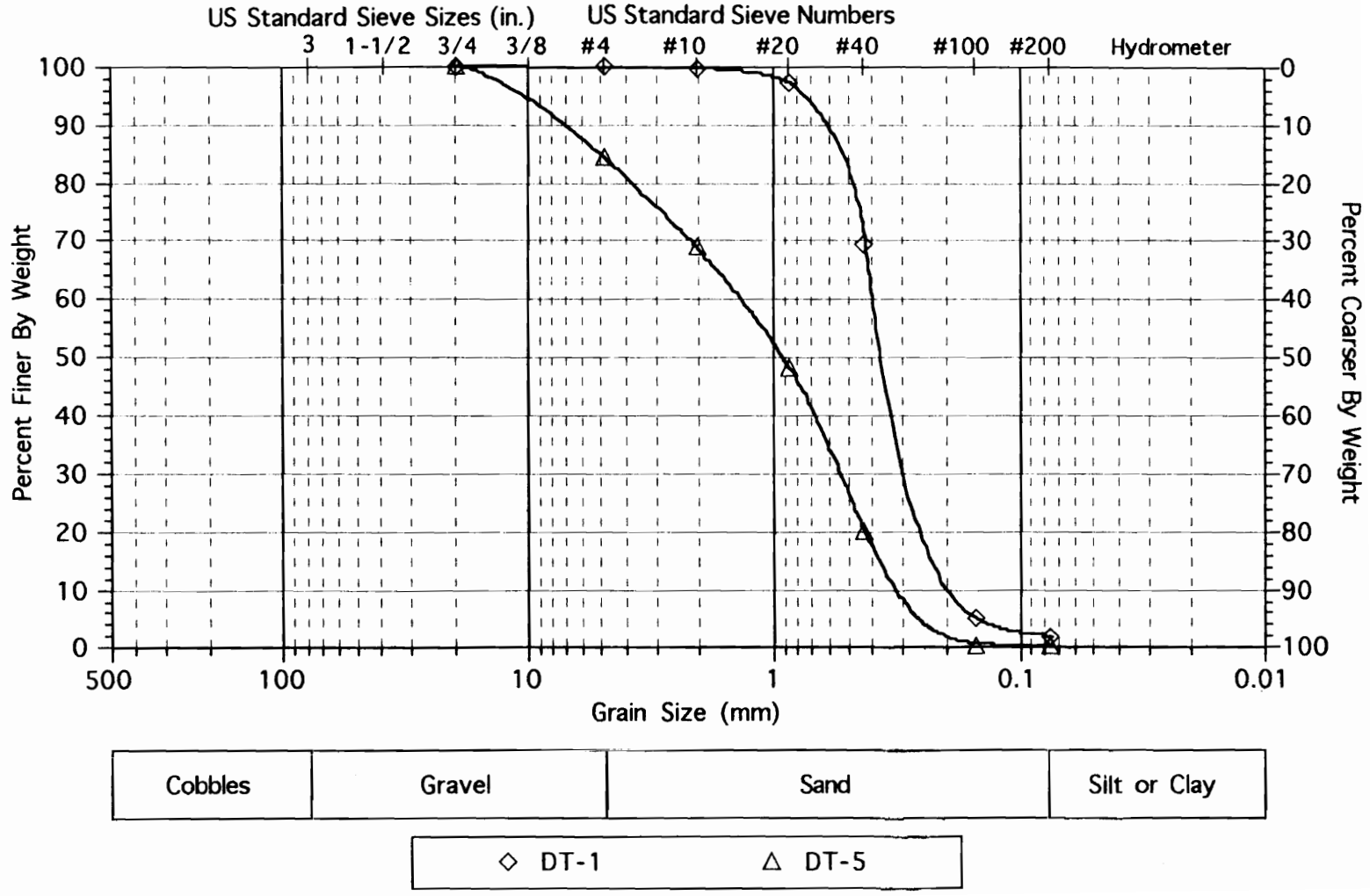

Site HM: In-Situ Density Tests #'s 2,4 and Dr Specimen

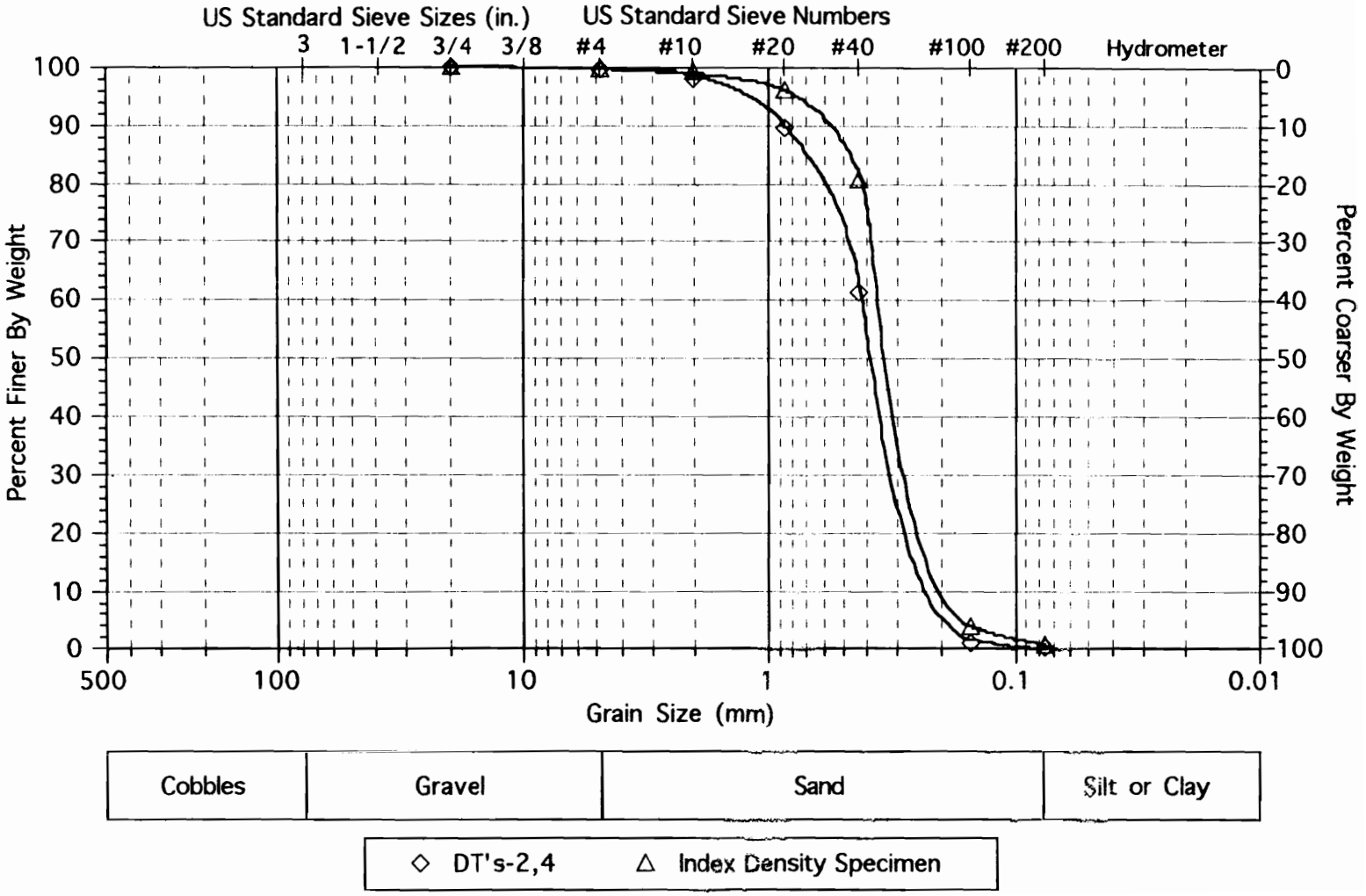

Site HM: In-Situ Density Tests #'s 3,6,7

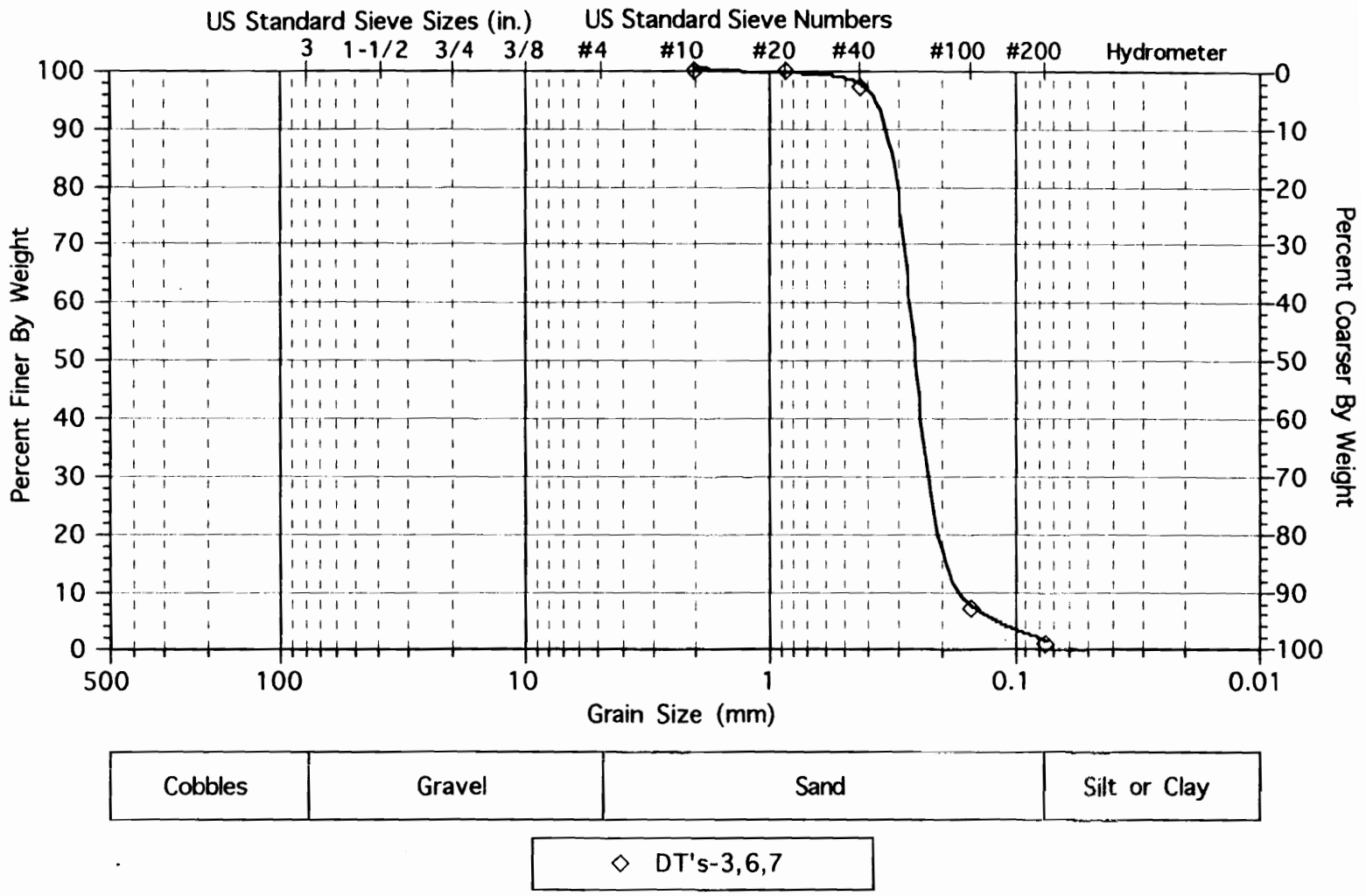

Grainsize Curves for Composite

Index Density and Bulk Samples

Composite Dr Specimen

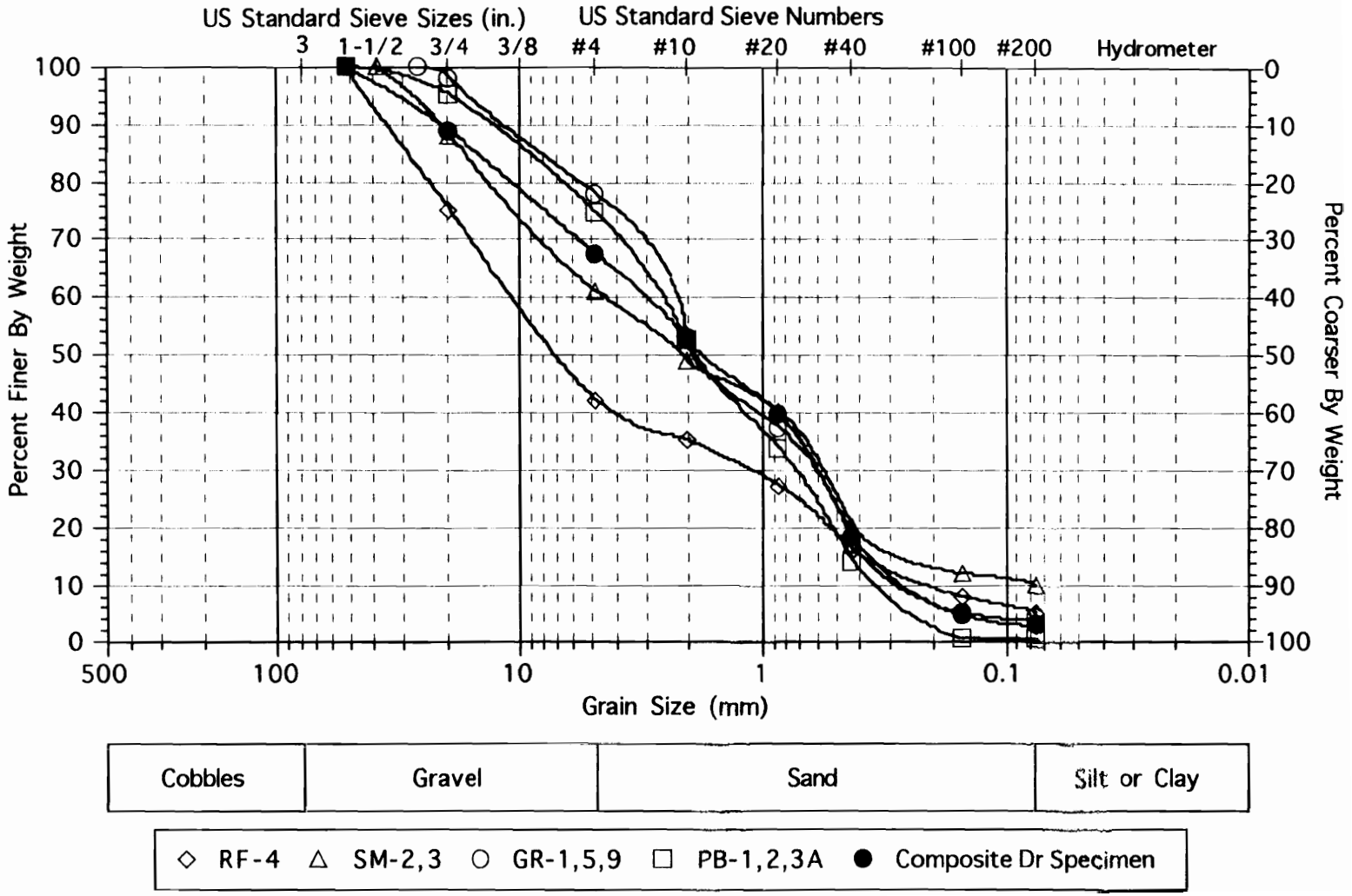

Grain Size Distributions: Sites RF,SM,VW Bulk Samples

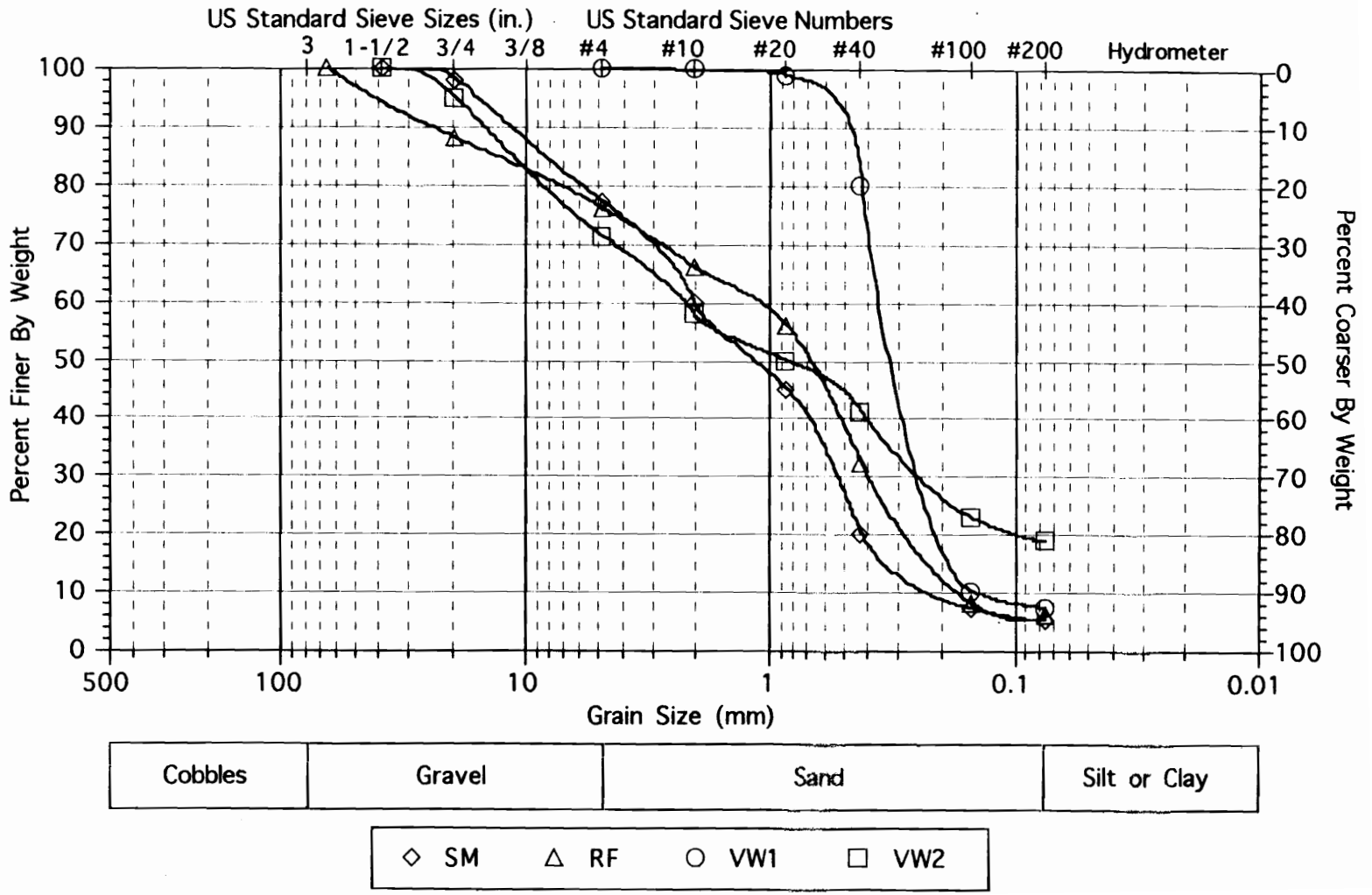

Specific Gravity Test Results

Specific Gravity Test Results

Vincennes Event		
Sample #	Gs	Soil Type
PL1-5	2.67	S
PL1-7	2.69	S
PL1-8	2.72	C
PL1-9	2.69	S
PL2-3	2.72	C
PL2-7	2.68	S
NP1-3	2.76	C
NP1-4	2.72	S
NP1-6	2.71	S
NP1-7	2.69	S
NP1-10	2.71	S
NP2-7	2.76	S
TH1-3	2.72	C
TH1-9	2.75	S
TH1-11	2.69	S
TH1-16	2.72	S
TH2-1	2.73	C
TH2-4	2.75	C
TH2-7	2.70	S
TH3-4	2.67	S
TH3-7	2.66	S
BG1-1	2.68	C
BG1-5	2.69	C
BG1-14	2.70	S
BG2-7	2.69	C
BG2-10	2.66	S
BG4-6	2.66	S
BG4-9	2.71	S
YO1-3	2.71	C
YO2-1	2.67	C
YO3-3	2.75	C
YO3-10	2.68	S
YO3-13	2.68	S
WO1-1	2.69	C
WO1-9	2.72	S
WO2-1	2.70	C
WO3-2	2.68	C
WO3-4	2.73	S
WO3-5	2.71	S
WO3-7	2.71	S
PA1-3	2.73	C
PA1-5	2.75	C
PA1-11	2.71	S
PA1-15	2.72	S
PA2-1	2.70	C
PA2-8	2.71	S
PA2-10	2.69	S
PA2-14	2.69	S
PA4-2	2.73	C
PA4-4	2.75	C
PA4-6	2.70	C
PA4-7	2.67	S

Samples Identified by site name abreviation and boring number, with individual sample numbers following the hyphen. See boring logs for location in profile.

Soil type is indicated based on predominant grain size
S=Sand
C=Clay

Specific Gravity Test Results

Vincennes Event		
Sample #	Gs	Soil Type
PA4-10	2.72	S
PA4-12	2.70	S
RF1-2	2.64	C
RF1-11	2.70	S
RF5-2	2.71	C
RF5-7	2.67	S
RF6-7	2.70	S
RF6-9	2.69	S
SM1-2	2.73	C
SM1-4	2.67	S
SM1-5	2.64	S
SM2-2	2.75	C
SM2-5	2.63	S
SM3-1	2.70	C
SM4-1	2.67	C
SM4-4	2.72	S
SM4-7	2.65	S
SM4-11	2.73	S
VW2-1	2.63	C
VW2-1	2.62	C
VW2-2	2.72	C
VW2-6	2.65	S
VW2-8	2.70	S
VW5-2	2.72	C
VW5-7	2.69	S
VW5-8	2.67	S
HA1-1	2.74	C
HA1-3	2.72	C
HA1-5	2.71	C
HA1-10	2.70	S
HA2-5	2.74	S
HA2-7	2.71	S
HA2-9	2.72	S
PB1-9	2.70	S
PB1-12	2.69	S
PB2-3	2.70	C
PB2-11	2.66	S
PB3-1	2.71	C
MA1-1	2.72	C
MA1-8	2.66	S
MA3-2	2.71	C
MA3-4	2.68	S
MA4-1	2.73	C
MA4-8	2.70	S
MA5-6	2.69	S

Specific Gravity Test Results

Vallonia Event		
Sample #	Gs	Soil Type
AZ1-1	2.75	C
AZ1-2	2.77	C
AZ1-5	2.72	S
AZ1-9	2.72	S
AZ2-1	2.74	C
AZ2-7	2.72	S
AZ2-9	2.73	S
AZ2-12	2.72	S
AZ3-2	2.72	C
AZ3-3	2.75	S
AZ3-8	2.74	S
AZ4-2	2.75	S
AZ4-4	2.72	S
SSP2-1	2.70	C
SSP1-6	2.74	S
SSP1-3	2.74	S
SSP2-7	2.70	S
SSP2-10	2.72	S
SSP2-13	2.71	S
SSP3-8	2.70	S
SP1-1	2.70	C
SP1-3	2.70	C
SP1-6	2.72	S
SP1-8	2.72	S
SP1-12	2.72	S
SP1-13	2.70	S

Waverly Event		
Sample #	Gs	Soil Type
SV1-2	2.76	C
SV1-4	2.76	S
SV1-11	2.76	S
SV2-6	2.74	S
SV2-9	2.73	S
MV1-2	2.73	C
MV1-4	2.73	S
MV1-8	2.71	S
MV2-3	2.69	C
MV2-10	2.71	S

Samples Identified by site name abreviation and boring number, with individual sample numbers following the hyphen. See boring logs for location in profile.

Soil type is indicated based on predominant grain size
S=Sand
C=Clay

Skelton Event		
Sample #	Gs	Soil Type
WA1-3	2.70	S
WA1-6	2.70	S
WA1-7	2.70	S
WA2-1	2.66	C
WA2-3	2.69	S
WA2-5	2.69	S
HM1-5	2.67	S
HM1-9	2.70	S
HM2-1	2.73	C
HM2-6	2.70	S
HM3-3	2.67	C
HM3-5	2.68	S
VC1-3	2.70	C
VC1-4	2.68	S
VC1-6	2.70	S
VC3-1	2.73	C
VC3-2	2.68	S
VC3-8	2.70	S
GR1-2	2.71	C
GR1-4	2.66	S
GR1-11	2.69	S
GR2-1	2.72	C
GR2-5	2.69	S
GR2-9	2.69	S
GR2-13	2.71	S
GR4-3	2.75	C

Summary of Specific Gravity Testing Results

Vincennes Event

	Soil Type	
Data	C	S
Average of Gs	2.71	2.69
Max of Gs	2.76	2.76
Min of Gs	2.62	2.63
StdDev of Gs	0.03	0.03
# of Samples Tested	39	58

Skelton Event

	Soil Type	
Data	C	S
Average of Gs	2.71	2.69
Max of Gs	2.75	2.71
Min of Gs	2.66	2.66
StdDev of Gs	0.03	0.01
# of Samples Tested	8	18

Index Density Specimens (coarse-grained)

	Event	
Data	Skelton	Vincennes
Average of Gs	2.68	2.69
Max of Gs	2.70	2.71
Min of Gs	2.65	2.67
StdDev of Gs	0.02	0.02
# of Samples Tested	10	9

Vallonia Event

	Soil Type	
Data	C	S
Average of Gs	2.73	2.72
Max of Gs	2.77	2.75
Min of Gs	2.70	2.70
StdDev of Gs	0.03	0.02
# of Samples Tested	7	19

Waverly Event

	Soil Type	
Data	C	S
Average of Gs	2.73	2.73
Max of Gs	2.76	2.76
Min of Gs	2.69	2.71
StdDev of Gs	0.04	0.02
# of Samples Tested	3	7

C: Clay
S: Sand

In-Situ and Index Density Test Results

Summary of In-Situ Relative Density Testing Results

In-Situ Test #	γ_d (pcf)	γ_{dmin} (pcf)	γ_{dmax} (pcf)	G_s	e	e_{max}	e_{min}	D_r (%)	Depth Within Liq'd Zone (ft)
RF1	119	114.5	134.7	2.71	0.42	0.48	0.26	25	1.5
RF2	122	114.5	134.7	2.71	0.39	0.48	0.26	41	0.5
RF3	120	114.5	134.7	2.71	0.41	0.48	0.26	31	1.0
RF4	127	117.8	145.3	2.70	0.33	0.43	0.16	38	2.0
SM1	108	106.4	132.1	2.68	0.55	0.57	0.27	8	1.5
SM2	120	111.7	135.8	2.70	0.40	0.51	0.24	39	1.0
SM3	114	111.7	135.8	2.70	0.48	0.51	0.24	11	2.0
SM4	108	106.4	132.1	2.68	0.55	0.57	0.27	8	2.0
SM5	99	89.0	111.0	2.67	0.68	0.87	0.50	51	1.0
SM6	104	89.0	111.0	2.67	0.60	0.87	0.50	73	0.5
PB1	123	111.5	129.5	2.69	0.36	0.51	0.30	67	1.0
PB2	131	111.5	129.5	2.69	0.28	0.51	0.30	107	4.0
PB3	108	103.9	122.7	2.67	0.54	0.60	0.36	25	7.5
PB3A	107	103.9	122.7	2.69	0.57	0.62	0.37	19	8.0
PB4	130	110.7	127.2	2.68	0.29	0.51	0.31	114	1.5
PB5	120	110.7	127.2	2.68	0.39	0.51	0.31	60	6.5
PB6	117	103.9	122.7	2.67	0.42	0.60	0.36	73	6.5
PB7A	101	92.7	110.8	2.67	0.65	0.80	0.50	50	0.5
MA1	106	94.2	111.8	2.69	0.58	0.78	0.50	71	5.0
MA2	94	90.2	109.2	2.69	0.79	0.86	0.54	23	2.0
MA3	104	90.2	109.2	2.69	0.61	0.86	0.54	76	6.5
MA4	93	90.2	109.2	2.69	0.80	0.86	0.54	17	2.5
GR1	102	101.7	123.7	2.65	0.62	0.63	0.34	2	1.5
GR2	101	98.0	121.4	2.67	0.65	0.70	0.37	15	5.0
GR3	107	98.0	121.4	2.67	0.56	0.70	0.37	44	5.5
GR4	105	95.3	122.0	2.66	0.58	0.74	0.36	42	3.5
GR5	108	101.7	123.7	2.65	0.53	0.63	0.34	33	1.5
GR6	103	95.3	122.0	2.66	0.61	0.74	0.36	34	3.5
GR7	100	95.3	122.0	2.66	0.66	0.74	0.36	21	3.5
GR8	98	93.2	112.8	2.68	0.71	0.79	0.48	28	2.0
GR9	104	101.7	123.7	2.65	0.59	0.63	0.34	12	2.5
HM1	97	83.2	114.2	2.67	0.72	1.00	0.46	52	2.0
HM2	103	92.4	111.8	2.69	0.63	0.82	0.50	59	8.0
HM3	98	88.4	110.0	2.69	0.71	0.90	0.53	50	5.5
HM4	100	92.4	111.8	2.69	0.68	0.82	0.50	44	2.0
HM5	121	109.6	124.3	2.70	0.39	0.54	0.36	80	9.0
HM6	96	88.4	110.0	2.69	0.75	0.90	0.53	40	4.0
HM7	97	88.4	110.0	2.69	0.73	0.90	0.53	45	3.5

Summary of Index Density Test Results

Index Density Sample #	γ_{dmin} (pcf)	γ_{dmax} (pcf)	G_s	e_{max}	e_{min}
RF1,2,3	114.5	134.7	2.71	0.48	0.26
RF4	117.8	145.3	2.70	0.43	0.16
SM1,4	106.4	132.1	2.68	0.57	0.27
SM2,3	111.7	135.8	2.70	0.51	0.24
SM5,6	89.0	111.0	2.67	0.87	0.50
PB1,2	111.5	129.5	2.69	0.51	0.30
PB3,6	103.9	122.7	2.67	0.60	0.36
PB4,5	110.7	127.2	2.68	0.51	0.31
PB7A	92.7	110.8	2.67	0.80	0.50
MA1	94.2	111.8	2.69	0.78	0.50
MA2,3,4	90.2	109.2	2.69	0.86	0.54
GR1,5,9	101.7	123.7	2.65	0.63	0.34
GR2,3	98.0	121.4	2.67	0.70	0.37
GR4,6,7	95.3	122.0	2.66	0.74	0.36
GR8	93.2	112.8	2.68	0.79	0.48
HM1	83.2	114.2	2.67	1.00	0.46
HM2,4	92.4	111.8	2.69	0.82	0.50
HM3,6,7	88.4	110.0	2.69	0.90	0.53
HM5	109.6	124.3	2.70	0.54	0.36

Comparison of Results Based on Alternative Test Procedures

Minimum Index Density Results		
Index Test #	Method C γ_{dmax}	Method A γ_{dmin}
GR8	93.2	
HM1	83.2	
MA2,3,4	90	
HM5	109.6	
GR4,6,7	94.5	95.3
PB1,2,3A	111.5	111.5
PB4,5	111.3	110.7
PB7,7A	92.5	92.7

Compare γ_{dmax} and γ_{dmin} results based on both large and small molds		
Test Mold Size	γ_{dmin}	γ_{dmax}
0.1 ft^3	111.9	134.3
0.5 ft^3	112.1	134.3

Specific Gravity Test Results for Index Density Specimens

Index Density Specimens		
Specimen #	Gs	Event
PB-1,2,3A	2.69	Vincennes
PB-3,6	2.67	Vincennes
PB-4,5	2.68	Vincennes
PB-7,7A	2.67	Vincennes
RF-1	2.71	Vincennes
RF-2,3,4	2.70	Vincennes
SM-1,4	2.68	Vincennes
SM-2,3	2.70	Vincennes
SM-5,6	2.67	Vincennes
GR-1,5,9	2.65	Skelton
GR-2,3	2.67	Skelton
GR-4,6,7	2.66	Skelton
GR-8	2.68	Skelton
HM-1	2.67	Skelton
HM-2	2.69	Skelton
HM-3	2.69	Skelton
HM-5	2.70	Skelton
MA-1	2.69	Skelton
MA-3	2.69	Skelton

Index density specimens are identified by site name abbreviation and density test numbers

Summary		
	Event	
Data	Skelton	Vincennes
Average Gs	2.68	2.69
Max Gs	2.70	2.71
Min Gs	2.65	2.67
StdDev of Gs	0.02	0.02

Appendix G:

Synthetic Ground Motions

Bedrock Motions

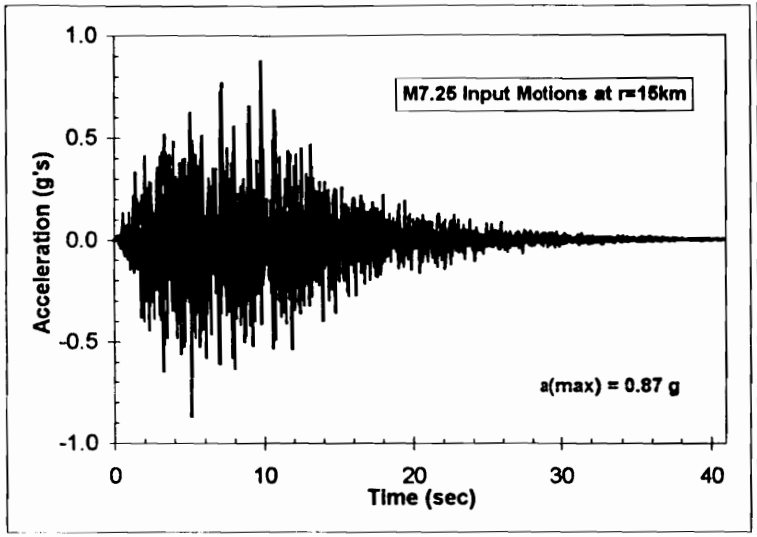

Wabash Valley Paleoseismic Liquefaction Study

ENA M7.25 Bedrock Motions Predicted Using a Stochastic Model Based on Atkinson and Boore (1995) Input Parameters

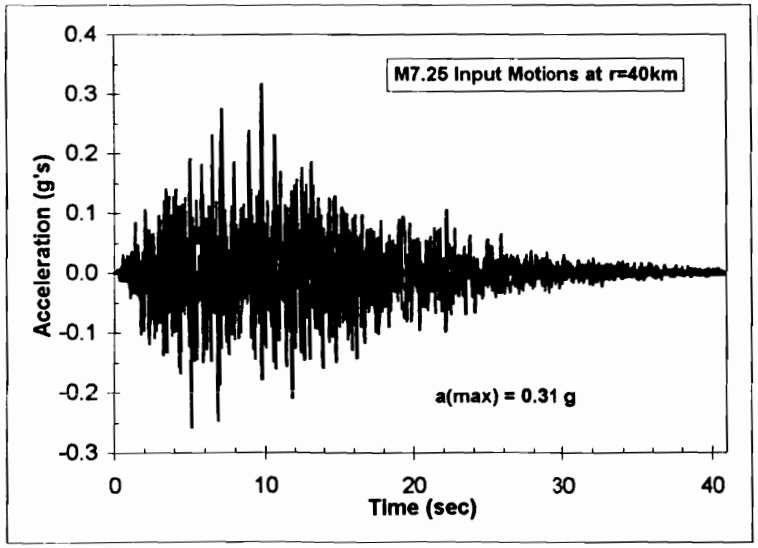

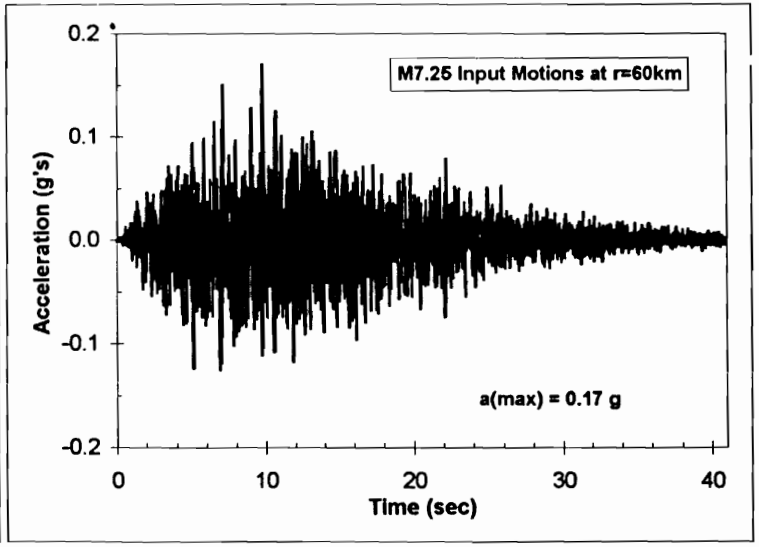

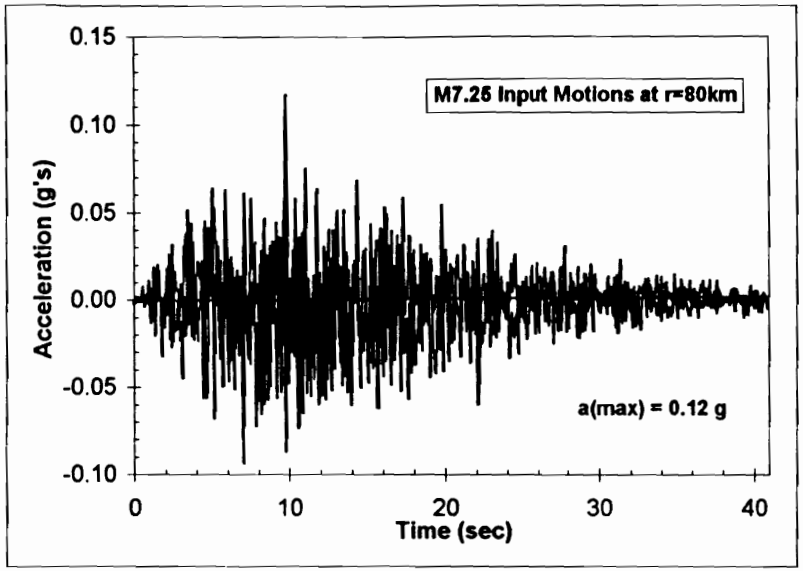

Wabash Valley Paleoseismic Liquefaction Study

ENA M7.25 Bedrock Motions Predicted Using a Stochastic Model Based on Atkinson and Boore (1995) Input Parameters

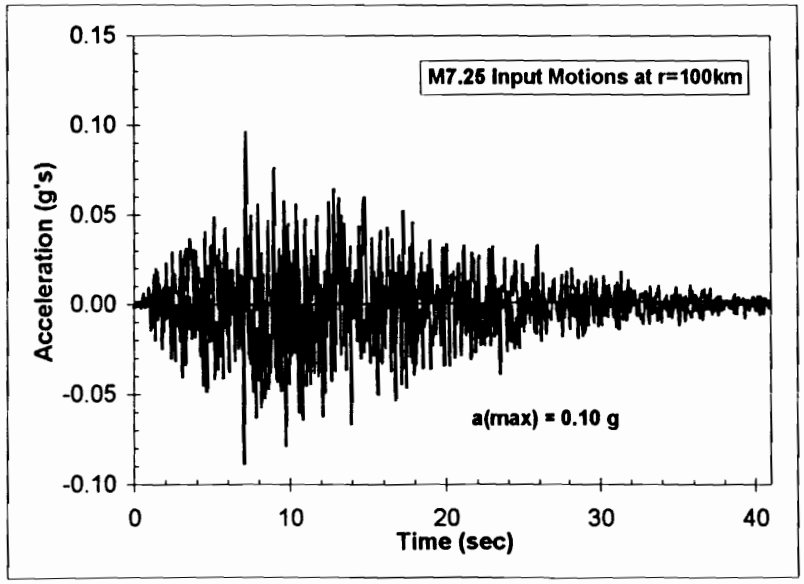

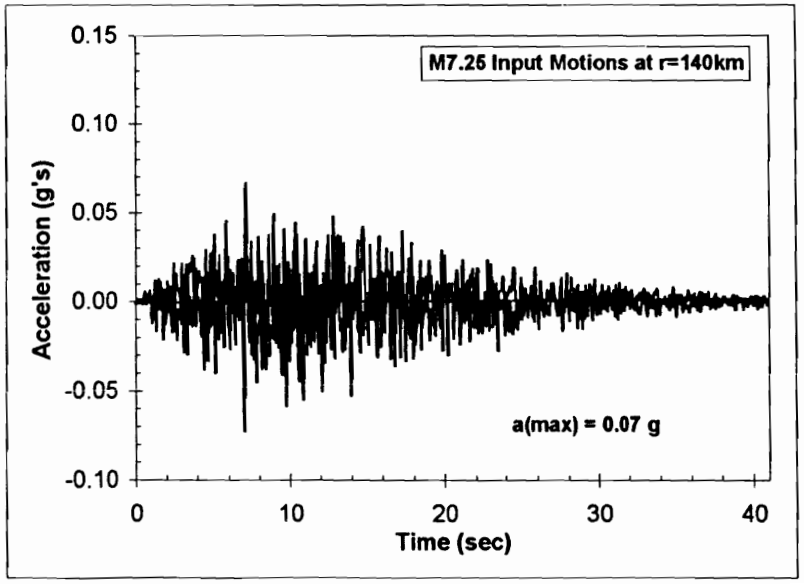

ENA M7.0 Bedrock Motions Predicted Using a Stochastic Model Based on Atkinson and Boore (1995) Input Parameters

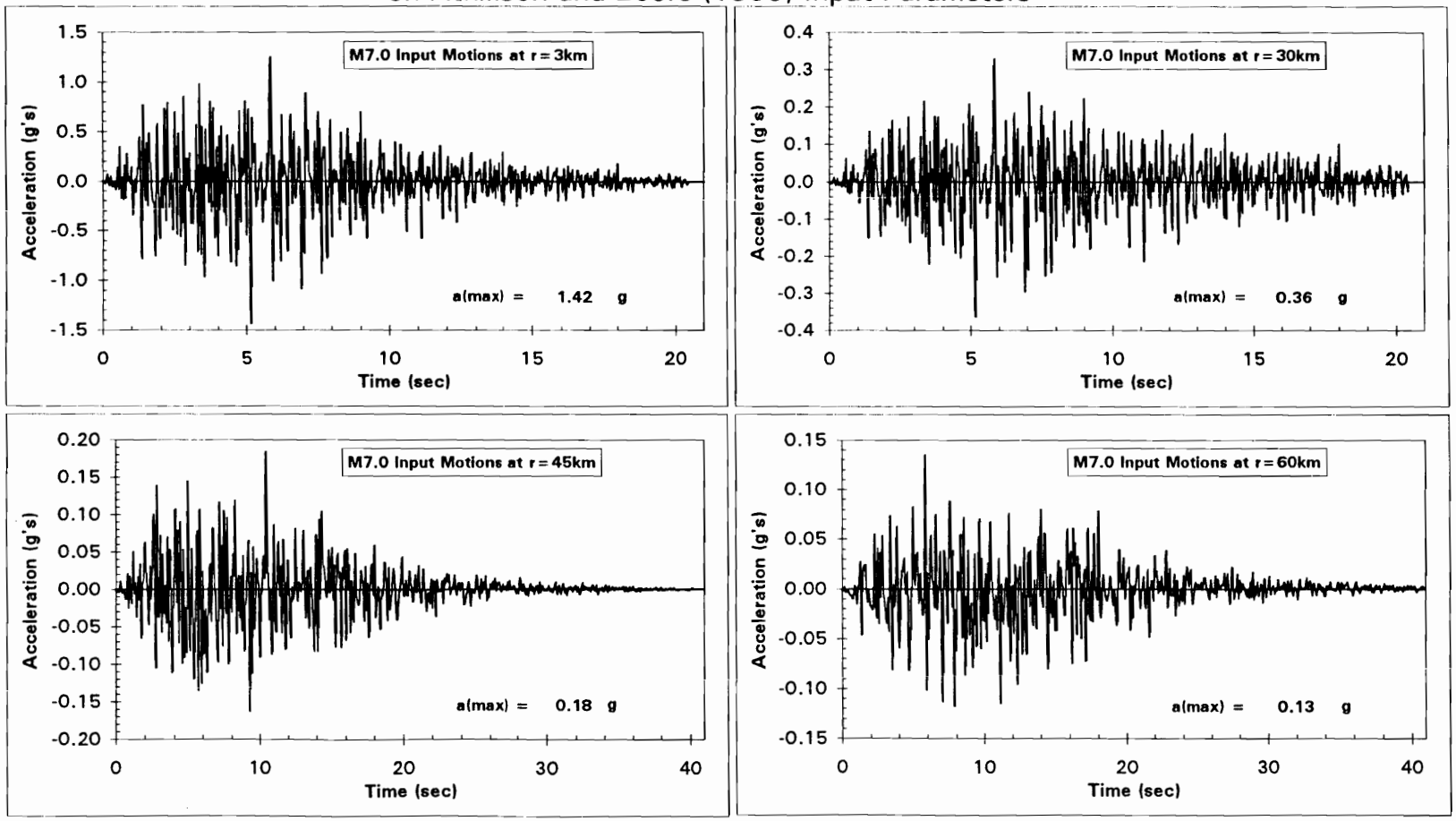

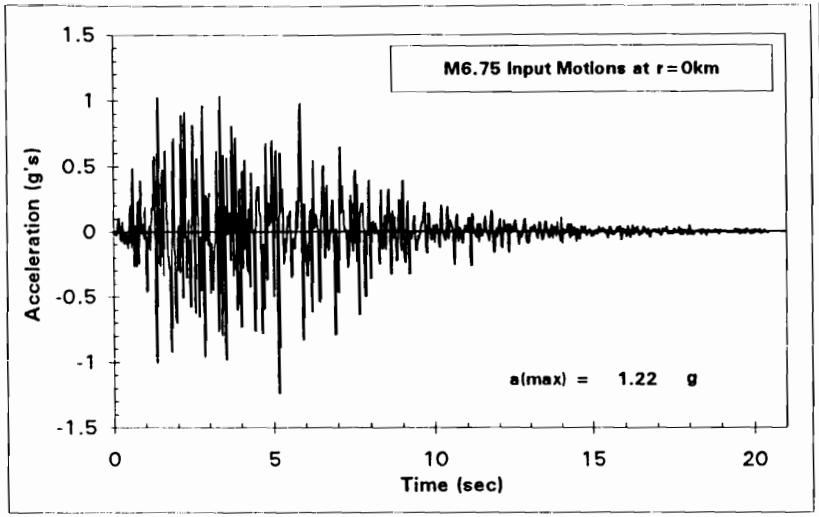

Wabash Valley Paleoseismic Liquefaction Study

ENA M6.75 Bedrock Motions Predicted Using a Stochastic Model Based on Atkinson and Boore (1995) Input Parameters

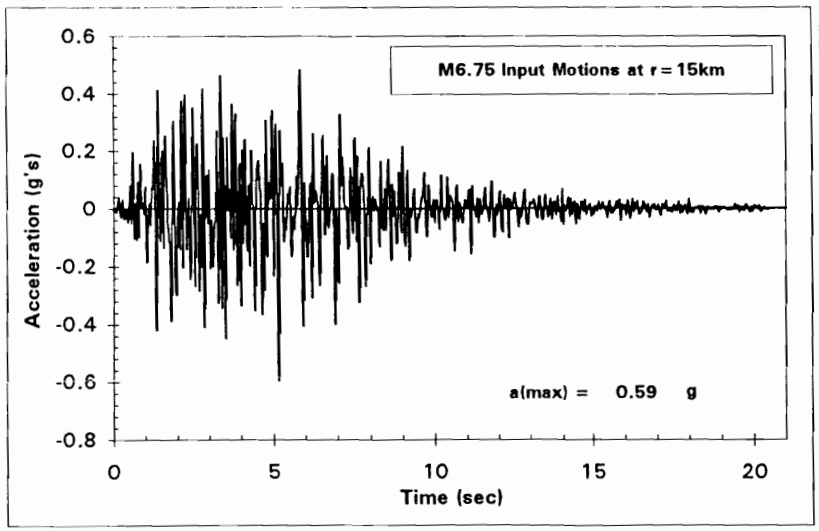

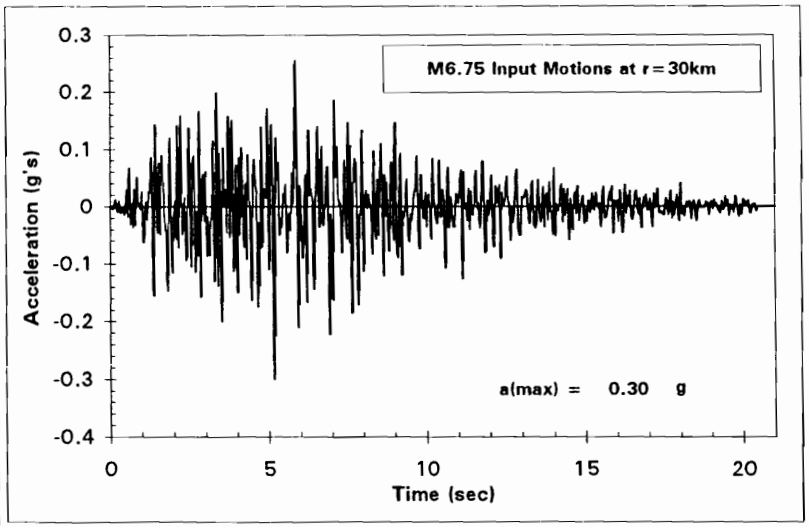

Predicted Surface Motions

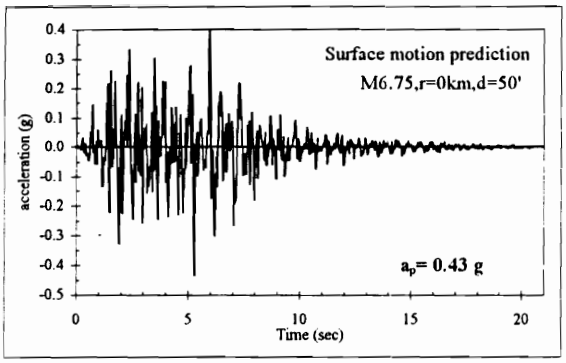

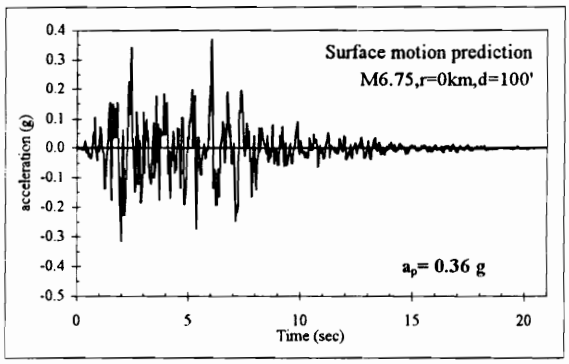

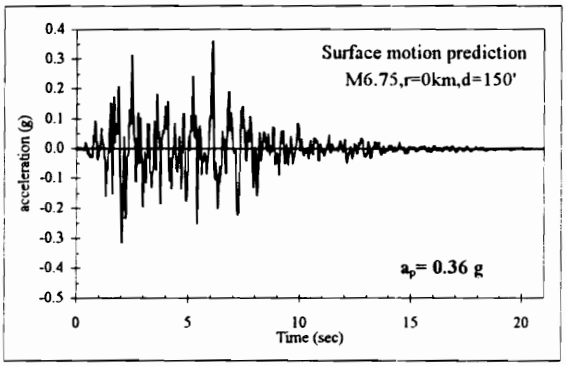

Surface motion predictions for a **M**6.75 ENA event affecting a site at an epicentral distance r = 0 km. Motions are for soil depths of 50 to 250 feet.

$$\frac{\text{average } a_p}{0.38 \text{ g}}$$

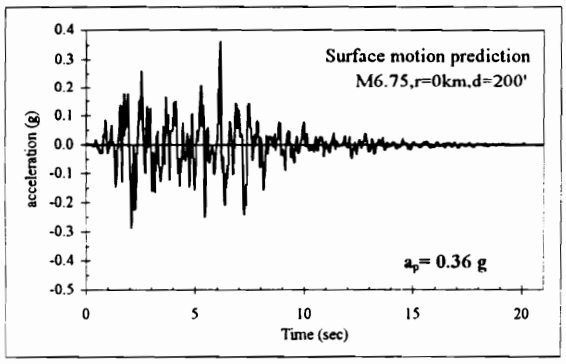

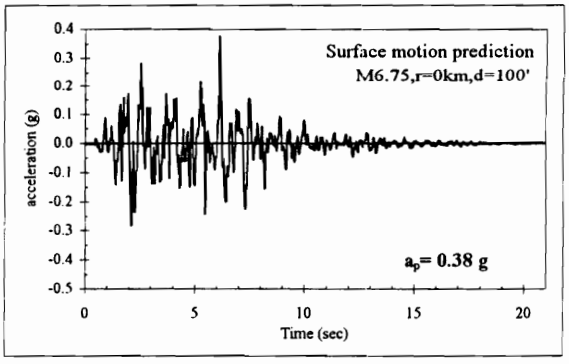

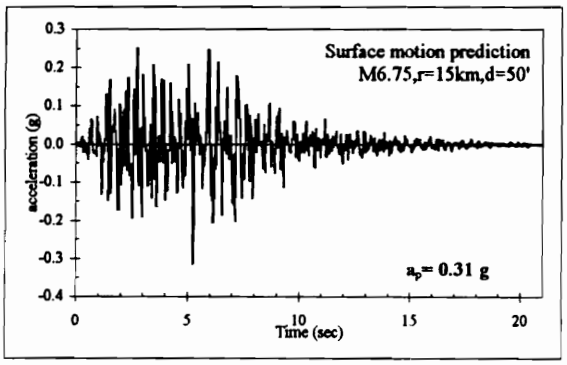

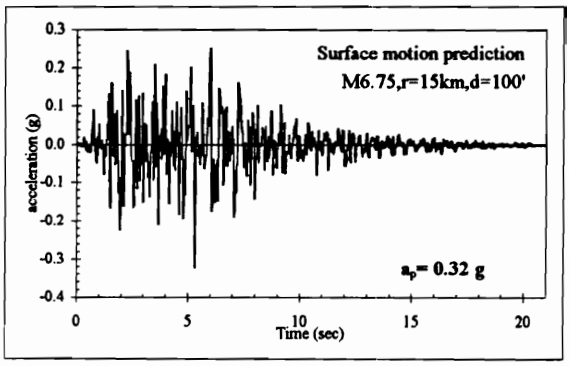

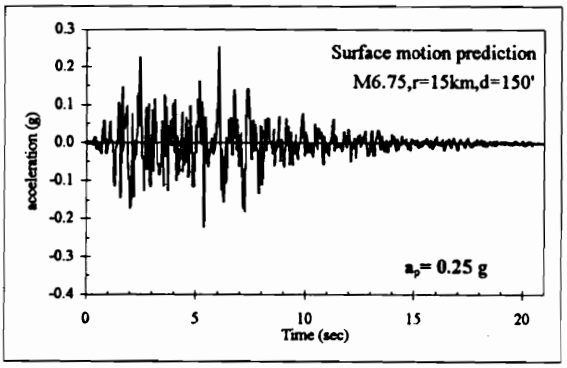

Surface motion predictions for a M6.75 ENA event affecting a site at an epicentral distance r = 15 km. Motions are for soil depths of 50 to 250 feet.

$$\frac{\text{average } a_p}{0.28 \text{ g}}$$

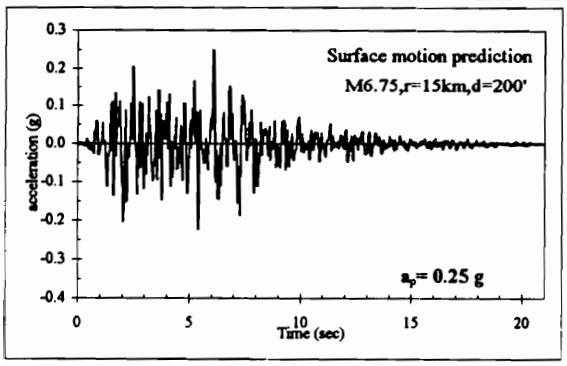

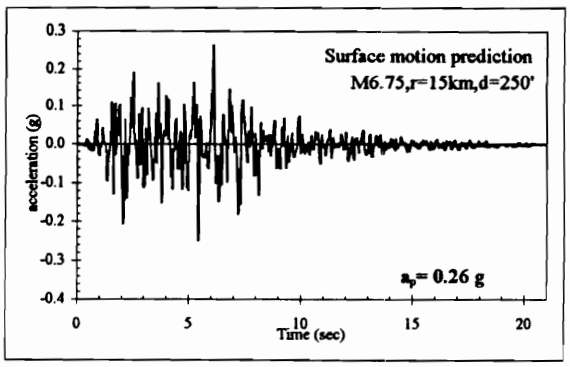

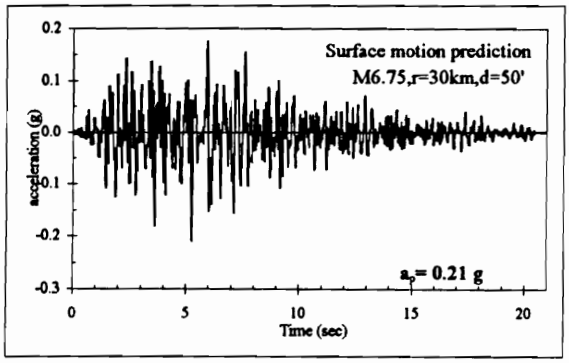

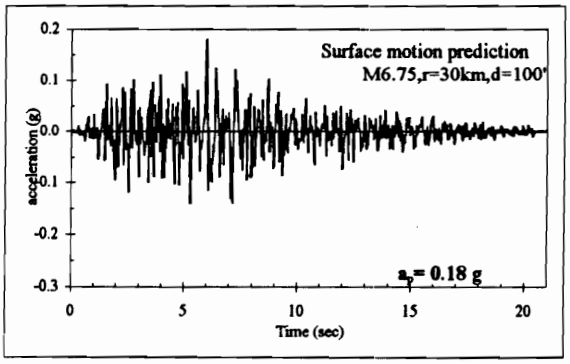

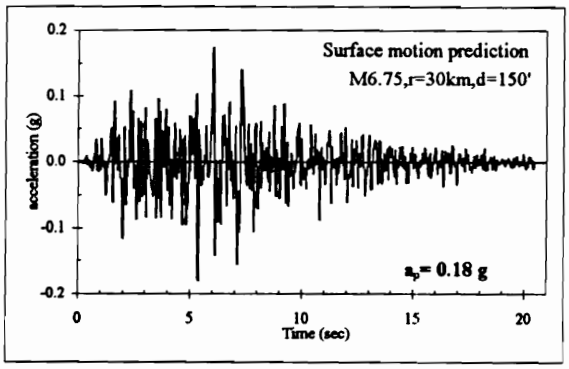

Surface motion predictions for a M6.75 ENA event affecting a site at an epicentral distance r = 30 km. Motions are for soil depths of 50 to 250 feet.

$$\frac{\text{average } a_p}{0.18 \text{ g}}$$

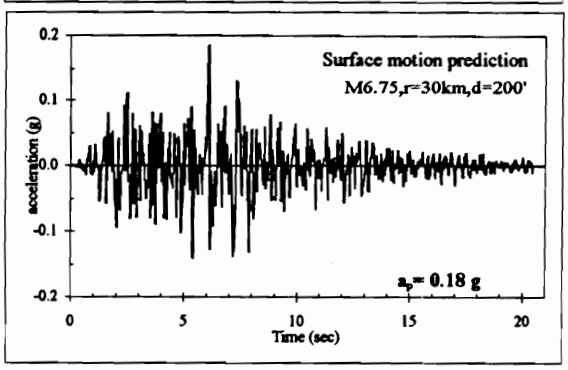

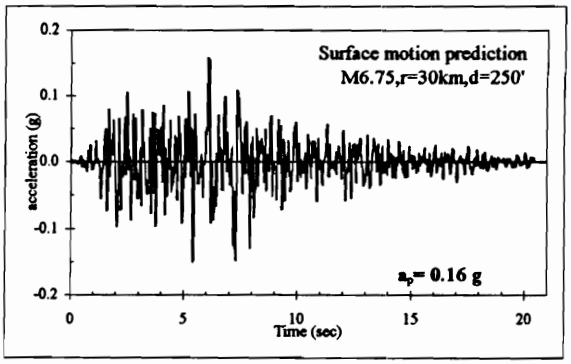

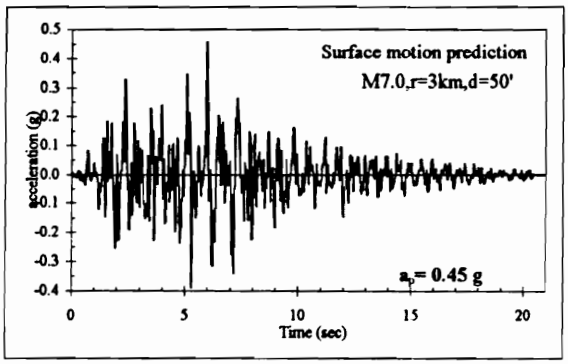

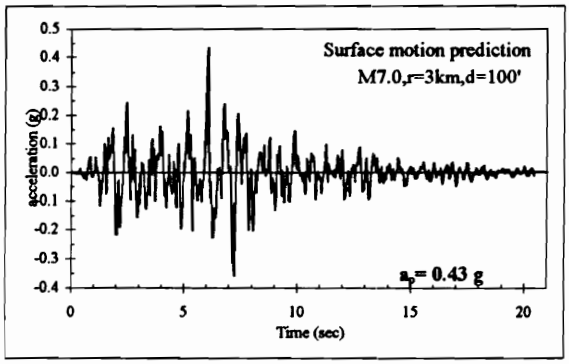

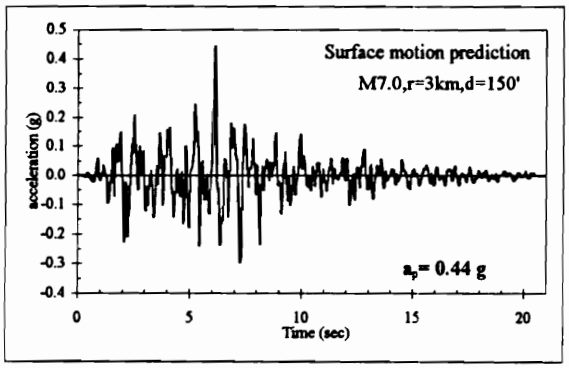

Surface motion predictions for a **M7.0** ENA event affecting a site at an epicentral distance r = 3 km. Motions are for soil depths of 50 to 250 feet.

average a_p
0.44 g

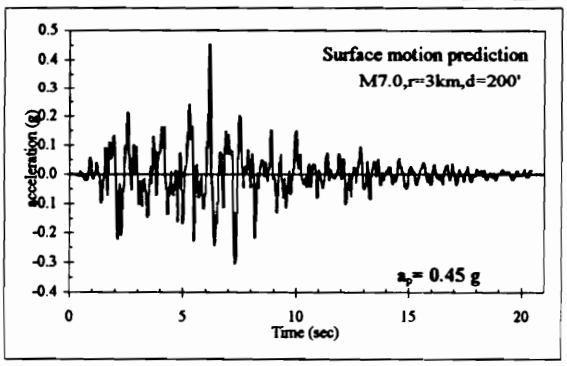

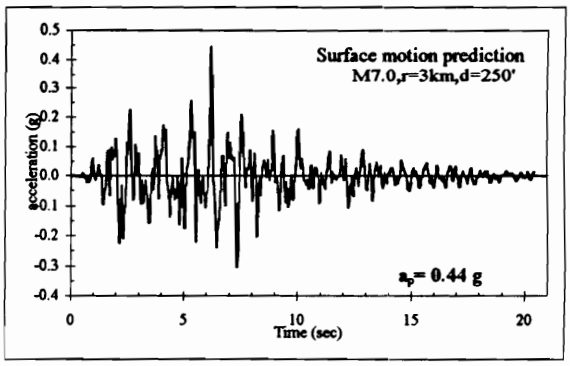

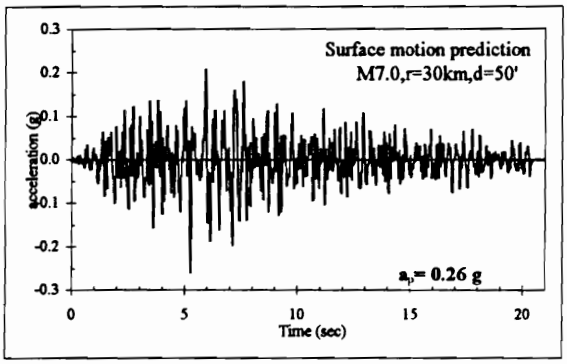

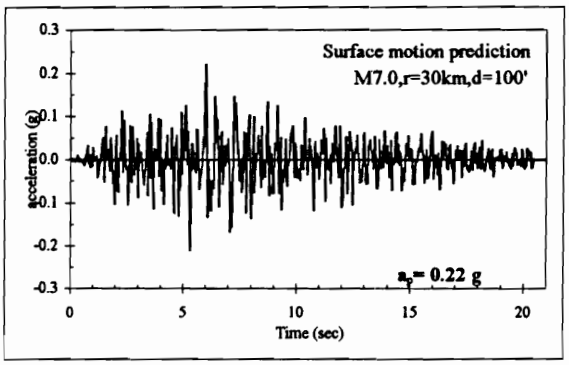

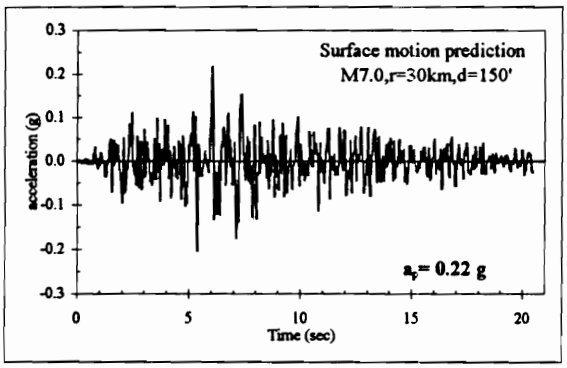

Surface motion predictions for a **M7.0** ENA event affecting a site at an epicentral distance r = 30 km. Motions are for soil depths of 50, to 250 feet.

$$\frac{\text{average } a_p}{0.22 \text{ g}}$$

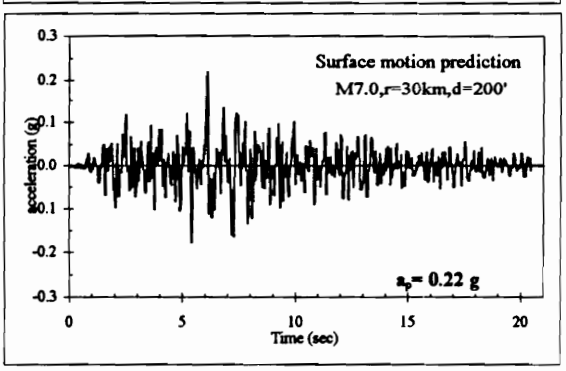

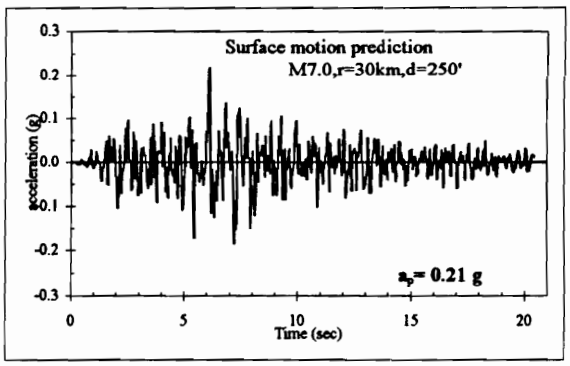

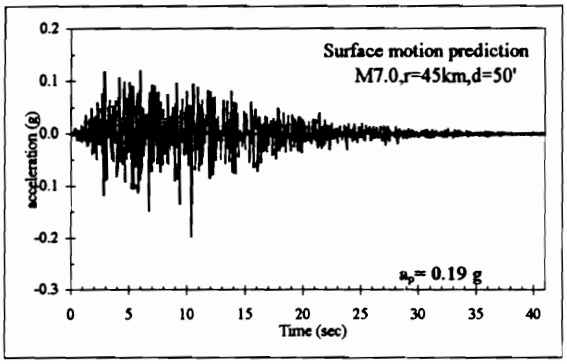

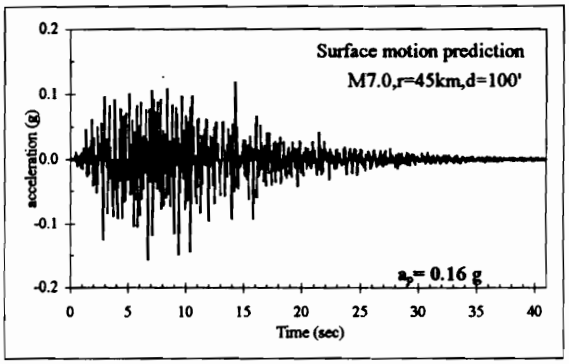

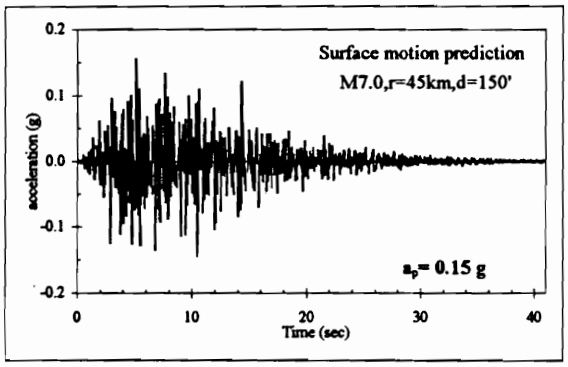

Surface motion predictions for a M7.0 ENA event affecting a site at an epicentral distance r = 45 km. Motions are for soil depths of 50 to 250 feet.

$$\frac{\text{average } a_p}{0.17 \text{ g}}$$

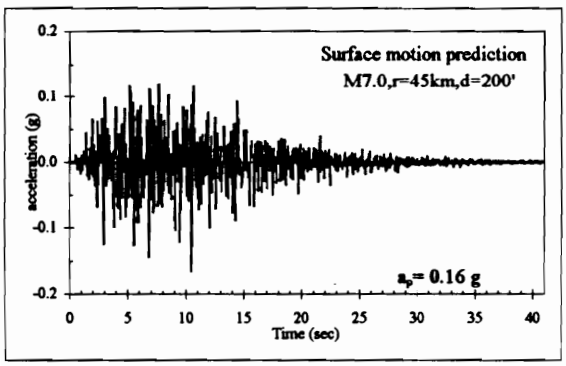

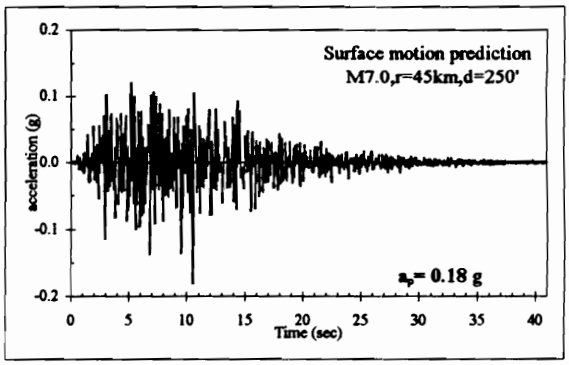

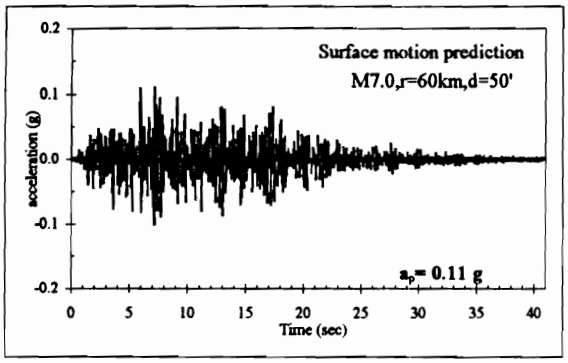

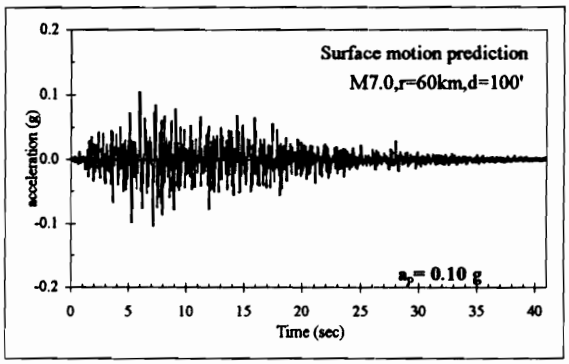

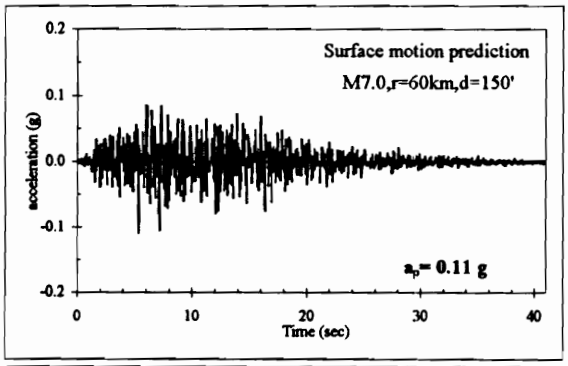

Surface motion predictions for a **M7.0** ENA event affecting a site at an epicentral distance r = 60 km. Motions are for soil depths of 50 to 250 feet.

$$\frac{\text{average } a_p}{0.11 \text{ g}}$$

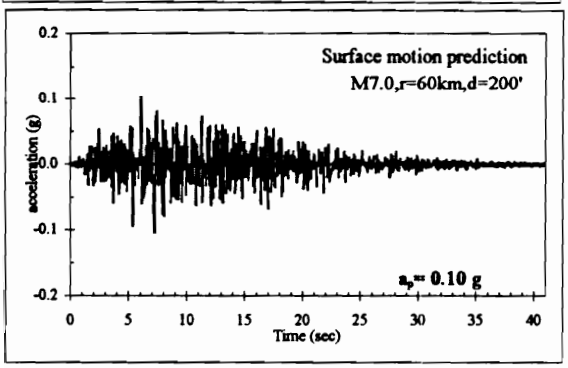

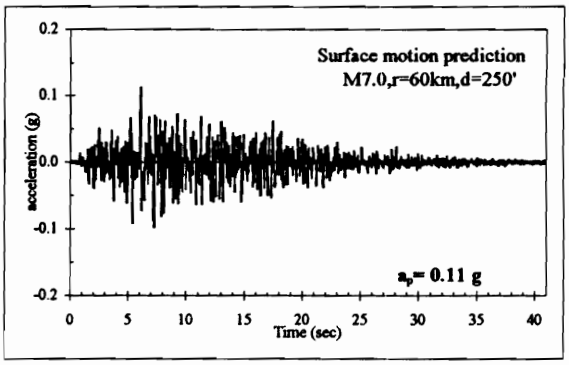

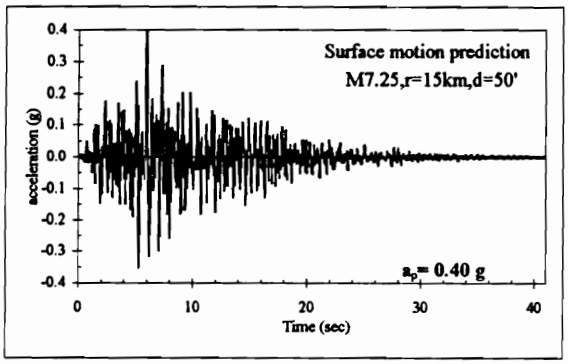

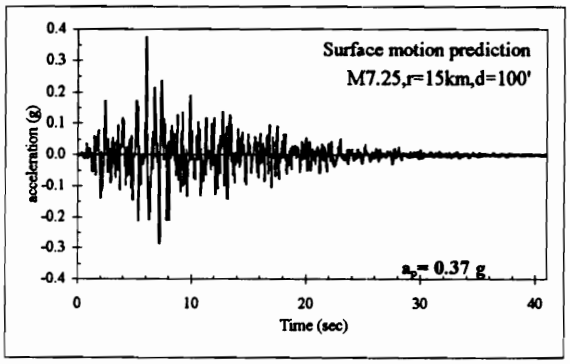

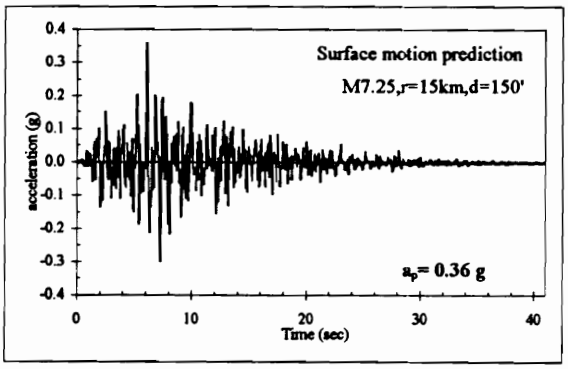

Surface motion predictions for a M7.25 ENA event affecting a site at an epicentral distance r = 15 km. Motions are for soil depths of 50 to 250 feet.

$$\frac{\text{average } a_p}{0.37 \text{ g}}$$

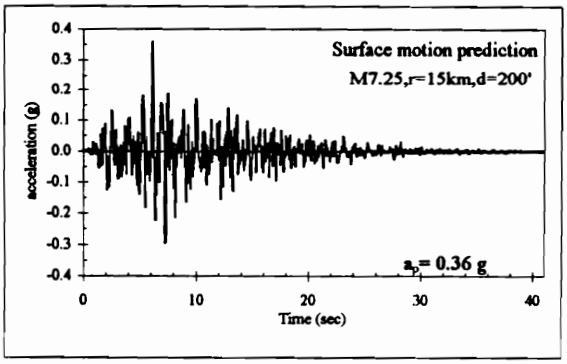

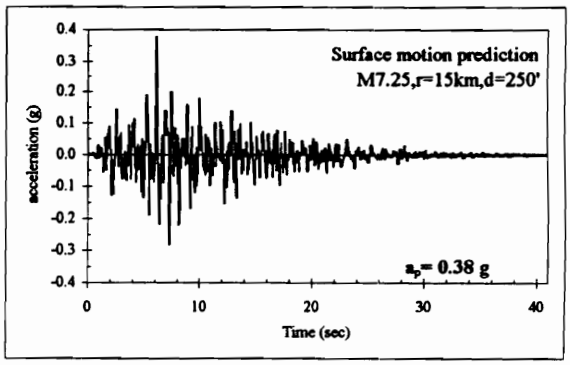

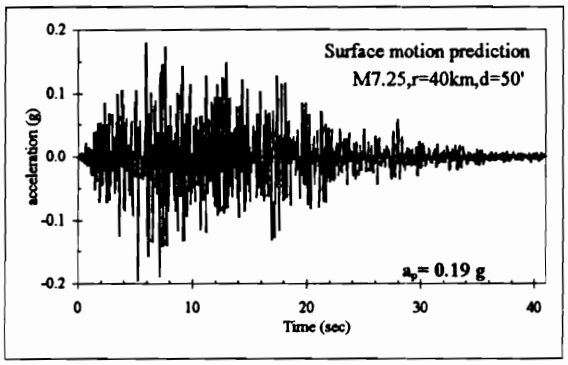

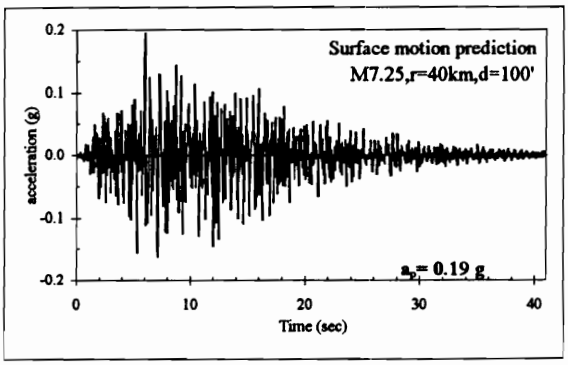

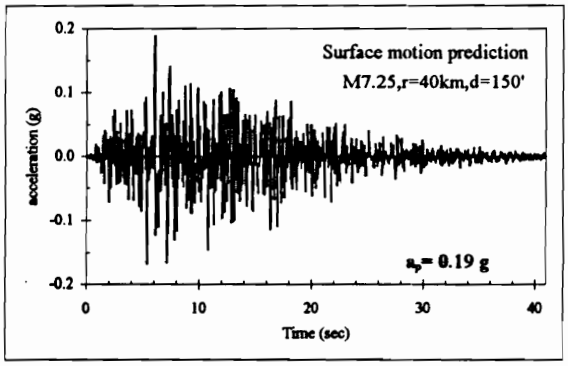

Surface motion predictions for a M7.25 ENA event affecting a site at an epicentral distance r = 40 km. Motions are for soil depths of 50 to 250 feet.

$$\frac{\text{average } a_p}{0.19 \text{ g}}$$

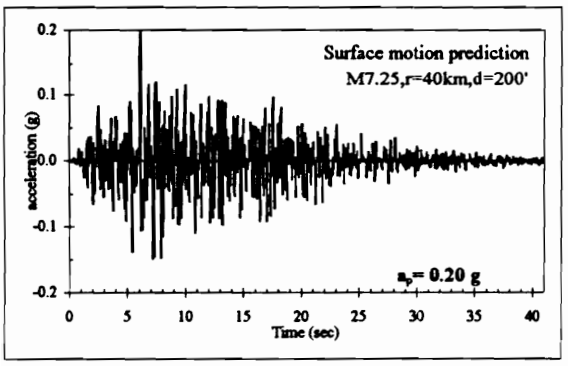

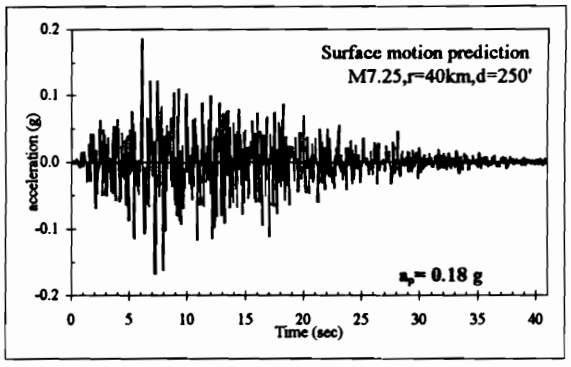

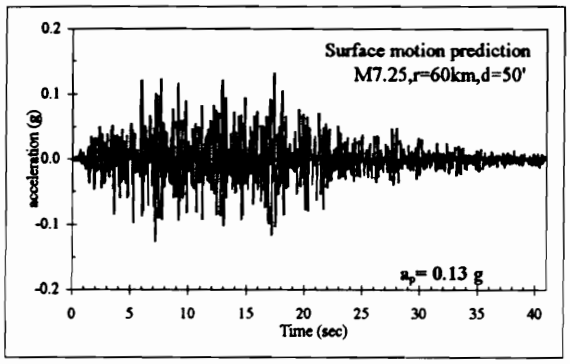

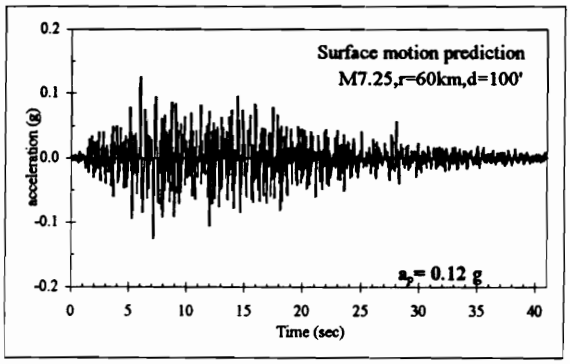

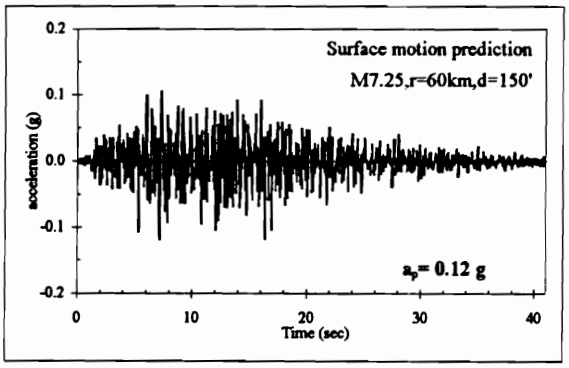

Surface motion predictions for a M7.25 ENA event affecting a site at an epicentral distance r = 60 km. Motions are for soil depths of 50 to 250 feet.

$$\frac{\text{average } a_p}{0.13 \text{ g}}$$

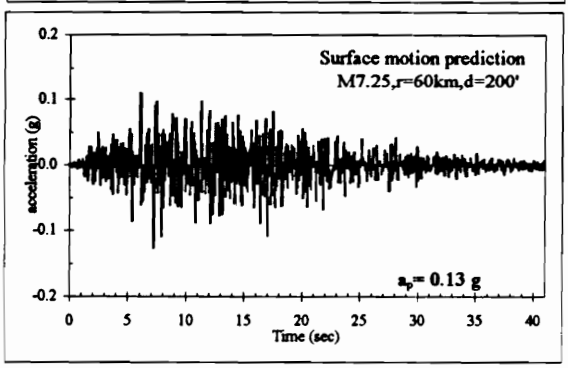

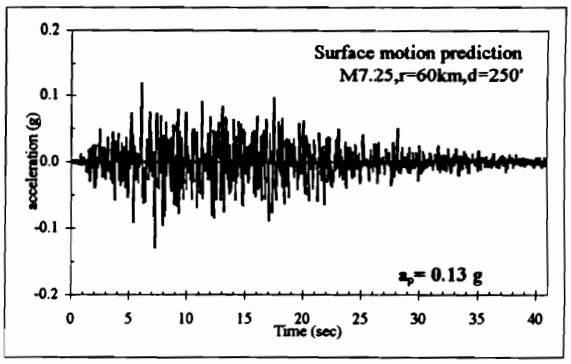

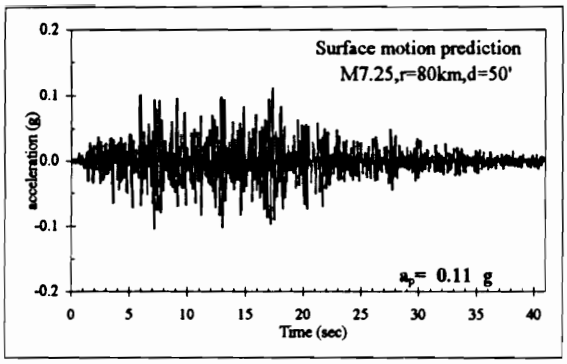

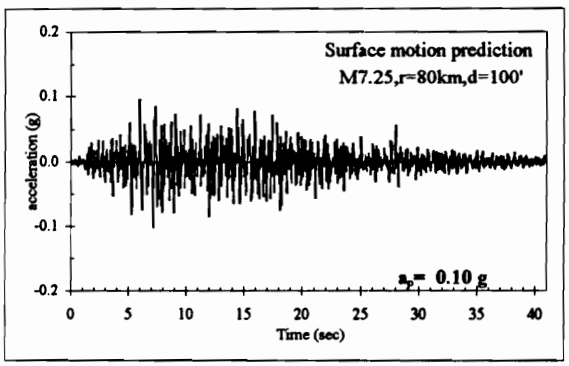

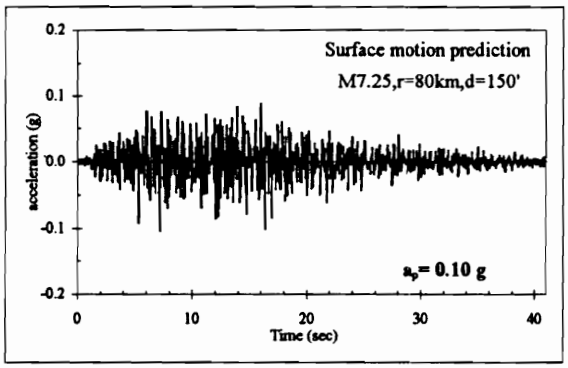

Surface motion predictions for a **M7.25** ENA event affecting a site at an epicentral distance r = 80 km. Motions are for soil depths of 50 to 250 feet.

$$\frac{\text{average } a_p}{0.10 \text{ g}}$$

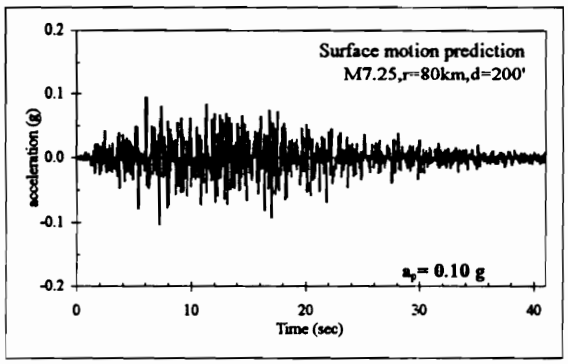

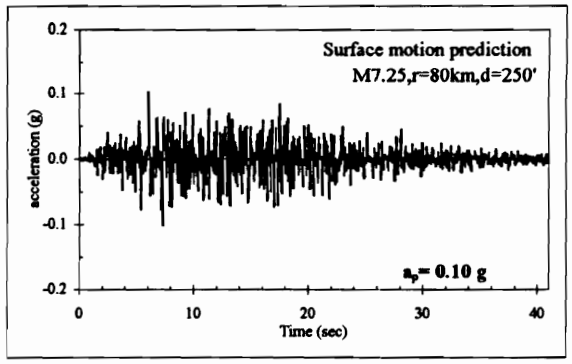

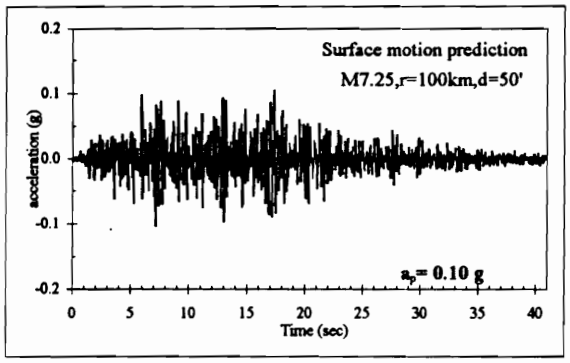

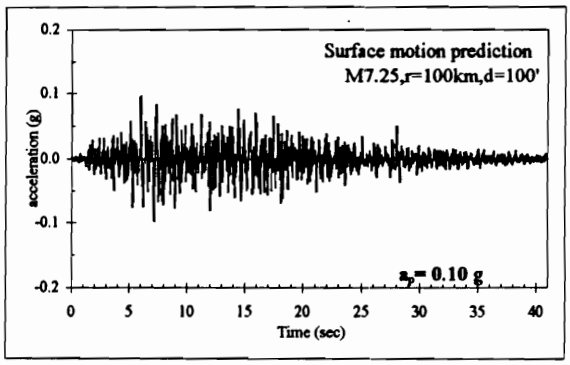

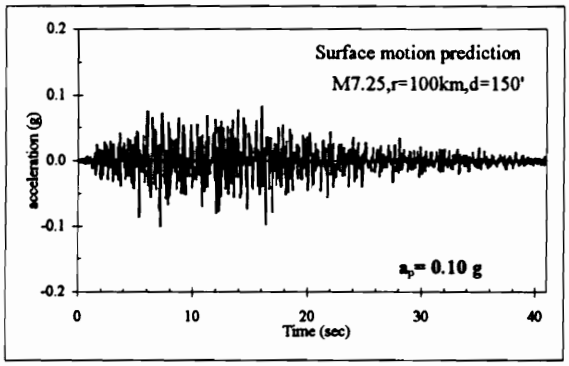

Surface motion predictions for a M7.25 ENA event affecting a site at an epicentral distance r = 100 km. Motions are for soil depths of 50 to 250 feet.

$$\frac{\text{average } a_p}{0.10 \text{ g}}$$

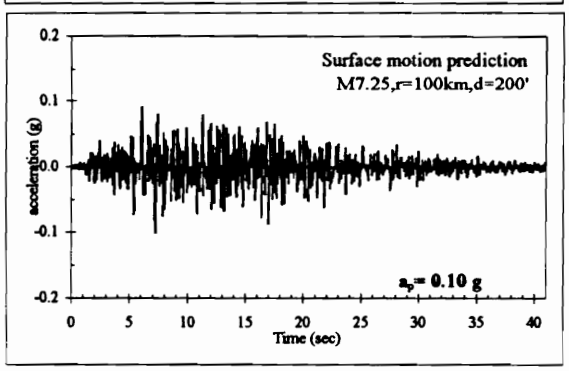

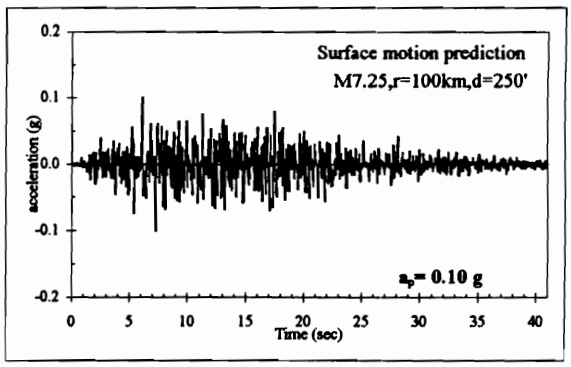

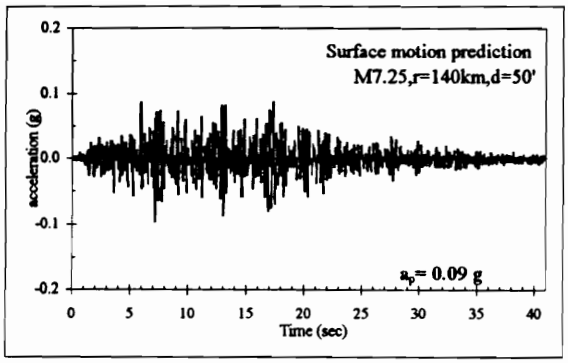

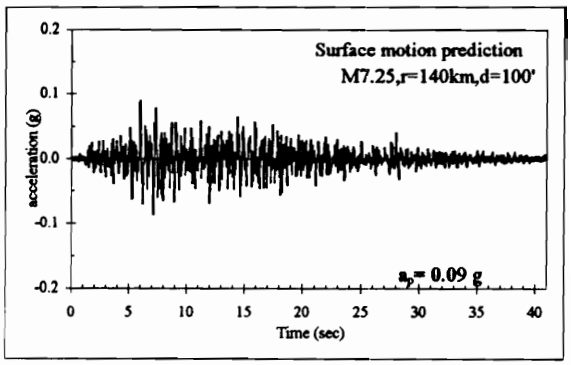

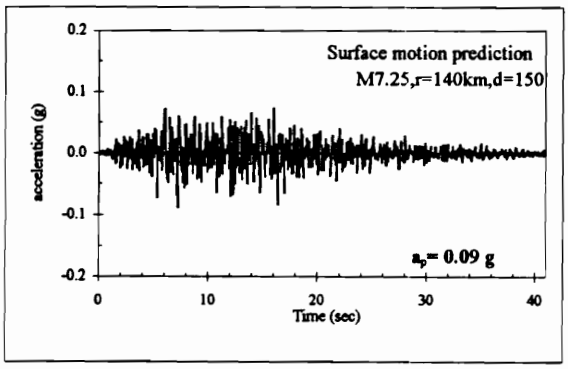

Surface motion predictions for a M7.25 ENA event affecting a site at an epicentral distance r = 140 km. Motions are for soil depths of 50 to 250 feet.

$$\frac{\text{average } a_p}{0.09 \text{ g}}$$

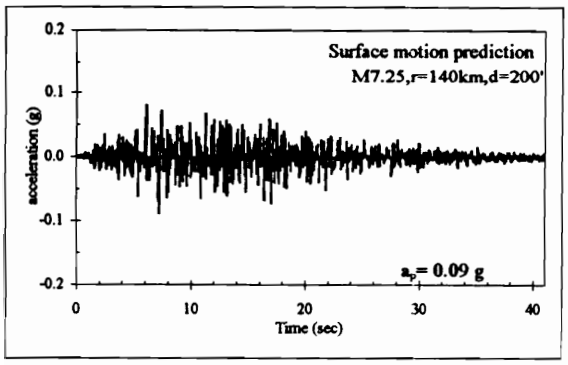

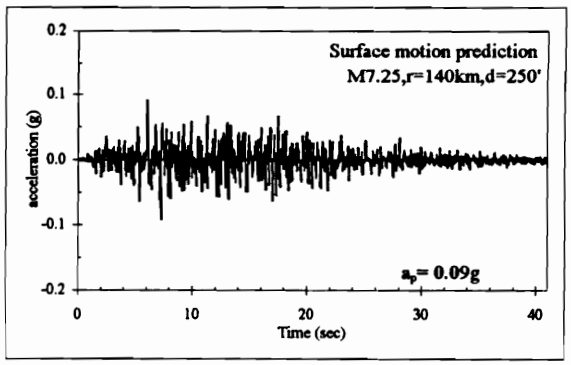

Change in Surface Response Prediction Due to Reduced Bedrock High Frequency Content

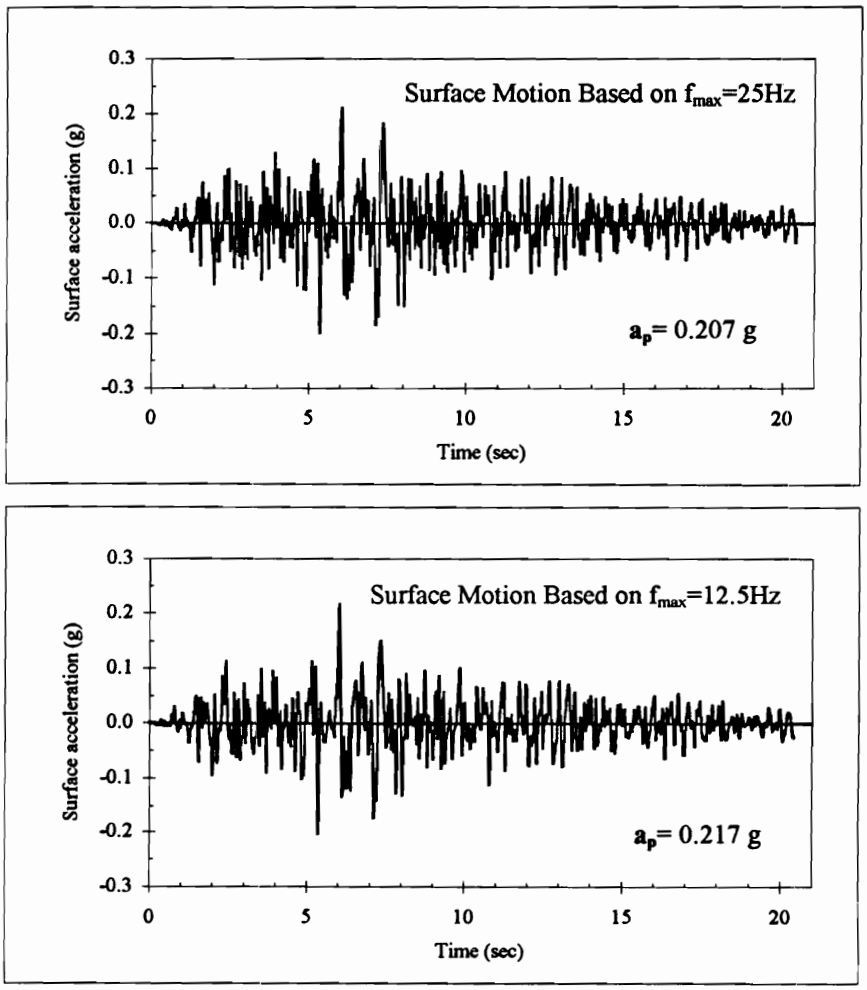

Comparison of Surface Motion Predictions based on f_{max} = 25Hz and 12.5Hz For A M7.0 Event at R= 30km, where soil depth is 150'.

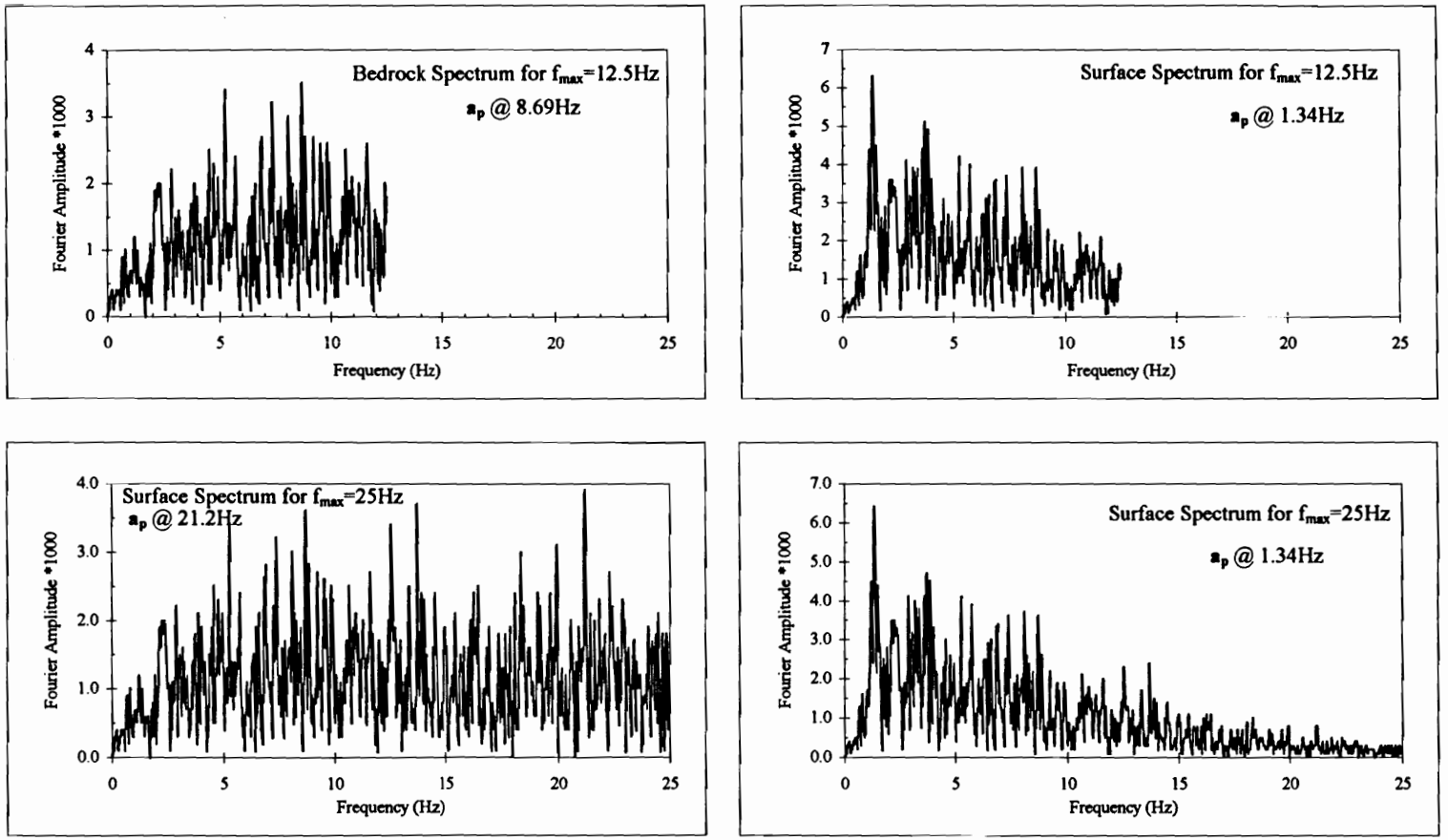

Comparison of Fourier Spectra Associated with Bedrock and Surface Motion Records Where f_{max} = 25Hz and 12.5Hz

Vita

Eric Clifton Pond was born October 21, 1958, in Sacramento, California. He was raised in Astoria, Oregon and Seattle, Washington. After graduating from Garfield High School he attended the University of Washington for two years studying Forestry. He returned to the University of Washington in 1983 to begin an undergraduate Civil Engineering degree program. After graduation in 1987 he was employed by the local geotechnical consulting firm of Rittenhouse-Zeman and Associates, initially as a technician, but was soon promoted to staff and senior staff level engineering positions.

In 1990, he began graduate studies at Virginia Polytechnic Institute and State University. While attending Virginia Tech he was employed as a teaching assistant for Professors G. Wayne Clough and Thomas L. Brandon. After receiving a Master of Science degree in Civil Engineering in 1992, he continued at Virginia Tech pursuing a Doctorate in Civil Engineering as a research associate under Professor James R. Martin, II. While pursuing his graduate degrees he co-authored a number of articles including:

Martin, J. R. and Pond, E. C. (1993) "Seismic Analysis Of Relict Liquefaction Features In Regions Of Infrequent Seismicity," National Research Council Transportation Research Board, Transportation Research Record 1411, pp. 53-60.

Obermeier, S. F., Martin, J. R., Frankel, A. D., Youd, T. L., Munson, P. J., Munson, C.A. and Pond, E. C. (1993) "Liquefaction Evidence For Strong Holocene Earthquake(s) In The Wabash Valley Of Southern Indiana-Illinois, With A Preliminary Estimate Of Magnitude," Unites States Geological Survey Professional Paper 1536, 28 pp.

Munson, P. J., Munson, C. A. and Pond, E. C. (1995) "Paleoliquefaction Evidence For A Strong Holocene Earthquake In South-Central Indiana," Geology, 23(4), 325-328.

Taylor, T., Fragaszy, R. J. and Pond, E. (1995) "Strength Of Gap-Graded Gravelly Soils," in Static and Dynamic Properties of Gravelly Soils, (Mark Evans and Richard Fragaszy, eds.), ASCE, Geotechnical Special Publications No. 56, 20-34.

Just prior to defending his Dissertation he presented the results of his research at the 1996 Seismological Society of America (SSA) Annual Conference in St. Louis. He is currently working on an article for the Seismological Research Letters (SRL) special issue on the Wabash Valley/Illinois Basin. He is a member of the American Society of Civil Engineers, International Society for Soil Mechanics and Foundation Engineering, Seismological Society of America, and Chi Epsilon National Civil Engineering Honor Society. He is registered as an EIT in Washington State.